Functionalized Biaryls as Building Blocks for Non-Aggregating Molecular Spoked Wheels

Dissertation

Zur Erlangung des Doktorgrades (Dr. rer. nat.)
der Mathematisch-Naturwissenschaftlichen Fakultät
der Rheinischen Friedrich-Wilhelms-Universität Bonn

vorgelegt von

Philipp Krämer

aus Troisdorf

Bonn

2024

Angefertigt mit Genehmigung der Mathematisch-Naturwissenschaftlichen Fakultät
der Rheinischen Friedrich-Wilhelms-Universität Bonn

Gutachter*in/Betreuer*in: Prof. Dr. Sigurd Höger
Gutachter*in: Prof. Dr. Andreas Gansäuer

Tag der Promotion: 20.12.2024
Erscheinungsjahr: 2025

Die vorliegende Arbeit wurde am Kekulé-Institut für Organische Chemie und Biochemie der Rheinischen Friedrich-Wilhelms-Universität Bonn in der Zeit von November 2020 bis Oktober 2024 unter der Leitung von Prof. Dr. Sigurd Höger angefertigt.

"Insanity is doing the same thing over and over and expecting different results."

Albert Einstein

Danksagung

Zuallererst möchte ich Herrn Prof. Dr. Sigurd Höger für die Aufnahme in den Arbeitskreis und die Vergabe des interessanten Themas danken. Ich habe das von Ihnen entgegengebrachte Vertrauen, die freie Möglichkeit zur eigenständigen Planung meiner Synthesen und Ihr offenes Ohr bezüglich neuer Themenvorschläge immer sehr geschätzt.

Des Weiteren danke ich Herrn Prof. Dr. Andreas Gansäuer für die Übernahme des Zweitgutachtens, das große Interesse an meiner Forschung trotz des unterschiedlichen Themengebiets und die stets hilfreichen Ideen, von denen diese Arbeit einige Male profitierte. Zudem danke ich Herrn Prof. Dr. Thomas Bredow und Herrn Prof. Dr. Lukas Schreiber für die Übernahme der weiteren Gutachten und die Teilnahme an der Prüfungskommission.

Ein großes Dankeschön gilt Maximilian Kersten, von dem ich die Grundlagen für eigenständiges, sauberes Arbeiten im Labor lernen durfte und für die tolle Betreuung während meiner Bachelor- und Masterarbeit, aus der sich eine gute Freundschaft entwickelt hat.

Ich möchte mich außerdem bei Ute Müller, Nils Schmickler und Alina Hilgers für die Zusammenarbeit im Labor 3.115 bedanken. Nicht zuletzt dank Euch bin ich immer gern dort gewesen, Danke für die schöne Zeit und die gemeinsamen Erlebnisse.

Anna Krönert und Christin Knabbe möchte ich für die tolle Zeit im Arbeitskreis, den vielen außeruniversitären Unternehmungen und der Freundschaft die sich aus der gemeinsamen Zeit entwickelt hat danken. Ebenfalls möchte ich mich bei Sarah Wentzke und Johanna Wollenweber für die Freundschaft und die schönen gemeinsamen Reisen durch Island, München und Irland bedanken.

Bei Laura zur Horst, Nils Denzer und Simon Rickert möchte ich mich ebenfalls für die tolle gemeinsame Zeit im Arbeitskreis bedanken.

David Ari Hofmeister und Jakob Gabriel aus der Arbeitsgruppe von Dr. Stefan-Sven Jester gilt mein Dank für die STM-Untersuchungen einiger meiner Moleküle.

Ein besonderer Dank gilt meinem Freund und Sportpartner Sebastian Höthker, mit dem zusammen ich während des Studiums und der Promotion Körper und Geist gestärkt habe, meistens gleichzeitig. Dein hoher Anspruch an wissenschaftliches Arbeiten hat mich oft ermutigt, mich mit manchen Problemen erneut auseinanderzusetzen und zum richtigen statt zum einfachen Ergebnis zu finden. Danke für deine bedingungslose Hilfsbereitschaft, dein Interesse und dein offenes Ohr.

Ich möchte mich außerdem bei Sarah Wentzke und Sophie Schimmelpfennig sowie Antonia Gres und Anna Stummer für die gute Zusammenarbeit und das Vertrauen während des Anfertigens der jeweiligen Master- beziehungsweise Bachelorarbeiten unter meiner Betreuung bedanken.

Ein weiterer Dank gilt Prof. Dr. Stefan Grimme, Dr. Andreas Hansen und Julia Kohn für die produktive Zusammenarbeit während den Arbeiten an der gemeinsamen Publikation.

Ulrike Blank und Dr. Jochen Möllmann danke ich für alle organisatorischen Hilfestellungen bei Problemen außerhalb der Laborarbeit.
Zudem möchte ich mich bei Benjamin Aymans für die gemeinsame Zeit während des Studiums und der lustigen Partnerarbeiten während diverser Praktika bedanken.
Ich bedanke mich außerdem bei allen ehemaligen Mitgliedern des Arbeitskreises Höger für die gemeinsame Zeit und den hilfreichen Austausch untereinander.
Zudem bedanke ich mich bei BIGS Chemistry sowie bei der GDCh für die finanzielle Bezuschussung diverser Forschungsreisen zu verschiedenen Konferenzen, die andernfalls nicht möglich gewesen wären.
Ein großer Dank gilt außerdem meinem besten Freund Simon Helwig für die Unterstützung und die gute Freundschaft während meines gesamten Studiums. Danke für deine stets offene Tür und deine tollen Ratschläge aus einem so anderen aber hilfreichen Blickwinkel. Außerdem bedanke ich mich bei Annkristin Lütz und Kerstin Besenbeck, ohne die die gemeinsame Zeit in unserem Nebenjob im Kino nicht so unterhaltsam gewesen wäre. Ich bin sehr froh, dass unsere Freundschaft diesen Job überdauert hat.
Ein wahnsinnig großer Dank gilt meiner Familie für die Finanzierung meines Studiums und die Unterstützung während meines gesamten Bildungswegs. Ohne eure ermutigende Erziehung hätte ich diesen Weg wahrscheinlich nicht eingeschlagen. Namentlich danken möchte ich meinen Eltern Thomas und Petra Krämer, meinem Bruder Torben Krämer und meinen Großeltern Helmut und Elfie Grützenbach sowie Friedhelm und Rita Krämer. Ebenfalls bedanken möchte ich mich bei Olaf und Barbara Trubel für die ständige Gastfreundschaft, die gemeinsamen Urlaube und das Zugehörigkeitsgefühl zu auch ihrer Familie.
Ein großer Dank gilt meiner Freundin Martha Trubel. Ohne dich hätte ich das Studium wahrscheinlich nicht geschafft, Danke für deine emotionale Unterstützung und für all die gemeinsamen Erinnerungen der letzten Jahre.
Der letzte Dank gilt Allen, die ich leider vergessen habe namentlich zu erwähnen. Auch Euch sei nochmal herzlich gedankt.

Contents

1 Abstract

Molecular spoked wheels (MSWs) showed to be synthetically accessible in various sizes and functionalization in the past. Due to their construction of not only phenylene- but also acetylene- and bisacetylene-units, some of the molecules turned out to decompose when stored under ambient conditions for too long. To overcome such decomposition, the employed structural motifs were limited to all-phenylene subunits, that were more inert towards ambient conditions, but revealed limits considering their lateral expansion. Within the final synthetic step, the formation of intermolecular bonds was observed instead of the desired intramolecular cyclization reaction. Detailed investigation came to the conclusion, that the open-framed precursors' tendencies to aggregate caused such intermolecular oligomerization.

Hence, this work deals with synthetic strategies to overcome the aggregation of all-phenylene MSW precursors. To do so, the established synthetic strategy was advanced. It was found to be helpful to introduce alkyl groups into the precursors' spokes to 1) maintain high solubility during its preparation and 2) to separate the open-framed precursors that is it insufficient for them to aggregate. Two promising building blocks are fluorene and biphenol.

Fluorene comes with the advantage, that it can be halogenated regioselectively in 2- and 7-position, allowing the construction of large, nearly linear aromatic precursor molecules *via* transition metal catalysis in few steps. Besides that, the mentioned alkyl groups can be introduced into the motif straightforward because of its acidic 9,9'-position. Biphenol can be alkylated with similar ease, since its two hydroxy groups can be utilized as strong nucleophiles as well under mild basic conditions. Due to its electronic properties, a late halogenation of (alkylated) biphenol is not possible, requiring an elaborate synthesis of the unit from two moieties.

The synthetic investigations of the final cyclization were supported by quantum chemical simulations predicting their outcome. Due to the slightly bent geometry of fluorene, the resulting MSWs become bowl-shaped, making it unclear, if a cyclization of the rim fragments can occur successfully in the final step. Thus, each cyclization step of the six-fold closure was investigated individually regarding the distance between both fragments as well as the strain introduced into the molecule after a successful bond formation. In the end, the predictions turned out to be in full accordance with the synthetic evidence.

The accessed MSWs were structurally proven *via* NMR spectroscopy and mass spectrometry and scanning tunnelling microscopy (STM), providing valuable insights into their geometry, the orientation of the newly introduced spoke unit and their packing on highly oriented pyrolytic graphite (HOPG).

2 Introduction

2.1 Carbon

Carbon forms the center of life as we know it. In organic chemistry, carbon's most prominent binding partners are hydrogen, nitrogen, oxygen and halogen atoms, while a broad variety of other atoms is described in literature as well. The introduction of amino acids in biology and biochemistry for example extends that list by sulfur (cysteine, methionine) and selenium (selenocysteine). Unlike most other atoms in organic chemistry, carbon also forms single- or multiple bonds to another carbon atoms to the extent of pure carbon compounds. The resulting all-carbon structures are referred to as allotropes as they are solids but feature different atomic constitutions[1] The most prominent examples for carbon allotropes are graphene, fullerene and diamond.

Graphene as the first and most common representative is entirely built from sp^2-hybridized carbon atoms and therefore forms two-dimensional, planar structures. In an angle of 120°, each carbon atom is surrounded by three other carbon atoms resulting in a honeycomb structure. Its hybridization combined with the planar arrangement makes graphene an excellent electric conductor due to the delocalization of π-electrons above and below the molecular plane. Graphene can also form non-covalent, three-dimensional structures. Here, multiple two-dimensional layers stack through weak *van-der-Waals* interactions forming a multi-layer structure, which is then known as graphite.[2] Those layers can easily be separated for example through very weak mechanical force, which is illustrated by its application as a material for pencil leads. A three-dimensional motif that is structurally reminiscent of graphene is the carbon nanotube. In theory, these tubes result of simply rolling up one monolayer and connecting its edges. The perimeter of the tube here is equal to the diameter of the flat monolayer.[3]

If the structure of a monolayer is slightly modified, for example by exchanging a distinct fraction of six-membered rings by five-membered rings, the monolayer will no longer remain flat and starts to curve. At a certain ratio the curvature introduced becomes so strong that it is possible to connect the edges resulting in a spherical, all-carbon structure. This highly symmetrical class of compounds is known as fullerenes. One prominent example for this class is the *Buckminster* fullerene consisting of exactly 60 carbon atoms. Its geometry consists of 32 faces, 20 hexagonal and 12 pentagonal faces, and forms a truncated icosahedron. The structure gained in fame especially in Europe due to its similarity to a common football.[4]

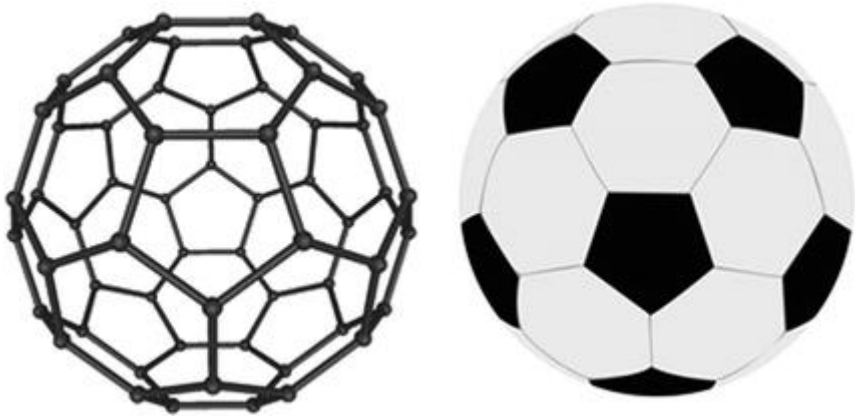

Figure 1: Similarity of *Buckminster* fullerene and a common football.[4]

In 1996, *Robert Floyd Curl Jr*, *Sir Harold Walter Kroto* and *Richard Errett Smalley* were awarded with the *Nobel* Prize in Chemistry for the discovery of fullerenes.[5]

The diamond modification of carbon is amongst its most famous representatives and even name-giving for a crystal structure. It is a cubically crystallizing, naturally occurring form of carbon and appears colorless and transparent if pure. In fact, various colors of diamonds are known, which result from heteroatoms contained within the structure as crystal defects. Technically, those colored diamonds are no longer carbon allotropes due to the impurities. Very characteristic for this crystal structure is its low atomic packing factor of 0.34, representing that only 34 % of the available space is actually occupied by atoms.[6] Additionally, diamond is the hardest material found on earth and positioned on top of the *Mohs* scale with a value of 10.[7] Due to its preciousness, diamond has its own measure of weight, which is given in *carat* and often used to determine its value. In 1907, that unit was standardized to exactly one-fifth of a gram resulting in the metric carat that is still used to quantify different gems.[8] Today, diamonds find application in jewelry but also in industry, for example as blades in scalpels or as material in drilling bits.

Due to modern techniques, it is also possible to craft fibers from carbon that open up a whole new area of usage. Carbon fiber is used in many fields because of its high impact-resistance paired with its lightweight. The combination of these three properties makes carbon fiber the preferred material for most sport equipment like rackets and bicycles. Additionally, in motorsports and in the sport cars industry, large parts of cars are crafted from carbon fiber to reduce the weight of the vehicle without losing stiffness. The incorporation was pushed to the limit by *Lamborghini* in the *Sesto Elemento* (ital.: “sixth element”) in 2010, with its name relating to the atomic number of carbon. Here, the company took the existing *Gallardo SuperLeggera LP 570-4* and substituted as many parts as possible through carbon fiber resulting in a weight loss of about one third which resulted in drastically improved performance regarding for example acceleration.[9]

Figure 2: *Lamborghini Sesto Elemento*, first presented in 2010, as an experimental study to explore the limits of carbon fiber incorporation into sports cars.[9]

2.2 Carbon-Carbon bond formation

Carbon not only forms covalent bonds to other elements but also to other carbon atoms. In nature as well as in organic synthesis, carbon-carbon bonds can be formed in many ways. With all the advances of the past 50 years, cross coupling reactions are amongst the most efficient and relevant methods. Anyways, since that class of reactions only became available in the early 1970s with the discovery of the first metal-*catalyzed* cross coupling by *Kumada*[10] and the subsequent refining work in cross coupling chemistry by *Negishi et al.*[11], it is important to understand how such bonds were formed prior to that discovery to better appreciate the impact of that work.

2.2.1 Transition metal-free carbon-carbon bond formations

Transition metal-free carbon-carbon bond formation reactions are not necessarily worse than the transition metal-catalyzed ones. In fact, some of the presented examples are not even possible through transition metal catalysis. Still, carbon-carbon bonds can be formed *via* all four "basic arithmetical operations" of organic chemistry: over pericyclic, cationic, anionic and radical pathways.

The most famous example of pericyclic bond formation is the *Diels-Alder* reaction. Discovered back in 1928, this reaction not just forms one but two bonds within one reaction step in a concerted fashion.[12] *Otto Diels* and *Kurt Alder* were rewarded with the *Nobel* Prize in Chemistry for their research in 1950.[13] The reaction occurs between a diene and a dienophile. Mechanistic investigations proved, that the reaction rate strongly depends on the electronic properties of both compounds and that it promotes the reaction rate the most, if both compounds are of contrary electronic properties.[14,15]

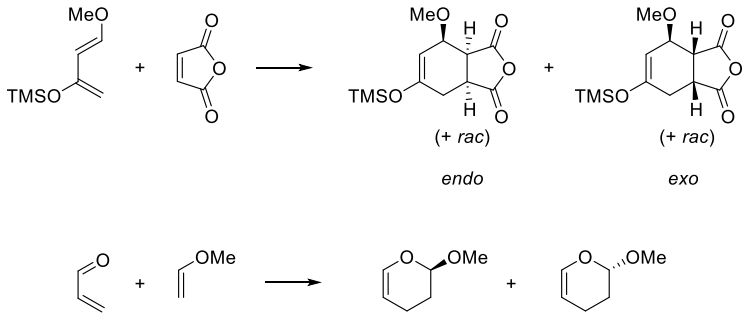

Scheme 1: *Diels-Alder* reaction with normal electron demand (electron-rich diene and electron-deficient dienophile) using the *Danishefsky* diene[16] (top) and *Diels-Alder* reaction with inverse electron demand (electron-deficient diene and electron-rich dienophile) between acrolein and methyl vinyl ether[17]; both yielding a mixture of enantiomers.

The formation of carbon-carbon bonds over cationic species is known for about 150 years. In 1877, *Charles Friedel* and *James Mason Crafts* discovered the mediating influence of metal halides in the preparation of alkylated and acylated aryl compounds.[18]

The reaction was amongst the first examples of an electrophilic aromatic substitution (S_EAr). It requires strong *Lewis* acids like $AlCl_3$ or $FeBr_3$ in order to activate the second reagent, an alkyl- or acyl-halide. Through formation of MX_4^- species (M = metal, X = halide), a carbo-cation is generated that can react with an arene in an S_EAr-reaction. The reaction inherits a high tolerance of functional groups at the arene, as long as they are not electron-withdrawing groups (EWG). Hence, a second substitution of already acylated compounds is only observed for alkylation reactions.[19]

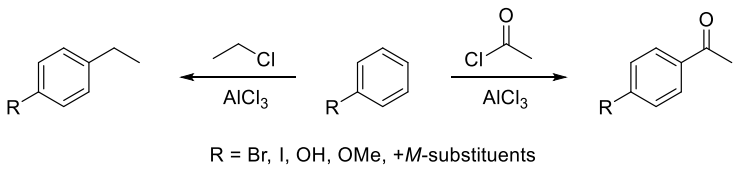

Scheme 2: Electrophilic aromatic substitution *via Friedel-Crafts* alkylation (left) and acylation (right). The second substitution of mono-substituted aryl compounds mostly happens in *para*-position for steric reasons.

Especially the preparation of acyl compounds is of high importance for both industry and research, as it gives access to for example relevant compounds for enolate chemistry.

An elementary way of anionic formations of carbon-carbon bonds is the nucleophilic substitution (S_N). In fact, the generation of carb-anions for S_N-reactions can be difficult and only few examples are described. The most prominent carbon nucleophile for such bond formation reactions is cyanide, frequently applied to convert different alkyl halides into nitriles, which can later be reacted into a broad scope of other functional groups. Hence, the introduction of cyanide is a very elegant method to extend a molecule by a single carbon unit.

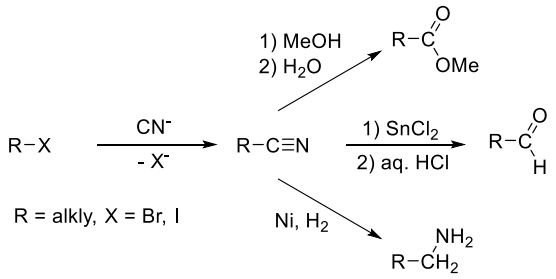

Scheme 3: Generation of nitriles from alkyl halides *via* nucleophilic substitution and further transformations of nitriles.[15]

A big field of anionic carbon-carbon bond formation reactions is opened up by enolate chemistry. In carbonyl compounds, especially the protons in *α*-position are acidic as a result of the strong mesomeric stabilization of the resulting anion through the carbonyl group. This is also the case for carbonyl compounds like the previously described methyl ketones.[15] Another example for the elimination of a proton can be found in fluorene, where the loss is highly favored due to the resulting aromatic anion.

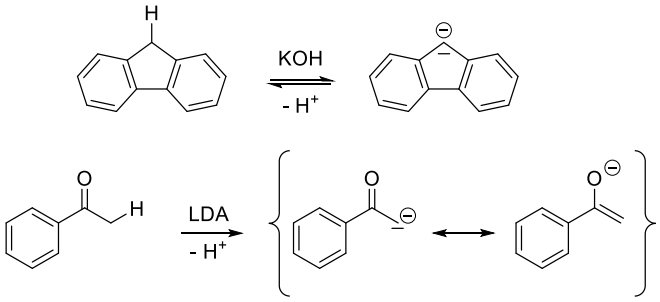

Scheme 4: Deprotonation of fluorene to achieve one fully conjugated system over two small individual conjugated systems (top) and deprotonation of acetophenone forming the corresponding stabilized enolate (bottom).

Even though fluorenyl anions are well stabilized through the extended aromatic system generated, they can be used as nucleophiles for example in S_N2-reactions with alkyl halides.[20]

The preparation of enolates, on the other hand, often requires low temperatures of -78 °C, specific solvents like THF and an air- and moisture-free atmosphere to be stabilized. Depending on the substrate and competitive reactions, the choice of base can influence the regioselectivity of deprotonation.[15]

Even though the preparation of enolates requires effort and precise conditions, their synthetic application is quite rewarding as they are a major component in aldol chemistry. To access such structures, either two aldehydes, two ketones or an aldehyde and a ketone need to be reacted.[15]

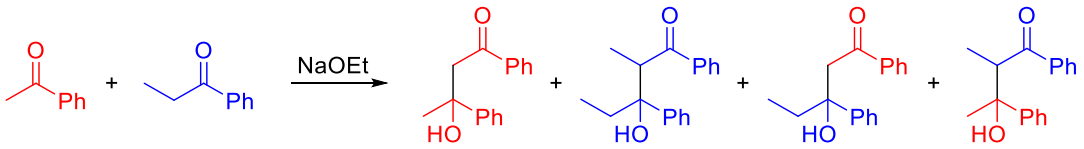

Scheme 5: Aldol reaction of a mixture of unsymmetrical ketones. Both ketones can form an enolate and either attack the same or the other type of ketone. For simplicity, stereochemistry is neglected here.

To avoid this, the choice of substrates can be changed to only one compound featuring acidic protons in *α*-position to the carbonyl group. This way, one product is obtained preferred because only one substrate can form an enolate, which reacts faster with the aldehyde than with another acetophenone. If the resulting aldol contains a proton between both oxygen-decorated groups, the molecule can additionally eliminate water in an aldol condensation under both acidic or basic conditions. Enoates are valuable, synthetic intermediates that are commonly employed as *Michael* acceptors.[21]

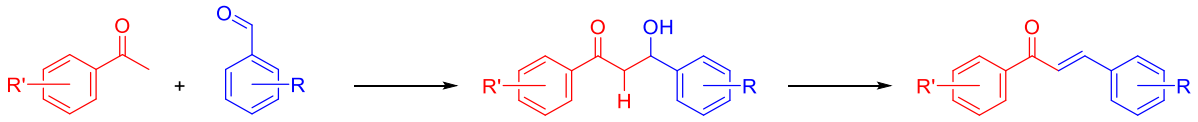

Scheme 6: Reaction of an acetophenone and an aldehyde into an aldol followed by an aldol condensation.[15]

A famous name reaction in aldol chemistry is the *Mannich* reaction. Through this method, *β*-amino carbonyl compounds can easily be prepared.[15]

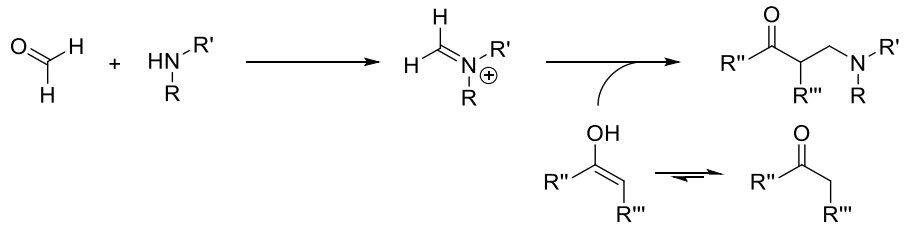

Scheme 7: Reaction example of the *Mannich* reaction forming the activated species in the first step, which is then reacted with the enolate form of a carbonyl compound into the desired product. All residues can be identical for this reaction.[15]

The chemistry around aldols is of high interest for many fields. Its simplest natural application is most likely within the citric acid cycle where stored energy is released from different nutrients.[22] On the other side, the 1,3-functionalization with oxygen-groups resulting from aldol reactions is a prominent motif for pharmaceutical applications. For example, the drug *Lipitor*, whose main pharmaceutically active agent is atorvastatin, that used to prevent cardiovascular disease, contains a functionalization that can be constructed through aldol reactions.[23] Besides the presented information, aldol reactions bring a broad scope of possibilities to synthesize chiral compounds in a stereoselective fashion. Since the field of stereoselective reactions is not of interest for this work, these possibilities and all theoretic discussions that come with it will not be further elaborated.

Radical carbon-carbon bond formations find their major application in polymer chemistry. Since polymers are inevitable for today's life and economy, those reactions are of major importance for life as we know it. Even though efficient polymerizations are also often performed *via* transition metal catalysis, there are still examples where no catalyst is required.

In order to polymerize a monomer radically, a radical needs to be generated first, in most cases through an initiator. To construct pure polymers, it can be helpful to choose a radical starter, that blends into the final polymer structure. An example for this is the radical polymerization of styrene starting from benzoyl peroxide.

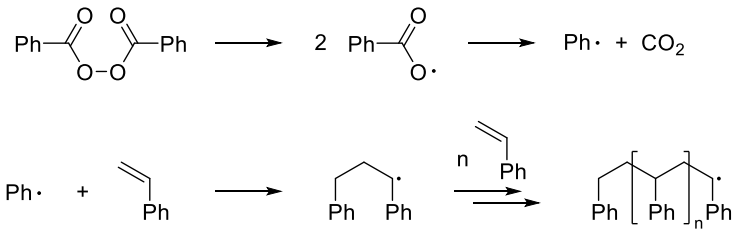

Scheme 8: Radical polymerization of styrene with benzoyl peroxide. The initiator is cleaved homolytically and after the loss of carbon dioxide, the generated phenyl radical can initiate the chain growth of polystyrene. The starter blends into the final structure as a phenyl group.

2.2.2 Transition metal-promoted carbon-carbon bond formations

Transition metal incorporation into the carbon-carbon bond formation process was first done by *Fritz Ullmann* and *Jean Bilecki* in 1901. Compared to the other reactions presented in the previous chapter, this method was unique as it was the only possibility to form sp^2-sp^2 bonds and create enlarged conjugated systems. To do so, different aryl halides were heated with copper yielding the respective biphenyl in a radical reaction pathway.[24] Still, the scope of this method was rather limited because it was only possible to synthesize symmetric biphenyls from two identical moieties reliably. Besides that, the strategy required high temperatures and tedious extraction of the residue, especially if the reaction was performed solvent-free in the melt.

It took more than 70 years to finally overcome these flaws with the discovery of cross coupling reactions.[10] Here, the radical pathway was exchanged for a reaction between a carbon electrophile and a carbon nucleophile. For the first time, these two compounds did not need to be identical, even though it is possible to form symmetric compounds on purpose. Additionally, the elevated temperatures were drastically reduced through the incorporation of a catalyst, that also made the use of an excess of copper metal obsolete.

Over the years, multiple cross coupling reactions were developed by various groups. While most of them agreed in the choice of an aryl halide as carbon electrophile, they varied most in the choice of the carbon nucleophile. As described in the previous chapter, the generation of carbon nucleophiles can be demanding and the scope of such stable compounds is limited. This scope can be drastically widened through the formation of covalent bonds between carbon and other elements of lower electronegativity, often metals. Examples for this are the generation of zinc organyls (*in situ*, *Negishi* coupling[11]), tin organyls (*Stille* coupling[25]) or copper aceylides (*in situ*, *Sonogashira* coupling[26]). Organyls of metalloids were used as well, such as boranes or pinacol boranes (*via Miyaura* reaction, *Suzuki* coupling[27]) or silanes (*Hiyama* coupling[28]). Through that, various methods that reliably form sp^2-sp^2 and sp-sp^2 carbon-carbon bonds were discovered.

Mechanistically, all cross couplings essentially consist of four key steps: oxidative addition, transmetalation, *trans-cis* isomerization and reductive elimination.

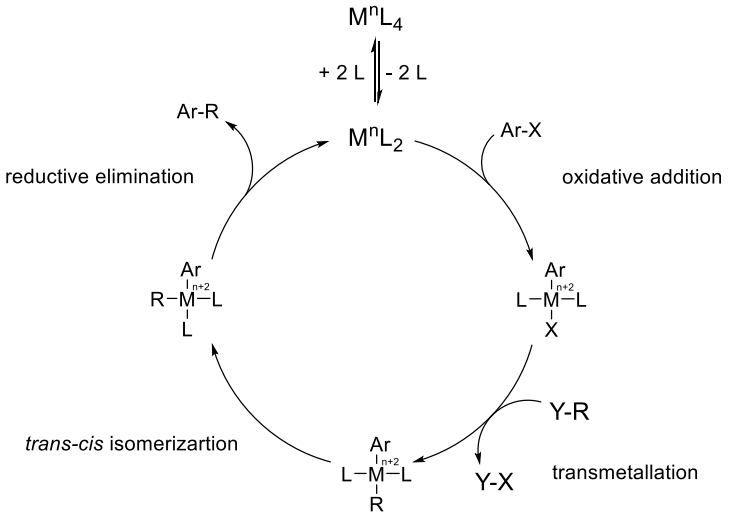

Scheme 9: Catalytic cycle of cross coupling reactions consisting of the four steps oxidative addition, transmetalation, *trans-cis* isomerization and reductive elimination.

The catalytic cycle in Scheme 9 features a lot of variables. Starting off with the catalyst, usually a late transition metal is chosen, typically from the tenth group. While nickel, palladium and platinum are all metals capable of catalyzing cross coupling reactions, they vary in one crucial point: their electronic properties. Neglecting the influence of the ligands, the more electron-rich a metal center is, the faster the oxidative addition of the aryl halide Ar-X occurs and *vice versa*. On the other hand, the reductive elimination occurs slower, the more electron-rich the metal center is and *vice versa*. As a consequence, palladium is the most prominently used metal as a catalyst for cross coupling reactions since it finds the best balance between both steps.[29]

For the ligands, a similar tendency can be observed. Very electron-rich ligands accelerate the oxidative addition as they make the metal more electron-rich, while electron-poor ligands slow down the tendency to cleave off the desired product in the reductive elimination step. Another aspect is the

ligand's size: it can be assumed, that large ligands hinder the oxidative addition through their bulky character while they promote the reductive elimination. Considering one of the most prominent cross coupling catalysts, $Pd(PPh_3)_4$, the complex contains four bulky ligands but is anyways one of the mostly used catalysts in cross coupling chemistry. The reason is, that the tetrahedral ML_4-type complex is not the active species. $Pd(PPh_3)_4$ is an 18 valence electron (VE) complex, that does neither lack any electrons, nor has any free coordination sites left. Instead, its proximity is too crowded due to four sterically demanding ligands. Their demand can be derived from the *Tolman* angle also known as the ligand cone angle. Considering the cone angle of 145° for PPh_3, it is no surprise that the complex loses not just one but up to two ligands spontaneously, while the latter can be seen as an equilibrium between the ML_3 and the ML_2 species.[30] Particularly, the linear ML_2-complex is now not just better accessible from a steric point of view, but also only a 14 VE complex that now benefits from an oxidative addition in order to re-acquire electrons. Thus, bulky ligands in a way promote the overall rate of the reaction by accelerating the formation of the active catalyst. For this reason, electron-rich and bulky ligands like PPh_3 are commonly used in cross coupling reactions.[29]

Since the *Suzuki* coupling is among the best studied cross coupling reactions regarding its mechanism and intermediates, it is an excellent example to explain cross coupling reactions in detail. Such mechanistic studies of the *Suzuki* coupling have found the oxidative addition to often be the rate-determining step of the reaction.[31] In this step, the transition metal center is oxidized reducing the added coupling fragment and therefore inverting its polarity. The addition turns the complex into a 16 VE complex, as it formally loses two electrons in the oxidation but gains four electrons through the two additional ligands. Apparently, the oxidative addition proceeds *via* a *cis*-complex, that rapidly rearranges into a less sterically hindered *trans*-complex.[32]

The subsequent transmetalation step is present in all cross coupling reactions, even though the applied reagent varies for all different name reactions. Identical for all of them is the bond metathesis between the M-X and the Y-R bonds yielding for example a transition metal complex with still two ligands and two coupling fragments. The *Suzuki* variant here has a unique characteristic amongst the cross coupling reactions, since an anion exchange takes place prior to the transmetalation, where the respective halide is substituted through hydroxide.[33] In an isomerization, the ligands are rearranged into a *cis*-conformation, which leads to a reductive elimination of both coupling fragments by forming the new C-C bond. One driving force here is the increased repulsion as a consequence of the rearrangement. Besides that, the elimination is also promoted by the transmetalation indirectly, as the introduction of a second coupling fragment further crowds the catalyst's ligand sphere. Again, the strength of the ligand repulsion depends on their size. Hence, *N*-heterocyclic carbenes (NHCs) are frequently used as ligands as well due to their increased bulkiness and supporting electronic properties.[34]

2.3 Biaryl compounds

Biaryl compounds are molecules of interest for both research and industry. Especially, since the advancements made in cross coupling chemistry, their spectrum of potential applicability has broadened. That chemistry enabled the formation of biaryls from two differently functionalized aryls in various patterns connected over one single bond. Furthermore, biaryls containing an additional bridging element such as fluorene and carbazole have garnered increasing attention. Biaryls are highly attractive monomers for oligomer and polymer chemistry as it is very easy to functionalize them regioselectively and polymerize the resulting organohalides.

2.3.1 Biphenyl and its relatives

Biphenyl is the simplest representative of the class of biaryls as it just consists of two phenyl groups corner-to-corner connected *via* a single bond. Like many other aromatic hydrocarbons, it is extracted as a byproduct in the work up process of black coal. Synthetically, biphenyl can either be prepared by recombination of two phenyl radicals or in a reaction of the diazonium salt of aniline and benzene, better known as *Gomberg-Bachmann* reaction.[35]

Biphenyl was found to perform great as fungicide inhibiting the growth of for example mold fungi. Hence, in the past, it was applied to the skin of citrus fruits.[36] Those treated fruit skins were found to be inedible to humans, which ended the use of biphenyl as a preservative in the European Union. Besides its outdated use as a fungicide, biphenyl has also technical applications, like being an additive for lithium-ion accumulators. If an electrochemical cell overcharges, biphenyl electropolymerizes at around 4.5 V and coats the electrodes, thereby preventing a thermal runaway of the accumulator.[37]

Contrary to the usual depiction of biphenyl, the molecule is not flat but twisted around the ring-connecting 1,1'-bond. Else, the *ortho*-hydrogen atoms would collide, which is obviously very unfavorable. Different studies showed the rotation angle to be around 44.4° with a low rotation barrier of approximately 1.4 kcal/mol at 273 K.[38] For comparison, the addition of one methyl groups in *ortho*-position of each ring drastically increases the barrier to 17.4 kcal/mol.[39] This tunable twisting limitation around the single bond was found to be useful for the application of biphenyl-based compounds as ligands.

2.3.1.1 Biphenyl-based compounds as ligands

As described before, the slight modification of biphenyl can influence the rotational barrier around the 1,1'-bond.[39] Most applications use a biphenyl derivative that is functionalized with another phenyl unit *via* edge connection along the 2,3-bond, known as 1,1'-binaphtyl. As explained for biphenyl already, the increased steric bulk of the annelated ring-systems prevents free rotation around the ring-interconnecting single bond, for naphthyl even stronger than for phenyl with a rotation barrier of 23.5 kcal/mol at 323 K.[40] Since there are two possible arrangements, two enantiomers can be distinguished due to the resulting axial chirality.

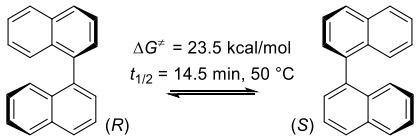

Scheme 10: 1,1'-Binaphthyl and its isomerization between both enantiomers.[40]

The use of an enantiomerically pure biaryl as a ligand in a transition-metal-catalyzed reaction can cause the biased formation of a specific product enantiomer. This may be of high importance, because sometimes, one isomer is of higher interest as outcome of a reaction, either in research or in the industry. An example for this are substrates that only have one naturally-occurring enantiomer making the access to the other enantiomer of high interest. With the use of the right chiral ligand or catalyst it is often possible to strongly influence the ratio of the yielded stereoisomers in favor of the desired outcome. If separated, binaphthyl derivatives can be used as enantiomerically pure, C_2-symmetric ligands in enantioselective catalysis.

While the applied stereoisomer plays an important role in the reaction, so does its functionalization and its overall geometry. The functionalization strongly affects the electronic properties of the ligand and therefore to a certain degree the resulting species' reactivity. Additionally, some functionalization is needed in all cases to bind the catalytically active metal to the chiral ligand. Common binding motifs to metals for binaphthyl ligands are hydroxy groups (for BINOL) and diphenyl phosphine (for BINAP).

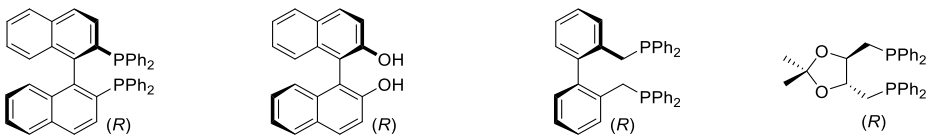

Figure 3: Chiral ligands BINAP, BINOL (bite angle: 93°),[41] BISBI (bite angle: 113°)[42] and DIOP (bite angle: 102°).[29]

Additionally, the size of functional groups can manipulate the so-called "bite angle", which describes the torsion angle between both coordination sites. The angle widens or shrinks as result of attractions or repulsions between the two moieties. Binaphthyl-based ligands are admired for their high flexibility. Due to the central axis, the bite angle can adapt to a broad variety of catalysts. Without going into too much detail, a fine tuning of the ligand's bite angle can be a powerful instrument to design a ligand

that fits to a very exclusive group of metals in terms of their radii enabling very selective binding and highly elaborated reaction conditions.

2.3.2 Fluorene

Another representative of the class of biaryls is fluorene. While both aryl moieties are connected similar to biphenyl, they are additionally bridged *via* a CH_2-group in 2- and 2'-position. The resulting formal cyclopentadiene central unit modifies the molecule's geometry and bends its backbone. Hence, fluorene cannot be assumed as a linear, planar molecule.

Similar to biphenyl, fluorene is also a byproduct obtained in the processing of black coal. Synthetically, it can be prepared as fluorenone in the *Pschorr* cyclization.[43] This reaction cyclizes a broad spectrum of compounds, diaryl ketones amongst others, intramolecularly *via* diazonium salts.[44]

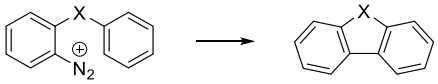

Scheme 11: *Pschorr* cyclization[43] of aromatic diazonium salts.[45]

The 9-position of fluorene is slightly acidic, indicated by a pK_a-value of 22.6 in DMSO.[46] The driving force behind this deprotonation is the formation of an aromatic anion, similar as for cyclopentadiene. Those formed anions are good nucleophiles and can react with electrophiles like alkyl halides, forming mono- or dialkylated fluorenes (compare chapter 2.2.1).[47]

The compound's demand for a full conjugation of its π-system was pivotal in the development of the fluorenylmethyloxycarbonyl (Fmoc) protecting group. Fmoc is used to protect amine groups as carbamates and can already be cleaved under mild basic conditions, making its cleavage very mild and therefore very prominent in peptide synthesis. Its inertness towards acidic conditions makes it very efficient in combination with acid-labile protecting groups. If two amino acids, one with a protected C-terminus and one with an protected N-terminus, are reacted, the resulting dimer can be grown from either terminus selectively if complementary protecting groups were installed in advance.[48]

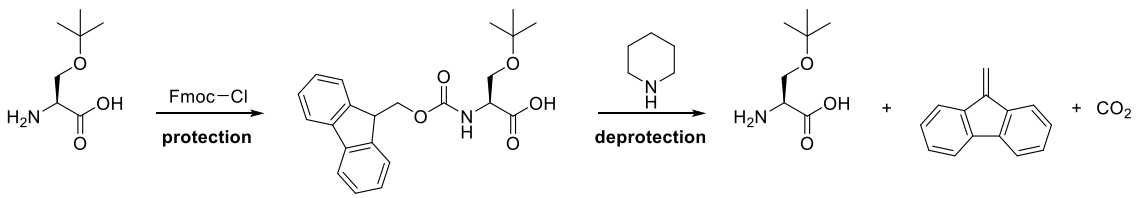

Scheme 12: Protection and deprotection of a serine with Fmoc. After the deprotection step, all previously installed groups are still intact as the substrate is recovered. The formed byproducts are dibenzofulvene and carbon dioxide.

Outside of synthetic applications, fluorenes find application as luminophores in polymer organic light-emitting diodes (OLEDs). Such polymer OLEDs are state of the art technology that can be used in almost every device requiring the emission of light ranging from room illumination to digital displays of any kind. Fluorene-derived polymers distinguish themselves from common LEDs in their emissive electroluminescent layer, that is made from an organic material emitting light when exposed to an electric current. Their inorganic counterpart here relies on monocrystalline, inorganic materials.

The full color spectrum can be emitted with polymer OLEDs through combination of the three primary colors red, green and blue. While different polymers of all three colors can be synthesized, there is no single polymer of unique substitution capable of emitting all three colors. Hence, three different polymers need to be combined to pointedly access the full spectrum of visible light. While red and green polymer OLEDs are well developed and literally shine through long life spans and high efficiency, blue polymer OLEDs have found to suffer from decomposition and a concomitant loss in brightness after shorter periods than the other two.[49]

Polyfluorene appeared to be a promising solution to that problem. Overall, the polymer is of rather flat character,[50] which leads to an overlap of the backbones' π-orbitals and therefore a full conjugation over the whole polymer. Besides that, the rigid backbone leads to a large band gap with blue emission. Interestingly, the band gap can be manipulated through substitution of the monomer or co-polymerization with other monomers, which means that different polyfluorene-based polymers can cover the whole visible spectrum of emission.[51]

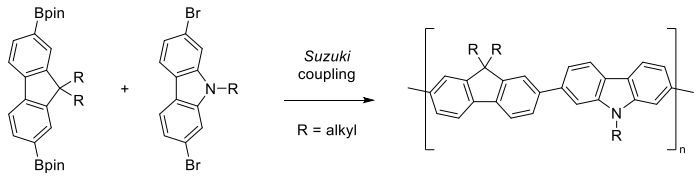

Scheme 13: Synthesis of a blue-emitting polymer by co-polymerization of a fluorene and a carbazole.[52]

Besides that, polyfluorene is known for its high thermal stability and its tunability regarding functionalization. The 9-position of fluorene is weakly acidic and can be alkylated easily, as mentioned before. This does not only influence the color of emission, but is an important aspect regarding the solubility of especially the polymer. Through increased solubility, a polymer can for example be applied more easily to a surface which allows for better control during the coating process resulting in thinner, more efficient films.[53]

While polyfluorenes sound to be promising OLED materials, they also bring their flaws. Polyfluorenes tend to form excimers or the polymers aggregate when exposed to electric current. Especially the latter is a problem, since the aggregation was found to be accompanied by a red shift in emission, tuning their desirable blue color towards green.[54]

To combat the aggregation, different strategies have been applied. Through construction of a branched monomer, the resulting branched polymer can no longer aggregate due to its own bulkiness. With such structures, luminescent quantum yields of 42 % were measured in the solid state. Unfortunately, this solution comes at the cost of a decreased processability due to chain entanglement and reduced solubility.[55]

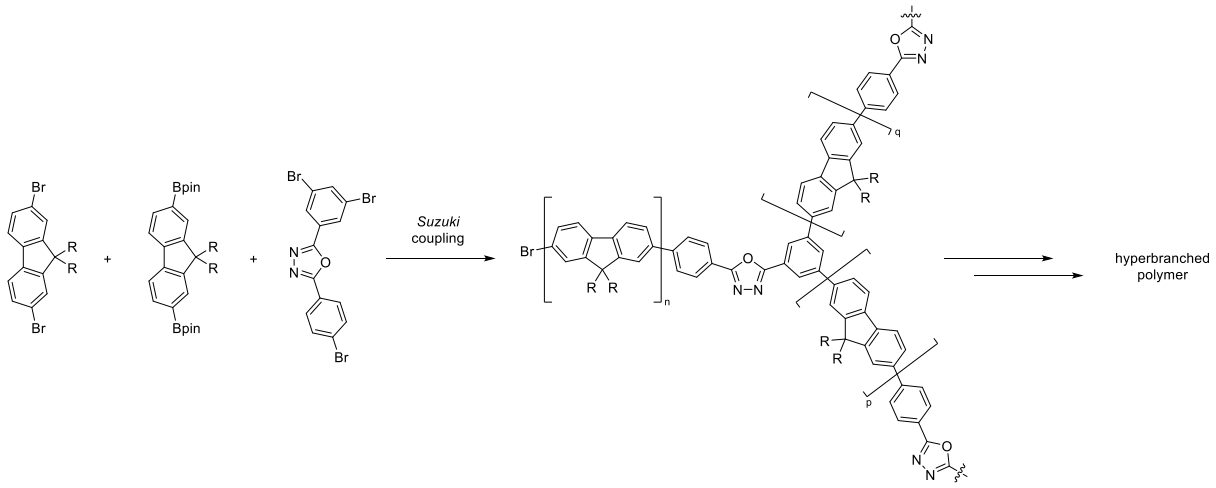

Scheme 14: Processing of a hyperbranched polymer *via Suzuki* coupling.[55]

Another strategy was the synthesis of star-shaped fluorene oligomers diverging from a central benzene unit. Here, two oligomers of similar size were connected *via* an acetylene and the resulting symmetric acetylene was trimerized.[56]

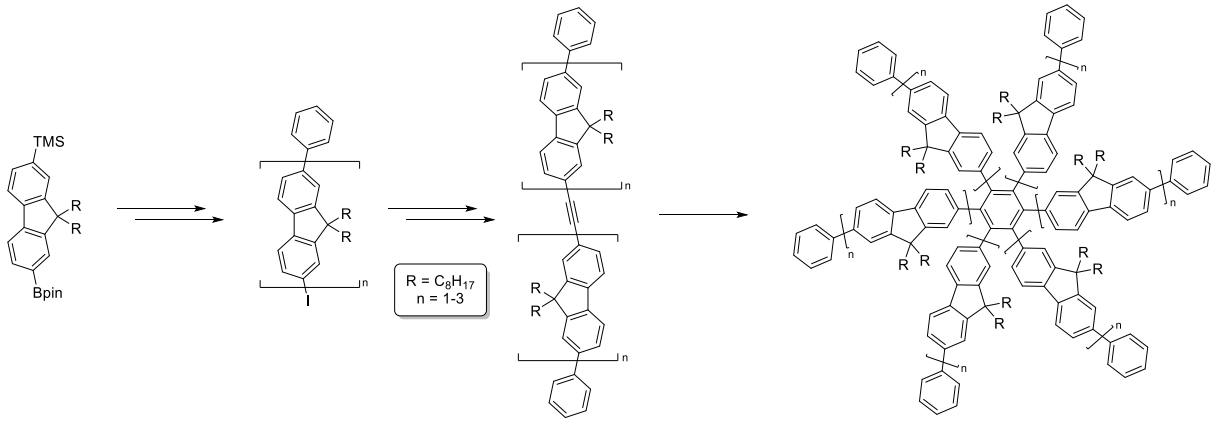

Scheme 15: Synthesis of a star-shaped polyfluorene.[56]

A direct correlation between the length of the oligofluorene arms and the absorption and emission maxima was found, stating that longer oligomers cause a red-shift for both parameters. Besides that, the undesired additional green emission within the spectra was no longer present, hinting at the absence of self-aggregating behavior. In fact, the star-shaped oligofluorenes adopt a certain alignment along one dimension resulting in a columnar structure in solid state according to X-ray diffraction.[56]

Even though both these solutions seem to minimize the problems regarding polyfluorene OLEDs, both do not find commercial application at the moment. Especially, the star-shaped oligomers seem promising for such applications, as they were found to be tunable regarding their emissions *via* suitable, additional end-capping, with for example nitrogen-containing functional groups like pyridines or carbazoles.[57] It appears that transition metal-based luminophores remain the most popular material for OLEDs, but with increasing scarcity of the required noble metals oligofluorenes may experience an immense growth in popularity in the next decades.

2.4 Cyclic structures

Structures consisting of more than two atoms that start and end in the same atom are considered as *cyclic* in organic chemistry. Hence, the smallest observed cyclic hydrocarbon is cyclopropane, consisting of three methylene groups linked in a triangular ring. In general, cyclic structures are found in a broad scope of size, functionalization and flexibility.

If such ring contains twelve or more atoms it is considered as *macrocycle*.[58] One representative class of compounds of macrocycles are cyclodextrins, which are of high interest in supramolecular chemistry. Cyclodextrins are compounds that can be obtained through enzymatic degradation of starch, which is a naturally occurring open-chained polysaccharide consisting of glucose molecules. In that enzymatic process, parts of the helical polysaccharide are cut out and cyclized through formation of 1,4-glycosidic bonds yielding a mixture of differently-sized cyclodextrins. The composition of that mixture depends on the used enzyme but usually the major share consists of the three main types named *α*-, *β*- and *γ*-cyclodextrin.[59]

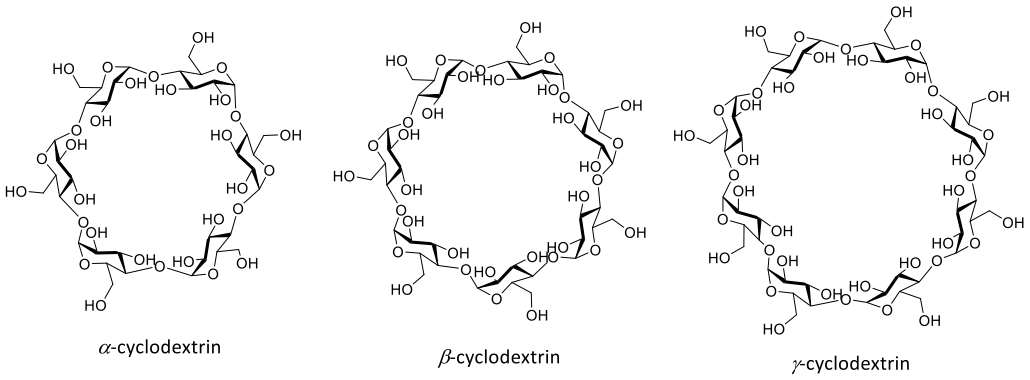

Figure 4: Chemical structures of the three main types of cyclodextrins: *α*-cyclodextrin (*n* = 6), *β*-cyclodextrin (*n* = 7) and *γ*-cyclodextrin (*n* = 8); where n equals the number of saccharide subunits in the backbone.[59]

The types differ in their perimeter, more specifically in the number of glucose subunits incorporated (Figure 4). Especially the main types are of high interest due to their characteristic geometry: the polysaccharide arranges in such way that hydrophilic groups are directed outwards. Furthermore, all

primary hydroxy groups sort to one end and all secondary hydroxy groups sort to the other end of the structure ending up in a three-dimensional, toroidal cone shape where the secondary hydroxy groups form the wider end.

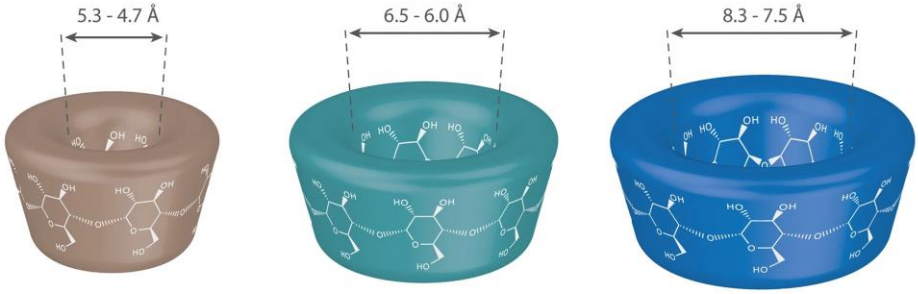

Figure 5: Schematic depiction of the three main types of cyclodextrins revealing their toroidal cone shape, the orientation of the primary and secondary hydroxy groups and their cavity size.[60]

As a consequence, the resulting cavity is comparatively hydrophobic and thus very attractive for hosting non-polar molecules. Hence, it is not surprising that cyclodextrins are a very popular motif of research within supramolecular chemistry, where such host-guest relations between molecules are a main topic of interest. The host properties of molecules like cyclodextrin can easily be tuned. Especially the hydroxy groups can be functionalized both fully or partially depending on carefully chosen conditions.[61]

Besides supramolecular research, cyclodextrins find application in a wide range of fields such as being utilized as stationary phases for chiral high-performance liquid chromatography (HPLC)[62] and they are also exploited due to their fragrance-binding properties in products like *Febreze*, that relies on the complexation of odor-causing molecules through *β*-cyclodextrins.[63] Cyclodextrins are also used for the delivery of drugs like hydrocortisone taken into the human body. By providing solubility and stability the drug can be transported safely through different parts of the body and only be released slowly up to the point of application.

Another very prominent class of cyclic compounds in chemistry are crown ethers. Just like cyclodextrins, they usually consist of a cyclic repeating monomer and also contain hetero-atoms like oxygen as the term *ether* implicates. The presence of these hetero-atoms gives the compounds strong donating properties and makes them excellent substrates for host-guest chemistry. The class of compounds was discovered by *Pedersen* in 1967 by accident, and described as a byproduct that forms stable complexes with many salts of *s*-block metals through complexation of the metal cations.[64]

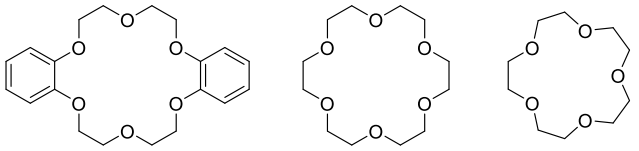

Figure 6: Dibenzo-18-crown-6 (left), 18-crown-6 (middle) and 15-crown-5 (right) for examples of crown ethers.

In fact, the compound *Pedersen* discovered was dibenzo-18-crown-6 (Figure 6, left), which formed due to a catechol contamination of his reaction. Under the basic conditions, two catechol molecules were connected *via* the ether linkage contained within the reaction mixture forming the cyclic ether.[64]

Over time, detailed investigations not only confirmed the ability of these compounds to form stable complexes with alkali metal cations, but also revealed that their size has a major impact on their coordination properties. By adaptation of the cavity size, it is possible to selectively complex different cations in the presence of each other. For example, potassium cations are perfectly complexed by 18-crown-6 (Figure 6, middle) but a complex formation with 15-crown-5 (Figure 6, right) is rarely observed because its cavity is too small to fit the ion.[65]

This complexation is frequently exploited because it makes inorganic salts soluble in many organic solvents. In some examples the complex formation can accelerate a reaction by suppressing ion bonding.[66] Besides that, the resulting complex enables a transfer of the inorganic salt between an aqueous and an organic phase, which allows the use of inorganic reagents in organic chemistry.[67] A prominent example for this is so-called *purple benzene*. Through complexation of the potassium cation with 18-crown-6, the inorganic salt becomes soluble in benzene. However, permanganate remains a potent oxidation agent which is why *purple benzene* is often used to oxidize various organic compounds.[68]

In another application, the crown ether is incorporated into the used catalyst. Here, 1-chloromethylnaphthalene was meant to be reduced with potassium formate under palladium catalysis.[69]

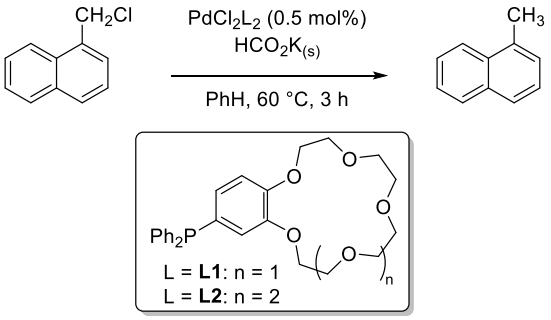

Catalyst	Yield (%)
$PdCl_2(PPh_3)_2$	17
$PdCl_2(PPh_3)_2$ + benzo-18-C-6	27
$PdCl_2$(**L1**)$_2$	39
$PdCl_2$(**L2**)$_2$	86

Scheme 16: Screening for the reduction of 1-chloromethylnaphthalene under palladium catalysis using different ligands.[69]

While the use of PPh_3 and benzo-18-crown-6 only yielded the desired reduction product in unsatisfactory yield, the design of phosphine ligands containing a covalently bound crown ether turned

out to be ground-breaking. A major advantage of this design is that the inorganic compound gains solubility in organic solvents through its complexation and additionally is transported directly to its application site. Thus, the palladium complex acts as a reduction as well as a and phase transfer catalyst within the presented reaction.[69]

A closely related class of compounds to crown ethers are cryptands. These polycyclic, multidentate compounds can also serve as ligands for metal cations, but instead of a single-ring structure they trap a cation in a cage-like three-dimensional structure. The name of this class is derived from a combination of the words “crypt” and “ligand” comparing the strong complexation to a final resting place. In terms of molecular design, the scope of heteroatoms is expanded for this class by nitrogen, which serves as a cross-linking point of the different rings but can also complex a potential guest with its electron pair.

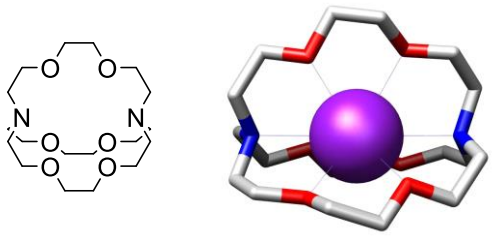

Figure 7: 2,2,2-cryptand molecular structure (left) and model of the cryptand complexing a potassium cation (purple, right).[70]

In 1987, *Charles J. Pedersen* was awarded with the *Nobel* Prize in Chemistry equally shared with *Donald J. Cram* and *Jean-Marie Lehn* “for their development and use of molecules with structure-specific interactions of high selectivity”, honoring their research on cryptands and crown ethers.[71]
As explained, both classes of compounds are available in different sizes and depending on the number of incorporated monomer units thereby widening their cavity. If enlarged too far, these compounds lose their property of interest, the ability as tightly-complexing hosts because they can adapt various conformations through additional degrees of freedom. Such macrocycles can be no longer be described as *shape-persistent*.

2.4.1 Shape-persistent cyclic structures

In contrast to just any cyclic compounds, shape-persistent cyclic structures are hardly deformable and have a preferred conformation. For the compound class of macrocycles, this inflexibility can be achieved through the incorporated building blocks. The cyclic structures discussed prior to this chapter mostly consisted of sp^3-hybridized carbon atoms and are therefore highly flexible. While acetylene and bisacetylene groups are less flexible, those building blocks are known to be still flexible despite their

rigid appearance. The incorporation of phenylene groups can be an effective method to actively stiffen the resulting structure.

For a cyclic compound to be defined as shape-persistent requires it to fulfil a certain criterion. For a shape-persistent macrocycle (SPM), its diameter *d* needs to be equal to its perimeter *p* divided by π. If that criterion is met, the backbone of the macrocycle is on average intact and not collapsed, so the structure can be seen as shape-persistent.[72]

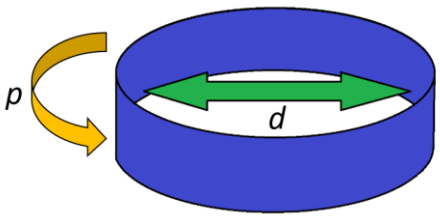

Figure 8: Schematic model of a shape-persistent macrocycle (blue), highlighting its diameter *d* (green) and its perimeter *p* (yellow).

2.4.2 Synthetic approaches towards shape-persistent macrocycles

As explained before, the incorporation of sp^3-hybridized atoms typically reduces the rigidity of the resulting macrocycle. Hence, the following strategies focus on constructing such molecules mainly through *sp*- and sp^2-hybridized atoms. As presented earlier within this work, such bonds can be easily formed *via* transition metal-catalyzed reactions like cross couplings (compare chapter 2.2.2).

In theory, macrocyclic structures can be prepared over thermodynamic and kinetic pathways and both methods have their benefits and drawbacks.

2.4.2.1 Thermodynamic synthetic strategies

Thermodynamically driven syntheses have the huge benefit of mainly relying on dynamic covalent chemistry (DCvC). In DCvC, the equilibration between different compounds is promoted to such degree, that a variety of different species coexist and are interconvertible *via* reversible reactions. This strategy comes at the advantage, that errors occurring during the reaction can still be corrected over the proceeding reversible reactions since the thermodynamic product is favored. To achieve that, undesired byproducts can also be disassembled and reassembled until the thermodynamic minimum is reached which obviously is beneficial for the overall yield. The equilibrium can also be affected, for example through addition of a specific template. Once the equilibrium has shifted to the right scope

of compounds, the template compound can be removed together with the desired compound if the system was designed properly.[73]

As for any thermodynamically driven process, its outcome can precisely be tuned by addressing the two main thermodynamic entities, enthalpy and entropy, and their influence can be broken down into two aspects. While the enthalpy depends on the bonds formed and cleaved during a process and the sum of the resulting energies, the entropy depends on the degrees of freedom of the investigated system. For the synthesis of macrocycles, both of these entities work against each other. This can be explained by comparing two polymers built of the identical number of monomers, with one of them adopting a cyclic and the other one in an open-chained structure. The cyclic polymer is enthalpically favored, as it requires one more bond formation than the open-chained one in order to cyclize. On the other hand, the open chained polymer is favored entropically due to its higher degrees of freedom. While this rivalry might appear to be a problem, it is of low impact as it can be controlled easily. Since the entropy of a system is strongly temperature-dependent, the outcome of the reaction can be manipulated through the choice of temperature. Besides that, the influence of the enthalpic component decreases with increasing size of the observed system. For example, for a polymer consisting of 1000 monomers the impact of the additional bond formation leading to a cyclic polymer after 1000 couplings compared to the open chained polymer after 999 couplings is comparatively tiny.[74]

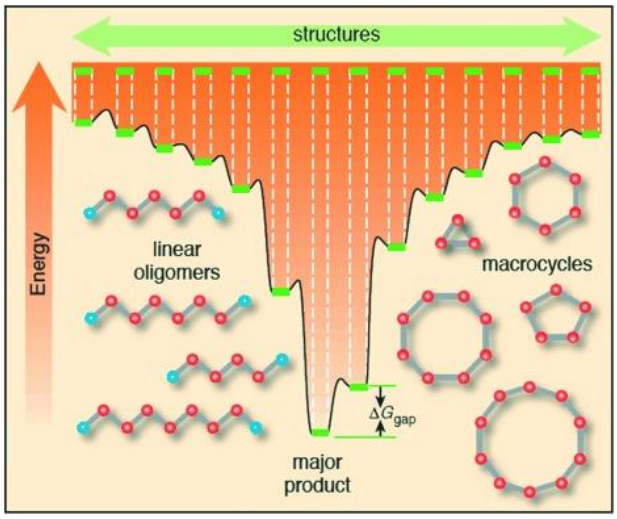

Figure 9: The energetic landscape resulting from a thermodynamically driven process. The most stable product ("major product", center) is the lowest in energy.[74]

As Figure 9 points out, the formed polymers are in theory interconvertible. For that, it is essential that the required energy barriers are low enough to be surpassed under the applied reaction conditions. In the end, the most stable product is the lowest in energy and formed as the major product. Anyways, the major product is not the only formed species. Since the method is a dynamic strategy and since the species separated by low energy barriers are in an equilibrium, it still yields a mixture of products.

The composition of the mixture depends on the stability of the formed compounds, while the most stable product usually forms the largest fraction.

One excellent example for the presented method was published by *Moore et al.* in 2002. The group managed to perform a cyclization of two moieties *via* imine formation in an outstanding yield of 95 % after optimizing the conditions. The formation of oligomers did not seem to be a problem here at all as the seemingly most stable compound was formed nearly exclusively.[75]

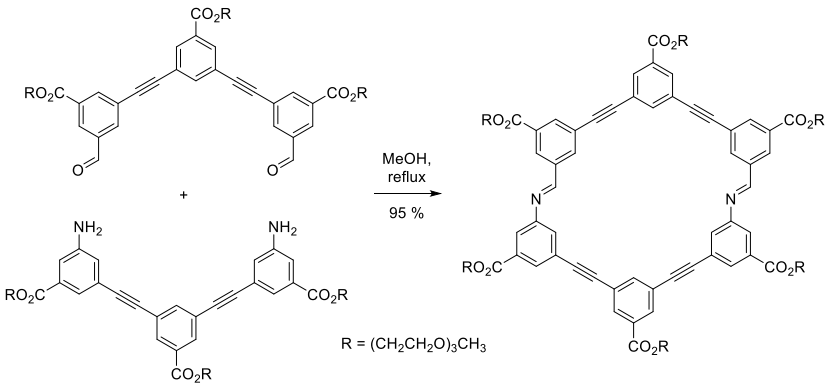

Scheme 17: Example for a thermodynamically driven cyclization reaction from two moieties *via* two formed imine bonds in nearly quantitative yield.[75]

The drawbacks of the thermodynamic approach are rather limited. First, it is not possible to synthesize strained cyclic systems applying this method. The resulting structures would be constructed of few monomers yielding rather small compounds, meaning that the enthalpy component cannot be neglected and the equilibrium is shifted towards open-chained compounds. Besides that, a strained system would display a low degree of freedom, thereby disfavoring its formation entropically. Secondly, while a "self-repairing" polymer growth seems desirable, this only works as long as all compounds remain soluble. Once a polymer reaches a size where it is no longer solubilized and precipitates, it can no longer be converted into other species. Besides that, it removes a tremendous amount of building blocks from the reaction strongly affecting the overall yield. The final drawback lies within the yielded mixture of products. Since all compounds are constructed from identical monomers, the polarity of the products becomes very similar, especially with increasing size. Even though this drawback is a problem of the kinetic approach as well, it still needs to be addressed before choosing this method.[74]

2.4.2.2 Kinetic synthetic strategy

The most characteristic aspect about kinetically driven synthetic strategies can also be construed as their first disadvantage because the reactions proceed irreversibly. Therefore, it is not possible to correct any synthetic errors within the molecules.

If not addressed properly, kinetically driven polymerisation reactions of monomers yield a broad distribution of open-chained and cyclic polymers. Hence, if aiming at only one desired species, like a small cyclic oligomer, it is obtained in only a very small yield.

Even though the presented characteristics sound like a drawback, this crude strategy can still find application. If both, the starting material and the required catalyst are extraordinarily cheap, the method can give easy access to one or more desired species despite the low yield. In the end, it might be possible that the overall yield of a synthetic route requiring ten steps to access a monomer is about equal to the lavish conditions suggested here. In contrast to the ten-step-method, the one-pot reaction on the other hand does consume less time and resources in order to access the monomer. Hence, at least from an economic point of view, the one-pot reaction can be worth a consideration.[74]

A simple example for this was published by *Staab et al.* in 1974. In a three-step synthesis, they prepared a copper acetylide from *m*-iodobenzaldehyde that was polymerized afterwards. With that approach, they were able to isolate the desired macrocycle from the statistical mixture in a yield of 4.6 % most likely at the cost of the formation of larger cyclic and open-chained oligomers.[76]

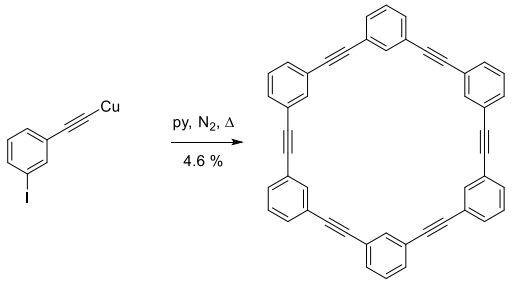

Scheme 18: Kinetically driven one-pot cyclization of copper *m*-iodophenylacetylide by *Staab et al*. yielding the desired cyclic compound in 4.6 %.

In order to avoid such low yields, macrocycles can also be synthesized from few multiple large precursors instead of many small ones. The concept here would be to build up as much of the final structure as possible prior to the cyclization so as few bonds as possible need to be formed in the cyclization step. By that, the number of side reactions can be reduced in favor of an improved yield. Theoretically, this leads to two options: 1) the macrocycle is either assembled from two moieties that are of different or identical functionalization or 2) an open-chained precursor to the macrocycle is fully synthesized and end-to-end cyclized in the final step. In fact, both methods were tested and applied in the past and will be presented in the following.

The first mentioned method synthesizes the macrocycle from two moieties, requiring the preparation of a more complex monomer over multiple steps. In an *Eglington-Glaser* coupling reaction, both moieties are connected in a moderate yield of 45 %. Even though the reaction was performed under high dilution the product was accompanied by the formation of larger oligomers distinctly lowering the yield.[77]

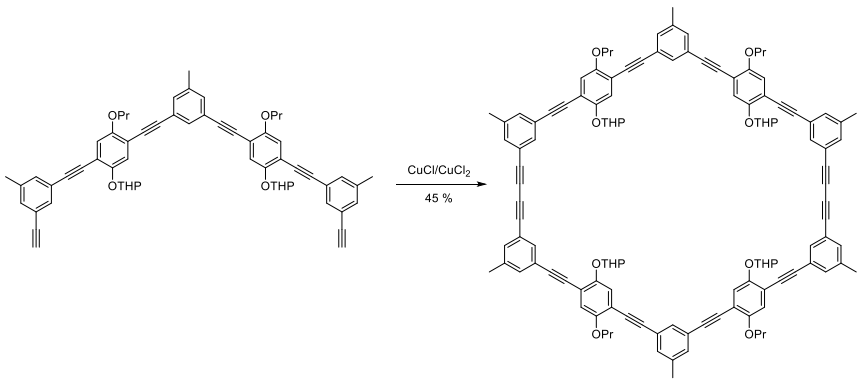

Scheme 19: Intermolecular cyclization of two macrocycle moieties in an *Eglington-Glaser* coupling.[77]

If smaller molecules or cyclic compounds are preferred, performing kinetically driven oligomerization reactions under high dilution conditions can favor their formation. At a lower concentration, the initially formed, open-chained dimer is less likely to encounter another reactive molecule thereby favoring an intramolecular coupling. High dilution is also suitable for open-chained oligomers that just need to cyclize, because in that case, both moieties are already connected and do not need to find another equivalent first.[74]

The second option tackles that cyclization problem by preparing an open-chained precursor from the monomers first and only closing the macrocycle in the final step. The desired macrocycle here was accessed in a *Sonogashira* coupling under *pseudo*-high dilution in 75 % successfully.[78]

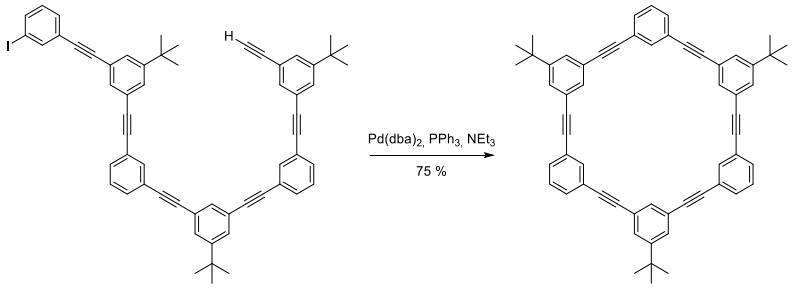

Scheme 20: Intramolecular cyclization of an open-chained oligomer into a macrocycle *via Sonogashira* coupling.[78]

The obvious drawback of this method is the careful and stepwise preparation of the precursor. Through complementary end protection and separate deprotection, it was possible to prepare the desired oligomer sizes in good to excellent yields. Interestingly, a minor decrease in the yield was observed for the cyclization step for each further enlargement of the open-chained oligomer.[79]

Apparently, high dilution conditions soon reach their limits, as especially for large-scale reactions it is undesirable to squander large amounts of solvents. Instead, a low concentrated catalyst solution can be prepared and the missing substrate can be added dissolved slowly over long periods of time. Such *pseudo*-high dilution conditions are designed to instantly consume or distribute the added drop of substrate to avoid any excess of monomer and hence, uncontrolled polymerization.[74]

Comparing both previous methods undoubtedly reveals some flaws. For the first option, the synthesis of precursors is either easy but a medium fraction of substrate is lost in the cyclization to higher molecular byproducts. In the second method, the cyclization yields a narrow scope of oligomer sizes but the synthesis of precursors is very demanding requiring multiple steps and keen control of the reaction conditions to not over-couple the substrates.

A very elegant method combining the best aspects of both strategies was published by *Höger et al*. in 1998. Here, a symmetric monomer was accessed in a four-step synthesis in excellent yields above 87 % for each step. Three equivalents of that monomer were attached to trimesic acid in an esterification step forming an open-framed precursor. Since all three fragments are connected to the identical central template group, the fragments are preorganized. Thus, an intermolecular coupling is rarely observed because the intramolecular coupling occurs way faster as a result of the proximity, especially under high dilution conditions. The effectiveness of this method is underlined by an incredible yield beyond 90 % for the cyclization step. Through the elaborate design of the covalent template bond *via* ester groups it is possible to easily cleave trimesic acid from the compound after the successful cyclization in nearly quantitative yield.[80]

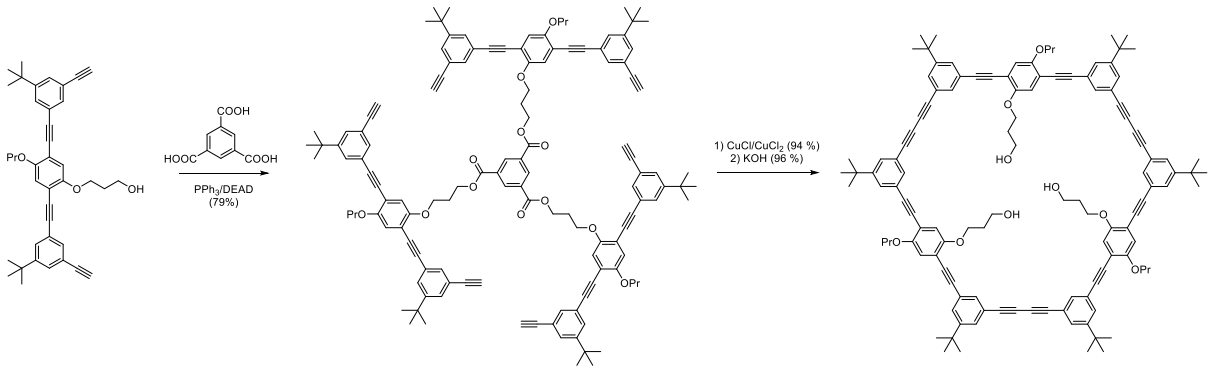

Scheme 21: Template-mediated cyclization strategy by *Höger et al*..[80]

2.4.3 Separation of macrocyclic structures

As discussed in the previous chapter in detail, most macrocycle syntheses yield not one but multiple species during the cyclization step. Since all compounds consist of the same monomer, separation *via* polarity is often extremely difficult. Despite the different connectivity, even cyclic and open-chained polymers can rarely be distinguished *via* their polarity. Instead, such product mixtures can be separated *via* gel permeation chromatography (GPC).

Similar to column chromatography, GPC also separates the mixture through columns but with way higher pressure than possible in common glass columns. The material of choice is a cross-linked, porous polystyrene (PS). In fact, columns with different pore sizes are commercially available so the

stationary phase can be adapted to the expected size of synthesized polymers. The cross-linked polymer is swelled in organic solvents like THF to form a gel that can then be used as a stationary phase. Under high pressure, an analyte solution (usually in THF as well) is then pumped through that gel and the outgoing liquid is analyzed with different detectors, for example an UV detector. On its way through the gel, the mixture passes differently sized pores and molecules that are small enough remain there for longer time than larger molecules. The smaller the analytes, the more pores they fit in, which means that these molecules are retarded the most and show the longest retention time to pass the column. On the other hand, larger molecules fit into less pores and travel faster. As a consequence, molecules of larger size are detected first. For large molecules that do not fit into any pores, no separation occurs. Hence, it is of high importance to choose the right pore size to make the separation as efficient as possible.[81]

Most available GPCs are equipped with a set of more than one column, sometimes also of different pore sizes. For more demanding separation processes in theory a large number of columns would be required to achieve a satisfactory separation. To overcome this, it is possible to recycle an analyte through the same set of columns repeatedly. Ideally, with each further cycle the compounds separate more until they can be identified as individual signals in the end. This method is known as recycling gel permeation chromatography (recGPC).

Based on the explained details, GPC can be described as a sub-category of size exclusion chromatography (SEC) because the intended separation is solely dependent on molecular size.

Contrary to recGPC, there is also a GPC-based method that only measures a single iteration called analytical GPC. The idea behind this tool is to separate the polymer mixture only so much, that it gives precious insight into the polymer distribution through UV detection of the injected analyte, which is usually gained after a single cycle. Thus, it is often used to check the progress of polymerisation reactions. Besides that, through this method it is possible to determine the molecular mass of the different observed compounds. Unfortunately, these values are often only of qualitative character because they are determined relative to the hydrodynamic radius of a polystyrene standard, which is a polymer with a low persistence length due to its high tendency to coil. Hence, especially for polymers of longer persistence length like rigid rod polymers, the molecular mass is often vastly overestimated. If a PS sample and a rigid rod polymer with identical molecular masses are investigated, they don’t necessarily adapt the same conformation. PS can be approximated as a coiled-up sphere while the rod is an elongated one-dimensional linear polymer. As a consequence, the length of the rod will be far longer than the length of a PS standard of identical mass, meaning that its retention time will be a lot shorter. Since the measured retention times only allow a quantification of the analyte's molecular weight based on its behavior as if it would be polystyrene, it is typically overestimated due to the spherical approximation. Anyways, those plots can be very helpful. Especially if the mass distribution

is overlayed with the elugram of compounds or precursors of known dimensions, its insights help interpret the size of the major formed compound or the progress of the reaction based on the consumed amount of substrate.

2.4.4 Structural proof of macrocyclic structures

Shape-persistent macrocycles are per definition found in one main conformation. Hence, it is of high interest to prove that main conformation and gain further insights into the atomic arrangement of the investigated compound. A typical tool for such insight is X-ray diffraction of single crystals revealing the packing between single molecules as well as bond lengths, angles and the overall structure within single molecules. For organic compounds, especially for the ones decorated with long solubilizing alkyl chains, it can be difficult to crystallize the analyte thereby excluding this method of structural elucidation.

Since many shape-persistent macrocycles consist of a mostly phenylene-based backbone or at least an extensive π-system, those molecules can easily self-assemble on suitable surfaces like gold or highly oriented pyrolytic graphite (HOPG). *Via* non-covalent interactions between the surface material and the molecules, the compound can form mono- and/or multilayers on top of the surface, in some cases even in very distinct and unique patterns.[82] One especially powerful tool to investigate such assemblies is scanning tunneling microscopy (STM) at the liquid/solid interface of HOPG. The method itself was developed by *Gerd Binning* and *Heinrich Rohrer*[83] who were both awarded equally the *Nobel* Prize in Physics in 1986.[84]

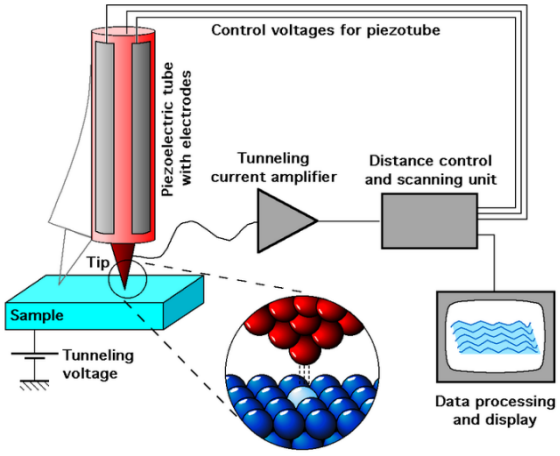

Figure 10: Simplified schematic setup of a scanning tunneling microscope (STM) highlighting all relevant components and their connectivity.[85]

This type of microscopy can visualize (macro)molecular structures down to a resolution of few *Ångströms*. For that, the investigated compound needs to be dissolved in a suitable solvent first.

1-Phenyloctane (PHO), 1,2,4-trichlorobenzene (TCB) and octanoic acid (OA) are all established solvents because on the one hand they were found to not adsorb on HOPG themselves and therefore not interfere with the analytes and on the other hand are not electrically conducting. In addition, they all have a low vapor pressure. Once the solution is applied to HOPG, the analyte starts to deposit from solution and covers the HOPG surface. The precise choice of concentration (generally 10^{-6} to 10^{-5} M) is essential for this step in order to generate thin but dense monolayers of the investigated compound. Too low concentrations prevent sufficient coverage of the HOPG surface or the molecules do not even adsorb at all while too high concentrations might lead to multilayers or overlapping of the molecules making it harder to distinguish single molecules and understand their behavior.[86]

Once a monolayer is formed, it can be visualized by hovering a metal tip over the surface while a voltage is applied (bias voltage). The tip is usually made of a platinum-iridium alloy, whose obvious drawback is its price but that is very inert towards ambient conditions. Hence, it forms no oxide layers that hinder the measurement of the tunneling current. STM investigations require a movement of the tip over the surface in such a precise manner, that a purely mechanical control is not feasible of. Instead, the tip is embedded into a piezoelectric ceramic tube, that mantles its other end. This way, it is possible to adjust the height and position of the tip on an *Ångström* scale by tiny changes in the applied bias voltage fitting the demands of any topologic environment.[87] Due to the difference in voltage between the surface and the tip, a current difference can be measured at each point the tip passes, creating a three-dimensional topographic image of occupied and unoccupied areas.[82] The measured current is influenced by the chemical structures regarding their height and adsorption, but also by their functionalization and electronic properties. Aromatic systems for example give higher currents than alkyl chains, which is why π-systems can be seen better as bright regions within the image.

The resolution and the pattern within the final image depend on various parameters. The resolution is strongly dependent on how strong the analyte interacts with HOPG. This strength increases with the size of the adsorbed backbone, but can also be influenced through decoration of the macrocycle, for example with alkyl chains that fix the macrocycle on HOPG stronger with increasing chain length due to additive *van der Waals* interactions. If a molecule adsorbs weakly to the surface or is not sufficiently fixed through decorating groups, it can be moved upon collision with the moving tip. As a result, the resolution of the molecules' outlines is lowered noticeably. The packing between different molecules on HOPG mainly depends on their outward functionalization. For molecules with bulky side groups of short chain length, the decorating groups avoid each other resulting in a dense packing of the compounds. Its stability depends on the adsorption of the backbones, as no packing supporting interactions are formed between the adsorbates. For molecules with long alkyl chains, those side

chains can interdigitate. As a consequence, those molecules form very distinct and repetitive patterns additionally stabilized through the interlocked side groups.

Besides single species investigations, mixing experiments on HOPG are possible as well. Here different packing driving phenomena[88] or the porous pattern of a single compound and the pattern after filling those pores through another compound[89] can be investigated.

In the past, STM investigations were not just used to prove the structure of many compounds but also falsified the characterization of some macrocyclic compounds as shape-persistent. While it was previously possible to postulate through quantum chemical calculations or from a single crystal investigation, that a macrocycle rather adapts a cyclohexane-like chair conformation if it reaches a certain size, a deformation in solution was never really observed.[90]

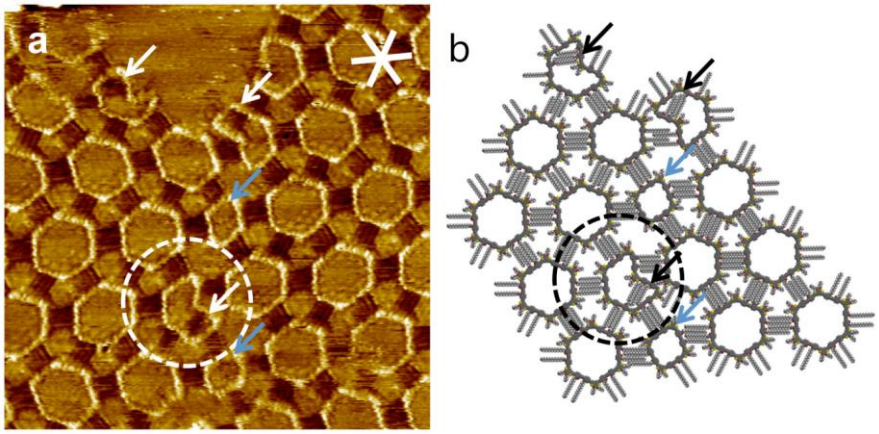

Figure 11: STM image (a) and model (b) of macrocycle mixing experiments by *Höger et al*. between the tetragonal and the hexagonal oligomer. Both images reveal the distortion and deformation of macrocycles that were assumed to be shape-persistent.[89]

STM mixing experiments of *Jester et al.* of a tetragonal and a hexagonal oligomer revealed not just that the square-shaped tetramers deform into a diamond-like polygon, but that some of the hexamers strongly deform as well. While most of the hexagons stayed intact, some of them featured one corner that pointed in- instead of outwards the ring clearly breaking with the concept of shape persistence.[89]

2.5 Molecular spoked wheels

When surpassing the persistence length, even macrocycles assumed as shape-persistent can deform or collapse as depicted in Figure 11. This problem can either be tackled by simply not further enlarging macrocyclic structures beyond their persistence length or by filling up the collapsing pore with supportive scaffolding. The latter was in fact realized by introducing a six-armed star armature that was covalently bound to each corner-phenylene of the macrocycle. Since all arms meet in the center

in a single phenylene, the resulting structure is highly symmetric and due to its resemblance given the name Molecular Spoked Wheel (MSW).

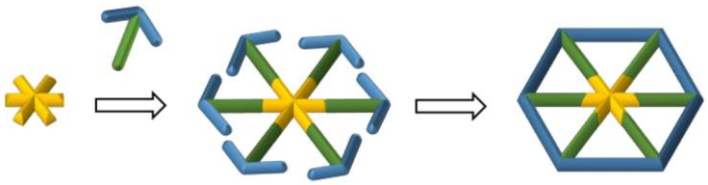

Figure 12: Schematic overview of the synthesis of a Molecular Spoked Wheel. The three main components are color-coded: a central hub module (yellow), six equally sized spoke modules (green) and the rim modules (blue) that form the molecule's backbone.[91]

The structure that can be clearly divided into three main components was first synthesized by *D. Mössinger* within his PhD studies. To do so, *Mössinger* chose an approach building up the desired compound from the center towards the rim of the MSW. With that, he synthesized the first MSW consisting of acetylene-, bisacetylene- and phenylene-units. The molecule was also decorated with 12 alkoxy groups at its spokes to promote and ensure the solubility of the final compound and all of its precursors.[92]

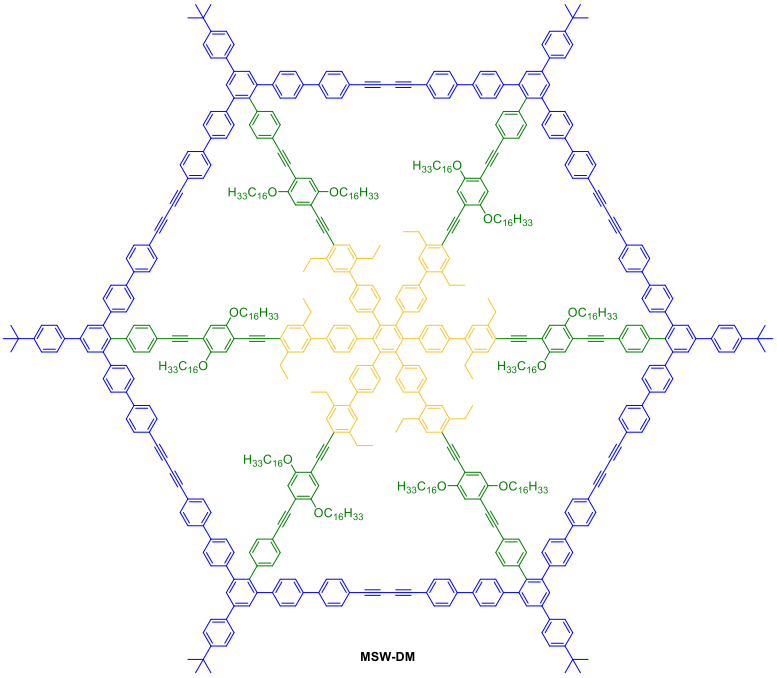

Figure 13: First ever synthesized MSW by *Mössinger* consisting of acetylene-, bisacetylene- and phenylene-units.[92]

As already mentioned, *Mössinger* chose an approach starting at the wheel's hub. The idea behind this strategy was to cut down the large structure into multiple building blocks, that were each synthesized separately and combined as late as possible. The high presence of acetylene- and phenylene groups also made cross coupling reactions a very powerful tool. While *Suzuki* coupling reactions are amongst the best methods to form bonds between two sp^2-hybridized carbon atoms, sp^2-sp bonds can be

formed *via Sonogashira* coupling. A side reaction usually observed in *Sonogashira* couplings is the *Glaser* coupling that consumes two terminal alkynes yielding a bisacetylene. As for the case of *Mössinger*, that reaction can also be exploited on purpose, for example to close the molecule's rim (compare Figure 13). The synthesis of the different components in separate routes additionally gives great control over their respective sizes. Since *Mössinger* intended to access a planar disk-like MSW, it was inevitable to him that the spoke segment and the edge segment are of identical dimensions. A different length would deform and bend the resulting MSW ending up with a bowl-shaped structure that might be accessible anyways, but was not striven for.[92]

Asides all planning, it was still not confirmed that the resulting structure would come out as a planar disk. To further investigate the impact of the spoke armature, molecular dynamics (MD) simulations regarding the shape-persistence of his molecule were performed. Here, the geometries of his targeted MSW, its open-framed precursor and a macrocycle only consisting of the MSW's backbone were compared.

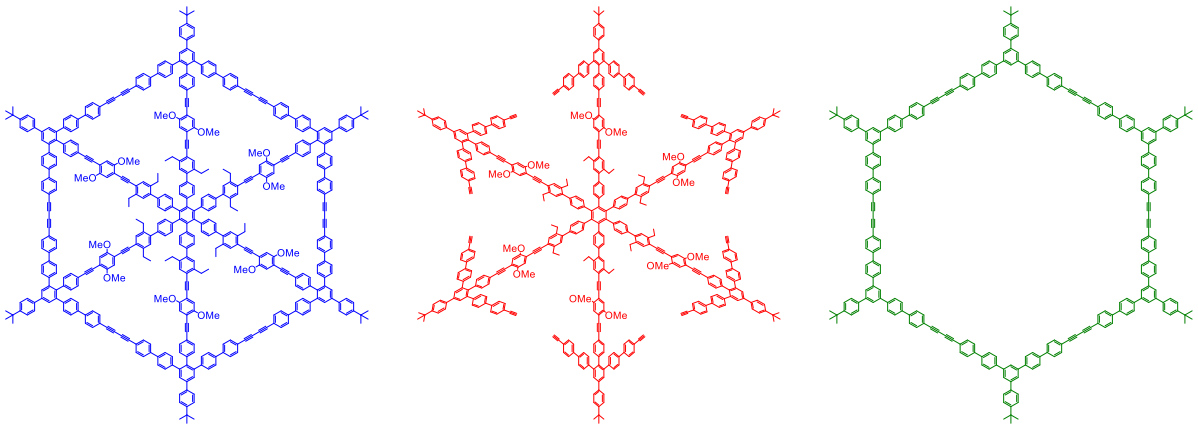

Figure 14: Investigated structures regarding the shape-persistence of the desired MSW (left, blue). For comparison, also its open-framed precursor (middle, red) and the macrocycle consisting of its backbone (right, green) are depicted. The alkyl chains are simplified as methyl groups to save computation time and resources.[92]

All three molecules were investigated over a time period of 500 ps. In that period, the distance between opposing corners was monitored as well as the angle between the opposing corners and the center of the molecule.

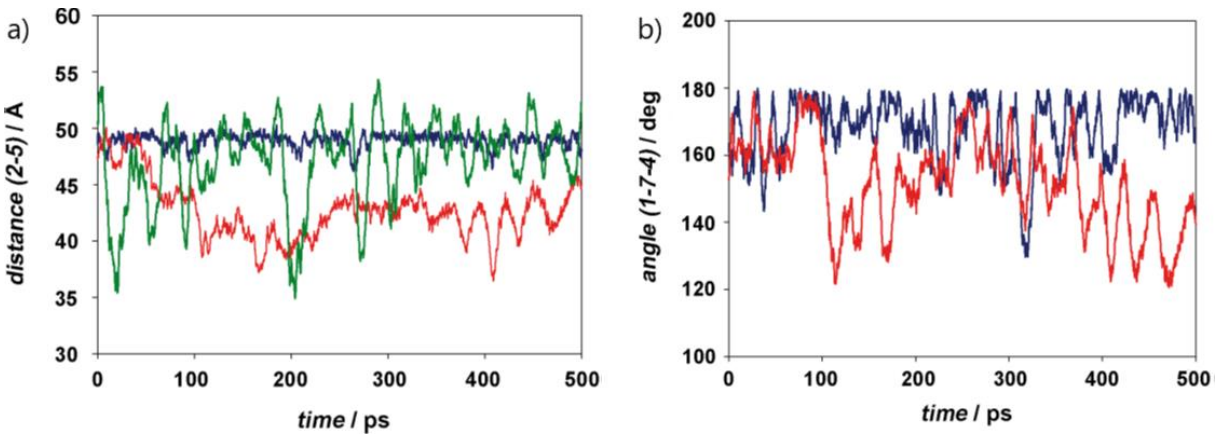

Figure 15: For both depictions the MSW is shown in blue, the open-framed precursor is shown in red and the macrocycle is shown in green. a) Distance investigation between opposing corners for the three described molecules over a time period of 500 ps. b) Angle investigations of the three molecules between two opposing corners over the molecule's center.

Figure 15 clearly shows that the strongest deformation through a change in corner distance is observed for the spokeless macrocycle (green). The precursor also shows increased flexibility, but that observation is not surprising due to the missing stiffness resulting from the unclosed rim. In fact, the precursor behaves like a star-shaped polymer which are known for their high flexibility. The MSW on the other hand does not appear to change in conformation a lot, as the corner-to-corner distance stays between 48 and 50 Å while the angle between two spokes stays between 160° and 180°, which resembles a planar molecule or a very flat boat geometry as *Mössinger* humbly stated.

The successful synthesis did not just allow access to the first MSW but also opened up a whole new class of macromolecular structures of interest since it proved that MSWs are indeed shape-persistent as anticipated.[92] *Mössinger* also did further research on MSWs and *Aggarwal* managed to use them for example as a seed for the growth of polymer strands from all six corners of the MSW's rim.[93]

The size limits of MSWs were expanded by *R. May* in 2014 with the synthesis of the largest MSW synthesized to this day. Also based on phenylenes, acetylenes and bisacetylenes, **MSW-RM** spanned a corner-to-corner diameter of 11.9 nm. Its structure as well as its shape persistence were proven by scanning tunneling microscopy (STM).[94]

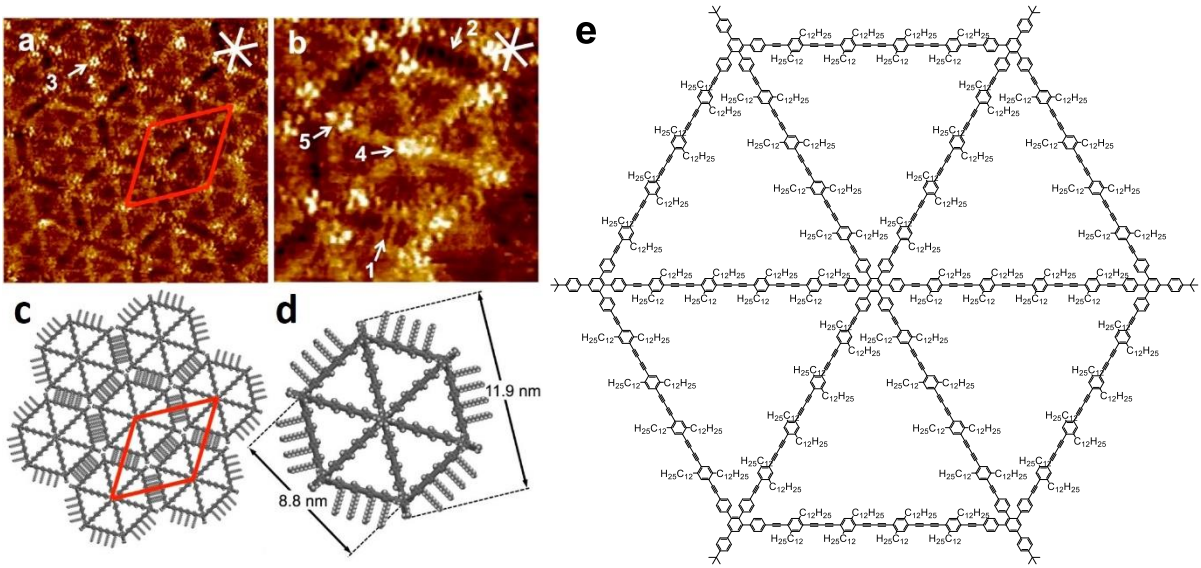

Figure 16: a) STM image of **MSW-RM** on HOPG at the solid-liquid-phase border (33 × 33 nm^2), showing a honeycomb setting of the respective molecules. The unit cell has the parameters $a = b$ = (10.8 ± 0,2) nm and γ = (60 ± 2)°; b) A single MSW at high resolution (15 × 15 nm^2); c) Reconstructed model of the MSW's packing on HOPG containing the interdigitation of all rim-connected alkyl chains and the unit cell (red). The alkyl chains on the spokes are neglected for better visibility; d) Model of a single MSW showing its corner-to-corner diameter as well as its edge-to-edge diameter. The alkyl chains on the spokes are neglected for better visibility; e) *Lewis* structure of **MSW-RM** with all side groups.[94]

A major drawback of this molecular design was discovered only over time. *May* found out, that some MSWs containing acetylenes and bisacetylenes cannot be stored over longer periods of time under ambient conditions. *Via* analytical GPC he discovered that over one year higher molecular species had formed even under exclusion of light. *May* assigned the signal to the connection of two macrocycles in an unfortunately irreversible reaction.

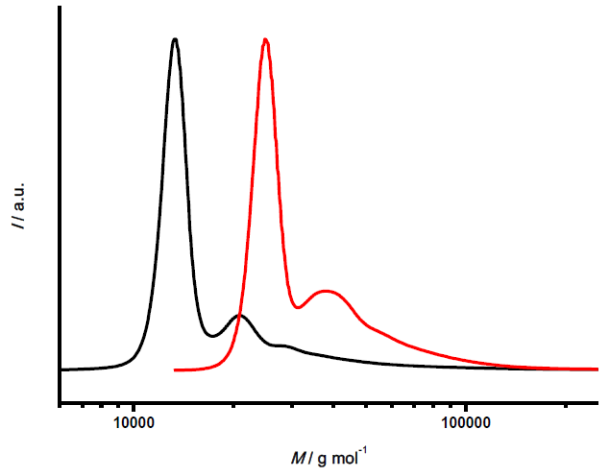

Figure 17: Analytical GPC elugram of two differently sized MSWs after storage for about one year at rt under the exclusion of light. The main signal represents the intact MSW while the shoulder was only visible after one year and corresponds to higher-molecular oligomers formed over time.[95]

Even though it was possible to synthesize the desired MSWs, the synthetic approach comes at a price. The route forced to perform and optimize multiple six-fold reactions to grow the structures and connect different components. This method relies on high and quantitative conversion of the substrates, but more importantly it can become difficult and time-consuming to separate the desired fully substituted compound from all the partly substituted byproducts and their various isomers.

2.5.1 All-Phenylene Molecular Spoked Wheels

The drawbacks of the route led to major refinements in the synthetic strategy towards MSWs. After the observations made by *May* regarding the stability of acetylene- and bisacetylene-groups within the structures, it was inevitable to fully remove them from MSWs. The easiest way to do so was to simply reduce the pool of structural motifs incorporated to just phenylene and oligophenylenes. Besides the vast improvement in inertness, the purposeful avoidance of acetylenes from the final structure allowed to incorporate acetylenes into the precursors to exclusively address them in one reaction step. This ground-breaking change became the key difference from the previous route and replaced the six-fold cross coupling previously required to access the open-framed precursor when *A. Idelson* developed a synthetic route for all-phenylene MSWs.[96]

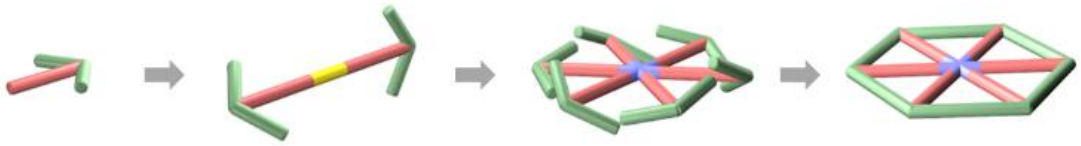

Figure 18: Synthetic strategy to access all-phenylene MSWs. Two anchor-shaped molecules (red+green) are connected through an acetylene (yellow). The acetylene can be trimerized (blue) into an open-framed precursor. The rim (green) is closed in the final reaction step yielding an MSW.[97]

As before, the strategy first focuses on the construction of an anchor shaped molecule. Afterwards, two anchor-shaped precursors are connected *via* an acetylene. This route no longer requires to pre-synthesize a hub molecule because it can be created *via* trimerization in a *Vollhardt* reaction.[98] Instead of performing a six-fold coupling, this reaction drastically reduces the amount of byproducts as well as facilitating the purification of the compound. Afterwards, the resulting open-framed precursor is closed in a six-fold *Yamamoto* coupling yielding the desired all-phenylene MSW with a perimeter of 18 phenylene units (“18 Ph-MSW”).[99]

The total synthesis of these all-phenylene MSWs starts with the synthesis of the spoke unit. In three steps, a functionalized biphenyl can be generated in a *Suzuki* coupling, and after exchanging the trimethylsilyl group for iodine (TMS-I exchange), the corresponding sodium aryl acetate is yielded as result of a simple deprotonation.

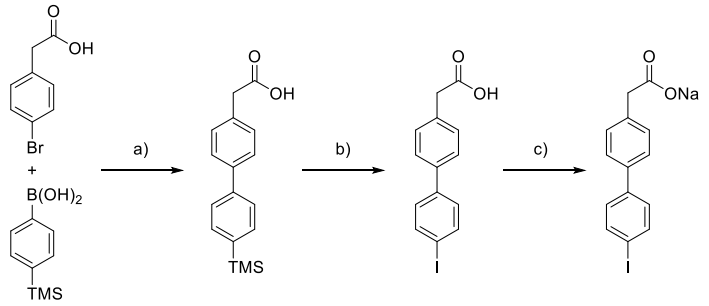

Scheme 22: a) $Pd_2(dba)_3$, K_2CO_3, toluene, water, 88 °C, 24 h, 75 %; b) ICl, DCM, 0 °C → r.t.; 2 h, 76 %; c) NaOMe, MeOH, rt, 2 h, quantitative yield.[96]

The obtained sodium aryl acetate is one of two compounds required for a *Zimmermann-Fischer* condensation.[100] The second compound, a pyrylium salt, can be synthesized from a diketone and a *Michael* acceptor or directly from two ketones and an aldehyde.

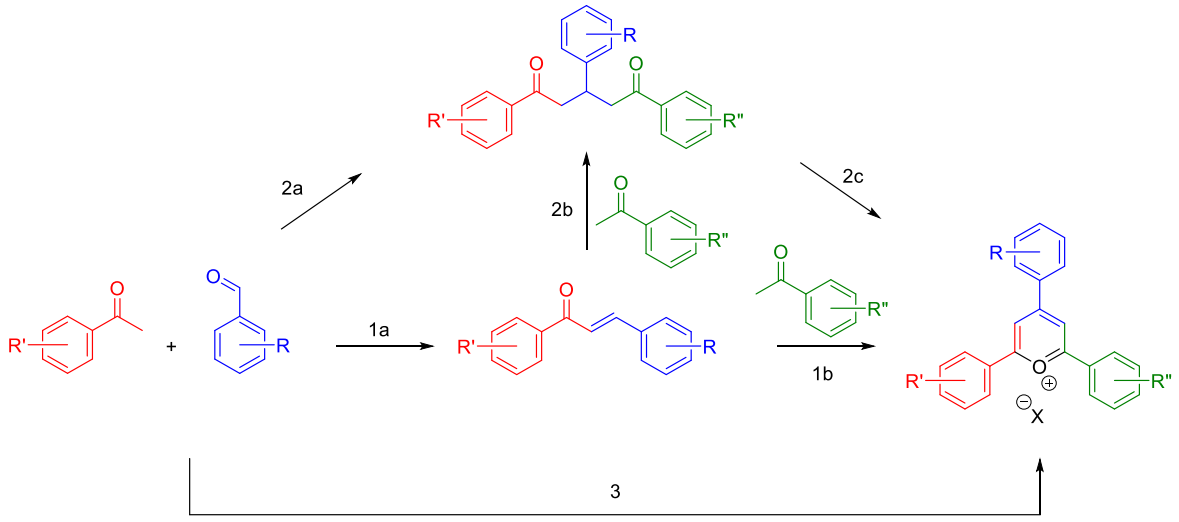

Scheme 23: Synthetic accessibility of pyrylium salts over three different routes *via* different intermediates.

The first path combines a benzaldehyde and an acetophenone under basic conditions yielding a *Michael* acceptor (Scheme 23, 1a). Subsequently, it can be reacted with another aromatic acetophenone and an acid yielding the desired pyrylium salt (Scheme 23, 1b).[101] The used acid here forms the counter ion of the final salt, which for the synthesis of MSWs is usually BF_4^-. A drawback of this method is that its maximum yield is limited to 50 % because for each formed pyrylium salt molecule, one equivalent of the *Michael* acceptor is consumed as substrate and one equivalent is consumed as a hydride scavenger.[102] Yet, a benefit of path 1b (Scheme 23) is that it allows for the synthesis of differently substituted pyrylium salts if the *Michael* acceptor is isolated.[21]

In the second path, the pyrylium salt is prepared *via* a 1,5-diketone intermediate. This diketone can either be synthesized from the described *Michael* acceptor (Scheme 23, 2b) or directly from a benzaldehyde with two equivalents of an aromatic acetophenone (Scheme 23, 2a). Here it is important, that for the latter method only symmetric 1,5-diketones are accessible. To perform the

cyclization of the diketone, an acid and an additional hydride scavenger (for example chalcone or triphenylmethanol) are added (Scheme 23, 2c).[103] Through the addition of such hydride scavengers the yield is no longer limited to 50 %.[102]

The third method accesses the pyrylium salt by combining both substrates and the acid in a one-pot reaction (Scheme 23, 3). Again, no asymmetric pyrylium salts are accessible this way. The reaction requires elevated temperatures, tends to give undesired byproducts and again consumes half of the *in situ* formed *Michael* acceptor as a hydride scavenger.[104]

In summary, the synthesis sequence of 1a, 2b and 2c (Scheme 23) gives the best synthetic results but is the most time-consuming as well. The intermediate isolation of the *Michael* acceptor avoids byproducts and therefore benefits the total yield. Furthermore, the yield is also boosted through the addition of a hydride scavenger. Anyways, in most cases, path 3 (Scheme 23) is the method of choice for two reasons. First, the substrates required usually are very cheap and the time saved in the one-pot method is chosen despite overall worse yield. Second, pyrylium salts are usually poorly soluble in most organic solvents, hence, they can easily be purified through precipitation and be used without further purification. Both other methods find their application nevertheless, as not all required pyrylium salts are symmetric or accessible over the direct one-pot method.[105,106]

In the case of *Idelson et al.*, the pyrylium salt was synthesized *via* the one-pot method. It is utilized in a *Zimmermann-Fischer* condensation, yielding a product that contained a methoxy group, which enables further functionalization.

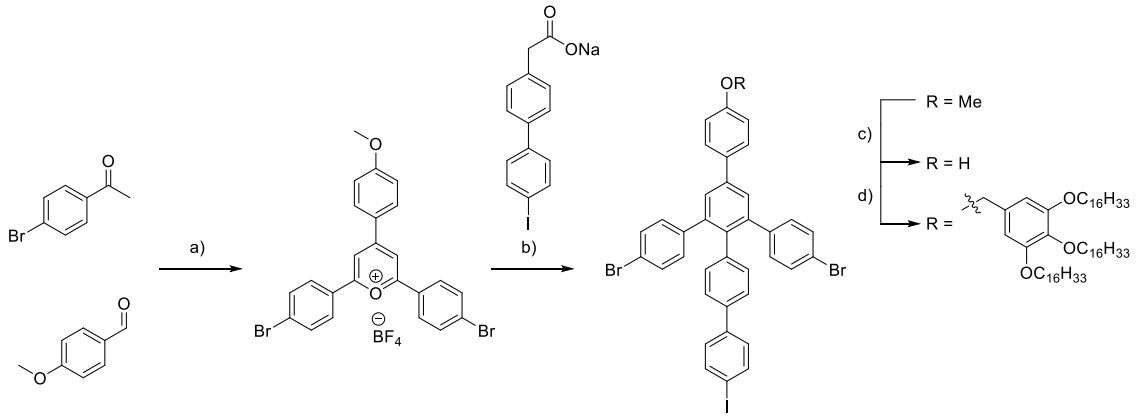

Scheme 24: $Et_2O{\cdot}BF_3$, 80° C, 3 h, 40 %, b) Bz_2O, 150 °C, 4 h, 40 %, c) BBr_3, DCM, -78 °C → rt, 18 h, 94 %, d) 1-(chloromethyl)-3,4,5-tris(hexadecyloxy)benzene[107], Cs_2CO_3, DMF, 100 °C, 18 h, 98 %.

The functionalization with the dendron molecule **68a**[107] (which will also find application later in the syntheses of this work) led to a MSW with very unique properties.[96]

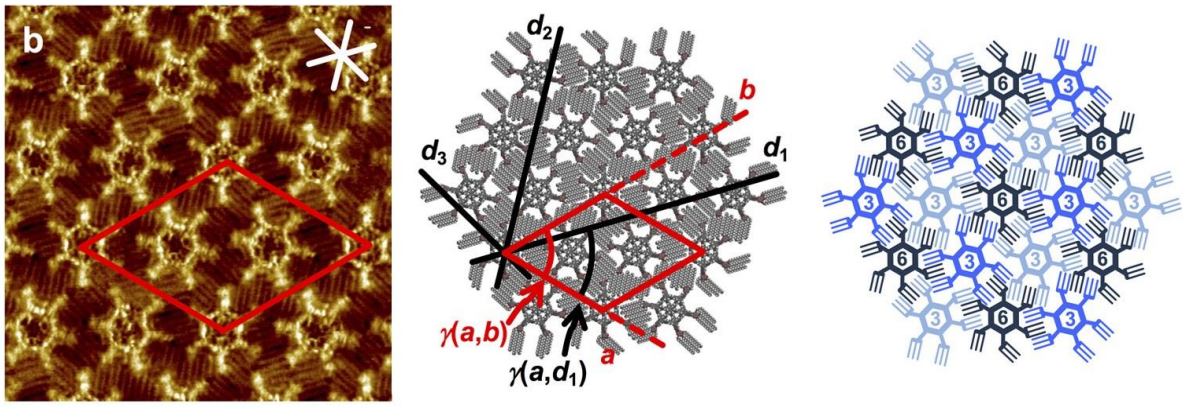

Figure 19: Depiction of **MSW-AI** adsorbing on HOPG. b) STM image (left) with the parameters: (25.2 × 25.2 nm^2, V_s = -1.8 V, I_t = 7 pA, c = 10^{-6} M in 1-phenyloctane (PHO); unit cell, a = (10.6 ± 0.2) nm, b = (10.6 ± 0.2) nm, $\gamma(a,b)$ = (60 ± 1)°; unit cell area, $A_{1b,B}$ = 97.3 nm^2; additional packing parameters, $\gamma(a,d_1)$ = (46 ± 1)°; molecular model of molecules on HOPG (center); simplified molecular model pointing out the coordination number of each MSW on HOPG (right).[96]

MSW-AI formed very organized patterns when investigated on HOPG. The molecules packed hexagonally with a unit cell containing three MSWs (Figure 19, left). All hexadecyl side chains are oriented along the HOPG main axes and three different backbone orientations of the molecules are observed, as depicted by the use of different colors (Figure 19, right).[96]

The most interesting aspect of that MSW was its liquid crystallinity. DSC measurements revealed the reversible formation of a mesophase at a temperature of 22 °C. This was the first time such a phenomenon was observed for a MSW.[96]

The newly developed synthetic strategy not only solved the problem of having to ensure a six-fold coupling to obtained an open-framed precursor to the MSW, but also gave new options. Since the anchor-shaped groups are connected to an acetylene successively, it is possible to functionalize both alkyne ends with different anchor-shaped molecules. *Sterzenbach* and *Schneiders* recognized that promising concept and developed a modified strategy[88] based on the method of *Idelson*.

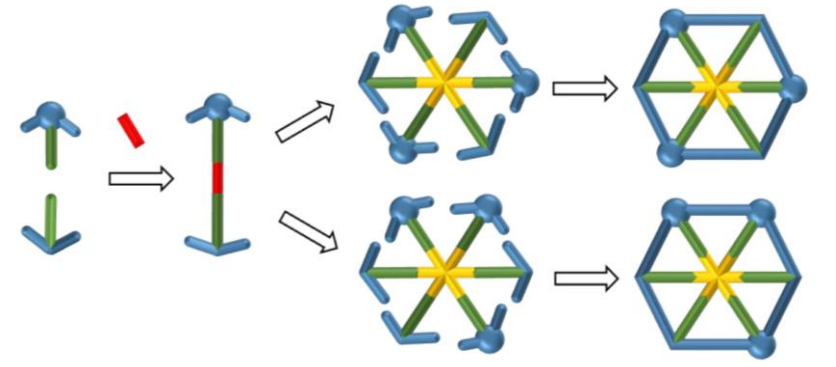

Figure 20: Schematic procedure for the synthesis of an asymmetric acetylene yielding two different MSWs of reduced symmetry.[108]

Since the resulting acetylene is no longer symmetric around the alkyne group its trimerization now yields not one but two isomers, a 1,2,4- and a 1,3,5-symmetric trimer in a ratio of 3:1 for statistical reasons.[108] This strategy was applied to synthesize asymmetric alkynes with head groups of complementary polarity. The first example was synthesized by *Schneiders* during her bachelor thesis under the supervision of *Sterzenbach*.[109]

Within the bachelor thesis, *Schneiders* and *Sterzenbach* focused on the synthesis of an MSW with a rim decorated with esters and dendron groups. They managed to access two MSWs that way over a course of 14 stages. For that, they synthesized two different anchor-shaped molecules that were then connected *via* an acetylene. The acetylene was introduced as a mono-TMS-protected alkyne to the dendron-functionalized anchor-shaped molecule and the TMS-group was cleaved afterwards. For the second *Sonogashira* reaction they used the freshly deprotected acetylene and the ester-functionalized second anchor-shaped molecule.

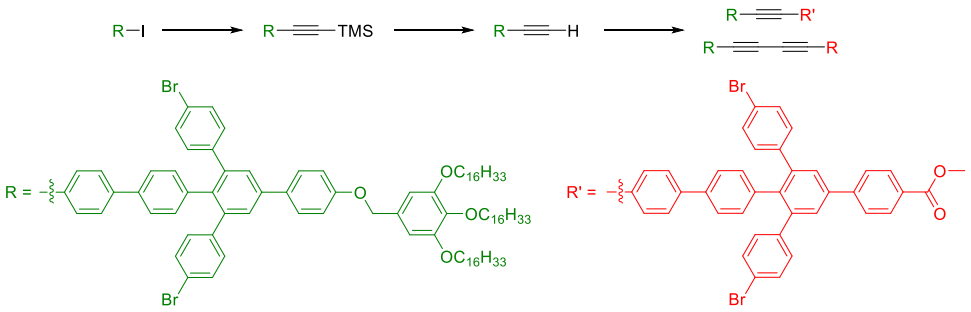

Scheme 25: Synthesis of *Schneiders*' symmetric acetylene and *Glaser* byproduct.

This method features a major advantage over the synthesis of symmetric acetylenes: for the symmetric approach, it can be extremely tedious to remove the *Glaser* byproduct since its size and polarity are nearly identical to the desired product. For the presented case the byproduct only features unpolar groups while the desired product also contains one polar ester group (compare Scheme 25). Thus, it is possible to separate both species through their difference in polarity *via* column chromatography easily while the dendron groups maintain sufficient solubility for both compounds.

The same concept was also exploited for the subsequent trimerization step. As mentioned, the trimerization of asymmetric acetylenes yields two different isomers.

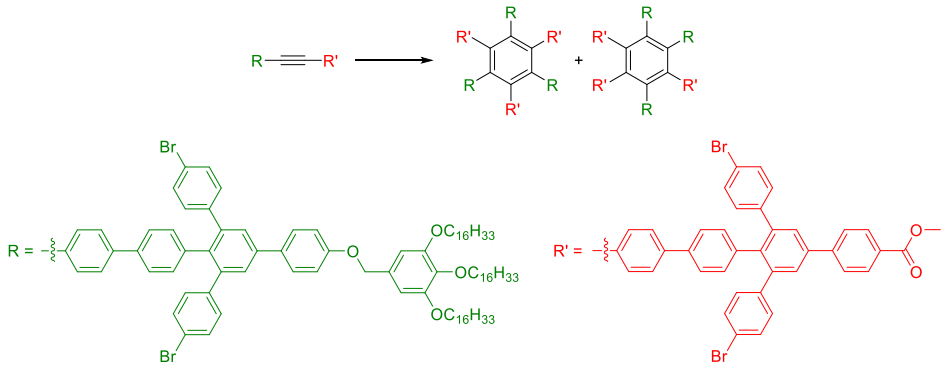

Scheme 26: Trimerization of asymmetric alkynes yielding two different open-framed precursors.

While usually the open-framed precursors were purified *via* recGPC, this is not immediately done for the presented example due to the near identical hydrodynamic radius of both trimers. Gratifyingly, the complementary polarity of the groups on the rim helps once again because it affects the overall dipole moment of the molecules. While for the 1,3,5-isomer, the dipole moment cancels out, the less symmetric 1,2,4-isomer has a dipole moment and can therefore be separated off *via* column chromatography. Afterwards, both fractions can be purified *via* recGPC yielding both trimers.[109]

Surprisingly, neither the trimers nor the closed MSWs after the following *Yamamoto* reactions were distinguishable *via* NMR- or MALDI mass spectrometry. Even though the spectra were not identical, it was not possible to assign the signals to one specific MSW.[108] Only the investigation *via* STM gave reliable insights into the connectivity of the respective isomer.[88]

Now that the isomers were assigned to the collected substances, *Sterzenbach* made an interesting observation. Through concentration NMR experiments, he found some signals to be shifting depending on the concentration. Only for low concentration, it was possible to identify sharp signals within the spectrum and confirm the molecular structure. *Sterzenbach* assigned the observed behavior of the molecules to a strong tendency of the MSWs to aggregate.[108] The phenomenon of aggregation through interaction of π-systems will be elucidated in more detail in chapter 2.6.

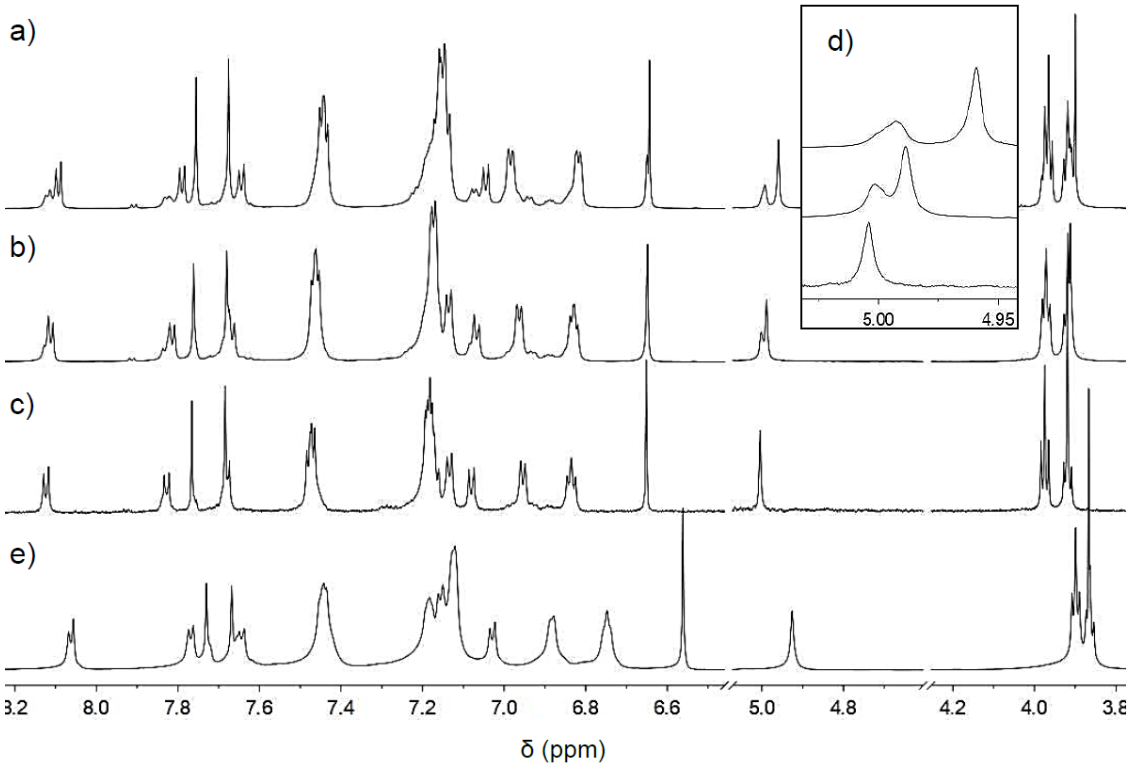

Figure 21: Investigations of *Schneiders*' 1,3,5-symmetric **MSW-TS** *via* ^{1}H-NMR spectroscopy in DCM at different concentrations (a-c): a) $1.57 \cdot 10^{-3}$ mol/L, b) $3.93 \cdot 10^{-4}$ mol/L, c) $4.92 \cdot 10^{-5}$ mol/L, d) zoomed excerpt of all three spectra a)-c) around 5.00 ppm, e) ^{1}H-NMR spectrum recorded in $C_2D_2Cl_4$ at $1.53 \cdot 10^{-3}$ mol/L.[108]

Both isomers of *Schneiders*' MSWs were in the following deprotected to yield the corresponding acids by *Sterzenbach* and re-functionalized as amides. All these re-functionalized MSWs showed the same aggregation tendency in their ^{1}H-NMR spectra as well.[108]

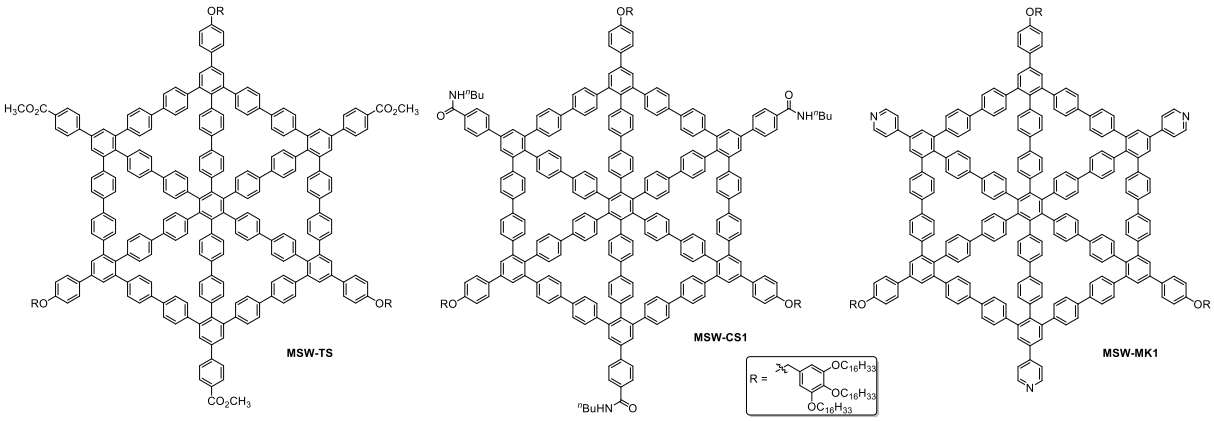

Figure 22: MSWs of lower symmetry synthesized by *Schneiders* (left)[109], *Sterzenbach* (center)[108] and *Kersten* (right).[105] All MSWs are decorated with dendron groups to ensure the solubility of the molecules and a second polar group to investigate different properties such as their packing driving character in STM.

Asides from esters, carboxylates and amides, MSWs of reduced symmetry were also prepared by *Kersten* within his PhD studies. For his work, he decided to synthesize a MSW decorated with the same dendron group as *Schneiders* and *Sterzenbach*, but chose pyridine as a polar head-group. He managed

to synthesize four additional MSWs with similar intended properties as his predecessors. Similar aggregation experiments surprisingly did not reveal any tendencies to aggregation for his molecules.[105]

Kersten's MSWs opened up an interesting opportunity, that the other two did not: While for all three presented MSWs both decorating groups are of complementary polarity and therefore give the molecules an amphiphilic character, only for the pyridyl-MSWs it is possible to additionally boost that character by formation of highly polar quaternary pyridinium salts. However, *Kersten* was not able to achieve such functionalization despite promising alkylation results with a test system.[105]

While all previously presented MSWs relied on solubility-promoting ether groups *L. zur Horst* explored the limits of all-phenylene based MSWs in her PhD studies. In her research, *zur Horst* took the term *all-phenylene* literally and synthesized an MSW exclusively consisting of phenylene groups. Hence, all corners of her **MSW-LzH** are functionalized with phenylene groups, making it essentially a combination of seven hexaphenylbenzenes.

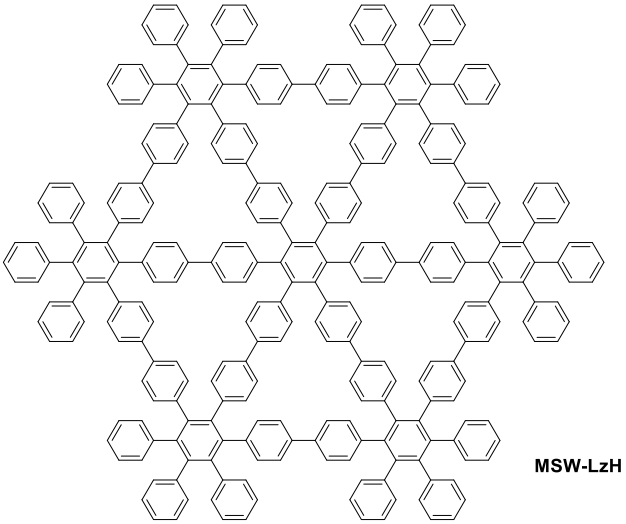

Figure 23: One target molecule of the work of *zur Horst* consisting of only phenylene groups.[106]

The special structure of the corner groups was achieved through the choice of a suitable pyrylium salt. Instead of 2,4,6-substituted salts as incorporated in most previously described examples, *zur Horst* prepared a pentasubstituted pyrylium salt.

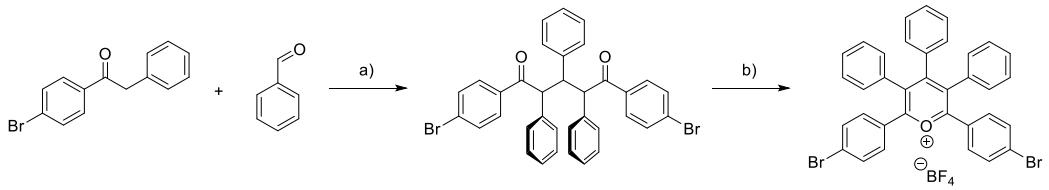

Scheme 27: Synthesis of *zur Horst*'s pentasubstituted pyrylium salt. a) KOH, EtOH, rt, 4 d, 61 %; b) 1) Ph_3COH, Ac_2O, 60 °C, 10 min, 2) aq. HBF_4 (48 %), 120 °C, 15 min, 3) 100 °C, 2 d, ≈82 %.[106]

Since it was not accessible over the direct path (compare Scheme 23), the intermediate 1,5-diketone was synthesized first. Besides that, it was not necessary to isolate the *Michael* acceptor since the resulting salt was meant to be symmetrical.

After synthesizing the anchor-shaped molecule in a *Zimmermann-Fischer* condensation, *zur Horst* developed and applied an elaborate strategy. For this, she first extended the anchor-shaped molecule by a CPD*i*PS-acetylene in a *Sonogashira* coupling.

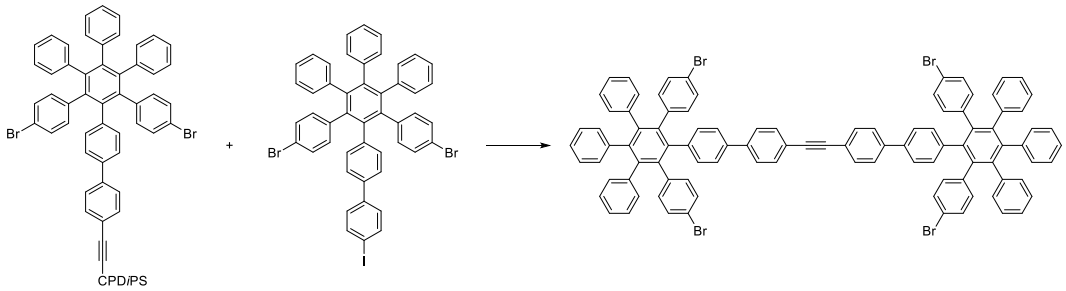

Scheme 28: Synthetic strategy for *zur Horst*'s symmetric acetylene. a) TBAF, $PdCl_2(PPh_3)_2$, PPh_3, CuI, THF/Piperidin (1:2), 18 h, rt, 71 %.

Instead of deprotecting and isolating the terminal alkyne, *zur Horst* dissolved the protected acetylene anchor and the iodo-substituted anchor under *Sonogashira* conditions and slowly added a solution of TBAF. Through that, the silyl protecting group was cleaved *in situ* over a longer period of time drastically reducing the formation of *Glaser* byproduct while shortening the total synthesis by one step. This sophisticated strategy gave the desired symmetric acetylene in an excellent yield of 71 %.[106]

As a consequence of the MSW's design choice, it was especially difficult to isolate the compound after the final step, as it obviously suffered from very poor solubility. Thus, a characterization *via* NMR spectroscopy was not possible. Instead, the molecule was characterized *via* MALDI mass spectrometry and the structure was finally proven *via* STM once again underlining the importance of this analytic tool in macrocycle chemistry.[106]

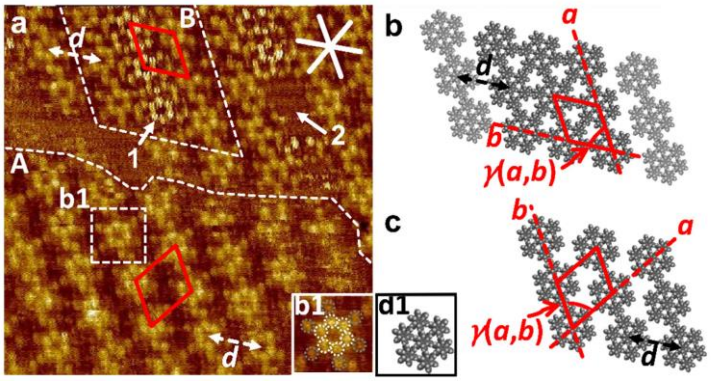

Figure 24: a) STM image of **MSW-LzH**: $c = 10^{-5}$ M in TCB, I_t = 30 pA, V_S = -1.85 V, 30 x 30 nm^2, tempered on HOPG for 20 s at 80 °C, the unit cell is depicted in red; b) supramolecular model of excerpt B: a = (3.8 ± 0.2) nm, b = (3.6 ± 0.2) nm, $\gamma(a, b)$ = (60 ± 1)°; c) supramolecular model of excerpt A: a = (4.3 ± 0.2) nm, b = (3.9 ± 0.2) nm, $\gamma(a, b)$ = (67 ± 1)°.

2.6 π-π interactions and aggregation

The 20th century was dominated by the research around covalent bonds and their formation. With the exponential advancements in technology especially towards the end of the century, new opportunities arose on how reactions can be surveilled and regarding the analysis of compounds. Fueled by these advancements, the field of supramolecular chemistry rose strongly in popularity.

Supramolecular chemistry is a branch of chemistry, that does not primarily revolve around covalent bonds but non-covalent interactions.[110] In general, those supramolecular interactions are weaker than most of the covalent bonds and therefore easier to cleave. On the other hand, it is exactly that weakness that makes them of such interest and that made it so hard to investigate them.

The list of supramolecular interactions lasts from very strong ion-ion interactions, which gain their strength from the attraction of complementary formal charges, down to weak *van der Waals* interactions, that only get strong if they are formed between enough atoms or groups due to their additive character. While supramolecular interactions are ever-present in vital processes and many of them are found and exploited in synthetic research as explained earlier (compare chapter 2.4), this chapter focuses on interactions found in π-systems.

The π-systems discussed within the limits of this work are mostly hydrocarbon-based, meaning they can be described as unpolar compounds, limiting the number of possible supramolecular interactions these compounds can make. The centrosymmetric shape of especially a benzene unit additionally disables the compound from having a dipole moment. Benzene molecules are nevertheless able to form strong interactions with ions and other benzene molecules, while the type of ions depends strongly on their functionalization. The reason for this is the inherent quadrupole moment.

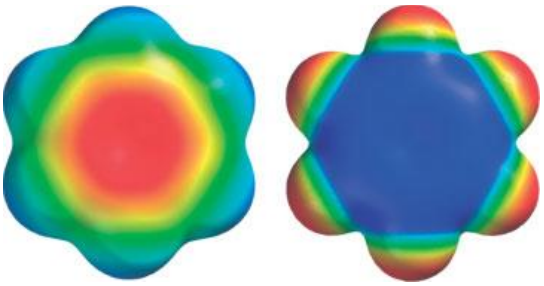

Figure 25: Electrostatic potential surfaces of benzene (left) and hexafluorobenzene (right) modelling their quadrupole moment. The color scheme indicates potentials between -60 kcal/mol (red) and 50 kcal/mol (blue).[111]

As Figure 25 shows, benzene features the highest electron density in the center of the molecule above (and below) the molecular plane instead of a symmetric distribution over the atoms and bonds. In strong contrast to that, the highest electron density in hexafluorobenzene can be found outside the ring at the strongly electron-withdrawing fluorine atoms. Summarizing, the quadrupole moment can be fully inverted by inverting the electronic properties of the substituting atoms or groups.

This is of importance to understand the interactions possible between two aryl groups displayed at the example of benzene and hexafluorobenzene in the following once again.

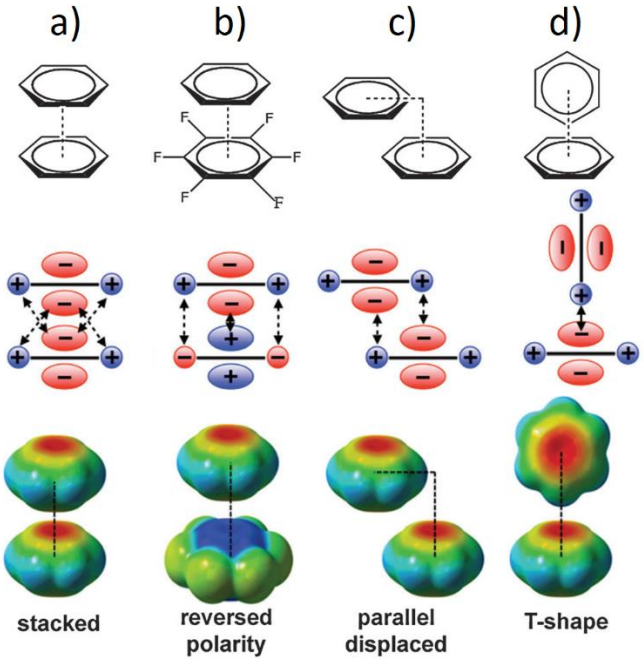

Figure 26: Molecular geometries and interactions between the quadrupole moments of both components and electrostatic potential surfaces of the participating molecules for four different cases of interactions of two π-systems.[112]

Even though the ecliptic stacking of two benzene molecules might appear the most intuitive, it is not observed as it leads to a repulsion of identically signed quadrupole moments (Figure 26a). Instead, the ecliptic packing is only observed for benzene derivates with opposing signs like benzene and hexafluorobenzene (Figure 26b). Two benzene molecules stack in a parallel displaced fashion to once again match opposite signs (Figure 26c). Of lower relevance for this work but explained for the sake of completeness is the T-shape arrangement. This edge-to-face conformation can only be observed between two compounds of similar oriented quadrupole moments due to alignment of complementary phases (Figure 26d).[112]

The attraction of different π-systems, that is often also referred to as π-stacking, was found to be an additive phenomenon. This means, that the tendency of π-stacking increases with the size of the conjugated system, especially for purely hydrocarbon-based and/or inflexible systems that maximize the interactions through preorganization.[110]

However, the stacking of π-systems is not necessarily something desirable, so there are common concepts to overcome this. One widely-used strategy is the decoration of the structure with long and/or branched alkyl chains, required to sufficiently boost the solubility. The group of *Mastalerz* chose another approach, when they researched on quinoxalinophenanthrophenazines (QPPs), large polyaromatic compounds with an extended π-system. Those compounds were found to form

face-to-face stacks when crystallized. Within their investigations, they analyzed the influence of *tert*-butyl, triptycene and a combination of both groups on the shifting between two molecules within the crystal structure.[113]

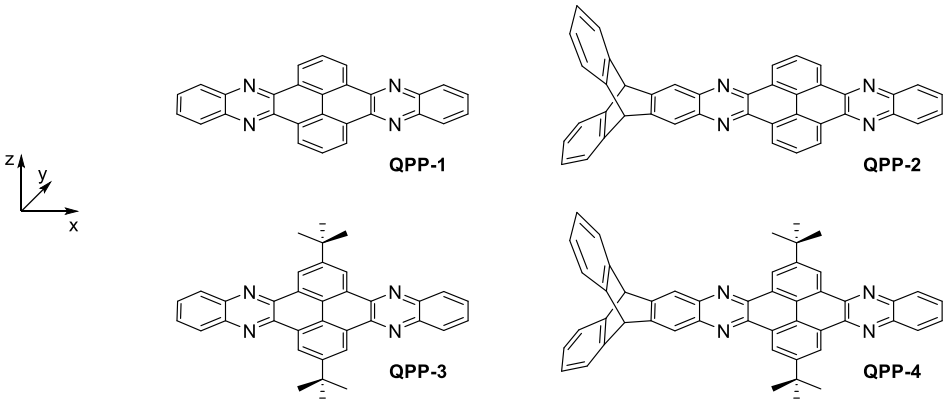

Figure 27: QPPs of different functionalization to be investigated regarding their crystal packaging.[113]

Interestingly, the presence of *tert*-butyl groups shifts both molecular planes strongly towards each other in x-direction for **QPP-3** by about 5 Å. The introduction of a triptycene end-cap strongly reduces that shift for **QPP-4** (0.28 Å) and **QPP-2** (0.01 Å). The influence of the off-centering is also reflected in the packing energies, as **QPP-4** and **QPP-3** were found to have higher absolute values than their counterparts. A reasonable explanation for this is the better overlap of quadrupole moments in the off-centered structure.[113]

Besides that, the end-capping turned out to have a massive influence onto the solubility. Compounds like **QPP-1** are poorly soluble due to the fact that they feature low degrees of freedom and lack any solubility-promoting group. As a consequence, the aromatic systems can pack closely and form crystals that no longer dissolve due to their strong interaction with each other. The end-capping and the *tert*-butyl groups enormously boost the solubility, especially for the twice-capped compounds.[114]

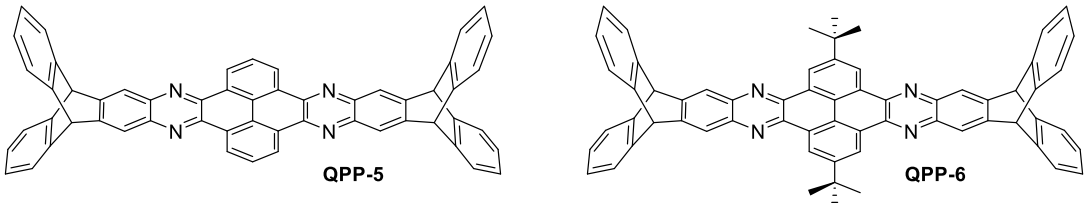

Figure 28: Twice-capped QPPs synthesized for the investigation of the solubility of different QPP compounds.[114]

While the solubility of **QPP-1** (0.25 mmol/L) increases by around the factor 4 through incorporating *tert*-butyl group (0.97 mmol/L, **QPP-3**), the bis-end-capped **QPP-1** results in solubility of 1.3 mmol/L (**QPP-5**) and the equivalent of **QPP-3** rises to 11.5 mmol/L (**QPP-6**), which is about 50 times the solubility of **QPP-1**. Additionally, the UV/Vis spectra of **QPP-3** and **QPP-6** in chloroform were compared.[114]

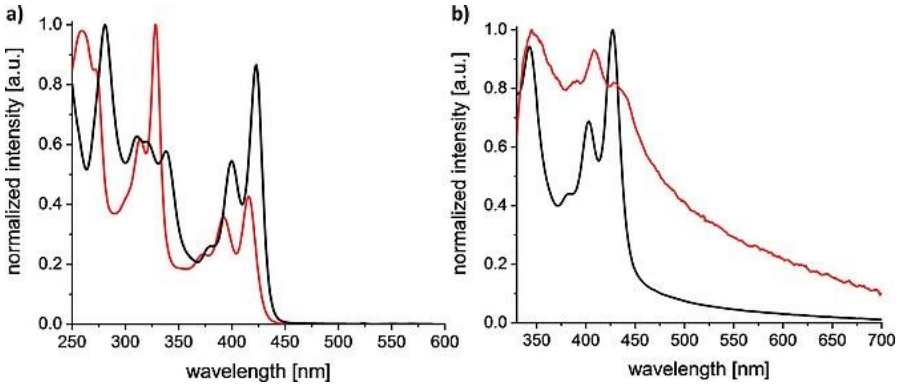

Figure 29: Comparison of the UV/Vis spectra of **QPP-3** (red) and **QPP-6** (black) dissolved in $CHCl_3$ (a) and as a film (b).[114]

Especially the spectrum recorded for the film shows a strong sharpening for the higher functionalized compound. Hence, *Mastalerz et al.* stated, that due to the increased solubility and the sharpening in the spectra, the aggregation of their compounds was reduced.[114]

Since the mostly flat, disk-shaped and fully conjugated systems by *Mastalerz et al*. are in a way similar to all-phenylene MSWs, both can be compared in some aspects. The poor solubility through the absence of solubility-promoting side groups was a problem for *zur Horst*'s **MSW-LzH** as well (compare chapter 2.5.1). Comparing her design to the previously presented findings, sparks the idea that her MSW also suffered from π-stacking additionally worsening its solubility.[106] Unfortunately, the latter can only be suggested since 1) the MSW was not soluble enough to record ^{1}H-NMR spectra of it, neither concentrated nor concentration-dependent and 2) the influence of all-hydrocarbon groups like triptycenes on π-stacking and the solubility of all-phenylene MSWs has not yet been investigated.
At the current state of research, the aggregation of precursors is what hindered *Sterzenbach* in the final cyclization step from enlarging all-phenylene MSWs. Even though he reported the aggregation of some of his MSWs in his PhD thesis (compare chapter 2.5.1), for the enlarged MSWs the combination of low steric hindrance and strong intermolecular attractions originating from the extended π-systems favored the intermolecular coupling of the precursors exclusively.[108] His synthetic efforts and observations will be elucidated in more detail in the following chapter.

3 Preliminary Work

As described, many all-phenylene MSWs were accessible in a broad scope of functionalization and with different symmetries. In the past, far larger structures than the presented all-phenylene MSWs were synthesized peaking in the synthesis of **MSW-RM** with 11.9 nm diameter (compare chapter 2.5).[94] Those structures were not all-phenylene-built as they featured acetylene- and butadiyne-units as well. While these units are very helpful to easily build up large structures due to their high reactivity in transition metal-catalyzed carbon-carbon bond formation reactions, they are unfortunately also very prone to decomposition or side reactions when stored under ambient conditions for longer time periods. In order to synthesize larger MSWs that are actually bench-stable over long times, it was necessary to rely on *Idelson*'s strategy employing only phenylene units as building blocks.

The first enlarging synthetic approach in that direction was undertaken by *C. Sterzenbach* during his PhD studies.[108] As the smallest possible enlargement step the MSW's edge was extended by one phenylene unit, resulting in a structure with a perimeter of 24 Ph units ("24 Ph-MSW"). Since five is an odd number, it was necessary to build the final structure from an asymmetric precursor. This was realized by synthesizing two different anchor-shaped precursors with identical spoke-length but different side group length.

Two different anchors were then connected *via* an acetylene group and trimerized in the following reaction step. The trimerization step yielded two different isomers that were both closed successfully, even though one was strongly distorted. Since **MSW-AI**, the "regular-sized" 18 Ph-MSW equivalent of *Sterzenbach*'s more symmetric MSW, was already synthesized by *Idelson* within the syntheses for her PhD studies,[96,115] it was possible to directly compare the results for both molecules. Especially for the final *Yamamoto* coupling, the yield for **MSW-AI** was with 74 %[115] drastically higher than for *Sterzenbach*'s **MSW-CS2** with only 17 %.[108]

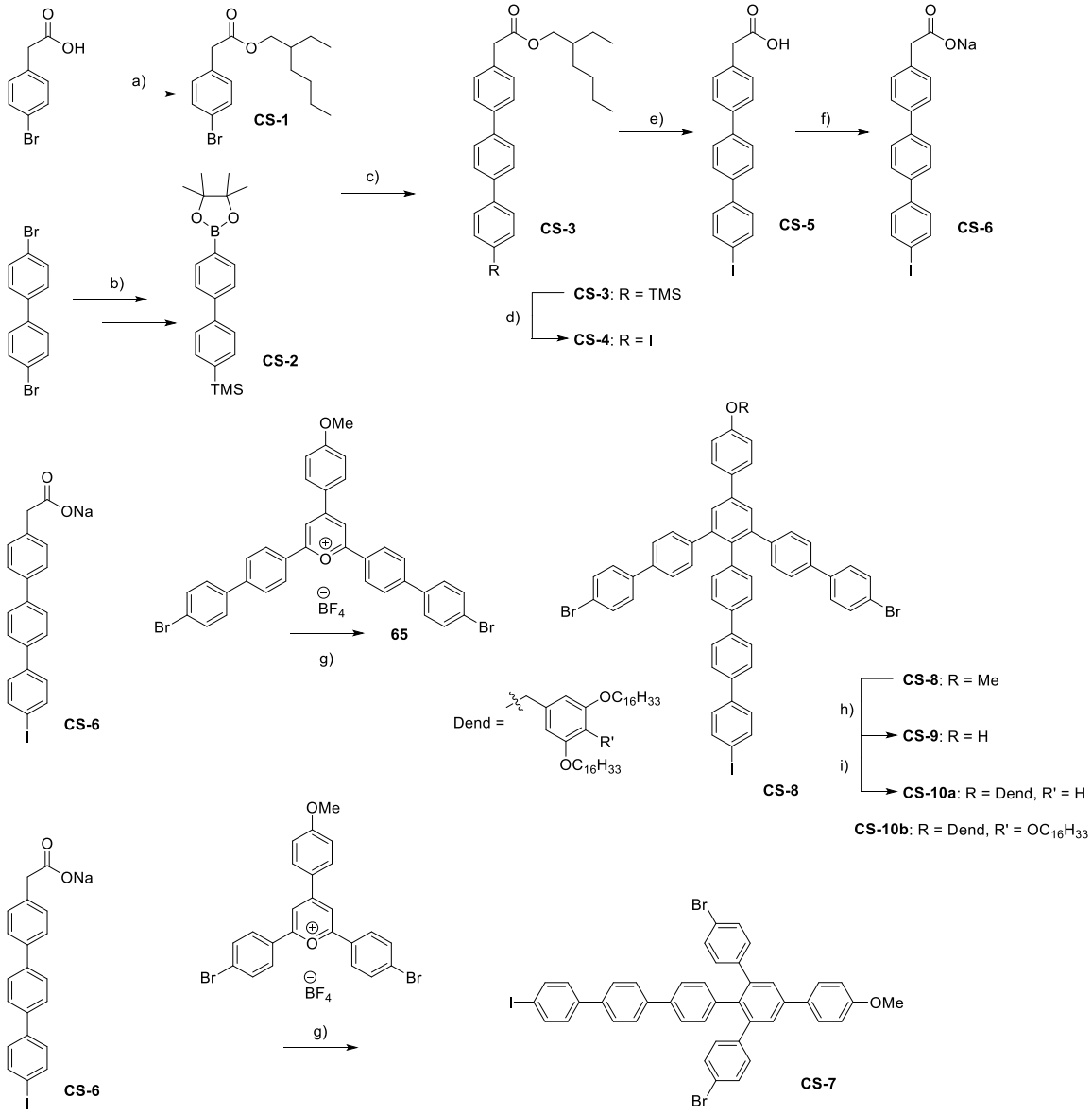

Scheme 29: Construction of two different anchor shaped molecules through variation of the pyrylium salt.
a) 2-ethyl-1-hexanol, TsOH, 70 °C, 18 h, 91 %; b) i) THF, *n*BuLi, -78 °C, 30 min; ii) TMSCl, 30 min, -78 °C → rt, 1 h; iii) *n*BuLi, -78 °C, 30 min; iv) 2-isopropoxy-4,4,5,5-tetramethyl-1,3,2-dioxaborolan, -78 °C → rt, 18 h, 60 %; c) K_2CO_3, PhMe, H_2O, PPh_3, $PdCl_2(PPh_3)_2$, 80 °C, 2 d, 56 %; d) ICl, DCM, 0 °C, 1.5 h, 99 %; e) LiOH, THF, H_2O, 60 °C, 1 d, 84 %; f) NaOMe, MeOH, 73 °C, 1 h, 100 %, g) Bz_2O, 150 °C, 4.5 h, 100 % h) BBr_3, DCM, rt, 2 d, 21 % (2 steps); i) **68b**, Cs_2CO_3, DMF, 100 °C, 19 h, 93 %.[108]

A further enlargement step to a 30 Ph-MSW was also attempted by *Sterzenbach*. For that even-numbered edge length no special synthesis was necessary, so a symmetric acetylene was synthesized from two identical anchor-shaped molecules. The special aspect about that synthesis is that the anchor-shaped molecules were no longer connected *via Sonogashira* couplings but in an one-pot two-fold *Suzuki* coupling. The urgency for this is that it is not possible to synthesize the required linear quaterphenylacetic acid as a spoke unit while maintaining sufficient solubility.[108] During his PhD, *S. Becker* attempted to synthesize a linear quaterphenyl acetophenone, which was not accessible for that exact reason, preventing the synthesis of the respective pyrylium salt.[116] For that

reason, it is essential to construct the spoke of the target molecule from at least two fragments and connect them in a late step. Fortunate about what first appeared to be a constraint was that **CS-8** (compare Scheme 29) was of suitable dimensions to be reused as an anchor-shaped compound if a matching new connection unit was synthetically accessible. The desired compound was received in a two-step synthesis following the instructions of *Takase et al.* in moderate yields.[117]

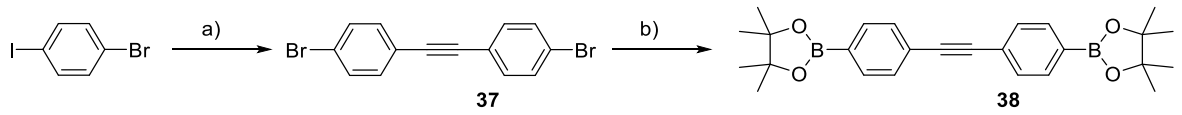

Scheme 30: a) $PdCl_2(PPh_3)_2$, PPh_3, CuI, TMS-acetylene, K_2CO_3, MeCN, MeOH, 15 h, rt, 81 %; b) Bis(pinacolato)diboron, $PdCl_2$(dppf), AcOK, DMF, 2 h, 105 °C, 58 %.

Even though the symmetric acetylene was trimerized successfully, it was not possible to isolate the desired **MSW-CS3** after the next step. Instead, a mixture of higher-molecular oligomers was received while the most dominant species appeared to be a molecule approximately twice the molecular weight of the targeted molecule, even though it was not possible to reliably characterize the species as a dimer. In order to facilitate the ring closure, the aryl halides were re-functionalized in an aromatic *Finkelstein* reaction.[118] A second closing attempt yielded tiny amounts of what at first appeared to be the desired species, but unfortunately was neither possible to be characterized *via* NMR spectroscopy nor mass spectrometry. Elucidation of the molecular structure of the isolated fraction *via* STM remained unsuccessful as well.

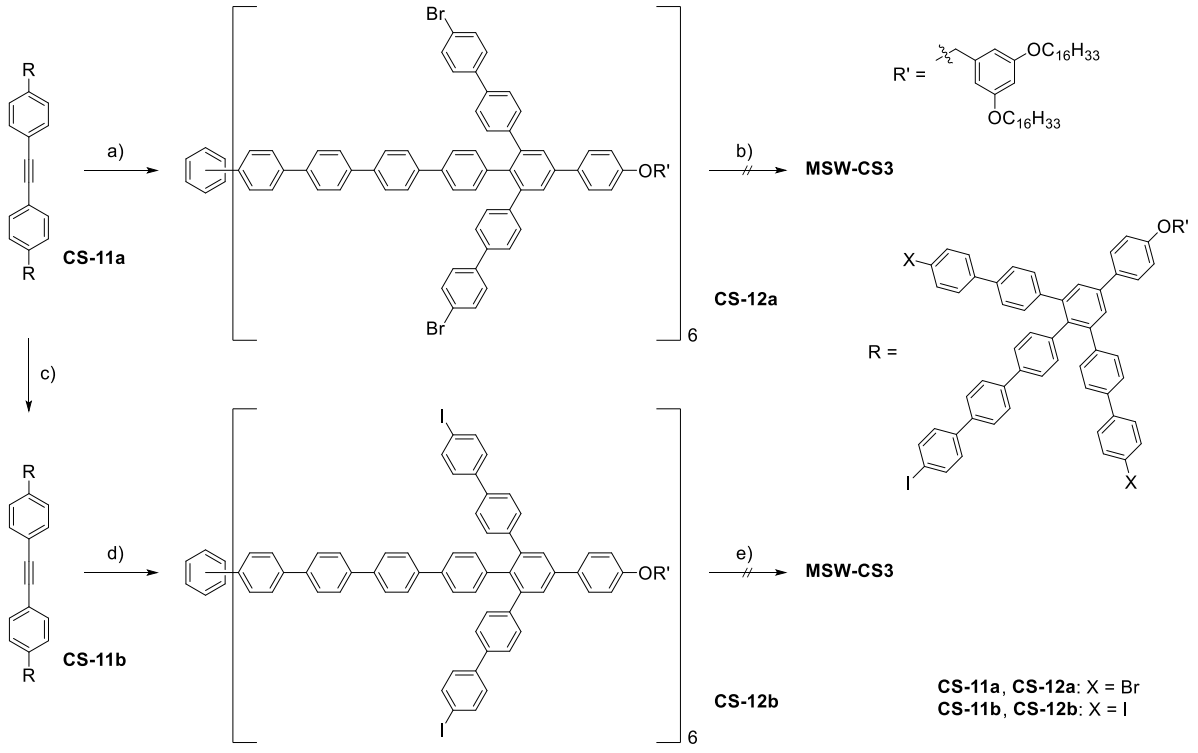

Scheme 31: a) $Co_2(CO)_8$, PhMe, 136 °C, 18 h, 49 %, b) various conditions, no yield, c) CuI, NaI, 1,4-dioxane, 125 °C, 18 h, 89 %; d) $Co_2(CO)_8$, PhMe, 135 °C, 18 h, 46 %, e) $Ni(COD)_2$, bipy, THF, COD, 120 °C (mw), traces.

Since the major product of the second cyclization attempt remained the unidentified species of higher molecular weight, further cyclization attempts were not carried out. It appeared that the intermolecular coupling was strongly favored over an intramolecular cyclization reaction. One possible explanation for that might be the extended π-systems of the precursors, increasing its tendency to aggregate and thus favor the intermolecular coupling due to the substrates' proximity. This hypothesis is also supported by the yield of **MSW-CS2** that strongly decreased to 17 % compared to **MSW-AI** that was obtained in 74 %. From these observations was concluded, that there was no possibility to access 30 Ph-MSWs without controlling the intermolecular distances.

After identifying the origin of the intermolecular side reactions, new designs were developed. In order to inhibit the aggregation of precursor molecules and ensure a certain distance between two molecules, alkyl chains were designated as spacing groups. Alkylated MSWs have been investigated in the past in various functionalization and even for all-phenylene MSWs. The problem about that approach is alkyl chains at the corners of the MSWs would be unable to prevent aggregation. This was also indirectly proven by *Sterzenbach* since his unsuccessful expansion attempt featured dendron-functionalized corners. Additionally, his 18 Ph-MSWs that revealed aggregation tendencies during concentration-dependent NMR-experiments were also partly decorated with dendron groups.[108] The best option for the implementation of alkyl chains was the alkylation of the spoke units and regarding synthetic strategies the field was narrowed down to three reasonable designs.

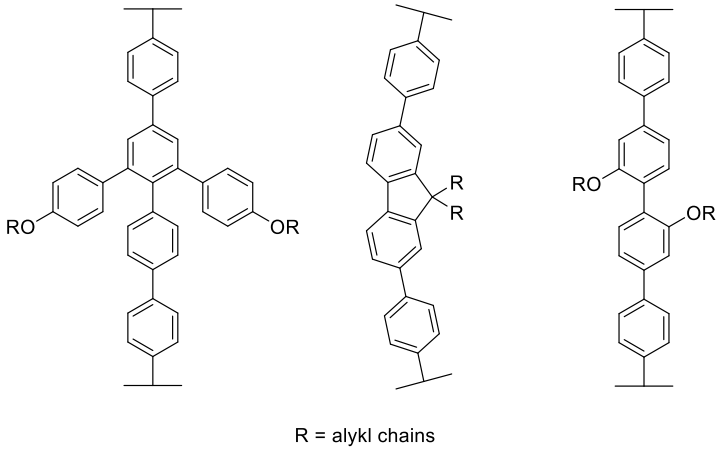

Figure 30: Modified designs of the spoke unit of potential 30 Ph-MSWs, alkoxy phenylenes as functional groups (left), alkylated fluorenes (center) and 2,2'-biphenol ethers.

The first design was investigated within my master thesis.[119] Incorporating the spoke unit into the usual anchor-shaped molecule results in an airplane-shaped geometry in which the alkoxy phenylenes resemble the horizontal stabilizers while the aryl halides resemble the large wings.

Synthetically, that airplane-shaped molecule was constructed from the respective sodium biaryl acetate that was described by *Idelson et al.* before.[96] The compound was yielded after a sequence of

two *Zimmermann-Fischer* condensations in moderate to acceptable yields similar to a blueprint of *Sterzenbach*.[108] The sequence of two of these reactions was very resource-draining, but led to the desired product in a few steps.

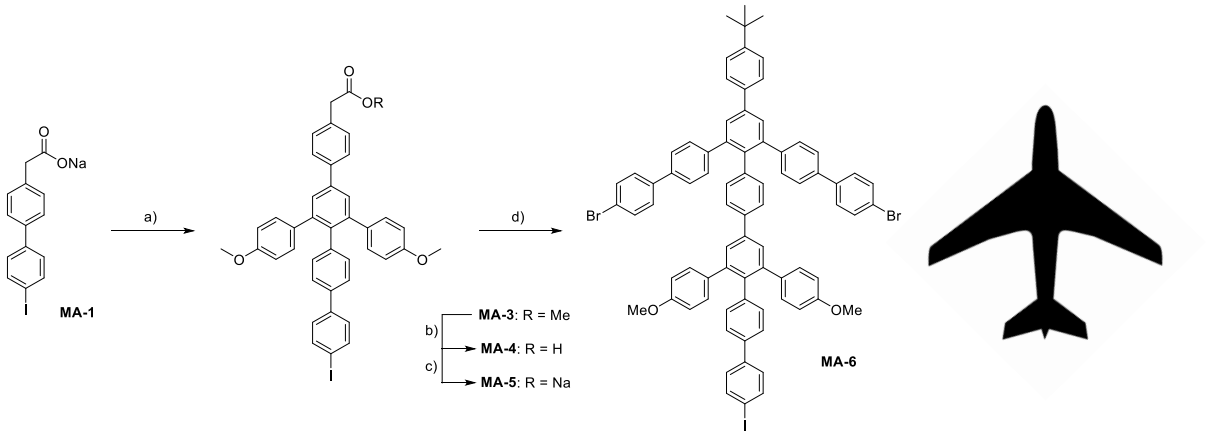

Scheme 32: Synthetic procedure (left) with schematic view of an airplane (right): a) **MA-2**, Ac_2O, 150 °C, 4 h, 24 %, b) $LiOH \cdot H_2O$, THF, H_2O, 60 °C, 91 %, c) NaOMe, MeOH, rt, 100 %, d) Bz_2O, **35**, 150 °C, 18 %.[119]

Unfortunately, it was neither possible to refunctionalize **MA-3** nor **MA-6** since the methyl ethers was not cleavable for either molecule under various conditions.

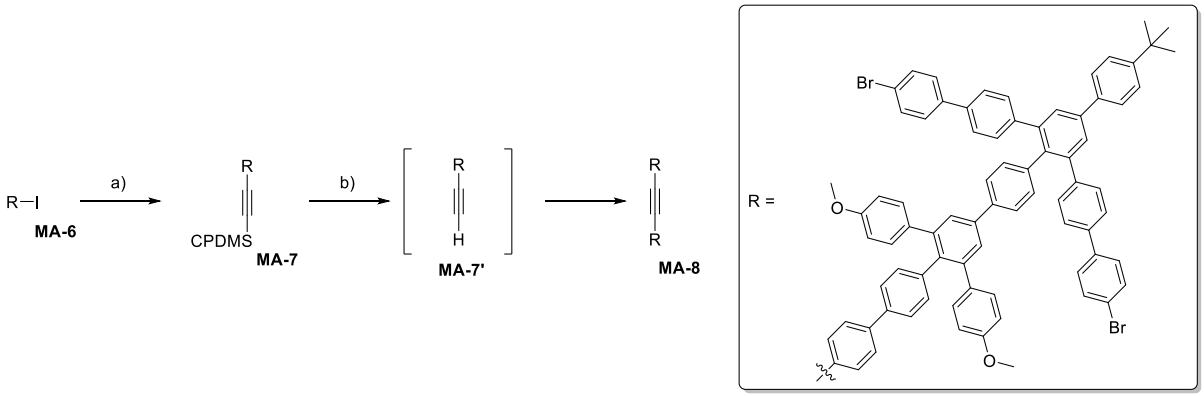

Scheme 33: a) $PdCl_2(PPh_3)_2$, PPh_3, CuI, CPDMS-acetylene, piperidine, THF, rt, 16.5 h, 71 %, b) **MA-5**, $Pd(PPh_3)_4$, CuI, piperidine, THF, TBAF, rt, 19 h, 61 %.

The planned synthesis proceeded with the phenyl methyl ethers anyways, forming a CPDMS-protected acetylene first *via Sonogashira* coupling. Adapting the strategy of *zur Horst*,[106] the compound was deprotected and coupled in another *Sonogashira* coupling with another equivalent of **MA-6** in a one-pot reaction. Even though there were no solubility-promoting groups except for the *tert*-butyl groups, **MA-8** was received in moderate yields over two steps. All deprotection efforts of **MA-8** were unsuccessful, which in the end led to the discontinuation of the project.[119]

The second concept was constructed around fluorene as a structural motif. Fluorene itself is very interesting as a substrate for many different reasons. First, the 9,9'-position of the fluorene is acidic and can therefore easily be functionalized with alkyl halides (compare chapter 2.3.2).[47] A second

benefit is, that due to the fluorene's chemical properties, its 2- and 7-position can easily be addressed with electrophiles like halogens. By this, it is very easy to synthesize slightly bent biaryl halides that are substrates for transition metal-catalyzed cross coupling reactions. Through this, it is fairly easy to build large organic structures like MSWs while incorporating fluorene into it adapting *Idelson*'s synthetic strategy.[96] The third aspect is that, opposite to the 4,4'-incorporated linear biphenyls, fluorenes introduce a curvature into the final structure. This curvature itself already influences the MSW's tendency to aggregate, because the final structure is no longer a planar disk but bowl-shaped. Once alkylated, the alkyl chains cover both sides inhibiting aggregation of the disks.

Within his PhD studies, *Kersten* began the investigations around fluorene-based MSWs before and parallel to the investigations of this work. *Kersten* first synthesized an 18 Ph-MSW since MSWs of that size proved to be more accessible and tended to aggregate in the past as well.[105]

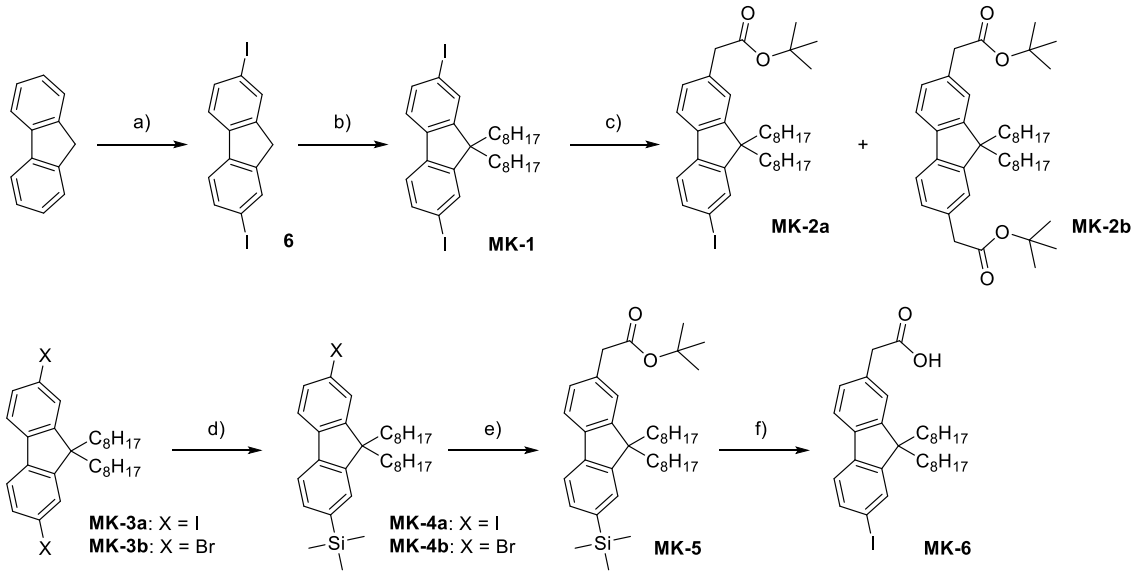

Scheme 34: a) I_2, H_5IO_6, HOAc, H_2O, H_2SO_4, 58 %, b) KO*t*Bu, $C_8H_{17}Br$, DMF, 48 %, c) Zn, *tert*-butyl bromoacetate, P(*t*Bu)$_3$, $Pd_2(dba)_3$, 0 % (**MK-2a**), d) *n*BuLi, THF, -78 °C, TMSCl, impure, e) Zn, *tert*-butyl bromoacetate, P(*t*Bu)$_3$, $Pd_2(dba)_3$, f) ICl, DCM, 37 %.

Kersten chose a symmetric approach in which he first synthesized a diiodofluorene that was alkylated subsequently. Afterwards, in a statistical *Hartwig α*-arylation *Kersten* attempted to introduce one equivalent of *tert*-butyl bromoacetate into his molecule.[120] When analyzing the crude product, it was found that no statistical product was formed but only the diester compound was isolated. The subsequent reaction yielded the product of an asymmetric TMS-protection of **MK-3a**. Unfortunately, **MK-6** was not accessible from **MK-4a** as *Kersten* only observed the product of dehalogenation during the coupling step when analyzing the crude product. The same route was attempted for the more stable respective dibromo-compounds. Again, the one-sided protection was possible exclusively, which solved two problems at once: first, *tert*-butyl bromoacetate can now be used in excess since no overfunctionalization is possible anymore. Second, at some point in the synthetic route it would have

been necessary to exchange bromine for iodine since their different reactivity must be exploited at a later point in order to maintain control over the reaction's regioselectivity. With a TMS group, a TMS-iodine exchange can be performed which works under very mild conditions and cleaves the labile ester at the same time. Usually, the bromine-iodine exchange is performed in an aromatic *Finkelstein* reaction. The problem with this reaction is that the product and the substrate usually do not differ in polarity, which makes it impossible to reliably check the progress of the reaction *via* thin layer chromatography (TLC) and separate them if the substrate is not fully converted. The rest of the synthetic route worked without any unexpected inconveniences yielding the desired **MSW-MK2**.[105]

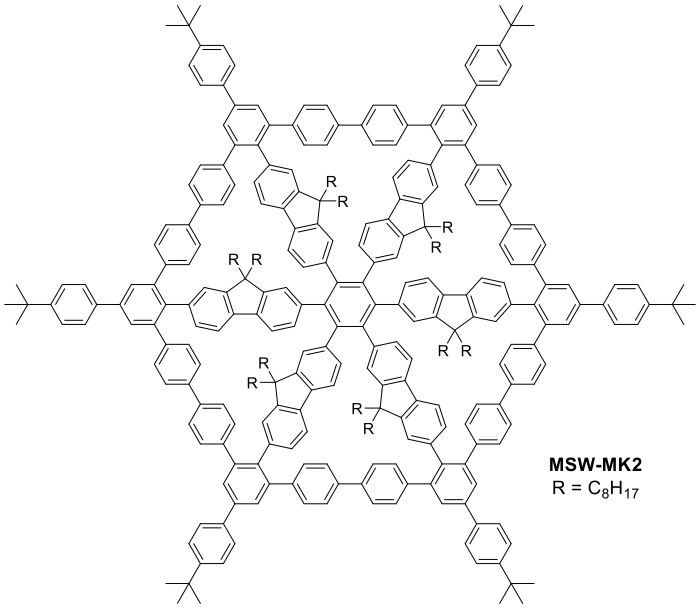

Figure 31: Molecular structure of *Kersten*'s **MSW-MK2**, all fluorene units are functionalized with two octyl chains.

After this success, *Kersten* began with the synthetic work for the size expansion. Other than *Sterzenbach*, *Kersten* first stuck to the synthetic strategy of building the full spoke contained within the anchor-shaped compound and link them *via Sonogashira* coupling. Due to the alkyl chains, solubility of the intermediates was not expected to be a problem. Since the spoke was expanded symmetrically, compound **MK-3b** was reused.

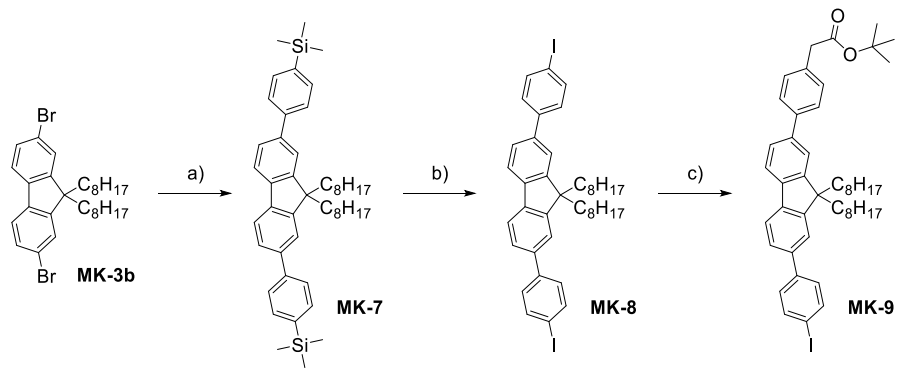

Scheme 35: a) 4-TMS-Phenylboronic acid, K_2CO_3, $Pd(PPh_3)_4$, PhMe/EtOH, 70 °C, 18 h, 61 %, b) ICl, DCM, 2 h, rt, 99 %, c) Zn, *tert*-butyl bromoacetate, $P(tBu)_3$, $Pd_2(dba)_3$, 80 °C, 18 h, no yield.

The simple TMS-protection was exchanged for a two-fold *Suzuki* coupling followed by a two-fold TMS-iodine exchange. This sequence was necessary and cannot be reduced to one step because 4-iodophenylboronic acid as an extender unit would have brought the risk of polymerizing before or after having successfully been coupled. Even though the synthesis of **MK-9** was accompanied by the byproduct of a two-fold coupling, a statistical coupling was possible. Unfortunately, both compounds were inseparable *via* column chromatography even though the retention factors suggested differently. After that setback, the synthetic planning of *Sterzenbach* was adapted to synthesize the desired spoke unit. The route used for **MSW-MK2** was reused and slightly modified by first exchanging the *Hartwig* *α*-arylation for a *Suzuki* coupling.[105]

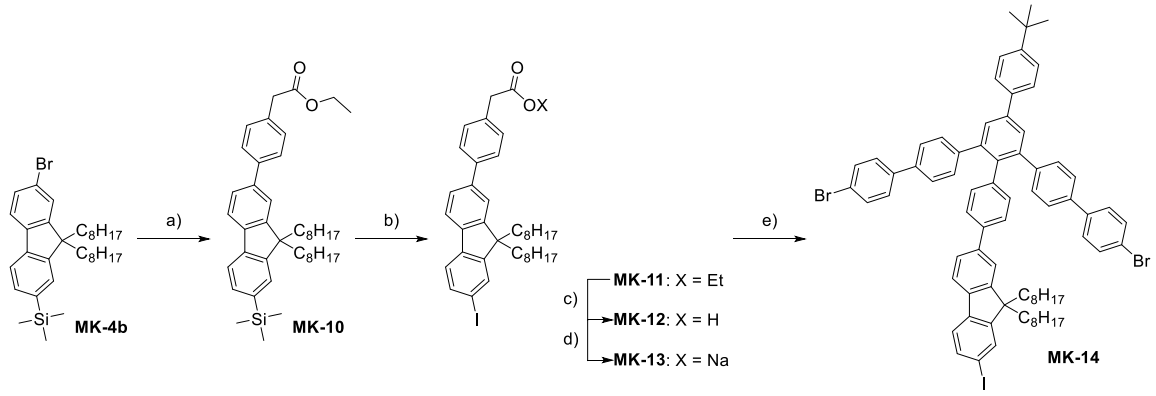

Scheme 36: a) **30**, K_2CO_3, $Pd(PPh_3)_4$, PhMe/EtOH, 70 °C, 18 h, 71 %; b) ICl, DCM, rt, 2 h, 99 %; c) $LiOH \cdot H_2O$, THF/H_2O, 50 °C, 2 h, 97 %; d) NaOMe, MeOH, rt, 1 h, 100 %, e) **35**, Bz_2O, 150 °C, 4 h, 26 %.

The *Sonogashira* coupling sequence was replaced by a two-fold *Suzuki* coupling.[108] Even though this sequence is shorter, the reaction yielded the desired symmetric acetylene in only 47 %, setting the method in the same range of yields as before.

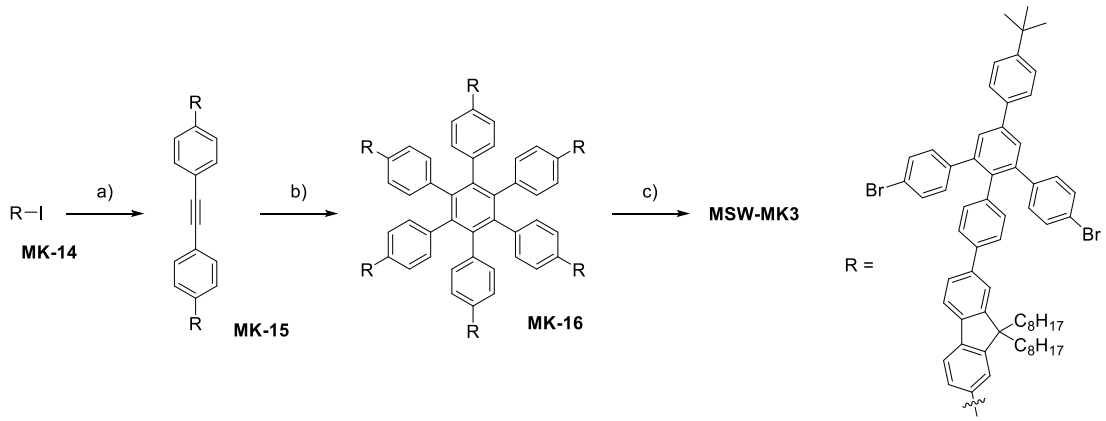

Scheme 37: a) **38**, $Pd(PPh_3)_4$, Cs_2CO_3, PhMe/H_2O, 50 °C, 4 d, 47 %; b) $Co_2(CO)_8$, PhMe, reflux, 22 h, 64 %; c) $Ni(COD)_2$, bipy, THF/COD, 120 °C (mw), 12 min, traces.

For the trimerization step, the yield approximately doubled from 31 % for the precursor of **MSW-MK2** to 64 %. *Kersten* stated that the increased space around the reactive center during the reaction benefited the successful trimerization for steric reasons. Other than *Sterzenbach*, *Kersten* did not

observe the formation of higher molecular species within the synthesis of **MSW-MK3**. Surprisingly, **MSW-MK3** was so poorly soluble, that he had massive problems with purifying and isolating the compound. As a consequence, the compound was not characterizable *via* NMR spectroscopy. In the end, it was necessary to isolate traces from the crude cyclization product *via Soxhlet* extraction, barely enough to prove the successful formation *via* MALDI mass spectrometry. An additional surprise was that it was possible to prove the structure of **MSW-MK3** *via* STM. Even though the compound was never designed for that purpose, **MSW-MK3** formed self-assembled monolayers on HOPG despite its non-planar geometry.[105]

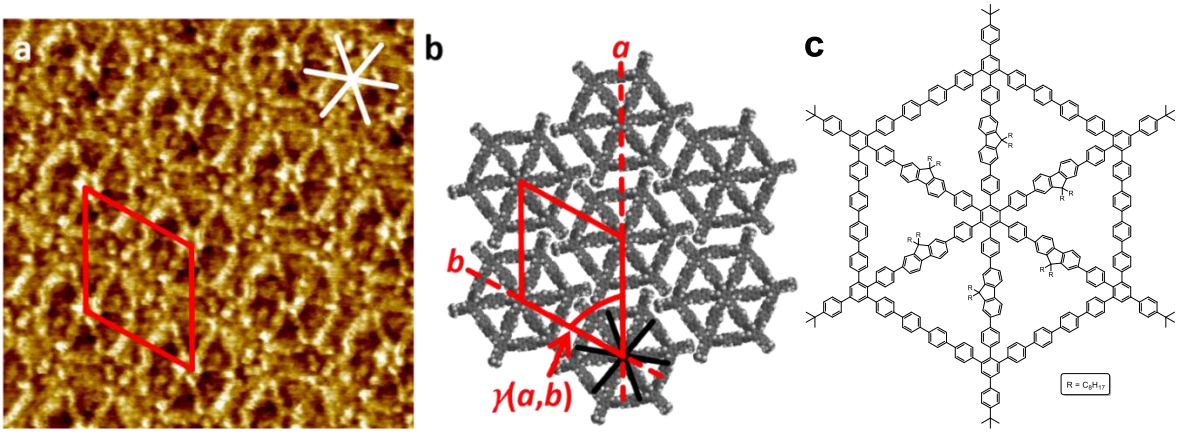

Figure 32: a) STM-recording of a self-assembled monolayer of **MSW-MK3** at the solid/liquid border of HOPG, $c = 3 \cdot 10^{-6}$ M in PHO, tempered at 80 °C for 20 s, 17 x 17 nm^2, V_s = -2.0 V, I_t = 35 pA; b) supramolecular model of a monolayer of **MSW-MK3** on HOPG, a = (5.3 ± 0.2) nm, b = (4.9 ± 0.2) nm, $\gamma(a, b)$ = (59 ± 2)°, all octyl chains pointing upwards into the liquid phase are cut from the depiction for better visibility; c) molecular structure of **MSW-MK3**.[105]

4 Aim of this Work

This work is intended to further investigate fluorene as a spoke-unit for Molecular Spoked Wheels. A general strategy for their incorporation was already proposed by *Kersten* within the limits of his work.[105] He managed to synthesize an 18 Ph-MSW with octyl-substituted fluorene spoke-units without a hitch and enlarged the structure into a 30 Ph-MSW afterwards. Regretfully, the latter structure suffered from poor solubility because the molecules' rims were only decorated with *tert*-butyl groups and the octyl groups seemed to not solubilize the structure sufficiently. To overcome this, the first structures of interest in this work are the respective hexadecyl-substituted 18 Ph-MSW and 30 Ph-MSW.

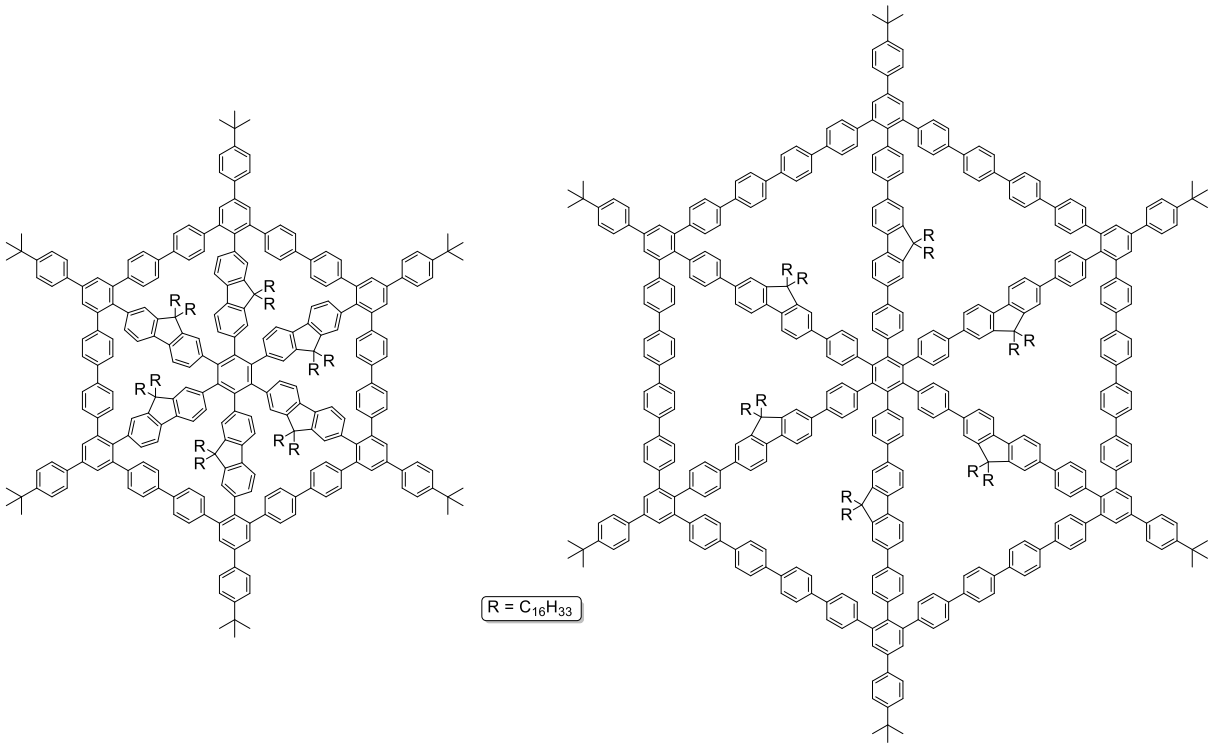

Figure 33: 18 Ph-MSW and 30 Ph-MSW with hexadecyl-substituted fluorene spoke-units as target structures for this work based on the molecules synthesized by *Kersten*.

The described 30 Ph-MSW is interesting for at least two reasons: First, it is of interest if the elongation of the incorporated alkyl chains is sufficient to make the molecule soluble enough to purify it *via* recGPC in order to record a full set of analytical data. Second, the alkyl chains might contribute to a lowered melting point of the structure, possibly even introducing liquid crystalline properties as first observed by *Idelson* for her dendron-functionalized 18 Ph-MSW.[96]

Since an enlargement of that 18 Ph-MSW was not possible for *Sterzenbach* due to aggregation of its precursors, a 30 Ph-MSW with the same rim decoration is of interest as well.[108]

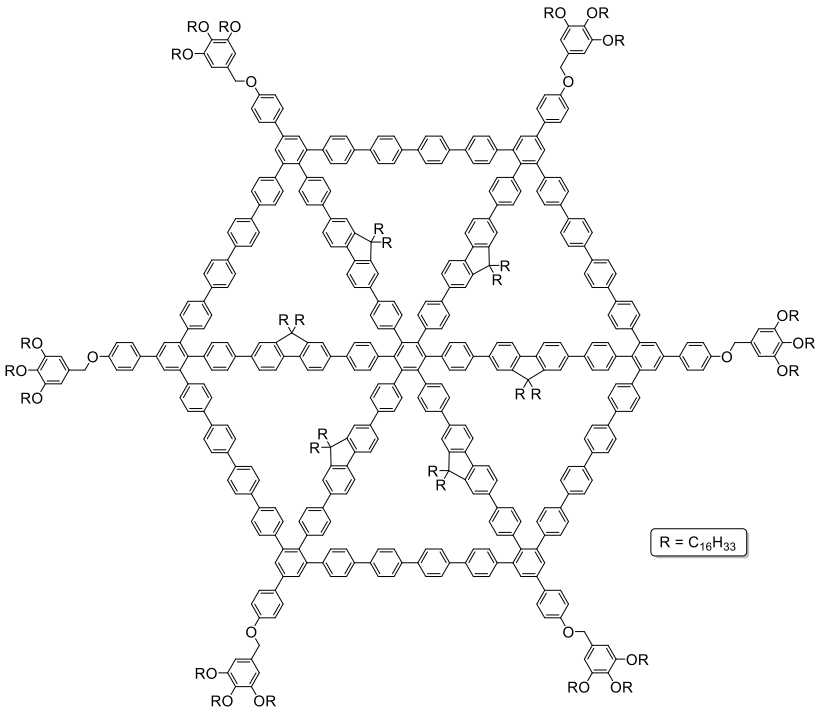

Figure 34: Fluorene-based 30 Ph-MSW decorated with dendron.

The introduction of more alkyl chains might once again influence the molecule's melting point and for sure drastically increase its solubility. Additionally, if any STM experiments with fluorene-based MSWs with hexadecyl chains are possible, this target structure has good chances to form ordered repetitive patterns on HOPG due to the packing-driving dendron groups.

If the synthesis of both 18 Ph-MSWs and 30 Ph-MSWs is successful, this might open the door to combine both structures and synthesize the first molecular cobweb (MCW).

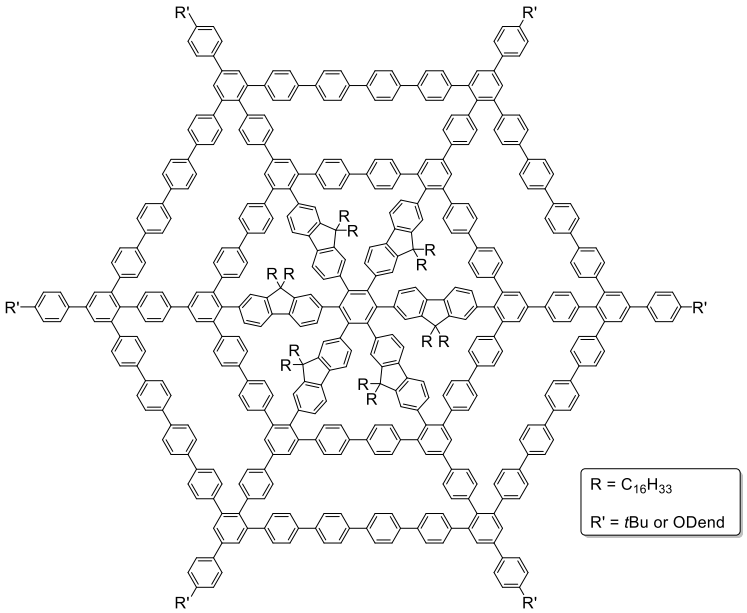

Figure 35: Concept for a molecular cobweb (MCW) with hexadecyl-substituted fluorene spokes. The rim functionalization can be realized with either *tert*-butyl or dendron groups.

Sterzenbach previously attempted to synthesize a similar structure within the limits of his PhD studies but this was unsuccessful due to formation of only higher-molecular species.[108] The synthesis of MCWs is poorly elucidated as the only known example was attempted by *Sterzenbach*. Access to this structure requires an elaborate route as especially the final step appears to be very challenging. Nevertheless, the double circle structure might lead to extremely rigid structures. The synthetic difficulty here is that both rims are designated to be closed in one reaction, which means that a twelve-fold *Yamamoto* coupling needs to be done. The chance of incomplete closure is overshadowed by the not yet disproven possibility of reactions between the inner- and the outer rim. The latter can be extremely dire because the incorporation of such defects is in theory possible up to the point of ten successful couplings.

5 Results and discussion

5.1 Fluorene-based Molecular Spoked Wheels

5.1.1 A hexadecyl-functionalized fluorene-based Molecular Spoked Wheel

Within his PhD studies, *Kersten* managed to successfully synthesize the first fluorene-based MSW containing octyl chains as aggregation-inhibiting spoke functionalization. When he enlarged that structure to a 30 Ph-MSW, it was barely soluble and he faced massive problems when isolating the final compound.[105] The most reasonable explanation for that problem is that the chain length was insufficient to keep **MSW-MK3** in solution. Hence, the aim of the first synthetic route of this work is the synthesis of a fluorene-based MSW with longer alkyl chains. Similar to *Kersten*, first, an 18 Ph-MSW was synthesized as a test system. The alkyl chains of choice for that project were hexadecyl chains, which are twice as long and therefore feature high potential to implement the desired solubility.
The first synthetic steps were done similar to the strategy of *Kersten* by brominating commercially available fluorene catalyzed by iron(III) chloride.[105]

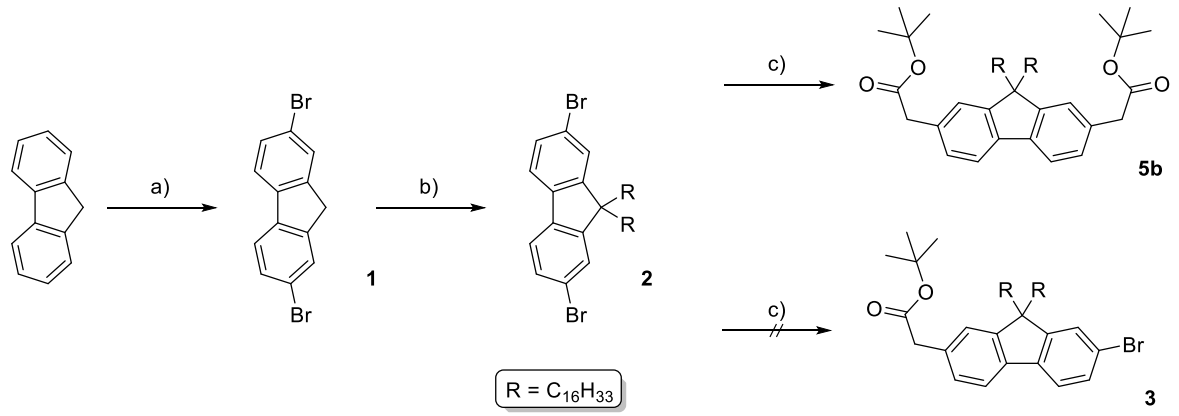

Scheme 38: a) $FeCl_3$, Br_2, $CHCl_3$, 0° C→rt, 2 h, 58 %; b) KOH, $C_{16}H_{33}Br$, KI, Bu_4NBr, acetone, H_2O, 80 °C, 48 h; c) *tert*-butyl bromoacetate, Zn, *XPhos*, $Pd_2(dba)_3$, THF, 90 °C, 48 h, 0 %.

Even though the simple elongation of the alkyl chains appears to be a reproduction of *Kersten*'s results, major differences were observed already at the second synthetic stage. In this reaction, the high acidity of the fluorene's 9-position is exploited to generate a mesomerically stabilized anionic carbon nucleophile that can react with alkyl bromides in an S_N2 reaction. Instead of using the more reactive alkyl iodide in the first place, the respective bromide was used since it is less viscous and hence easier to handle. To exploit the iodide's higher reactivity anyways, to this and all other alkylations of that type, substoichiometric amounts of potassium iodide were added. This way, the alkyl bromide can be

re-functionalized *in situ* to generate a more reactive compound. Since iodide is cleaved off in a successful alkylation anyway, only catalytic amounts of potassium iodide are needed.

While *Kersten* optimized his alkylation in the work up *via* distillation of the crude product removing large parts of the overstoichiometrically employed octyl bromide, this strategy cannot be applied to the given reaction. Hexadecyl bromide can only be evaporated at 190 °C at 1 mbar making a distillation entirely inapplicable. Instead, a very exhausting chromatographic purification was performed. The incorporated alkyl bromide is highly unpolar but the same is true for **2** as it does not comprise a single polar atom. For that reason, the required chromatography needs to be performed with especially long columns since both compounds barely separate even in pure cyclohexane. At this point it is important to mention, that recrystallization from now on was no option for purification in any of the following reactions due to the immense solubility of all alkylated compounds and the oily or waxy behavior of all early stages.

The following statistical *Hartwig* α-arylation[120] was attempted even though *Kersten* did not achieve any successes here for his substrates. The required zinc organyl is generated *in situ* from commercially available ethyl bromoacetate and zinc powder. The latter was freshly activated through stirring in aq. HCl, filtered off and dried overnight. Anyway, **3** was not accessible in the contemplated statistical reaction as only the formation of undesired, twice reacted **5b** was observed. Hence, a one-sided bromine-TMS exchange was performed.

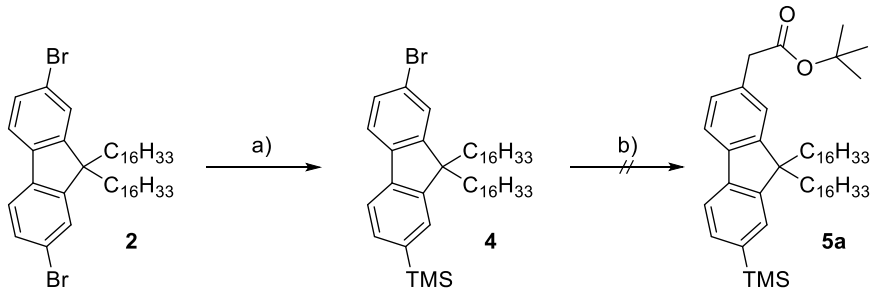

Scheme 39: a) *n*BuLi, TMSCl, THF, -78 °C → rt, 4 h; b) *tert*-butyl bromoacetate, Zn, *XPhos*, $Pd_2(dba)_3$, THF, 90 °C, 48 h, 0 %.

Sadly, it was not possible to separate **4** from unreacted **2** because the introduction of TMS did not influence the polarity of the compound. Since ethyl bromoacetate was used in excess this time, all remains of **2** should be converted into **5b** while **4** can now only be converted into **5a** as it cannot undergo a two-fold coupling due to the TMS-protection. Both resulting compounds should differ enough in polarity to separate them easily. Unfortunately, only the side reaction forming **5b** was observed while **4** was only recovered. This again stands in contrast to *Kersten*'s results as he managed to obtain the monosubstituted compound from this reaction. Additionally, when reproducing the α-arylation, it was found, that the reaction also works without an additional activation of zinc as long as the metal is added in an excess. Since that was also the case for the first approaches, the activation was superfluous and skipped for subsequent applications.

In order to exclude bromine as possible reason for the unsuccessful coupling, the same synthetic sequence was attempted with the respective diiodofluorenes as it was hoped that the C-I bond was more prone towards palladium chemistry.

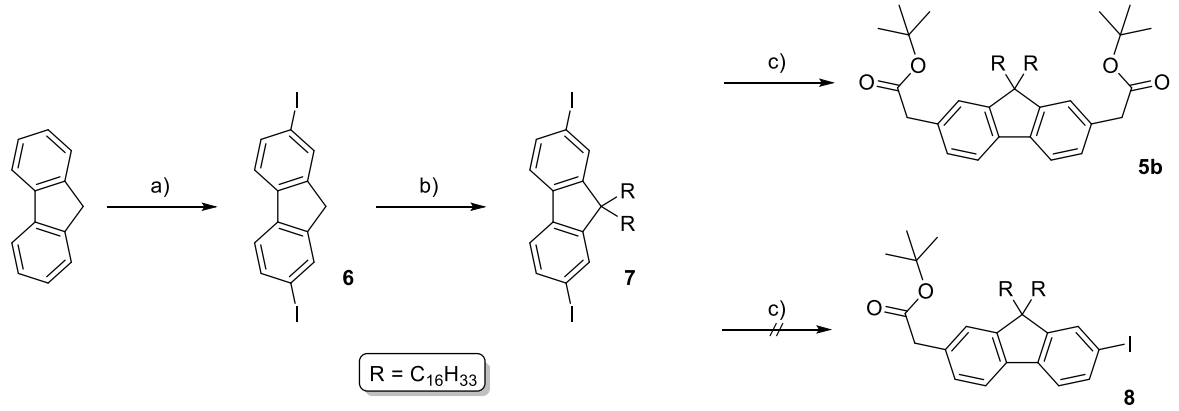

Scheme 40: a) I_2, HIO_3, AcOH, CCl_4, H_2SO_4, 80 °C, 22 h, 50 %; b) KOH, $C_{16}H_{33}Br$, KI, Bu_4NBr, acetone, H_2O, 80 °C, 48 h, 77 %; c) *tert*-butyl bromoacetate, Zn, *XPhos*, $Pd_2(dba)_3$, THF, 90 °C, 48 h, 0 %.

This synthetic strategy brought the same problems as its bromine counterpart. Since iodine is even less polar than bromine, the replacement did not benefit the purification step isolating **7**. A statistical reaction of **7** also failed and again only byproduct **5b** was received. The respective TMS-I exchange yielded a product-substrate mixture as well, that was reacted afterwards in a *Hartwig α*-arylation reaction once again yielding only **5b** next to recovered substrate.

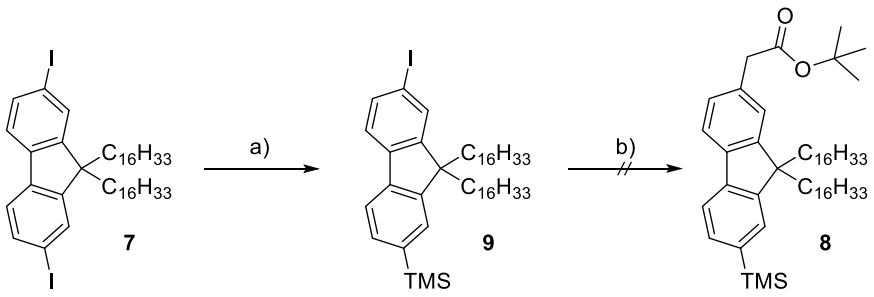

Scheme 41: a) *n*BuLi, TMSCl, THF, -78 °C → rt, overnight; b) *tert*-butyl bromoacetate, Zn, *XPhos*, $Pd_2(dba)_3$, THF, 90 °C, 48 h, 0 %.

At this point, the route needed to be re-conceptualized. Instead of symmetric 2,7-dihalogenated fluorenes, an asymmetric fluorene was considered. The idea behind this was, that the *α*-arylation should no longer bring any problems in terms of over-functionalization, as there is only one possible reaction side in the modified substrate. Due to the electronic properties of fluorene, it should be easy to introduce the iodine afterwards.[121] Since this sequence was performed in early stages of this work, the conversion of 2-iodofluorene was not considered yet. However, the applicability of that compound will be discussed within the synthesis of **MSW-C** (see chapter 5.1.3). For now, the new fluorene derivate of choice was 2-bromofluorene. The change of the substrate also cut two steps from *Kersten*'s

route, on the one hand the halogenation of fluorene and on the other hand the protection of the second binding site. This way, this modification potentially saves time, resources and boosts the overall yield.

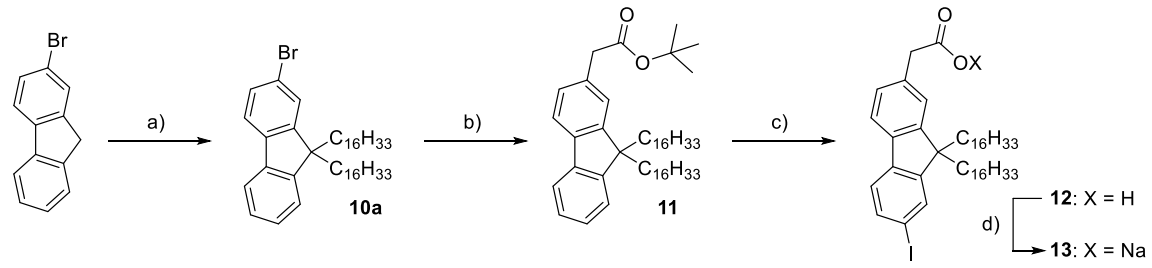

Scheme 42: a) KOH, $C_{16}H_{33}Br$, KI, Bu_4NBr, acetone, H_2O, 80 °C, 48 h, 65 %; b) *tert*-butyl bromoacetate, Zn, *XPhos*, $Pd_2(dba)_3$, THF, 90 °C, 48 h, 77 %; c) I_2, HIO_3, AcOH, CCl_4, H_2SO_4, 80 C, 4.5 h, 88 %; d) NaO*t*Bu, *t*BuOH, 3 h, 30 °C, 100 %.

Once again, the alkylation of 2-bromofluorene brought the same problems already discussed for the similar substrates. After tedious removal of surplus 1-bromohexadecane, the *Hartwig α*-arylation was attempted with **10a**. Surprisingly, already the first attempt yielded **11**, but in poor yields. Since in the literature, *Hartwig et al*. present the screening of different ligands,[122] some experiments with other catalyst systems were investigated.

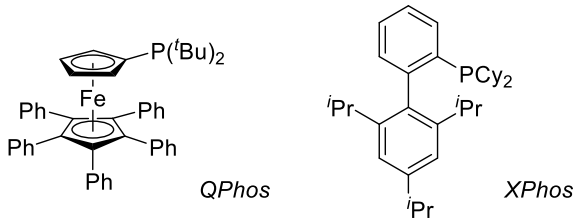

Figure 36: *QPhos* (left) and *XPhos* (right) as examples for phosphine ligands tested for the *Hartwig α*-arylation.[122]

QPhos was tested as ligand for the conversion of **2** and **7**, but this system also failed to yield the desired respective products. The excellent results of *S. Rickert* with *XPhos*[123] made the use of that ligand promising for two reasons. First, *XPhos* is a lot cheaper than P(*t*Bu)$_3$ and *QPhos*. Second, it is air-stable and therefore not required to be stored in a glove box. Through this, its handling is far easier and it can be added to the reaction mixture already before the step of purging the reaction mixture with argon. Additionally, the work up of the reaction was drastically facilitated. Before, it happened to be a problem to separate the phases following the aqueous work up, since only one phase was observable which was visibly clouded by finely distributed metal particles of palladium and zinc. By filtering the reaction solution through a plug of $MgSO_4$ twice, the plug became denser after the first filtration and minor parts of the metal compounds passed through. After re-filtration, only the clear crude product solution passed the plug. This technique was applied to the synthesis of all metal-catalyzed couplings involved in the construction of spoke fragments in the following. The optimization of conditions boosted the yield of this step to a maximum of 77 %.

As already described, after the successful coupling, an electrophilic iodination was performed. While at first, very harsh and unfavorable conditions were applied containing concentrated sulfuric acid and tetrachlorocarbon,[121] the conditions were later switched to iodine monochloride in DCM.[105] Nonetheless, both applied conditions did not just introduce the iodine substituent but additionally cleaved the *tert*-butyl ester in the same reaction step. This indirectly solved another problem: the exchange of hydrogen for iodine barely affects the compound's polarity. For that reason, the compound can hardly be purified *via* column chromatography. The combination with the ester cleavage in the same reaction step facilitated the purification drastically due to the impactful alteration in polarity.

Through the addition of sodium methanolate in methanol the acidic proton is exchanged for sodium generating a sodium acetate. These conditions have been used for the syntheses of MSWs for years without any inconveniences. Surprisingly, for this substrate it was not possible to quantitatively remove methanol under reduced pressure, which led to problems for the following reaction step. Since in the past, no solubility-promoting groups were involved in the construction of the spoke, that problem might result from an interaction of the alkyl groups with methanol and hence, was never observed. The interesting thing here is, that this problem was never observed by *Kersten* and his similar molecules.[105] Still, this observation is another major difference resulting from the apparently simple elongation of the alkyl chains. Interestingly, this problem was fully eradicated by switching sodium methanolate for sodium *tert*-butoxide and implementing the corresponding alcohol as solvent. Even though *tert*-butanol evaporates at more elevated temperatures, it was unmitigatedly removed yielding **13** quantitatively.

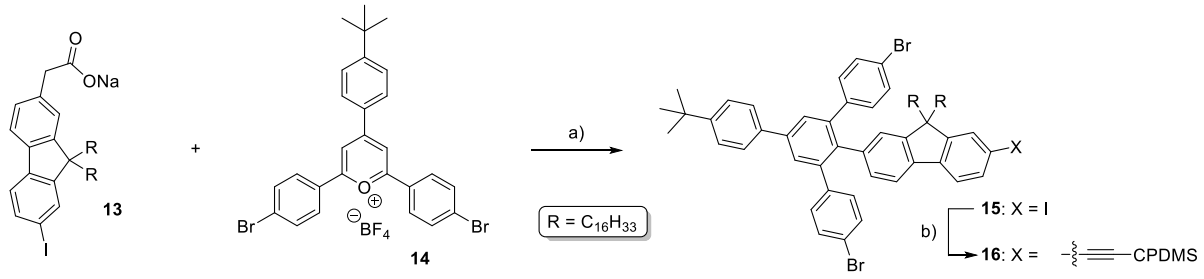

Scheme 43: a) Bz_2O, 150 °C, 4 h, 8 %; b) CPDMS-acetylene, $PdCl_2(PPh_3)_2$, PPh_3, CuI, THF, piperidine, rt, 21 h, 23 %.

13 is one of two compounds that are employed in the subsequent *Zimmermann-Fischer* condensation. The second compound is a pyrylium salt, in this case **14**, that was synthesized by *Kersten* in such high quantity[105] that besides this work two other students' works benefited from his diligence. With the *Zimmermann-Fischer* condensation, a high-functionalized arene is accessible in only one reaction step, while usually reactions leading to such complex molecules take several steps that suffer from incomplete conversions as well as selectivity-problems. For that reason, it is advantageous to build such compounds in one-pot reactions instead of troublesome cross coupling sequences. The downside

of this reaction is that it ordinarily gives moderate to low yields as well as sometimes inseparable byproducts. For the presented example, only 8 % of **15** were isolated while a mixed fraction was also collected containing mainly **15**. Instead of being disposed, that mixed fraction was used in a *Sonogashira* coupling essaying to separate **15** as CPDMS-acetylene **16**, because that compound is required for the proceeding route anyways. Not only was pure **16** received here, but valuable substance was saved through conversion this way saving time as well as resources.

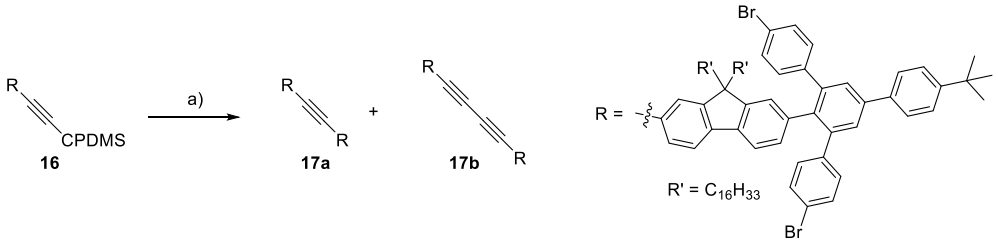

Scheme 44: a) $Pd(PPh_3)_4$, PPh_3, CuI, TBAF, THF, piperidine, rt, 22 h, 26 %.

16 then became subject of another *Sonogashira* coupling. In order to be a suitable substrate, **16** was deprotected *in situ* and converted into **17a**. This method was adapted from the investigations of *zur Horst* within her PhD studies.[106] The idea behind this one-pot reaction is to provide all required compounds for the *Sonogashira* coupling and slowly add a solution of TBAF afterwards. This way, a freshly deprotected acetylene can immediately be coupled with an aryl iodide. Ideally, this fully suppresses the homo-coupling byproduct resulting from a *Glaser* coupling that can occur under the same conditions.

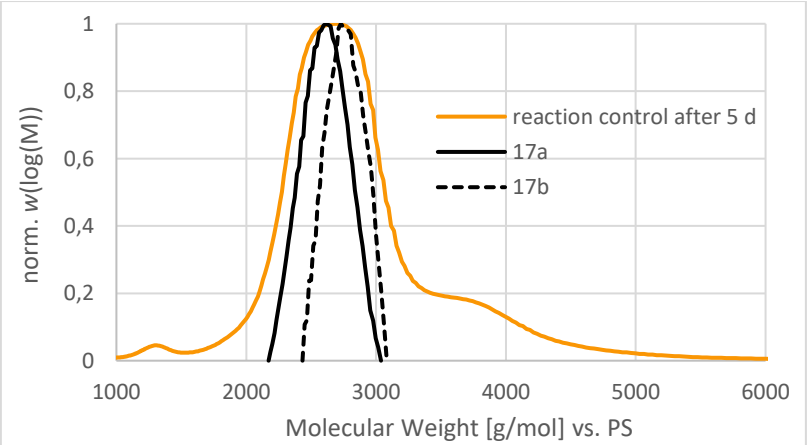

Figure 37: Molar mass distribution (THF, *vs* PS) as reaction control of the synthesis of **17a** *via* analytical GPC after five days with **17a** and **17b** as reference.

Reaction control *via* analytical GPC (THF, *vs* PS) showed the formation of a main signal within the correct molecular weight region. Disturbingly, that signal was wider than expected seemingly not being caused by just one compound. Unfortunately, the widening could be assigned to the *Glaser* coupling product found *via* MALDI-spectrometry, which was a bigger problem than first expected. For the synthesis of asymmetric acetylenes, the byproduct is no problem because due to the complementary

polarity of the end groups, the byproduct can easily be separated *via* column chromatography (compare chapter 2.5.1). For symmetric acetylenes as presented here, the target molecule and the respective byproduct are essentially identical in polarity, which makes a separation *via* polarity impossible.

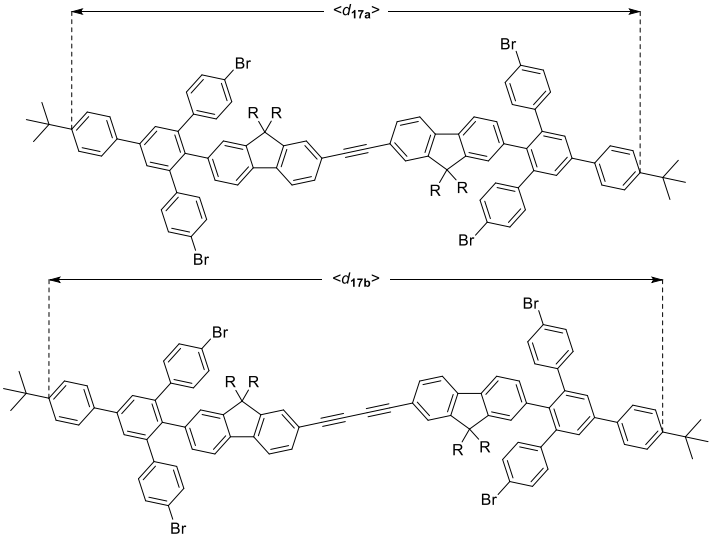

Figure 38: Molecular geometries and average end-to-end distances <d_{17a}> and <d_{17b}> of the *Sonogashira* product and the *Glaser* byproduct derived from MD simulations by *J. Kohn*.

Normally, compounds of that dimension can be isolated *via* size-exclusion chromatography or more specifically recycling gel permeation chromatography. If two compounds are that similar in size, recGPC is extremely difficult since their size varies in just one acetylene group. For the presented example, the difference in molecular weight only is around 1 %. The average lengths of both products were calculated in MD simulations to be <d_{17a}> = 32.8 Å and <d_{17b}> = 35.1 Å, uncovering that **17b** is only 6 % longer. The calculations were performed by *J. Kohn*, more details on the applied methods can be found in chapter 9.3 that deals with computational methods applied for this work.

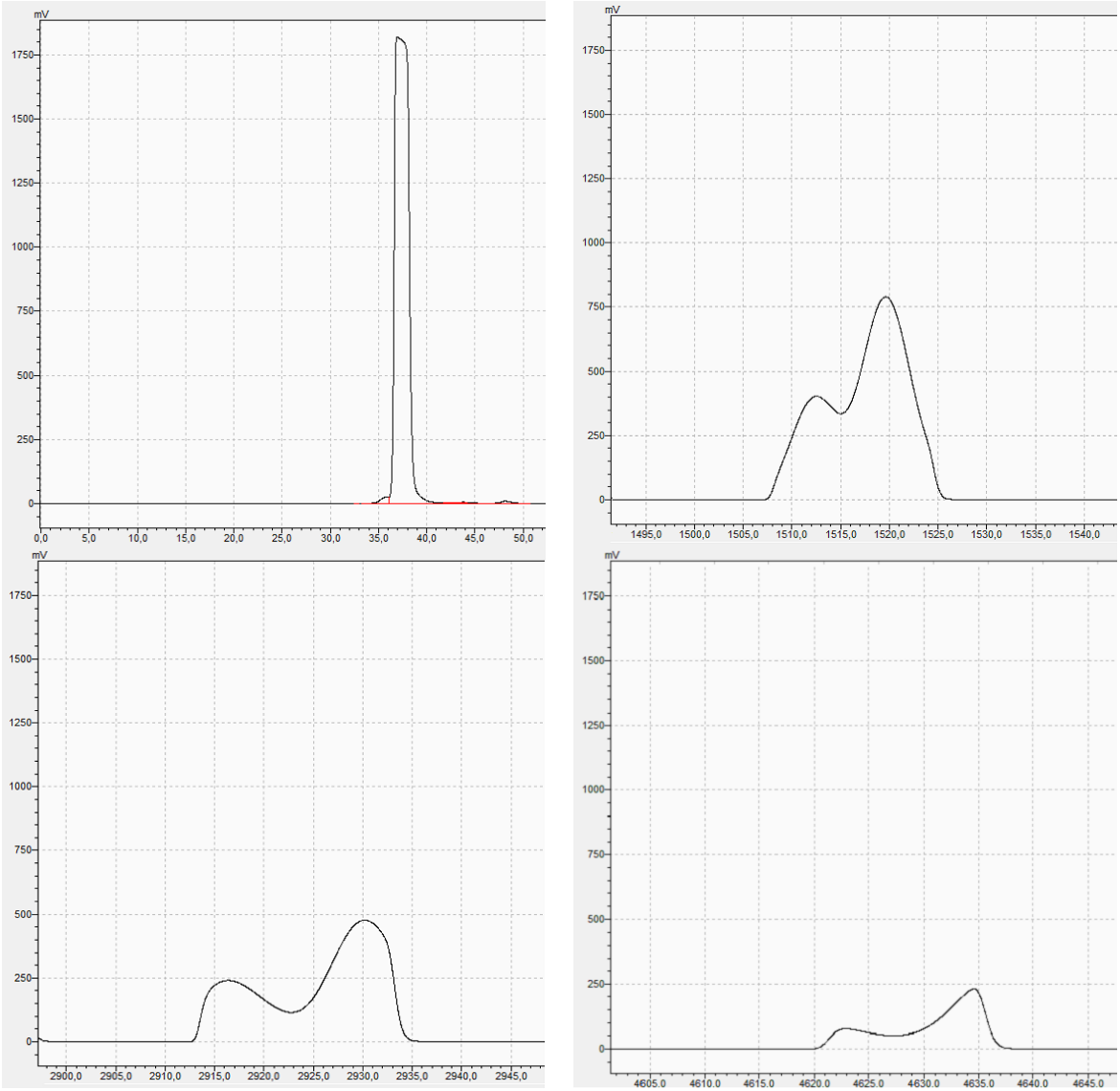

Figure 39: Elugram of recGPC of the separation of **17a** and **17b** showing the mixture after the first cycle (top, left), after one day (top, right), after two days (bottom, left) and at the moment of final separation (bottom, right). The smaller left peak corresponds to **17b** while the higher one was identified as **17a**.

Figure 39 displays the separation of **17a** and **17b**. It was against all odds possible to separate both compounds over very long recycling times, as the spectra in Figure 40 confirm. This was an extraordinary success because as already explained, the likeliness of separating nearly identical compounds that way was vanishingly low.

Figure 39 shows, the signals loose intensity over time while broadening. This has two reasons: first, through recyclization the mixture is distributed more over the columns with increasing time, which in the end also leads to the anticipated separation. Second, every day the outer edges were trimmed to collect fractions of both compounds that were far apart enough from each other to be sufficiently pure. The lower the minimum between both signals gets, the cleaner the collected fractions will be.

This way, after the full elution period the minimum was below a value of 50 mV, which about two days earlier was around 350 mV.

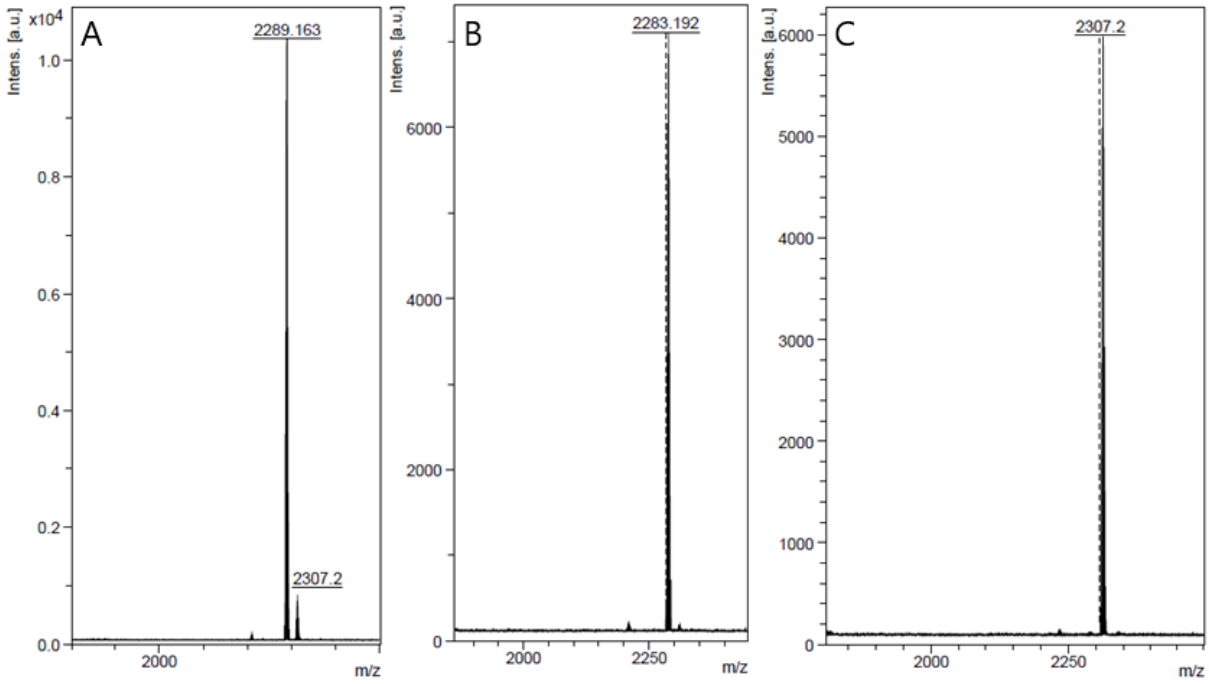

Figure 40: MALDI mass spectra of **17a** and **17b**; displayed for the mixture of both compounds prior to the purification (A), isolated **17a** (B) and isolated **17b**, proving the success of separation *via* recGPC.

The thorough separation of both compounds might appear picky and superabundant, but in fact is of utmost importance for the next reaction step. If both compounds are not separated exhaustively, one molecule of bisacetylene can consume up to two equivalents of acetylene creating a mixed arene during the trimerization that is useless for all further investigations.

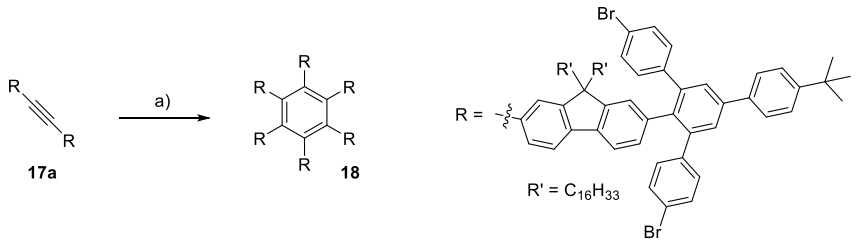

Scheme 45: a) $Co_2(CO)_8$, PhMe, 120 °C, 15 h, traces.

The trimerization was carried out under the conditions developed by *Idelson et al.* that were applied to the syntheses of multiple MSWs before.[96] The progress of reaction was checked *via* analytical GPC multiple times since the formation of product only proceeded slowly.

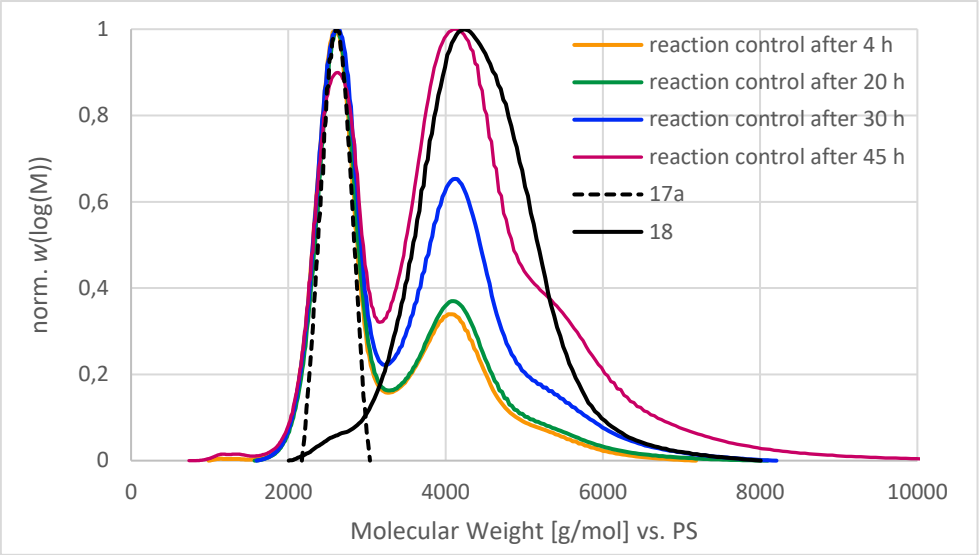

Figure 41: Molar mass distribution (THF, *vs* PS) as reaction control of the synthesis of **18** *via* analytical GPC after different periods of time with a fraction containing **18** as a reference.

Even though more catalyst was added twice, the conversion stayed low and the reaction was terminated after 45 hours. Devastatingly, after all the efforts put into the isolation of **17a**, the desired trimer was only isolated in traces. Its concentration was so low that it was only proven *via* MALDI spectrometry within a mixed fraction. It was not possible to perform the final reaction step with the collected amount of **18**. A possible explanation for the poor conversion during the trimerization might be the bulkiness of the hexadecyl chains. During the trimerization, the reactive center becomes very crowded and the chain groups most likely repulse each other. This might be the major difference from *Kersten*'s results and explains why his trimer was far better accessible isolated in moderate yields.[105]
As a consequence, the synthetic efforts towards **MSW-A** were discontinued.
The experimental efforts towards **MSW-A** were also published in 2024.[97]

5.1.2 A less crowded fluorene-based Molecular spoked wheel

After identifying the crowdedness around the center as a main problem during the synthesis of **MSW-A**, the follow-up idea was to decrowd the center while keeping the alkyl chain's length constant. This was meant to be realized by incorporating the chains as alkoxy phenylenes still in 9-position of the fluorene.[124]
To do so, the route was started from commercially available fluorenone.

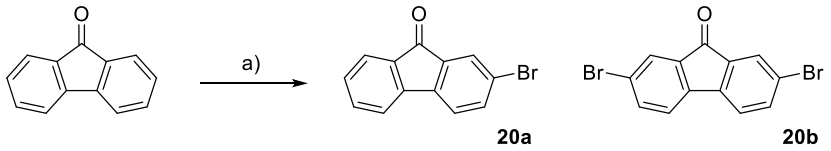

Scheme 46: a) Br_2, $FeCl_3$, $CHCl_3$, rt, overnight, 22 % (**20a**).

This time, the desired product was the mono-brominated compound **20a** while **20b** was only yielded in traces. A reasonable explanation might be the impact of the electron-withdrawing carbonyl group that does not interfere with the needed regioselectivity of the bromination but acts deactivating towards substitution reactions in general. The next type of reaction does not seem very straighforward at first. Two phenol equivalents are introduced here *via* electrophilic aromatic substitution.[125]

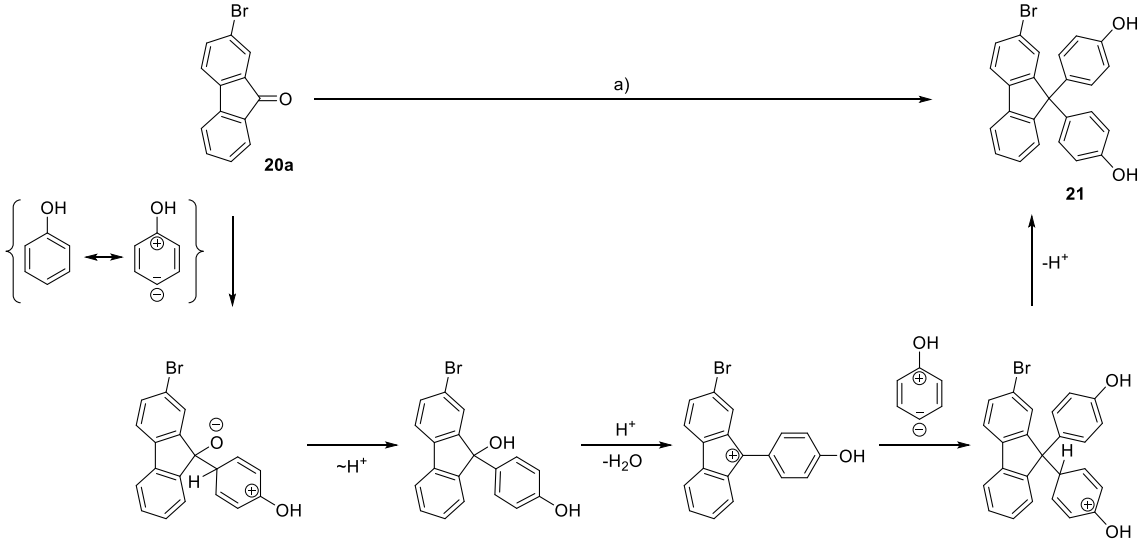

Scheme 47: Proposed mechanism for the formation of **21** *via* S_EAr; a) MsOH, PhOH, 50 °C, 46 h, 61 %.

Through its acceptor-substituted 9-position, the carbonyl carbon atom of **20a** becomes highly electrophilic and can therefore be attacked by an equivalent of phenol. Due to the donating character of its hydroxy group, phenol features an increased electron density in *ortho*- and *para*-position, while the *para*-position here turned out to be more reactive for steric reasons. After the first substitution, water is cleaved off generating a mesomerically stabilized carbocation that undergoes another substitution yielding **21**.[15]

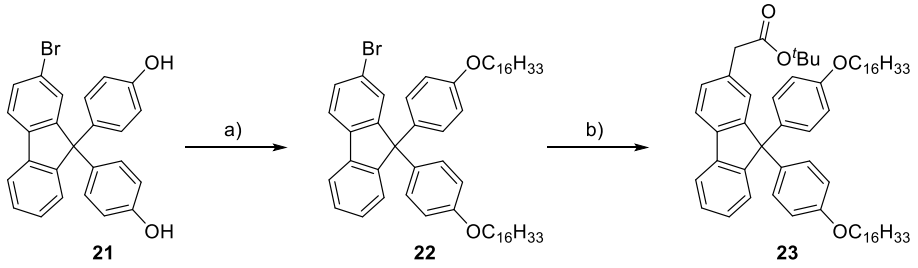

Scheme 48: a) KOH, $C_{16}H_{33}Br$, KI, Bu_4NBr, acetone, H_2O, 80 °C, 50 h, 89 %; b) *tert*-butyl bromoacetate, Zn, *XPhos*, $Pd_2(dba)_3$, THF, 80 °C, 17 h, 78 %.

In contrast to the previous alkylations, the synthesis of **22** did not pose any problems. Especially the purification was very straightforward since the presence of ethers made the molecule slightly more polar and granted an easy separation from overstoichiometrically employed hexadecyl bromide. The *Hartwig* reaction was carried out under similar conditions as for the synthesis of **11** giving the product in 78 % yield.[120]

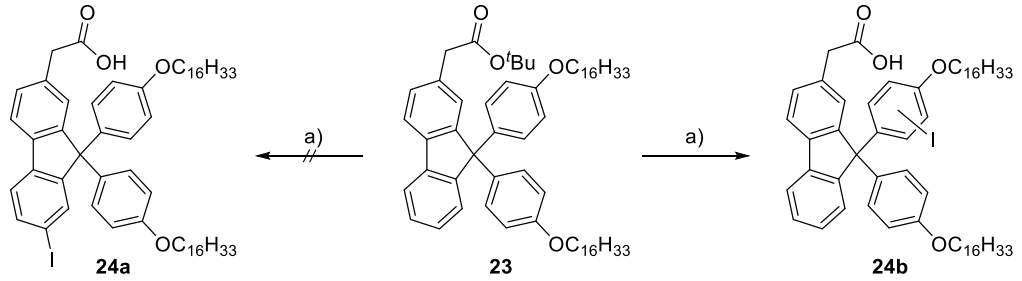

Scheme 49: a) I_2, HIO_3, AcOH, CCl_4, H_2SO_4, 80 C, 4.5 h, 50 %.

Something that should have been clear in the first place is the anticipated iodination of **23** will not yield the desired product. Instead of an iodination in 7-position of the fluorene unit, the *ortho*-positions of the alkoxy phenylene units are much stronger activated for substitution due to their neighboring electron-donating ether groups. Also proven synthetically, the conversion only yielded **24b**.

Since the desired spoke compound was not accessible through this route, a symmetric approach was reconsidered. The synthetic planning was oriented around the synthesis of **23** and executed by *Thorsten Taschler* up to **27** within the limits of the bachelor studies' module 6.1.1 in 2021 under my supervision.

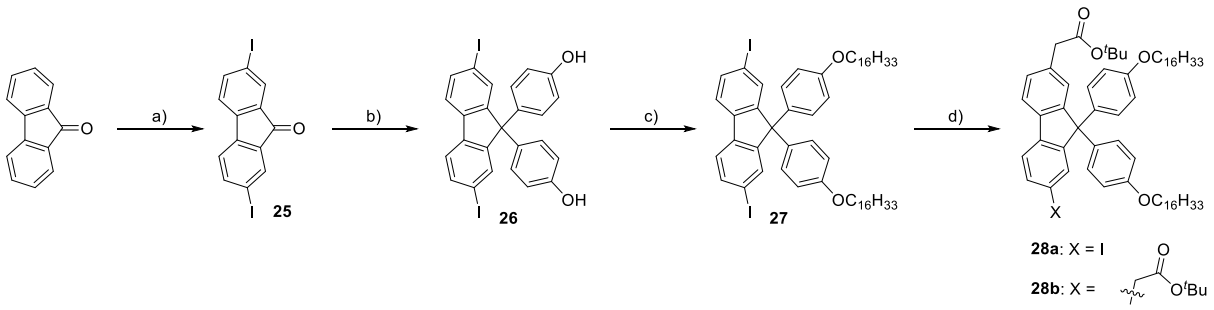

Scheme 50: a) I_2, HIO_3, AcOH, CCl_4, H_2SO_4, 80 C, overnight, 83 %; b) MsOH, PhOH, 50 °C, 6 h; c) KOH, $C_{16}H_{33}Br$, KI, Bu_4NBr, acetone, H_2O, 80 °C, 72 h, 91 % (two steps); d) *tert*-butyl bromoacetate, Zn, *XPhos*, $Pd_2(dba)_3$, THF, 90 °C, 48 h, 0 % (**28a**).

Even though it seems counter-intuitive to go back to this approach after the exclusive observation of bifunctionalization in all previous attempts, this time the substrate features two electron-rich arenes. It was hoped that after the reductive elimination palladium would move towards that high electron density instead of inserting into the second carbon-iodine bond.[124]

In contrast to the bromination (compare Scheme 46), the iodination only yielded bifunctionalized product. Both following steps worked in excellent yields. Even though the phenolation solidified during

stirring despite constant heating it was still possible to isolate **27** over two steps in 91 %.[124] Unfortunately, the *Hartwig* reaction[120] once more failed to deliver the anticipated product as only the formation of **28b** was observed carrying the synthetic route towards **MSW-B** to an early grave. Nevertheless, the general idea of alkoxy phenyl-substituted spokes will be reapproached during the synthesis of **MSW-E** in chapter 4.1.5 in a modified fashion.

5.1.3 The lateral expansion of a fluorene-based Molecular Spoked Wheel

After two frustrating setbacks the enlargement of **MSW-A** was attempted anyways. While *Kersten* was able to synthesize a MSW of identical size with octyl chains, his MSW was practically insoluble.[105] For that reason, the extension to hexadecyl chains should yield a MSW that can easily be purified and investigated and proved *via* more analytical methods than just MALDI mass spectrometry and STM.

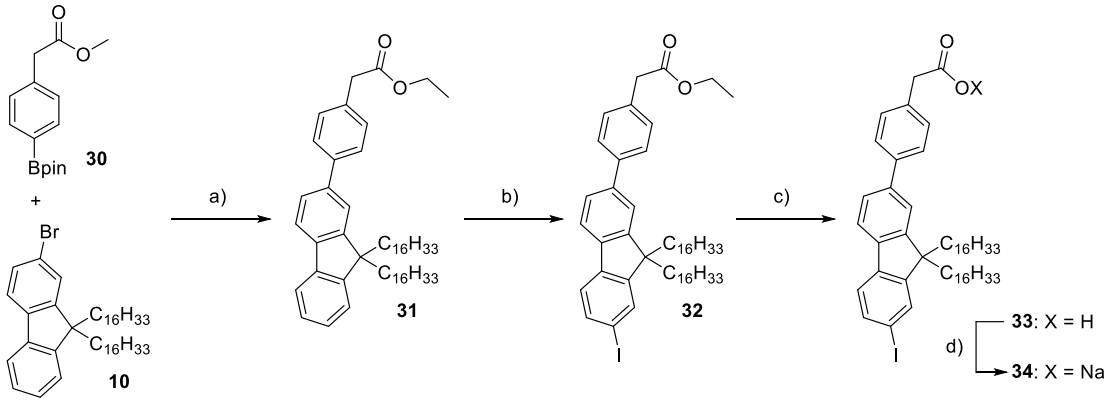

Scheme 51: a) K_2CO_3, $PdCl_2(PPh_3)_2$, PPh_3, PhMe, EtOH, 70 °C, 48 h, 75 %; b) ICl, DCM, rt, overnight, 98 %; c) $LiOH \cdot H_2O$, THF, H_2O, 60 °C, 19 h, 96 %; d) NaO*t*Bu, *t*BuOH, 3 h, 40 °C, 100 %.

For the enlargement of the spoke unit, the *Hartwig* α-arylation[120] was exchanged for a *Suzuki* coupling. Thus, ethyl bromoacetate was substituted for **30** as a boronic acid or its respective pinacol ester is required for that coupling. The reaction was performed in a solvent mixture consisting of toluene and ethanol that was used for the respective reaction by *Kersten* as well. As for his coupling, the use of ethanol came with a trans-esterification from the methyl to the ethyl aryl acetate. Since the ester is cleaved a few steps later anyways, this was not seen as a problem and did not turn out to become one.[105] Additionally, the reaction time seemed to have a strong influence on the yield, as doubling the reaction time from one to two days nearly doubled the yield from 40 % to 75 %.[126]
Other than before, the ethyl ester was not cleaved during the iodination requiring a further reaction step. Since the iodination was performed in 98 % yield and the subsequent ester cleavage gave the respective carboxylic acid in 96 % yield, the additional reaction step did not turn out to be a noteworthy

drawback. **34** was then synthesized by a simple deprotonation but based on the positive experiences during the synthesis of **13**, sodium *tert*-butoxide was used yielding **34** quantitatively.

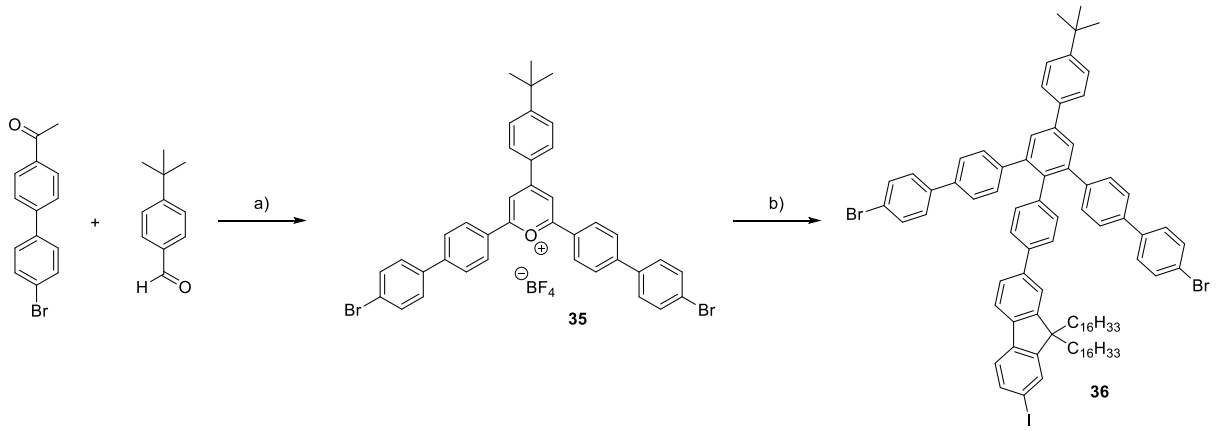

Scheme 52: a) $Et_2O{\cdot}BF_3$, DCE, 80 °C, 4 h, 36 %; b) Bz_2O, 150 °C, 4 h, 41 %.

As already explained, for a *Zimmermann-Fischer* condensation, a pyrylium salt and a sodium aryl acetate are required. This time, the pyrylium salt was not sourced from *Kersten*'s work but synthesized directly from the commercially available precursors 4'-(4-bromophenyl)acetophenone and 4-*tert*-butylbenzaldehyde.[108] The following condensation was performed in benzoic anhydride and yielded **36** in 41 % yield.

The subsequent step was performed adapting the strategy *Sterzenbach* developed for the synthesis of his enlarged symmetric acetylene[108] that was successfully adapted by *Kersten* for fluorene-based MSWs already.[105] The central unit **38** was first sourced from *Sterzenbach*'s leftover compounds and afterwards attempted to be reproduced.

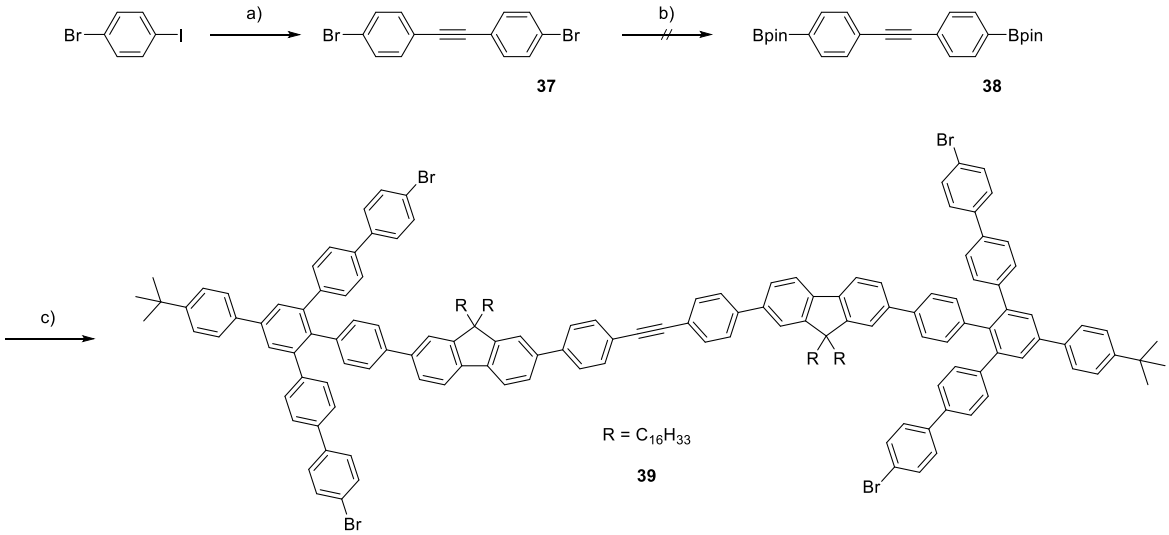

Scheme 53: a) $PdCl_2(PPh_3)_2$, PPh_3, CuI, THF, piperidine, rt, 21 h, 23 %; b) KOAc, $B_2(pin)_2$ $PdCl_2(dppf)$, DMF, 105 °C, overnight, 0 %; c) **36**, Cs_2CO_3, $Pd(PPh_3)_4$, PhMe, H_2O, 50 °C, 5 d, 32 %.

For the synthesis of its precursor **37**, again a similar coupling with *in situ* deprotection sequence was applied, that yielded the desired compound in a moderate yield.[127] Unfortunately, it was not possible to execute the subsequent *Miyaura* borylation successfully under the given conditions.[117] To preclude any flaws resulting from the synthesized **37** and to avoid a comparatively pricey reproduction, **37** was purchased and the conversion was tested again. After various attempts, **38** was also not accessible through the commercially available compound. Instead, **38** was purchased for a seemingly expensive price of around 100 euros per gram, but one gram is more than sufficient for screening purposes, as one test reaction consumed around 50 mg. Considering the resources consumed for the alternative two-step procedure as well as the required time, this price is more than reasonable in comparison.

Starting from **38**, the synthesis of **39** was investigated. The reaction requires highly elaborate conditions as **36** contains three halogen atoms, that may each be susceptible to *Suzuki* couplings. To exploit the higher reactivity of iodine over bromine, the reaction temperature can only be slightly elevated. While the *Sonogashira* reaction can be carried out at room temperature to fully suppress the reaction of aryl bromides, this did not work for similar substrates in *Suzuki* couplings in the past. Thus, the reaction temperature is limited to 50 °C while the reaction time is extended to five days to ensure a high conversion since these conditions performed best for *Sterzenbach*'s and *Kersten*'s investigations.[105,108]

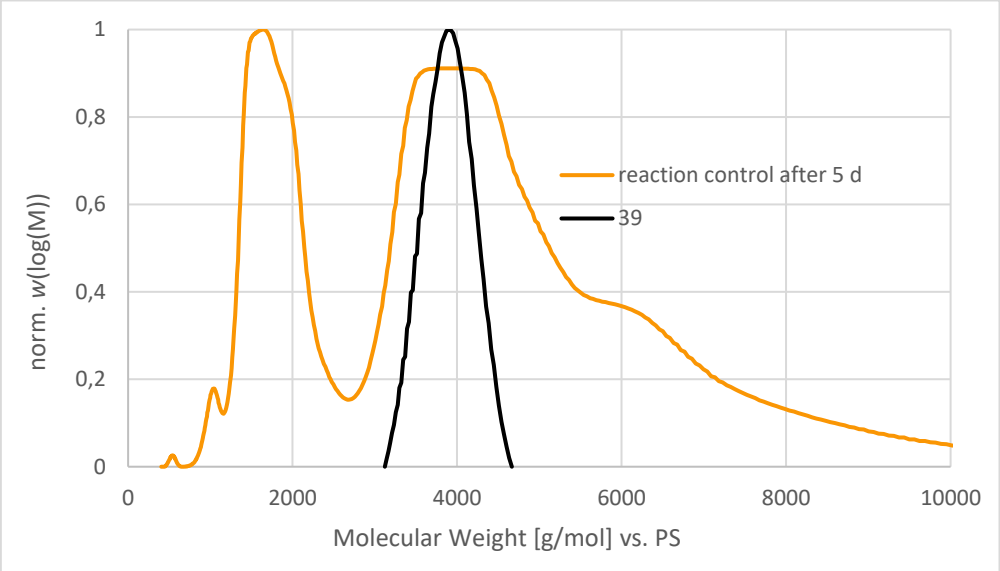

Figure 42: Molar mass distribution (THF, *vs* PS) as reaction control of the synthesis of **39** *via* analytical GPC after five days with the isolated compound as a reference.

Even though these conditions were carefully chosen, some of the substrate still seemed to have reacted at the wrong position, as recGPC revealed the formation of multiple additional species with some of them being of larger size than **39**. Since the structure of the byproducts was not reliably clarified, it is only possible to speculate over their composition. MALDI mass spectrometry nevertheless suggested the formation of higher-molecular species as signals were observed in the respective areas

of size. Anyways, **39** was isolated in 32 %, which was sufficient to continue the work for now, but nevertheless unpleasant considering that two-thirds of the synthesized compound was lost.

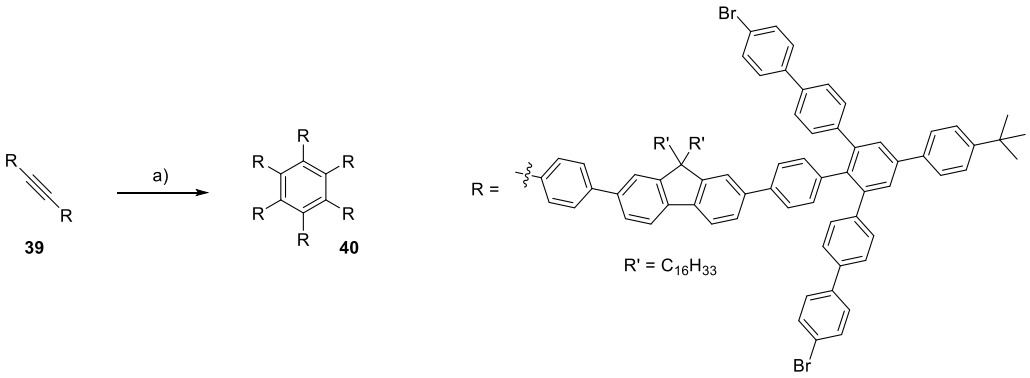

Scheme 54: a) $Co_2(CO)_8$, PhMe, 120 °C, 5 h, 56 %.

Compared to the trimerization step leading to **18** that barely yielded any product, the synthesis of **40** gave the desired product in a moderate yield of 56 %.[96] This drastic increase in yield undoubtedly supports the hypothesis of the overcrowded reactive center for the preparation of **17a**.

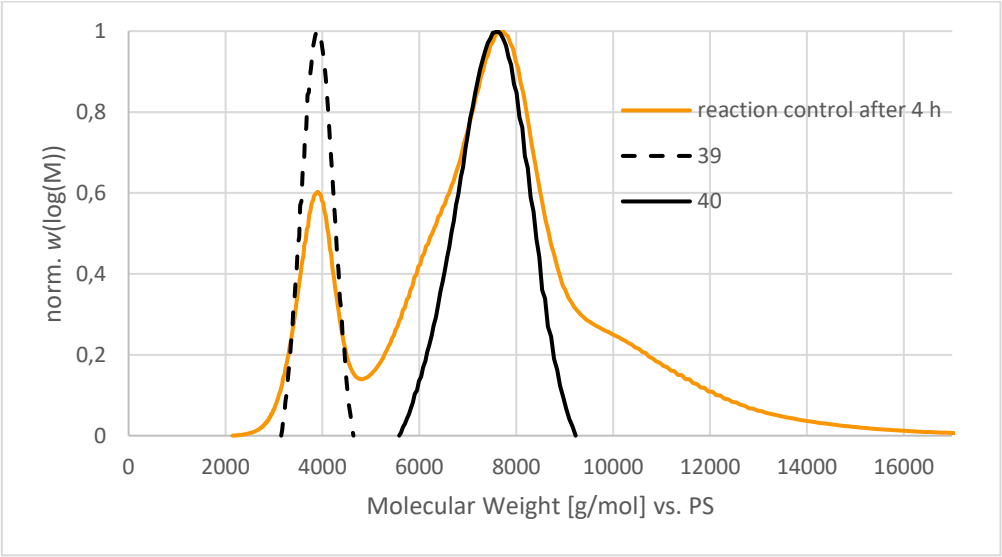

Figure 43: Molar mass distribution (THF, *vs* PS) as reaction control of the synthesis of **40** *via* analytical GPC with the substrate and the isolated compound as a reference.

The additional space also seemed to affect the reaction rate, as analytical GPC suggested **40** to be the main species within the mixture after only four hours. The final step of the synthetic route was performed successfully as well yielding the first MSW of this work.

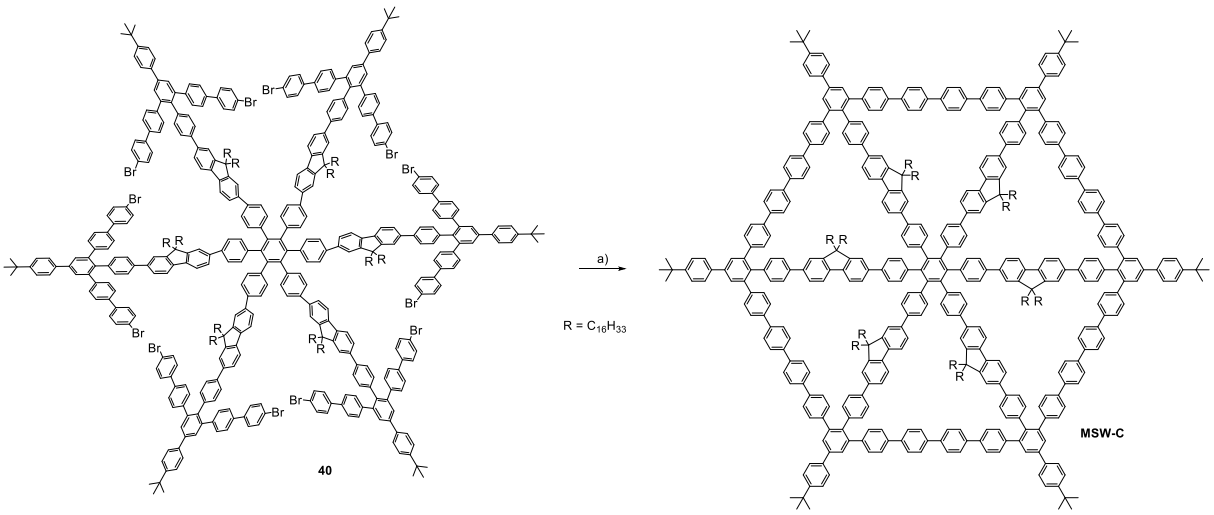

Scheme 55: a) $Ni(COD)_2$, bipy, THF, COD, 12 min, 300 W, 120 °C (mw), 43 %.

40 was cyclized in a microwave reactor under the exclusion of light and air. The applied harsh conditions proved to be successful in the past in many other works and appear to be necessary in order to perform the six-fold closure of that structure all in one reaction.[96]

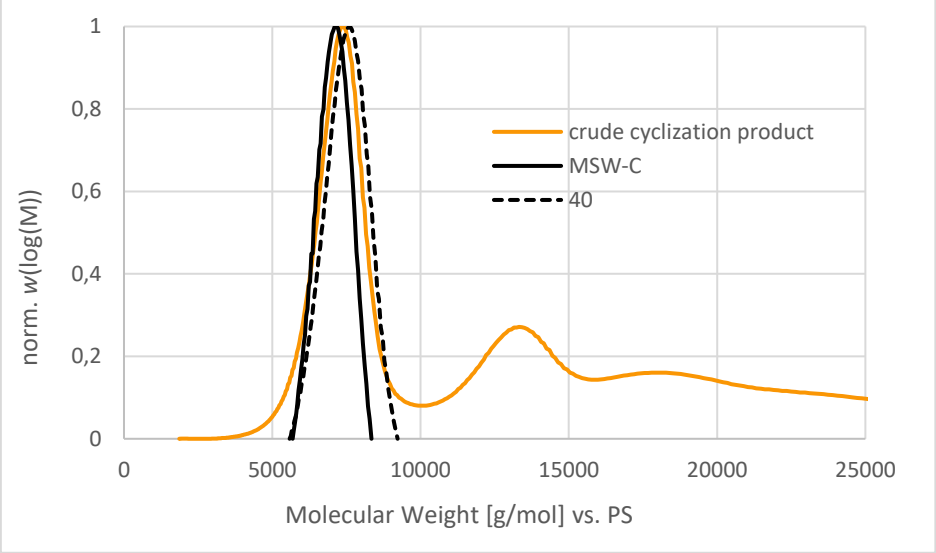

Figure 44: Molar mass distribution (THF, *vs* PS) as reaction control of the synthesis of **MSW-C** *via* analytical GPC showing the crude cyclization product after filtering column chromatography with the isolated compound as a reference.

In the end, the substrate was closed while a small amount of an impurity was revealed by MALDI mass spectrometry. It was not possible to remove the impurity *via* recGPC.

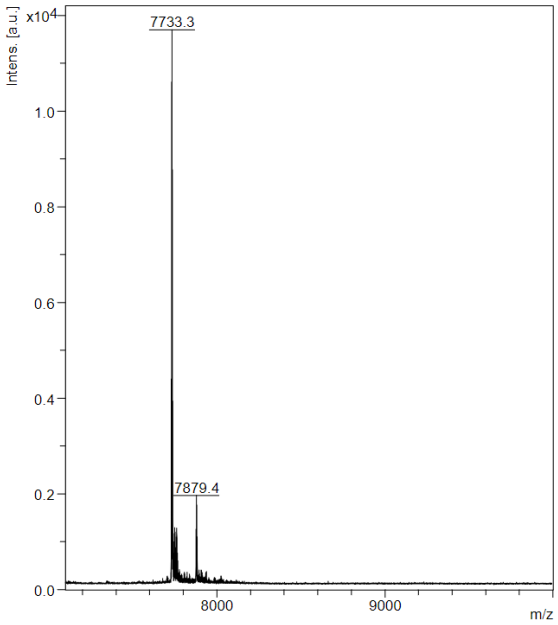

Figure 45: MALDI mass spectrum (matrix: DCTB) of **MSW-C** (left signal, calculated as 7732.2 Da) showing also unidentified impurities (right signal).

Interestingly, the presence of that byproduct was only present in MALDI mass spectrometry but not observed in any other analytical method. The final synthetic step of this and other MSWs was carefully investigated and illustrated in a cooperation with *Julia Kohn* from the group of *Prof. Dr. Stefan Grimme*. The revelatory results of this will be presented in chapter 6.[97]

In fact, **MSW-C** was characterized *via* mass spectrometry, ^{1}H- and ^{13}C-NMR spectroscopy successfully, making it the first 30 Ph-MSW yielding a full data set.

In order to investigate the aggregation of the received MSW, ^{1}H-NMR experiments at different concentrations were undertaken. In a concentration range between 10^{-3} mol/L and 10^{-5} mol/L, *Sterzenbach* observed shifting of some signals in ^{1}H-NMR spectra and sharpening of the respective signals with decreasing concentration.[108] Similar experiments were performed for **MSW-C** in three different concentrations, that were impossible for **MSW-MK3** due to its poor solubility.[105]

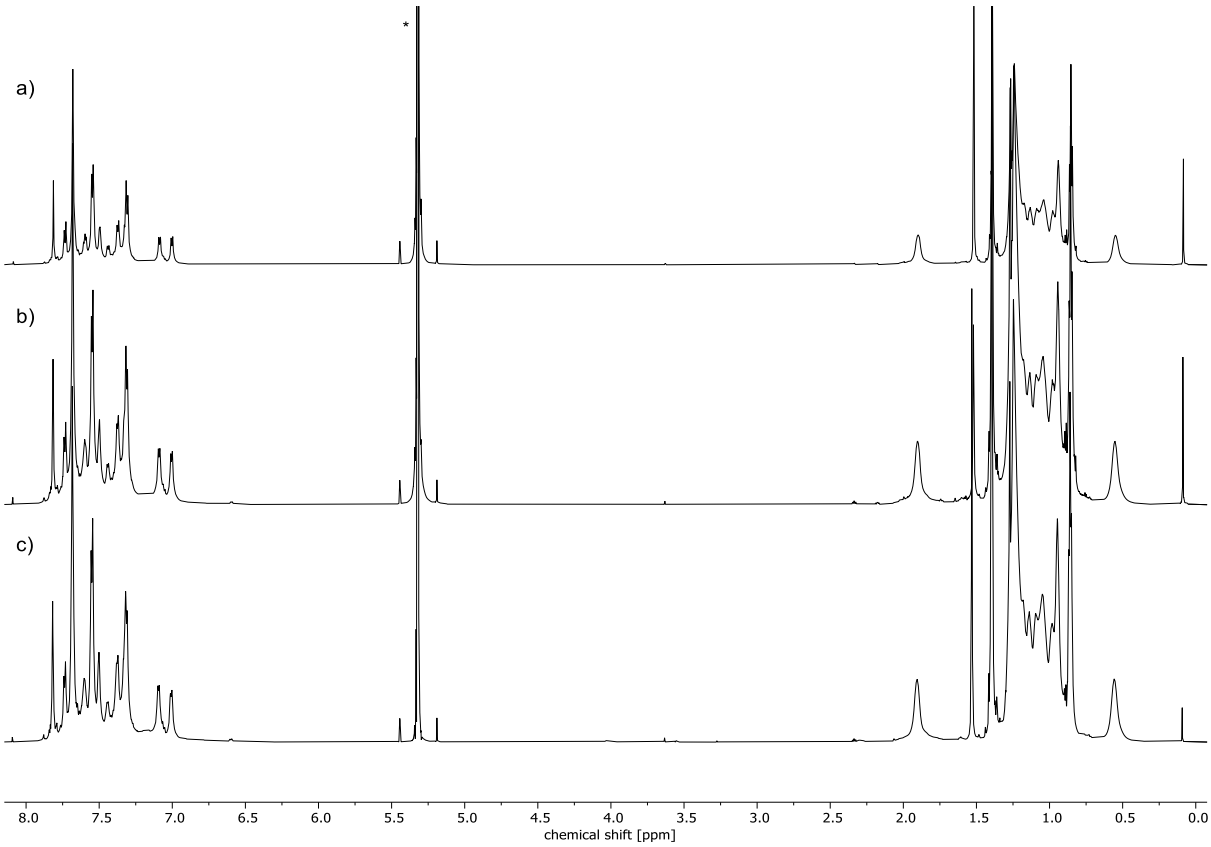

Figure 46: ^{1}H-NMR experiments of **MSW-C**, all recorded in CD_2Cl_2 (marked with *) at room temperature (700 MHz): $9.1 \cdot 10^{-4}$ mol/L (a), $1.84 \cdot 10^{-3}$ mol/L (b), $3.68 \cdot 10^{-3}$ mol/L (c).

A comparison of the spectra proves that the phenomena described by *Sterzenbach* do not seem to be present for **MSW-C**. Figure 46 neither shows a shifting of signals, nor do any signals change in multiplicity and sharpness. Thus, the inhibition of aggregation was proven for a fluorene-based MSW with spectral data for the first time, instead of relying on the MSW's accessibility as only proof.[105]

MSW-C was also investigated via ^{1}H-NMR spectroscopy at variable temperature. Over the investigated area of 243 K to 373 K, no dynamic changes were yielded. Instead, only a temperature-dependent sharpening of the signals was observed.

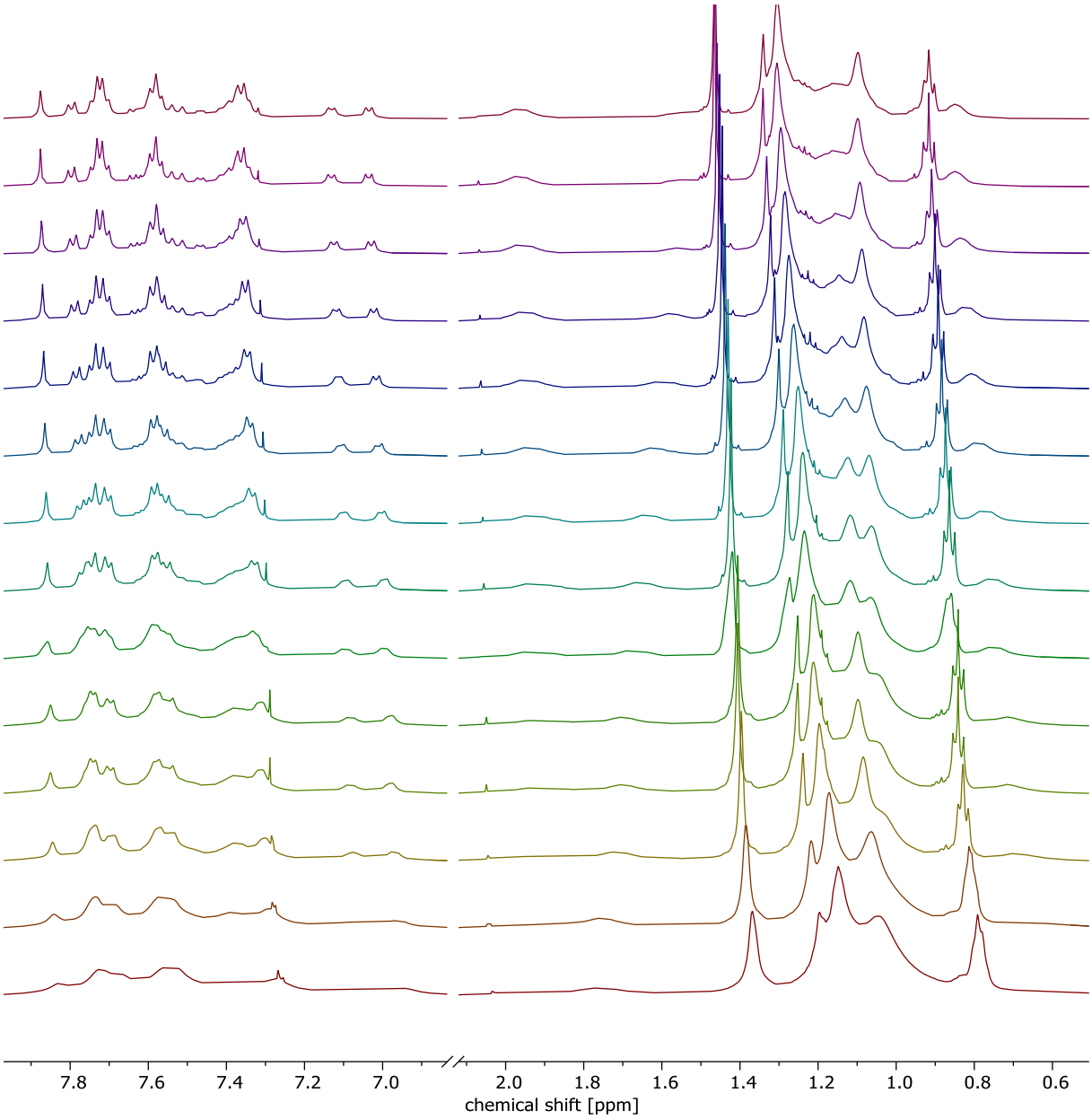

Figure 47: ^{1}H-NMR spectra of **MSW-C** recorded at various temperatures. All spectra were recorded in $C_2D_2Cl_4$ in the range between 243 K (bottom) to 373 K (top). The spectra overview was cropped for better visibility.

The experimental results of **MSW-C** were also published in 2024.[97]

5.1.4 Fluorene-based Molecular Spoked Wheel precursors for late functionalization

The successful synthesis of **MSW-C** sparked the interest in enlarged MSWs with longer side chains. Following the successful synthesis of two 30 Ph-MSWs, the limits of possible side chain lengths and their influence on physical properties became the next topic of interest.

At this point, a new strategy was considered: if it was possible to synthesize chain-free precursors and functionalize them as late as possible, this method would grant access to a broad scope of MSWs in very few steps.

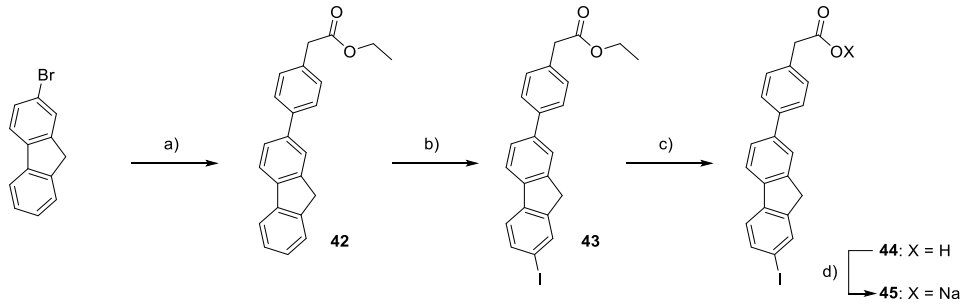

Scheme 56: a) **30**, K_2CO_3, $PdCl_2(PPh_3)_2$, PPh_3, PhMe, EtOH, 90 °C, overnight, 79 %; b) ICl, DCM, rt, overnight, 94 %; c) $LiOH \cdot H_2O$, THF, H_2O, 60 °C, 19 h, 92 %; d) NaO*t*Bu, *t*BuOH, 3 h, 40 °C, 100 %.

The synthesis of **45** is in a way a direct reproduction of the synthesis of **34** and will therefore not be described as detailed. For the first step, the conditions developed by *Kersten* were once again reapplied[105] ending up in a yield of 79 % very similar to its alkylated equivalent. Again, a trans-esterification was observed yielding **43**. Both the iodination as well as the ester hydrolysis worked in excellent yields above 90 % followed by a quantitative cation exchange yielding **45** by applying the *tert*-butanol system as before. **46** was subsequently accessed in another *Zimmermann-Fischer* condensation.

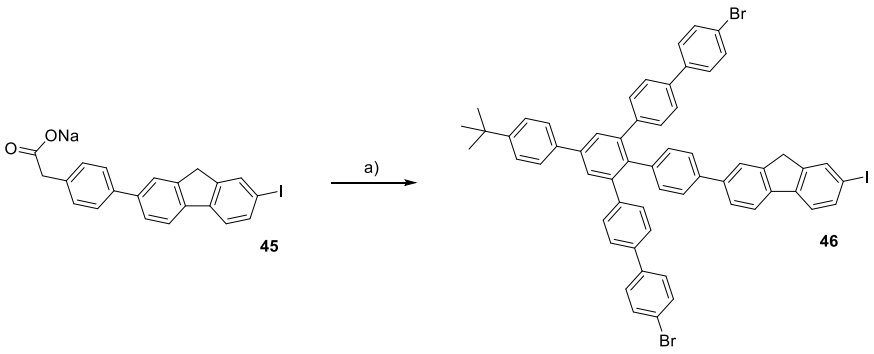

Scheme 57: a) **35**, Bz_2O, 4 h, 150 °C, 24 %.

The first alkyl group of interest was the C_{30} chain, as it was the only commercially available chain with a noteworthy difference in length compared to hexadecyl chains. Unfortunately, it was only available as triacontanol and analogous compounds with longer chain length are very expensive.

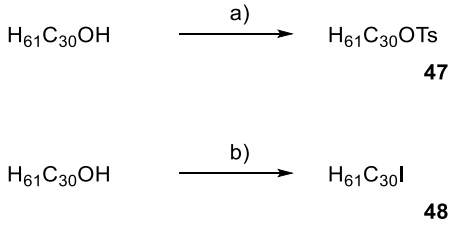

Scheme 58: a) K_2CO_3, TsCl, THF, reflux, overnight, 68 %; b) PPh_3, I_2, imidazole, DCM, 0 °C → rt, overnight, 20 %.

While the tosylate was accessible in a moderate yield of 68 %[128], to respective alkyl iodide was received in only 20 %.[129] Due to the high price and the low conversion triacontyl-groups were eliminated as possible new chains for MSWs. Anyways, the received substances were used for at least some investigations.

Due to the small collected amounts of alkylation reagents, only a functionalization of **46** with synthesized **47** was attempted. Unfortunately, no product was isolated.

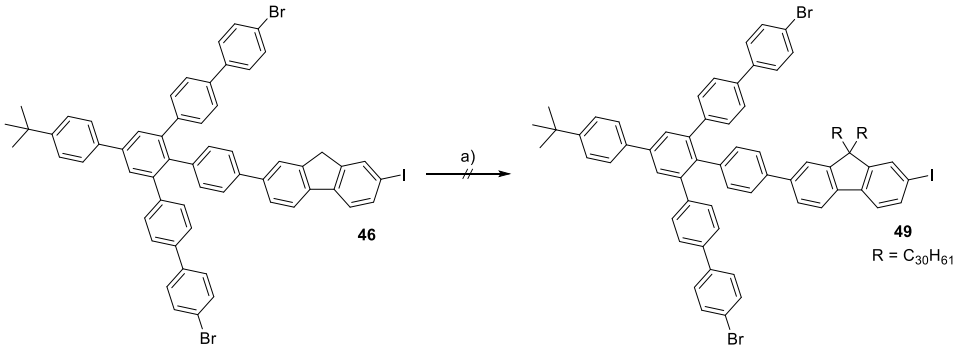

Scheme 59: a) KOH, **47**, Bu_4NBr, acetone, H_2O, 80 °C, 3 d, 0 %.

Because large linear chains were not available easily for further investigation, the introduction of a branched chain was the closest design. Even though the cavity for the 30 Ph-MSWs is bigger than for 18 Ph-MSWs, the introduction of a chain directly at its branch-position on the one hand is very difficult, on the other hand introduces massive potential steric hindrance. To eliminate such risk, the chain was introduced as 19-(3-iodopropyl)heptatriacontane.[130] Since the synthetic investigation of **49** consumed all the available substance of **46**, it needed to be reproduced.

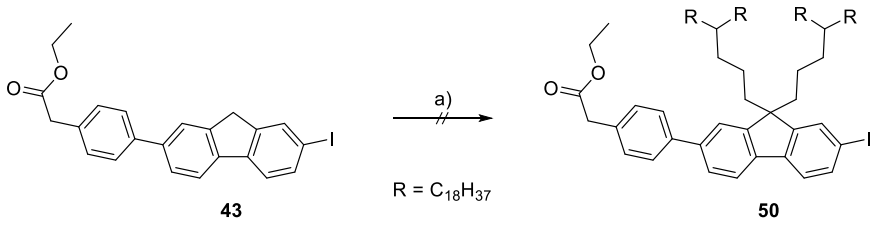

Scheme 60: a) 19-(3-iodopropyl)heptatriacontane, KOH, $C_{16}H_{33}Br$, KI, Bu_4NBr, acetone, H_2O, 80 °C, 68 h, 0 %.

Hence, 19-(3-iodopropyl)heptatriacontane was reacted with reproduced **43** to test if the alkyl halide was attachable to the less hindered precursor already. Unfortunately, after purification *via* column

chromatography no isolated fraction was identified as product. Retrospectively, the poor choice of KOH as base most likely hydrolyzed the ester, which made the resulting **44** very insoluble in organic solvents and removed it from the reaction.

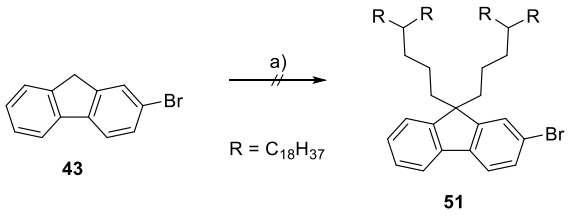

Scheme 61: a) KOH, $C_{16}H_{33}Br$, KI, Bu_4NBr, acetone, H_2O, 80 °C, 40 h, 0 %.

The same reaction conditions were applied to 2-bromofluorene to see if the alkylation works with the sterically least demanding substrate at all.[130] Even though KOH was used as base again, this time there were no cleavable groups present. For unknown reasons, no alkylation of the substrate was observed after two days. The interesting thing about this is that not even singly alkylated byproduct was observed as only the substrate was recovered.

Over all described syntheses in this subchapter, one problem grew in importance that was not considered during synthetic planning. If the alkylation is performed at a late stage, more groups can hinder it. On the one hand, it can be sterically more difficult to access the designated binding position, because 1) other groups attached to the substrate, 2) a single alkylation already shielding the bonding position or 3) a combination of both.

Hence, this subchapter concludes in acceptance that the tedious work up of early functionalization is preferable over late diversification of substrates in low to no yields, discontinuing the efforts towards **MSW-D**.

5.1.5 An alkoxy phenylene-substituted enlarged fluorene spoke

The development of the synthetic route for the late functionalization of MSWs brought up some new ideas for the synthesis of an alkoxy phenyl-substituted fluorene-based 30 Ph-MSW.

In order to construct the spoke, 2-bromfluorenone was utilized as starting material, beginning the synthesis in a similar manner as for **43**.

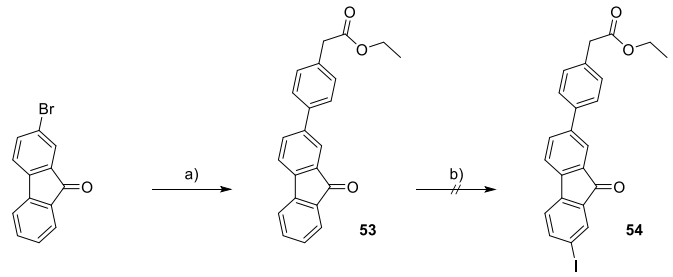

Scheme 62: a) **30**, K_2CO_3, $PdCl_2(PPh_3)_2$, PPh_3, PhMe, EtOH, 100 °C, 19 h, 86 %; b) ICl, DCM, rt, overnight, 0 %.

While the *Suzuki* coupling gave **53** in 86 % yield, the iodination of the resulting fluorenone was unsuccessful. Other than before, the 9-position was no longer formally a methylene group but now an electron-withdrawing ketone group that strongly deactivates the substrate towards further substitution.

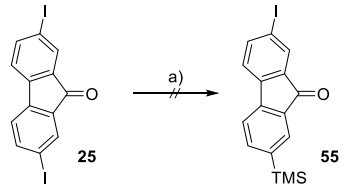

Scheme 63: a) *n*BuLi, TMSCl, THF, -78 °C → rt, 4 h, 0 %.

Alternatively, it was attempted to temporarily mask one binding site of previously prepared **25** with TMS to exploit its directing effect towards an iodine-TMS exchange later on. For the presented example, the substitution unfortunately did happen on neither side as **55** was not accessible this way. While for the reaction of **23** the alkoxy phenyl groups were the most electron-rich groups in the molecule, this property might be invertible by substituting the phenol groups' oxygen atoms with electron-withdrawing groups prior to the iodination. By that, the iodination should be destined to favor the 7-position of the fluorene again. Additionally, the deactivating groups should be distanced enough from the designated reacting position and beyond that, not in mesomeric resonance with it due to the quaternary carbon-atom in 9-position.

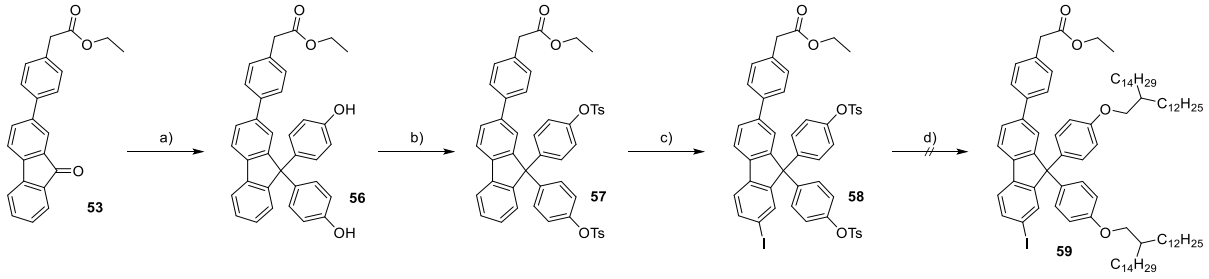

Scheme 64: a) MsOH, PhOH, 50 °C, 20 h, 73 %; b) TsCl, K_2CO_3, THF, 0 °C → rt, 4 h, 72 %; c) I_2, HIO_3, AcOH, $CHCl_3$, 80 °C, overnight, 29 %; d) KOH, 13-(Iodomethyl)heptacosane, KI, Bu_4NBr, acetone, H_2O, 80 °C, 48 h, 0 %.

Firstly, the phenolation of **53** yielded diol **56** in 73 % without any inconveniences.[124] In order to decrease the phenolic arenes' nucleophilicity is was decided to mask the free alcohols as tosylates. Hence, the following tosylation successfully gave **57** in 72 %.[128] The good conversion of **56** is also supported through the mentioned quaternary carbon in 7-position. Thus, both phenols are not conjugated, which means that a successful tosylation of the first one does not deactivate the second one for a further tosylation. Unfortunately, the preparations only gave 29 % of product in the subsequent iodination. It is difficult to say if in the end the electron-withdrawing groups still influenced the molecule's overall reactivity leading to that low conversion, but what needs to be emphasized here is that the sequence worked as planned. In ^{13}C-NMR spectroscopy, it is extremely easy to distinguish different regioisomers of aromatic iodination reactions, especially for the presented compounds. Usually, the signal for the iodine-functionalized carbon is met around 90 ppm for the 7-position of fluorene. The iodinated *ortho*-position of the phenol groups on the other hand generates a signal at 80.2 ppm (compare **24a**). For the just presented reaction, the only observed signal in that region is located at 93.3 ppm unequivocally confirming the formation of only the desired product. For the following reaction, it was decided to cleave the tosyl esters *in situ* as the alkylation of phenols required an excess of base anyways. The added water should enable the hydrolysis while also dissolving KOH and incorporating it into the reaction due to the good miscibility of the used acetone and water. After two days, the progress of reaction was checked *via* thin-layer chromatography, revealing that barely any product had formed. Through purification *via* column chromatography, it was not possible to separate and isolate the desired fraction. Due to the poor conversion within the iodination step, the synthetic results of **57** were not reproduced to further investigate its alkylation. Instead, **43** was oxidized successfully yielding **54** in the end.[131]

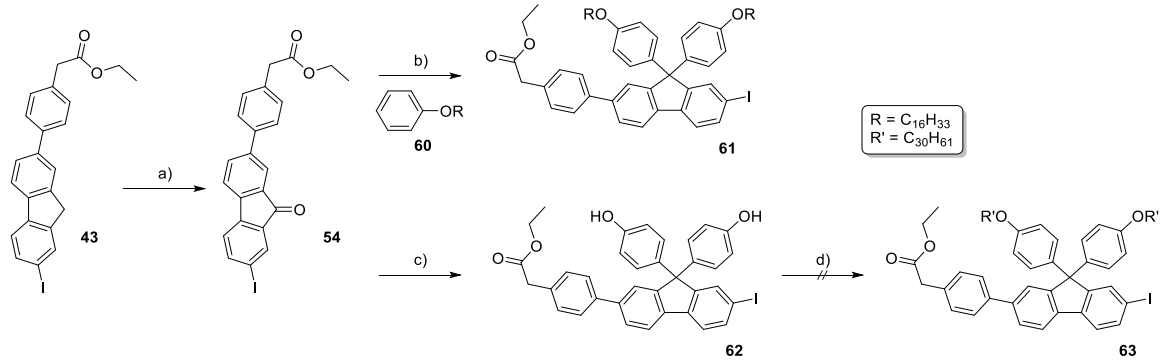

Scheme 65: a) $FeCl_3 \cdot 6\ H_2O$, *t*BuOOH, 2-pinacolic acid, pyridine, MeCN, rt, overnight, 81 %; b) MsOH, 50 °C, 48 h, 12 %; c) MsOH, PhOH, 50 °C, overnight, 91 %; d) **48**, KOH, KI, Bu_4NBr, acetone, H_2O, 80 °C, 48 h, 0 %.

Phenol was alkylated with 1-bromohexadecane under basic conditions in an excellent yield of 95 %, attempting to introduce two equivalents into **54**. While the formation of product was observed, it was only yielded in 12 %, too poor to proceed the investigation of this route. Instead, common phenol substituted the carbonyl function yielding **62**, in promising 91 %.[124] Despite all efforts, it was not

possible to functionalize **62**, once again denying the access of an alkoxy phenyl-substituted fluorene as a precursor, in this case for **MSW-E**.

5.1.6 Highly soluble fluorene-based Molecular Spoked Wheels

After the successes of the synthesis of **MSW-B** and its drastically improved solubility over **MSW-MK3**,[105] the next project of this work aimed at further improving this property by introducing more alkyl chains. As mentioned before, all-phenylene 18 Ph-MSWs with liquid-crystalline properties were synthesized.[96] After investigations of **MSW-MK3** and **MSW-B** both showed that these molecules did not possess that property (see melting point experiments in chapter 7.1), another molecular structure was designed containing elements of both **MSW-B** as well as of **MSW-AI**.[96] Therefore, a new anchor-shaped molecule decorated with a dendron unit should be implemented into the design as done by *Idelson* while maintaining the alkyl chains attached to the fluorene as in **MSW-B**. The fusion of both these molecules was attempted first by *A. Gres* in 2022 within her bachelor thesis up to symmetric acetylene **71a** under my supervision.[126] The poor yield of **71a** yet required the reproduction of her results in order to attempt a trimerization.

Pyrylium salt **65** was synthesized prior to *Gres*' work from the commercially available compounds *p*-anisaldehyde and 4'-(4-bromophenyl)acetophenone in 48 % yield.[108]

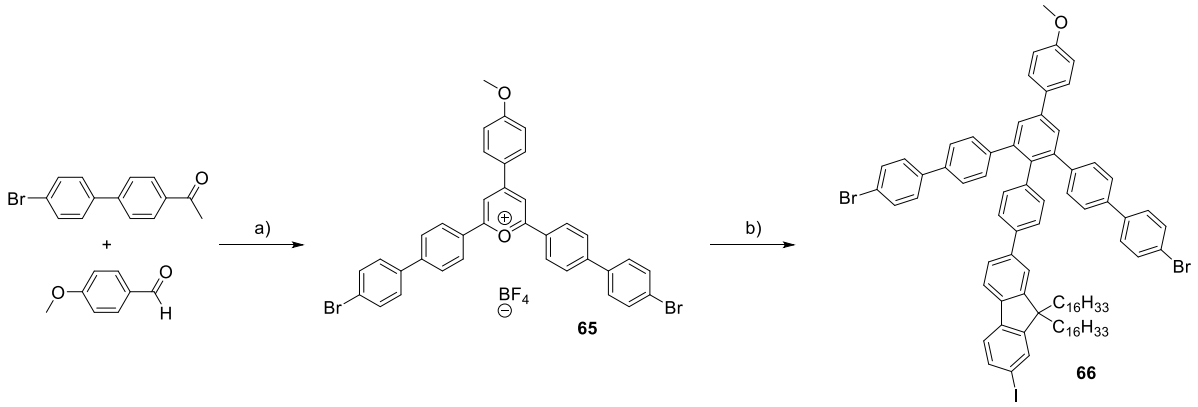

Scheme 66: a) $Et_2O{\cdot}BF_3$, DCE, 80 °C, 4 h, 48 %; b) **34**, Bz_2O, 150 °C, 4 h, 56 %.

Since this pyrylium salt was synthesized *via* the direct method (compare Scheme 23), the yield of 48 % is an excellent outcome, as it is capped at 50 % due to the consumption of its own intermediate as scavenger.[104]

65 was then condensed with the previously described **34** in a *Zimmermann-Fischer* reaction in a melt of benzoic anhydride in 56 %, which was far beyond average for the substrates prepared within this work.[126]

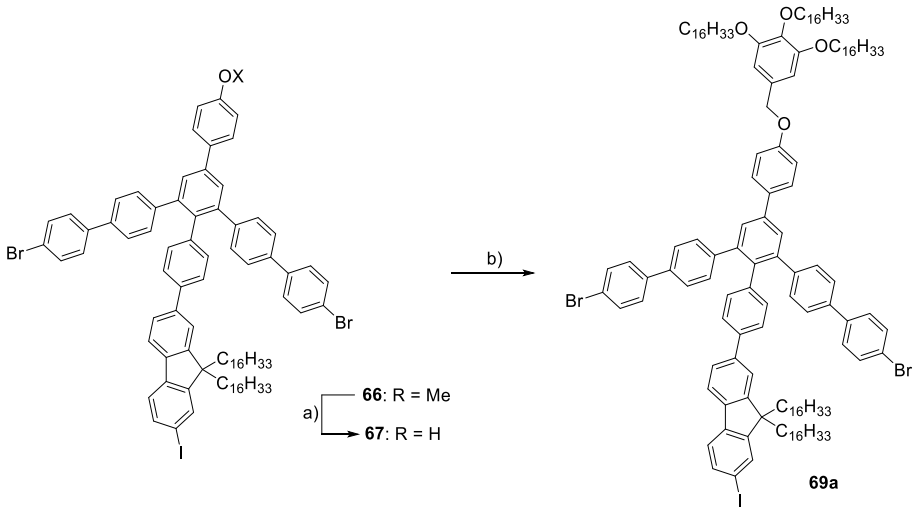

Scheme 67: a) BBr_3, DCM, -78 °C → rt, overnight, 96 %; b) **68a**, Cs_2CO_3, DMF, 100 °C, 48 h, 75 %.

The deprotection of **66** using BBr_3 in DCM was performed in near-quantitative yields of 96 %, followed by an etherification with **68a** that was introduced in an S_N2 reaction with the respective benzylic chloride. **68a** was prepared following the synthetic protocol of *Percec et al*. by *U. Müller*.[107]

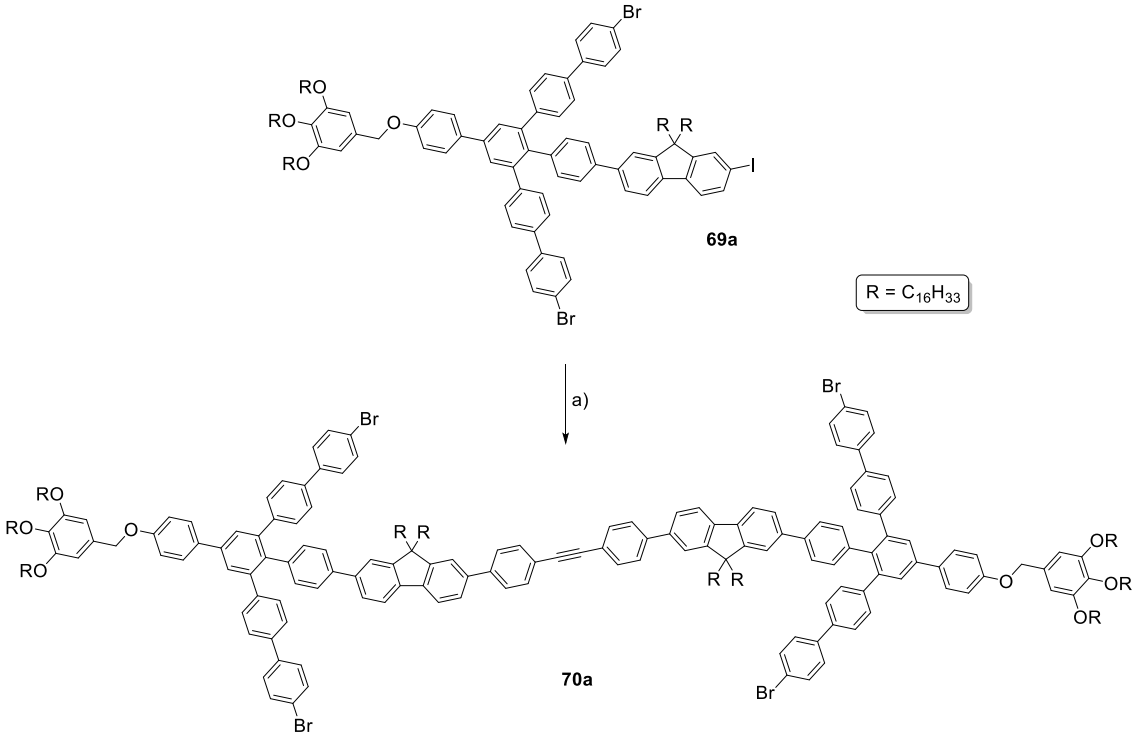

Scheme 68: a) **38**, Cs_2CO_3, $Pd(PPh_3)_4$, THF, H_2O, 50 °C, 5 d, 17 %.

70a was prepared following the same strategy as for **39**.[108] Again, the bromine-iodine selectivity is the crunch point in this reaction. It needs to be carried out at moderate temperatures to promote an ideally exclusive reaction at the iodine functionality. The flipside to this method is that the reduction of temperature strongly affects the yield that in many cases cannot be compensated by extension of the reaction time.

Table 1: Reaction conditions for the two-fold *Suzuki* reaction for the formation of **70a**. The first attempt was performed by *A. Gres* within the limits of her bachelor thesis under my supervision, the second attempt was performed reproducing her observations. Both attempts were reacted for five days at 50 °C, catalzed by $Pd(PPh_3)_4$.

#	*catalyst charge*	*solvent [mL]*	*equivalents (69a)*	*yield [%]*
1	18 mol%	PhMe/H_2O (10/0.3)	2.07	15
2	15 mol%	THF/H_2O (4/0.2)	3.92	17

In order to boost the yield, it was attempted to change the solvent and the concentration of the reaction, unfortunately without any major impact. It is extremely difficult to screen for reaction conditions for such complex systems, as the aryl halide here only is accessible over multiple steps and therefore very costly. Additionally, test systems are no option as well since compounds of similar functionalization and dimension are not commercially available and would take several synthetic steps to access as well.

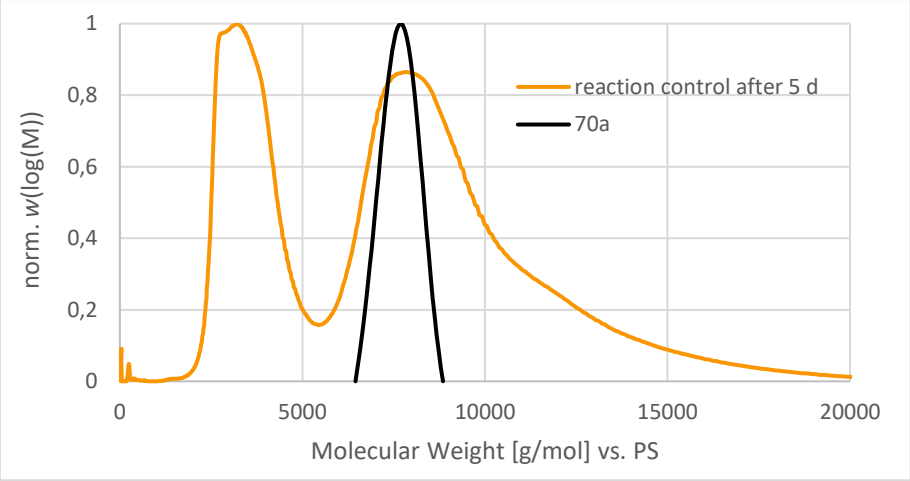

Figure 48: Molar mass distribution (THF, *vs* PS) as reaction control of the synthesis of **70a** *via* analytical GPC showing the crude product mixture after five days with the isolated compound as a reference. Due to the high similarity, only the first synthetic attempt is plotted.

Gratifyingly, both attempts yielded enough substance after recGPC to proceed with the synthesis.

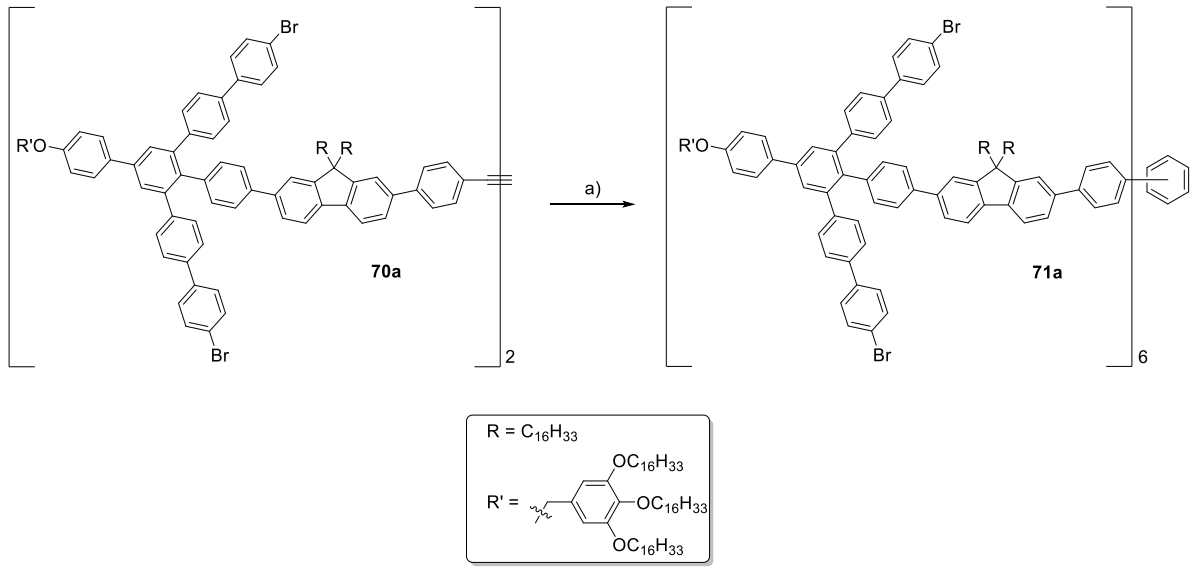

Scheme 69: a) $Co_2(CO)_8$, PhMe, 120 °C, 5 d, 15 %.

Other than for **40**, the synthesis of **71a** did not work out as easily. The main problem here was that the formed product was accompanied by a species that, according to mass spectrometry, appeared to be a dimeric species of **70a**. Even though it was possible to isolate both **71a** and the byproduct *via* recGPC, it was unfortunately not possible to fully characterize the byproduct. NMR spectroscopy gave clean spectra for ^{1}H- and ^{13}C-experiments and it was possible to identify the anchor-shaped groups but not how they are connected. Since this dimeric species seemed to be the favored product, the reaction time needed to be extended to five days.

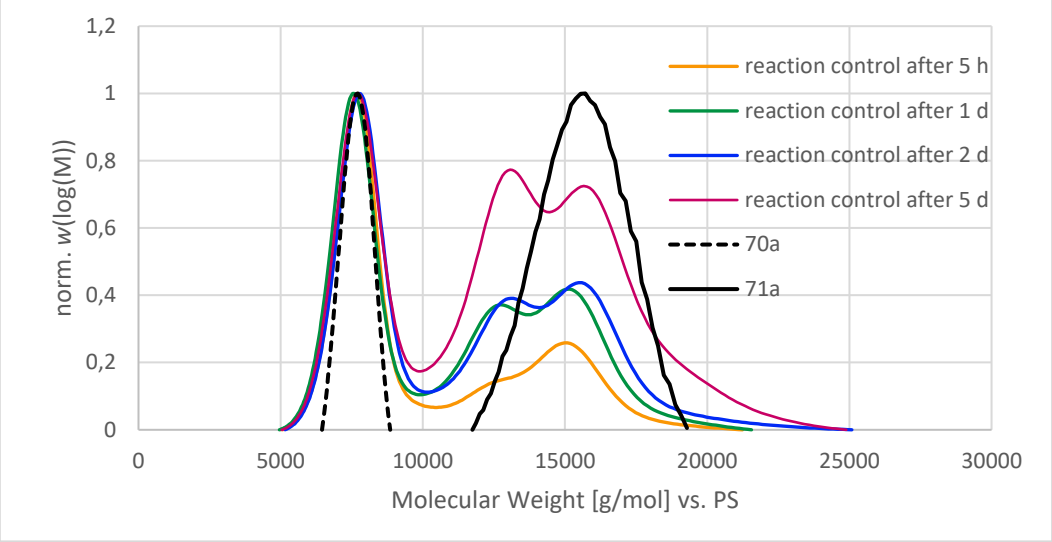

Figure 49: Molar mass distribution (THF, *vs* PS) as reaction control of the synthesis of **71a** *via* analytical GPC showing the crude cyclization product after various periods of time with the isolated compound as a reference.

Nevertheless, it was possible to fully characterize **71a** *via* NMR spectroscopy and MALDI spectrometry. For the final synthetic step of this route, the open-framed trimer was cyclized in a microwave reactor under high dilution conditions. This proved to be the most effective method for a six-fold reaction like

this while the low concentration additionally lowers the probability of two intermolecular coupling reactions.

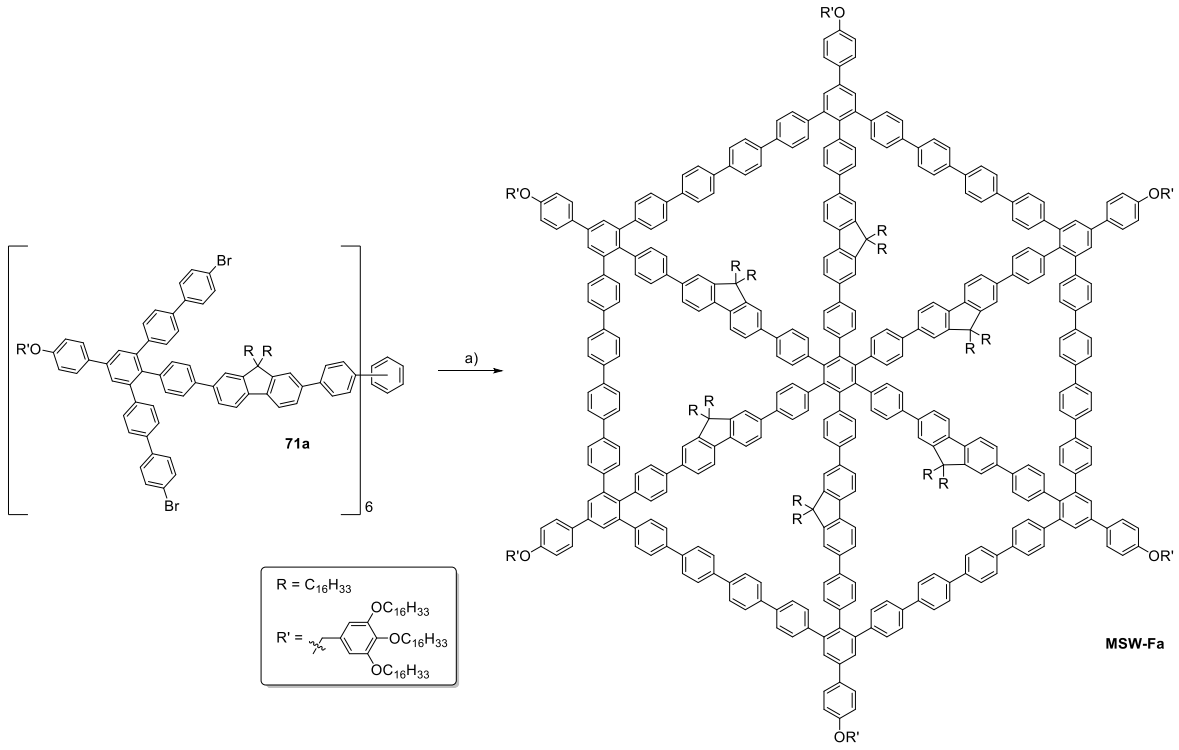

Scheme 70: a) $Ni(COD)_2$, bipy, THF, COD, 12 min, 300 W, 120 °C (mw), 60 %.

The elugram of analytical GPC shows the presence of a signal of marginally smaller molecular mass compared to the precursor.

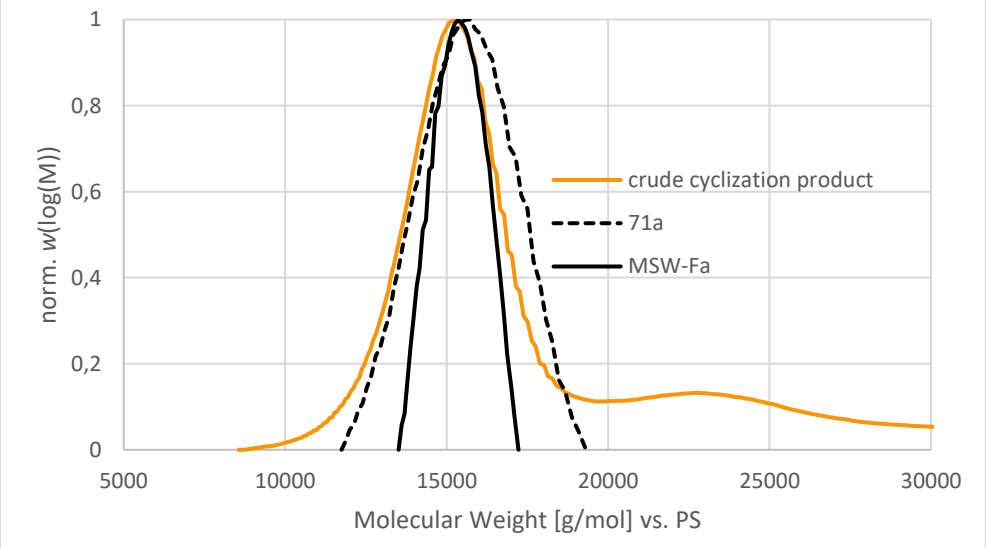

Figure 50: Molar mass distribution (THF, *vs* PS) as reaction control of the synthesis of **MSW-Fa** *via* analytical GPC showing the crude cyclization product after filtering column chromatography with the isolated compound and **71a** as a reference.

This signal can be assigned to the target structure since the rim closure harshly limits the rotational freedom of the rim segments diminishing the hydrodynamic radius, which makes the newly formed

species appear smaller. The reaction vessel yielded **MSW-Fa** in 60 % (5.3 mg), which was enough to generate a complete data set.

^{1}H-NMR experiments in similar concentrations as for **MSW-C** once again showed no signs of shifting signals or any of them changing in shape. This was considered as further proof of the aggregation-inhibiting effect of the hexadecyl-functionalized spokes.

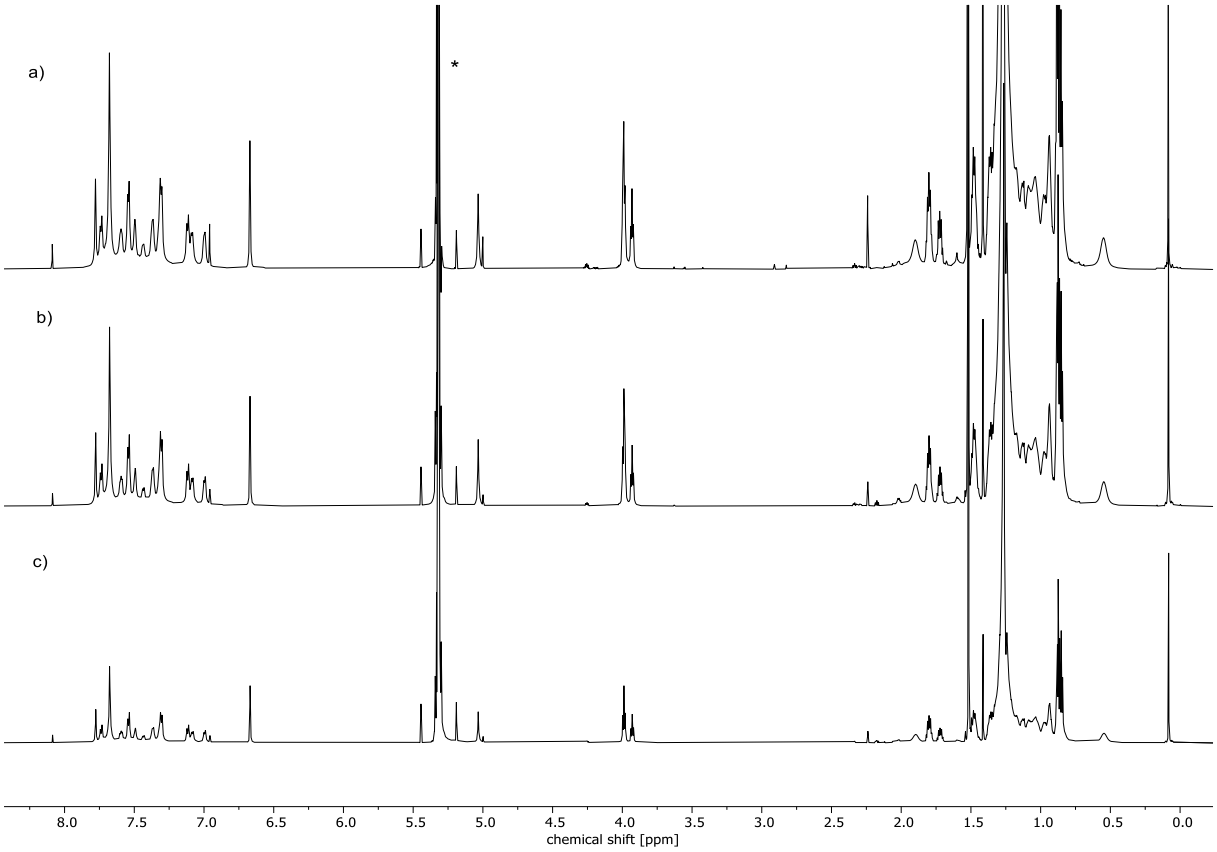

Figure 51: ^{1}H-NMR experiments of **MSW-Fa**, all recorded in CD_2Cl_2 (marked with *) at room temperature (700 MHz): a) $3.44 \cdot 10^{-3}$ mol/L, b) $1.72 \cdot 10^{-3}$ mol/L, c) $8.6 \cdot 10^{-4}$ mol/L.

The experimental results of **MSW-Fa** were also published in 2024.[97]

Similar to **MSW-Fa** it is of interest to synthesize a MSW decorated with a slightly different dendron unit and compare the molecules' properties in different experiments afterwards. Since the functionalization is done at a rather late stage during the synthesis, the modification is straightforward. Hence, **67** was reacted with the dialkoxy-functionalized dendron **68b**, once again prepared reproducing the instructions of *Percec et al.* by *U. Müller*.[107]

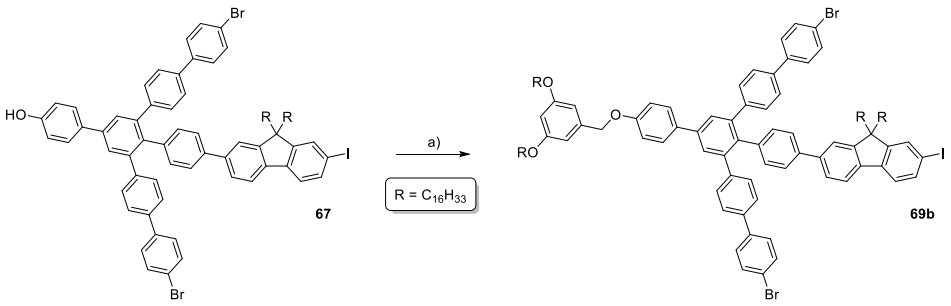

Scheme 71: a) **68b**, Cs_2CO_3, DMF, 100 °C, 48 h, 95 %.

During purification *via* column chromatography, an intense purple coloring accompanied the product band moving down the silica. The most likely explanation for this is the de-iodination of the compound. This observation was further supported by MALDI spectrometry.

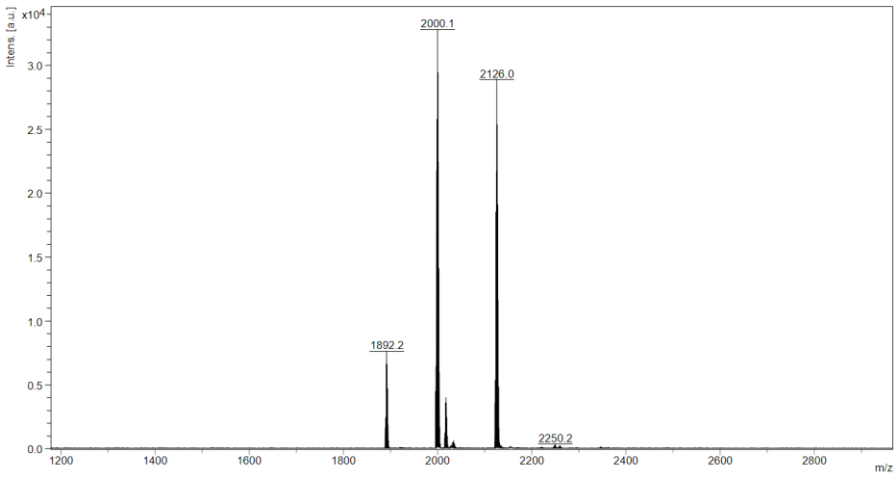

Figure 52: MALDI mass spectrum of **69b**. The spectrum shows the silver adduct of **69b** (*m*/*z* = 2126.0), the molecule peak (*m*/*z* = 2018.1), the de-iodinated compound as a silver adduct (*m*/*z* = 2000.1) and the de-iodinated product (*m*/*z* = 1892.2).

While in some examples, de-iodination occurs during the measuring process of MALDI mass spectrometry in small amounts, the species here had similar intensities corresponding to a significant amount of de-iodinated species. As before, both compounds were impossible to separate, so the mixture was converted into the symmetric alkyne in another two-fold *Suzuki* coupling.

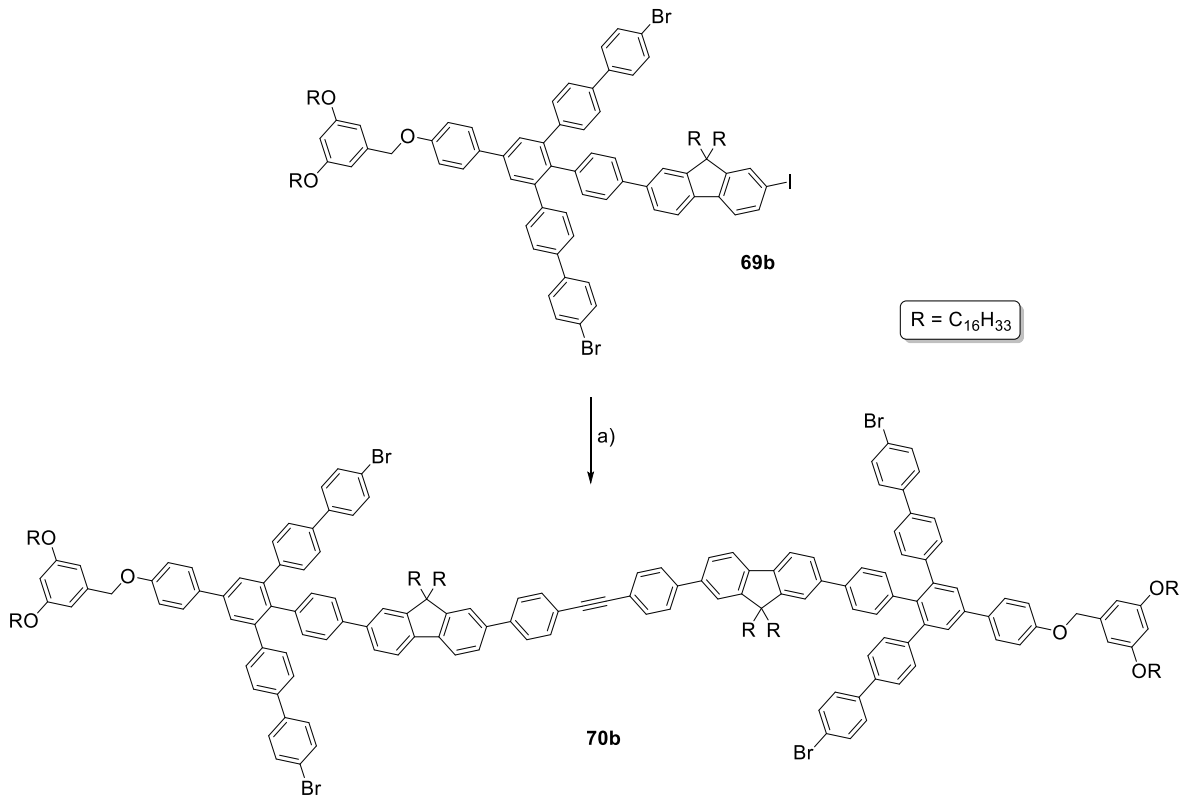

Scheme 72: a) **38**, Cs_2CO_3, $Pd(PPh_3)_4$, THF, H_2O, 50 °C, 5 d, 10 %.

Unfortunately, the conversion for this reaction was even lower than for the closely related alkyne **70a**. Even though the maximum yield is very likely perturbed by the de-iodinated byproduct from the previous step, **70b** is still yielded in poor amounts. The synthetic route was proceeded anyways, since enough substance was collected to attempt the subsequent trimerization.

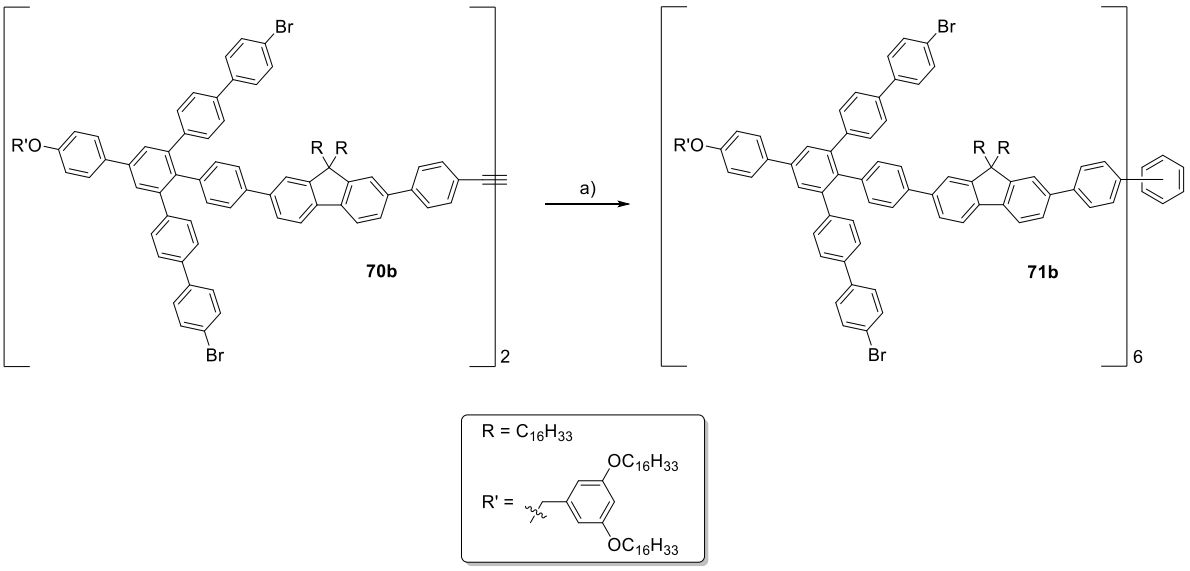

Scheme 73: a) $Co_2(CO)_8$, PhMe, 120 °C, 2 d, 34 %.

As before, the *Vollhardt* reaction yields the target compound as the main product. Similar as for the synthesis of **71a**, an unidentified dimeric species is obtained as well, whose structure could not be

derived. The following elugram shows the ratios of the different species after different periods of time. Fortunately, this time the trimer was formed as major product in about twice the yield of **71a**.

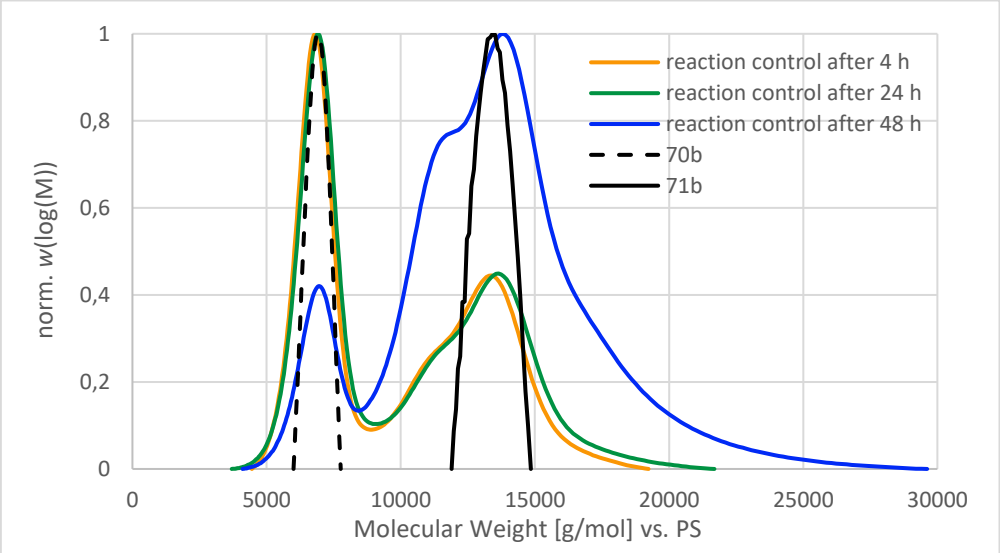

Figure 53: Molar mass distribution (THF, *vs* PS) as reaction control of the synthesis of **71b** *via* analytical GPC showing the crude cyclization product after various periods of time with the isolated compound as a reference.

Since 10.5 mg of the desired trimer were collected after recGPC in a yield of 34 %, the reaction yielded enough substance to attempt the final cyclization in another six-fold *Yamamoto* coupling.

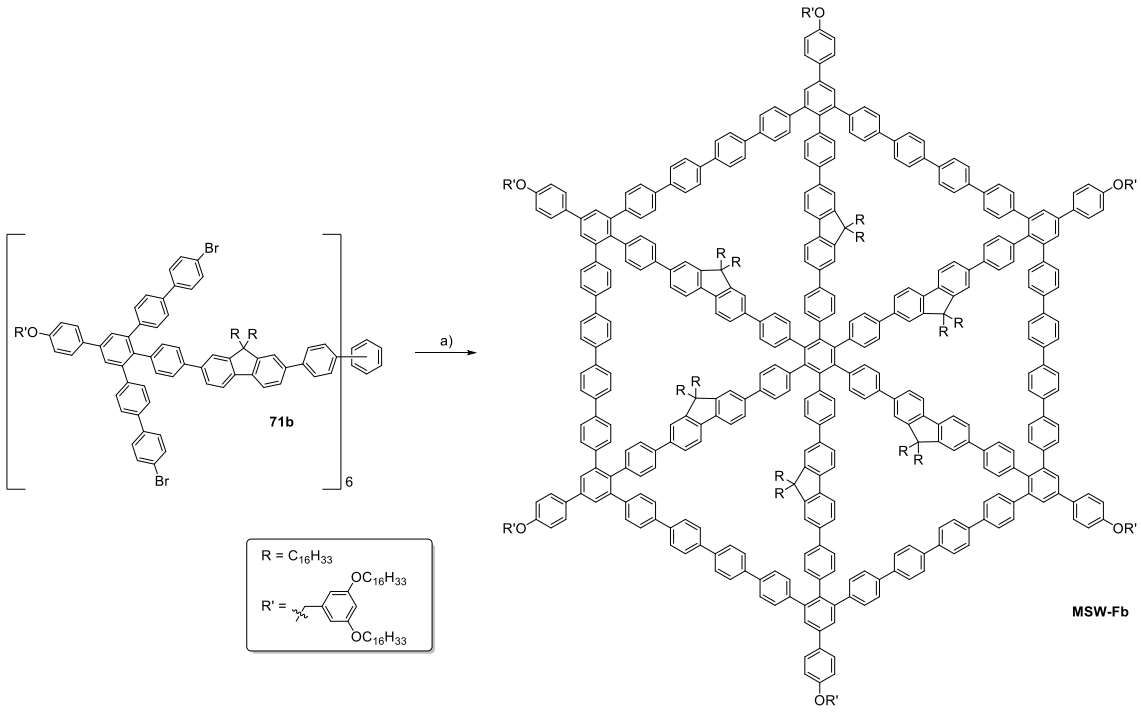

Scheme 74: a) $Ni(COD)_2$, bipy, THF, COD, 12 min, 300 W, 120 °C (mw), 35 %.

After the cyclization reaction, the crude product was pre-purified by filtration column chromatography and isolated *via* recGPC. The following elugram shows the formation of the MSW as the main product.

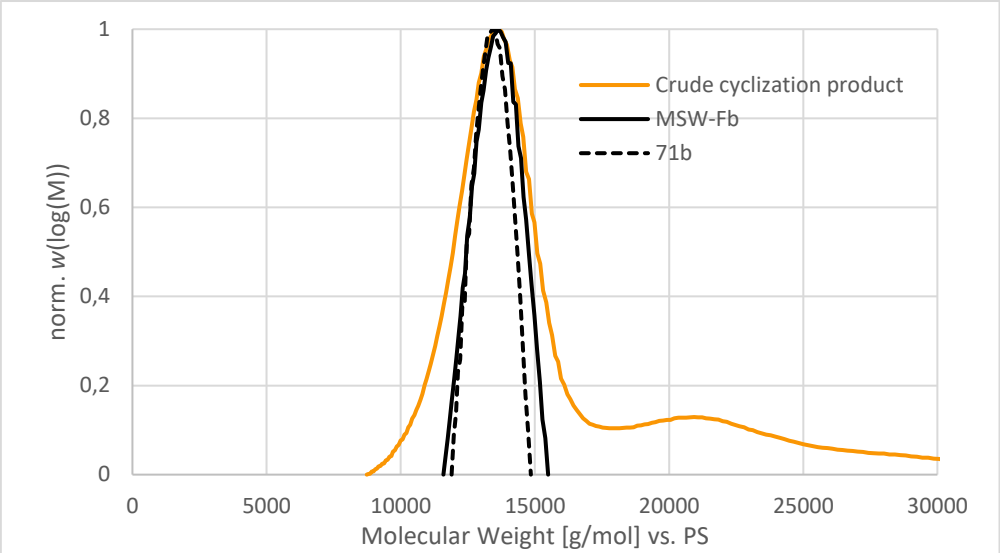

Figure 54: Molar mass distribution (THF, *vs* PS) as reaction control of the synthesis of **MSW-Fb** *via* analytical GPC showing the crude cyclization product after filtering column chromatography with the isolated compound and **71b** as a reference.

The hydrodynamic radius of **MSW-Fb** is slightly smaller than for precursor **71b** resulting from the reduced degrees of freedom. Hence, the elugram suggests the formation of the desired MSW. *Via* NMR spectroscopy and MALDI mass spectrometry it was possible to finally prove the structure. Due to its high similarity to **MSW-Fa**, **MSW-Fb** was not investigated regarding concentration-dependent characteristics *via* ^{1}H-NMR spectroscopy.

5.2 Molecular Cobwebs

Molecular Cobwebs (MCWs) are structures closely related to MSWs. While they are identical in size compared to the 30 Ph-MSWs, they vary in a vital point as they consist of not one but two rims. The obvious problem accompanying their synthesis is that in the final reaction step not one but two rims must be closed in a twelve-fold instead of a six-fold reaction, which might lead to several problems. While there are no known synthesized examples for this class of compounds, one example was already investigated by *C. Sterzenbach* within the limits of his PhD research.[108]

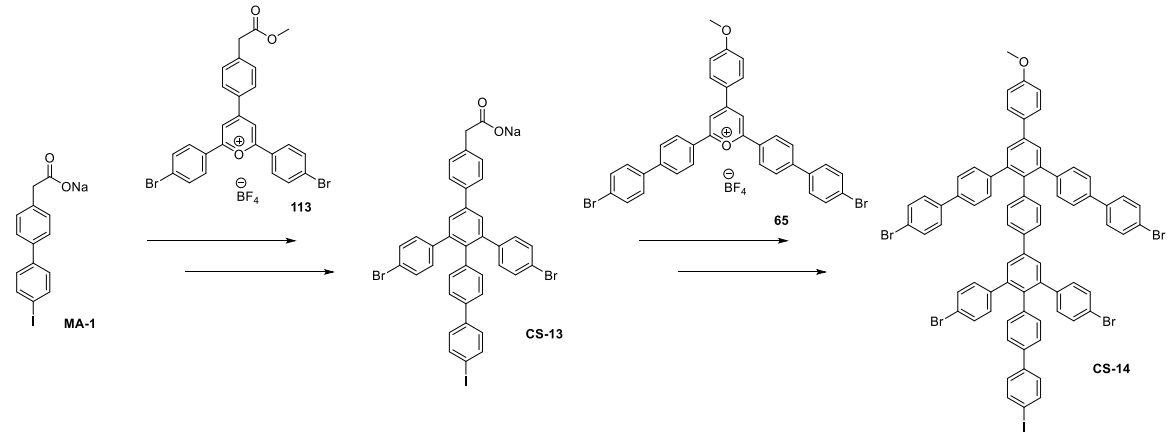

Scheme 75: Abbreviated schematic strategy of *Sterzenbach* attempting to synthesize an anchor-shaped molecule leading to a Molecular Cobweb (MCW).[108]

Sterzenbach modified his already existent synthetic route for an 18 Ph-MSW by exchanging the head functionalization of its anchor-shaped molecule for another acetic ester. From that, it was possible to convert the species into the corresponding sodium aryl acetate and perform a second *Zimmermann-Fischer* condensation. This procedure also formed the blueprint for the conception and synthesis of **MA-8** (compare chapter 3), which was successfully synthesized as part of my master thesis. *Sterzenbach* managed to proceed his route up the respective trimer but failed to close the molecule's rim in the final stage. The most likely explanation for this was once again the aggregation of precursors leading to intermolecular couplings as he observed mainly the formation of compounds twice the mass of his MCW.[108] Thus, the alkylation of the structure's spokes might once again cancel that problem.

5.2.1 A fluorene-based Molecular Cobweb

For the conception of this work's MCWs, different aspects were considered. In order to inhibit the aggregation of the precursors, alkyl chain-carrying spokes are inevitable, making fluorene a promising substrate. Following *Sterzenbach*'s approach, the target structure needs to have at least the dimension of a 30 Ph-MSW. The work of *Kersten* elucidated, that structures with such diameters are not soluble if their spokes are functionalized with octyl chains. Hexadecyl chains on the other hand sufficiently improve the solubility of 30 Ph-MSWs as the synthesis of **MSW-C** proved (compare chapter 5.1.3). Additionally, the incorporation of hexadecyl groups comes at the price of an additional spacing phenylene group between the acetylene- and the fluorene-unit, which turned out to be inevitable to successfully trimerize the symmetric alkyne as the synthesis of **18** affirmed (compare chapter 5.1.1). Hence, the only reasonable way to incorporate fluorene into a MCW is to decorate its spokes with hexadecyl chains and insert a spacer unit between the fluorene unit and its hub.

Due to the great synthetic results for the fluorene-based 30 Ph-MSWs with hexadecyl chains, the most intuitive idea for a MCW was to simply extend a 30 Ph-MSWs by a second rim around the existing MSW.

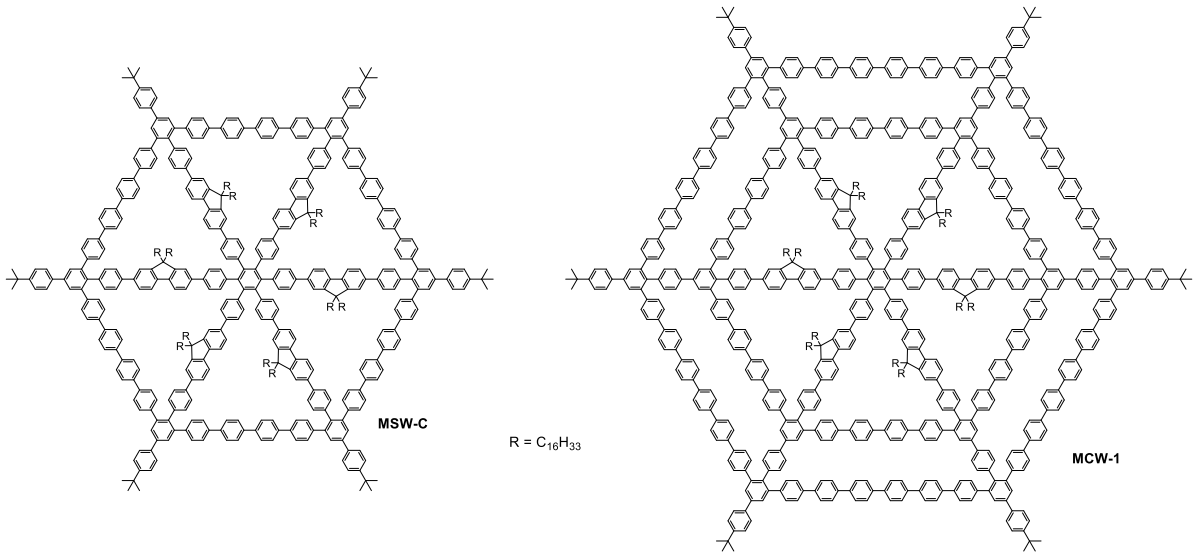

Figure 55: Conception of a MCW derived from the synthetically accessible structure of **MSW-C**.

A structure of that dimension can unfortunately not be prepared. The pyrylium salt for a macrocyclic structure with an edge length of eight phenylene-units requires an unfunctionalized, linear terphenyl acetophenone, that is neither commercially available nor can be accessed easily if being processed without any solubilizing groups. *S. Becker* faced that exact problem during his PhD studies.[116]

Summarizing, to successfully design the simplest possible fluorene-based MCW it is necessary to 1) incorporate hexadecyl chains into the spokes, 2) implement a spacer phenylene between the hub and the fluorene-unit and 3) not exceed an edge length of six phenylenes because terphenyl acetophenone can already cause massive problems within its own synthesis.

Considering these restrictions, a new path was envisioned. The idea was to design the smallest possible fluorene-based anchor-shaped molecule for the inner rim as a fusion of **13** as well as *Sterzenbach*'s extender **113** and connect it to **35** after conversion into the sodium aryl acetate.[108]

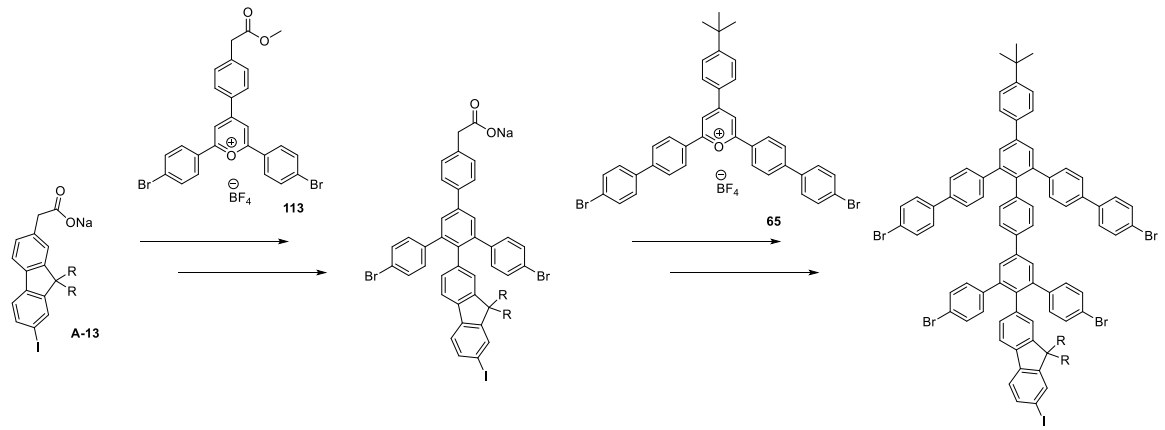

Scheme 76: Concept for the synthesis of a plane-shaped molecule leading to a fluorene-based MCW.

Afterwards, the resulting airplane-shaped molecule should be converted into the respective symmetric acetylene by connecting two equivalents *via* **38**. This clearly distorts the final structure compared to the previously presented MSWs because usually, the distance between hub and rim d_s is equal to the edge length d_e between two spokes.

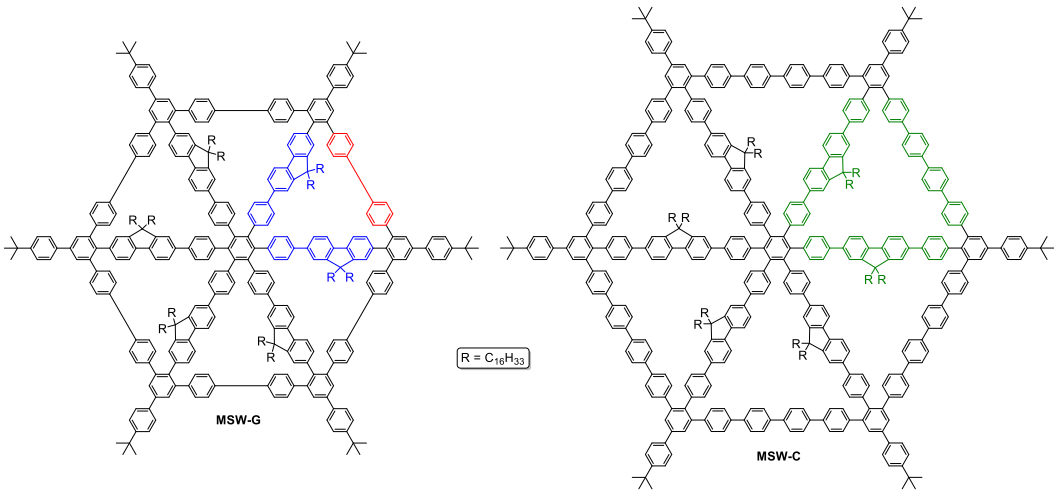

Figure 56: Symmetry comparison of **MSW-G** and **MSW-B**. For **MSW-C** both distances are equal ($d_s = d_e$, green), for **MSW-G** the distance between hub and rim d_s (blue) is longer than the edge length d_e (red) breaking the symmetry ($d_s \neq d_e$).

This rule would be fulfilled by **MCW-1** (compare Figure 55) but is hurt in a MCW based on **MSW-G** due to the additional spacer phenylene unit between the hub and the fluorene units.

Since the strictness of this rule was never investigated, it is unknown if the extended diameter affects the final rim closures. In order to not waste too much time and resources on such a fluid concept, **MSW-G** only constructed of the MCW's inner rim is synthesized as a model system first to investigate the potential strain.

Luckily, the model system may be synthesized from **16** and **38** in a two-fold *Suzuki* coupling.

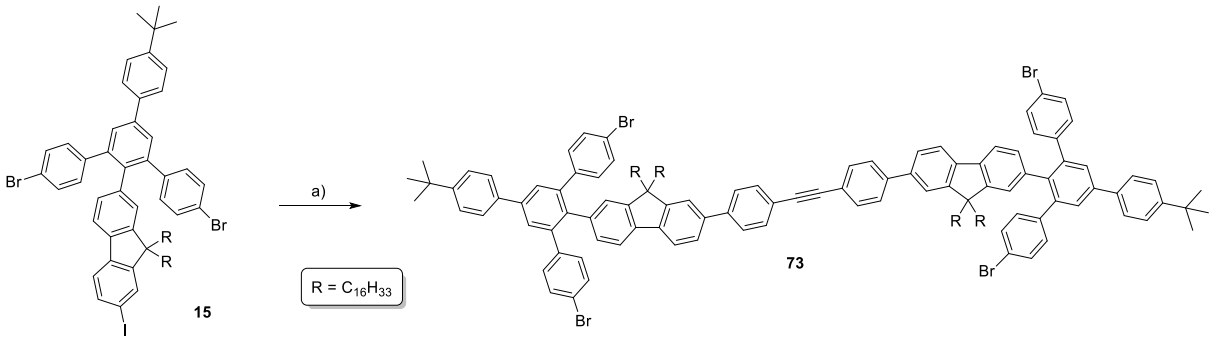

Scheme 77: Synthesis of **73**, performed under various conditions as displayed in table 2.

While the synthesis appears to be very simple, it took some attempts to optimize the conditions for this reaction step, while *optimize* here means to not just waste medium amounts of **15** in one-digit yield reactions. The conditions applied are listed in the following table.

Table 2: Reaction conditions investigated for the two-fold *Suzuki* coupling yielding **73**.

#	catalyst	base	solvent	Yield [%]
1	$Pd(PPh_3)_4$	Cs_2CO_3	PhMe : H_2O (45:1)	20
2	$Pd(PPh_3)_4$	Cs_2CO_3	PhMe : H_2O (23:1)	10
3	$Pd_2(dba)_3$, $P(tBu)_3 \cdot HBF_4$	CsF	PhMe	0
4	$Pd(PPh_3)_2Cl_2$, PPh_3	K_2CO_3	PhMe : EtOH (2:1)	<1
5	$Pd(PPh_3)_4$	K_2CO_3	PhMe : H_2O : EtOH (8:1:1)	6
6	$Pd(PPh_3)_4$	Cs_2CO_3	PhMe : H_2O : EtOH (8:1:1)	21

Screening of the reaction conditions showed a strong dependence of the yield regarding the solvent composition. In the second attempt, doubling the amount of water used in the first attempt halved the yield of the reaction. In another approach, cesium fluoride was employed that is a commonly used as a base in organic reactions due to its low nucleophilicity and the weak interaction between cesium and fluoride. While $P(tBu)_3$ needs to be stored under inert atmosphere and can therefore be difficult to handle, $P(tBu)_3 \cdot HBF_4$ is inert to atmospheric conditions. Unfortunately, reproducing the conditions of *Müller et al.* did not yield the desired product.[132] The conditions developed for the synthesis of **73** only yielded the desired compound in traces. A slight modification of those conditions seemed to show, that the incorporation of water is essential for the reaction. Finally, exchanging potassium carbonate (K_2CO_3) for cesium carbonate (Cs_2CO_3) boosted the yield to a maximum of 21 %.

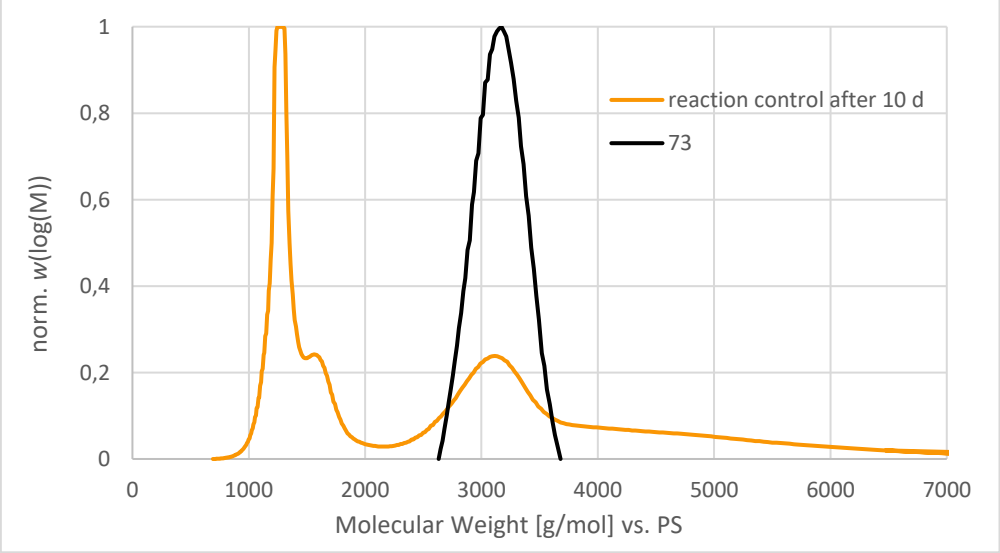

Figure 57: Molar mass distribution (THF, *vs* PS) as reaction control of the synthesis of **73** *via* analytical GPC showing the crude cyclization product after ten days with the isolated compound as a reference.

Since sufficient amounts of **73** were yielded overall, the reaction was not further investigated and the substrate was trimerized in a cobalt-catalyzed *Vollhardt* reaction.

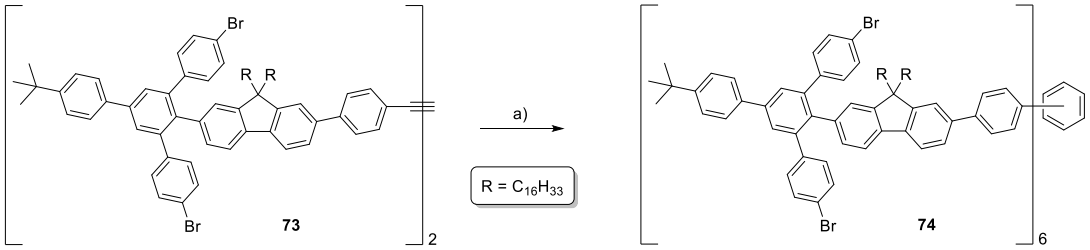

Scheme 78: a) $Co_2(CO)_8$, PhMe, 130 °C, 4 h, 41 %.

As usual, the reaction was carried out in toluene using $Co_2(CO)_8$ as a catalyst. The incorporation of the spacer phenylene in combination with the shortened bromide-containing side groups seemed to have a significant impact on the trimerization. The gained space between the outward-bound groups resulting from the de-crowding spacer phenylene units sped up the reaction that much, that the reaction control *via* analytical GPC after only four hours found the trimer to be the predominant species.

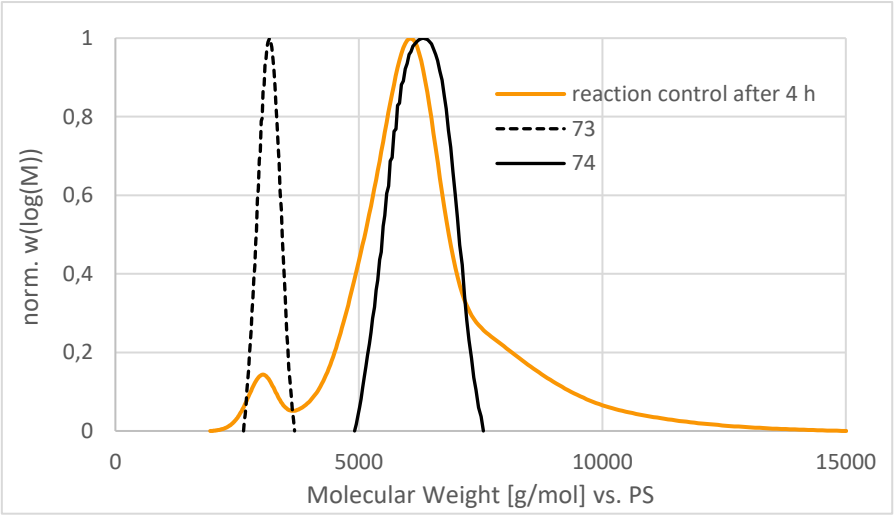

Figure 58: Molar mass distribution (THF, *vs* PS) as reaction control of the synthesis of **74** *via* analytical GPC showing the crude cyclization product after four hours with the isolated compound and **73** as reference.

The final reaction step for the test system was performed in a microwave reactor once again. Here, the outer rim was attempted to be closed in six-fold *Yamamoto* coupling.

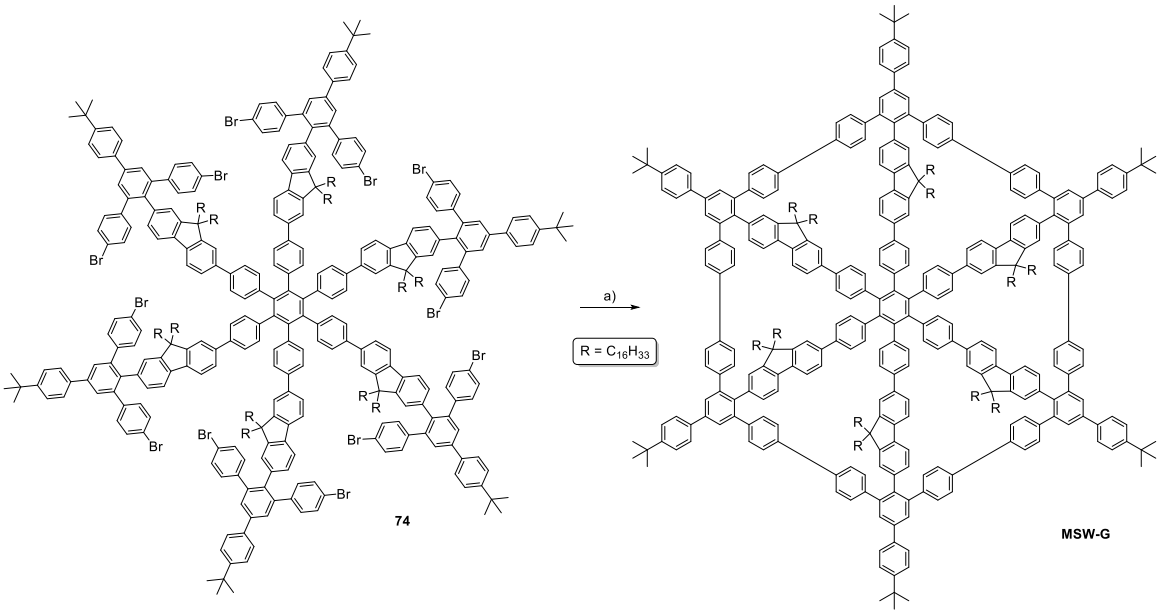

Scheme 79: a) $Ni(COD)_2$, bipy, THF, COD, 12 min, 300 W, 120 °C (mw), 0 %.

The reaction mixtures from all reaction vessels were combined and pre-purified *via* filtering column chromatography to remove all metal salts. Afterwards, the crude product was further purified *via* recGPC.

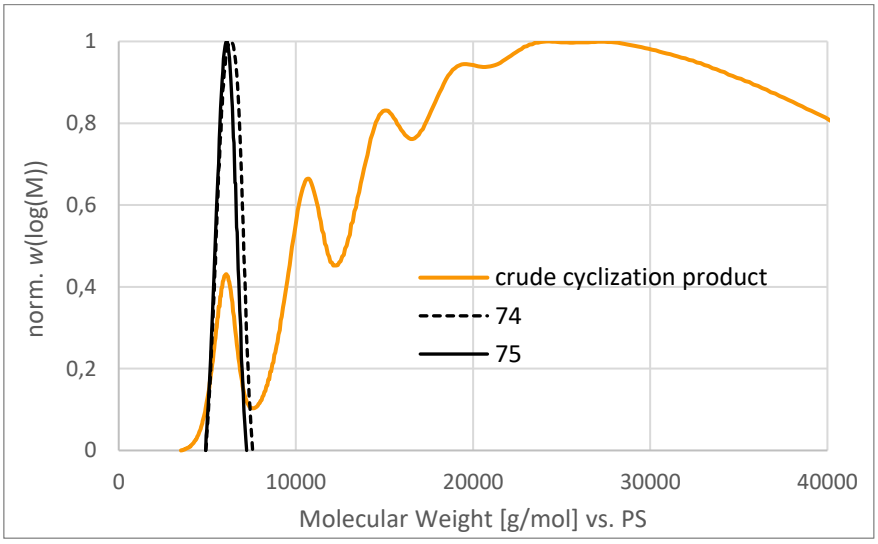

Figure 59: Molar mass distribution (THF, *vs* PS) as reaction control of the synthesis of **MSW-G** *via* analytical GPC showing the crude cyclization product after filtering column chromatography with the isolated compound **74** and **75** as reference. The elugram was cropped for visibility reasons and due to the lack of further identifiable peaks.

As the elugram reveals, the resulting species is lower in its hydrodynamic radius, which indicates a rim closure as already explained before. The formation of species of higher hydrodynamic radii on the other hand was concerning. Hence, the crude product was investigated *via* MALDI spectrometry, as depicted in the following.

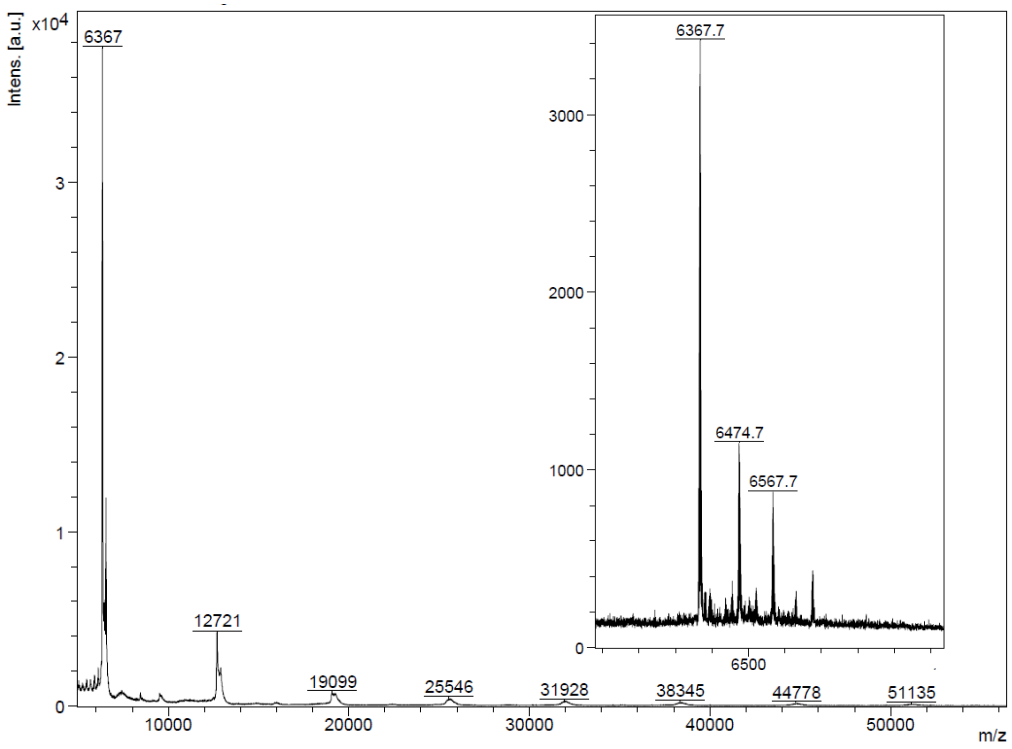

Figure 60: MALDI mass spectrum with added silver salts of the crude cyclization product and zoomed excerpt of the product region.

The spectrum shows, that the higher radii are seemingly caused by higher-molecular weight species that are undoubtedly present within the crude product mixture. While it is no problem to separate them from the desired compound, it was unexpected that they formed at all in the presence of alkylated spokes. The more extraordinary thing is the signal corresponding to the target molecule. With a value of *m*/*z* = 6367 the molecule appears to be three atomic units too heavy. Due to very precise measuring in the region around the product, this deviation is out of tolerance to result of a technical imprecision or an error. Instead, the idea that a dehalogenation in the final of the six couplings took place over the full closure of the structure manifested itself and assigned the found signal as $[MH_2+H]^+$. MH_2 is in the following referred to as **75**. Considering this allocation, the noise-dominated ^{1}H-NMR spectrum now made sense since **75** is strongly de-symmetrized through the dehalogenation resulting in split up and overlapping signals that are no longer identical. Keen-eyed analysis of the MALDI spectrum also discerns that aside from the molecule signal no other dehalogenated species or signals of still halogen-carrying unclosed precursors are present within. Conclusively, it appears that the overall closure of **74** worked while only the final coupling failed.

A very plausible hypothesis for this is the increasing strain with each further connection of two neighboring ring fragments. Such strain was also predicted by quantum chemical simulations that will be further elucidated in chapter 6. As stated in the discussion of the design, the contempt against the ratio between edge- and spoke-length leads to a strained MSW due to the distortion of its precursor.

Because of the stiffening of the structure accompanying every additionally formed bond, only the final bond formation was unsuccessful due to a too large distance between the two coupling positions in an intermediate too rigid to adapt to the intended reaction.
The synthetic efforts towards **MSW-G** were also published in 2024.[97]

5.2.2 A biphenol-based Molecular Cobweb

After the detailed investigation around fluorene-based MCWs, the failure of the final synthetic step towards **MSW-G** put the research on fluorene for further MCWs to rest for now. A substrate that seemed convenient to substitute fluorene was biphenyl, more specifically 2,2'-biphenol ethers. Similar to fluorene, the implementation of two alkyl chains is possible with that substrate, while the compound is more flexible due to its rotational freedom around the biphenyl-bond. Beyond that, the molecule is not curved, which allows the synthesis of planar MSWs and MCWs again. While planar MSWs, for example, tend to have a higher affinity towards aggregation as learned from the work of *Sterzenbach*,[108] the molecules presented in this chapter should not be prone to aggregate since they are still alkoxy-substituted forcing them to stay distant. While at least one alkyl chain is at a similar distance to the designated target structures' hub as in the fluorene equivalent, a cyclotrimerization is possibly more facile as the chains might not interfere as strongly with the reactive center as before due to the mentioned higher rotational freedom.
The main problem 2,2'-biphenol-based spokes were not taken into account for so long is the construction of the spoke. For fluorene, the procedure is straightforward. A halogenated fluorene is either purchased or prepared, subsequently alkylated, converted into the convenient ester and if not already present, iodine is implemented. For 2,2'-biphenol, that path is not possible. While already halogenated 2,2'-biphenol derivates are hardly available, their one-step preparation is not possible due to their strongly electron-donating *+M* substituents. The hydroxy groups strictly direct any electrophilic aromatic substitution (S_EAr) halogenations into 4-/4'- and 6-/6'-position exclusively.[15]

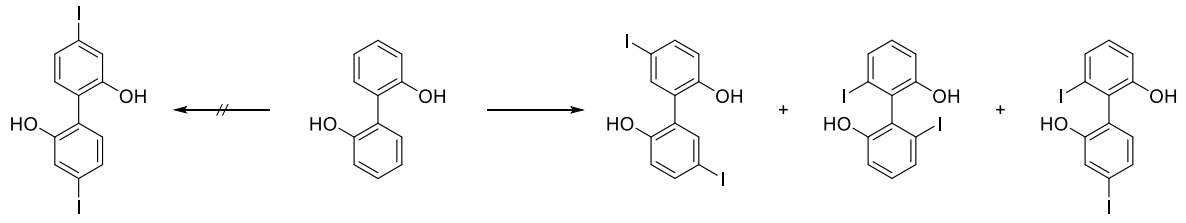

Scheme 80: Iodination of 2,2'-biphenol with the desired outcome (left) and the observable outcome (right). The reaction was not performed and the shown outcome follows elementary organic chemistry rules.[15]

Due to the presented complication, the spoke cannot be constructed from the central biphenol-unit straight away but needs to be built from two separate pre-functionalized arenes. In a work of *He et al.*,

a procedure yielding a 4,4'-diiodinated biphenol methyl ether is described. That compound is obtained from an *Ullmann* coupling of two identical moieties *via* multiple steps. It includes many compounds that suffer from poor solubility as they were purified through *Soxhlet* extraction.[133] This appeared concerning, since poor solubility can also mean that the conversion of the respective compound is poor because they only participate sparsely in a reaction due to their low availability in solution. To avoid this, their approach was slightly modified through an early alkylation to avoid that susceptibility.

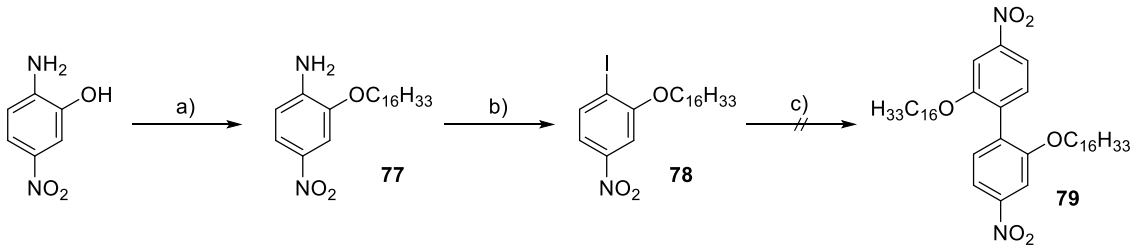

Scheme 81: a) KOH, $C_{16}H_{33}Br$, KI, Bu_4NBr, acetone, H_2O, 80 °C, overnight, 81 %; b) *p*-TsOH·H_2O, $NaNO_2$, KI, MeCN, H_2O, 0 °C → rt, 70 %; c) Cu, 200 °C, overnight, 0 %.

The developed route commences from commercially available 2-amino-5-nitrophenol, which is decorated with a hexadecyl ether early on. Subsequently, an iodine functionality is generated from the amine group of **77** in a *Sandmeyer*-type reaction. These reactions are a very elegant way to functionalize arenes with atoms or groups that usually cannot be introduced with such low effort. The only requirement for this is the presence of an amino group that is *in situ* converted into a diazonium salt. Since *Sandmeyer*-type reactions do not proceed *via* the S_EAr mechanism, their regioselectivity is not determined by any directing effects of other substituents but solely controlled by the position of the diazonium group. Beyond that, while some *Sandmeyer*-type reactions require the presence of copper ions as oxidant, the iodination can be easily done with potassium iodide since iodide is able to reduce the diazonium group itself. Hence, it was possible to access a position in a substrate exclusively, that would not have been addressed as selective in an S_EAr of 3-nitrophenol.[15] **78** was then attempted to be homo-coupled in an *Ullmann* coupling.[24] The reaction conditions for this reaction were harsh as it was performed solely in the melt of the substrate at 200 °C.[133] Despite all efforts, it was not possible to isolate any of **79**. A likely explanation for the unsuccessful coupling is the strong repulsion originating from the hexadecyl-groups that are right next to the designated reactive center. As a consequence, the investigation of that route was not proceeded.

Instead, the results of *He et al.* were reproduced starting from commercially available 4-nitro-*o*-anisidine.[133]

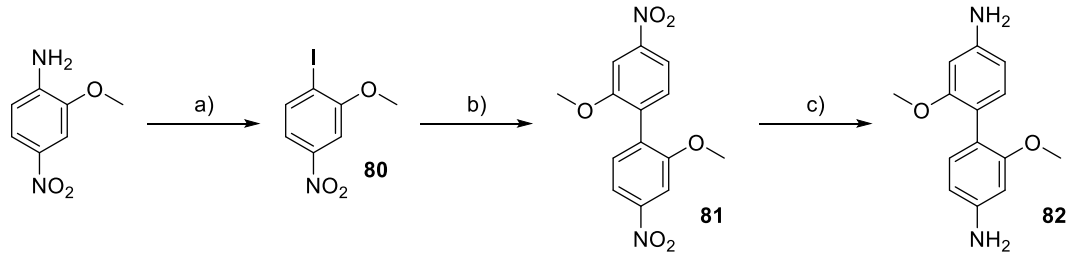

Scheme 82: a) *p*-TsOH·H_2O, $NaNO_2$, KI, MeCN, H_2O, 0 °C → rt, 70 %; b) Cu, DMF, 140 °C, overnight, 44 %; c) Sn, HCl, EtOH, 90 °C, overnight, 79 %.

As depicted, *He et al.* synthesizes **81** in a similar fashion. They start with the iodination of the amine group in the first step before doing an *Ullmann* coupling to homo-couple the arene into the biphenol ether. The feature of **81** is the presence of the nitro group. While for the previous reaction steps, a highly polar and deactivating group implies to be an obstacle, it can be seen as a "protected iodine". **81** can be reduced with tin metal in refluxing aq. HCl to diamine **82**, which is the substrate for another *Sandmeyer*-type reaction. In this fashion, two iodine functionalities can be generated in three steps uncompetitively and without any regioselectivity issues.[133]

While in theory such syntheses seem straightforward, their reproduction can often be demanding. The preparation of **80** was very difficult, as the reaction temperature needed to be controlled accurately. If the combined solution of sodium nitrite and potassium iodide was added only slightly too fast or if the temperature just slightly surpassed 4 °C, the mixture immediately started to foam vigorously due to the formation of nitrogen gas. Anyways, it was possible to synthesize the compound in good yields after staying within the described parameters.

The *Ullmann* coupling was reproduced as well under different conditions since the reproduction of the conditions provided in literature gave mediocre yields. While it was possible to replace the reaction in melt with DMF as solvent and therefore reduce the temperature from 200 °C to 140 °C, the yield did not improve after the still necessary *Soxhlet* extraction and remained at 44 %. Reduction of **81** then gave **82** after another *Soxhlet* extraction in a good yield of 79 %.[133]

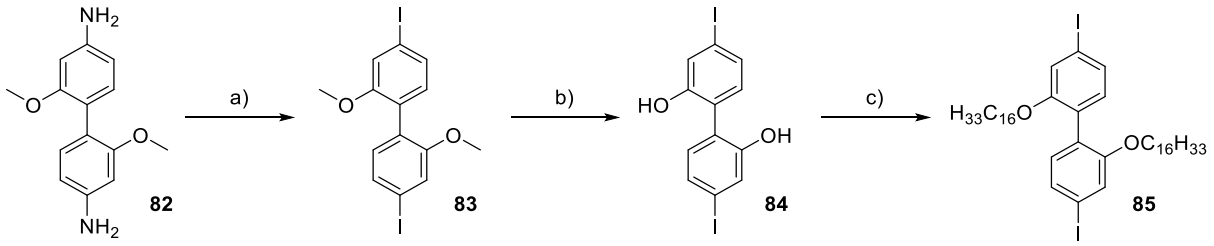

Scheme 83: a) HCl, $NaNO_2$, KI, H_2O, 0 °C → rt, 48 %; b) BBr_3, DCM, -78 °C → rt, overnight, 92 %; c) K_2CO_3, $C_{16}H_{33}Br$, KI, acetone, 60 °C, 46 h, 96 %.

82 was then iodinated in a two-fold *Sandmeyer*-type reaction. Gratifyingly, this conversion was not as sensitive to temperature as the preparation of **80** and worked without any foaming. The solution was

added to the mixture slowly but **83** was yielded in only 48 %. The low outcome might result from the two-fold conversion. A drawback of *Sandmeyer*-type reactions is their susceptibility to side reactions. Since the diazonium exchange can also be performed with water and the reagent solution is added aqueously, water might be a competitor. Due to the poor solubility, it was not possible to add sodium nitrite and potassium iodide as acetonitrilic solution. Besides that, *Sandmeyer*-type reactions occur over radical pathways that can tend to broaden the scope of byproducts.

In order to finally introduce the alkyl chains, the methyl ethers needed to be cleaved first. As before, a reliable method to do so is through the addition of a solution of BBr_3 at low temperature. Quenching with water and removal of the organic solvent under reduced pressure precipitated pure **84** in excellent yields of 92 %.[133]

The subsequent alkylation brought two welcome surprises with it. First, the reaction worked in excellent yields of 96 %. Second, the purification worked incredibly easy compared to the alkylation of fluorene. For fluorene, it was extremely tedious to remove any excess of alkyl chain due to the similar polarity of the product and the alkyl halide. For **85** this is not the case since the presence of ethers increases its polarity yielding pure product after medium to short columns.[133]

As already for the fluorene derivates it was attempted to access the required ester in a statistical reaction. This time, due to the rotational freedom around the biphenyl bond and the bulky side chains the substrate is no longer planar, which should impede the active palladium species from moving coordinated along the molecule and insert into the second carbon-iodine bond.[105]

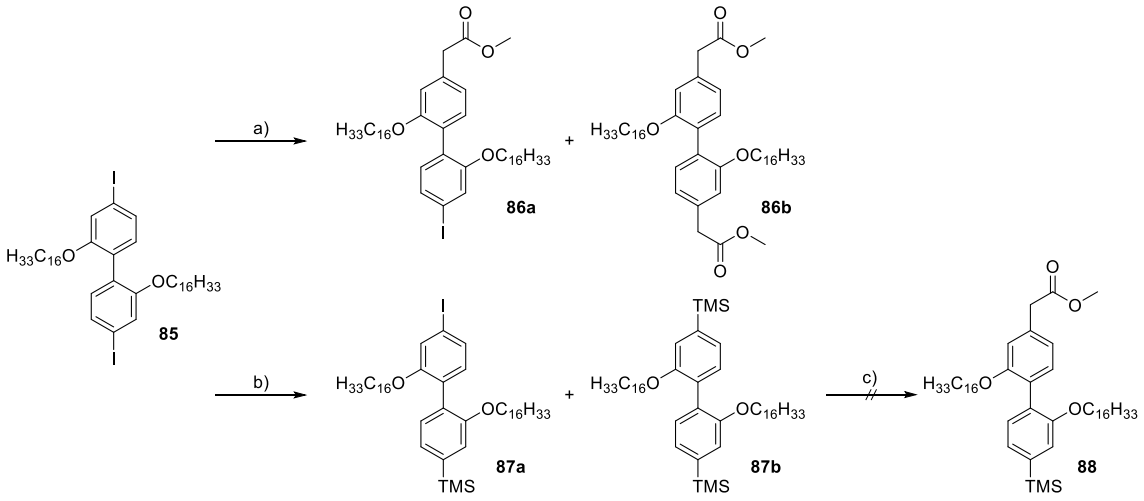

Scheme 84: a) *tert*-butyl bromoacetate, Zn, *XPhos*, $Pd_2(dba)_3$, THF, 50 °C, 46 h, 9 % (**86a**), 30 % (**86b**); b) *n*BuLi, TMSCl, THF, -78 °C → rt, 4 h; c) *tert*-butyl bromoacetate, Zn, *XPhos*, $Pd_2(dba)_3$, THF, 50 °C, 70 h, 0 %.

It was in fact possible to isolate **86a** in 9 % while the main product remained **86b** with 30 %. Even though it was possible to recover 48 % of the substrate, this method did not seem ideal. Instead, a one-sided protection of **85** was aimed at. Other than for the fluorene equivalent, this time also twice protected **87b** was found within the crude product. Due to the vanishing differences in polarity of **85**,

87a and **87b**, it was not possible to separate the mixture. Instead, the separation was planned after the next reaction step, because **87b** would not react at all here, remains of **85** would be converted into **86b** and targeted **88** should be easily separable from both byproducts. Investigation of the crude product of the followed step instead only revealed the formation of both byproducts in about equal amounts. The synthetic modification of the route of *He et al.* was discontinued here.

After two synthetic setbacks, the third approach towards a biphenol-based spoke was self-developed *via* an asymmetric approach. The idea was to introduce the acetic acid function already from the beginning to avoid any selectivity problems. The biphenyl bond was supposed to be formed *via* a *Suzuki* coupling. Since that reaction requires an aryl boronic acid and an aryl halide, two combinations of moieties are possible because both can be incorporated as either functional group host.

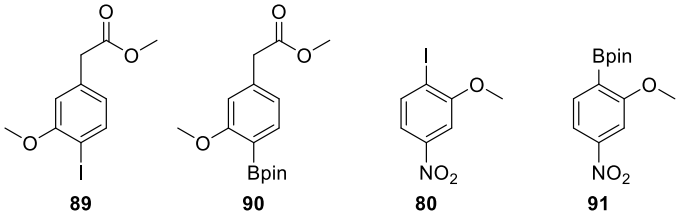

Figure 61: Four precursors for the asymmetric assembly of a biphenol-based spoke *via* two different Suzuki coupling pathways.

To optimize the reaction, all four components were synthesized first and utilized in a brief screening afterwards. Since both boronic esters needed to be prepared, their respective precursor served as coupling partner for the opposite boronic ester.

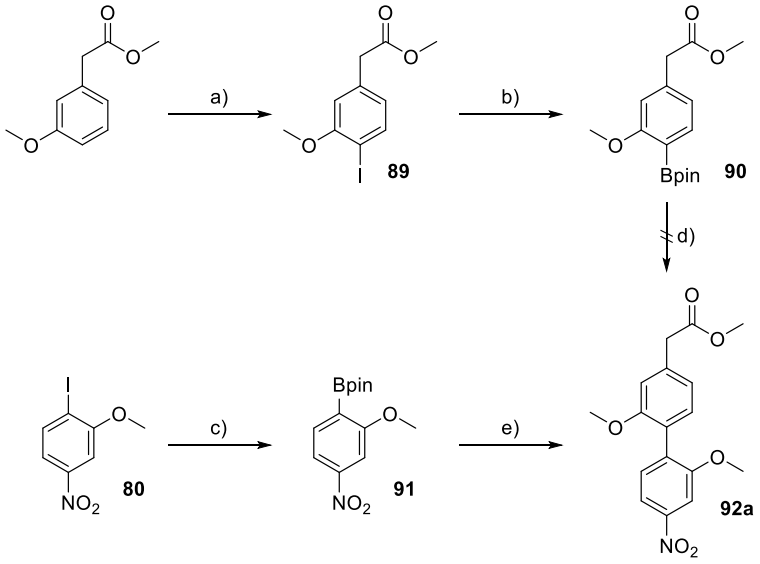

Scheme 85: a) ICl, DCM, rt, overnight, 86 %; b) KOAc, B_2pin_2, $PdCl_2(dppf)$, DMF, 105 °C, 17 h, 57 %; c) KOAc, B_2pin_2, $PdCl_2(dppf)$, DMF, 105 °C, overnight, 31 %; d) **80**, K_2CO_3, $PdCl_2(PPh_3)_2$, PPh_3, THF, 65 °C, 20 h, 0 %; e) **89**, K_2CO_3, $PdCl_2(PPh_3)_2$, PPh_3, THF, 70 °C, 48 h, 73 %.

Starting from commercially available methyl 3-methoxyphenylacetate the first component was synthesized *via* iodination under the same conditions as **32** before.[105] In theory, the iodination regioselectivity is not limited only to the 4-position but can also access the 2- and 6-position. In fact, both other isomers were observed during the synthesis.

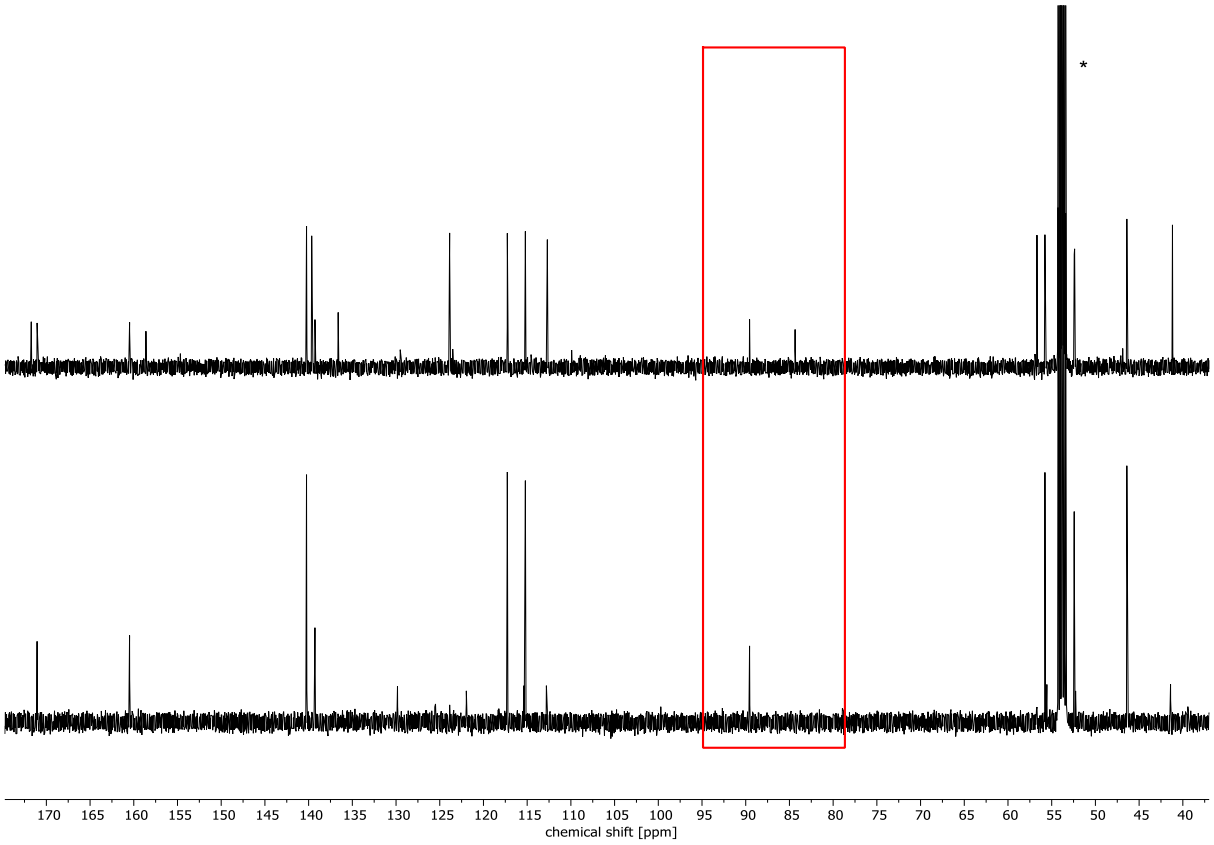

Figure 62: ^{13}C-NMR spectra in CD_2Cl_2 of mixed fraction of **89** and a regioisomer (top) and isolated **89** (bottom), the area with the signals corresponding to the iodinated carbon atoms is marked with the red box, the solvent is marked with *.

As mentioned before, the carbon-signal resulting from iodination of phenylenes can be observed in ^{13}C-NMR spectra nearly exclusively for the described substrates in the area around 90 ppm. On top of that, the regioisomers were observed to all feature individual shifts for their respective iodinated carbon atom, which enabled facile distinguishing after purification. In accordance with theory, the signal at 89.6 ppm can be assigned to **89** while the signal at 84.4 ppm is caused by an iodination in 2-position characterized through the high-field shift of the most shielded position.

Gratifyingly, it was possible to isolate **89** as the main isomer in 86 % after column chromatography. In a *Miyaura* borylation, **89** was converted into the respective pinacol ester in 57 % yield. The synthesis of **91** only worked about half as good while the same *Miyaura* reaction conditions yielded the pinacol ester in only 31 %.[117]

The comparison of both coupling pairs ended on a surprising result: While the synthesis of **89** and **90** worked in higher yields than for their counter parts, the coupling of **90** with commercially available **80** was unsuccessful. The synthesis of **92a** on the other hand peaked at a yield of 73 %.

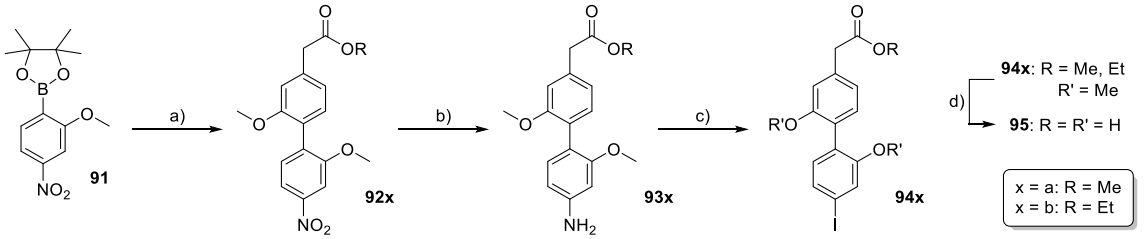

Scheme 86: a) (a): **89**, K_2CO_3, $PdCl_2(PPh_3)_2$, PPh_3, THF, 70 °C, 48 h, 73 %; (b): **89**, K_2CO_3, $PdCl_2(PPh_3)_2$, PPh_3, PhMe, EtOH, 80 °C, 48 h, 54 %; b) $SnCl_2$, EtOH, 90 °C, overnight, 77 % (**93a**), mixed fraction (**93b**); c) *p*-TsOH·H_2O, $NaNO_2$, KI, MeCN, H_2O, 0 °C → rt, 80 % (**94a**), 46 % (**94b**, yield over two steps); d) BBr_3, DCM, -78 °C → rt, overnight, 88 %.

On the way to that peak, different reaction conditions were investigated. As before, the choice of solvent in one case led to a trans-esterification influencing the molecular structure. Since the ester was planned to be cleaved later anyways, this was not seen as problem.

In the same fashioned sequence as described by *He et al.*, **92a** and **92b** were reduced into the respective amines. The conversion of **92a** was at first performed with tin in aq. HCl as before.[133] In fact, those harsh and acidic conditions cleaved the ester, which in theory was not a problem for the following reaction steps but turned out to be an obstacle for the purification. Due to the successful reduction accompanied by the cleaved ester, the resulting product was an amino acid. Those compounds tend to form a zwitter-ionic structure, which obviously interacts strongly with polar silica gel. Thus, it was not possible to recover the species from column chromatography. To avoid the presence of HCl, tin was substituted by adding tin(II) chloride instead of generating it *in situ*. Overall, the conversion of **92a** into **94a** worked in 62 % over two steps, while the respective ethyl ester was only converted in 46 % over two steps.

Deprotection of the methyl ethers with BBr_3 ended in a global deprotection for both **94a** and **94b** instead.

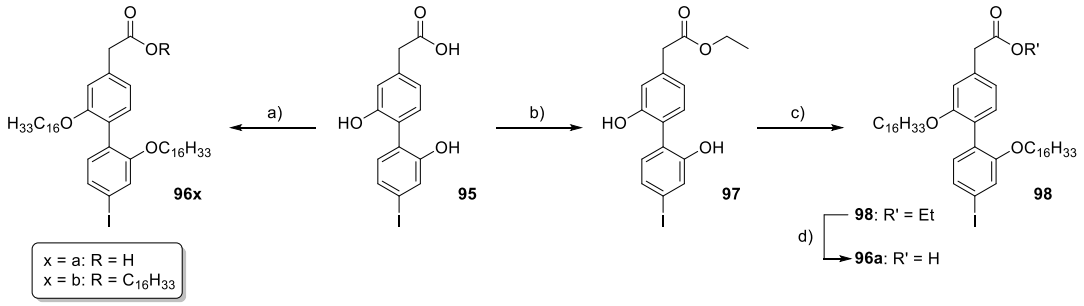

Scheme 87: a) K_2CO_3, $C_{16}H_{33}Br$, KI, acetone, 60 °C, 20 h, 8 % (**96a**), 28 % (**96b**); b) H_2SO_4, EtOH, 90 °C, overnight, 85 %; c) K_2CO_3, KI, 18-C-6, $C_{16}H_{33}Br$, acetone, 60 °C, 5 d, 46 %; d) LiOH·H_2O, THF, H_2O, 60 °C, 20 h, 98 %.

The conversion of **95** gave the desired compound in poor yields. The main product of the reaction was hexadecyl ester **96b** in 28 % yield accompanied by the desired acid **96a** in only 8 % yield. Since the ester cleavage of **96b** was unsuccessful, the route was slightly modified over the step of reprotecting the acid function of **95**. The esterification yielded **97** in 85 % without further purification and the

additional ethyl group increased its solubility drastically in hopes of contributing to a higher conversion in the following etherification step. Frustratingly, the previously successful conditions of *He et al.* only yielded **98** in 36 %.[133] Even though alternative conditions boosted the yield to 46 % through the incorporation of 18-C-6,[134] still large amounts of substance are lost at a late stage.

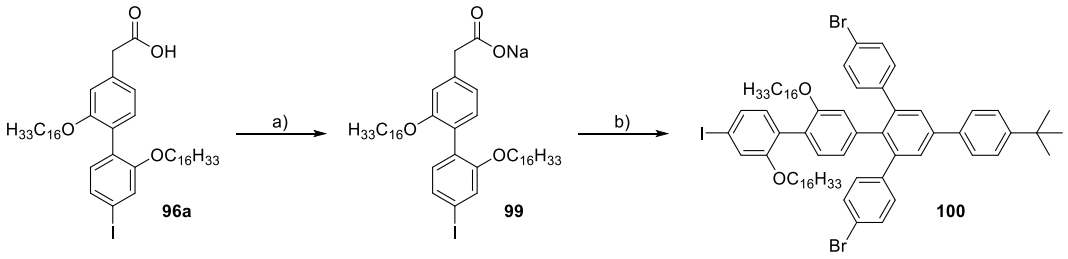

Scheme 88: a) NaO*t*Bu, HO*t*Bu, 40 C, 2.5 h, 100 %; b) **14**, Bz_2O, 150 °C, 4 h, 30 %.

The quantitative conversion of **96a** into the corresponding sodium aryl acetate **99** finally completed the synthesis of the biphenol-based spoke unit. The followed *Zimmermann-Fischer* reaction yielded the anchor-shaped molecule **100** in 30 %.

After the problematic separation of **17a** (compare chapter 5.1.1), the following synthesis of symmetric alkyne **102** was faced deferentially. The possibility of *Glaser*-byproduct formation that consumes precious substrate, but, more importantly, whose separation is time-consuming was too big of a threat to consider *Sonogashira* couplings especially at such a late stage. *Eichler et al.* proposed a forceful solution to that problem. In their work they published a method to access symmetric diarylacetylenes in one-pot syntheses from various aryl halides that were reacted with bis(tributylstannyl)acetylene in a two-fold *Stille* coupling.[135] While the group synthesized the central unit themselves, it was found to be commercially available and therefore purchased.

To see if this reaction was applicable to the desired systems, a test system for the one-pot reaction was investigated first. Since biphenol ether halides are hardly commercially available and the synthesis of a spoke-like model system would be nearly as consuming as reproducing the spoke, it was decided to start from a simple replacement in the guise of 4-iodobiphenyl.

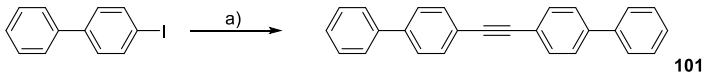

Scheme 89: a) Bis(tributylstannyl)acetylene, $Pd(PPh_3)_4$, PhMe, 50 °C, 3 d, 35 %.

From crude product MALDI mass spectrometry, it was learned, that in fact product was formed. Problematic on the other hand was the presence of tributylstannyl species even after column chromatography revealed by NMR spectroscopy. Due to the high affinity of tin to form stable tin-fluorine bonds, literature states those impurities can be removed through treatment with potassium fluoride precipitating tributylstannyl fluoride. Unfortunately, neither vigorous shaking of a

crude product solution with aq. 1 M KF solution for several minutes, nor stirring the mixture overnight in different solvent constellations removed the impurities in a measurable amount.

Harrowven et al. developed a method that seems rather dubious at first. They stated, that the replacement of ten weight-percent of silica through potassium carbonate in the stationary phase of column chromatography removes stannyl impurities down to a level of 15 ppm.[136] Anyhow, the application of such column chromatography isolated **101** in 35 % fully removing any stannyl impurities according to NMR spectroscopy.

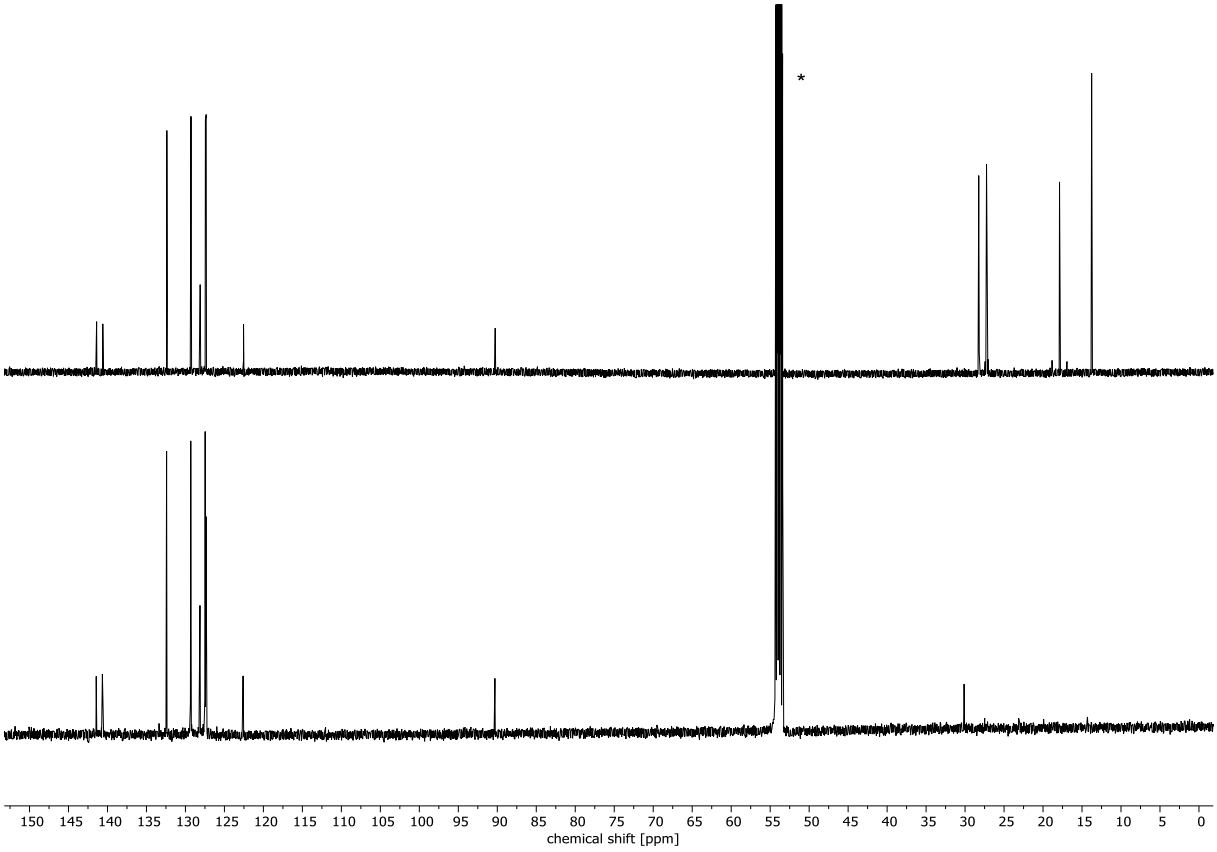

Figure 63: ^{13}C-NMR spectra of the fraction containing mainly **101** after column chromatography using silica as the stationary phase (top) and after column chromatography using silica:K_2CO_3 (9:1) (bottom).[136] In the top spectrum, signals caused by tributylstannyl-based byproducts are clearly visible in the region between 30 and 10 ppm. Those signals fully vanish after the latter purification method.

To put this seemingly medium yield into perspective, the conversion of **15** into similar-sized **17a** only yielded the symmetric acetylene in 6 % over two steps. Except **39** (that was received in 32 % yield), all other symmetric acetylenes synthesized up to this point were received in a maximum of 21 % in one-pot syntheses, ranking the method of *Eichler et al.* as the most promising strategy for the synthesis of **102** yet.

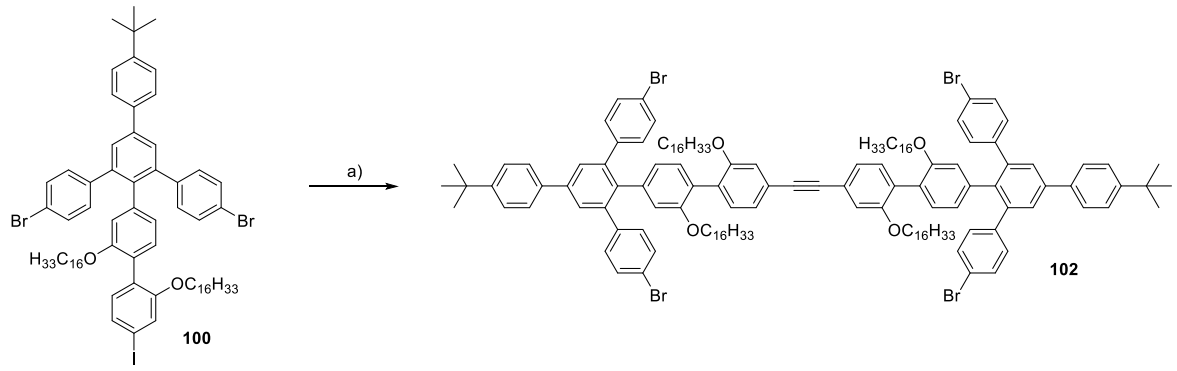

Scheme 90: a) Bis(tributylstannyl)acetylene, $Pd(PPh_3)_4$, PhMe, 50 °C, 6 d, 78 %.

The outcome of the reaction surpassed any hopes and expectations by far. After five days of reaction, the progress of the reaction was investigated *via* analytical GPC.

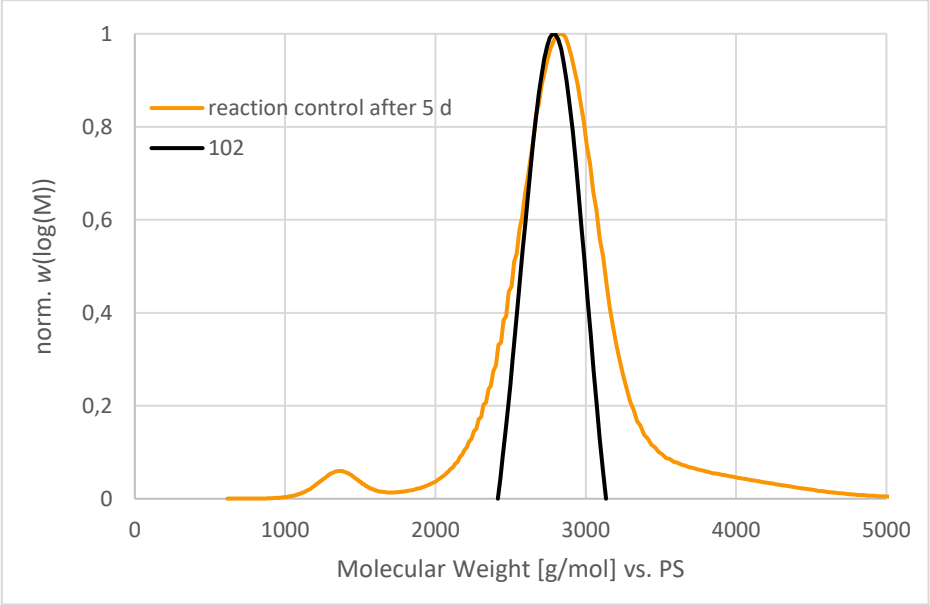

Figure 64: Molar mass distribution (THF, *vs* PS) as reaction control of the synthesis of **102** *via* analytical GPC showing the crude product mixture after six days with the isolated compound as a reference.

As the elugram revealed, **102** was the main product formed. The crude product was pre-purified *via* column chromatography using the stationary phase suggested by *Harrowven et al.*[136] and further purified *via* recGPC in THF. Since THF is stabilized with BHT during that process, it needs to be removed from the collected fractions through precipitation of the products from methanol. After these three purification steps, **102** was yielded in incredible 78 %. To put this in perspective once again, 78 % equals 88 % per step in a two-step *Sonogashira* pathway, which was neither achieved for the synthesis of **18** nor by *Kersten* for his octyl-equivalent that was isolated in 38 % yield over two steps.[105] Beyond that, MALDI mass spectrometry of the crude product mixture revealed the exclusive reaction of the C-I bond over the C-Br bond showing the absence of any bromine-related coupling products resulting in a fully

iodine-selective conversion. This was observed for no other symmetric alkyne prepared within this work to that degree.

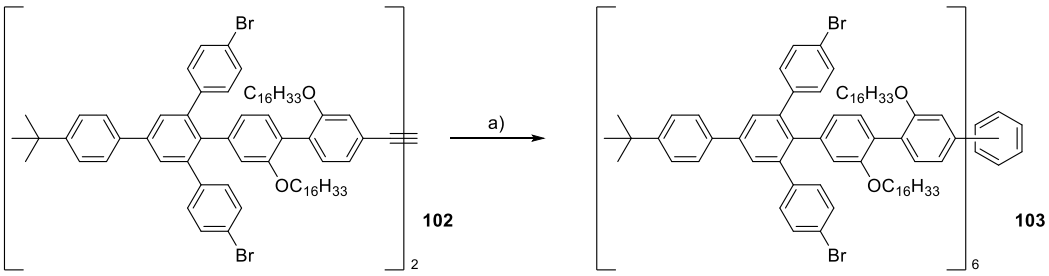

Scheme 91: a) $Co_2(CO)_8$, PhMe, 135 °C, 5 d, 5 %.

Subsequently, the successfully isolated alkyne was trimerized in a *Vollhardt* reaction. Reaction control after different periods of times showed that the formation of the desired product only proceeded slowly.

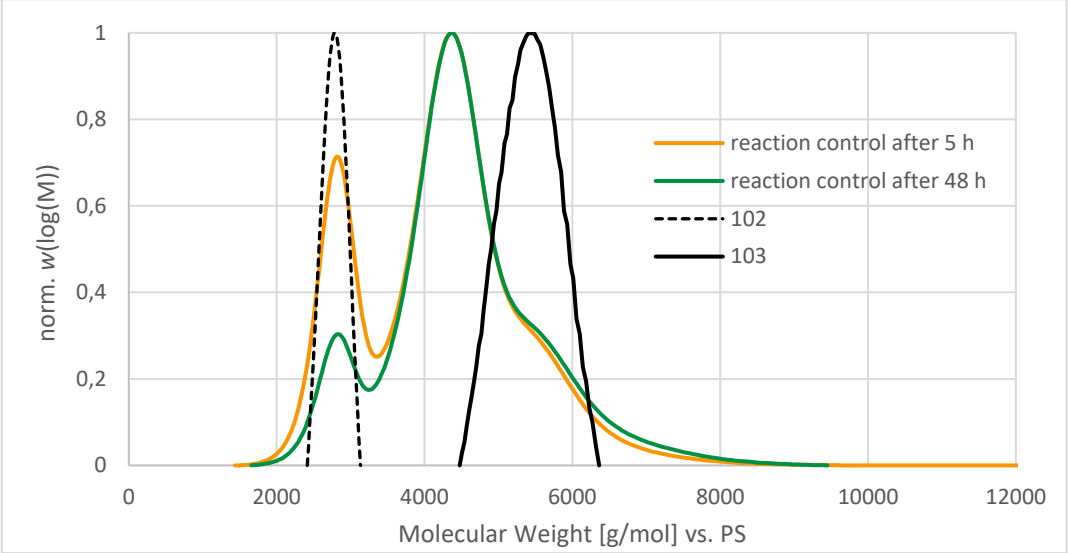

Figure 65: Molar mass distribution (THF, *vs* PS) as reaction control of the synthesis of **103** *via* analytical GPC showing the crude cyclization product after different periods of time with the isolated compound and precursor **102** as reference.

Purification of the crude cyclization product *via* recGPC yielded **103** in only 5 %. To boost the conversion, the synthesis was reproduced but this time, the progress of the reaction was checked every day and more catalyst was added afterwards. Details on the amounts added can be found in the experimental discussion (compare chapter 9.4).

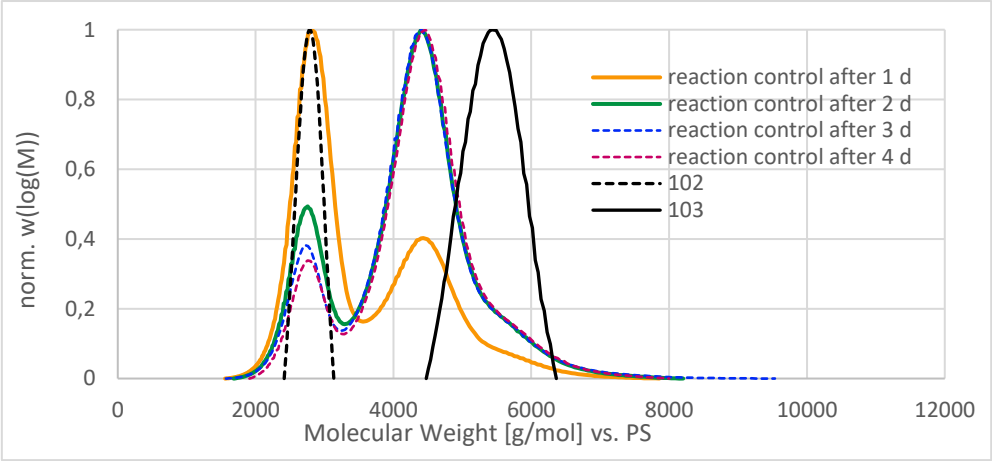

Figure 66: Molar mass distribution (THF, *vs* PS) as reaction control of the second synthetic approach of **103** *via* analytical GPC showing the crude cyclization product every 24 h with the isolated compound and precursor **102** as a reference. This time, for better visibility all reaction controls are displayed as dotted lines.

The elugram reveals that after 48 h no further formation of **103** is observed, while **102** seems to get consumed until the reaction was terminated. Beyond that, **103** is again not the main product formed because it can be identified as a shoulder of a signal corresponding to an unidentified species of smaller hydrodynamic radius. In the end, after recGPC the yield of **103** was still limited to 5 %. For unknown reasons, **103** could only be characterized *via* MALDI mass spectrometry. NMR spectra recorded at either room temperature or 100 °C did not deliver any evaluable data.

As predicted, the trimerization step might be a bottleneck for the synthesis of **MSW-H**. Similar to the synthesis of **18** the bulk introduced through the hexadecyl chains might acutely hinder the reaction explaining the low rate of formation. This hypothesis is further underlined through the constant addition of fresh catalyst ensuring the presence of an active species over the full reaction time. While it was unclear if the additional flexibility of biphenol over fluorene would positively influence the formation of the trimer, in a way this assumption was confirmed. Yet a yield of 5 % is far from desirable, it is a clear increase compared to **18** that was only accessible in traces and not fully isolated. The increase is in fact that big, that enough substance was collected to approach the final reaction step, which was not possible with **18**.

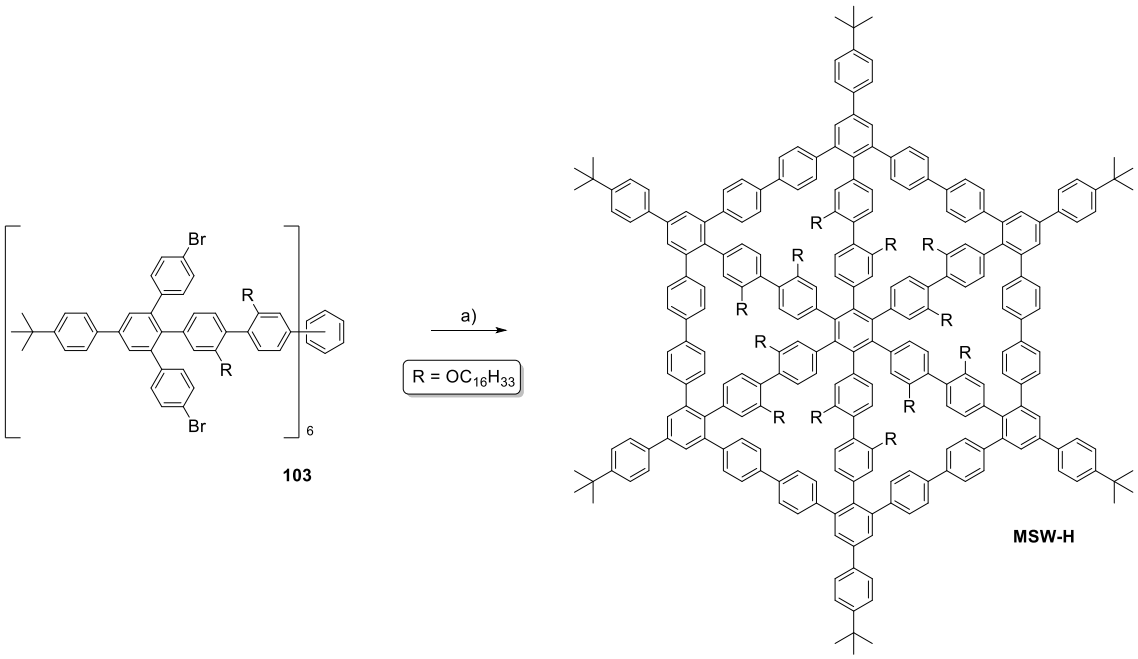

Scheme 92: a) $Ni(COD)_2$, bipy, THF, COD, 12 min, 300 W, 120 °C (mw), 75 %.

The six-fold *Yamamoto* reaction was carried out in a microwave reactor under the same conditions presented for the syntheses of the other MSWs of this work. The conversion was checked afterwards *via* analytical GPC as depicted in the following.

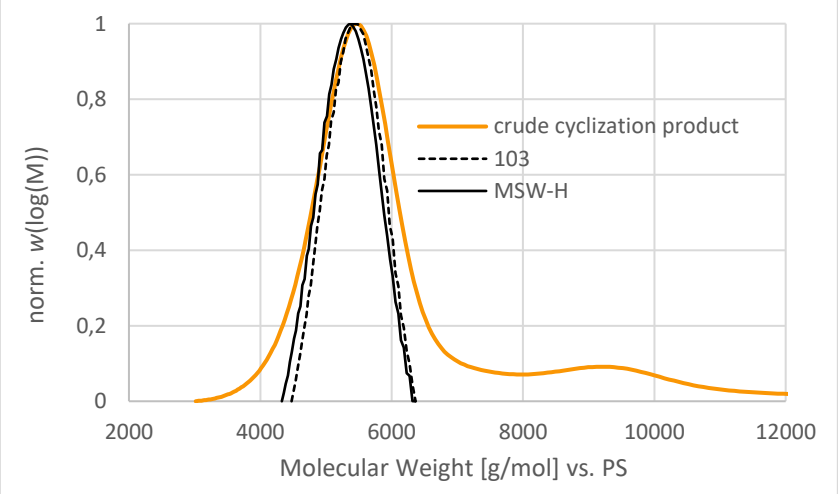

Figure 67: Molar mass distribution (THF, *vs* PS) as reaction control of the synthesis of **MSW-H** *via* analytical GPC showing the crude cyclization product after filtering column chromatography with the isolated compound and precursor **103** as a reference.

Even though the reaction control *via* analytical GPC does not suggest the formation of **MSW-H**, it was possible to isolate the desired compound in an excellent yield of 75 % *via* recGPC as the main product. With a collected amount of 6.6 mg, it was possible to record a full data set of the described compound. Unfortunately, the ^{1}H-NMR spectrum was not very informative because it was mostly noise-dominated at both room temperature and 100 °C, which is a behavior that was also observed for its precursor

103. The close proximity of different phenylenes and the molecule's high symmetry lead to overlayed signals slightly shifted towards each other and therefore a spectrum of low significance. In contrast to that, its ^{13}C-NMR spectrum delivers all the anticipated signals individually, where the concentration for **103** was too low to identify those. MALDI mass spectrometry finally confirms the formation of **MSW-H**. Even though **MSW-H** was accessible as a model system, the bottleneck within the trimerization step discouraged from continuing the investigations regarding biphenol-based spokes as suitable substrates for MCW preparations for now.

5.3 Investigation of symmetric acetylene preparation conditions

The synthetic breakthrough for the synthesis of **102** sparked the interest in *Stille* couplings as the new preferred method for the syntheses of symmetric alkynes as precursors for MSWs. After the many setbacks resulting from low conversions in the two-fold *Suzuki* couplings, there was plenty of room for improvement.

Hence, a new central unit was necessary. Since the respective stannyl compound was not commercially available, it needed to be prepared from **37**.

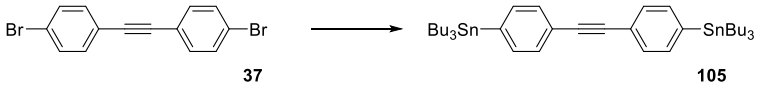

37 **105**

Scheme 93: Synthesis of the central building block **105** as a symmetric acetylene precursor for MSWs, attempted under various conditions (compare Table 3).

The synthesis of **105** required a diverse screening of conditions regarding the utilized organometallic compounds, the stannyl source and the solvent.

The first investigated conditions involved the formation of an organolithium compound at low temperatures through addition of *n*BuLi, where lithium is then exchanged with the desired stannyl group.[137] Investigation of the crude product only suggested dehalogenation of **37**. Substituting *n*BuLi with the more reactive *s*BuLi did not change the outcome. In the third attempt, a palladium-catalyzed stannylation was tried. The *Stille* coupling can proceed without the presence of any base, thus, there is strong competition between the desired Br-$SnBu_3$ exchange and an undesired *Stille* coupling of the generated tin organyl with the substrate. Investigation of the crude product revealed the latter to be dominant under the applied conditions evidenced by the formation of oligomers.[138] Even though the preparation of *Grignard* reagents is often taught to undergrad students already, its practical execution can be demanding. The most difficult aspect about this reaction is to keep it free of moisture while magnesium needs to be stripped off its oxide layer. Unfortunately, neither the activation of magnesium with diluted HCl nor the *in situ*-activation through the addition of crumbs of molecular iodine led to

any observable formation of a *Grignard* reagent. The method proposed by *Nechaev et al.* finally led to the desired compound. Their catalytic system consisting of $Pd(OAc)_2$ and PCy_3 yielded **105** in 43 % while generating only small amounts of oligomers.[138]

An overview over the reaction conditions investigated for the preparation of **105** is given in the following.

Table 3: Overview over the screened reaction conditions for the synthesis of **105**.

#	*Metalation compound*	*Stannyl source*	*Solvent*	*Yield [%]*
1	*n*BuLi (1.6M)	Bu_3SnCl	THF	0
2	*s*BuLi (1.4M)	Bu_3SnCl	THF	0
3	$PdCl_2(PPh_3)_2$	Bu_6Sn_2	toluene	0
5	Mg	Bu_3SnCl	THF	0
6	$Pd(OAc)_2$, PCy_3	Bu_6Sn_2	-	43

Once **105** was accessible, its applicability needed to be elucidated. Since the breakthrough regarding the preparation conditions of **105** was made during the synthesis of **MSW-Fb**, its acetylene precursor became the test system for the following screening.

As presented, the synthesis of a symmetric acetylene requires an anchor-shaped molecule like **69b** and a central unit. While the connection *via* **38** was sufficiently discussed already, it was unclear if the poor yields can be boosted in a reaction carried out under *Stille* conditions. First, the conditions yielding **102** in an excellent yield were applied and second, the conditions published by *Keay et al.* were employed finding that the use of tri(2-furyl)phosphine (TFP) as a ligand in *Stille* couplings can have a positive impact on the reaction's yield.[139]

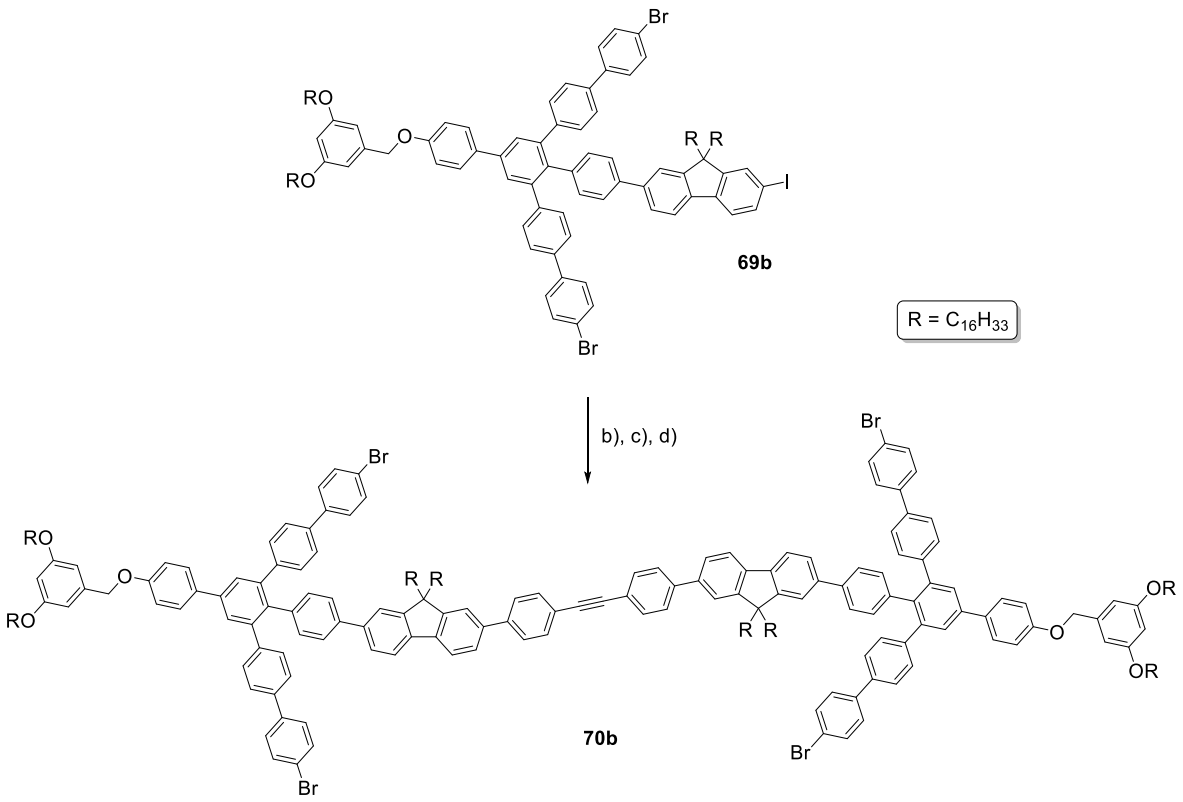

Scheme 94: Synthesis of **70b** investigated under various conditions. b) **38**, Cs_2CO_3, $Pd(PPh_3)_4$, PhMe, H_2O, 50 °C, 5 d, 10 %; c) **105**, $Pd(PPh_3)_4$, PhMe, 50 °C, 5 d, 1 %; d) **105**, $Pd_2(dba)_3$, TFP, PhMe, 50 °C, 5 d, 4 %.

Unfortunately, it was not possible to improve the yield through *Stille* couplings. The reproduced conditions were only able to yield 1 % of **70b** while the conditions of *Keay et al*. gave the product in 4 % yield.[139] The applied *Suzuki* conditions yielded 10 % of the desired species, as discussed in detail before (compare chapter 5.1.6).

Since the achieved results were not nearly satisfying, the conditions for **102** needed to be reproduced more accurately. To closer match the substrates, **70b** needed to be elongated by one phenylene unit in order to make use of bis(tributylstannyl)acetylene again. To avoid the bromine-iodine selectivity problem in substrates like **69b** it was decided to perform the elongation at an earlier stage.

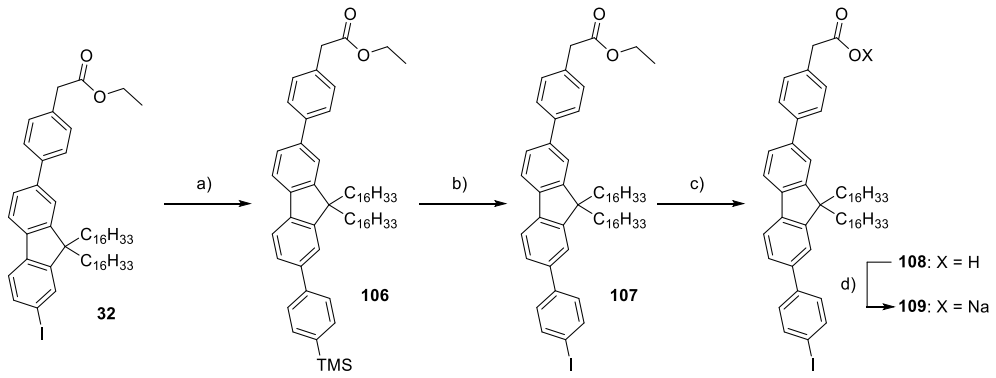

Scheme 95: a) 4-(Trimethylsilyl)phenyl boronic acid, K_2CO_3, $PdCl_2(PPh_3)_2$, PPh_3, PhMe, EtOH, 90 °C, overnight, 39 %; b) ICl, DCM, rt, overnight, 99 %, c) $LiOH \cdot H_2O$, THF, H_2O, 60 °C, 20 h, 99 %; d) NaO*t*Bu, HO*t*Bu, 40 °C, 3 h, 100 %.

Starting from **32**, the elongation was performed in another *Suzuki* coupling adding 4-trimethylsilyl phenylboronic acid. In the first attempt, this reaction was carried out in a mixture of toluene and water using $Pd_2(dba)_3$ as catalyst.[96] The conversion of the reaction was not quantitative, ending in a product-substrate mixture that was impossible to separate due to the similar polarity of both compounds. Applying the catalyst system already used for the synthesis of **31** yet only gave **106** in 39 % yield, but it was possible to isolate the desired product. The following sequence of iodination, ester cleavage and ion exchange worked in almost quantitative fashion. Hence, their purification worked straightforwardly and without complications.

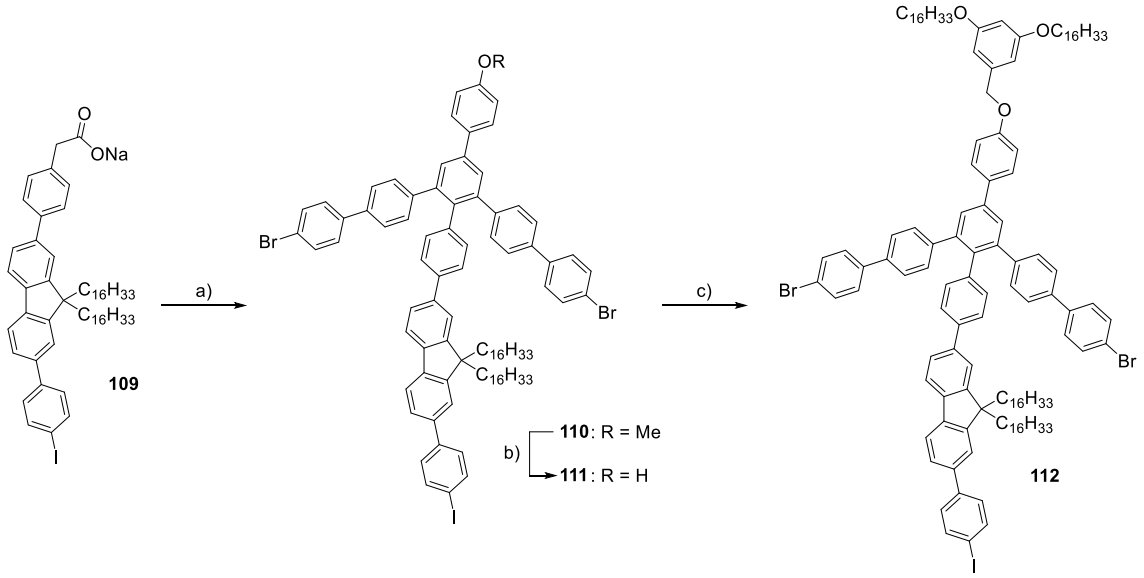

Scheme 96: a) Bz_2O, 150 °C, 5 h, 21 %; b) BBr_3, DCM, -78 °C → rt, overnight, 80 %; c) **68b**, Cs_2CO_3, DMF, 100 °C, 48 h, 65 %.

The subsequent *Zimmermann-Fischer* condensation between **109** and **65** yielded the targeted anchor-shaped compound in 21 %. As before, the anchor-shaped compound was deprotected in 80 % and re-functionalized with **68b** yielding the final coupling moiety in 65 %, but with impurities of remaining **68b** that could not be separated off *via* column chromatography.

With **112** finally prepared, its conversion into a symmetric alkyne was to be investigated.

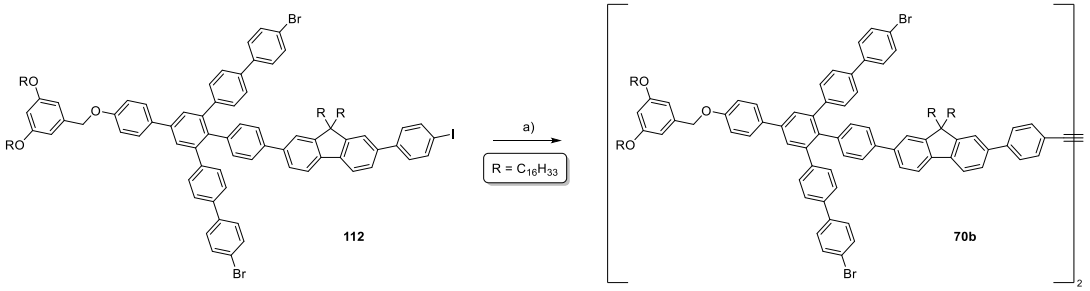

Scheme 97: a) Bis(tributylstannyl)acetylene, $Pd(PPh_3)_4$, PhMe, 50 °C, 5 d, 46 %.

Sadly, it was only possible to test **112** in one reaction as it was only obtained in 102.5 mg impurely. Thus, it was decided to apply the conditions successfully utilized in the synthesis of **102** instead of the untested catalyst system consisting of $Pd_2(dba)_3$ and TFP.

After five days, the progress of reaction was monitored *via* analytical GPC as usual.

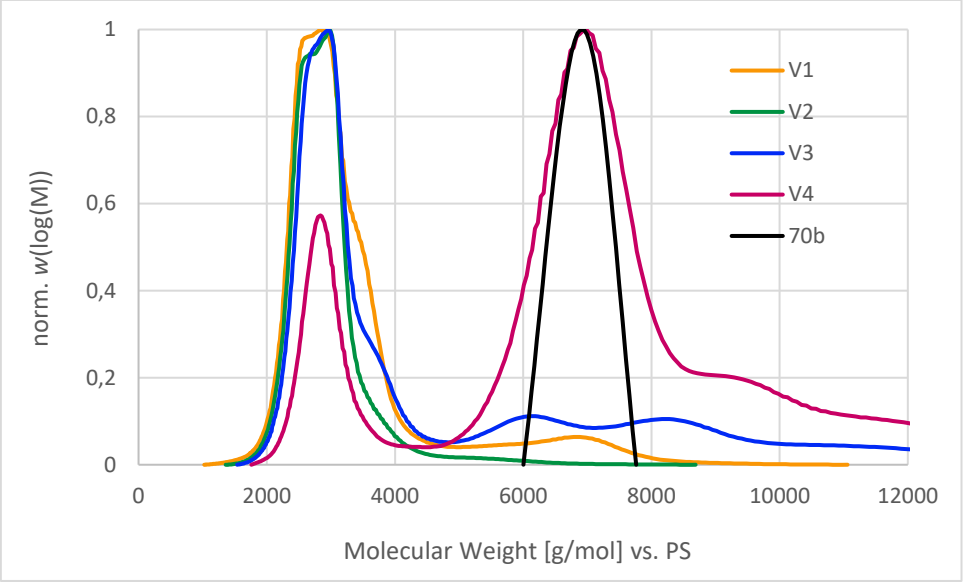

Scheme 98: Molar mass distribution (THF, *vs* PS) as reaction control of the synthesis of **70b** *via* analytical GPC showing the crude product mixture of four different reaction conditions (V1-V4, compare Table 4) after filtering column chromatography with the isolated compound **70b** as a reference.

The elugram shows one species to be formed majorly with a large gap towards the next signal. From this, two things can be learned: first, it appears that the desired compound was formed as the main product, as it has the highest signal intensity and second, that no single-coupled product was formed due to the missing corresponding signal. The crude product was pre-purified *via* column chromatography (SiO_2:K_2CO_3 9:1) as **102** before,[136] and **70b** was isolated *via* recGPC. Astonishingly, the compound was received in 46 % yield by far surpassing any other applied conditions. While this yield is lower than for the synthesis of **102**, the impurity of **112** needs to be taken into account formally lowering the maximum possible outcome. Despite that, the applied *Stille* conditions turned out to be unrivaled once more.

Summarizing, it can be said that all applied conditions yielded the product. Interestingly, the *Stille* conditions only gave the desired compound in a good yield for the *sp*-sp^2 coupling systems. The distinguishing benefit is that **106** even though being a bottleneck regarding the total yield can be prepared on a gram scale in advance, because its work up is straightforward *via* column chromatography. Starting on a larger scale, the same amount of anchor-shaped precursor can be prepared, but followed by a far more efficient two-fold coupling. The real advance here only gets clear considering the limits of recGPC separation. For such syntheses, one injection takes about 8 h of separation time while being capped to about 30 mg per injection. Assuming the synthesis of **70b** with

a crude product mixture of about 180 mg, the separation requires a minimum of two days. With so much effort put into one stage, it makes a tremendous difference if 13 mg or 50 mg are yielded after a very time-consuming separation.

The preferred conditions should therefore be chosen based on the overall efficiency of the method instead of simply on its yields. Anyways, the results for all four conditions tested are displayed in the following table compactly.

Table 4: Overview of the reaction conditions applied for the synthesis of **70b** from **69b** and **112**, all carried out at 50 °C over five days under argon atmosphere.

#	*Substrate*	*Central unit*	*Catalyst*	*Solvent*	*Yield [%]*
V1	**69b**	**38**	$Pd(PPh_3)_4$	PhMe/ H_2O	10
V2	**69b**	**105**	$Pd(PPh_3)_4$	PhMe	1
V3	**69b**	**105**	$Pd_2(dba)_3$, TFP	PhMe	4
V4	**112**	$(Bu_3Sn)_2C_2$	$Pd(PPh_3)_4$	PhMe	46

6 Quantum Chemical Investigations

The incorporation of fluorene redesigning *Sterzenbach*'s approach in order to access a 30 Ph-MSW brought certain risks with it. Due to the curved nature of fluorene, it was unclear if the open-framed trimer would be closable as the curvature tilts all anchor-shaped groups out of the plane. Hence, it might be possible that the necessary distance for their connection cannot be reached. *J. Kohn* from the *Grimme* group consented to do quantum chemical calculations on that issue.

The first step for *Kohn* was investigate the mechanism of the *Yamamoto* coupling. With these simulations, it was not the aim to elucidate all intermediates and to propose a new mechanism for the reaction, but to investigate the behavior and geometry of the MSW-precursors over the reaction. To investigate the mechanism of the reaction, it needs to be understood first.

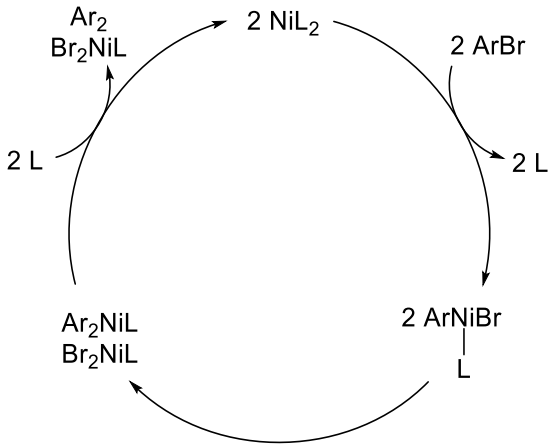

Scheme 99: Postulated cycle proposed by *Yamamoto*.[99] L represents bidentate ligand here.

In the first reaction step, an oxidative addition to the Ni complex takes place under the loss of one ligand. Two of the formed mixed species react in a transmetalation into the diaryl and the dibromo nickel compound. While the diaryl species reductively eliminates a biaryl and enters another cycle, the dibromo compound does not. Therefore, this reaction cannot be seen as catalysis.

Kohn translated the observations made by *Yamamoto et al.*[99] into a quantum chemical equivalent elucidating geometries and relations between the intermediates at the model system of bromobenzene.

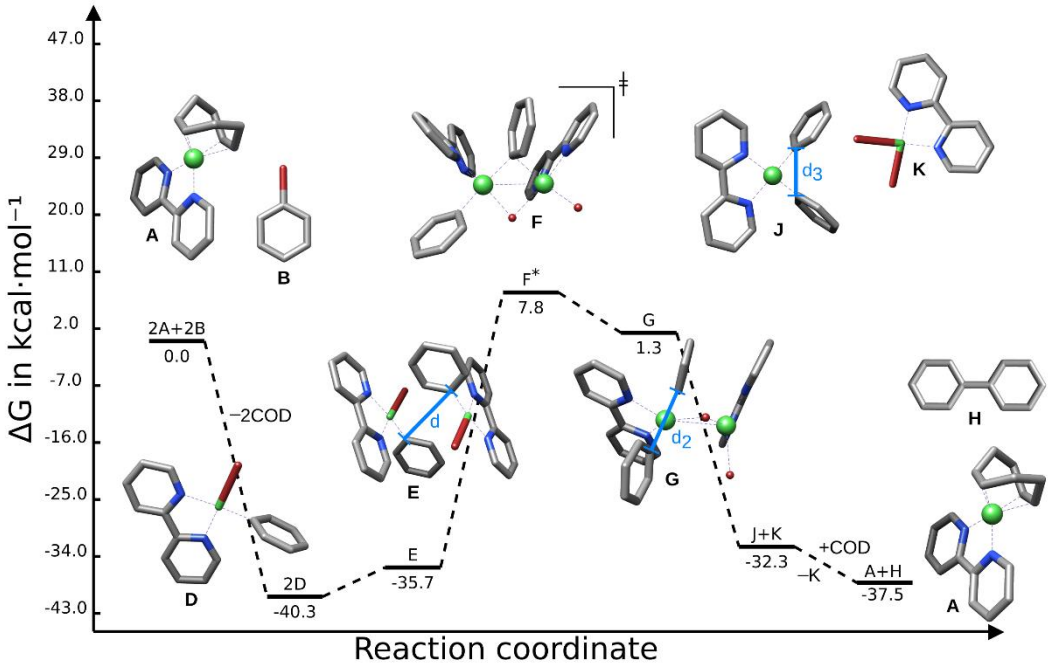

Figure 68: Quantum chemical investigation of all relevant steps within the nickel-mediated *Yamamoto* coupling of two equivalents of bromobenzene (**B**). The applied metal species is Ni(COD)(bipy) (**A**), that is converted into Ni(bipy) as active species.

Figure 68 graphically shows the results of *Kohn*'s investigations. A step of utmost importance is found at intermediate **E**. Here, two equivalents of the oxidative addition-complex PhNiBr(bipy) approach each other before forming transition state **F**. Complex **E** elucidates the distance *d* between the bromine-functionalized carbon atoms (Figure 68, blue) that needs to be reached at least for **F** to form. While for two separate, unhindered molecules like bromobenzene this may seem irrelevant, it is highly relevant for the synthesis of MSWs, as here both bromobenzene molecules are covalently bound in the open-framed precursor. Thus, the precursor needs to be able to change its conformation in such way, that an adequate distance *d* can be reached if a successful closure of two rim fragments should occur within a MSW. For bromobenzene, that distance was found to be *d* = 5.4 Å.

To find out if that distance can be reached during the closing process of MSWs, the sequence of closure must be investigated as well. Since complex structures like MSWs do not necessarily close clockwise and due to the harsh applied conditions in the presence of an excess of the mediating metal, all possible closure paths need to be taken into account to yield an accurate simulation.

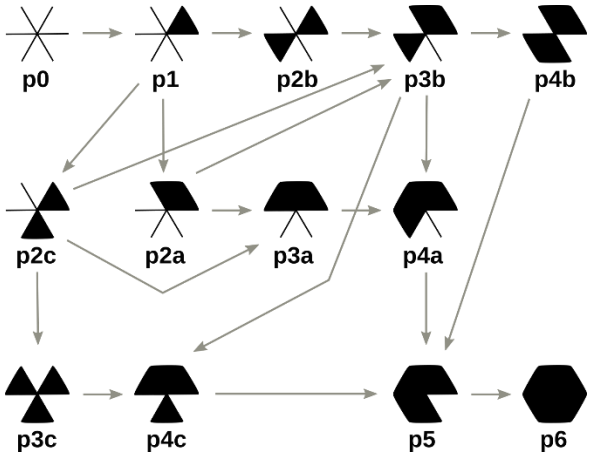

Scheme 100: Schematic overview over all possible intermediates of the six-fold *Yamamoto* coupling starting from an open-framed precursor (**p0**) towards the closed MSW (**p6**). Filled triangles represent closed bonds while voids represent open connection positions.

For a successful closure, a second aspect needs to be considered. Besides the distance *d* that needs to be reached, investigations regarding the strain, that a newly formed bond introduces into the system, needs to be considered as well. Fortunately, a highly suitable reference system was synthesized by *G. Ohlendorf* in the past. *Ohlendorf* synthesized cyclophanes attached to quinquephenylenes, that were cyclized in the final step in a two-fold *Yamamoto* coupling under identical conditions as MSWs.[140]

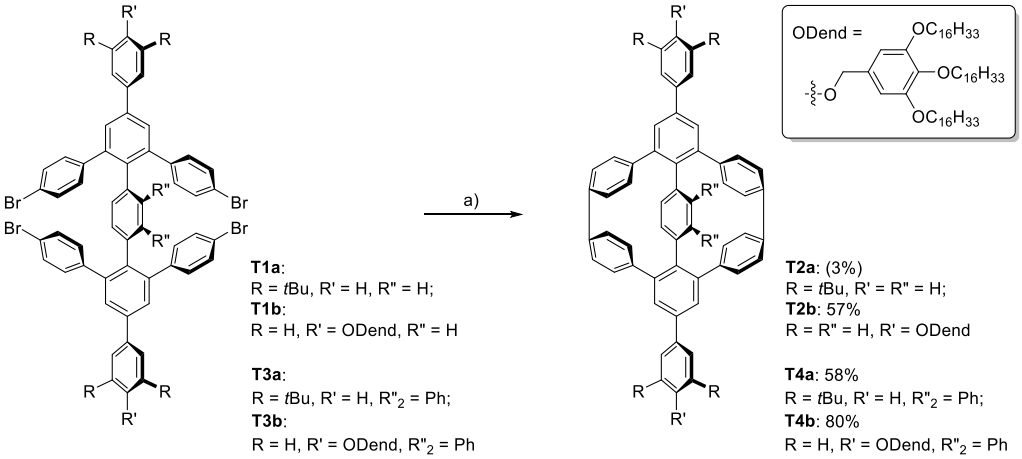

Scheme 101: Synthetic efforts of *Ohlendorf* yielding different cyclophanes in one-pot reactions (left). a) $Ni(COD)_2$, bipy, THF, COD, 12 min, 300 W, 120 °C (mw).[140]

From these systems, it was known that they achieved excellent results under identical conditions and that they were closed successfully despite the undeniable introduced strain resulting from each further coupling. *Kohn* calculated the strain energies for **T2a** and **T4a** to save computational resources assuming the dendron groups had only minor influence on the strain-introducing steps. From that demanding system, a threshold of about 35 kcal/mol per ring closure was derived as a reference.

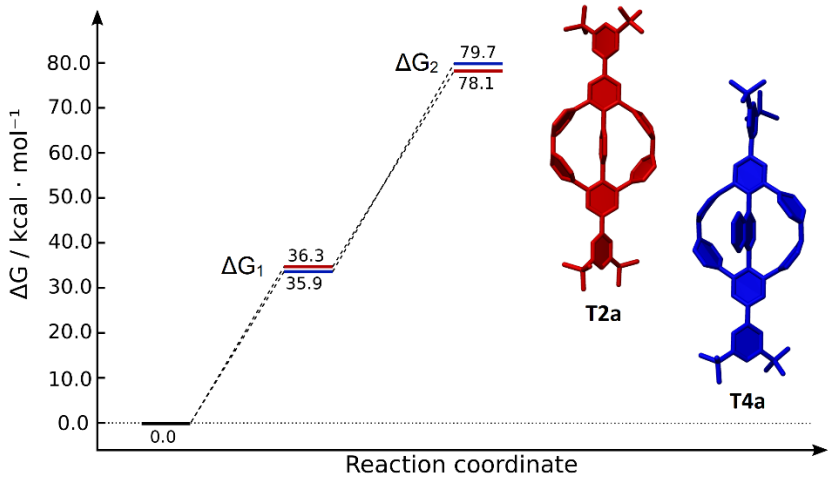

Figure 69: The resulting free *Gibbs* energies for the single couplings steps are presented as diagram for **T2a** (red) and **T4a** (blue).

Summarizing, the quantum chemical simulations found that both coupling fragments need to approach to a distance d = 5.4 Å to from a bond. If the strain introduced into the system through that bond formation is below 35 kcal/mol, a stable bond can be formed.

The concept was applied to **MSW-MK2** first, computing the distances d of all intermediates as well as the free *Gibbs* energies. The results are depicted in the following.

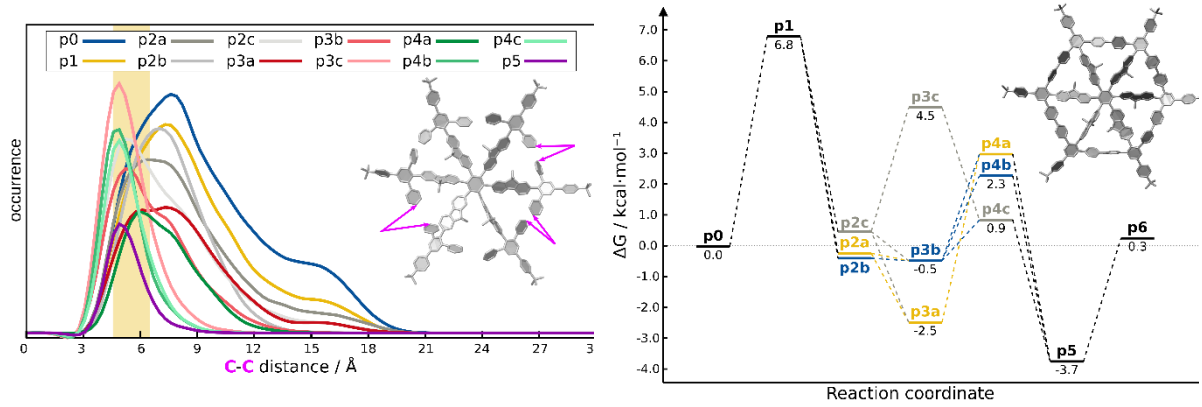

Figure 70: Investigation of the distance criterion for all intermediates of **MSW-MK2**, the yellow area marks the range, where a coupling can occur (left); corresponding free *Gibbs* energies of all coupling intermediates (right).

The simulations confirm that a fluorene-based 18 Ph-MSW should be accessible according to both criteria. The average distance between both connecting carbon atoms shows high occurrence of the required distance for all coupling intermediates. Besides that, the maximum strain introduced during all coupling steps is at 6.8 kcal/mol, which is far below the computed cyclophane threshold. Besides that, **p6** is only 0.3 kcal/mol higher in energy than **p0**. Assuming that its open-framed precursor is not a strained system, **MSW-MK2** can be assumed as an unstrained compound. In accordance to the simulation, *Kersten* was able to successfully synthesize **MSW-MK2**.[105] Since the developed method relies on the accessibility of the trimer, it predicted a successful closure for **MSW-A** as well. As

explained, **18** was only accessible in traces (compare chapter 5.1.1), that prediction cannot be validated.

From the synthetic drawback of **MSW-A** the importance of a spacing phenylene unit between the fluorene and the rim was learned. As stated during the synthetic discussion, the design of the resulting **MSW-G** strongly deforms the structure of the compound.

First, the designed target structure was modelled to get a feeling how strained **MSW-G** would in theory be. For comparision, **MSW-C** was modelled as well, but both structures are depicted without their alkyl chains for better visibility.

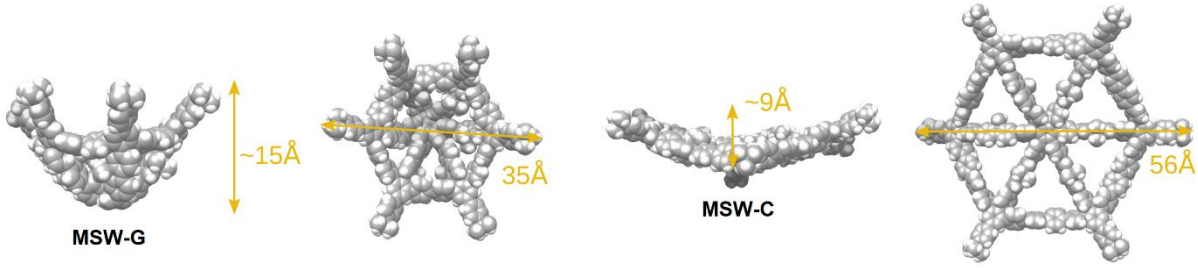

Figure 71: Quantum chemical modelling of **MSW-G** (left) and **MSW-C** (right), both structures are illustrated in profile and from the top.

The visualization reveals that the structure in fact is highly strained and instead of a slightly convex bowl like **MSW-C**, **MSW-G** is better described as basket-shaped. The structure and its precursing intermediates were examined under the same criteria as before.

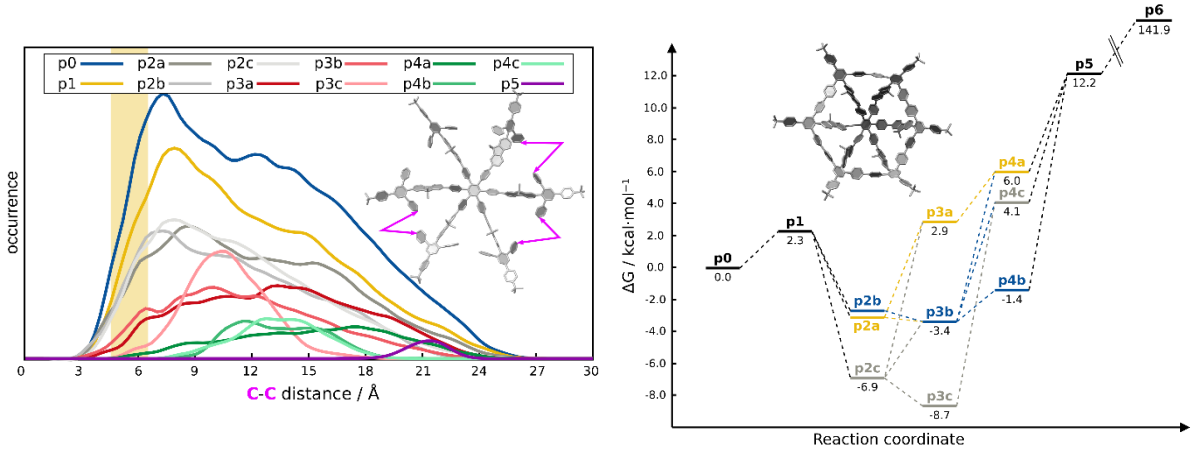

Figure 72: Investigation of the distance criterion for all intermediates of **MSW-G**, the yellow area marks the range, where a coupling can occur (left); corresponding free *Gibbs* energies of all coupling intermediates (right).

Comparing the results for **MSW-G** to the results yielded for **MSW-MK2** reveals major differences. For **MSW-G** the maxima are now strongly shifted towards longer distances. In theory, the position of the maxima is not important as long as some occurrence of the right distance is observed, as it is the case for **p4a** (compare Figure 72, left, green). Within **p5**, there is no occurrence of distances shorter than 19 Å (compare Figure 72, left, purple), suggesting that this intermediate cannot form another

intramolecular bond. Considering the free *Gibbs* energies underlines that statement, as the formation of **p6** overshoots the threshold derived from *Ohlendorf*'s systems by far (ΔG_{p6} = 141.9 kcal/mol, Figure 72, right). Interestingly, this simulation exactly confirmed the observed incomplete closure of **MSW-G** yielding only **75**, already discussed earlier in more detail (compare chapter 5.2.2).

To determine if the synthetic attempts towards **MSW-G** were unsuccessful due to the curvature introduced by the fluorene-based spoke units, theoretical investigations towards a biphenyl spoke-based MSW were made following the same criteria as before.

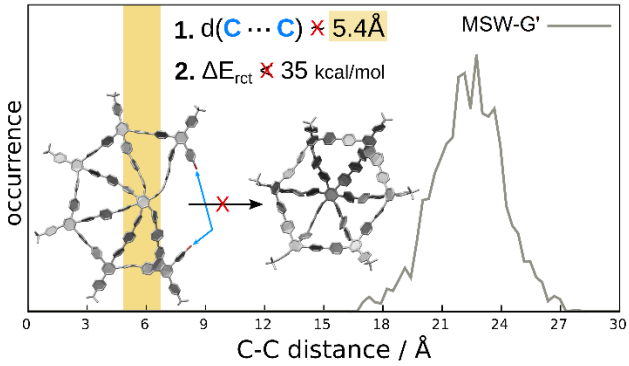

Figure 73: Investigation of the distance criterion in final coupling step towards the theoretical **MSW-G'**.

As learned for the previous MSWs, the final coupling step is the most critical bond formation in the cyclization process. The distribution in Figure 73 shows that with a minimal distance of about 17 Å the distance criterion cannot be met for **MSW-G'**. The computation of the free *Gibbs* energy for that step yielded a strain of 67.1 kcal/mol. Summarizing, it can be said that fluorene as a spoke unit definitely hindered the formation of **MSW-G** since both computed parameters are lower for **MSW-G'**. Still, the formation of **MSW-G'** is predicted to be unsuccessful meaning that the failure of the synthesis of **MSW-G** cannot be attested to fluorene alone but most notably the molecular design.

Furthermore, the synthetic accessibility of a 30 Ph-MSW was examined. Since those compounds were previously not accessible and their preparation led to the formation of oligomeric species, the insights gotten from the simulations were precious.

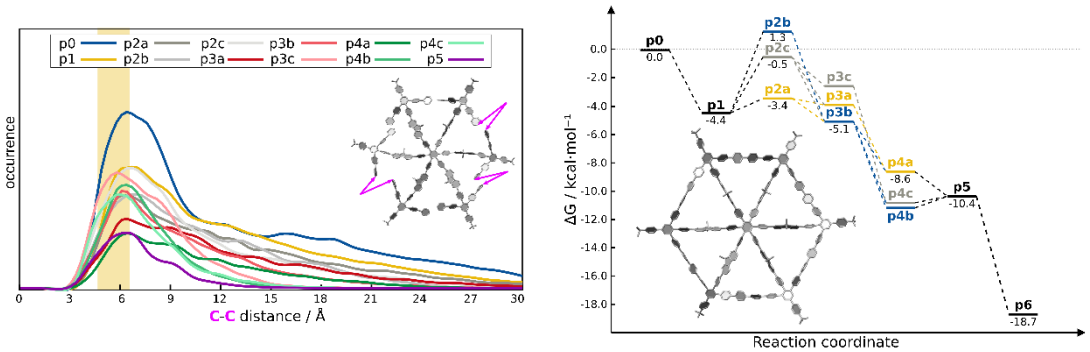

Figure 74: Investigation of the distance criterion for all intermediates of **MSW-G**, the yellow area marks the range, where a coupling can occur (left); corresponding free *Gibbs* energies of all coupling intermediates (right).

From the distance investigations, a few things were learned. First, the longer distances were observed for the formation of **MSW-C**. Since all components of that system are elongated compared to **MSW-MK2** and **MSW-G**, this was not concerning. Second, for this case all occurrence maxima were located within the yellow area, meaning that all required bonds are highly likely to be closable. Especially, this observation is of high importance for *Sterzenbach*'s work because that means that MSWs with spoke and rim fragments of identical length (compare chapter 5.2) are in theory closable. Hence, it is likely that **MSW-CS3** would have been accessible from a steric point of view and the formation of higher-molecular byproducts was observed as dominant competitive reaction.
The free *Gibbs* energies indicating the strain within the proceeding closure of the molecule overall decrease with each formed bond. As a consequence, the MSW seems to be far better accessible, perhaps also due to the increased pore sizes in between the spokes and the corresponding reduced crowdedness. The lower free *Gibbs* energy compared to **40** suggests that **MSW-C** is not strained at all. This assumption is underlined by its barely curved backbone (compare Figure 71).

Summarizing, the method developed in cooperation with the *Grimme* group is able to precisely predict if the final *Yamamoto* coupling for different systems is possible. Beyond that, the method is able to not only determine if the full closure is possible, but also to identify the critical coupling step up to where a partly closure would be realizable.
The computational insights gained for the synthesis of differently sized MSWs were also published in 2024.[97]

With the success on all three discussed systems, a more complex system was investigated as well. During the synthetic investigation of MCWs, the question grew in interest if couplings between the inner and the outer rim could occur during the simultaneous closure of both rims. After the setback in the trimerization step yielding **103** and hence, discontinuing the synthetic efforts towards MCWs, the computation results were of even higher interest. Based on the previous investigations, it was known that the intra-rim couplings are possible since the investigated system consists of an 18 Ph-MSW surrounded by a 30 Ph-MSW. For the following investigations, therefore, only the inter-rim couplings were analyzed.

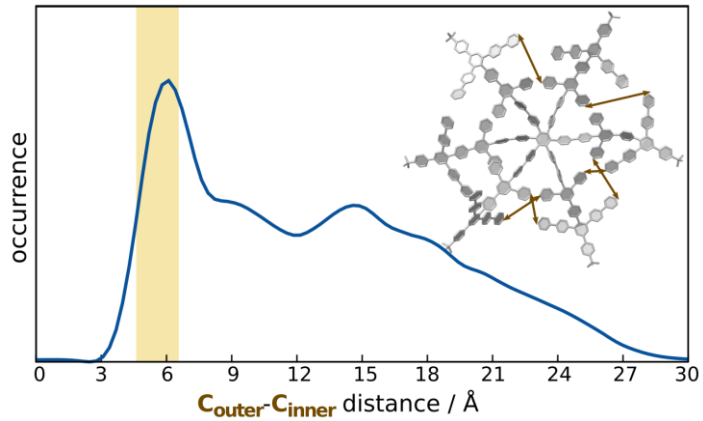

Figure 75: Distribution of the distances between bromine-functionalized carbon atoms for the inter-rim coupling step possibly occurring during the twelve-fold *Yamamoto* coupling. The yellow area marks the distance range in which a reaction is in theory possible.

The simulation unfortunately reveals that in a system designed in the given dimensions, inter-rim couplings can occur according to the distance between both rims. Besides, only one inter-rim coupling ruins a whole molecule for further investigation and the incorporation of such defects is possible up to the tenth coupling, depending on the order of bond formations. Thus, the intended strategy bears a high risk if applied to synthesize the first MCW from a quantum chemical point of view.

7 Analytical Investigations of the MSWs

7.1 Physical properties

After **MSW-AI** showed to have liquid crystalline properties and formed a mesophase at 22 °C already, these properties were assumed to originate from its long alkyl chains.[115] MSWs decorated with plenty of alkyl chains like fluorene-based MSWs were promising compounds to also feature those properties. Hence, *Kersten* investigated the behavior of his molecules when heated on a microscope. Sadly, over the whole surveilled temperature range, no melting of the molecules was perceived below 250 °C.[105] The elongation of the MSWs' alkyl chains was hence seen as a promising option to shift the melting point into the observable limits.

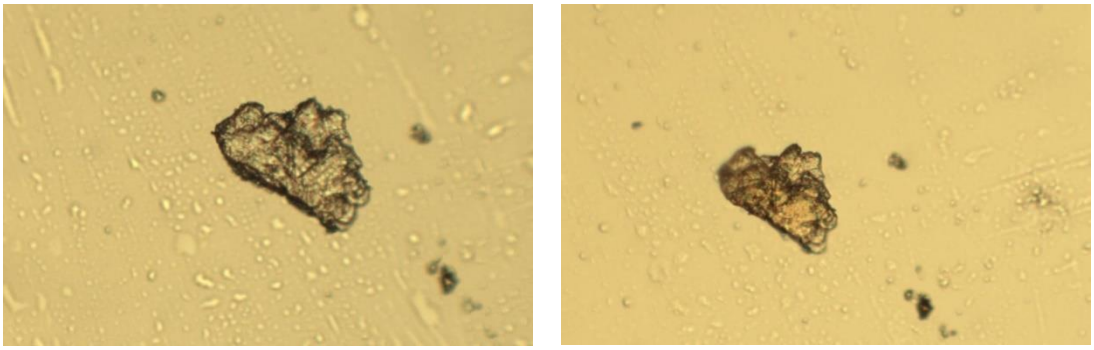

Figure 76: Thermal investigations of **MSW-C** *via* a microscope at 25 °C (left) and 250 °C (right).

The investigation of **MSW-C** was performed with a microscope in a temperature range between 25 °C and 250 °C. However, the compound did not melt within the investigable region. Besides that, no change in the behavior, color or shape of the sample was observed within the analysis. **MSW-Fa** was investigated under the same conditions.

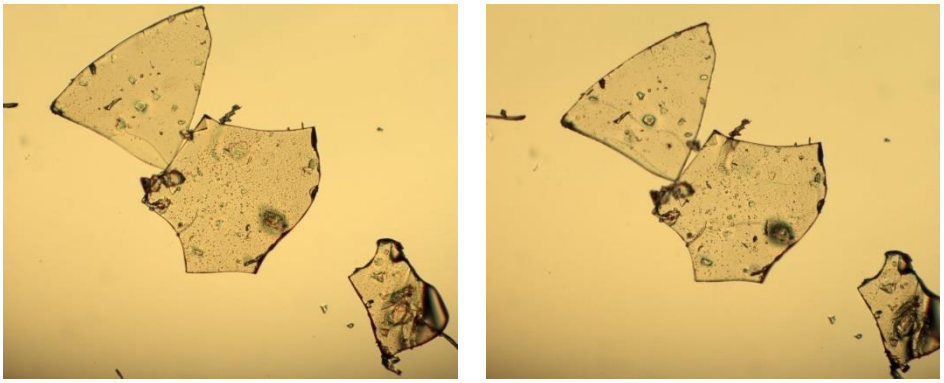

Figure 77: Thermal investigations of **MSW-Fa** *via* microscope at 25 °C (left) and 250 °C (right).

As for **MSW-C**, **MSW-Fa** did not melt within the investigated temperature range. Its optical properties did not change neither. **MSW-Fb** was not investigated as it was decorated with fewer melting point-reducing alkyl chains.

7.2 Optical properties

To elucidate their optical properties, all successfully synthesized MSWs of thus work were investigated regarding their absorption and emission as displayed in the following.

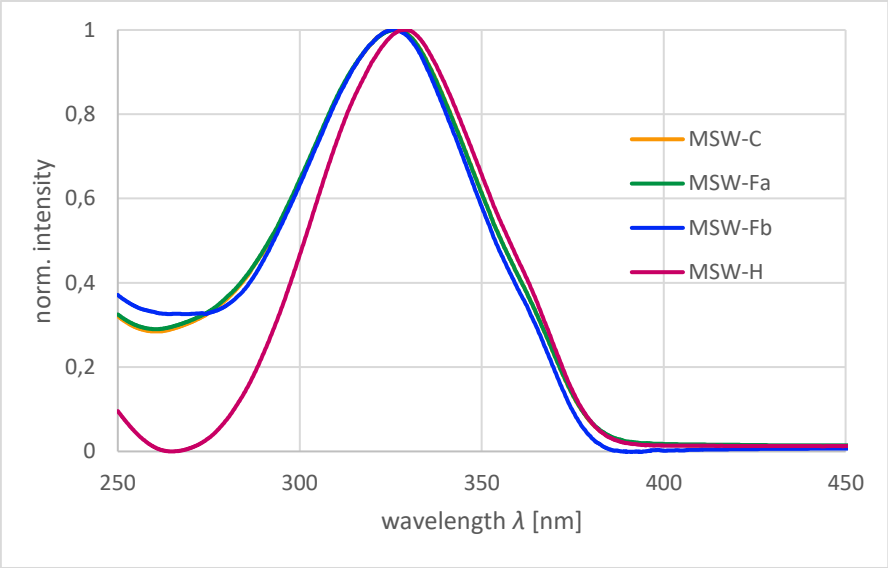

Figure 78: UV/Vis absorption spectra of all MSWs accessible within this work. Displayed are **MSW-C** (λ_{max} = 325.8 nm, orange), **MSW-Fa** (λ_{max} = 326.6 nm, green), **MSW-Fb** (λ_{max} = 326.6 nm, blue) and **MSW-H** (λ_{max} = 328.6 nm, pink); all spectra were measured in DCM.

The absorption spectra of all MSWs appear very similar. Nevertheless, **MSW-H** features a minimum at short wavelengths that is lower in intensity than for the 30 Ph-MSWs. Apart from that, the difference in size barely affects the displayed spectra.

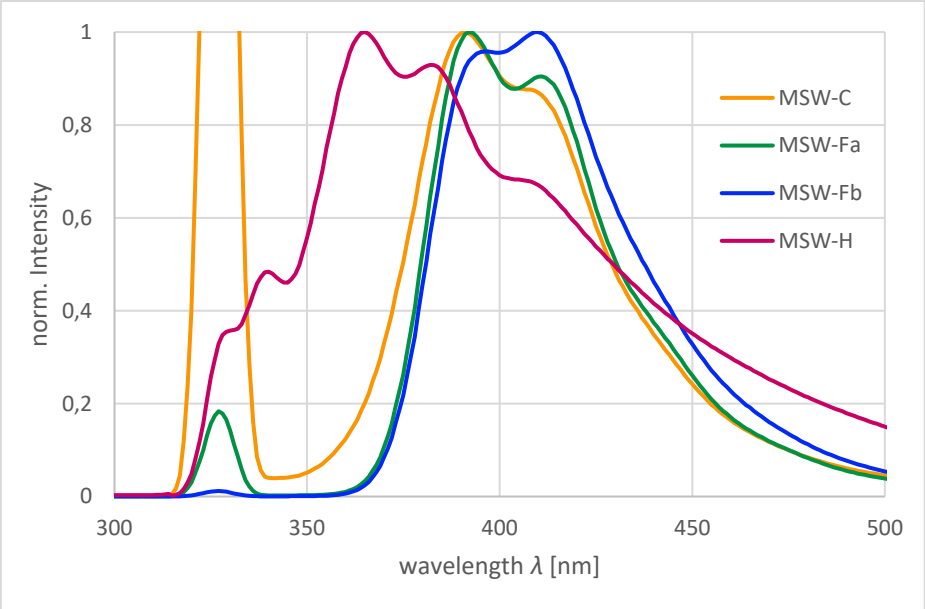

Figure 79: Fluorescence emission spectra of all MSWs accessible within this work. Displayed are **MSW-C** (λ_{max} = 391 nm, orange), **MSW-Fa** (λ_{max} = 392 nm, green), **MSW-Fb** (λ_{max} = 410 nm, blue) and **MSW-H** (λ_{max} = 365 nm, pink); all spectra were measured in DCM. All samples were excited with the wavelength of their emission maxima.

For the emission spectra, the size of the MSWs seems to be of high impact. The only 18 Ph-MSW **MSW-H** yields a total of four maxima (λ_1 = 340 nm, λ_2 = 365 nm, λ_3 = 382 nm, λ_4 = 411 nm), where λ_2 forms the global maximum. **MSW-H** is the only investigated MSW of this chapter featuring two blue-shifted emission maxima (λ_1, λ_2). The maxima λ_3 and λ_4 can be found within the 30 Ph-MSWs as well within a deviation of about 10 nm. The emission spectra of all 30 Ph-MSWs are similar, as they all contain two maxima at alike wavelengths. While **MSW-C** and **MSW-Fa** showed their global maxima at 391 nm (**MSW-C**) and 392 nm (**MSW-Fa**), the red-shifted second maximum of **MSW-Fb** (λ_{max} = 410 nm) turned out to be of higher intensity.

It is important to point out that it is difficult to compare the spectra of **MSW-H** to the other MSWs. **MSW-H** is not just the only 18 Ph-MSW investigated here, but also the only biphenol spoke-based MSW. This means, that its electronic and geometric properties strongly differ from the fluorene-based compounds discussed and hence, deviations from their behavior are not unlikely. However, it is interesting that such different molecules yield nearly identical absorbance spectra but drastically differ in emission. The *Stokes* shift of **MSW-H** is the shortest of all analyzed molecules.

7.3 STM investigations

Even though fluorene-based MSWs were never designed to adsorb on HOPG, *Kersten*'s work proved that their visualization utilizing STM is possible at the example of **MSW-MK3**.[105] Hence, it was of interest if the MSWs prepared within this work would also form self-assembled monolayers (SAMs) on HOPG.

The first molecule of interest was **MSW-C** as it is structurally highly reminiscent of **MSW-MK3**. A solution of **MSW-C** in PHO (10^{-5} M) was prepared and a single droplet of it was applied to a HOPG sample. The sample was heated to 100 °C for 30 s and allowed to cool to rt afterwards. The subsequent STM investigations at the solid/liquid interface of HOPG and the solution unveiled a dense packing of the molecules. The packing also showed random defects within the ordered packing, indicated by the white arrow (compare Figure 80).

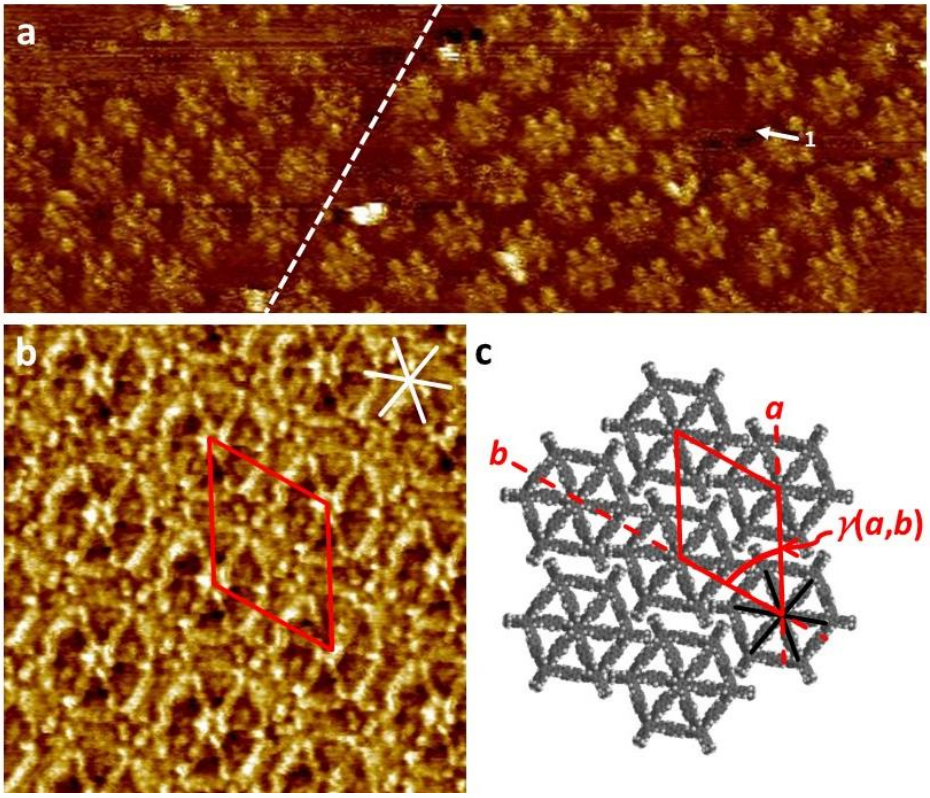

Figure 80: a) STM image of **MSW-C** at the liquid/solid interface. Image parameters: c = 1 × 10^{-5} M, 26.6 × 80 nm^2, *vs* = -1.8 V, I_t = 6 pA, internal scanner calibration; b) STM image of **MSW-MK3** for comparative reasons. Depicted is a SAM at the solid/liquid interface of HOPG and a PHO solution (c = 3 × 10^{-6} M) of the analyte, tempered at 80 °C for 20 s, image parameters: 17 × 17 nm^2, *vs* = -2.0 V, I_t = 35 pA; c) supramolecular model of the SAM of **MSW-MK3**, a = (5.3 ± 0.2) nm, b = (4.9 ± 0.2) nm, γ(a,b) = (59 ± 2)°, all octyl chains attached to the fluorene units are oriented into the liquid phase and omitted for better visibility.[105]

The lower resolution as compared to **MSW-MK3** results from the longer alkyl chains pointing into the solution. Due to their length, they are more likely to collide with the tip additionally hindering the

recording of a highly resolved image. Besides that, the rim of **MSW-C** does not feature any decoration additionally fixing the molecule on the HOPG surface. As a consequence, every collision with the STM tip can slightly move the molecules furthermore lowering the resolution. Due to the bad resolution, it is not possible to determine a unit cell and to give information about its parameters. For *Kersten*'s molecule, the adsorption of their backbones alone seemed to be sufficient to keep all molecules in position. The molecules of **MSW-MK3** orient parallelly in close proximity with their backbones and spokes oriented along the HOPG main axes (± 2°) and their *tert*-butyl groups avoid each other (compare Figure 80c). Additionally, the packing of **MSW-MK3** was a lot denser than for **MSW-C** even though they are of identical diameter and rim functionalization.

MSW-Fa was not found to form any SAMs in PHO independent of the concentration. A solution of **MSW-Fa** in TCB ($c = 10^{-4}$ M) adsorbed in a hexagonal pattern on HOPG, visualized at the solid/liquid interface of HOPG and the solution *via* STM.

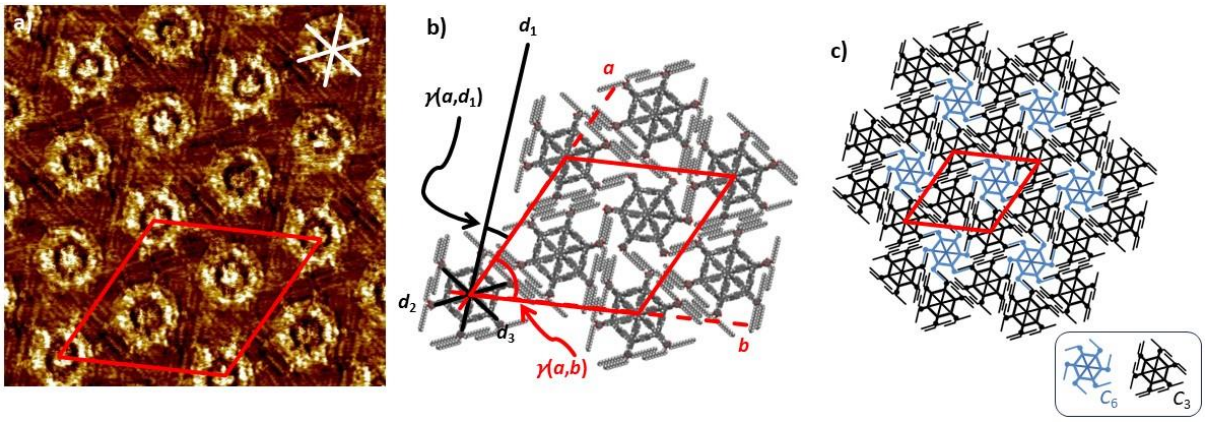

Figure 81: a) STM image of **MSW-Fa** at the solid/liquid interface of HOPG and a TCB solution (c = 10^{-4} M), tempered at 80 °C for 20 s, the unit cell is depicted in red, image parameters: 30 × 30 nm^2, V_s = -0.67 V, I_t = 109 pA; b) supramolecular model of the SAM, $a = b$ = (13.3 ± 0.2) nm, $\gamma(a,b)$ = (62 ± 2)°, $\gamma(a,d_1)$ = (21 ± 2)°, all hexadecyl chains attached to the fluorene units are oriented into the liquid phase and neglected for better visibility, the unit cell is depicted in red; c) Schematic model of the packing of a SAM of **MSW-Fa**. It consists of C_3-symmetric (black) and C_6-symmetric (blue) conformers, with their coordination numbers covering the spoke segments.

Interestingly, **MSW-Fa** formed a unique pattern. As depicted in Figure 81c), the packing consists of different conformers. A C_6-symmetric molecule (blue) is surrounded by six C_3-symmetric molecules (black). Each C_3-symmetric molecule on the other hand is surrounded by three C_3-symmetric and three C_6-symmetric molecules alternately. Here, the C_3-symmetric molecules' backbones align along the HOPG main axes and the C_6-symmetric molecules orient their backbones along the armchair directions of HOPG (compare Figure 81b). All alkyl chains attached to the fluorene units are not visible and point most likely upwards into the liquid phase. The alkyl chains of the dendron groups are visible as medium bright lines in between the bright backbones and separate individual molecules from each other. Still, the alkoxy chains of both conformers behave differently. 15 of the 18 hexadecyloxy side chains of the

C_3-symmetric conformer adsorb on HOPG and are oriented along the three main axes directions of HOPG. Their other side chains point upwards into the liquid phase as well and hence cannot be detected. The C_6-symmetric conformer results of a lower adsorption ratio of its rim-decorating dendron groups. Here, only six of the 18 hexadecyloxy side chains are adsorbed on HOPG. They are oriented along the three main axis directions of HOPG, all other chains once again point upwards and are indetectable. Keen-eyed observation of the C_3-symmetric conformer points out its triangular-alike shape resulting of the hexadecyloxy groups' alignment, but lacking the geometrically required corners. Instead, small gaps can be observed enabling an interdigitation within the resulting pores of the adsorbed alkoxy chains of the C_6-symmetric conformers. Coincidently, the nanopattern of **MSW-Fa** is identical with the pattern observed for the adsorption of **MSW-AI** regarding the coordination numbers of the different conformers despite their different perimeter. Nevertheless, their interdigitation pattern is not fully identical because the alkoxy chains of the individual dendron groups of **MSW-AI** are all oriented in the same direction while they split up for **MSW-Fa**.[96]

The STM results for **MSW-C** and **MSW-Fa** were also published in 2024.[97]

STM investigations of **MSW-Fb** revealed the formation of self-assembled monolayers as well. Dissolved in TCB, it was possible to visualize such monolayers at the solid/liquid interface of HOPG.

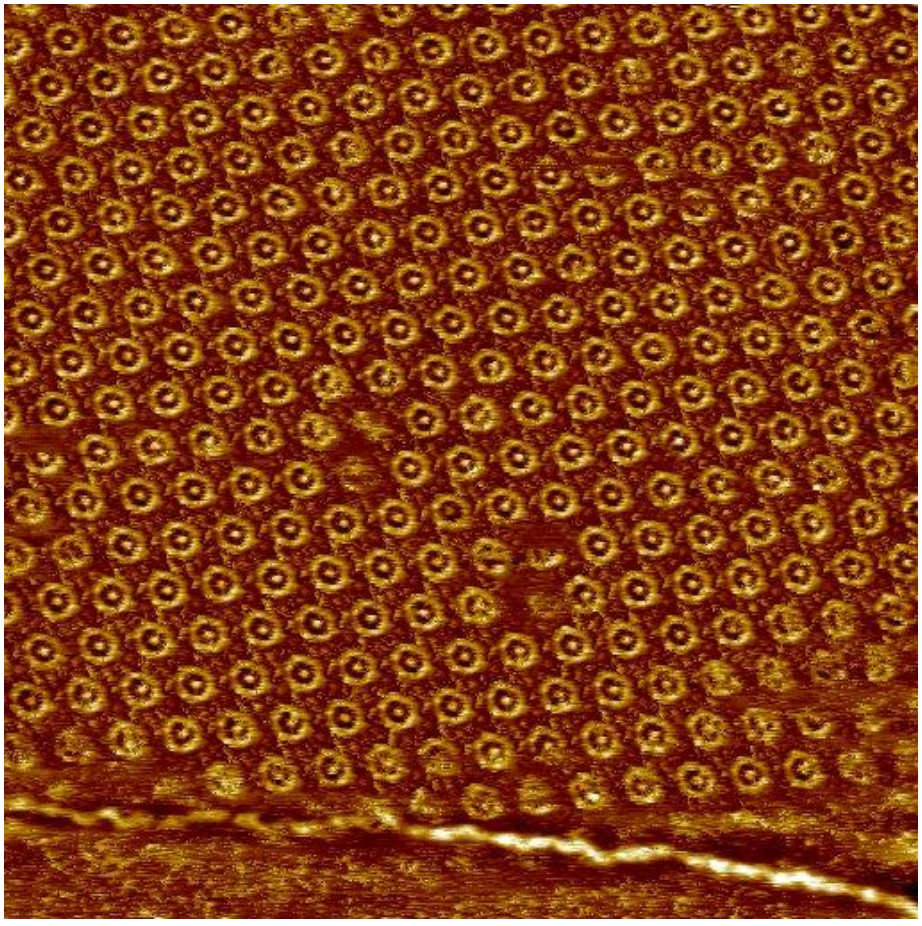

Figure 82: STM image of **MSW-Fb** at the solid/liquid interface of HOPG and a TCB solution (c = 10^{-4} M), tempered at 80 °C for 20 s, image parameters: 130 × 130 nm^2, V_s = -0.9 V, I_t = 13 pA.

Despite all efforts, it was not possible to record higher resolved images of **MSW-Fb** within the time limits of this project. Thus, it is not possible to identify the orientation of the rim-decorating alkyl chains and imply any unique packing of the MSWs or different conformers. Besides that, without that information it is not possible to reliably determine a unit cell and its parameters. Nevertheless, it can be clearly identified that **MSW-Fb** forms a repetitive pattern covering a large area. The assembled molecules orient in a slightly distorted honeycomb pattern, where each individual MSW is surrounded by six other molecules (compare Figure 82).

For **MSW-H**, it was not possible to record any images of SAMs on HOPG. The reason for this lies within its molecular design. Similar to **MSW-MK2**, the six-fold *Yamamoto* coupling yields a mixture of statistic conformers. Those conformers result of the orientation of the alkyl- or alkoxy-decorated units during the closing steps. Once closed, the conformers are no longer interconvertible as the pores within the MSW are too small to thread the chains through them. To adsorb on HOPG, it is necessary for all alkyl chains to orient in one direction maximizing the interaction of the MSW's backbone with the surface material (compare Figure 83).

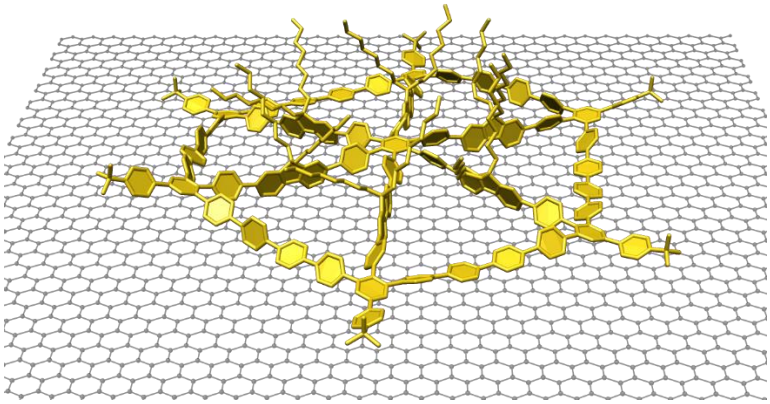

Figure 83: Quantum chemical model of a single molecule of **MSW-MK3** adsorbing on a HOPG cutout. For this conformer, all alkyl chains are pointing upwards into the solvent phase maximizing the adsorption of its backbone on the surface.

Quantum chemical simulations also supported spoke-functionalized 18 Ph-MSWs to not be interconvertible, hindered by a rotational barrier of 31.1 kcal/mol. 30 Ph-MSWs were found to be interconvertible between the rotamers. Here, the barrier was computed to be only 8.1 kcal/mol. This higher rotational freedom leads to the formation of repetitive SAMs through facile isomerization for the 30 Ph-MSWs exclusively as described within this chapter.

8 Summary & Outlook

During the course of this work, several new insights regarding the field of MSWs were gained. Overall, it was possible to synthesize four different MSWs, the routes of two additional molecules were proceeded unsuccessful up to the stage of the trimer.

Within of this work, it was possible to synthesize three differently decorated 30 Ph-MSWs. For the first time ever, it was possible to fully characterize an all-phenylene MSW of these dimensions *via* NMR spectroscopy and MALDI-spectrometry.

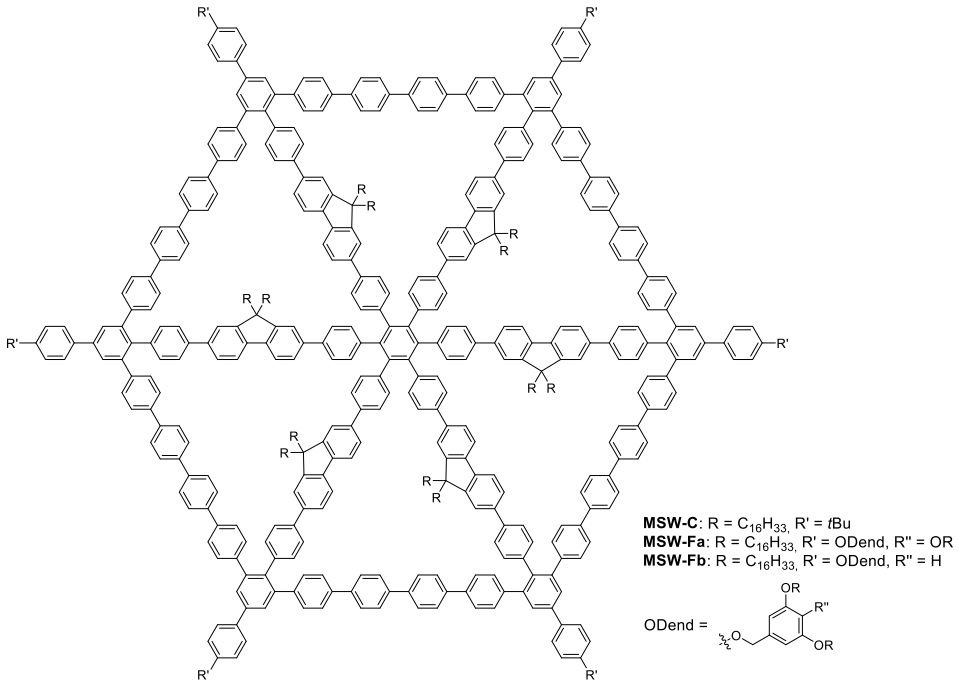

Figure 84: Overview over the successfully accessed 30 Ph-MSWs of this work.

Via STM investigations, it was possible to prove the structure of all three molecules. While for **MSW-C** and **MSW-Fb** the resolution was acceptable and only few insights regarding the molecule's packing were obtained, **MSW-Fa** gave well resolved images that enabled the identification of a unit cell and all its parameters. A comparison of both images did not grant the anticipated revelations within the given time limits.

Unfortunately, the synthetic progression of **MSW-A** was discontinued after poor yields in the trimerization of its symmetric acetylene. Nevertheless, this drawback gave precious insight into the steric demand of the trimerization step and led to the purposeful incorporation of a spacing phenylene unit between the reactive acetylene center and the fluorene unit. The impact of that modification was proven with the synthesis of **74** as well as the syntheses of all 30 Ph-MSWs presented previously.

The synthesis of **MSW-G** marks another unsuccessful synthetic route that this time failed during the final cyclization step of the MSW's rim. However, this drawback turned out to be essential to develop

a method that predicts the accessibility of strained cyclization products *via Yamamoto* coupling in the future. **MSW-G** was the only MSW that was confirmed to not be closable within synthetic conditions *via* quantum chemical simulations and hence served as a precious proof of concept. This method was also applied to **MSW-MK2**[105] and **MSW-C** again modelling the actual synthetic outcome correctly.

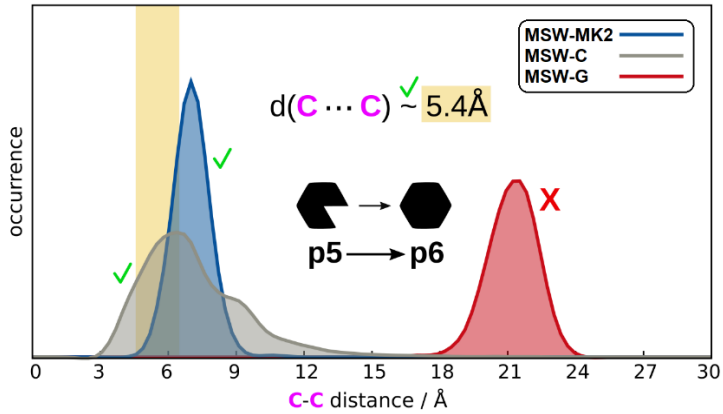

Figure 85: Distance criterion of the final cyclization step *via Yamamoto* coupling for **MSW-MK2**, **MSW-C** and **MSW-G**. The criterion attests only the successful formation of **MSW-MK2** and **MSW-C**. These exact results were reproduced synthetically.

The second focus of this work revolved around the synthesis of a biphenol-based MSW. **MSW-H** that was designed as a test system, was prepared successfully, but the synthetic pathway to it was dominated by drawbacks and poor yields. Especially, the low yield of the trimerization of **102** did not suggest to attempt the synthesis of an MCW. On the other hand, it was learned that the substitution of fluorene through the more flexible biphenol had in fact an influence on the trimerization step because even though its yield was poor for **103**, enough substance was collected to finish the synthetic route accessing the MSW.

The third and final part of this work dealt with the synthesis of symmetric acetylenes as precursors for MSWs and MCWs. Over the course of this work, this stage turned out to become a bottleneck at a late stage within the synthesis, which made it extremely challenging to improve this synthetic step. After the *Sonogashira* reaction was accompanied by a challenging separation of the *Glaser* byproduct, it was substituted through a two-fold *Suzuki* coupling. The testing of different substrates revealed that the byproduct was avoided that way but the low yield still made this reaction not favorable. Only direct connection of the substrates to the acetylene group in a two-fold *Stille* coupling was in the end able to overcome this issue and became a promising method for future synthetic attempts towards MSWs and MCWs.

Learning from the results of this work, *A. Roth* is currently working on a modified version of **MSW-H** within the limits of his master thesis under the supervision of *S. Schimmelpfennig*. As presented earlier, the absence of an unsubstituted spacing phenylene unit hinders the trimerization of symmetric alkynes

decorated with long alkyl chains for both fluorene- and biphenol-based MSWs. Hence, the modification removes the inner alkoxy chain of each spoke of **MSW-H**.[141]

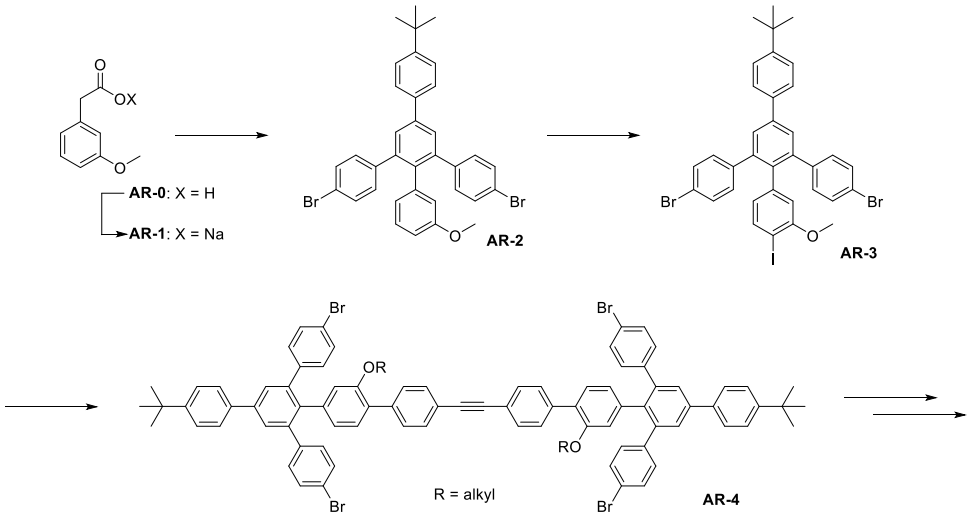

Scheme 102: Modified synthetic approach investigated by *Roth*.[141]

Schimmelpfennig herself is investigating the enlargement of biphenol-based MSWs. Continuing the research of her master thesis under my supervision, *Schimmelpfennig* is currently exploring the synthesis of a 30 Ph-MSW equivalent of **MSW-H**. Again, this structure is of interest regarding its behavior during the trimerization step. Besides that, she would access the first planar 30 Ph-MSW. This geometry is also of special interest for STM investigations, as it is not clear if the molecule adsorbs to HOPG at all and how its alkoxy chains arrange if it does.[142]

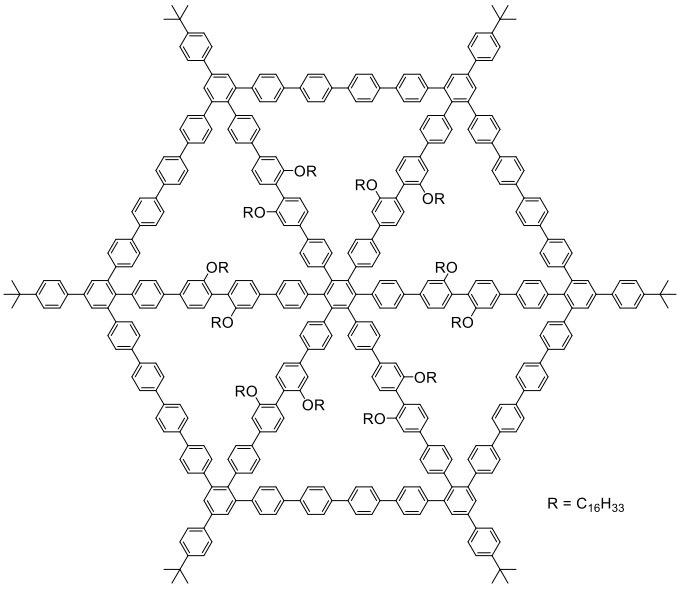

Figure 86: Target structure of *Schimmelpfennig* as 30 Ph-MSW-equivalent of **MSW-H**.[142]

Proceeding the research of this work, it is of interest to further pursue the synthesis of MCWs. If *Roth*'s MSW can be accessed successfully, its expansion by a second rim would be an interesting approach. Learning from the quantum chemical simulations, the introduction of two different halides into the

rim fragments is inevitable to be able to close both rims subsequently without any defects. Different reactivities were already observed by *Yamamoto et al.* in their original publication,[99] but not for the reaction within a microwave reactor. Thus, investigations regarding the reactivity of different aryl halides under microwave conditions are reasonable prior to the synthesis of the MCW.

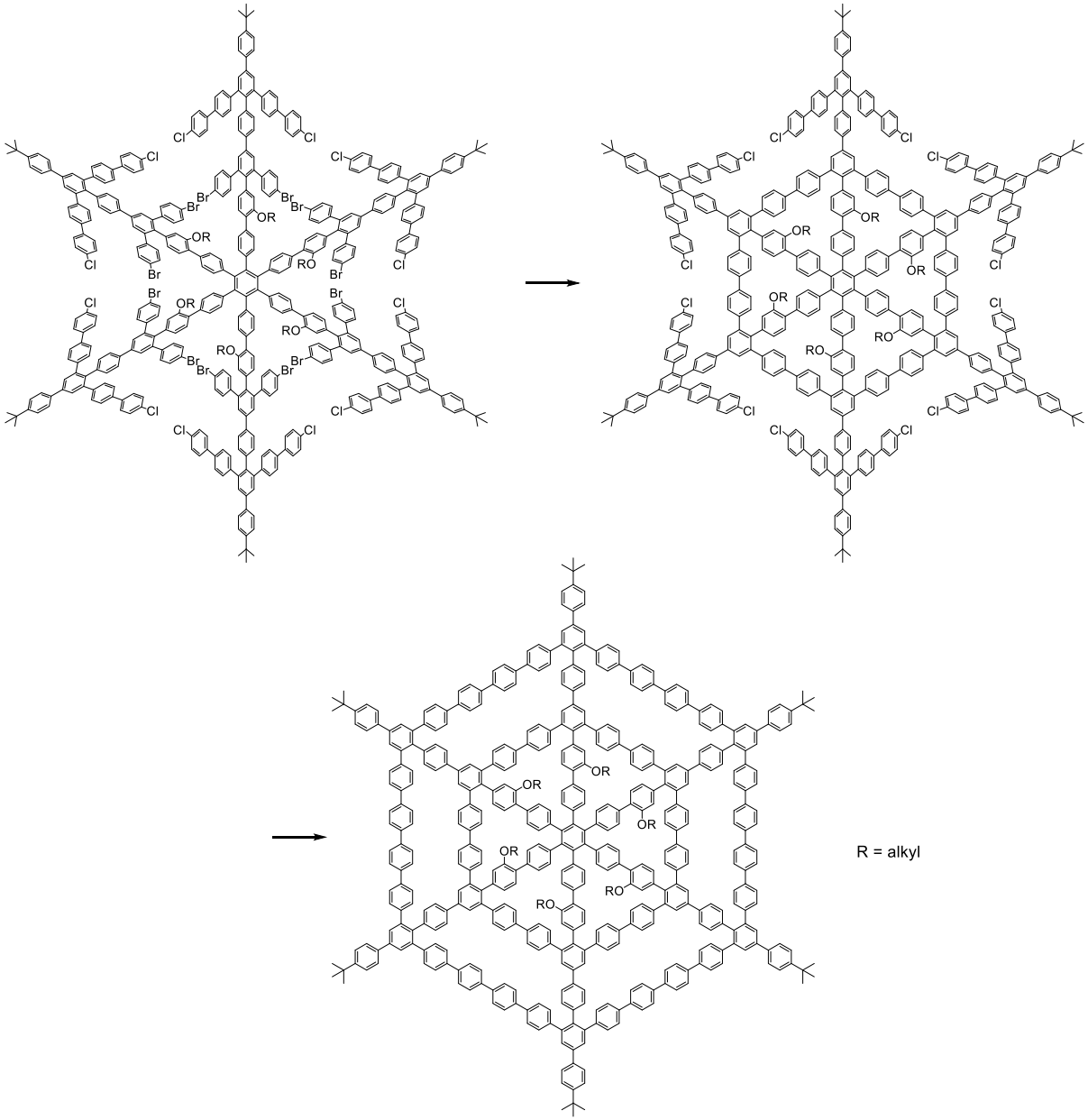

Scheme 103: Synthesis of a MCW exploiting different reactivities of different aryl halides within the *Yamamoto* coupling.

9 Experimental discussion

9.1 General aspects

All chemicals were used without any further purification. All moisture- or air-sensitive reactions were performed under *Schlenk*-conditions and argon atmosphere. Dry reaction solvents were taken from an MB SPS 800 drying plant of the company *MBraun*. The solvents DCM, cyclohexane and ethyl acetate were distilled before usage. All other solvents used were commercially available and used without any further purification.

CPDMS-acetylene was synthesized according to literature procedures by *U. Müller*.[143] Piperidine was distilled under argon atmosphere over CaH_2 before being used. Air- and/or moisture-sensitive compounds and catalysts were stored in a glove box under argon atmosphere and added to the reaction as late as possible.

9.2 Technical aspects

The purification of the crude products *via* column chromatography was performed with silica gel 60 of the company *Acros Organics* (0.040-0.063 mm). The separation was surveilled by the use of TLC Silica gel 60 F254 plates (175-225 μm silica gel with fluorescence indicator) produced by the company *Merck*. The TLC plates were analyzed with the help of UV lamps carrying two Bulbs (wavelength λ_1 = 254 nm and λ_2 = 366 nm).

All ^{1}H- and ^{13}C NMR spectra were measured with devices of the *Bruker* company. The models Avance I 300 (^{1}H: 300 MHz, ^{13}C: 76 MHz), Avance I 400 (^{1}H: 400 MHz, ^{13}C: 100 MHz), Avance I 500 (^{1}H: 499 MHz, ^{13}C: 125 MHz), Avance III HD Ascend 500 (^{1}H: 500 MHz, ^{13}C: 125 MHz) and Avance III HD Ascend 700 (^{1}H: 700 MHz, ^{13}C: 176 MHz) were used. The analyzed chemicals were dissolved in deuterated solvents produced by the *Deutero* company. All measured spectra were analyzed with the software MestReNova 8.0.1. A *MAT 90*- or a *MAT 95 XL* sector field device were used to record the EI mass spectra, produced by the company *Thermo Finnigan*. All MALDI spectra were recorded using a MALDI ultrafleXtreme TOF/TOF mass spectrometer by *Bruker Daltonik*. ESI spectra (pos/neg) were measured with a LTQ Orbitrap XL manufactured by *Thermo Fischer Scientifc*.

The analytical GPC used for reaction control of later stages consisted of components by the company *Agilent Technologies* (pump: IsoPump G1310A, autosampler: ALS G1329A, UV-detector: VWD G1314B, RI-detector: RID G1362A, columns: four column-set, (PSS *Polymer Standard Service* GmbH, polystyrene, 8 mm 25 × 300 mm; porosity: 102, 103, 105/ 106 Å), three column-set (PSS *Polymer*

Standard Service GmbH, polystyrene, 8 mm × 300 mm, 102, 103, 105 Å)). The used eluent comes from the company *VWR*, using BHT as stabilizer. The recGPC used for some purification steps consists of components by *Shimadzu* (pump: LC-20 AD, deaerator: DGU-20 A3, autosampler: SIL-20 A HT, UV-detector: SPD-20 A, column reactor: CTO-20 AC, fraction collector: FRC-10 A, switch valve: FCV-10 A, system controller: CBM-20A, columns: three column set, PSS *Polymer Standard Service* GmbH, polystyrene, 20 mm × 300 mm, porosity: 103 Å). The THF used as eluent was also drawn from *VWR*. If separations were performed BHT-free, the solvent was distilled under reduced pressure prior to use.
STM investigations were performed under ambient conditions at the solution/solid interface, utilizing HOPG and different solvents for the analyte solutions. 2 μl of an analyte solution were applied onto a freshly cleaved HOPG. HOPG was commercially available from TipsNano (*via* Anfatec) in ZYB-SS quality. The sample was thermally annealed at elevated temperature for at least 20 s to promote the two-dimensional mobility of the molecules on the surface. Afterwards, it was allowed to cool to room temperature. Bias voltages and tunneling currents varied for all investigated samples and are given with the respective images. An Agilent 5500 scanning probe microscope is placed on a Halcyonics actively isolated microscopy workstation and shielded from external noise through a self-built box. The used Pt/Ir (80/20) tips were cut with scissors and modified *via* short voltage pulses until meeting satisfactory properties. For calibration of the final image, a second image with reduced bias voltage is recorded as reference. Here, the atomic lattice of HOPG is better visible, serving as calibration grid to precisely align the images. Data processing and image calibration were done using the SPIP 5 (Image Metrology) software package. The supramolecular modelling visualized alongside the STM images within this work was created using backbone geometries optimized with the inherent tools of *Spartan* ’16 and ’18. The missing alkyl-/alkoxy chains were added manually afterwards according to the observed angles within the STM measurements to save computational resources.
For the optical investigations of the prepared MSWs, UV/Vis spectra were recorded using a *PerkinElmer* LAMBDA 365+ UV/Vis spectrometer. The fluorescence spectra were recorded with an RF-6000 spectro fluorophotometer manufactured by *Shimadzu*.

9.3 Computational Details

All structures were constructed in Avogadro.[144] Most calculations were carried out using the xtb program package V6.6.1,[145,146] all exceptions are explicitly stated. Evaluation of radial distribution functions (RDF) was performed with VMD.[147] Geometry optimization and molecular dynamics (MD) at the GFN-FF[148] level of theory were performed for all structures, applying ALPB[149] as an implicit solvent model with THF as solvent. All MDs were performed in an NVT ensemble at 393 K, step length of 2 fs, increased hydrogen mass of 4 a.u. for stability reasons, total length of 500 ps, and no bonds

constrained from breaking *via* the SHAKE algorithm. The first 30% of each trajectory were assigned to the equilibration phase and discarded. RDFs were calculated between all pairs of neighboring carbon atoms potentially able to couple *via Yamamoto* coupling. Reaction free *Gibbs* energies for the rim closure of the investigated MSWs were calculated at the r²SCAN-3c(COSMO(THF)) level of theory.[150,151] Thermal contributions in the modified rigid-rotator-harmonic-oscillator approximation (mRRHO) derived from the biased Hessian approach (bhess) at GFN2-xTB level of theory[145,151] were also considered. The electronic and solvation energy were computed using Turbomole 7.5.1.[152] The energetic minimum structures yielded from the GFN-FF(ALPB(THF)) MDs were re-optimized at the r²SCAN-3c(COSMO(THF)) level.

To simulate the reaction path of the *Yamamoto* coupling, the computation was conducted using the growing string method (GSM)[153] as the method of choice as contained in ORCA[154] 5.0.4 at the B97-3c(CPCM(DMF)) level of theory[155]. The resulting reactants were re-optimized afterwards at the r²SCAN-3c(CPCM(DMF)) level in ORCA and reaction free *Gibbs* energies were calculated using Turbomole employing hybrid DFT single point energies at the ωB97X-3c(COSMO(DMF)) level[156] and thermal contributions by bhess. All computational studies were performed by *J. Kohn*.

9.4 Syntheses

Compound **1** (PK-026)

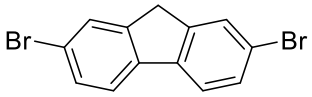

This synthesis applies a procedure published by Göbel et al.[157]

In a round-bottom flask, fluorene (10.02 g, 60.25 mmol, 1.000 eq.) and $FeCl_3$ (0.371 g, 2.29 mmol, 0.038 eq.) were suspended in $CHCl_3$ (70 mL) and cooled to 0 °C. Then, a solution of bromine (6.50 mL, 130 mmol, 2.16 eq.) in $CHCl_3$ (20 mL) was slowly added dropwise. After 25 minutes of addition, the mixture was stirred for two hours at room temperature. The reaction was quenched by adding aq. $NaHSO_3$ solution (40 %). The phases were separated and the aqueous layer was extracted with DCM three times. The combined organic layers were washed with water and brine, dried over magnesium sulfate and the solvent was removed under reduced pressure until the product started to crystallize. The flask was then cooled in a freezer for 20 minutes. Afterwards the product was filtered off and **1** was received in 58 % as a colorless solid (11.35 g, 35.04 mmol).

Chemical formula: $C_{13}H_8Br_2$

Molecular weight: 324.02 g/mol

^{1}H-NMR (500 MHz, CD_2Cl_2, 298 K), *δ* [ppm]

7.67 - 7.65 (m, 2 H), 7.62 - 7.59 (d, *J* = 8.1 Hz, 2 H), 7.51 - 7.48 (m, 2 H), 3.85 (s, 2 H).

^{13}C-NMR (126 MHz, CD_2Cl_2, 298 K), *δ* [ppm]

145.5, 140.0, 130.4, 128.6, 121.6, 121.2, 37.0.

MS (EI, 70 eV), *m/z* (%)

324.0 (87) $[M]^{\bullet+}$, 243.0 (100) $[M\text{-}Br]^+$, 164.0 (31) $[M\text{-}2\ Br]^+$; calculated: 323.9 Da.

Compound **2** (PK-027)

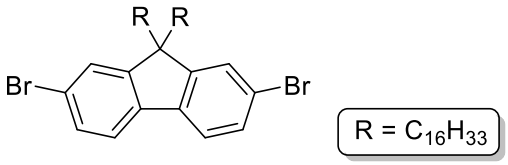

This synthesis applies a procedure published by Ponmuthu et al.[47]

1 (5.001 g, 15.44 mmol, 1.000 eq.) and KOH (4.002 g, 71.32 mmol, 4.621 eq.) were suspended in a mixture of acetone (80 mL) and water (7.5 mL). Potassium iodide (0.256 g, 1.54 mmol, 0.0999 eq.), NBu_4Br (0.500 g, 1.55 mmol, 0.101 eq.) and 1-bromohexadecane (10.0 mL, 32.7 mmol, 2.12 eq.) were added and the mixture was heated to 80 °C for 24 hours. After checking the progress of the reaction *via* TLC, ten percent of the used amounts of potassium iodide, NBu_4Br and 1-bromohexadecane were

additionally added and the reaction was continued for another 24 hours. The mixture was allowed to cool to room temperature, the solvent was removed under reduced pressure and the residue was dissolved in DCM and water. The phases were separated and the aqueous layer was extracted with DCM four times. The combined organic layers were washed with water, aq. HCl (2M) and brine and dried over magnesium sulfate. After removal of the solvent under reduced pressure, the crude product was purified *via* column chromatography (SiO_2, Cy, R_f = 0.9), receiving the product as pale-yellow solid (12.63 g, 1.059 eq.). It was not possible to determine the yield because the ^{1}H-NMR spectrum revealed leftovers of unreacted 1-bromohexadecane.

Chemical formula: $C_{45}H_{72}Br_2$

Molecular weight: 772.88 g/mol

^{1}H-NMR (500 MHz, CD_2Cl_2, 298 K), δ [ppm]

7.57 - 7.55 (dd, *J* = 7.9 Hz, *J* = 0.7 Hz, 2 H), 7.49 - 7.45 (m, 4 H), 1.96 - 1.92 (m, 4 H), 1.26 (bs, 56 H), 0.90 - 0.86 (t, *J* = 7.1 Hz, 6 H).

^{13}C-NMR (126 MHz, CD_2Cl_2, 298 K), δ [ppm]

143.2, 138.2, 130.0, 127.6, 120.4, 120.0, 32.9, 32.6, 30.3, 30.2, 30.2, 30.1, 30.1, 30.0, 29.7, 29.4, 28.7, 24.4, 23.1, 14.5.

MS (EI, 70 eV), *m*/*z* (%)

772.3 (100) $[M]^{\bullet+}$, 322.8 (31) $[M\text{-}C_{16}H_{33}\text{-}C_{16}H_{33}]^+$; calculated: 772.4 Da.

Compound **4** (PK-028)

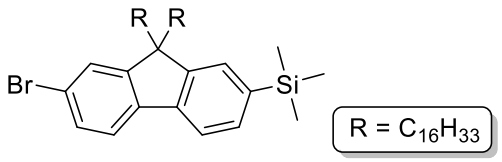

This synthesis applies a procedure published by Suranna et al.[158]

Under *Schlenk* conditions, **2** (900 mg, 1.17 mmol, 1.00 eq.) was dissolved in dry THF (30 mL), that was freshly distilled over sodium. The solution was cooled to -78 °C and a solution of *n*BuLi (0.80 mL, 1.28 mmol, 1.10 eq., 1.6M in hexane) was added dropwise and afterwards stirred for one hour. After adding TMSCl (0.30 mL, 2.36 mmol, 2.03 eq.) the mixture was allowed to warm to room temperature and stirred for three hours. The mixture was diluted with DCM and water, and the phases were separated. The aqueous layer was extracted with DCM three times. The combined organic layers were washed with water and brine and dried over magnesium sulfate. After removal of the solvent under reduced pressure, the crude product was purified *via* column chromatography (SiO_2, Cy, R_f = 0.85). The product could not be separated from the substrate due to their similar polarity. It was therefore not possible to determine the yield or to provide reliable spectra.

Chemical formula: $C_{48}H_{81}BrSi$

Molecular weight: 766.17 g/mol

Compound **5a** (PK-029)

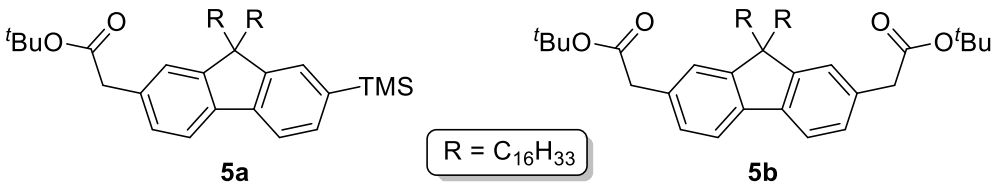

5a **5b**

This synthesis applies a procedure published by Hartwig et al.[122]

Zinc powder was stirred in aq. HCl (1M) for 30 min to strip off its oxide layer. After filtering off, it was dried under vacuum overnight. Activated zinc powder (270 mg, 4.13 mmol, 6.74 eq.) was then placed in a flamed *Schlenk* flask. Freshly distilled THF (10 mL) and *tert*-butyl bromoacetate (0.30 mL, 2.03 mmol, 3.31 eq.) were added and the mixture was refluxed until it became a clear solution. Afterwards, **4** (470 mg, 0.613 mmol, 1.00 eq.), PPh_3 (28.4 mg, 0.140 mmol, 0.229 eq.) and $Pd_2(dba)_3$ (25.7 mg, 28.1 μmol, 0.0458 eq.) were added and the mixture was heated to 90 °C for 22 hours. After cooling to room temperature, the mixture was diluted with DCM and water and the phases were separated. The aqueous layer was extracted with DCM three times. The combined organic layers were washed with water and brine and dried over sodium sulfate. After removal of the solvent under reduced pressure, the crude product was purified *via* column chromatography (SiO_2, Cy:DCM 1:1). The reaction yielded byproduct **5b** as colorless oil in 26 % (0.132 g, 0.156 mmol) as well as recovering **4** in 45 % (210 mg, 0.274 mmol). The desired product **5a** was not obtained.

5a:

Chemical formula: $C_{54}H_{92}O_2Si$

Molecular weight: 801.41 g/mol

5b:

Chemical formula: $C_{57}H_{94}O_4$

Molecular weight: 843.38 g/mol

Compound **6** (PK-030)

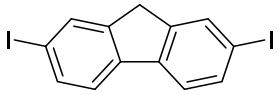

Fluorene (3.005 g, 18.08 mmol, 1.000 eq.), iodine (3.441 g, 13.56 mmol, 0.750 eq.) and iodic acid (1.503 g, 8.546 mmol, 0.473 eq.) were suspended in a mixture of glacial acetic acid (40 mL) and carbon tetrachloride (3 mL). After adding concentrated sulfuric acid (2 mL), the mixture was heated to 80 °C for 22 hours. After cooling to room temperature, the formed precipitate was filtered off. The filtrate was washed with aq. $NaHSO_3$ solution (20 %), dried over sodium sulfate and the solvent was removed under reduced pressure. The residue and the previously separated precipitate were recrystallized from isopropanol yielding **6** in 50 % (3.775 g, 9.033 mmol).

Chemical formula: $C_{13}H_8I_2$

Molecular weight: 418.02 g/mol

^{1}H-NMR (500 MHz, $CDCl_3$, 298 K), δ [ppm]

7.88 - 7.86 (m, 2 H), 7.71 - 7.69 (m, 2 H), 7.51 - 7.48 (d, J = 8.0 Hz, 2 H), 3.83 (s, 2 H).

^{13}C-NMR (126 MHz, CD_2Cl_2, 298 K), δ [ppm]

145.0, 140.5, 136.1, 134.3, 121.7, 92.6, 36.4.

MS (EI, 70 eV), *m/z* (%)

417.9 (100) $[M]^{\bullet+}$, 290.9 (43) $[M\text{-}I]^+$, 164.0 (33) $[M\text{-}2\ I]^+$; calculated: 417.9 Da.

Compound **7** (PK-031)

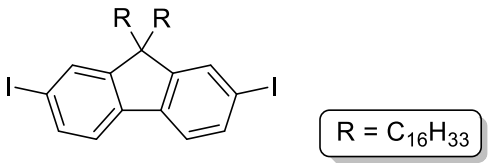

This synthesis applies a procedure published by Ponmuthu et al.[47]

6 (999 mg, 2.39 mmol, 1.00 eq.) and NaOH (2.011 g, 50.29 mmol, 21.03 eq.) were dissolved in a mixture of toluene (30 mL) and water (4 mL). NBu_4Br (122 mg, 0.379 mmol, 0.159 eq.) and 1-bromohexadecane (1.70 mL, 5.56 mmol, 2.33 eq.) were added and the mixture was heated to 80 °C for 24 hours. After checking the progress of the reaction *via* TLC, NBu_4Br (122 mg, 0.379 mmol, 0.158 eq.) and 1-bromohexadecane (1.7 mL, 5.6 mmol, 2.3 eq.) were additionally added and the reaction was continued for another 24 hours. After cooling to room temperature, the mixture was diluted with DCM and water. The phases were separated and the aqueous layer was extracted with DCM four times. The combined organic layers were washed with water and brine and dried over sodium sulfate. After removal of the solvent under reduced pressure, the crude product was purified

via column chromatography (SiO_2, Cy, R_f = 0.8), receiving the product in 77 % as a pale-yellow oil (1.598 g, 1.837 mmol).

Chemical formula: $C_{45}H_{72}I_2$

Molecular weight: 866.88 g/mol

^{1}H-NMR (400 MHz, $CDCl_3$, 298 K), δ [ppm]

7.66 - 7.63 (m, 4 H), 7.41 - 7.39 (d, J = 8.3 Hz, 2 H), 1.90 - 1.80 (m, 4 H), 1.26 (bs, 56 H), 0.91 - 0.87 (t, J = 7.1 Hz, 6 H).

^{13}C-NMR (126 MHz, CD_2Cl_2, 298 K), δ [ppm]

145.0, 140.5, 136.1, 134.3, 121.7, 92.6, 31.9, 29.4, 29.4, 29.4, 29.3, 29.3, 29.3, 29.3, 29.2, 29.2, 29.1, 29.0, 23.3, 22.7, 13.9.

MS (EI, 70 eV), *m*/*z* (%)

866.4 (100) $[M]^{\bullet+}$; calculated: 866.4 Da.

Compound **3**/**8** (PK-033/ PK-032, PK-036)

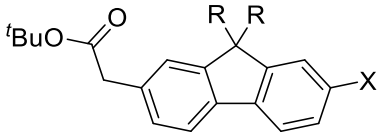

3: X = Br
8: X = I
R = $C_{16}H_{33}$

This synthesis applies a procedure published by Hartwig et al.[122]

The reaction was performed twice using two different substrates, as displayed in the following tables. Zinc powder was stirred in aq. HCl (1M) for 30 min to activate it. After filtering off, it was dried under vacuum overnight. Activated zinc powder was then placed in a *Schlenk* flask and the flask was dried and purged with argon. Under *Schlenk* conditions, dry THF and *tert*-butyl bromoacetate were added and the mixture was refluxed until it became a clear solution. Afterwards, the respective dihalo-fluorene, *QPhos* and $Pd_2(dba)_3$ were added and the mixture was heated to 90 °C for 16 hours. TLC revealed the formation of **5b** exceptionally in presence of the respective substrate. The mixture was in both cases discarded.

Table 5: Reaction conditions applied for the synthesis of **3**.

For 3:	m [mg]	V [mL]	n [μmol]	eq.
2	202	-	261	1.00
zinc	40.1	-	613	2.35
ethyl bromoacetate	-	0.04	271	1.04
QPhos	11.1	-	15.6	0.0598
$Pd_2(dba)_3$	13.0	-	14.0	0.054
THF	-	20	-	-

Table 6: Reaction conditions applied for the synthesis of **8**.

For 8:	m[mg]	V [mL]	n [μmol]	eq.
7	202	-	2328	1.000
Zinc powder	40.8	-	624	2.68
ethyl bromoacetate	-	0.04	271	1.16
QPhos	9.8	-	14	0.059
$Pd_2(dba)_3$	13.0	-	14.2	0.0601
THF	-	30	-	-

Compound **9** (PK-034)

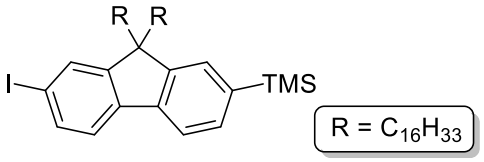

This synthesis applies a procedure published by Suranna et al.[158]

Under *Schlenk* conditions, **7** (0.203 g, 0.234 mmol, 1.000 eq.) was dissolved in dry THF (20 mL). The solution was cooled to -78 °C and a solution of *n*BuLi (1.70 mL, 0.272 mmol, 1.16 eq.; 1.6M in hexane) was added dropwise and afterwards stirred for one hour. After adding TMSCl (50 μL, 0.39 mmol, 1.68 eq.), the mixture was allowed to warm to room temperature and stirred overnight. The mixture was diluted with DCM and water and the phases were separated. The aqueous layer was extracted with DCM twice. The combined organic layers were washed brine and dried over magnesium sulfate. After removal of the solvent under reduced pressure, the crude product was purified *via* column chromatography (SiO_2, DCM, R_f = 0.85). The product could not be separated from substrate **7** due to their similar polarity. It was therefore not possible to determine the yield or provide reasonable spectral data.

Chemical formula: $C_{48}H_{81}ISi$

Molecular weight: 813.17 g/mol

Compound **10a** (PK-035)

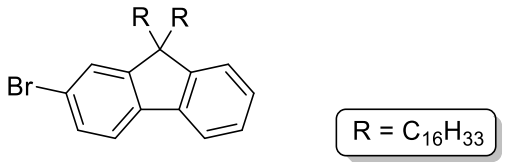

This synthesis applies a procedure published by Ponumuthu et al.[47]

2-bromofluorene (3.067 g, 12.51 mmol, 1.000 eq.) and KOH (2.841 g, 50.64 mmol, 4.047 eq.) were dissolved in a mixture of acetone (40 mL) and water (4 mL). NBu_4Br (0.376 g, 1.17 mmol, 0.093 eq.) and 1-bromohexadecane (7.30 mL, 23.9 mmol, 1.91 eq.) were added and the mixture was heated to 80 °C for 70 hours. After cooling to room temperature, the residue was diluted with DCM and water. The phases were separated and the aqueous layer was extracted with DCM three times. The combined organic layers were washed with water, aq. HCl (1M) and brine and dried over magnesium sulfate. After removal of the solvent under reduced pressure, the crude product was purified *via* column chromatography (SiO_2, Cy, R_f = 0.9), receiving the product in 65 % as a colorless solid (5.632 g, 8.116 mmol).

Chemical formula: $C_{45}H_{73}Br$

Molecular weight: 693.98 g/mol

^{1}H-NMR (500 MHz, CD_2Cl_2, 298 K), δ [ppm]

7.70 - 7.67 (m, 1 H), 7.59 - 7.57 (d, *J* = 8.0 Hz, 1 H), 7.50 (d, *J* = 1.8 Hz, 1 H), 7.47 - 7.44 (d, *J* = 1.8 Hz, 1 H), 7.35 - 7.31 (m, 3 H), 1.99 - 1.94 (m, 4 H), 1.89 - 1.83 (m, 4 H), 1.28 (s, 52 H), 0.91 - 0.88 (t, *J* = 6.8 Hz, 6 H).

^{13}C-NMR (126 MHz, CD_2Cl_2, 298 K), δ [ppm]

153.7, 151.0, 140.9, 140.7, 130.4, 128.1, 127.5, 126.8, 123.5, 121.6, 121.5, 120.3, 56.0, 54.0, 40.8, 34.8, 33.6, 32.6, 30.4, 30.3, 30.2, 30.2, 30.1, 30.0, 29.9, 29.4, 28.8, 24.4, 23.3, 14.5.

MS (EI, 70 eV), *m/z* (%)

694.0 (45) $[M]^{\bullet+}$, 469.2 (15) $[M\text{-}C_{16}H_{33}]^+$, 388.2 (14) $[M\text{-}C_{16}H_{33}\text{-}Br]^+$, 244.9 (29) $[M\text{-}2\ C_{16}H_{33}]^+$; calculated: 692.5 Da.

Compound **10b**

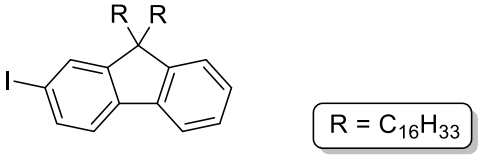

This synthesis applies a procedure published by Ponumuthu et al.[47]

2-Iodofluorene (1.000 g, 3.425 mmol, 1.000 eq.) and KOH (1.240 g, 22.09 mmol, 6.451 eq.) were dissolved in a mixture of acetone (20 mL) and water (3 mL). NBu_4Br (0.501 g, 1.55 mmol, 0.454 eq.) and 1-bromohexadecane (2.1 mL, 6.9 mmol, 2.01 eq.) were added and the mixture was heated to 70 °C for 48 h. After cooling to room temperature, the residue was diluted with DCM and aq. HCl (2M). The phases were separated and the aqueous layer was extracted with DCM three times. The combined organic layers were washed with brine and dried over magnesium sulfate. After removal of the solvent under reduced pressure, the crude product was purified *via* column chromatography (SiO_2, Cy, R_f = 0.77), receiving the product in 55 % as a colorless solid (1.392 g, 1.879 mmol).

Chemical formula: $C_{45}H_{73}I$

Molecular weight: 740.98 g/mol

^{1}H-NMR (500 MHz, CD_2Cl_2, 298 K), δ [ppm]

7.70 - 7.65 (m, 3 H), 7.48 - 7.46 (d, J = 8.0 Hz, 1 H), 7.34 - 7.32 (m, 3 H), 1.99 - 1.90 (m, 4 H), 1.27 (bs, 56 H), 0.90 - 0.86 (t, J = 7.1 Hz, 6 H).

^{13}C-NMR (126 MHz, CD_2Cl_2, 298 K), δ [ppm]

153.0, 149.9, 140.6, 139.9, 135.5, 131.9, 127.4, 126.6, 122.7, 121.1, 119.5, 92.1, 55.1, 31.7, 29.7, 29.5, 29.5, 29.4, 29.4, 29.4, 29.4, 29.3, 29.3, 29.1, 29.0, 23.5, 22.5, 13.7.

MS (EI, 70 eV), *m/z* (%)

740.5 (100) $[M]^{\bullet+}$; calculated: 740.5 Da.

Compound **11** (PK-037)

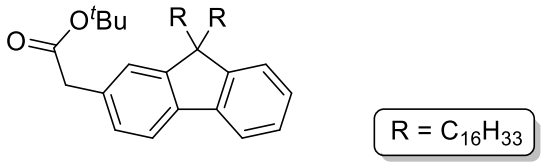

This synthesis applies a procedure published by Hartwig et al.[122]

Zinc powder was stirred in aq. HCl (1M) for 30 min to activate it. After filtering off, it was dried under vacuum overnight. Under *Schlenk* conditions, zinc powder (2.502 g, 38.26 mmol, 13.28 eq.) and *tert*-butyl bromoacetate (5.70 mL, 38.6 mmol, 13.4 eq.) were suspended in dry THF (30 mL) and the mixture was heated to 60 °C for three hours. After adding **10a** (2.000 g, 2.882 mmol, 1.000 eq.), *XPhos* (0.207 g, 0.434 mmol, 0.151 eq.) and $Pd_2(dba)_3$ (0.271 g, 0.296 mmol, 0.103 eq.), the mixture was

heated to 80 °C for 17 hours. After cooling to room temperature, the mixture was diluted with DCM and aq. HCl (1M), the phases were separated and the aqueous layer was extracted with DCM four times. The combined organic layers were washed with aq. HCl (1M) and brine and dried over magnesium sulfate. After removal of the solvent under reduced pressure, the crude product was purified *via* column chromatography (SiO_2, Cy:DCM 1:1, R_f = 0.55), receiving the product as a colorless solid (1.622 g, 2.224 mmol) in 77 % yield.

Chemical formula: $C_{51}H_{84}O_2$

Molecular weight: 729.23 g/mol

^{1}H-NMR (500 MHz, CD_2Cl_2, 298 K), δ [ppm]

7.70 - 7.68 (m, 1 H), 7.66 - 7.63 (d, *J* = 7.7 Hz, 1 H), 7.36 - 7.27 (m, 4 H), 7.24 - 7.21 (dd, *J* = 7.8 Hz, *J* = 1.6 Hz, 1 H), 3.58 (s, 2 H), 2.00 - 1.95 (m, 4 H), 1.42 (*s*, 9 H), 1.27 (bs, 56 H), 0.91 - 0.87 (t, *J* = 6.9 Hz, 6 H).

^{13}C-NMR (126 MHz, CD_2Cl_2, 298 K), δ [ppm]

171.2, 151.4, 151.2, 141.4, 140.3, 134.4, 128.2, 127.3, 127.1, 124.1, 123.3, 119.9, 114.3, 80.8, 55.4, 40.9, 34.6, 33.4, 32.4, 30.2, 30.2, 30.1, 30.0, 30.0, 29.9, 29.8, 29.3, 28.7, 28.2, 27.4, 24.3, 23.2, 14.4.

MS (EI, 70 eV), *m*/*z* (%)

728.6 (100) $[M]^{\bullet+}$, 672.5 (44) $[M\text{-}C_4H_9]^+$, 503.3 (25) $[M\text{-}C_{16}H_{33}]^+$; calculated: 728.7 Da.

Compound **12** (PK-038)

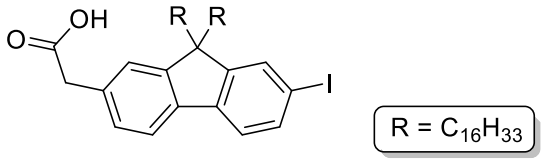

11 (203 mg, 0.279 mmol, 1.000 eq.), iodine (53.8 mg, 0.212 mmol, 0.760 eq.) and iodic acid (26.1 mg, 0.148 mmol, 0.532 eq.) were suspended in a mixture of glacial acetic acid (20 mL) and carbon tetrachloride (2 mL). After adding concentrated sulfuric acid (0.05 mL), the mixture was heated to 80 °C for 4.5 hours. After cooling to room temperature, the mixture was diluted with DCM and aq. $NaHSO_3$ solution (40 %), the phases were separated and the aqueous layer was extracted with DCM twice. The combined organic layers were washed with brine and dried over magnesium sulfate. After removal of the solvent under reduced pressure, the crude product was purified *via* column chromatography (SiO_2, DCM, R_f = 0.3), receiving the product as a brown oil (196 mg, 0.246 mmol) in 88 %.

Chemical formula: $C_{47}H_{75}IO_2$

Molecular weight: 799.02 g/mol

^{1}H-NMR (400 MHz, CD_2Cl_2, 298 K), δ [ppm]

7.67 - 7.63 (m, 2 H), 7.46 - 7.44 (d, *J* = 8.0 Hz, 1 H), 7.36 - 7.24 (m, 3 H), 3.73 (s, 2 H), 2.00 - 1.92 (m, 4 H), 1.28 (bs, 56 H), 0.91 - 0.87 (t, *J* = 6.9 Hz, 6 H).

^{13}C-NMR (126 MHz, CD_2Cl_2, 298 K), δ [ppm]

177.3, 153.3, 150.6, 140.4, 139.2, 135.8, 133.0, 132.1, 128.1, 124.1, 121.3, 119.7, 92.3, 55.3, 40.0, 34.6, 33.4, 32.4, 30.2, 30.2, 30.1, 30.0, 30.0, 29.9, 29.8, 29.3, 28.7, 28.2, 27.4, 24.3, 23.2, 14.4.

MS (EI, 70 eV), *m/z* (%)

798.4 (8) $[M]^{\bullet+}$; calculated: 798.5 Da.

Compound **13** (PK-041)

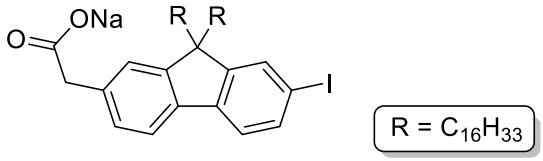

In a round-bottom flask, *tert*-butanol (40 mL) was molten at 30 °C. **12** (855 mg, 1.07 mmol, 1.00 eq.) and sodium *tert*-butoxide (0.103 g, 1.07 mmol, 1.00 eq.) were added and the mixture was stirred three hours at 30 °C. The solvent was removed under reduced pressure yielding **13** as pale-brown solid (886 mg, 1.08 mmol) in quantitative yield.

Chemical formula: $C_{47}H_{74}IO_2Na$

Molecular weight: 821.00 g/mol

Due to the similarity of **13** *and* **12***, no spectra were recorded.*

Compound **14**

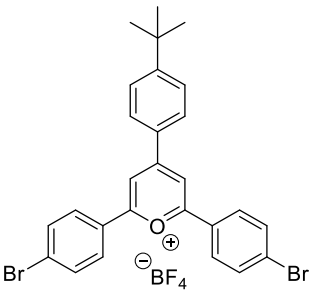

Chemical formula: $C_{27}H_{23}BBr_2F_4O$

Molecular weight: 610.09 g/mol

14 *was synthesized by M. Kersten during his PhD studies.*[105]

Compound **15** (PK-043)

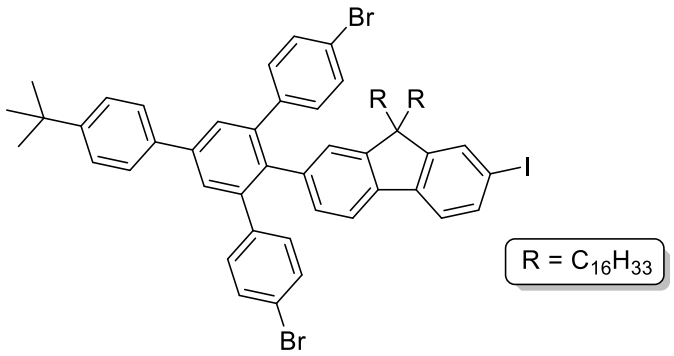

This synthesis applies a procedure published by Idelson et al.[96]

13 (886 mg, 1.08 mmol, 1.00 eq.) and **14** (801 mg, 1.31 mmol, 1.22 eq.) were placed in a round bottom flask. Benzoic anhydride (4.977 g, 22.00 mmol, 20.38 eq.) was added and the mixture was heated to 150 °C for four hours. Sublimed benzoic anhydride was molten by external heating every 15 minutes so that it drops back down into the melt. The crude product was purified *via* column chromatography (SiO_2, Cy:DCM 20:1, R_f = 0.85) successfully removing large parts of benzoic anhydride and substrate leftovers. Afterwards, the desired compound was isolated *via* column chromatography (SiO_2, Cy, R_f = 0.8) yielding **15** as a pale-yellow glass-like solid (111 mg, 88.4 μmol) in 8 %. Additionally, another fraction was collected separately containing mainly **15** with slight impurities (276 mg) that could not be removed.

Chemical formula: $C_{73}H_{95}Br_2I$

Molecular weight: 1259.28 g/mol

^{1}H-NMR (500 MHz, CD_2Cl_2, 298 K), δ [ppm]

7.71 - 7.61 (m, 6 H), 7.54 – 7.50 (d, J = 8.2 Hz, 2 H), 7.45 - 7.37 (m, 2 H), 7.30 – 7.27 (d, J = 8.5 Hz, 4 H), 7.10 - 7.06 (dd, J = 8.6 Hz, J = 6.9 Hz, 4 H), 6.95 - 6.93 (dd, J = 6.5 Hz, J = 1.6 Hz, 1 H), 6.88 - 6.84 (m, 1 H), 1.87 - 1.76 (m, 4 H), 1.74 - 1.67 (m, 4 H), 1.39 (s, 9 H), 1.28 (bs, 52 H), 0.90 (t, J = 6.9 Hz, 6 H).

^{13}C-NMR (126 MHz, CD_2Cl_2, 298 K), δ [ppm]

154.0, 151.6, 151.6, 151.5, 150.8, 150.2, 142.0, 141.5, 141.4, 138.9, 136.4, 132.6, 132.2, 132.2, 131.4, 131.3, 128.8, 128.7, 127.3, 126.5, 126.5, 123.4, 121.2, 121.2, 92.9, 55.4, 40.8, 40.7, 35.1, 32.6, 31.7, 30.7, 30.7, 30.3, 30.3, 30.3, 30.1, 30.1, 30.0, 27.6, 23.3, 14.6.

MS (MALDI-pos, DCTB) *m/z* (%)

1256.5 (60) $[M]^{\bullet+}$, 1130.6 (100) $[M\text{-}I]^+$; calculated: 1258.5 Da.

Compound **16** (PK-044)

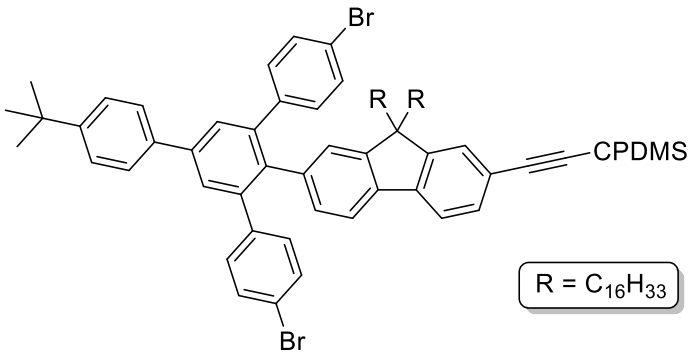

This synthesis applies an unpublished procedure by zur Horst.[106]

An impure fraction of **15** (181 mg, 144 μmol, 1.000 eq.), $PdCl_2(PPh_3)_2$ (8.3 mg, 11.8 μmol, 0.082 eq.), CuI (10.8 mg, 56.7 μmol, 0.395 eq.) and PPh_3 (8.3 mg, 29.7 μmol, 0.207 eq.) were placed in a *Schlenk* flask, which was evacuated and purged with argon three times. The compounds were suspended in dry THF (15 mL) and freshly distilled piperidine (10 mL) and the mixture was purged with argon for 30 minutes. After adding CPDMS-acetylene (39.2 mg, 259 μmol, 1.80 eq.) the mixture was stirred 21 hours. The solution was diluted with DCM and aq. HCl (1M), the phases were separated and the aqueous layer was extracted with DCM seven times. The combined organic layers were washed with aq. EDTA (0.1M) and brine and dried over magnesium sulfate. After removal of the solvent under reduced pressure, the crude product was purified *via* column chromatography (SiO_2, Cy:DCM 3:1, R_f = 0.4), receiving the product as pale-yellow glass-like solid (42.4 mg, 33.1 μmol) in 23 % yield.

Chemical formula: $C_{81}H_{107}Br_2NSi$

Molecular weight: 1282.65 g/mol

^{1}H-NMR (500 MHz, CD_2Cl_2, 298 K), δ [ppm]

7.67 - 7.64 (d, *J* = 9.5 Hz, 4 H), 7.58 - 7.55 (dd, *J* = 7.8 Hz, *J* = 0.7 Hz, 1 H), 7.53 - 7.50 (d, *J* = 8.5 Hz, 2 H), 7.43 - 7.40 (d, *J* = 7.8 Hz, 2 H), 7.38 (s, 1 H), 7.30 - 7.27 (d, *J* = 8.5 Hz, 4 H), 7.08 - 7.05 (d, *J* = 8.5 Hz, 4 H), 6.94 - 6.93 (d, *J* = 0.7 Hz, 1 H), 6.88 - 6.85 (dd, *J* = 7.8 Hz, *J* = 1.5 Hz, 1 H), 2.47 - 2.43 (t, *J* = 7.0 Hz, 2 H), 1.89 - 1.77 (m, 4 H), 1.73 - 1.66 (m, 2 H), 1.38 (s, 9 H), 1.26 (bs, 52 H), 0.90 - 0.85 (m, 8 H), 0.42 - 0.33 (m, 4 H), 0.28* (s, 6 H).

^{13}C-NMR (126 MHz, CD_2Cl_2, 298 K), δ [ppm]

151.6, 151.5, 151.1, 142.1, 142.0, 141.4, 140.8, 139.2, 139.1, 138.6, 137.6, 132.2, 131.8, 131.5, 131.3, 131.0, 130.8, 130.5, 128.7, 127.5, 127.2, 126.9, 126.7, 126.5, 121.2, 107.9, 92.5, 55.5, 40.8, 35.1, 32.5, 32.4, 31.7, 30.7, 30.4, 30.3, 30.3, 30.3, 30.3, 30.3, 30.2, 30.0, 27.5, 24.4, 24.1, 23.3, 21.3, 21.0, 16.3, 14.5, -1.5*.

MS (MALDI-pos, DCTB) *m/z* (%)

1281.6 (100) $[M]^{\bullet+}$; calculated: 1281.7 Da.

*Signals marked with * feature satellites from couplings with isotopes of low abundance.*

Compound **17a** (PK-047)

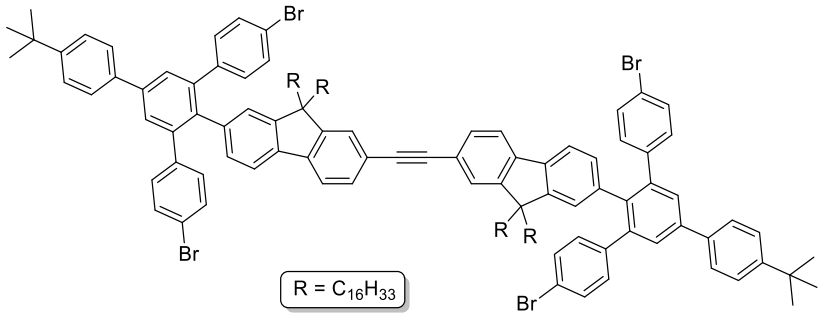

This synthesis applies an unpublished procedure by zur Horst.[106]

15 (155 mg, 123 μmol, 1.21 eq.), **16** (131 mg, 102 μmol, 1.00 eq.) and CuI (5.4 mg, 28 μmol, 0.28 eq.) were placed in a *Schlenk* flask and the flask was evacuated and purged with argon three times. Dry THF (15 mL) and freshly distilled piperidine (10 mL) were added and the resulting solution was purged with argon for 50 minutes. After adding $Pd(PPh_3)_4$ (13.2 mg, 11.4 μmol, 0.112 eq.) and TBAF (0.1 mL, 0.4 mmol, 3.4 eq.), the mixture was stirred 22 hours at room temperature. The solution was diluted with DCM and aq. HCl (1M), the phases were separated and the aqueous layer was extracted with DCM three times. The combined organic layers were washed with brine and dried over magnesium sulfate. After removal of the solvent under reduced pressure, the crude product was pre-purified *via* column chromatography (SiO_2, Cy:EA 100:1, R_f = 0.4) and isolated *via* recGPC (THF, unstabilized) yielding **17a** as a yellow solid in 26 % (61.3 mg, 26.8 μmol).

Chemical formula: $C_{148}H_{190}Br_4$

Molecular weight: 2288.76 g/mol

^{1}H-NMR (500 MHz, CD_2Cl_2, 298 K), δ [ppm]

7.67 (s, 4 H), 7.67 - 7.64 (m, 4 H), 7.63 - 7.60 (d, *J* = 7.8 Hz, 2 H), 7.53 - 7.51 (d, *J* = 8.6 Hz, 4 H), 7.51 - 7.47 (m, 4 H), 7.44 - 7.42 (d, *J* = 7.8 Hz, 2 H), 7.30 - 7.28 (d, *J* = 8.6 Hz, 8 H), 7.09 - 7.06 (d, *J* = 8.5 Hz, 8 H), 6.94 (m, 2 H), 6.88 - 6.85 (dd, *J* = 7.8 Hz, *J* = 1.5 Hz, 2 H), 1.87 - 1.80 (m, 8 H), 1.76 - 1.67 (m, 8 H), 1.38 (s, 18 H), 1.25 (bs, 104 H), 0.90 - 0.86 (t, *J* = 6.9 Hz, 12 H).

^{13}C-NMR (126 MHz, CD_2Cl_2, 298 K), δ [ppm]

151.0, 150.5, 141.4, 141.0, 140.8, 140.2, 138.8, 137.0, 131.6, 130.7, 130.4, 130.0, 128.1, 126.6, 126.3, 125.9, 125.8, 120.6, 119.7, 119.2, 90.5, 54.9, 40.2, 34.5, 31.9, 31.0, 30.1, 29.7, 29.7, 29.7, 29.6, 29.5, 29.3, 27.7, 23.7, 22.7, 22.1, 13.9.

MS (MALDI-pos, DCTB) *m/z* (%)

2289.2 (100) $[M]^{\bullet+}$; calculated: 2287.2 Da.

Compound **18** (PK-058)

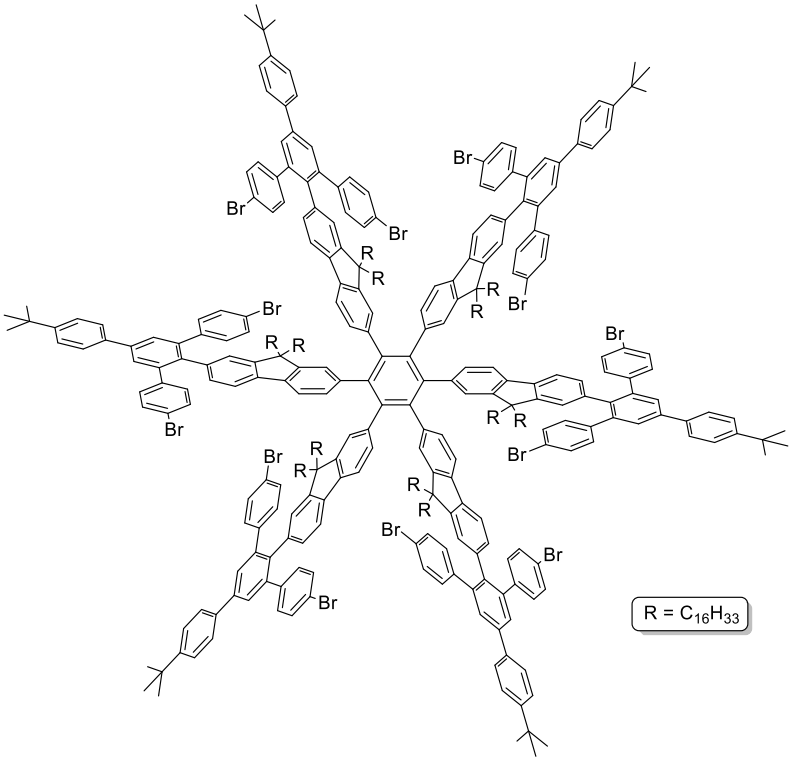

This synthesis applies a procedure published by Idelson et al.[96]

17 (61.3 mg, 26.8 μmol, 1.00 eq.) was dissolved in toluene (15 mL) and purged with argon for one hour. After adding $Co_2(CO)_8$ (2.5 mg, 7.3 μmol, 0.27 eq.), the mixture was heated to 120 °C. After four hours, the progress of the reaction was checked *via* analytical GPC. Due to the low conversion, the reaction was continued for an additional 16 hours. The conversion was checked again, more $Co_2(CO)_8$ (1.7 mg, 5.0 μmol, 0.19 eq.) was added and the reaction was continued for an additional ten hours. To increase the turnover, $Co_2(CO)_8$ (1.2 mg, 3.5 μmol, 0.13 eq.) was added one last time. After 15 hours, the mixture was allowed to cool to room temperature and the solvent was removed under reduced pressure. Afterwards, the crude product was pre-purified by filtering column chromatography (SiO_2, DCM, R_f = 0.9). It was only possible to collect analytical amounts from recGPC (THF, unstabilized). Hence, **18** was only found *via* MALDI mass spectrometry in traces.

Chemical formula: $C_{444}H_{570}Br_{12}$

Molecular weight: 6866.29 g/mol

MS (MALDI-pos, DCTB), *m/z* (%)

6866.5 (8) $[M]^{\bullet+}$; calculated: 6861.5 Da.

Compound **20b** (PK-039)

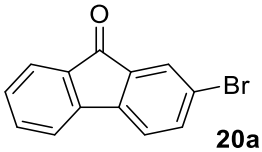

20a

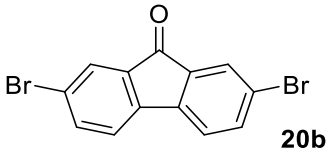

20b

This synthesis applies a procedure published by Göbel et al.[157]

To a suspension of 9-fluorenone (5.001 g, 27.75 mmol, 1.000 eq.) and $FeCl_3$ (301 mg, 1.86 mmol, 0.0669 eq.) in $CHCl_3$ (40 mL) a solution of bromine (3.00 mL, 60.1 mmol, 2.17 eq.) in $CHCl_3$ (10 mL) was added dropwise over a period of one hour. Afterwards, the mixture was stirred overnight. The formed precipitate was filtered off and dissolved in DCM. The resulting solution was washed three times with aq. $NaHSO_3$ solution (40 %), once with brine and dried over sodium sulfate. The crude product was purified *via* column chromatography (SiO_2, Cy:DCM 1:2), receiving **20a** (1.576 g, 6.083 mmol, R_f = 0.4) in 22 % yield as well as **20b** in analytical amounts (R_f = 0.5) both as yellow solids.

20a:

Chemical formula: $C_{13}H_7BrO$

Molecular weight: 259.10 g/mol

^{1}H-NMR (500 MHz, CD_2Cl_2, 298 K), δ [ppm]

7.73 (dd, *J* = 1.9 Hz, *J* = 0.5 Hz, 1 H), 7.65 - 7.62 (m, 2 H), 7.56 - 7.51 (m, 2 H), 7.45 - 7.43 (dd, *J* = 7.9 Hz, *J* = 0.5 Hz, 1 H), 7.36 - 7.32 (td, *J* = 7.2 Hz, *J* = 1.5 Hz, 1 H).

^{13}C-NMR (126 MHz, CD_2Cl_2, 298 K), δ [ppm]

192.5, 144.0, 143.5, 137.5, 136.2, 135.5, 134.1, 129.8, 127.6, 124.7, 123.2, 122.3, 121.0.

MS (EI, 70 eV), *m/z* (%)

258.1 (100) $[M\text{-}H]^{\bullet+}$, 179.1 (7) $[M\text{-}Br]^+$, 151.1 (65) $[M\text{-}Br\text{-}CO]^+$; calculated: 258.0 Da.

20b:

Chemical formula: $C_{13}H_6Br_2O$

Molecular weight: 338.00 g/mol

^{1}H-NMR (400 MHz, CD_2Cl_2, 298 K), δ [ppm]

7.75 - 7.73 (dd, *J* = 1.9 Hz, *J* = 0.5 Hz, 2 H), 7.66 - 7.63 (dd, *J* = 7.9 Hz, *J* = 1.9 Hz, 2 H), 7.43 - 7.40 (dd, *J* = 8.0 Hz, *J* = 0.5 Hz, 2 H).

^{13}C-NMR (126 MHz, CD_2Cl_2, 298 K), δ [ppm]

191.1, 142.7, 137.9, 135.7, 127.9, 123.6, 122.5.

MS (EI, 70 eV), *m/z* (%)

338.0 (100) $[M]^{\bullet+}$, 229.1 (20) $[M\text{-}Br\text{-}CO]^+$, 150.1 (53) $[M\text{-}2\ Br\text{-}CO]^+$; calculated: 337.9 Da.

Compound **21** (PK-040)

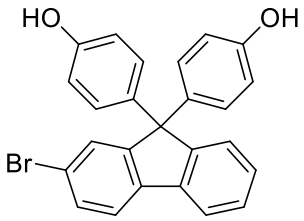

This synthesis applies a procedure published by Abashev et al.[124]

20a (960.7 mg, 3.708 mmol, 1.000 eq.) was suspended in phenol (3.806 g, 40.45 mmol, 10.91 eq.) and the mixture was heated to 50 °C until the phenol was fully molten. After adding methanesulfonic acid (3.80 mL, 58.5 mmol, 15.8 eq.), the mixture was stirred for 46 hours at 50 °C. The mixture was allowed to cool to room temperature, the suspension was poured into water and a red viscous liquid was filtered off. The oil was dissolved in DCM and the solvent was removed under reduced pressure until the product began to crystallize. The suspension was stored in a freezer for 30 minutes and the precipitate was filtered off. The volume of the filtrate was reduced once more and the previous procedure was repeated until no more precipitate formed. The desired product was isolated as a colorless solid (967 mg, 2.25 mmol) in 61 %.

Chemical formula: $C_{25}H_{17}BrO_2$

Molecular weight: 429.31 g/mol

^{1}H-NMR (500 MHz, DMSO-*d*6, 298 K), *δ* [ppm]

9.35 (bs, 2 H), 7.92 - 7-89 (d, *J* = 7.5 Hz, 1 H), 7.87 - 7.84 (d, *J* = 8.0 Hz, 1 H), 7.57 - 7.54 (dd, *J* = 8.1 Hz, *J* = 1.8 Hz, 1 H), 7.49 (d, *J* = 1.8 Hz, 1 H), 7.39 - 7.30 (m, 3 H), 6.90 - 6.86 (d, *J* = 8.8 Hz, 4 H), 6.65 - 6.62 (d, *J* = 8.7 Hz, 4 H).

^{13}C-NMR (126 MHz, DMSO-*d*6, 298 K), *δ* [ppm]

156.6, 154.5, 152.0, 139.2, 138.6, 135.7, 130.8, 129.1, 128.0, 126.4, 122.9, 121.0, 115.6, 64.3.

MS (EI, 70 eV), *m/z* (%)

428.0 (27) $[M]^{\bullet+}$, 349.0 (100) $[M\text{-}Br]^+$; calculated: 428.0 Da.

Compound **22** (PK-042)

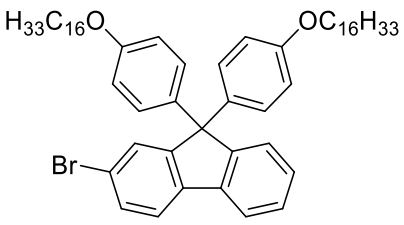

21 (958 mg, 2.23 mmol, 1.00 eq.) and KOH (490 mg, 8.73 mmol, 3.91 eq.) were dissolved in a mixture of acetone (20 mL) and water (2 mL). NBu_4Br (103 mg, 0.320 mmol, 0.144 eq.) and 1-bromohexadecane (1.30 mL, 4.25 mmol, 1.91 eq.) were added and the mixture was heated to 80 °C

for 50 hours. After cooling to room temperature, the solvent was removed under reduced pressure and the residue was dissolved in DCM and water. The phases were separated and the aqueous layer was extracted with DCM four times. The combined organic layers were washed with water, aq. HCl (2M) and brine and dried over magnesium sulfate. After removal of the solvent under reduced pressure, the crude product was purified *via* column chromatography (SiO_2, DCM, R_f = 0.9), receiving the product as colorless solid (1.745 g, 1.987 mmol) in 89 % yield.

Chemical formula: $C_{57}H_{81}BrO_2$

Molecular weight: 878.18 g/mol

^{1}H-NMR (500 MHz, CD_2Cl_2, 298 K), δ [ppm]

7.77 - 7.75 (d, *J* = 8.4 Hz, 1 H), 7.67 - 7.65 (d, *J* = 7.9 Hz, 1 H), 7.52 - 7.49 (m, 2 H), 7.39 - 7.35 (m, 2 H), 7.33 - 7.29 (m, 1 H), 7.10 - 7.06 (d, *J* = 8.9 Hz, 4 H), 6.79 - 6.74 (d, *J* = 8.9 Hz, 4 H), 3.92 - 3.89 (t, *J* = 6.6 Hz, 4 H), 1.78 - 1.72 (p, *J* = 6.7 Hz, 4 H), 1.47 - 1.41 (p, *J* = 7.3 Hz, 4 H), 1.29 (bs, 48 H), 0.92 - 0.88 (t, *J* = 6.6 Hz, 6 H).

^{13}C-NMR (126 MHz, CD_2Cl_2, 298 K), δ [ppm]

158.7, 154.5, 152.2, 139.5, 139.2, 137.4, 131.0, 129.4, 128.5, 128.0, 122.1, 121.6, 120.7, 114.6, 68.5, 64.8, 32.4, 30.2, 30.2, 30.1, 30.1, 30.1, 30.1, 29.9, 29.8, 29.7, 26.5, 23.2, 14.4.

MS (MALDI-pos, DCTB), *m*/*z* (%)

878.5 (100) $[M]^{\bullet+}$; calculated: 876.5 Da.

Compound **23** (PK-045)

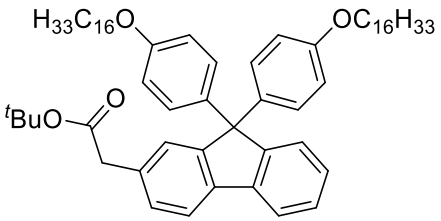

This synthesis applies a procedure published by Hartwig et al.[122]

Zinc powder was stirred in aq. HCl (1M) for 30 min to activate it. After filtering off, it was dried under vacuum overnight. Under *Schlenk* conditions, zinc powder (1.113 g, 17.03 mmol, 14.98 eq.) and *tert*-butyl bromoacetate (2.50 mL, 16.9 mmol, 14.9 eq.) were suspended in dry THF (20 mL) and the mixture was heated to 60 °C for three hours. After adding **22** (999 mg, 1.14 mmol, 1.00 eq.), *XPhos* (82.6 mg, 0.173 mmol, 0.152 eq.) and $Pd_2(dba)_3$ (101 mg, 0.110 mmol, 0.0968 eq.) the mixture was heated to 80 °C for 17 hours. After cooling to room temperature, the mixture was diluted with DCM and aq. HCl (1M), the phases were separated and the aqueous layer was extracted with DCM four times. The combined organic layers were washed with aq. HCl (1M) and brine and dried over sodium sulfate. After removal of the solvent under reduced pressure, the crude product was purified *via*

column chromatography (SiO_2, Cy:DCM 2:1, R_f = 0.3), receiving the product as a pale-yellow oil (806 mg, 0.883 mmol) in 78 %.

Chemical formula: $C_{63}H_{92}O_4$

Molecular weight: 913.43 g/mol

^{1}H-NMR (500 MHz, CD_2Cl_2, 298 K), δ [ppm]

7.77 - 7.70 (m, 2 H), 7.39 - 7.33 (m, 2 H), 7.29 - 7.24 (m, 3 H), 7.10 - 7.06 (d, *J* = 8.9 Hz, 4 H), 6.76 - 6.72 (d, *J* = 8.9 Hz, 4 H), 3.91 - 3.87 (t, *J* = 6.6 Hz, 4 H), 3.51 (s, 2 H), 1.77 - 1.89 (p, *J* = 6.7 Hz, 4 H), 1.44 (s, 9 H), 1.27 (bs, 52 H), 0.91 - 0.87 (t, *J* = 6.6 Hz, 6 H).

^{13}C-NMR (126 MHz, CD_2Cl_2, 298 K), δ [ppm]

171.0, 158.5, 152.5, 152.5, 140.1, 139.0, 138.1, 135.0, 129.4, 129.2, 128.9, 127.9, 127.8, 127.1, 126.3, 120.5, 118.2, 114.5, 81.0, 68.4, 64.6, 43.4, 32.4, 30.1, 30.1, 30.1, 30.1, 30.0, 30.0, 29.8, 29.8, 29.7, 28.1, 27.4, 26.5, 23.1, 14.3.

MS (MALDI-pos, DCTB), *m*/*z* (%)

912.7 (100) $[M]^{\bullet+}$; calculated: 912.7 Da.

Compound **24a** (PK-046)

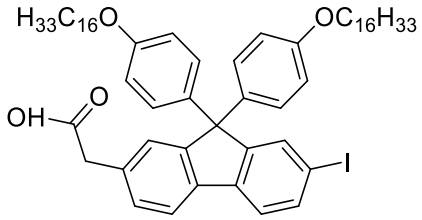

23 (778 mg, 0.852 mmol, 1.00 eq.), iodine (165 mg, 0.650 mmol, 0.763 eq.) and iodic acid (71.1 mg, 0.404 mmol, 0.475 eq.) were suspended in a mixture of glacial acetic acid (50 mL) and carbon tetrachloride (5 mL). After adding concentrated sulfuric acid (0.1 mL), the mixture was heated to 80 °C for 4.5 hours. The mixture was allowed to cool to room temperature, diluted with DCM and aq. $NaHSO_3$ solution (39 %), the phases were separated and the aqueous layer was extracted three times with DCM. The combined organic layers were washed with brine and dried over magnesium sulfate. The desired product was synthetically not accessible.

Chemical formula: $C_{59}H_{83}IO_4$

Molecular weight: 983.21 g/mol

Compound **25** (PK-TT-01)

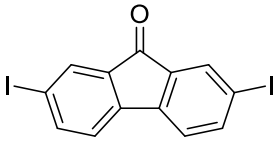

This synthesis applies a procedure published by Abashev et al.[124]

Fluorenone (10.02 g, 55.58 mmol, 1.000 eq.), iodine (10.57 g, 41.65 mmol, 0.749 eq.) and iodic acid (5.018 g, 28.53 mmol, 0.513 eq.) were suspended in a mixture of glacial acetic acid (100 mL), concentrated sulfuric acid (10 mL) and $CHCl_3$ (6 mL) and the mixture was heated to 80 °C overnight. After cooling to room temperature, the formed precipitate was collected and washed with water. After recrystallization from isopropanol, the product was yielded as a yellow solid (19.82 g, 45.90 mmol) in 83 %.

Chemical formula: $C_{13}H_6I_2$

Molecular weight: 432.00 g/mol

^{1}H-NMR (400 MHz, CD_2Cl_2, 298 K), δ [ppm]

7.93 – 7.91 (d, J = 1.6 Hz, 2 H), 7.86 – 7.84 (dd, J = 7.9 Hz, J = 1.7 Hz, 2 H), 7.31 – 7.29 (d, J = 7.9 Hz, 2 H).

^{13}C-NMR (126 MHz, CD_2Cl_2, 298 K), δ [ppm]

191.3, 144.0, 143.5, 135.4, 133.8, 122.8, 94.9.

MS (EI, 70 eV), *m/z* (%)

431.8 (100) $[M]^{\bullet+}$, 304.9 (20) $[M\text{-}I]^{\bullet+}$; calculated: 431.9 Da.

This molecule was synthesized by Thorsten Taschler within the limits of the module BCh 6.1.1 in 2021. The synthetic strategy is reproduced from his protocols.

Compound **26** (PK-TT-02)

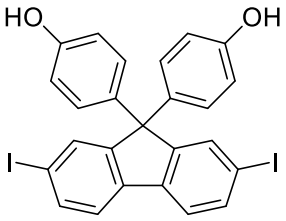

This synthesis applies a procedure published by Abashev et al.[124]

25 (5.008 g, 11.59 mmol, 1.000 eq.) and phenol (12.05 g, 128.0 mmol, 11.04 eq.) were placed in a round-bottom flask and methanesulfonic acid (12.0 mL, 184.7 mmol, 15.93 eq.) was rapidly added over two minutes. The suspension was heated to 50 °C for six hours. Due to solidification of the suspension, the reaction was stopped and allowed to cool to room temperature. After dissolving in acetone, the product was precipitated twice from water, yielding the product as a colorless solid (6.866 g).

It was not possible to determine a reasonable yield since it was possible to recognize remains of the yellow-colored substrate in the colorless crude product. The substrate was most likely not fully converted due to the solidification of the mixture.

Chemical formula: $C_{25}H_{16}I_2O_2$

Molecular weight: 602.21 g/mol

^{1}H-NMR (500 MHz, CD_2Cl_2, 298 K), δ [ppm]

8.40 (s, 2 H), 7.74 (m, 4 H), 7.73 – 7.71 (m, 2 H), 7.05 – 7.02 (d, J = 9.8 Hz, 4 H), 6.80 - 6.76 (d, J = 9.8 Hz, 4 H).

^{13}C-NMR (126 MHz, CD_2Cl_2, 298 K), δ [ppm]

157.4, 155.1, 139.5, 137.5, 136.3, 135.8, 129.9, 123.3, 116.1, 93.8, 65.2.

MS (EI, 70 eV), *m/z* (%)

601.9 (100) $[M]^{\bullet+}$, 475.0 (97) $[M\text{-}I]^+$, 349.1 (20) $[M\text{-}2\ I]^+$, 255.0 (18) $[M\text{-}2\ I\text{-}C_6H_4OH]^+$; calculated: 601.9 Da.

This molecule was synthesized by Thorsten Taschler within the limits of the module BCh 6.1.1 in 2021. The synthetic strategy is reproduced from his protocols.

Compound **27** (PK-TT-03)

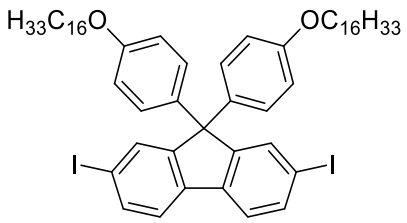

This synthesis applies a procedure published by Abashev et al.[124]

26 (6.866 g, 11.40 mmol), KOH (2.505 g, 44.64 mmol), NBu_4Br (0.534 g, 1.674 mmol) and potassium iodide (0.576 g, 3.471 mmol) were suspended in a mixture of acetone (100 mL) and water (10 mL). After adding 1-bromohexadecane (6.70 mL, 21.9 mmol), the mixture was heated to 80 °C for three days. After cooling to room temperature, the solvent was removed under reduced pressure and the residue was suspended in DCM and water. The phases were separated and the aqueous phase was extracted with DCM three times. The combined organic layers were washed with aq. HCl (10 %) and brine, dried over magnesium sulfate and the solvent was removed under reduced pressure. The crude product was purified *via* column chromatography (SiO_2, Cy:DCM 1:1), receiving the desired product (11.10 g, 10.56 mmol) in 91 % yield over two steps as a pale-yellow resin.

Chemical formula: $C_{57}H_{80}I_2O_2$

Molecular weight: 1051.07 g/mol

^{1}H-NMR (500 MHz, CD_2Cl_2, 298 K), δ [ppm]

7.69 (m, 4 H) 7.52 – 7.49 (d, 2 H, *J* = 8.0 Hz), 7.05 – 7.01 (d, 4 H, *J* = 10 Hz), 6.78 – 6.75 (d, 4 H, *J* = 10 Hz), 3.92 – 3.89 (t, 4 H), 1.77 – 1.70 (p, *J* = 6.6 Hz, 4 H), 1.36 – 1.26 (m, 52 H), 0.91 – 0.86 (t, *J* = 6.7 Hz, 6 H).

^{13}C-NMR (126 MHz, CD_2Cl_2, 298 K), δ [ppm]

158.8, 154.2, 139.0, 137.1, 136.8, 135.4, 129.5, 122.4, 114.6, 93.7, 68.5, 64.7, 34.2, 33.1, 32.4, 30.2, 30.1, 30.0, 29.9, 29.8, 29.7, 29.6, 29.4, 28.6, 27.3, 27.3, 26.4, 23.1, 14.3.

MS (MALDI-pos, DCTB), *m*/*z* (%)

1050.4 (100) $[M+H]^+$; calculated: 1050.4 Da.

This molecule was synthesized by Thorsten Taschler within the limits of the module BCh 6.1.1 in 2021. The synthetic strategy is reproduced from his protocols.

Compound **28a**/**28b** (PK-051)

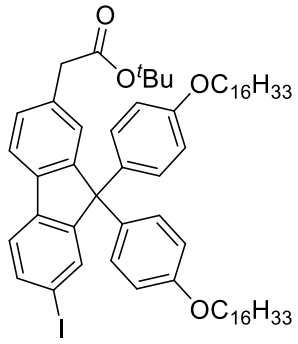

28a

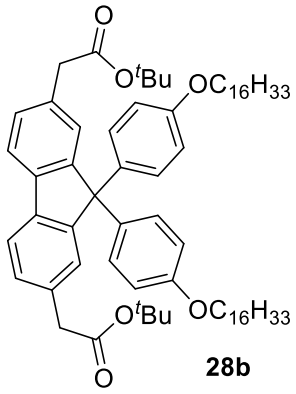

28b

This synthesis applies a procedure published by Hartwig et al.[122]

Zinc powder was stirred in aq. HCl (1M) for 30 min to activate it. After filtering off, it was dried under vacuum overnight. Under *Schlenk* conditions, zinc powder (0.060 g, 0.92 mmol, 0.87 eq.) and *tert*-butyl bromoacetate (0.14 mL, 0.95 mmol, 0.90 eq.) were suspended in dry THF (20 mL) and the mixture was heated to 60 °C for three hours. After adding **27** (1.112 g, 1.058 mmol, 1.000 eq.), *XPhos* (70.2 mg, 0.147 mmol, 0.139 eq.) and $Pd_2(dba)_3$ (115 mg, 0.126 mmol, 0.119 eq.), the mixture was heated to 80 °C for 17 hours. After cooling to room temperature, the mixture was diluted with DCM and aq. HCl (1M), the phases were separated and the aqueous layer was extracted with DCM four times. The combined organic layers were washed with aq. HCl (1M) and brine and dried over sodium sulfate. After removal of the solvent under reduced pressure, the residue was purified *via* column chromatography (SiO_2, Cy:DCM). None of the isolated fractions contained **28a**.

28a:

Chemical formula: $C_{63}H_{91}IO_4$

Molecular weight: 1039.32 g/mol

28b

Chemical formula: $C_{69}H_{102}O_6$

Molecular weight: 1027.57 g/mol

Compound **30**

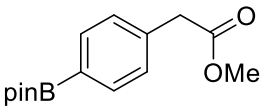

Chemical formula: $C_{15}H_{21}BO_4$

Molecular weight: 276.14 g/mol

30 *was commercially available and used without further purification.*

Compound **31** (PK-052)

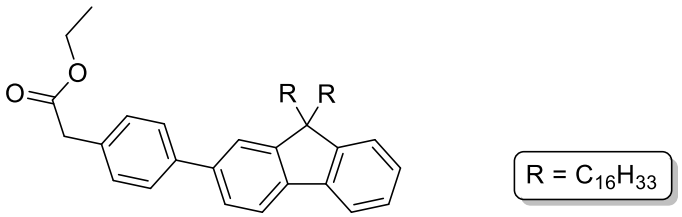

Version **a**:[105]

10a (3.020 g, 4.351 mmol, 1.000 eq.), K_2CO_3 (3.035 g, 21.96 mmol, 5.05 eq.), **30** (1.280 g, 4.634 mmol, 1.060 eq.) and PPh_3 (0.503 g, 0.433 mmol, 0.100 eq.) were dissolved in a mixture of toluene (60 mL) and ethanol (40 mL) and purged with argon for one hour. $PdCl_2(PPh_3)_2$ (0.503 g, 0.716 mmol, 0.165 eq.) was added and the mixture was heated to 70 °C for 48 h. After cooling to room temperature, the mixture was diluted with water and DCM and neutralized using aq. HCl (1M). After separating the phases, the aqueous layer was extracted three times with DCM. The combined organic layers were washed with brine twice and dried over magnesium sulfate. After removal of the solvent under reduced pressure, the crude product was purified *via* column chromatography (SiO_2, Cy:DCM 1:1, R_f = 0.71), receiving the product as a yellow oil (2.518 g, 3.239 mmol) in 75 %.

Version **b**:[105]

10b (1.392 g, 1.879 mmol, 1.000 eq.), K_2CO_3 (1.002 g, 7.253 mmol, 3.860 eq.), **30** (0.571 g, 2.069 mmol, 1.101 eq.) and PPh_3 (99.1 mg, 0.377 mmol, 0.201 eq.) were dissolved in a mixture of toluene (20 mL) and ethanol (10 mL) and purged with argon for one hour. $PdCl_2(PPh_3)_2$ (7.1 mg, 0.101 mmol, 0.054 eq.) was added and the mixture was heated to 80 °C for 46 h. After cooling to room temperature, the

solvent was removed under reduced pressure and the residue was suspended in DCM and aq. HCl (2M). The phases were separated and the aqueous layer was extracted three times with DCM. The combined organic layers were washed with brine and dried over magnesium sulfate. After removal of the solvent under reduced pressure, the crude product was purified *via* column chromatography (SiO_2, Cy:DCM 2:1, R_f = 0.5), receiving the product as yellow oil (999 mg, 1.29 mmol) in 68 %.

Chemical formula: $C_{55}H_{84}O_2$

Molecular weight: 777.28 g/mol

^{1}H-NMR (500 MHz, CD_2Cl_2, 298 K), δ [ppm]

7.79 - 7.77 (d, *J* = 8.3 Hz, 1 H), 7.76 - 7.73 (m, 1 H), 7.67 - 7.64 (d, *J* = 8.2 Hz, 2 H), 7.61 - 7.58 (m, 2 H), 7.40 - 7.37 (d, *J* = 8.5 Hz, 3 H), 7.37 - 7.30 (m, 2 H), 4.20 - 4.15 (q, *J* = 7.1 Hz, 2 H), 3.68 (s, 2 H), 2.05 - 2.01 (m, 4 H), 1.30 - 1.28 (m, 3 H), 1.27 (s, 56 H), 0.91 - 0.88 (t, *J* = 7.0 Hz, 6 H).

^{13}C-NMR (126 MHz, CD_2Cl_2, 298 K), δ [ppm]

171.8, 151.9, 151.5, 141.2, 140.9, 140.8, 140.0, 130.2, 127.6, 123.4, 121.9, 120.3, 120.1, 61.3, 55.6, 40.8, 32.4, 30.5, 30.2, 30.2, 30.1, 30.1, 30.1, 30.1, 30.0, 30.0, 30.0, 29.9, 29.8, 29.7, 29.2, 28.6, 14.5, 14.3.

MS (MALDI-pos, DCTB) *m/z* (%)

776.6 (100) $[M]^{\bullet+}$; calculated: 776.7 Da.

Compound **32** (PK-053)

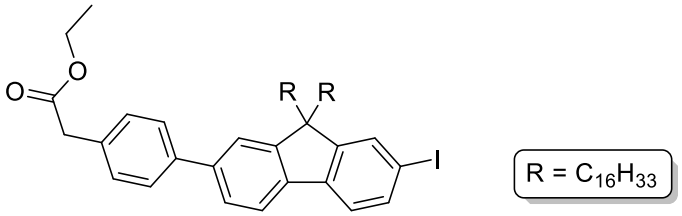

This synthesis applies a procedure published by Idelson et al.[96]

31 (1.937 g, 2.493 mmol, 1.000 eq.) was dissolved in DCM (25 mL) and the solution was purged with argon for 30 min. Iodine monochloride (2.50 mL, 2.50 mmol, 1.00 eq., 1M in DCM) was added and the mixture was stirred overnight at room temperature under the exclusion of light. The reaction was quenched by adding aq. $NaHSO_3$ solution (39 %), the phases were separated and the aqueous layer was extracted three times with DCM. The combined organic layers were washed with brine and dried over magnesium sulfate. After removal of the solvent under reduced pressure, the crude product was purified *via* column chromatography (SiO_2, DCM:Cy 1:1, R_f = 0.55), receiving the product as a pale-yellow oil (2.203 g, 2.439 mmol) in 98 %.

Chemical formula: $C_{55}H_{83}IO_2$

Molecular weight: 903.17 g/mol

^{1}H-NMR (500 MHz, CD_2Cl_2, 298 K), δ [ppm]

7.76 - 7.72 (m, 2 H), 7.70 - 7.67 (dd, *J* = 7.9 Hz, *J* = 1.6 Hz, 1 H), 7.65 - 7.62 (d, *J* = 8.2 Hz, 2 H), 7.60 - 7.56 (m, 2 H), 7.51 - 7.48 (d, *J* = 8.0 Hz, 1 H), 7.39 - 7.36 (d, *J* = 8.3 Hz, 2 H), 4.18 - 4.14 (q, *J* = 7.1 Hz, 2 H), 3.67 (s, 2 H), 2.05 - 1.94 (m, 4 H), 1.28 - 1.27 (m, 3 H), 1.26 (bs, 56 H), 0.90 - 0.87 (t, *J* = 7.0 Hz, 6 H).

^{13}C-NMR (126 MHz, CD_2Cl_2, 298 K), δ [ppm]

171.3, 153.5, 150.9, 140.5, 140.2, 140.1, 139.4, 132.2, 129.7, 127.1, 121.4, 120.0, 92.3, 60.8, 55.4, 40.8, 31.9, 29.9, 29.7, 29.6, 29.6, 29.6, 29.6, 29.6, 29.5, 29.5, 29.3, 29.2, 23.7, 22.7, 14.0, 13.9.

MS (MALDI-pos, DCTB) *m/z* (%)

902.5 (50) $[M]^{\bullet+}$, 776.7 (100) $[M\text{-}I]^+$; calculated: 902.5 Da.

Compound **33** (PK-054)

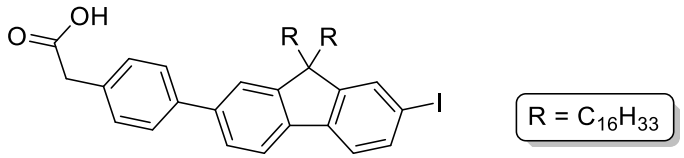

32 (1.235 g, 1.368 mmol, 1.000 eq.) was dissolved in a mixture of THF (20 mL) and water (4 mL). After adding $LiOH{\cdot}H_2O$ (1.000 g, 23.80 mmol, 17.40 eq.), the mixture was heated to 60 °C for 19 hours. The reaction mixture was diluted with DCM and neutralized using aq. HCl (2M). After phase separation, the aqueous layer was extracted three times using DCM. The combined organic phases were washed once with brine, dried over magnesium sulfate and the solvent was removed under reduced pressure. The crude product was purified *via* column chromatography (SiO_2, DCM, R_f = 0.1), receiving the product as a yellow oil (1.150 g, 1.314 mmol) in 96 %.

Chemical formula: $C_{53}H_{79}IO_2$

Molecular weight: 875.12 g/mol

^{1}H-NMR (500 MHz, CD_2Cl_2, 298 K), δ [ppm]

7.76 - 7.72 (m, 2 H), 7.69 - 7.67 (dd, *J* = 7.9 Hz, *J* = 1.6 Hz, 1 H), 7.65 - 7.63 (d, *J* = 8.2 Hz, 2 H), 7.60 - 7.56 (m, 2 H), 7.50 - 7.48 (d, *J* = 8.0 Hz, 1 H), 7.40 - 7.38 (d, *J* = 8.4 Hz, 2 H), 3.74 (s, 2 H), 2.03 - 1.94 (m, 4 H), 1.25 (bs, 56 H), 0.89 - 0.86 (t, *J* = 6.9 Hz, 6 H).

^{13}C-NMR (126 MHz, CD_2Cl_2, 298 K), δ [ppm]

177.0, 151.3, 140.9, 139.9, 136.3, 133.1, 132.6, 130.3, 127.7, 126.4, 121.9, 120.5, 92.8, 55.9, 40.6, 32.4, 30.4, 30.3, 30.1, 30.1, 30.1, 30.0, 30.0, 30.0, 29.8, 29.6, 24.2, 23.1, 14.3.

MS (EI, 70 eV), *m/z* (%)

874.6 (60) $[M]^{\bullet+}$, 749.7 (40) $[M\text{-}I]^{+}\cdot$; calculated: 874.5 Da.

Compound **34** (PK-055)

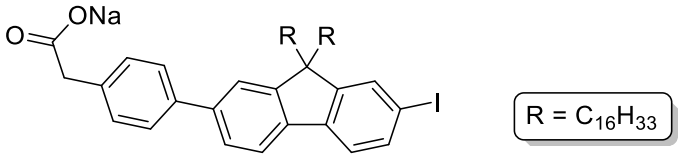

In a round-bottom flask, *tert*-butanol (40 mL) was molten at 30 °C. **33** (1.120 g, 1.280 mmol, 1.000 eq.) and sodium *tert*-butoxide (0.119 g, 1.23 mmol, 0.963 eq.) were added and the mixture was stirred three hours at 40 °C. The solvent was removed under reduced pressure yielding the product as pale-yellow solid in quantitative yield.

Chemical formula: $C_{53}H_{78}IO_2Na$

Molecular weight: 897.10 g/mol

Due to the similarity of **34** *and* **33***, no spectra were recorded.*

Compound **35** (PK-006)

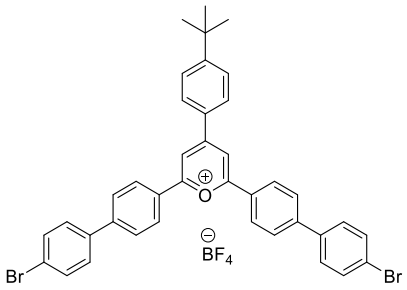

This synthesis applies a procedure published by Kotra et al.[104]

A *Schlenk* flask was equipped with 4'-(4-bromophenyl)acetophenone (10.08 g, 36.63 mmol, 1.976 eq.) and evacuated and flooded with argon three times. Afterwards, 4-*tert*-butylbenzaldehyde (3.10 mL, 18.5 mmol, 1.00 eq.) and boron trifluoride diethyl etherate (14.0 mL, 111 mmol, 5.96 eq.) were added, the mixture was diluted with dichloroethane (11 mL) and the solution was heated to 80 °C for four hours. After cooling to room temperature, the suspension was suspended in DCM and precipitated from diethyl ether. The precipitate was filtered off and the precipitation step was repeated one more time. The received solid was dried overnight under vacuum yielding the product as an orange-red solid in 36 % (5.142 g, 6.746 mmol).

Chemical formula: $C_{39}H_{31}Br_2OBF_4$

Molecular Weight: 762.28 g/mol

^{1}H-NMR (500 MHz, DMSO-*d*6, 298 K), *δ* [ppm]

9.14 (s, 2 H), 8.66 – 8.63 (d, *J* = 8.6 Hz, 4 H), 8.57 – 8.54 (d, *J* = 8.6 Hz, 2 H), 8.12 – 8.09 (d, *J* = 8.6 Hz, 4 H), 7.87 – 7.84 (d, *J* = 8.6 Hz, 4 H), 7.80-7.74 (m, 6 H), 1.40 (s, 9 H).

^{13}C-NMR (126 MHz, DMSO-*d*6, 298 K), *δ* [ppm]

169.6, 164.8, 159.6, 145.2, 137.8, 132.6, 130.7, 130.4, 130.0, 129.8, 128.9, 128.2, 127.3, 123.3, 115.1, 35.8, 31.2.

MS (ESI+), *m*/*z* (%)

673.07 (50) $[M\text{-}BF_4]^+$; calculated: 760.0 Da.

Compound **36** (PK-056)

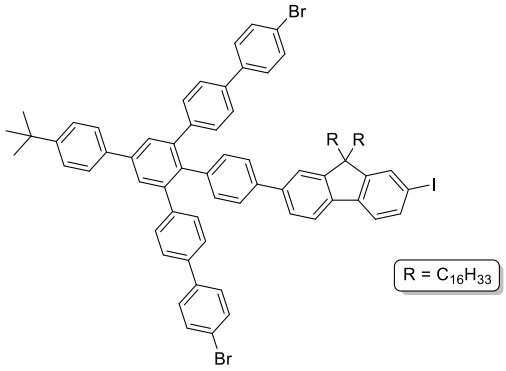

This synthesis applies a procedure published by Idelson et al.[96]

34 (316 mg, 0.352 mmol, 1.00 eq.) and **35** (305 mg, 0.401 mmol, 1.14 eq.) were placed in a round bottom flask. Benzoic anhydride (1.53 g, 6.78 mmol, 19.2 eq.) was added and the mixture was heated to 150 °C for four hours. Sublimed benzoic anhydride was molten by external heating every 15 minutes so that it drops back down into the solution. The mixture was allowed to cool to room temperature. The crude product was purified *via* column chromatography (SiO_2, CH:DCM 10:1, R_f = 0.5) yielding the desired product as a pale-yellow glass-like solid (215 mg, 0.144 mmol) in 41 %.

Chemical formula: $C_{91}H_{107}Br_2I$

Molecular weight: 1487.57 g/mol

^{1}H-NMR (500 MHz, CD_2Cl_2, 298 K), *δ* [ppm]

7.74 (s, 2 H), 7.70 - 7.65 (m, 4 H), 7.55 - 7.50 (m, 8 H), 7.48 - 7.45 (m, 8 H), 7.43 - 7.41 (d, *J* = 8.4 Hz, 2 H), 7.32 - 7.30 (d, *J* = 8.4 Hz, 4 H), 7.10 - 7.08 (d, *J* = 8.2 Hz, 2 H), 7.00 - 6.94 (m, 2 H), 1.98 - 1.92 (m, 4 H), 1.38 (s, 9 H), 1.25 (bs, 48 H), 1.04 - 0.98 (m, 8 H), 0.88 - 0.85 (t, *J* = 7.1 Hz, 6 H).

^{13}C-NMR (126 MHz, CD_2Cl_2, 298 K), δ [ppm]

153.9, 151.4, 151.3, 142.5, 142.0, 140.9, 140.5, 140.3, 139.9, 139.8, 139.2, 138.9, 138.1, 137.8, 137.7, 136.3, 135.5, 133.7, 132.7, 132.2, 131.0, 130.7, 129.8, 128.9, 128.8, 127.1, 126.7, 126.5, 126.4, 121.8, 121.3, 120.4, 92.8, 55.9, 40.6, 34.9, 32.4, 31.5, 30.3, 30.1, 30.1, 30.1, 30.0, 30.0, 30.0, 29.8, 29.6, 27.4, 24.2, 23.1, 14.3.

MS (MALDI-pos, DCTB) *m/z* (%)

1486.6 (100) $[M-H]^+$; calculated: 1484.6 Da.

Compound **37** (PK-022)

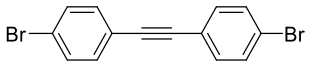

37 *was synthesized adapting the instructions of Mandali et al.*[127]

In a *Schlenk* flask, 1-bromo-4-iodobenzene (2.003 g, 7.081 mmol, 1.000 eq.), K_2CO_3 (2.002 g, 14.48 mmol, 2.045 eq.), PPh_3 (103 mg, 0.394 mmol, 0.0556 eq.) and CuI (142 mg, 0.747 mmol, 0.106 eq.) were suspended in MeCN (20 mL) and methanol (10 mL) and the mixture was purged with argon for 40 min. Afterwards, TMS-acetylene (1.020 g, 3.970 mmol, 0.561 eq.) and $PdCl_2(PPh_3)_2$ (142 mg, 1.45 mmol, 0.205 eq.) were added and the mixture was stirred at room temperature overnight. The mixture was diluted with aq. HCl (1M) and the phases were separated. The aqueous phase was extracted three times with DCM, the phases were separated and the combined organic phase was washed with aq. EDTA (0.1M) and brine and dried over magnesium sulfate. After removal of the solvent under reduced pressure the crude product was isolated *via* column chromatography (SiO_2, Cy, R_f = 0.6) yielding the product (947 mg, 2.82 mmol) as a pale-yellow solid in 78 %.[127]

Chemical formula: $C_{14}H_8Br_2$

Molecular weight: 336.03 g/mol

^{1}H-NMR (500 MHz, CD_2Cl_2, 298 K), δ [ppm]

7.50 - 7.47 (d, *J* = 8.6 Hz, 4 H), 7.39 - 7.36 (d, *J* = 8.4 Hz, 4 H).

^{13}C-NMR (126 MHz, CD_2Cl_2, 298 K), δ [ppm]

109.8, 108.5, 99.6, 98.7, 66.2.

MS (EI, 70 eV), *m/z* (%)

335.8 (100) $[M]^{\bullet+}$, 176.0 (58) $[M-2\ Br]^+$; calculated: 335.9 Da.

Compound **38** (PK-023)

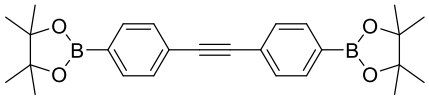

38 *was synthesized adapting the instructions of Takase et al.*[117]

In a flamed *Schlenk* flask, **37** (501 mg, 1.49 mmol, 1.00 eq.), potassium acetate (902 mg, 9.19 mmol, 6.16 eq.) and bis(pinacolato)diboron (858 mg, 3.38 mmol, 2.27 eq.) were suspended in dry DMF (15 mL), $PdCl_2$(dppf) (60 mg, 82 μmol, 0.055 eq.) was added and the mixture was heated to 105 °C overnight. After cooling to room temperature, the mixture was diluted with aq. HCl (1M) and the phases were separated. The aqueous phase was extracted four times with DCM, the phases were separated and the combined organic phase was washed with aq. EDTA (0.1M), water and brine and dried over magnesium sulfate. After removal of the solvent under reduced pressure, the residue was purified *via* column chromatography (SiO_2, DCM:Cy 5:1), but it was not possible to isolate the desired compound.

Chemical formula: $C_{26}H_{32}B_2O_4$

Molecular weight: 430.16 g/mol

Since **38** *was synthetically not accessible, the compound was purchased and used without further purification.*

Compound **39** (PK-057)

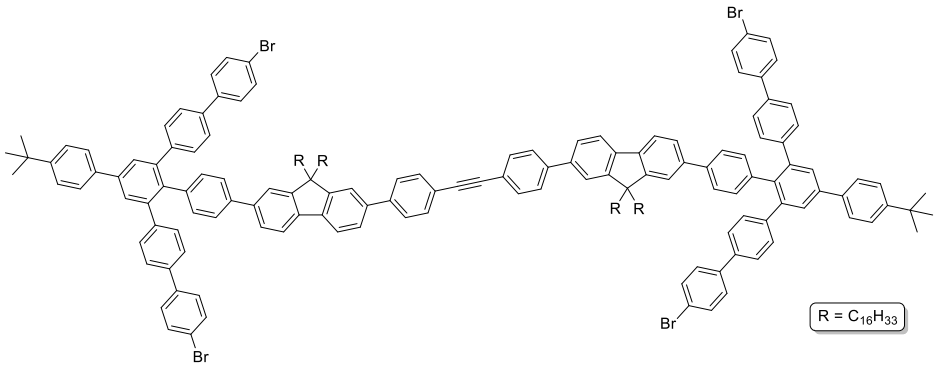

36 (351 mg, 0.236 mmol, 2.04 eq.), Cs_2CO_3 (245 mg, 0.751 mmol, 6.48 eq.) and **38** (49.9 mg, 0.116 mmol, 1.00 eq.) were placed in a flask under *Schlenk* conditions. The mixture was suspended in a mixture of toluene (7.5 mL) and water (0.2 mL) and purged with argon for one hour. $Pd(PPh_3)_4$ (28.0 mg, 24.2 μmol, 0.209 eq.) was added and the mixture was heated to 50 °C for five days. After cooling to room temperature, the mixture was diluted with water and DCM and neutralized using aq. HCl (1M). After separating the phases, the aqueous layer was extracted three times with DCM. The combined organic layers were washed twice with brine and dried over magnesium sulfate. After removal of the solvent under reduced pressure, the crude product was purified *via* recGPC (THF, unstabilized), receiving the product as a yellow solid (106.3 mg, 36.7 μmol) in 32 %.

Chemical formula: $C_{196}H_{222}Br_4$

Molecular weight: 2897.55 g/mol

^{1}H-NMR (700 MHz, CD_2Cl_2, 298 K), δ [ppm]

7.79 - 7.77 (d, *J* = 7.8 Hz, 4 H), 7.75 (s, 4 H), 7.75 - 7.70 (m, 12 H), 7.68 - 7.66 (d, *J* = 8.2 Hz, 4 H), 7.64-7.62 (m, 4 H), 7.55-7.53 (m, 16 H), 7.49-7.46 (m, 16 H), 7.45 (s, *J* = 8.2 Hz, 4 H), 7.34 - 7.31 (d, *J* = 8.3 Hz, 8 H), 7.12 - 7.10 (d, *J* = 8.1 Hz, 4 H), 2.07-1.99 (m, 8 H), 1.39 (s, 18 H), 1.25 (bs, 112 H), 0.79 (t, 12 H, *J* = 7.3 Hz).

^{13}C-NMR (176 MHz, CD_2Cl_2, 298 K), δ [ppm]

152.4, 152.4, 151.5, 142.7, 142.2, 142.0, 141.1, 140.7, 140.6, 140.0, 140.0, 139.6, 139.5, 138.3, 138.0, 137.8, 132.8, 132.5, 132.4, 131.2, 129.1, 128.9, 127.6, 127.3, 126.7, 126.5, 126.5, 126.5, 126.3, 126.0, 122.5, 122.0, 121.9, 121.6, 120.6, 120.6, 90.6, 55.9, 40.9, 35.1, 32.3, 31.7, 30.7, 30.5, 29.7, 24.4, 23.2, 14.4.

MS (MALDI-pos, DCTB) *m/z* (%)

2897.4 (100) $[M]^{\bullet+}$; calculated: 2897.4 Da.

Compound **40** (PK-059)

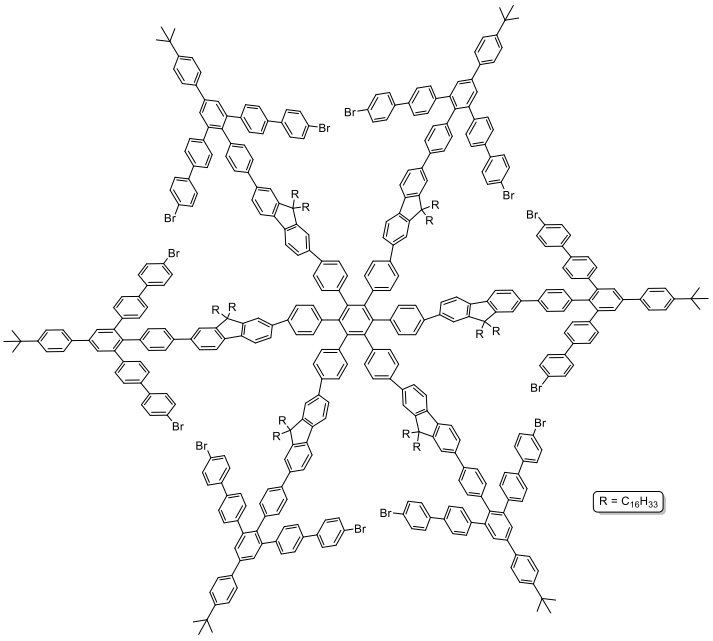

This synthesis applies a procedure published by Idelson et al.[96]

39 (106.3 mg, 36.68 μmol, 1.000 eq.) was dissolved in toluene (15 mL) and purged with argon for one hour. After adding $Co_2(CO)_8$ (3.9 mg, 11 μmol, 0.31 eq.), the mixture was heated to 120 °C. After five hours, the progress of the reaction was checked *via* analytical GPC. The mixture was allowed to cool to room temperature and the solvent was removed under reduced pressure. Afterwards, the crude product was purified by column chromatography (SiO_2, DCM, R_f = 0.9). The desired product was isolated *via* recGPC (THF, unstabilized) as a yellow solid (59.8 mg, 6.90 μmol) in 56 % yield.

Chemical formula: $C_{588}H_{666}Br_{12}$

Molecular weight: 8692.64 g/mol

^{1}H-NMR (700 MHz, CD_2Cl_2, 298 K), δ [ppm]

7.74 (s, 12 H), 7.70 - 7.68 (d, J = 8.5 Hz, 12 H), 7.67 - 7.63 (m, 12 H), 7.55 - 7.49 (m, 48 H), 7.48 - 7.45 (m, 48 H), 7.43 - 7.38 (m, 24 H), 7.33 - 7.29 (m, 36 H), 7.11 - 7.06 (m, 24 H), 1.38 (s, 54 H), 1.22 (bs, 360 H), 0.88 - 0.85 (t, J = 7.1 Hz, 36 H).

^{13}C-NMR (176 MHz, CD_2Cl_2, 298 K), δ [ppm]

152.0, 151.3, 142.5, 142.0, 140.8, 140.6, 140.5, 140.3, 140.3, 140.0, 140.0, 139.6, 139.5, 139.4, 139.0, 138.7, 138.1, 137.8, 137.7, 132.6, 132.2, 131.0, 129.4, 128.9, 128.8, 128.6, 127.1, 126.5, 126.3, 126.0, 125.9, 121.8, 121.5, 121.3, 120.3, 55.7, 42.3, 40.8, 36.4, 34.9, 33.7, 32.4, 31.5, 30.4, 30.1, 30.1, 30.0, 29.8, 28.1, 27.5, 26.0, 23. 1, 22.6, 14.3.

MS (MALDI-pos, DCTB) *m/z* (%)

8692.5 (100) $[M]^{\bullet+}$; calculated: 8687.1 Da.

Compound **MSW-C** (PK-060)

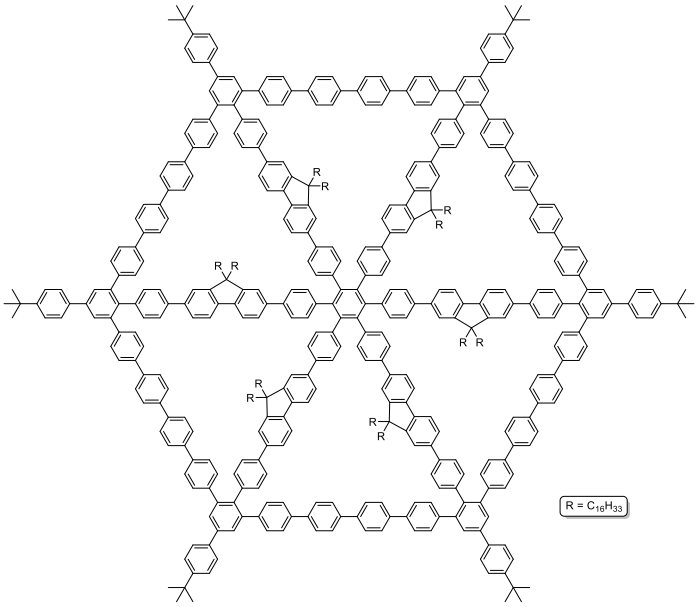

This synthesis applies a procedure published by Idelson et al.[96]

Inside a glove box, **40** (59.8 mg, 6.87 μmol, 1.00 eq.) was equally distributed to six microwave-tubes. Each tube was equipped with $Ni(COD)_2$ (5.0 mg, 18 μmol) and 2,2´-bipyridine (1.0 mg, 6.3 μmol). Under the exclusion of light, each tube was filled with a solvent mixture consisting of THF and COD (32:1, 8.25 mL), immediately sealed and heated in a microwave reactor (12 min, 300 W, 120 °C). The product was purified *via* filtration through a plug of silica gel (DCM) and subsequent recGPC (THF, unstabilized) to give **MSW-C** (22.6 mg, 2.9 μmol) as a pale-yellow solid in 43 % yield.

Chemical formula: $C_{588}H_{666}$

Molecular weight: 7733.80 g/mol

^{1}H-NMR (700 MHz, CD_2Cl_2, 298 K), δ [ppm]

7.82 (s, 12 H), 7.75 - 7.73 (d, *J* = 7.8 Hz, 12 H), 7.68 (s, 48 H), 7.62 - 7.58 (m, 12 H), 7.56 - 7.54 (d, *J* = 7.9 Hz, 36 H), 7.50 (s, 12 H), 7.39 - 7.30 (m, 60 H), 7.11 - 7.07 (d, *J* = 7.9 Hz, 12 H), 7.01 - 6.98 (d, *J* = 7.9 Hz, 12 H), 1.39 (s, 54 H), 1.25 - 0.93 (m, 360 H), 0.87 - 0.84 (m, 36 H).

^{13}C-NMR (176 MHz, CD_2Cl_2, 298 K), δ [ppm]

152.1, 151.3, 142.7, 141.6, 141.0, 140.4, 139.7, 138.9, 138.6, 137.8, 132.7, 132.5, 131.0, 128.2, 127.6, 127.1, 126.4, 126.1, 125.7, 121.0, 120.2, 34.9, 32.4, 31.5, 30.4, 30.2, 30.2, 30.1, 30.1, 30.1, 30.0, 30.0, 29.8, 29.7, 24.2, 23.1, 14.3.

MS (MALDI-pos, DCTB) *m/z* (%)

7733.3 (100) $[M+H]^+$; calculated: 7732.2 Da.

Compound **42** (PK-073, PK-088)

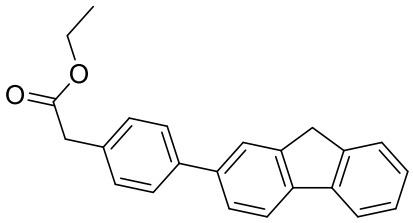

2-Bromofluorene (554 mg, 2.26 mmol, 1.00 eq.), **30** (697 mg, 2.52 mmol, 1.12 eq.), K_2CO_3 (1.015 g, 7.347 mmol, 3.250 eq.) and PPh_3 (100 mg, 0.382 mmol, 0.169 eq.) were suspended in a mixture of toluene (35 mL) and ethanol (25 mL) and purged with argon for one hour. $Pd(PPh_3)_2Cl_2$ (75.0 mg, 0.107 mmol, 0.047 eq.) was added and the mixture was heated to 90 °C overnight. After cooling to room temperature, the solvent was removed under reduced pressure. The residue was suspended in DCM and aq. HCl (2M), the phases were separated and the aqueous layer was extracted three times with DCM. The combined organic layers were washed once with water, once with brine and dried over magnesium sulfate. After removal of the solvent under reduced pressure, the crude product was purified *via* column chromatography (SiO_2, Cy:DCM 3:1, R_f = 0.23) yielding the desired product as a colorless solid (590 mg, 1.80 mmol) in 79 %.

Chemical formula: $C_{23}H_{20}O_2$

Molecular weight: 328.41 g/mol

^{1}H-NMR (500 MHz, CD_2Cl_2, 298 K), δ [ppm]

7.88 - 7.85 (d, *J* = 8.0 Hz, 1 H), 7.84 - 7.81 (d, *J* = 7.5 Hz, 1 H), 7.81 - 7.80 (d, *J* = 1.0 Hz, 1 H), 7.66 - 7.62 (m, 3 H), 7.60 - 7.57 (dt, *J* = 7.3 Hz, *J* = 1.0 Hz, 1 H), 7.43 - 7.36 (m, 3 H), 7.35 - 7.31 (td, *J* = 7.4 Hz, *J* = 1.2 Hz, 1 H), 4.20 - 4.14 (q, *J* = 7.1 Hz, 2 H), 3.98 (s, 2 H), 3.67 (s, 2 H), 1.31 - 1.26 (t, *J* = 7.1 Hz, 3 H).

^{13}C-NMR (126 MHz, CD_2Cl_2, 298 K), δ [ppm]

171.8, 144.5, 144.0, 141.7, 141.3, 140.5, 139.7, 133.8, 130.2, 127.5, 127.2, 127.2, 126.2, 125.5, 124.0, 120.5, 120.3, 61.3, 41.3, 37.4, 14.4.

MS (EI, 70 eV), *m/z* (%)

329.2 (100) $[M+H]^+$, 255.1 (82) $[M\text{-}CO_2Et]^+$; calculated: 328.2 Da.

Compound **43** (PK-074)

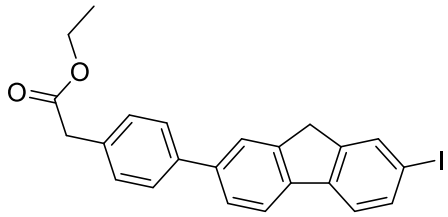

This synthesis applies a procedure published by Idelson et al.[96]

42 (590 mg, 1.80 mmol, 1.00 eq.) was dissolved in DCM (20 mL) and a solution of iodine monochloride (1.80 mL, 1.80 mmol, 1.00 eq., 1M in DCM) was slowly added dropwise. The solution was stirred at room temperature under the exclusion of light overnight. After adding an aq. $NaHSO_3$ solution (40 %) until the organic phase decolored, the phases were separated. The aqueous phase was extracted three times with DCM afterwards and the combined organic phases were washed with brine once and dried over magnesium sulfate. After removal of the solvent, the crude product was purified *via* column chromatography (SiO_2, DCM) yielding the desired product as a pale-orange solid (769 mg, 1.69 mmol) in 94 %.

Chemical formula: $C_{23}H_{19}IO_2$

Molecular weight: 454.31 g/mol

^{1}H-NMR (500 MHz, CD_2Cl_2, 298 K), δ [ppm]

7.87 - 7.85 (d, *J* = 7.9 Hz, 1 H), 7.84 - 7.81 (dt, *J* = 7.6 Hz, *J* = 1.0 Hz, 1 H), 7.81 - 7.80 (q, *J* = 0.8 Hz, 1 H), 7.67 - 7.63 (m, 3 H), 7.60 - 7.57 (dt, *J* = 7.3 Hz, *J* = 1.0 Hz, 1 H), 7.35 - 7.30 (td, *J* = 7.4 Hz, *J* = 1.2 Hz, 1 H), 4.20 - 4.14 (q, *J* = 7.1 Hz, 2 H), 3.98 (s, 2 H), 3.67 (s, 2 H), 1.30 - 1.26 (t, *J* = 7.1 Hz, 3 H).

^{13}C-NMR (126 MHz, CD_2Cl_2, 298 K), δ [ppm]

171.4, 145.9, 143.6, 141.0, 140.0, 139.9, 139.9, 135.8, 134.2, 133.6, 129.8, 127.1, 126.0, 123.6, 121.6, 120.3, 91.7, 60.9, 40.9, 36.7, 26.9, 14.0.

MS (EI, 70 eV), *m/z* (%)

454.0 (21) $[M]^{\bullet+}$, 381.0 (7) $[M\text{-}CO_2Et]^+$, 328.1 (98) $[M\text{-}I]^+$, 255.1 (100) $[M\text{-}CO_2Et\text{-}I]^+$; calculated: 454.0 Da.

Compound **44** (PK-075)

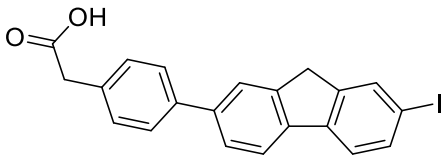

43 (251 mg, 0.552 mmol, 1.00 eq.) was dissolved in a mixture of THF (20 mL) and water (4 mL). After adding $LiOH \cdot H_2O$ (402.4 mg, 9.590 mmol, 17.4 eq.), the mixture was heated to 60 °C for 19 hours. The reaction mixture was diluted with DCM and neutralized using aq. HCl (2M). After phase separation, the aqueous layer was extracted three times using DCM. The combined organic phases were washed once with brine, dried over magnesium sulfate and the solvent was removed under reduced pressure. The crude product was purified *via* column chromatography (SiO_2, DCM:EA 1:1, $R_f = 0.5$), receiving the product as a yellow solid (216 mg, 0.919 mmol) in 92 %.

Chemical formula: $C_{21}H_{15}IO_2$

Molecular weight: 426.25 g/mol

Due to its poor solubility, it was not possible to record any reasonable spectra of **44**.

Compound **45** (PK-076)

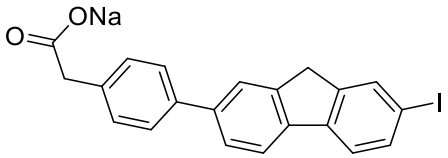

In a round-bottom flask, *tert*-butanol (40 mL) was molten at 30 °C. **44** (201 mg, 0.472 mmol, 1.00 eq.) and sodium *tert*-butoxide (45.0 mg, 0.468 mmol, 0.992 eq.) were added and the mixture was stirred for three hours at 40 °C. The solvent was removed under reduced pressure yielding the product as a yellow solid in quantitative yield.

Chemical formula: $C_{21}H_{15}IO_2Na$

Molecular weight: 448.24 g/mol

Due to its poor solubility, it was not possible to record any reasonable spectra of **45**.

Compound **46** (PK-078)

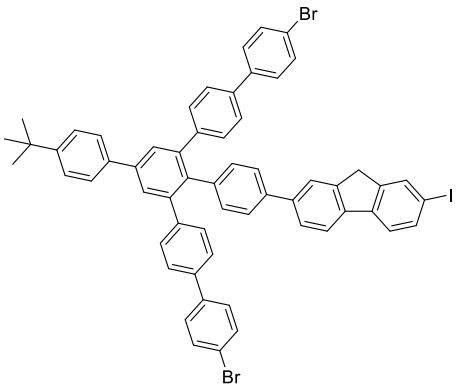

This synthesis applies a procedure published by Idelson et al.[96]

45 (1.402 g, 3.128 mmol, 1.000 eq.) and **35** (2.399 g, 3.148 mmol, 1.006 eq.) were placed in a round bottom flask. Benzoic anhydride (9.39 g, 41.5 mmol, 13.3 eq.) was added and the mixture was heated to 150 °C for four hours. Sublimed benzoic anhydride was molten by external heating every 15 minutes so that it drops back down into the solution. The mixture was allowed to cool to room temperature. The crude product was purified *via* column chromatography (SiO_2, CH:DCM 5:2, R_f = 0.5) yielding the desired product as a pale-yellow glass-like solid (0.764 g, 0.735 mmol) in 24 %.

Chemical formula: $C_{59}H_{43}Br_2I$

Molecular weight: 1038.71 g/mol

^{1}H-NMR (500 MHz, CD_2Cl_2, 298 K), δ [ppm]

7.74 (s, 2 H), 7.71 - 7.68 (m, 4 H), 7.55 - 7.51 (dd, *J* = 8.7 Hz, *J* = 1.2 Hz, 6 H), 7.47 - 7.43 (m, 8 H), 7.40 - 7.37 (d, *J* = 8.2 Hz, 2 H), 7.31 - 7.28 (d, *J* = 8.4 Hz, 4 H), 7.08 - 7.05 (d, *J* = 8.3 Hz, 2 H), 3.87 (s, 2 H), 1.38 (s, 9 H).

^{13}C-NMR (126 MHz, CD_2Cl_2, 298 K), δ [ppm]

151.3, 146.3, 143.9, 142.4, 141.9, 141.4, 140.5, 140.2, 140.0, 139.9, 139.9, 139.0, 138.1, 137.8, 137.7, 136.2, 134.6, 132.7, 132.4, 132.2, 131.0, 128.9, 128.7, 127.1, 126.5, 126.3, 126.3, 126.1, 123.7, 121.9, 121.8, 120.6, 92.1, 37.1, 34.9, 31.5.

MS (MALDI-pos, DCTB) *m/z* (%)

1038.1 (100) $[M]^{\bullet+}$, 912.2 (24) $[M\text{-}I]^+$; calculated: 1036.08 Da.

Compound **47** (PK-081)

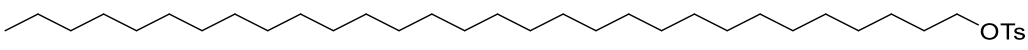

47 *was synthesized adapting the instructions of Mandali et al.*[128]

Triacontanol (115 mg, 0.263 mmol, 1.00 eq.), K_2CO_3 (301 mg, 2.18 mmol, 8.29 eq.) and tosyl chloride (402 mg, 2.11 mmol, 8.03 eq.) were suspended in THF (15 mL) and water (3 mL) and the mixture was refluxed overnight. After cooling to room temperature, the solvent was removed under reduced pressure and the residue was suspended in $CHCl_3$ and water. The phases were separated and the

aqueous phase was extracted three times using $CHCl_3$. The combined organic layers were washed with aq. HCl (1M) and brine once each, dried over magnesium sulfate and the solvent was removed under reduced pressure. The crude product was purified *via* column chromatography (SiO_2, Cy:EA 10:1), receiving the product as a yellow oil (105 mg, 0.177 mmol) in 68 %.

Chemical formula: $C_{37}H_{68}O_3S$

Molecular weight: 593.01 g/mol

^{1}H-NMR (400 MHz, $CDCl_3$, 298 K), δ [ppm]

7.95 - 7.91 (d, *J* = 8.5 Hz, 2 H), 7.43 - 7.39 (d, *J* = 8.1 Hz, 2 H), 3.66 - 3.63 (t, *J* = 6.6 Hz, 2 H), 2.49 (s, 3 H), 1.60 - 1.53 (p, *J* = 6.6 Hz, 4 H), 1.25 (bs, 52 H), 0.90 - 0.88 (t, *J* = 6.9 Hz, 3 H).

^{13}C-NMR (126 MHz, CD_2Cl_2, 298 K), δ [ppm]

146.9, 131.7, 130.4, 127.2, 63.3, 33.0, 32.1, 29.9, 29.8, 29.8, 29.8, 29.8, 29.6, 29.5, 25.9, 22.0, 14.3.

MS (EI, 70 eV), *m/z* (%)

421.4 (15) $[C_{30}H_{61}]^+$, 407.4 (16) $[C_{29}H_{59}]^+$, 393.4 (17) $[C_{28}H_{57}]^+$, 379.4 (18) $[C_{27}H_{55}]^+$, 365.4 (18) $[C_{26}H_{53}]^+$, 351.3 (18) $[C_{25}H_{51}]^+$, 337.3 (22) $[C_{24}H_{49}]^+$, 323.3 (23) $[C_{23}H_{47}]^+$, 309.3 (23) $[C_{22}H_{45}]^+$, 295.3 (25) $[C_{21}H_{43}]^+$, 281.3 (27) $[C_{20}H_{41}]^+$, 267.3 (28) $[C_{19}H_{39}]^+$, 253.2 (33) $[C_{18}H_{37}]^+$, 239.2 (35) $[C_{17}H_{35}]^+$, 225.2 (37) $[C_{16}H_{33}]^+$, 211.2 (38) $[C_{15}H_{31}]^+$, 197.2 (40) $[C_{14}H_{29}]^+$, 183.1 (5) $[C_{13}H_{27}]^+$, 169.1 (6) $[C_{12}H_{25}]^+$, 155.1 (7) $[C_{11}H_{23}]^+$, 141.1 (8) $[C_{10}H_{21}]^+$, 125.1 (10) $[C_9H_{19}]^+$, 111.0 (18) $[C_8H_{17}]^+$, 97.0 (35) $[C_7H_{15}]^+$, 85.0 (52) $[C_6H_{13}]^+$, 71.1 (73) $[C_5H_{11}]^+$, 57.1 (100) $[C_4H_9]^+$; calculated: 592.5 Da.

Compound **48** (PK-086)

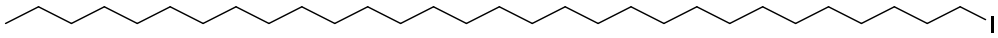

48 *was synthesized adapting the instructions of Yoon et al.*[129]

Tricontanol (201 mg, 0.458 mmol, 1.00 eq.), imidazole (51.7 mg, 0.759 mmol, 1.66 eq.) and triphenylphosphine (156 mg, 0.593 mmol, 1.30 eq.) were suspended in DCM and purged with argon for 30 min. The mixture was cooled in an ice bath and iodine (207 mg, 0.815 mmol, 1.78 eq.) was added. Afterwards, the mixture was allowed to warm to room temperature and stirred overnight. To the solution, aq. $NaHSO_3$ (40 %) was added, the phases were separated and the aqueous phase was extracted three times using DCM. The combined organic layers were washed with brine once, dried over magnesium sulfate and the solvent was removed under reduced pressure. The crude product was purified *via* column chromatography (SiO_2, DCM, R_f = 0.4), receiving the product as a yellow oil (50.5 mg, 92.0 μmol) in 20 % yield.

Chemical formula: $C_{30}H_{61}I$

Molecular weight: 548.72 g/mol

^{1}H-NMR (500 MHz, CD_2Cl_2, 298 K), δ [ppm]

1.26 (bs, 58 H), 0.91 - 0.88 (t, J = 6.8 Hz, 3 H).

^{13}C-NMR (126 MHz, CD_2Cl_2, 298 K), δ [ppm]

32.1, 30.2, 29.9, 29.8, 29.8, 29.7, 29.6, 29.5, 29.3, 29.1, 28.7, 27.4, 27.3, 27.1, 22.9, 14.3, 7.4.

MS (EI, 70 eV), *m/z* (%)

421.4 (15) $[C_{30}H_{61}]^+$, 407.4 (16) $[C_{29}H_{59}]^+$, 393.4 (17) $[C_{28}H_{57}]^+$, 379.4 (18) $[C_{27}H_{55}]^+$, 365.4 (18) $[C_{26}H_{53}]^+$, 351.3 (18) $[C_{25}H_{51}]^+$, 337.3 (22) $[C_{24}H_{49}]^+$, 323.3 (23) $[C_{23}H_{47}]^+$, 309.3 (23) $[C_{22}H_{45}]^+$, 295.3 (25) $[C_{21}H_{43}]^+$, 281.3 (27) $[C_{20}H_{41}]^+$, 267.3 (28) $[C_{19}H_{39}]^+$, 253.2 (33) $[C_{18}H_{37}]^+$, 239.2 (35) $[C_{17}H_{35}]^+$, 225.2 (37) $[C_{16}H_{33}]^+$, 211.2 (38) $[C_{15}H_{31}]^+$, 197.2 (40) $[C_{14}H_{29}]^+$, 183.1 (5) $[C_{13}H_{27}]^+$, 169.1 (6) $[C_{12}H_{25}]^+$, 155.1 (7) $[C_{11}H_{23}]^+$, 141.1 (8) $[C_{10}H_{21}]^+$, 125.1 (10) $[C_9H_{19}]^+$, 111.0 (18) $[C_8H_{17}]^+$, 97.0 (35) $[C_7H_{15}]^+$, 85.0 (52) $[C_6H_{13}]^+$, 71.1 (73) $[C_5H_{11}]^+$, 57.1 (100) $[C_4H_9]^+$; calculated: 548.4 Da.

Compound **49** (PK-082)

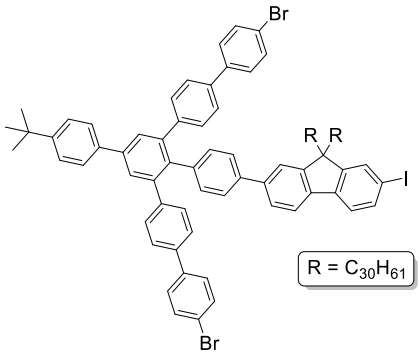

This synthesis applies a procedure published by Ponumuthu et al.[47]

48 (42.2 mg, 40.6 μmol, 1.00 eq.), **47** (52.2 mg, 88.0 μmol, 2.17 eq), KOH (51.1 mg, 0.911 mmol, 22.4 eq.) and Bu_4NBr (10.3 mg, 32.0 μmol, 0.786 eq.) were suspended in acetone (15 mL) and water (2 mL) and the mixture was heated to 80 °C for 70 h. After removal of the solvent, the residue was suspended in water and DCM and the phases were separated. The aqueous phase was extracted four times with DCM. The combined organic layers were washed with aq. HCl (2M) and brine, dried over magnesium sulfate and the solvent was removed under reduced pressure. The residue was purified *via* column chromatography (SiO_2, Cy:DCM 2:1). No isolated fraction was identified as the desired species.

Chemical formula: $C_{119}H_{163}Br_2I$

Molecular weight: 1880.33 g/mol

Compound **50** (PK-077)

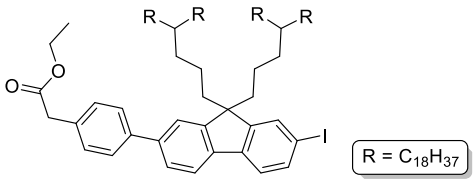

43 (252 mg, 0.555 mmol, 1.00 eq.), KOH (150 mg, 2.68 mmol, 4.82 eq.), 19-(3-iodopropyl)heptatriacontane (748 mg, 1.09 mmol, 1.96 eq.) and Bu_4NBr (54.2 mg, 0.168 mmol, 0.303 eq.) were suspended in acetone (20 mL) and water (2 mL) and heated to 80 °C for 68 h. After removal of the solvent under reduced pressure, the residue was suspended in aq. HCl (2M) and DCM and the phases were separated. The aqueous phase was extracted five times with DCM. The combined organic layers were washed with aq. HCl (2M) and brine, dried over magnesium sulphate and the solvent was removed under reduced pressure. The residue was purified *via* column chromatography (SiO_2, Cy:DCM 1:1). No isolated fraction was identified as neither the desired species nor the singly alkylated byproduct.

Chemical formula: $C_{103}H_{179}IO_2$

Molecular weight: 1576.47 g/mol

Compound **51** (PK-079)

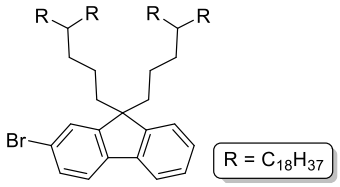

This synthesis applies a procedure published by Ponumuthu et al.[47]

2-Bromofluorene (201 mg, 0.820 mmol, 1.00 eq.), KOH (202 mg, 3.61 mmol, 4.40 eq.), 19-(3-iodopropyl)heptatriacontane (2.008 g, 2.913 mmol, 3.554 eq.) and Bu_4NBr (83.8 mg, 0.260 mmol, 0.317 eq.) were suspended in acetone (20 mL) and water (4 mL) and heated to 80 °C for 40 h. After removal of the solvent under reduced pressure, the residue was suspended in aq. HCl (2M) and DCM and the phases were separated. The aqueous phase was extracted three times with DCM. The combined organic layers were washed with brine, dried over magnesium sulphate and the solvent was removed under reduced pressure. The residue was purified *via* column chromatography (SiO_2, Cy). No isolated fraction was identified as neither the desired species nor the singly alkylated byproduct.

Chemical formula: $C_{93}H_{169}Br$

Molecular weight: 1367.28 g/mol

Compound **53** (PK-062, PK-080, PK-085)

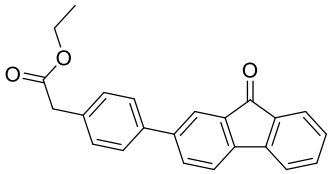

2-Bromofluorenone (2.008 g, 7.750 mmol, 1.000 eq.), K_2CO_3 (2.910 g, 21.05 mmol, 2.717 eq.) and **30** (2.276 g, 8.241 mmol, 1.063 eq.) were dissolved in a mixture of dioxane (35 mL) and ethanol (25 mL) and purged with argon for one hour. $PdCl_2(PPh_3)_2$ (298 mg, 0.424 mmol, 0.0548 eq.) was added and the mixture was heated to 100 °C for 19 hours. After cooling to room temperature, the mixture was diluted with water and DCM and neutralized using aq. HCl (2M). The phases were separated and the aqueous layer was extracted three times with DCM. The combined organic layers were washed with brine and dried over magnesium sulfate. After removal of the solvent under reduced pressure, the crude product was purified *via* column chromatography (SiO_2, Cy:DCM 1:3, R_f = 0.3), receiving the product as a yellow oil (2.285 g, 6.674 mmol) in 86 % yield.

Chemical formula: $C_{23}H_{18}O_3$

Molecular weight: 342.39 g/mol

^{1}H-NMR (500 MHz, CD_2Cl_2, 298 K), δ [ppm]

7.86 (dd, *J* = 1.8 Hz, *J* = 0.7 Hz, 1 H), 7.75 - 7.72 (dd, *J* = 7.8 Hz, *J* = 1.8 Hz, 1 H), 7.65 - 7.62 (dt, *J* = 7.3 Hz, *J* = 0.9 Hz, 1 H), 7.61 - 7.58 (m, 3 H), 7.57 - 7.55 (dt, *J* = 7.4 Hz, *J* = 1.0 Hz, 1 H), 7.53 - 7.49 (td, *J* = 7.4 Hz, *J* = 1.2 Hz, 1 H), 7.39 - 7.37 (d, *J* = 8.6 Hz, 2 H), 7.33 - 7.29 (td, *J* = 7.4 Hz, *J* = 1.1 Hz, 1 H), 4.19 - 4.14 (q, *J* = 7.1 Hz, 2 H), 3.67 (s, 2 H), 1.29 - 1.25 (t, *J* = 7.1 Hz, 3 H).

^{13}C-NMR (126 MHz, CD_2Cl_2, 298 K), δ [ppm]

193.8, 171.7, 144.6, 143.6, 142.1, 138.9, 135.2, 134.8, 134.7, 133.5, 130.8, 130.3, 129.4, 127.2, 124.5, 122.9, 121.2, 120.9, 61.3, 41.2, 14.4.

MS (EI, 70 eV), *m/z* (%)

342.1 (64) $[M]^{\bullet+}$, 269.1 (100) $[M\text{-}CO_2Et]^+$, 180.1 (24) $[C_{13}H_7O+H]^+$; calculated: 342.1 Da.

Compound **54** (PK-064)

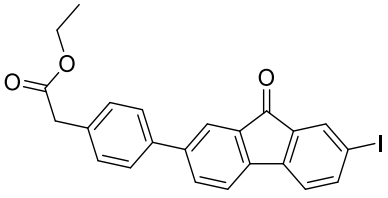

Version A:[96]

53 (399 mg, 1.17 mmol, 1.00 eq.) was dissolved in dry DCM (15 mL) in a flamed round-bottom flask under argon atmosphere. After slowly adding a solution of iodine monochloride (1.30 mL, 1.30 mmol,

1.11 eq., 1M in DCM) dropwise, the mixture was stirred under the exclusion of light overnight. The progress of the reaction was checked *via* TLC, but no formation of any product was observed.

Version B:[131]

Under argon atmosphere, iron(III) chloride (6.6 mg, 0.041 mmol, 0.046 eq.) and 2-picolinic acid (10.9 mg, 88.5 μmol, 0.100 eq.) were suspended in a mixture of acetonitrile (15 mL) and freshly distilled pyridine (3 mL). After adding **43** (402 mg, 0.885 mmol, 1.00 eq.), an aqueous solution of *tert*-butyl hydroperoxide (0.50 mL, 5.2 mmol, 5.9 eq., 70 % in H_2O) was slowly added dropwise. The reaction was stirred overnight at room temperature. After removal of the solvent under reduced pressure, the residue was suspended in DCM and aq. HCl (2M). After separating the phases, the aqueous layer was extracted three times with DCM. The combined organic layers were washed with brine and dried over magnesium sulfate. After removal of the solvent under reduced pressure, the crude product was purified *via* column chromatography (SiO_2, Cy:DCM 1:3, R_f = 0.6), receiving the product as a pale-yellow solid (334 mg, 0.714 mmol) in 81 % yield.

Chemical formula: $C_{23}H_{17}O_3I$

Molecular weight: 468.29 g/mol

^{1}H-NMR (500 MHz, CD_2Cl_2, 298 K), δ [ppm]

7.98 - 7.92 (m, 1 H), 7.88 - 7.85 (m, 2 H), 7.78 - 7.75 (m, 1 H), 7.61 - 7.58 (ddd, *J* = 7.9 Hz, *J* = 2.0 Hz, *J* = 0.9 Hz, 3 H), 7.39 - 7.37 (dd, *J* = 7.9 Hz, *J* = 0.6 Hz, 2 H), 7.35 - 7.33 (dd, *J* = 7.8 Hz, *J* = 0.5 Hz, 1 H), 4.18 - 4.13 (q, *J* = 7.1 Hz, 2 H), 3.66 (s, 2 H), 1.28 - 1.25 (t, *J* = 7.1 Hz, 3 H).

^{13}C-NMR (126 MHz, CD_2Cl_2, 298 K), δ [ppm]

192.5, 171.7, 143.9, 143.7, 142.9, 142.7, 138.7, 136.4, 134.9, 134.5, 133.8, 133.5, 130.4, 127.2, 123.1, 122.6, 121.4, 94.1, 61.3, 41.3, 14.4.

MS (EI, 70 eV), *m/z* (%)

468.0 (100) $[M]^{\bullet+}$, 394.4 (97) $[M\text{-}CO_2Et]^+$, 268.0 (31) $[M\text{-}CO_2Et\text{-}I]^+$; calculated: 468.0 Da.

Compound **55** (PK-065)

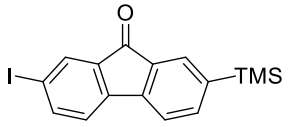

This synthesis applies a procedure published by Suranna et al.[158]

Under *Schlenk* conditions, **25** (502 mg, 1.16 mmol, 1.00 eq.) was dissolved in dry THF (20 mL), the mixture was cooled to -78 °C and *s*BuLi (0.90 mL, 1.3 mmol, 1.1 eq., 1.4M in Cy) was slowly added dropwise. After stirring for one hour, TMSCl (0.30 mL, 2.4 mmol, 2.0 eq.) was added and the mixture was allowed to warm to room temperature and stirred for 42 h. The mixture was diluted with DCM

and aq. HCl (2M). After separating the phases, the aqueous layer was extracted three times with DCM. The combined organic layers were washed with brine and dried over magnesium sulfate. After removal of the solvent under reduced pressure, the crude product was purified *via* column chromatography (SiO_2, Cy:DCM 1:2). It was not possible to isolate the desired product.

Chemical formula: $C_{16}H_{15}IOSi$

Molecular weight: 378.28 g/mol

Compound **56** (PK-066)

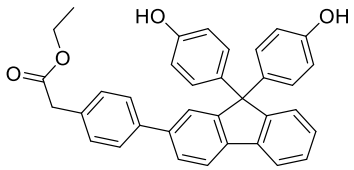

This synthesis applies a procedure published by Abashev et al.[124]

53 (501 mg, 1.46 mmol, 1.00 eq.) and phenol (1.50 g, 15.9 mmol, 10.9 eq.) were suspended in $CHCl_3$ (10 mL) and the mixture was heated to 50 °C. After adding methanesulfonic acid (1.50 mL, 23.1 mmol, 15.8 eq.) the mixture was stirred for 20 hours at 50 °C. After cooling to room temperature, the crude product was dissolved in DCM and purified *via* column chromatography (SiO_2, DCM, R_f = 0.6) yielding the desired product (550 mg, 1.07 mmol) in 73 % as an orange resin.

Chemical formula: $C_{35}H_{28}O_4$

Molecular weight: 512.61 g/mol

^{1}H-NMR (500 MHz, CD_2Cl_2, 298 K), δ [ppm]

7.85 - 7.83 (dd, *J* = 7.7 Hz, *J* = 0.8 Hz, 1 H), 7.81 - 7.79 (m, 1 H), 7.62 - 7.59 (m, 2 H), 7.55 - 7.52 (d, *J* = 8.2 Hz, 2 H), 7.40 - 7.63 (m, 2 H), 7.33 - 7.31 (d, *J* = 8.5 Hz, 2 H), 7.30 - 7.27 (m, 1 H), 7.11 - 7.07 (d, *J* = 8.8 Hz, 4 H), 6.71 - 6.67 (d, *J* = 8.8 Hz, 4 H), 4.17 - 4.12 (q, *J* = 7.1 Hz, 2 H), 3.64 (s, 2 H), 1.26 - 1.23 (t, *J* = 7.2 Hz, 3 H).

^{13}C-NMR (126 MHz, CD_2Cl_2, 298 K), δ [ppm]

171.6, 154.8, 152.6, 140.3, 139.5, 139.2, 137.8, 133.5, 129.7, 129.3, 127.7, 127.5, 127.1, 126.4, 126.0, 124.6, 120.5, 120.3, 115.0, 64.3, 61.0, 40.9, 14.0.

MS (EI, 70 eV), *m*/*z* (%)

512.2 (100) $[M]^{\bullet+}$, 439.2 (14) $[M\text{-}CO_2Et]^+$, 149.2 (8) $[M\text{-}C_6H_4OH]^+$, 346.2 (8) $[M\text{-}CO_2Et\text{-}C_6H_4OH]^+$; calculated: 512.2 Da.

Compound **57** (PK-067)

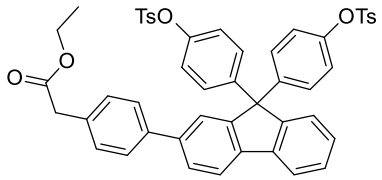

This synthesis applies a procedure published by Lei et al.[128]

56 (456 mg, 0.889 mmol, 1.00 eq.) and K_2CO_3 (452 mg, 3.27 mmol, 3.67 eq.) were suspended in a mixture of THF (15 mL) and water (5 mL) and cooled in an ice bath. A solution of tosyl chloride (401 mg, 2.10 mmol, 2.36 eq.) in THF (10 mL) was slowly added dropwise and the mixture was stirred for 10 min at 0 °C. After removal of the ice bath, the mixture was allowed to warm to room temperature and stirred for 4 h. The suspension was diluted with DCM and water and the phases were separated. The aqueous phase was extracted with DCM twice and the combined organic layers were washed brine and dried over magnesium sulfate. After removal of the solvent under reduced pressure, the crude product was purified *via* column chromatography (SiO_2, DCM:Cy 5:1, R_f = 0.5) yielding the desired product as a colorless solid (527 mg, 0.642 mmol) in 72 %.

Chemical formula: $C_{49}H_{40}O_8S_2$

Molecular weight: 820.97 g/mol

^{1}H-NMR (500 MHz, CD_2Cl_2, 298 K), δ [ppm]

7.86 - 7.84 (d, *J* = 7.9 Hz, 1 H), 7.82 - 7.80 (d, *J* = 7.6 Hz, 1 H), 7.68 - 7.65 (d, *J* = 8.4 Hz, 4 H), 7.64 (d, *J* = 1.6 Hz, 1 H), 7.53 - 7.50 (m, 3 H), 7.43 - 7.40 (ddd, *J* = 7.6 Hz, *J* = 6.2 Hz, *J* = 2.3 Hz, 1 H), 7.36 - 7.34 (d, *J* = 8.2 Hz, 2 H), 7.32 (m, 2 H), 7.29 - 7.27 (dd, *J* = 8.6 Hz, *J* = 0.7 Hz, 4 H), 7.15 - 7.11 (d, *J* = 8.9 Hz, 4 H), 6.88 - 6.85 (d, *J* = 8.9 Hz, 4 H), 4.17 - 4.12 (q, *J* = 7.1 Hz, 2 H), 3.65 (s, 2 H), 2.40 (s, 6 H), 1.27 - 1.24 (t, *J* = 7.1 Hz, 3 H).

^{13}C-NMR (126 MHz, CD_2Cl_2, 298 K), δ [ppm]

171.7, 151.4, 150.9, 149.0, 146.1, 144.8, 141.1, 140.1, 140.0, 139.6, 134.2, 132.8, 130.2, 129.7, 128.7, 128.5, 128.4, 127.5, 127.4, 126.3, 124.9, 122.6, 121.9, 121.2, 120.9, 65.0, 61.3, 41.2, 21.8, 14.4.

MS (MALDI-TOF pos, DCTB), *m*/*z* (%)

820.2 (100) $[M]^{\bullet+}$; calculated: 820.2 Da.

Compound **58** (PK-068)

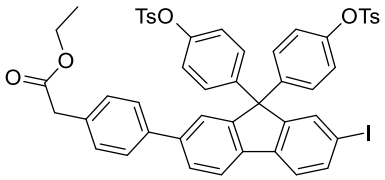

This synthesis applies a procedure published by Grisorio et al.[125]

57 (227 mg, 0.277 mmol, 1.00 eq.), iodine (76.7 mg, 0.302 mmol, 1.09 eq.) and iodic acid (40.5 mg, 0.230 mmol, 0.830 eq.) were suspended in a mixture of acetic acid (20 mL) and $CHCl_3$ (4 mL) and heated to 80 °C overnight. The mixture was cooled to room temperature, the reaction was terminated through addition of aq. $NaHSO_3$ solution and the suspension was diluted with DCM. The phases were separated, the aqueous phase was extracted three times with DCM and the combined organic layers were washed with brine and dried over magnesium sulfate. After removal of the solvent under reduced pressure, the crude product was purified *via* column chromatography (SiO_2, DCM, R_f = 0.5) yielding the desired product as yellow crystals (75.4 mg, 79.6 μmol) in 29 %.

Chemical formula: $C_{49}H_{39}O_8S_2$

Molecular weight: 946.87 g/mol

^{1}H-NMR (500 MHz, CD_2Cl_2, 298 K), δ [ppm]

7.85 - 7.82 (d, *J* = 8.4 Hz, 1 H), 7.77 - 7.75 (dd, *J* = 8.0 Hz, *J* = 1.5 Hz, 1 H), 7.70 - 7.64 (m, 6 H), 7.59 - 7.57 (d, *J* = 8.0 Hz, 1 H), 7.54 - 7.50 (m, 3 H), 7.36 - 7.35 (m, 7 H), 7.12 - 7.05 (d, *J* = 8.9 Hz, 4 H), 6.92 - 6.87 (d, *J* = 8.9 Hz, 4 H), 4.18 - 4.13 (q, *J* = 7.1 Hz, 2 H), 3.66 (s, 2 H), 2.40 (s, 6 H), 1.29 - 1.25 (t, *J* = 7.1 Hz, 3 H).

^{13}C-NMR (126 MHz, CD_2Cl_2, 298 K), δ [ppm]

171.7, 153.1, 151.1, 149.2, 146.2, 144.1, 141.8, 139.8, 138.5, 137.6, 135.3, 134.4, 132.7, 132.7, 130.2, 130.2, 129.6, 128.7, 127.5, 125.6, 124.8, 122.8, 122.6, 121.3, 93.3, 65.0, 61.3, 41.2, 21.8, 14.4.

MS (MALDI-TOF pos, DCTB), *m*/*z* (%)

946.1 (100) $[M]^{\bullet+}$; calculated: 946.1 Da.

Compound **59** (PK-070)

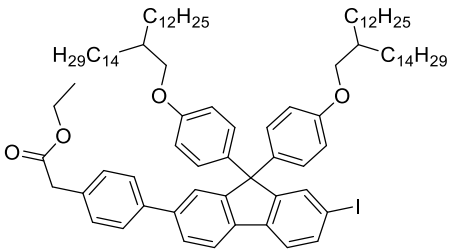

This synthesis applies a procedure published by Abashev et al.[124]

58 (255 mg, 0.270 mmol, 1.00 eq.), 13-(iodomethyl)heptacosane (279 mg, 0.536 mmol, 1.99 eq.), KOH (52.1 mg, 0.929 mmol, 3.44 eq.) and NBu_4Br (172.6 g, 0.535 mmol, 1.99 eq.) were suspended in a mixture of acetone (16 mL) and water (8 mL) and the mixture was heated to 80 °C for 47 h. The mixture was allowed to cool to room temperature, diluted with DCM and aq. HCl (1M) and the phases were separated. The aqueous phase was extracted three times with DCM, the combined organic layers were washed with brine, dried over magnesium sulfate and the solvent was removed under reduced pressure. The residue was purified *via* column chromatography (SiO_2, DCM:Cy 5:1). It was not possible to isolate any desired product.

Chemical formula: $C_{89}H_{135}IO_4$

Molecular weight: 1395.96 g/mol

Compound **60** (PK-063)

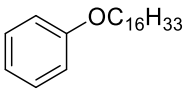

This synthesis applies a procedure published by Abashev et al.[124]

Phenol (2.012 g, 21.38 mmol, 1.000 eq.) and KOH (4.005 g, 71.39 mmol, 3.339 eq.) were dissolved in a mixture of acetone (40 mL) and water (4 mL). NBu_4Br (0.701 g, 2.17 mmol, 0.102 eq.) and 1-bromohexadecane (7.5 mL, 25 mmol, 1.2 eq.) were added and the mixture was heated to 80 °C for 70 hours. After cooling to room temperature, the residue was diluted with DCM and water. The phases were separated and the aqueous layer was extracted with DCM three times. The combined organic layers were washed with water, aq. HCl (1M) and brine and dried over magnesium sulfate. After removal of the solvent under reduced pressure, the crude product was purified *via* column chromatography (SiO_2, Cy:DCM 3:2, R_f = 0.7), receiving the product in 95 % as a colorless solid (6.436 g, 20.20 mmol).

Chemical formula: $C_{22}H_{38}O$

Molecular weight: 318.55 g/mol

^{1}H-NMR (500 MHz, CD_2Cl_2, 298 K), δ [ppm]

7.30 - 7.24 (m, 2 H), 6.94 - 6.87 (m, 3 H), 3.98 - 3.93 (t, *J* = 6.6 Hz, 2 H), 1.82 - 1.73 (p, *J* = 6.7 Hz, 2 H), 1.50 - 1.41 (m, 2 H), 1.28 (bs, 24 H), 0.92 - 0.88 (t, *J* = 6.9 Hz, 3 H).

^{13}C-NMR (126 MHz, CD_2Cl_2, 298 K), δ [ppm]

159.7, 129.8, 120.8, 114.8, 68.3, 32.4, 30.2, 30.2, 30.1, 30.1, 30.1, 30.1, 29.9, 29.8, 29.8, 26.5, 23.2, 14.3.

Compound **61** (PK-092)

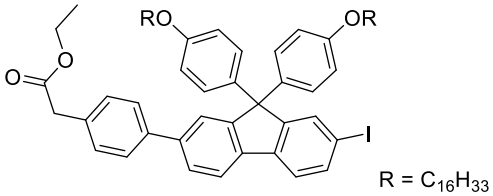

This synthesis applies a procedure published by Abashev et al.[124]

54 (203 mg, 0.433 mmol, 1.00 eq.) and **60** (410 mg, 1.29 mmol, 2.97 eq.) were suspended in $CHCl_3$ (5 mL) and the mixture was heated to 50 °C. After adding methanesulfonic acid (0.4 mL, 6.2 mmol, 14 eq.), the mixture was stirred for 20 hours at 50 °C. After cooling to room temperature, the crude product was dissolved in DCM and purified *via* column chromatography (SiO_2, Cy:DCM, R_f = 0.4) yielding the desired product (58 mg, 54 μmol) in 12 % as an orange resin.

Chemical formula: $C_{67}H_{91}IO_4$

Molecular weight: 1087.37 g/mol

^{1}H-NMR (500 MHz, CD_2Cl_2, 298 K), δ [ppm]

7.83 - 7.80 (d, *J* = 7.9 Hz, 1 H), 7.72 - 7.70 (m, 2 H), 7.63 - 7.61 (dd, *J* = 7.9 Hz, *J* = 1.7 Hz, 1 H), 7.60 - 7.55 (m, 2 H), 7.54 - 7.52 (d, *J* = 8.2 Hz, 2 H), 7.34 - 7.32 (d, *J* = 8.0 Hz, 2 H), 7.13 - 7.10 (d, *J* = 6.6 Hz, *J* = 8.8 Hz, 4 H), 6.78 - 6.76 (d, *J* = 8.9 Hz, 4 H), 4.16 - 4.13 (q, *J* = 7.1 Hz, 2 H), 3.91 - 3.88 (t, *J* = 6.6 Hz, 4 H), 3.64 (s, 2 H), 1.76 - 1.71 (p, *J* = 6.8 Hz, 4 H), 1.45 - 1.40 (p, *J* = 7.5 Hz, 4 H), 1.36 - 1.22 (m, 51 H), 0.91 - 0.88 (t, *J* = 7.0 Hz, 6 H).

^{13}C-NMR (126 MHz, CD_2Cl_2, 298 K), δ [ppm]

171.7, 158.7, 154.8, 152.8, 141.3, 140.1, 139.7, 138.5, 137.4, 137.3, 137.0, 135.5, 134.1, 130.2, 129.4, 127.6, 124.9, 122.4, 121.1, 114.7, 93.1, 68.5, 64.8, 61.3, 41.3, 32.4, 30.1, 30.1, 30.1, 30.1, 30.0, 30.0, 29.8, 29.8, 29.7, 26.4, 23.1, 14.4, 14.3.

MS (MALDI-TOF pos, DCTB), *m*/*z* (%)

1086.6 (100) $[M]^{\bullet+}$; calculated: 1086.6 Da.

Compound **62** (PK-090)

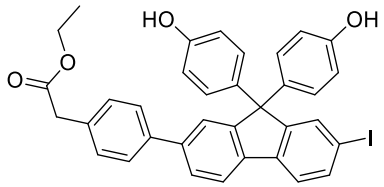

This synthesis applies a procedure published by Abashev et al.[124]

54 (94.5 mg, 0.202 mmol, 1.00 eq.) and phenol (1.00 g, 10.6 mmol, 52.7 eq.) were heated to 50 °C under vigorous stirring. After adding methanesulfonic acid (0.20 mL, 3.1 mmol, 15 eq.) the mixture was heated for 20 hours at 50 °C. After cooling to room temperature, the crude product was dissolved in DCM and purified *via* column chromatography (SiO_2, DCM:EA 5:1, R_f = 0.6) yielding the desired product (118 mg, 0.184 mmol) in 91 % as a colorless solid.

Chemical formula: $C_{35}H_{27}IO_4$

Molecular weight: 638.50 g/mol

^{1}H-NMR (500 MHz, acetone-*d*6, 298 K), *δ* [ppm]

7.95 - 7.92 (d, *J* = 7.9 Hz, 1 H), 7.83 (d, *J* = 1.5 Hz, 1 H), 7.76- -7.70 (m, 3 H), 7.68 - 7.65 (m, 1 H), 7.59 - 7.76 (d, *J* = 8.2 Hz, 2 H), 7.44 - 7.34 (m, 3 H), 7.11 - 7.08 (d, *J* = 8.7 Hz, 4 H), 6.77 - 6.74 (d, *J* = 8.9 Hz, 4 H), 4.13 - 4.08 (q, *J* = 7.2 Hz, 2 H), 3.65 (s, 2 H), 1.21 - 1.18 (t, *J* = 7.1 Hz 3 H).

^{13}C-NMR (126 MHz, acetone-*d*6, 298 K), *δ* [ppm]

170.1, 156.4, 154.9, 152.8, 140.9, 139.4, 138.1, 136.5, 136.2, 135.1, 134.1, 129.9, 129.1, 126.9, 126.4, 124.3, 122.3, 120.9, 115.2, 92.2, 64.4, 60.3, 59.7, 40.3, 13.7.

MS (MALDI-TOF pos, DCTB), *m*/*z* (%)

638.1 (100) $[M]^{\bullet+}$; calculated: 638.10 Da.

Compound **63** (PK-091)

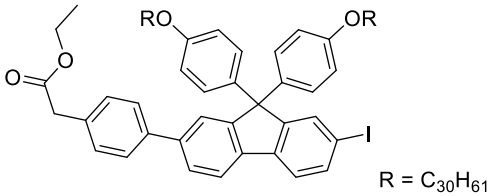

This synthesis applies a procedure published by Abashev et al.[124]

62 (136 mg, 0.212 mmol, 1.00 eq.) and KOH (51 mg, 0.911 mmol, 4.29 eq.) were dissolved in a mixture of acetone (20 mL) and water (4 mL). NBu_4Br (30 mg, 92 *µ*mol, 0.43 eq.) and **48** (225 mg, 0.411 mmol, 1.94 eq.) were added and the mixture was heated to 80 °C for 48 h. After cooling to room temperature, the residue was diluted with DCM and water. The phases were separated and the aqueous layer was extracted with DCM three times. The combined organic layers were washed with water, aq. HCl (1M) and brine and dried over magnesium sulfate. After removal of the solvent under reduced pressure, the

crude product was purified *via* column chromatography (SiO_2, DCM). It was not possible to successfully isolate **63**.

Chemical formula: $C_{95}H_{147}IO_4$

Molecular weight: 1480.12 g/mol

Compound **65** (PK-104)

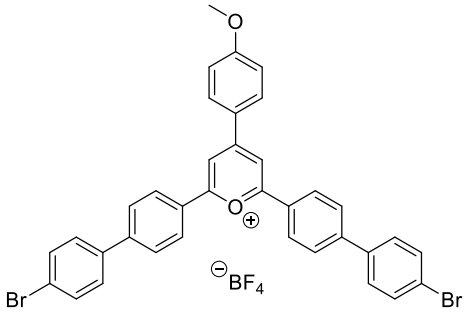

This synthesis applies a procedure published by Kotra et al.[104]

4'-(4-Bromophenyl)acetophenone (18.2 g, 66.2 mmol, 2.01 eq.) and *p*-anisaldehyde (4.0 mL, 33 mmol, 1.00 eq.) were suspended in DCE (15 mL), the mixture was purged with argon and $Et_2O{\cdot}BF_3$ (10.0 mL, 78.9 mmol, 2.40 eq.) was slowly added dropwise afterwards. The mixture was heated to 80 °C for 4 h. After cooling to room temperature, the residue was dropped into diethyl ether precipitating the crude product. The crude product was collected, dissolved in DCM and precipitated from diethyl ether again. The precipitate was dried overnight yielding **65** as a crimson solid (12.15 g, 15.94 mmol) in 48 %.

Chemical formula: $C_{26}H_{25}BBr_2F_4O_2$

Molecular weight: 736.21 g/mol

^{1}H-NMR (500 MHz, DMSO-*d6*, 298 K), *δ* [ppm]

9.06 (s, 2 H), 8.74 – 8.70 (d, *J* = 8.8 Hz, 2H), 8.64 – 8.60 (d, *J* = 8.3 Hz, 4H), 8.11 – 8.06 (d, *J* = 8.5 Hz, 4H), 7.87 – 8.72 (d, *J* = 8.6 Hz, 4H), 7.78 – 7.73 (d, *J* = 8.6 Hz, 4H), 7.34 – 7.29 (d, *J* = 8.9 Hz, 2H), 4.00 (s, 3H).

^{13}C-NMR (126 MHz, DMSO-*d*6, 298 K), *δ* [ppm]

168.2, 165.9, 163.1, 144.4, 137.3, 133.1, 132.1, 129.2, 129.2, 128.5, 127.7, 124.4, 122.7, 115.6, 113.2, 56.3.

MS (ESI+), *m*/*z* (%)

649.0 (100) $[M\text{-}BF_4]^+$; calculated: 734.0 Da.

Compound **66** (PK-AG-08)

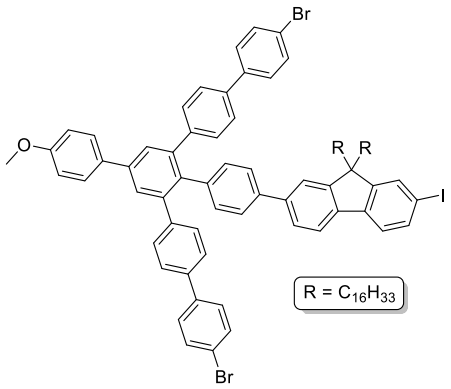

This synthesis applies a procedure published by Idelson et al.[96]

34 (509 mg, 0.568 mmol, 1.00 eq.), **65** (424 mg, 0.577 mmol, 1.02 eq.) and benzoic anhydride (2.01 g, 8.89 mmol, 15.7 eq.) were mixed and heated to 150 °C for 4 h. Sublimed benzoic anhydride was molten back into the flask by external heating with a heat gun every 15 minutes. The mixture was allowed to cool to rt and the crude product was purified *via* column chromatography (SiO_2, Cy:DCM 10:1, R_f = 0.22) yielding **66** (468 mg, 0.320 mmol, 56 %) as a yellow oil.

Chemical formula: $C_{88}H_{101}Br_2IO$

Molecular weight: 1461.49 g/mol

^{1}H-NMR (500 MHz, CD_2Cl_2, 298 K), δ [ppm]

7.70 (s, 2 H), 7.69 - 7.63 (m, 4 H), 7.55 - 7.50 (m, 6 H), 7.50 - 7.49 (m, 10 H), 7.43 – 7.40 (d, *J* = 8.3 Hz, 2 H), 7.32 – 7.28 (d, *J* = 8.2 Hz, 4 H), 7.09 – 7.06 (d, *J* = 8.7 Hz, 2 H), 7.04 – 7.01 (d, *J* = 8.9 Hz, 2 H), 3.86 (s, 3 H), 1.98-1.91 (m, 4 H), 1.31-1.00 (m, 56 H), 0.89 – 0.84 (t, *J* = 6.5 Hz, 6 H).

^{13}C-NMR (126 MHz, CD_2Cl_2, 298 K), δ [ppm]

160.2, 154.0, 151.5, 142.6, 142.2, 141.0, 140.4, 140.0, 139.3, 139.1, 138.3, 137.5, 136.4, 133.1, 132.8, 132.4, 131.1, 129.1, 128.6, 126.7, 126.5, 121.9, 121.5, 120.6, 114.90, 92.9, 55.97, 40.7, 32.5, 30.2, 27.5, 24.3, 23.3, 14.5.

MS (MALDI-TOF pos, DCTB), *m*/*z* (%)

1458.5 (100) $[M]^{\bullet+}$, 1332.6 (35) $[M\text{-}I]^+$; calculated: 1458.53 Da.

Compound **67** (PK-AG-09)

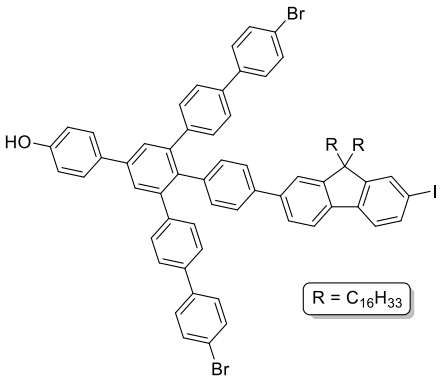

This synthesis applies a procedure published by Idelson et al.[96]

66 (577 mg, 0.395 mmol, 1.00 eq.) was dissolved in dry DCM (20 mL), purged with argon for 15 min and cooled to -78 °C. A solution of BBr_3 (2.0 mL, 2.0 mmol, 5.1 eq., 1M in DCM) was slowly added dropwise and the mixture was stirred for 18 h at room temperature. After adding water, the mixture was stirred for another 15 min. The phases were separated and the aqueous layer was extracted with DCM. The combined organic layers were washed with water and brine, dried over magnesium sulfate and the solvent was removed under reduced pressure. After purification *via* column chromatography (SiO_2, DCM:Cy 2:1, R_f = 0.39) the product was received as a colorless solid (547 mg, 0.378 mmol) in 96 %.

Chemical formula: $C_{87}H_{99}Br_2IO$

Molecular weight: 1447.46 g/mol

^{1}H-NMR (500 MHz, CD_2Cl_2, 298 K), δ [ppm]

7.69 (s, 2 H), 7.67 - 7.63 (m, 4 H), 7.55 - 7.49 (m, 6 H), 7.48 - 7.44 (m, 10 H), 7.43-7.40 (m, 2 H), 7.32 – 7.28 (d, *J* = 8.4 Hz, 2 H), 7.09 – 7.06 (d, *J* = 8.6 Hz, 2 H), 6.97 – 6.94 (d, *J* = 8.5 Hz, 2 H), 1.95 - 1.93 (m, 4 H), 1.24 - 1.01 (m, 58 H), 0.88 – 0.84 (t, *J* = 7.0 Hz, 6 H).

^{13}C-NMR (126 MHz, CD_2Cl_2, 298 K), δ [ppm]

156.3, 154.0, 151.5, 142.6, 142.2, 141.0, 140.4, 140.0, 139.3, 138.3, 137.6, 136.4, 133.4, 132.8, 132.4, 131.1, 129.0, 128.9, 128.6, 126.7, 126.5, 121.9, 121.5, 116.3, 92.9, 56.0, 40.7, 32.5, 30.5, 30.2, 29.9, 27.5, 24.3, 23.3, 14.5.

MS (MALDI-TOF pos, DCTB), *m*/*z* (%)

1444.5 (100) $[M]^{\bullet+}$, 1318.6 (35) $[M\text{-}I]^+$; calculated: 1444.5 Da.

Compound **68a**

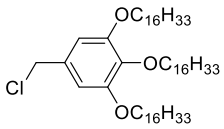

Chemical formula: $C_{55}H_{103}ClO_3$

Molecular weight: 847.88 g/mol

68a *was synthesized following the instructions of Percec et al. by U. Müller.*[107]

Compound **69a** (PK-AG-10)

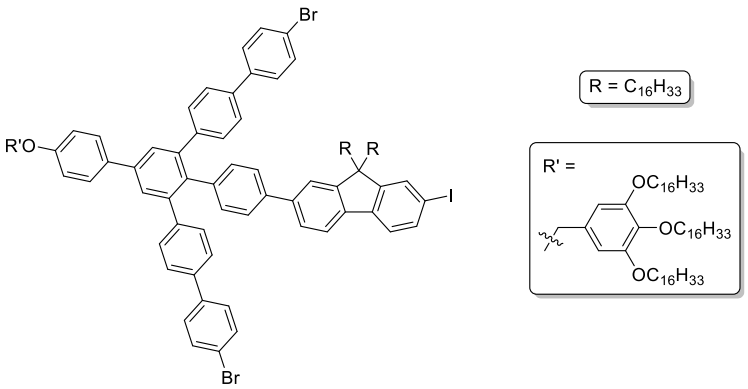

This synthesis applies a procedure published by Idelson et al.[96]

67 (402 mg, 0.278 mmol, 1.00 eq.), **68a** (471 mg, 0.554 mmol, 1.99 eq.) and Cs_2CO_3 (306 mg, 0.921 mmol, 3.31 eq.) were suspended in DMF (25 mL). The mixture was purged with argon for 30 min and heated for 48 h at 100 °C. After cooling to room temperature, the residue was suspended in DCM and aq. HCl (1M). The phases were separated and the aqueous layer was extracted with DCM three times. The combined organic layers were washed with brine, dried over magnesium sulfate and the solvent was removed under reduced pressure. After purification *via* column chromatography (SiO_2, Cy:DCM 1:1, R_f = 0.83), the product was received as an orange solid (473 mg, 0.209 mmol) in 75 % yield.

Chemical formula: $C_{142}H_{201}Br_2IO_4$

Molecular weight: 2258.88 g/mol

^{1}H-NMR (500 MHz, CD_2Cl_2, 298 K), δ [ppm]

7.71-7.65 (m, 6 H), 7.55 – 7.52 (d, *J* = 6.4 Hz, 4 H), 7.52 - 7.50 (m, 2 H), 7.48 - 7.45 (m, 8 H), 7.45 - 7.40 (m, 2 H), 7.36-7.28 (m, 6 H), 7.32 – 7.29 (dd, *J* = 6.2 Hz, *J* = 2.3 Hz, 5 H), 7.11 – 7.07 (t, *J* = 9.1 Hz, *J* = 8.6 Hz, 4 H), 6.66 (s, 2 H), 5.02 (s, 2 H), 4.00 - 3.96 (t, *J* = 6.5 Hz, 4 H), 3.94 – 3.91 (t, *J* = 6.6 Hz, 2 H), 1.98 - 1.92 (m, 4 H), 1.80 - 1.70 (m, 6 H), 1.53 (s, 10 H), 1.43 (s, 14 H), 1.30 - 1.23 (m, 95 H), 1.01 (s, 10 H), 0.89 - 0.85 (m, 15 H).

^{13}C-NMR (126 MHz, CD_2Cl_2, 298 K), δ [ppm]

159.3, 153.9, 152.0, 151.5, 151.5, 142.6, 142.2, 140.0, 139.3, 138.3, 137.6, 136.4, 133.5, 132.8, 132.5, 132.4, 131.1, 129.0, 126.7, 126.4, 123.5, 121.9, 121.5, 120.4, 115.8, 106.5, 92.9, 73.9, 71.0, 69.6, 56.0, 55.7, 40.8, 32.5, 30.9, 30.2, 27.5, 26.7, 24.3, 23.3, 14.5.

MS (MALDI-TOF pos, DCTB), *m*/*z* (%)

2278.4 (65) $[M+Na]^+$, 2258.3 (100) $[M]^{\bullet+}$; calculated: 2258.3 Da.

Compound **70a** (PK-AG-11)

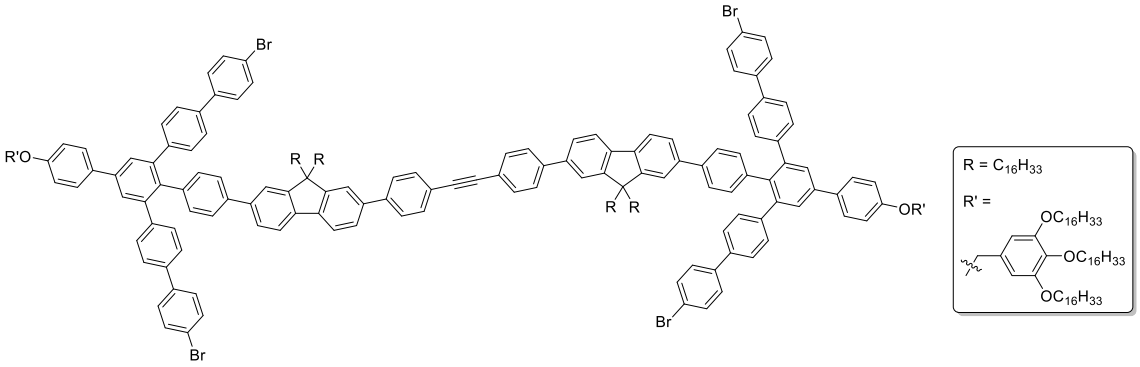

Under argon atmosphere, **69a** (1.452 g, 0.643 mmol, 3.92 eq.), **38** (70.5 mg, 0.164 mmol, 1.00 eq) and Cs_2CO_3 (348 mg, 1.07 mmol, 6.51 eq) were dissolved in THF (4 mL) and water (0.2 mL). The solution was purged with argon for 1 h before adding $Pd(PPh_3)_4$ (29.3 mg, 25.4 μmol, 0.15 eq). The mixture was stirred at 50 °C for 5 d. After cooling to room temperature, the mixture was diluted with water and aq. HCl (1M). The phases were separated and the aqueous layer was extracted with DCM. The combined organic layer was washed with water and brine, dried over magnesium sulfate and the solvent was removed under reduced pressure. After pre-purification *via* column chromatography (SiO_2, Cy:DCM 3:1), the crude product was isolated *via* recGPC (THF, unstabilized) yielding **70a** (122.5 mg, 27.6 μmol, 17 %) as a pale yellow solid.

Chemical formula: $C_{298}H_{410}Br_4O_8$

Molecular weight: 4432.84 g/mol

^{1}H-NMR (500 MHz, CD_2Cl_2, 298 K), δ [ppm]

7.75 - 7.61 (m, 24 H), 7.57 - 7.51 (m, 12 H), 7.49 - 7.43 (m, 20 H), 7.57 - 7.44 (m, 32 H), 7.34 – 7.29 (d, *J* = 8.4 Hz, 8 H), 7.11 - 7.07 (m, 8 H), 6.66 (s, 4 H), 5.02 (s, 4 H), 4.01 - 3.97 (t, *J* = 6.5 Hz, 8 H), 3.96 – 3.92 (t, *J* = 6.6 Hz, 4 H), 1.82 - 1.71 (m, 12 H), 1.54 (s, 6 H), 1.34 - 1.21 (m, 238 H), 0.88 (m, 30 H).

^{13}C-NMR (126 MHz, CD_2Cl_2, 298 K), δ [ppm]

159.4, 153.9, 152.4, 142.7, 142.2, 140.0, 138.3, 132.6, 132.4, 131.2, 129.1, 128.7, 127.6, 126.6, 121.9, 115.9, 108.6, 106.5, 90.5, 73.9, 71.0, 69.6, 68.2, 55.9, 40.9, 32.6, 30.9, 30.2, 26.8, 24.5, 23.3, 14.5.

MS (MALDI-TOF pos, DCTB), *m/z* (%)

5252.7 (50) $[M+C_{55}H_{103}O_3]^+$, 4440.0 (100) $[M]^{\bullet+}$; calculated: 4439.9 Da.

Compound **71a** (PK-109)

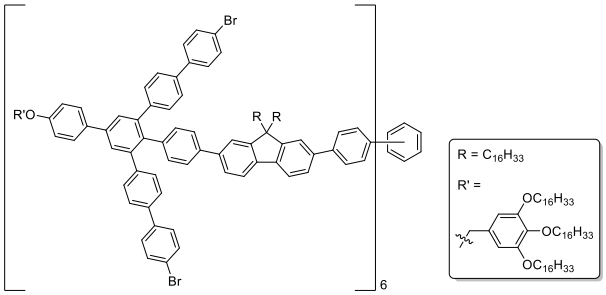

This synthesis applies a procedure published by Idelson et al.[96]

Under argon atmosphere, **70a** (122.5 mg, 27.6 μmol, 1.00 eq.) was dissolved in toluene (15 mL) and the solution was purged with argon for 1 h. $Co_2(CO)_8$ (3.0 mg, 8.8 μmol, 0.32 eq.) was added and the mixture was stirred at 120 °C for 5 h. After reaction control, another portion of $Co_2(CO)_8$ (4.8 mg, 14 μmol, 0.52 eq.) was added and the mixture was stirred for 48 h at 120 °C. The same procedure was repeated and more $Co_2(CO)_8$ (6.7 mg, 19 μmol, 0.71 eq.) was added. The reaction mixture was allowed to cool to room temperature and the solvent was removed under reduced pressure. After pre-purification *via* column chromatography (SiO_2, DCM), the product was isolated *via* recGPC (THF, BHT-stabilized) and precipitated from methanol to give **71a** (18.9 mg, 1.40 μmol, 15 %) as a pale-yellow glassy solid.

Chemical formula: $C_{894}H_{1230}Br_{12}O_{24}$

Molecular weight: 13320.5 g/mol

^{1}H-NMR (700 MHz, CD_2Cl_2, 298 K), δ [ppm]

7.71 (s, 18 H), 7.70 (s, 6 H), 7.68 - 7.63 (m, 12 H), 7.52 - 7.50 (d, *J* = 8.6 Hz, 48 H), 7.48 - 7.45 (dd, *J*= 2.2 Hz, *J* = 8.1 Hz, 42 H), 7.43 - 7.38 (m, 24 H), 7.34 - 7.30 (m, 36 H), 7.12 - 7.07 (m, 30 H), 6.66 (s, 12 H), 5.02 (s, 12 H), 4.00 - 3.97 (t, *J* = 6.5 Hz, 24 H), 3.94 - 3.92 (t, *J* = 6.6 Hz, 12 H), 1.83 - 1.78 (m, 24 H), 1.75 - 1.70 (m, 12 H), 1.51 - 1.45 (m, 36 H), 1.28 (bs, 792 H), 0.90 - 0.87 (m, 54 H), 0.86 - 0.83 (t, *J* = 7.1 Hz, 36 H).

^{13}C-NMR (176 MHz, CD_2Cl_2, 298 K), δ [ppm]

159.2, 153.7, 152.1, 151.9, 142.5, 142.0, 140.8, 140.6, 140.3, 140.2, 140.0, 139.9, 139.6, 139.4, 139.0, 138.7, 138.2, 138.1, 137.5, 136.2, 133.3, 132.7, 132.4, 132.2, 131.0, 129.8, 128.9, 128.6, 128.5, 126.5, 126.3, 126.1, 125.8, 121.8, 121.5, 121.3, 120.3, 115.7, 106.3, 73.8, 70.9, 69.5, 55.7, 40.8, 34.5, 32.4, 32.4, 30.8, 30.5, 30.5, 30.2, 30.2, 30.2, 30.1, 30.1, 30.1, 30.0, 29.9, 29.8, 29.8, 29.7, 26.6, 26.6, 24.3, 23.1, 21.2, 14.3, 14.3.

MS (MALDI-TOF pos, DCTB), *m*/*z* (%)

13425.9 (100) $[M+Ag]^+$, 12618.6 (52) $[M+Ag\text{-}Dend]^+$, 12618.6 (20) $[M+Ag\text{-}2\ Dend]^+$; calculated: 13314.5 Da.

Compound **MSW-Fa** (PK-110)

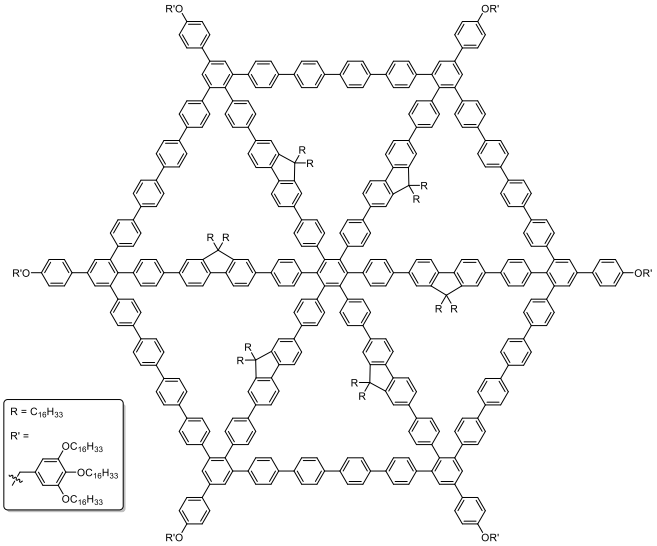

This synthesis applies a procedure published by Idelson et al.[96]

Inside a glove box, **71a** (9.5 mg, 0.71 μmol, 1.0 eq.) was placed in a microwave tube and equipped with $Ni(COD)_2$ (14.0 mg, 50.4 μmol) and 2,2´-bipyridine (14.0 mg, 88.2 μmol). Under the exclusion of light, the tube was filled with a solvent mixture consisting of THF and COD (32:1, 8.25 mL), immediately sealed and heated in a microwave reactor (12 min, 300 W, 120 °C). The product was purified *via* filtration through a plug of silica gel (DCM) and subsequent recGPC (THF, unstabilized) yielding **MSW-Fa** (5.3 mg, 0.86 μmol, 60 %) as a pale-yellow solid.

Chemical formula: $C_{894}H_{1230}O_{24}$

Molecular weight: 12361.65 g/mol

^{1}H-NMR (700 MHz, CD_2Cl_2, 298 K), δ [ppm]

7.79 - 7.65 (m, 72 H), 7.60 (s, 12 H), 7.56 - 7.53 (d, *J* = 8.5 Hz, 24 H), 7.51 - 7.41 (m, 24 H), 7.38 - 7.29 (m, 48 H), 7.13 - 7.07 (m, 24 H), 7.01 - 6.95 (m, 12 H), 6.67 (s, 12 H), 5.03 (s, 12 H), 4.00 - 3.97 (t, *J* = 6.4 Hz, 24 H), 3.94 - 3.91 (t, *J* = 6.6 Hz, 12 H), 1.82 - 1.78 (p, *J* = 6.6 Hz, 24 H), 1.75 - 1.70 (p, *J* = 6.7 Hz, 12 H), 1.51 - 1.44 (m, 48 H), 1.28 (bs, 780 H), 0.89 - 0.84 (m, 90 H).

^{13}C-NMR (176 MHz, CD_2Cl_2, 298 K), δ [ppm]

159.2, 153.7, 152.0, 151.9, 142.7, 141.6, 140.4, 141.0, 139.7, 139.1, 138.6, 138.2, 136.2, 132.7, 132.4, 130.9, 129.8, 128.7, 128.6, 128.0, 127.5, 126. 3, 126.1, 125.8, 121.0, 120.2, 115.7, 106.3, 73.8, 70.9, 69.5, 55.9, 40.6, 34.5, 32.4, 32.4, 32.4, 30.8, 30.5, 30.4, 30.2, 30.2, 30.2, 30.1, 30.1, 30.1, 30.1, 30.1, 30.0, 29.9, 29.8, 29.8, 29.8, 29.6, 26.6, 26.6, 24.4, 24.2, 23.1, 23.1, 21.2, 14.3, 14.3.

MS (MALDI-TOF pos, DCTB), *m/z* (%)

12469.6 (100) $[M+Ag]^+$, 11657.7 (62) $[M\text{-}Dend+Ag]^+$, 10846.3 (11) $[M\text{-}2\ Dend+Ag]^+$; calculated: 12356.5 Da.

Compound **68b**

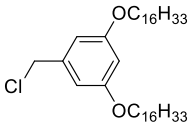

Chemical formula: $C_{39}H_{71}ClO_2$

Molecular weight: 607.45 g/mol

68b *was synthesized following the instructions of Percec et al. by U. Müller.*[107]

Compound **69b** (PK-157)

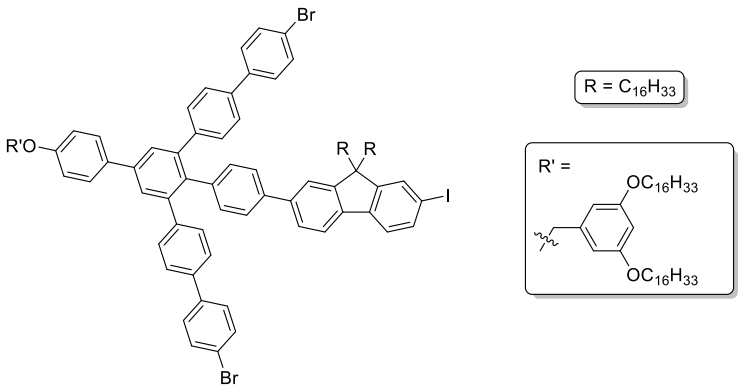

This synthesis applies a procedure published by Idelson et al.[96]

67 (339 mg, 0.235 mmol, 1.00 eq.), **68b** (161 mg, 0.264 mmol, 1.13 eq.) and Cs_2CO_3 (236 mg, 0.725 mmol, 3.09 eq.) were suspended in DMF (15 mL) and the mixture was stirred for 48 h at 100 °C. After cooling to room temperature, the solvent was removed under reduced pressure and the residue was suspended in DCM and aq. HCl (2M). The phases were separated and the aqueous layer was extracted with DCM four times. The combined organic layers were washed with brine, dried over magnesium sulfate and the solvent was removed under reduced pressure. After purification *via* column chromatography (SiO_2, Cy:DCM 2:1, R_f = 0.45) the product was received as a pale-yellow resin (0.450 g, 0.223 mmol) in 95 % yield.

Chemical formula: $C_{126}H_{169}Br_2IO_3$

Molecular weight: 2018.45 g/mol

^{1}H-NMR (500 MHz, CD_2Cl_2, 298 K), δ [ppm]

7.70 (d, *J* = 1.0 Hz, 2 H), 7.69 (m, 3 H), 7.68 (d, *J* = 1.0 Hz, 1 H), 7.67 - 7.65 (dd, *J* = 7.6 Hz, *J* = 1.9 Hz, 1 H), 7.54 - 7.51 (m, 6 H), 7.48 - 7.44 (m, 10 H), 7.44 - 7.40 (dd, *J* = 8.2 Hz, *J* = 6.2 Hz, 2 H), 7.32 - 7.29 (m, 5 H), 7.10 - 7.07 (dd, *J* = 8.5 Hz, *J* = 4.4 Hz, 4 H), 6.58 (d, *J* = 2.2 Hz, 2 H), 6.40 (t, *J* = 2.3 Hz, 1 H), 3.96 - 3.93 (t, *J* = 6.6 Hz, 4 H), 1.99 - 1.91 (m, 4 H), 1.79 - 1.73 (p, *J* = 6.6 Hz, 4 H), 1.48 - 1.41 (m, 4 H), 1.27 (bs, 104 H), 0.90 - 0.60 (m, 12 H).

^{13}C-NMR (126 MHz, CD_2Cl_2, 298 K), δ [ppm]

161.0, 159.1, 153.9, 151.9, 151.3, 142.5, 142.0, 140.9, 140.3, 139.9, 139.7, 139.4, 139.2, 138.9, 138.1, 137.4, 136.2, 133.3, 132.7, 132.2, 131.0, 128.9, 128.9, 128.5, 128.5, 126.5, 126.3, 123.4, 121.8, 121.3, 120.4, 115.7, 106.0, 104.0, 101.0, 92.8, 70.4, 68.6, 55.9, 32.4, 30.4, 30.3, 30.1, 30.1, 30.1, 30.0, 30.0, 30.0, 29.8, 29.8, 29.7, 29.6, 26.5, 24.2, 23.1, 14.3.

MS (MALDI-TOF pos, DCTB), *m*/*z* (%)

2126.0 (88) $[M+Ag]^+$, 2018.1 (16) $[M]^+$, 2000.1 (100) $[M-I+Ag]^+$, 1892.2 (19) $[M-I]^+$; calculated: 2018.1 Da.

Compound **70b** (PK-159, PK-168)

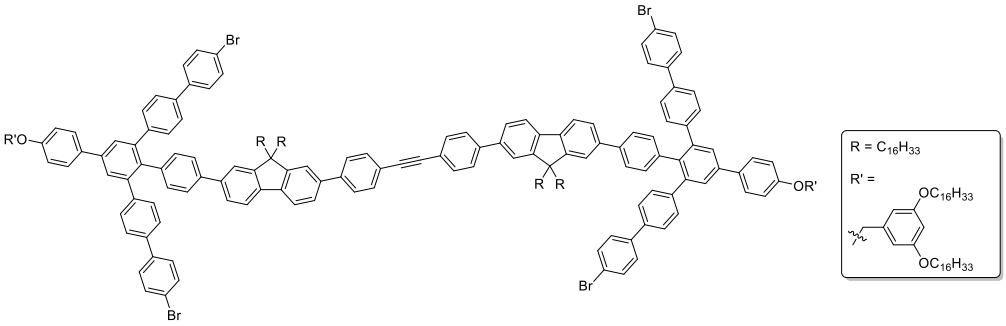

V1:

Inside a glove box, a *Schlenk* tube containing **69b** (150 mg, 74.3 μmol, 2.20 eq.) and Cs_2CO_3 (75.6 mg, 232 μmol, 6.88 eq.) was equipped with **38** (14.5 mg, 33.7 μmol, 1.00 eq.) and $Pd(PPh_3)_4$ (4.5 mg, 3.9 μmol, 0.12 eq.) and the mixture was diluted with toluene (3.5 mL). Outside the glove box, water (0.2 mL) was added and the mixture was heated to 50 °C for five days. The solvent was removed under reduced pressure and after pre-purification *via* column chromatography (SiO_2, Cy:DCM 3:1), the crude product was purified *via* recGPC (THF, unstabilized) to give **70b** (13.8 mg, 3.5 μmol) as a pale yellow solid in 10 % yield.

V2:

Inside a glove box, a *Schlenk* tube containing **69b** (150 mg, 74.3 μmol, 2.04 eq.) and **105** (27.5 mg, 36.4 μmol, 1.00 eq.) was equipped with $Pd(PPh_3)_4$ (3.8 mg, 3.3 μmol, 0.090 eq.) and the mixture was diluted with toluene (4 mL). Outside the glove box, the mixture was heated to 50 °C for five days. The solvent was removed under reduced pressure and after pre-purification *via* column chromatography (SiO_2:K_2CO_3 9:1,DCM),[136] the crude product was purified *via* recGPC (THF, unstabilized) to give **70b** (1.5 mg, 0.4 μmol) as a pale yellow solid in 1 % yield.

V3:[139]

Inside a glove box, a *Schlenk* tube containing **69b** (150 mg, 74.3 μmol, 2.17 eq.), **105** (25.9 mg, 34.2 μmol, 1.00 eq.), $Pd_2(dba)_3$ (1.8 mg, 2.0 μmol, 0.057 eq.) and TFP (1.9 mg, 8.2 μmol, 0.24 eq.) was diluted with toluene (4 mL). Outside the glove box, the mixture was heated to 50 °C for five days. The solvent was removed under reduced pressure and after pre-purification *via* column chromatography (SiO_2:K_2CO_3 9:1, DCM),[136] the crude product was purified *via* recGPC (THF, unstabilized) to give **70b** (4.9 mg, 1.2 μmol) as a pale yellow solid in 4 % yield.

V4:[135]

Inside a glove box, a *Schlenk* tube containing **112** (103 mg, 48.9 μmol, 2.90 eq.) and bis(tributylstannyl)acetylene (10.2 mg, 16.9 μmol, 1.00 eq.) was equipped with $Pd(PPh_3)_4$ (2.2 mg, 1.9 μmol, 0.11 eq.) and the mixture was diluted with toluene (2 mL). Outside the glove box, the mixture was heated to 50 °C for five days. The solvent was removed under reduced pressure and after pre-purification *via* column chromatography (SiO_2:K_2CO_3 9:1, DCM),[136] the crude product was isolated *via* recGPC (THF, unstabilized) to give **70b** (30,6 mg, 7.7 μmol) as a yellow solid in 46 % yield.

Chemical formula: $C_{266}H_{346}Br_4O_6$

Molecular weight: 3959.30 g/mol

^{1}H-NMR (500 MHz, CD_2Cl_2, 298 K), δ [ppm]

7.79-7.77 (d, *J* = 8.1 Hz, 4 H), 7.74 - 7.72 (d, *J* = 7.8 Hz, 4 H), 7.72 - 7.70 (d, *J* = 4.7 Hz, 4 H), 7.70 (s, 4 H), 7.70 - 7.67 (m, 8 H), 7.67 - 7.65 (d, *J* = 8.1 Hz, 4 H), 7.64 - 7.62 (m, 4 H), 7.57 - 7.53 (m, 12 H), 7.48 - 7.46 (dd, *J* = 8.6 Hz, *J* = 2.7 Hz, 16 H), 7.46 - 7.44 (d, *J* = 8.3 Hz, 4 H), 7.11 - 7.09 (d, *J* = 8.3 Hz, 8 H), 6.59 (d, *J* = 2.3 Hz, 4 H), 6.41 (t, *J* = 2.3 Hz, 2 H), 5.06 (s, 4 H), 3.97 - 3.94 (t, *J* = 6.6 Hz, 8 H), 1.79 - 1.75 (m, 8 H), 1.48 - 1.43 (m, 8 H), 1.28 (bs, 216 H), 0.90 - 0.86 (dt, *J* = 13.0 Hz, *J* = 7.0 Hz, 24 H).

^{13}C-NMR (126 MHz, CD_2Cl_2, 298 K), δ [ppm]

160.6, 158.7, 151.8, 142.1, 141.6, 141.4, 140.5, 140.0, 139.8, 139.5, 139.4, 139.3, 139.1, 138.9, 138.4, 137.7, 137.0, 132.9, 132.9, 132.3, 132.0, 131.9, 131.8, 130.6, 128.5, 128.1, 128.1, 127.0, 126.1, 125.9, 125.8, 122.0, 121.4, 121.4, 121.0, 120.1, 120.0, 115.3, 105.6, 100.6, 90.1, 70.0, 68.1, 67.8, 55.4, 32.0, 30.0, 29.7, 29.7, 29.7, 29.7, 29.7, 29.7, 29.6, 29.6, 29.6, 29.6, 29.4, 29.4, 29.3, 29.2, 26.0, 25.6, 23.8, 22.7, 13.9.

MS (MALDI-TOF pos, DCTB), *m*/*z* (%)

4067.4 (100) $[M+Ag]^+$, 3959.4 (37) $[M]^{\bullet+}$; calculated: 3958.4 Da.

Compound **71b** (PK-165, PK-169)

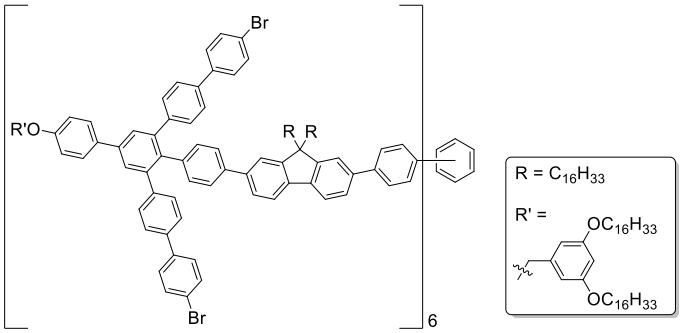

This synthesis applies a procedure published by Idelson et al.[96]

Inside a glove box, **70b** (30.6 mg, 7.7 μmol, 1.00 eq) was dissolved in dry toluene (15 mL). $Co_2(CO)_8$ (1.1 mg, 3.2 μmol, 0.42 eq) was added and the mixture was stirred at 120 °C for 4 h. After reaction control *via* analytical GPC, the mixture was heated for an additional 20 h. The progress of the reaction was checked again, more $Co_2(CO)_8$ (1.2 mg, 3.5 μmol, 0.45 eq.) was added and the reaction was continued for further 24 h. The mixture was allowed to cool to room temperature and the solvent was removed under reduced pressure. After pre-purification *via* column chromatography (SiO_2, DCM), the product was isolated *via* recGPC (THF, unstabilized) to give **71b** (10.5 mg, 0.9 μmol, 34 %) as a pale-yellow glassy solid.

Chemical formula: $C_{798}H_{1038}Br_{12}O_{18}$

Molecular weight: 11877.91 g/mol

^{1}H-NMR (700 MHz, CD_2Cl_2, 298 K), δ [ppm]

7.82 - 7.78 (m, 24 H), 7.74 - 7.69 (m, 12 H), 7.61 - 7.58 (d, *J* = 8.2 Hz, 24 H), 7.54 - 7.50 (d, *J* = 8.5 Hz, 60 H), 7.47 - 7.43 (d, *J* = 7.2 Hz, 24 H), 7.41 - 7.37 (d, *J* = 7.9 Hz, 36 H), 7.21 - 7.16 (t, *J* = 8.7 Hz, 24 H), 7.14 - 7.11 (d, *J* = 7.8 Hz, 12 H), 6.70 (s, 12 H), 6.53 (s, 6 H), 5.15 (s, 12 H), 4.09 - 4.05 (t, *J* = 6.6 Hz, 24 H), 4.05 - 4.02 (t, *J* = 6.7 Hz, 24 H), 1.91 - 1.84 (p, *J* = 7.0 Hz, 24 H), 1.60 - 1.53 (p, *J* = 7.1 Hz, 24 H), 1.39 (bs, 624 H), 1.01 - 0.97 (t, *J* = 6.5 Hz, 36 H), 0.97 - 0.93 (t, *J* = 6.7 Hz, 36 H).

^{13}C-NMR (176 MHz, CD_2Cl_2, 298 K), δ [ppm]

160.6, 158.7, 151.6, 142.1, 141.6, 140.1, 139.8, 139.5, 139.3, 138.9, 138.3, 137.7, 137.1, 132.9, 132.2, 131.8, 130.6, 128.5, 128.1, 126.1, 125.9, 121.4, 120.9, 119.8, 115.3, 108.0, 105.6, 100.6, 70.0, 67.8, 67.6, 55.3, 40.4, 31.9, 30.0, 29.7, 29.7, 29.7, 29.7, 29.7, 29.6, 29.6, 29.6, 29.4, 29.4, 29.3, 29.2, 29.1, 29.1, 26.0, 25.6, 25.2, 23.9, 22.7, 22.2, 13.9, 13.9.

MS (MALDI-TOF pos, DCTB), *m/z* (%)

11985.2 $[M+Ag]^+$, 11878.7 (28) $[M+H]^+$; calculated: 11872.1 Da.

Compound **MSW-Fb** (PK-170)

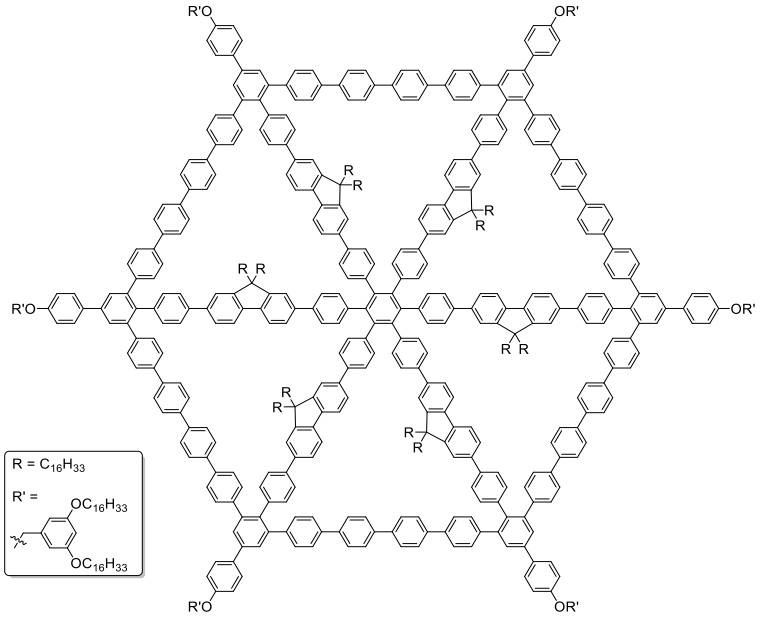

This synthesis applies a procedure published by Idelson et al.[96]

Inside a glove box, **71b** (10.5 mg, 0.884 μmol, 1.00 eq.) was placed in a microwave tube and equipped with $Ni(COD)_2$ (11.4 mg, 41.4 μmol) and 2,2´-bipyridine (12.3 mg, 78.8 μmol). Under the exclusion of light, the tube was filled with a solvent mixture consisting of THF and COD (32:1, 8.25 mL), immediately sealed and heated in a microwave reactor (12 min, 300 W, 120 °C). The product was purified by filtration through a plug of silica gel (DCM) and subsequent recGPC (THF, unstabilized) to give **MSW-Fb** as a yellow solid (3.4 mg, 0.311 μmol) in 35 % yield.

Chemical formula: $C_{798}H_{1038}O_{18}$

Molecular weight: 10919.06 g/mol

^{1}H-NMR (700 MHz, CD_2Cl_2, 298 K), δ [ppm]

7.77 (s, 12 H), 7.75 - 7.71 (d, *J* = 8.4 Hz, 24 H), 7.68 (s, 36 H), 7.62 - 7.58 (m, 12 H), 7.56 - 7.52 (d, *J* = 7.8 Hz, 36 H), 7.50 (s, 12 H), 7.39 - 7.35 (d, *J* = 7.8 Hz, 18 H), 7.33 - 7.28 (d, *J* = 7.6 Hz, 30 H), 7.14 - 7.07 (m, 24 H), 7.02 - 6.98 (d, *J* = 7.8 Hz, 12 H), 6.59 (s, 12 H), 6.41 (s, 6 H), 5.08 (s, 12 H), 4.05 - 3.93 (m, 48 H), 1.80 - 1.73 (p, *J* = 6.8 Hz, 24 H), 1.27 (bs, 648 H), 0.90 - 0.84 (m, 72 H).

^{13}C-NMR (176 MHz, CD_2Cl_2, 298 K), δ [ppm]

161.1, 159.2, 152.1, 142.4, 141.4, 140.1, 139.8, 138.4, 133.7, 132.7, 131.0, 128.3, 127.6, 126.4, 120.9, 120.2, 115.8, 106.1, 101.1, 32.4, 30.2, 30.1, 30.1, 30.1, 29.8, 29.8, 29.7, 26.5, 25.7, 24.3, 23.1, 14.3.

MS (MALDI-TOF pos, DCTB), *m*/*z* (%)

10923 (92) $[M]^{\bullet+}$; calculated: 10915.0 Da.

Compound **73** (PK-103)

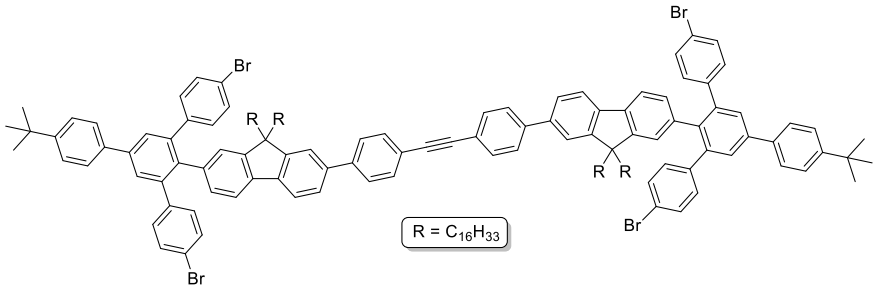

Under argon atmosphere, **15** (389 mg, 0.309 μmol, 2.16 eq.), **38** (61.5 mg, 143.0 μmol, 1.00 eq) and Cs_2CO_3 (321 mg, 984 μmol, 6.89 eq) were dissolved in THF (4.0 mL), ethanol (0.5 mL) and water (0.5 mL). The solution was purged with argon for 1 h before adding $Pd(PPh_3)_4$ (11.9 mg, 7.20 μmol, 0.07 eq). The mixture was stirred at 50 °C for 5 d. After cooling to room temperature, the mixture was diluted with water and aq. HCl (1 M). The phases were separated and the aqueous layer was extracted with DCM. The combined organic layer was washed with water and brine, dried over magnesium sulfate and the solvent was removed under reduced pressure. After pre-purification *via* column chromatography (SiO_2, DCM), **73** was purified by recGPC (THF, unstabilized) to give **73** as a pale-yellow solid (72.5 mg, 29.7 μmol) in 21 % yield.

Chemical formula: $C_{160}H_{198}Br_4$

Molecular weight: 2440.96 g/mol

^{1}H-NMR (700 MHz, CD_2Cl_2, 298 K), δ [ppm]

7.71 - 7.67 (m, 12 H), 7.67 - 7.64 (t, *J* = 8.5 Hz, 8 H), 7.61 - 7.59 (dd, *J* = 7.8 Hz, *J* = 1.7 Hz, 2 H), 7.56 (d, *J* = 1.8 Hz, 2 H), 7.53 - 7.51 (d, *J* = 8.4 Hz, 2 H), 7.47 - 7.45 (d, *J* = 7.7 Hz, 2 H), 7.31 - 7.28 (d, *J* = 8.6 Hz, 8 H), 7.10 - 7.08 (d, *J* = 8.6 Hz, 8 H), 6.96 (s, 2 H), 6.88 - 6.86 (dd, *J* = 7.6 Hz, *J* = 1.5 Hz, 2 H), 1.93 - 1.87 (m, 4 H), 1.78 - 1.72 (m, 4 H), 1.38 (s, 18 H), 1.25 (bs, 112 H), 0.89 - 0.86 (t, *J* = 7.1 Hz, 12 H).

^{13}C-NMR (176 MHz, CD_2Cl_2, 298 K), δ [ppm]

151.7, 151.0, 150.9, 150.5, 150.1, 142.1, 141.4, 140.9, 140.1, 139.0, 138.3, 138.1, 138.0, 137.2, 137.1, 131.9, 131.6, 130.7, 128.8, 128.3, 128.1, 126.9, 126.6, 125.9, 121.9, 121.2, 120.6, 120.0, 90.0, 54.9, 40.1, 34.5, 31.9, 31.0, 30.0, 30.0, 29.7, 29.6, 29.4, 29.3, 23.7, 22.7, 13.9.

MS (MALDI-TOF pos, DCTB), *m*/*z* (%)

2441.2 (100) $[M]^{\bullet+}$; calculated: 2441.2 Da.

Compound **74** (PK-115)

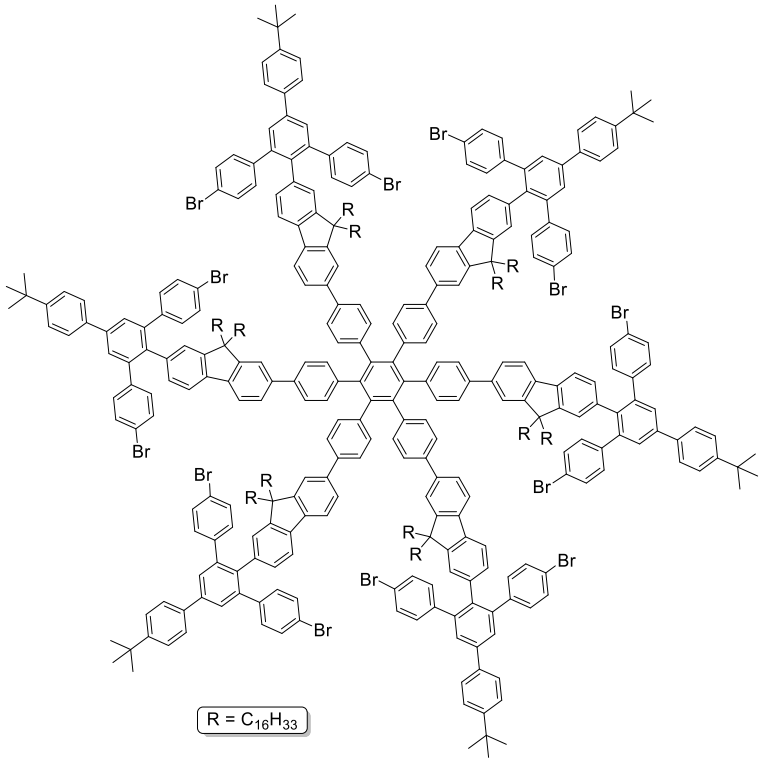

This synthesis applies a procedure published by Idelson et al.[96]

Under argon atmosphere, **73** (136 mg, 55.6 μmol, 1.00 eq.) was dissolved in toluene (10 mL) and purged with argon for 1 h. After adding $Co_2(CO)_8$ (3.8 mg, 11 μmol, 0.20 eq.), the mixture was heated to 130 °C. After 4 h, the progress of the reaction was checked *via* analytical GPC. The mixture was allowed to cool to rt and the solvent was removed under reduced pressure. The product was purified by filtration through a plug of silica gel (DCM) and subsequent recGPC (THF, unstabilized) to give **74** as a yellow solid (56.2 mg, 7.70 μmol) in 41 % yield.

Chemical formula: $C_{480}H_{594}Br_{12}$

Molecular weight: 7322.88 g/mol

^{1}H-NMR (500 MHz, CD_2Cl_2, 373 K), δ [ppm]

7.69 - 7.66 (d, *J* = 7.2 Hz, 24 H), 7.52 - 7.49 (d, *J* = 8.6 Hz, 12 H), 7.42 - 7.38 (m, 12 H), 7.36 - 7.33 (dd, *J* = 7.9 Hz, *J* = 1.5 Hz, 6 H), 7.31 - 7.25 (m, 42 H), 7.12 - 7.06 (m, 36 H), 6.94 - 6.92 (d, *J* = 1.6 Hz, 6 H), 6.87 - 6.84 (dd, *J* = 7.8 Hz, *J* = 1.5 Hz, 6 H), 1.42 (s, 54 H), 1.29 (bs, 360 H), 0.92 - 0.89 (t, *J* = 7.0 Hz, 36 H).

^{13}C-NMR (176 MHz, CD_2Cl_2, 298 K), δ [ppm]

152.0, 151.9, 151.4, 150.8, 141.9, 141.4, 140.6, 140.4, 140.1, 139.7, 138.6, 138.2, 137.6, 136.3, 132.6, 132.1, 131.2, 130.7, 128.7, 128.6, 127.1, 126.4, 126.3, 125.8, 121.4, 121.1, 120.3, 119.4, 40.7, 34.9, 34.5, 32.4, 31.5, 30.7, 30.5, 30.3, 30.2, 30.2, 30.1, 29.9, 24.3, 23.2, 21.3, 14.4.

MS (MALDI-TOF pos, DCTB), *m/z* (%)

7430.7 (100) $[M+Ag]^+$, 7351.8 (23) $[M+Ag+H-Br]^+$, 7322.8 (30) $[M]^{\bullet+}$; calculated: 7317.7 Da.

Compound **MSW-G** (PK-117)

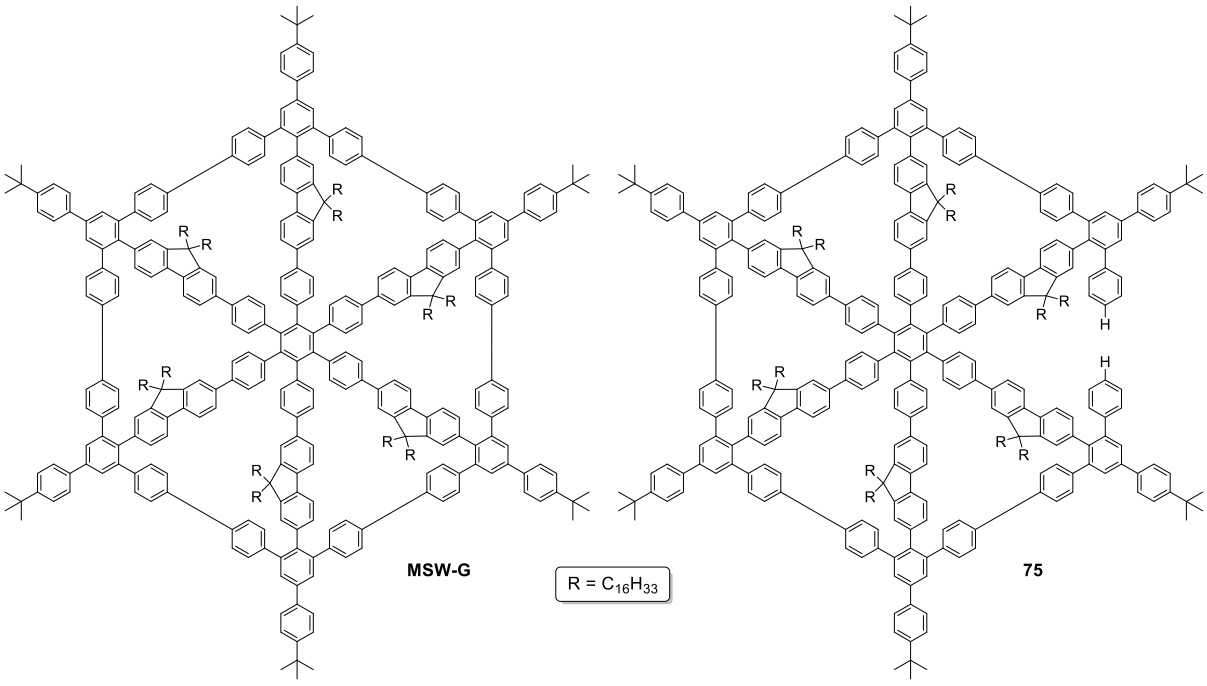

This synthesis applies a procedure published by Idelson et al.[96]

Inside a glove box, **74** (40.9 mg, 5.58 μmol, 1.00 eq) was equally distributed to seven microwave-tubes. Each tube was equipped with $Ni(COD)_2$ (12.0 mg, 43.5 μmol) and 2,2´-bipyridine (12.0 mg, 75.0 μmol). Under the exclusion of light, each tube was filled with a solvent mixture consisting of THF and COD (32:1, 8.25 mL), immediately sealed and heated in a microwave reactor (12 min, 300 W, 120 °C). The solvent was removed under reduced pressure and after pre-purification *via* column chromatography (SiO_2, DCM), **74** was isolated using recGPC (THF, unstabilized) in traces. **MSW-G** was not obtained.

MSW-G

Chemical formula: $C_{480}H_{594}$

Molecular weight: 6364.03 g/mol

75

Chemical formula: $C_{480}H_{594}$

Molecular weight: 6366.03 g/mol

MS (MALDI-pos, DCTB), *m/z* (%)

6474.6 (21) $[M+Ag]^+$, 6367.7 (100) $[M+H]^+$; calculated: 6365.7 Da.

Compound **77** (PK-113)

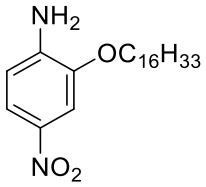

This synthesis applies a procedure published by He et al.[133]

2-Amino-5-nitrophenol (1.004 g, 6.512 mmol, 1.000 eq.), KOH (1.052 g, 18.76 mmol, 2.880 eq.), substoichiometric amounts of potassium iodide, NBu_4Br (0.206 g, 0.639 mmol, 0.0981 eq.) and 1-bromohexadecane (2.1 mL, 6.9 mmol, 1.1 eq.) were dissolved in a mixture of acetone (15 mL) and water (2 mL) and heated to 80 °C overnight. The solvent was removed under reduced pressure, the residue was suspended in EA and aq. HCl (2M) and the phases were separated. The aqueous phase was extracted four times with EA and the combined organic phases were washed with brine and dried over magnesium sulfate. After removal of the solvent under reduced pressure, the crude product was purified *via* column chromatography (SiO_2, Cy:DCM 1:3, R_f = 0.55) yielding the desired product (2.002 g, 5.289 mmol) as a yellow oil in 81 %.

Chemical formula: $C_{22}H_{38}N_2O_3$

Molecular weight: 378.56 g/mol

^{1}H-NMR (500 MHz, CD_2Cl_2, 298 K), δ [ppm]

7.78 - 7.75 (dd, *J* = 6.9 Hz, 1 H), 7.65 - 7.63 (d, *J* = 2.3 Hz, 1 H), 6.67 - 6.64 (d, *J* = 8.7 Hz, 1 H), 4.62 (bs, 2 H), 4.10 - 4.06 (t, *J* = 6.5 Hz, 2 H), 1.88 - 1.80 (m, 2 H), 1.52 - 1.44 (m, 2 H), 1.27 (bs, 24 H), 0.90 - 0.86 (t, *J* = 6.9 Hz, 3 H).

^{13}C-NMR (126 MHz, CD_2Cl_2, 298 K), δ [ppm]

145.4, 144.0, 139.0, 119.1, 112.0, 106.9, 69.4, 32.3, 30.1, 30.1, 30.1, 30.0, 30.0, 29.8, 29.4, 27.3, 26.4, 23.1, 14.3.

MS (EI, 70 eV), *m/z* (%)

378.3 (23) $[M]^{\bullet+}$, 154.0 (100) $[M\text{-}C_{16}H_{32}]^+$; calculated: 378.3 Da.

Compound **78** (PK-114)

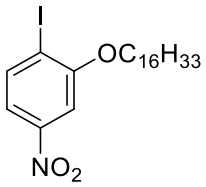

This synthesis applies a procedure published by He et al.[133]

77 (2.002 g, 5.288 mmol, 1.000 eq.) and *p*-TsOH·H_2O (7.601 g, 14.79 mmol, 2.796 eq.) were suspended in THF (30 mL) and the mixture was cooled to 0 °C in an ice bath. A mixture of sodium nitrite (711 mg, 10.3 mmol, 1.95 eq.) and potassium iodide (2.095 g, 12.62 mmol, 2.386 eq.) dissolved in water (15 mL) was slowly added dropwise while constantly keeping the temperature below 4 °C. After stirring for 30 min, the mixture was allowed to warm to room temperature and was stirred overnight. The reaction was quenched through addition of aq. $NaHSO_3$ (40 %) and was neutralized with aq. $NaHCO_3$ (10 %). After removal of the organic solvent under reduced pressure, the aqueous residue was diluted with DCM and the phases were separated. The aqueous phase was extracted three times with DCM, the combined organic phases were washed with brine and dried over magnesium sulfate. After removal of the solvent under reduced pressure, the crude product was purified *via* column chromatography (SiO_2, Cy:DCM 1:2, R_f = 0.83) yielding the desired product as an orange solid (1.823 g, 3.725 mmol) in 70 %.

Chemical formula: $C_{22}H_{36}INO_3$

Molecular weight: 489.44 g/mol

^{1}H-NMR (500 MHz, CD_2Cl_2, 298 K), δ [ppm]

7.98 - 7.96 (d, *J* = 8.5 Hz, 1 H), 7.61 - 7.59 (d, *J* = 2.4 Hz, 1 H) 7.57 - 7.54 (dd, *J* = 8.5 Hz, *J* = 2.5 Hz, 1 H), 4.14 - 4.10 (t, *J* = 6.4 Hz, 2 H), 1.90 - 1.84 (m, 2 H), 1.57 - 1.51 (m, 2 H), 1.27 (bs, 24 H), 0.90 - 0.87 (t, *J* = 6.9 Hz, 3 H).

^{13}C-NMR (126 MHz, CD_2Cl_2, 298 K), δ [ppm]

158.8, 149.7, 140.1, 116.9, 106.4, 95.7, 70.5, 32.3, 30.1, 30.1, 30.0, 29.9, 29.8, 29.6, 29.2, 27.3, 26.4, 23.1, 14.3.

MS (EI, 70 eV), *m/z* (%)

489.2 (14) $[M]^{\bullet+}$, 363.3 (13) $[M\text{-}I+H]^+$, 125.1 (12) $[M\text{-}I\text{-}C_{16}H_{32}]^+$; calculated: 489.2 Da.

Compound **79** (PK-116)

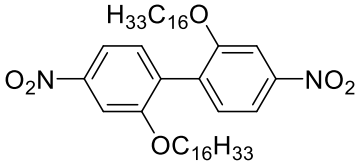

This synthesis applies a procedure published by He et al.[133]

78 (796 mg, 1.63 mmol, 1.00 eq.) and copper powder (798 mg, 12.6 mmol, 7.72 eq.) were heated to 200 °C and the formed melt was stirred overnight. After cooling to room temperature, the resulting solid was purified *via* column chromatography (SiO_2, Cy:DCM 1:1). It was not possible to isolate the desired product.

Chemical formula: $C_{44}H_{72}N_2O_6$

Molecular weight: 725.07 g/mol

Compound **80** (PK-118)

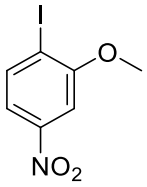

This synthesis applies a procedure published by He et al.[133]

2-Methoxy-4-nitroanilin (5.034 g, 29.94 mmol, 1.000 eq.) and *p*-TsOH·H_2O (16.95 g, 89.08 mmol, 2.975 eq.) were suspended in acetonitrile (120 mL) and the mixture was cooled to 0 °C in an ice bath. A mixture of sodium nitrite (4.107 g, 59.52 mmol, 1.988 eq.) and potassium iodide (13.38 g, 80.59 mmol, 2.692 eq.) dissolved in water (20 mL) was slowly added dropwise while constantly keeping the temperature below 4 °C. After stirring for 30 min, the mixture was allowed to warm to room temperature and was stirred overnight. The reaction was quenched through addition of aq. $NaHSO_3$ (40 %) and aq. $NaHCO_3$ (10 %), which caused the precipitation of a yellow solid. The solid was collected and recrystallized from ethanol yielding the desired product as a yellow solid (6.788 g, 24.33 mmol) in 81 %.

Chemical formula: $C_7H_6INO_3$

Molecular weight: 279.03 g/mol

^{1}H-NMR (500 MHz, CD_2Cl_2, 298 K), δ [ppm]

8.00 - 7.98 (d, J = 8.5 Hz, 1 H), 7.63 (m, 1 H), 7.29 (s, 1 H), 4.02 (s, 3 H).

^{13}C-NMR (126 MHz, CD_2Cl_2, 298 K), δ [ppm]

158.8, 149.3, 139.8, 117.0, 105.2, 95.0, 56.9.

MS (EI, 70 eV), *m/z* (%)

278.9 (100) $[M]^{\bullet+}$, 217.9 (14) $[M\text{-}CH_3\text{-}NO_2]^+$; calculated: 278.9 Da.

Compound **81** (PK-119)

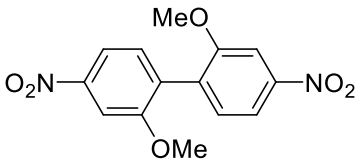

This synthesis applies a procedure published by He et al.[133]

80 (5.005 g, 17.94 mmol, 1.000 eq.) and copper powder (5.014 g, 78.91 mmol, 4.399 eq.) were suspended in DMF (25 mL) and the mixture was heated to 140 °C overnight. The solvent was removed under reduced pressure and the residue was extracted with $CHCl_3$ under reflux for 3.5 h. The suspension was filtrated and the filtrate was concentrated under reduced pressure until the precipitation of the crude product began. The flask was stored in a fridge overnight to promote precipitation. The precipitate was collected yielding the desired product as a crimson solid (1.189 g, 3.909 mmol) in 44 %.

Chemical formula: $C_{14}H_{12}N_2O_6$

Molecular weight: 304.26 g/mol

^{1}H-NMR (500 MHz, CD_2Cl_2, 298 K), δ [ppm]

7.94 – 7.91 (dd, J = 8.4 Hz, J = 2.1 Hz, 2 H), 7.84 (d, J = 2.2 Hz, 7.40 – 7.35 (d, J = 8.4 Hz, 2 H), 3.29 (s, 6 H).

^{13}C-NMR (126 MHz, CD_2Cl_2, 298 K), δ [ppm]

157.3, 148.9, 132.5, 131.5, 115.7, 106.1, 56.2.

MS (EI, 70 eV), *m*/*z* (%)

304.1 (100) $[M]^{\bullet+}$; calculated: 304.1 Da.

Compound **82** (PK-120)

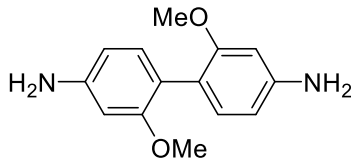

This synthesis applies a procedure published by He et al.[133]

81 (2.268 g, 7.455 mmol, 1.000 eq.) was suspended in a mixture of ethanol (20 mL) and concentrated HCl (40 mL). Tin powder (5.082 g, 42.81 mmol, 5.742 eq.) was added in one portion and the mixture was heated to 90 °C under the initial formation of fume overnight. After cooling to room temperature, the reaction was quenched with an aq. NaOH (10 %) and the precipitate was collected. The resulting solid was collected *via Soxhlet* extraction for 72 h using $CHCl_3$. The filtrate was cooled and the resulting precipitate was separated and washed with ice-cold $CHCl_3$ yielding the desired product as a colorless solid (1.435 g, 5.875 mmol) in 79 %.

Chemical formula: $C_{14}H_{16}N_2O_2$

Molecular weight: 244.29 g/mol

^{1}H-NMR (500 MHz, CD_2Cl_2, 298 K), δ [ppm]

7.02 - 6.99 (dd, J = 8.3 Hz, J = 2.1 Hz, 2 H), 6.34 - 6.30 (m, 4 H), 3.72 (s, 6 H), 3.66 (s, 4 H).

^{13}C-NMR (126 MHz, CD_2Cl_2, 298 K), δ [ppm]

158.2, 146.8, 132.5, 118.4, 107.2, 99.2, 55.7.

MS (EI, 70 eV), *m/z* (%)

244.1 (100) $[M]^{\bullet+}$, 229.1 (17) $[M\text{-}CH_3]^+$, 214.1 (30) $[M\text{-}2\ CH_3]^+$, 198.1 (35) $[C_{12}H_{10}N_2O]^+$; calculated: 244.12 Da.

Compound **83** (PK-121)

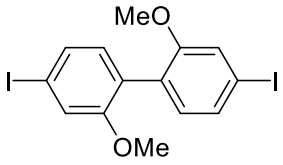

This synthesis applies a procedure published by He et al.[133]

82 (1.435 g, 5.875 mmol, 1.000 eq.) was suspended in a mixture of concentrated HCl (11.0 mL, 145 mmol, 24.7 eq.) and water (30 mL) and the suspension was cooled in an ice bath. A solution of sodium nitrite (1.312 g, 19.01 mmol, 3.235 eq.) in water (10 mL) was slowly added dropwise constantly keeping the temperature below 4 °C. After stirring for 20 min, an aqueous solution of potassium iodide (6.008 g, 36.19 mmol, 6.160 eq.) was slowly added dropwise keeping the temperature below 4 °C. The mixture was stirred overnight and was allowed to warm to room temperature. The formed solid was collected, suspended in DCM and washed with aq. HCl (1M) and aq. $NaHSO_3$ (40 %). After removal of the solvent under reduced pressure, the crude product was purified *via* column chromatography (SiO_2, Cy:DCM 3:1, R_f = 0.5) yielding the desired product as a colorless solid (1.314 g, 2.819 mmol) in 48 %.

Chemical formula: $C_{14}H_{12}I_2O_2$

Molecular weight: 466.06 g/mol

^{1}H-NMR (500 MHz, CD_2Cl_2, 298 K), δ [ppm]

7.35 - 7.31 (dd, J = 7.9 Hz, J = 1.9 Hz, 2 H), 7.29 - 7.26 (d, J = 1.6 Hz, 2 H), 6.91 - 6.88 (d, J = 7.9 Hz, 2 H), 3.72 (s, 6 H).

^{13}C-NMR (126 MHz, CD_2Cl_2, 298 K), δ [ppm]

157.5, 132.7, 129.8, 126.7, 120.6, 93.7, 56.1.

MS (EI, 70 eV), *m/z* (%)

465.9 (100) $[M]^{\bullet+}$; calculated: 465.9 Da.

Compound **84** (PK-122)

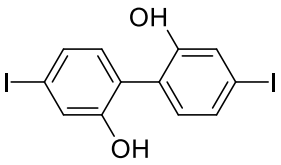

This synthesis applies a procedure published by He et al.[133]

83 (1.709 g, 3.666 mmol, 1.000 eq.) was dissolved in dry DCM (20 mL) and the solution was cooled to -78 °C. After slowly adding a solution of boron tribromide (15.0 mL, 15.0 mmol, 4.09 eq., 1M in DCM), the mixture was allowed to warm to room temperature overnight. The reaction was terminated through the addition of water and the organic solvent was removed under reduced pressure. The formed precipitate was collected by filtration and dried overnight yielding the desired product as a colorless solid (1.479 g, 0.921 mmol) in 92 %.

Chemical formula: $C_{12}H_8I_2O_2$

Molecular weight: 438.00 g/mol

^{1}H-NMR (500 MHz, CD_2Cl_2, 298 K), δ [ppm]

7.40 - 7.37 (m, 4 H), 6.99 - 6.96 (m, 2 H).

^{13}C-NMR (126 MHz, CD_2Cl_2, 298 K), δ [ppm]

154.1, 133.2, 131.3, 126.4, 124.6, 94.6.

MS (EI, 70 eV), *m/z* (%)

437.8 (100) $[M]^{\bullet+}$; calculated: 437.9 Da.

Compound **85** (PK-123)

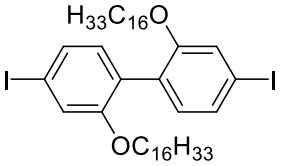

This synthesis applies a procedure published by He et al.[133]

84 (1.479 g, 3.378 mmol, 1.000 eq.), K_2CO_3 (2.807 g, 20.31 mmol, 6.013 eq.), substoichiometric amounts potassium iodide and 1-bromohexadecane (4.10 mL, 13.4 mmol, 3.97 eq.) were suspended in acetone and the mixture was heated to 60 °C for 46 h. After cooling to room temperature, the solvent was removed under reduced pressure, the residue was diluted with DCM and aq. HCl (2M) and the phases were separated. The aqueous phase was extracted three times with DCM, the combined organic layers were washed with brine and dried over magnesium sulfate. After removal of the solvent under reduced pressure, the crude product was purified *via* column chromatography (SiO_2, Cy:DCM 5:1, R_f = 0.9) yielding the desired product as a colorless solid (2.866 g, 3.231 mmol) in 96 %.

Chemical formula: $C_{44}H_{72}I_2O_2$

Molecular weight: 886.87 g/mol

^{1}H-NMR (500 MHz, CD_2Cl_2, 298 K), δ [ppm]

7.31 - 7.28 (dd, *J* = 8.0 Hz, *J* = 1.6 Hz, 2 H), 7.25 (d, *J* = 1.6 Hz, 2 H), 6.92 - 6.90 (d, *J* = 8.0 Hz, 2 H), 3.89 - 3.86 (t, *J* = 6.6 Hz, 4 H), 1.32-1.22 (m, 56 H), 0.90 - 0.87 (t, *J* = 6.8 Hz, 6 H).

^{13}C-NMR (126 MHz, CD_2Cl_2, 298 K), δ [ppm]

157.6, 133.2, 129.7, 127.5, 121.8, 93.6, 69.3, 32.5, 30.3, 30.3, 30.2, 30.2, 30.0, 29.8, 29.6, 27.5, 26.5, 23.3, 14.5.

MS (EI, 70 eV), *m/z* (%)

886.3 (100) $[M]^{\bullet+}$, 662.1 (14) $[M\text{-}C_{16}H_{33}]^+$, 437.8 (32) $[C_{22}H_{31}IO]^{\cdot+}$; calculated: 886.4 Da.

Compound **86a**/**86b** (PK-124)

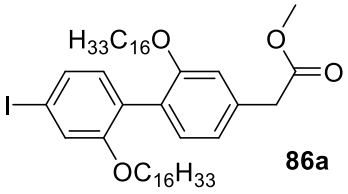

86a

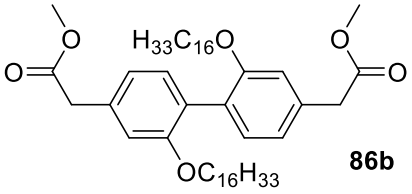

86b

This synthesis applies a procedure published by Hartwig et al.[122]

In a flamed *Schlenk* flask, zinc powder (500 mg, 7.65 mmol, 22.1 eq.), **85** (307 mg, 0.346 mmol, 1.00 eq.) and methyl-2-bromoacetate (40.0 μL, 0.423 mmol, 1.22 eq.) were suspended in THF (15 mL) and the mixture was heated to 40 °C for 30 min. *XPhos* (20.7 mg, 43.4 μmol, 0.126 eq.) and $Pd_2(dba)_2$ (15.4 mg, 16.8 μmol, 0.0486 eq.) were added and the mixture was heated to 50 °C for 46 h. After cooling to room temperature, the solvent was removed under reduced pressure, the residue was diluted with DCM and aq. HCl (2M) and the phases were separated. The aqueous phase was extracted with DCM three times, the combined organic layers were washed with brine and dried over magnesium sulfate. After removal of the solvent under reduced pressure, the residue was purified *via* column chromatography (SiO_2, Cy:DCM 2:1) yielding **86a** (26.9 mg, 32.3 μmol, R_f = 0.6) in 9 %, **86b** (81.3 mg, 104 μmol, R_f = 0.1) in 30 % and recovering the substrate (146 mg, 164 μmol, R_f = 0.9) in 48 %.

86a

Chemical formula: $C_{47}H_{77}IO_4$

Molecular weight: 833.03 g/mol

^{1}H-NMR (500 MHz, CD_2Cl_2, 298 K), δ [ppm]

7.32 - 7.29 (dd, *J* = 7.9 Hz, *J* = 1.6 Hz, 1 H), 7.26 (d, *J* = 1.6 Hz, 1 H), 7.15 - 7.13 (m, 1 H), 6.96 - 6.93 (d, *J* = 7.9 Hz, 1 H), 6.87 - 6.85 (m, 2 H), 3.93 - 3.87 (m, 4 H), 3.70 (s, 3 H), 3.64 (s, 2 H), 1.66 - 1.60 (m, 4 H), 1.28 (bs, 52 H), 0.91 - 0.87 (t, *J* = 6.9 Hz, 6 H).

^{13}C-NMR (126 MHz, CD_2Cl_2, 298 K), δ [ppm]

171.8, 157.2, 156.5, 134.9, 133.0, 131.2, 129.1, 127.6, 125.8, 121.1, 120.8, 119.8, 113.0, 92.6, 68.7, 68.4, 51.9, 41.1, 31.9, 29.7, 29.7, 29.6, 29.6, 29.6, 29.4, 29.4, 29.3, 29.2, 29.0, 26.0, 25.9, 22.7, 13.9.

86b

Chemical formula: $C_{50}H_{82}O_6$

Molecular weight: 779.20 g/mol

^{1}H-NMR (500 MHz, CD_2Cl_2, 298 K), δ [ppm]

7.20 - 7.17 (d, *J* = 8.1 Hz, 2 H), 6.89 - 6.86 (m, 4 H), 3.95 - 3.92 (t, *J* = 6.7 Hz, 4 H), 3.72 (s, 6 H), 3.66 (s, 4 H), 1.69 - 1.62 (p, *J* = 6.9 Hz, 4 H), 1.28 (bs, 52 H), 0.92 - 0.88 (t, *J* = 6.7 Hz, 6 H).

^{13}C-NMR (126 MHz, CD_2Cl_2, 298 K), δ [ppm]

172.3, 157.0, 134.9, 132.0, 127.0, 121.2, 113.4, 68.8, 52.3, 41.6, 32.4, 30.2, 30.2, 30.1, 30.1, 30.1, 29.8, 29.7, 26.4, 23.2, 14.3.

Compound **87a**/**87b** (PK-126)

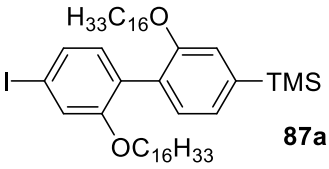

87a

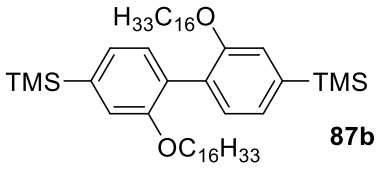

87b

This synthesis applies a procedure published by Suranna et al.[158]

85 (505 mg, 0.606 mmol, 1.00 eq.) was dissolved in dry THF (15 mL) in a flamed *Schlenk* tube and the resulting solution was cooled to -78 °C. A solution of *n*BuLi (0.25 mL, 0.63 mmol, 1.1 eq., 2.5M in hexane) was slowly added dropwise and the cooled mixture was stirred for 45 min. Afterwards, TMSCl (0.20 mL, 1.6 mmol, 2.8 eq.) was added and the mixture was allowed to warm to room temperature overnight. The solvent was removed under reduced pressure, the residue was diluted with DCM and water and the phases were separated. The aqueous phase was extracted four times with DCM, the combined organic layers were washed with brine and dried over magnesium sulfate. After removal of the solvent under reduced pressure, the residue was purified *via* column chromatography (SiO_2, Cy:DCM 2:1). It was only possible to isolate a mixture (505 mg) of **87a** and **87b** making it impossible to give individual yields.

87a

Chemical formula: $C_{47}H_{81}IO_2Si$

Molecular weight: 833.15 g/mol

87b

Chemical formula: $C_{50}H_{90}O_2Si_2$

Molecular weight: 779.44 g/mol

Compound **88** (PK-127)

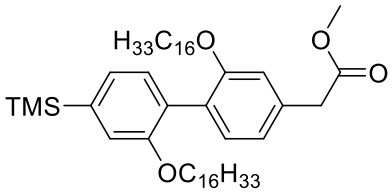

This synthesis applies a procedure published by Suranna et al.[158]

In a flamed *Schlenk* flask, zinc powder (503 mg, 7.70 mmol) and methyl-2-bromoacetate (90 µL, 7.8 mmol) were suspended in THF (30 mL) and the mixture was heated to 40 °C for 30 min. After adding mixture of **87a** and **87b** (505 mg), *XPhos* (29.8 mg, 62.5 µmol) and $Pd_2(dba)_2$ (30.1 mg, 32.9 µmol) were added and the suspension was heated to 50 °C for 70 h. After cooling to room temperature, the solvent was removed under reduced pressure, the residue was diluted with DCM and aq. HCl (1M) and the phases were separated. The aqueous phase was extracted three times with DCM, the combined organic layers were washed with brine and dried over magnesium sulfate. After removal of the solvent under reduced pressure, the residue was purified *via* column chromatography (SiO_2, Cy:DCM 1:1) yielding **87b** (167 mg, 0.214 mmol) in 38 % and **86b** (190 mg, 0.220 mmol) in 39 %. The desired product was not isolated.

Chemical formula: $C_{50}H_{86}O_4Si$

Molecular weight: 779.32 g/mol

Compound **89** (PK-130)

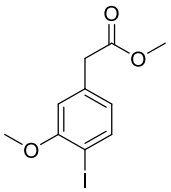

This synthesis applies a procedure published by Idelson et al.[96]

Methyl 3-methoxyphenylacetate (2.0 mL, 12 mmol, 1.0 eq.) was dissolved in DCM (20 mL) and purged with argon for 30 min. A solution of iodine monochloride (12.5 mL, 12.5 mmol, 1.01 eq., 1M in DCM) was added and the mixture was stirred overnight under the exclusion of light. The reaction was terminated through the addition of aq. $NaHSO_3$ (40 %) and the phases were separated. The aqueous phase was extracted with DCM four times, the combined organic layers were washed with brine and dried over magnesium sulfate. After removal of the solvent under reduced pressure, the residue was

purified *via* column chromatography (SiO_2, Cy:DCM 1:2, R_f = 0.5) yielding the desired product as a colorless oil (3.261 g, 10.65 mmol) in 86 %.

Chemical formula: $C_{10}H_{11}IO_3$

Molecular weight: 306.10 g/mol

^{1}H-NMR (500 MHz, CD_2Cl_2, 298 K), δ [ppm]

7.72 - 7.70 (d, J = 8.7 Hz, 1 H), 6.87 (d, J = 3.1 Hz, 1 H), 6.62 - 6.59 (dd, J = 8.7 Hz, J = 3.1 Hz, 1 H), 3.78 (s, 3 H), 3.75 (s, 2 H), 3.70 (s, 3 H).

^{13}C-NMR (126 MHz, CD_2Cl_2, 298 K), δ [ppm]

171.1, 160.5, 140.2, 139.3, 117.3, 115.2, 89.6, 55.8, 52.4, 46.4.

MS (APCI), *m*/*z* (%)

307.0 (46) $[M+H]^+$, 247.0 (14) $[M\text{-}CO_2Me]^+$, 180.0 (100) $[M\text{-}I]^+$; calculated: 306.0 Da.

Compound **90** (PK-131)

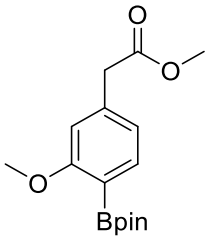

This synthesis applies a procedure published by Takase et al.[117]

89 (493 mg, 1.61 mmol, 1.00 eq.) was dissolved in DMF (15 mL). Potassium acetate (703 mg, 7.17 mmol, 4.45 eq.) and bis(pinacolato)diboron (413 mg, 1.63 mmol, 1.01 eq.) were added and the mixture was purged with argon for 30 min. $PdCl_2$(dppf) (58.5 mg, 80.1 μmol, 0.0496 eq.) was added and the mixture was heated to 105 °C for 17 h. The solvent was removed under reduced pressure, the residue was suspended in DCM and poured two times through the same plug of magnesium sulfate to remove remaining transition metal species and salts. The filtrate was washed with aq. HCl (1M), brine and dried over magnesium sulfate. After removal of the solvent under reduced pressure, the residue was purified *via* column chromatography (SiO_2, DCM:EA 20:1, R_f = 0.17 in Cy:DCM 1:12) yielding the desired product as an amber-colored oil (280 mg, 0.916 mmol) in 57 %.

Chemical formula: $C_{16}H_{23}BO_5$

Molecular weight: 306.17 g/mol

^{1}H-NMR (500 MHz, CD_2Cl_2, 298 K), δ [ppm]

7.74 - 7.72 (d, J = 8.3 Hz, 1 H), 6.81 - 6.79 (dd, J = 8.3 Hz, J = 2.5 Hz, 1 H), 6.72 (d, J = 2.5 Hz, 1 H), 3.91 (s, 2 H), 3.80 (s, 3 H), 3.65 (s, 3 H), 1.29 (s, 12 H).

^{13}C-NMR (126 MHz, CD_2Cl_2, 298 K), δ [ppm]

172.5, 161.8, 142.7, 137.7, 116.2, 111.3, 83.3, 55.0, 51.5, 40.8, 24.5.

MS (APCI), *m/z* (%)

307.2 (100) $[M+H]^+$; calculated: 306.2 Da.

Compound **91** (PK-129, PK-135)

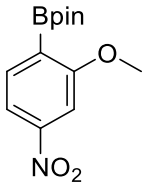

This synthesis applies a procedure published by Takase et al.[117]

A flamed *Schlenk* tube was equipped with 2-iodo-5-nitroanisole (502 mg, 1.80 mmol, 1.00 eq.), potassium acetate (703 mg, 7.17 mmol, 4.45 eq.), bis(pinacolato)diboron (413 mg, 1.63 mmol, 1.01 eq.) and $PdCl_2$(dppf) (51.4 mg, 73.2 μmol, 0.0407 eq.). The compounds were suspended in dry DMF (40 mL) and the mixture was heated to 105 °C overnight. After cooling to room temperature, the solvent was removed under reduced pressure. The residue was suspended in DCM and aq. HCl (1M) and the phases were separated. The aqueous phase was extracted five times with DCM, the combined organic layers were washed with brine and dried over magnesium sulfate. After removal of the solvent under reduced pressure, the residue was purified *via* column chromatography (SiO_2, Cy:DCM 5:1, R_f = 0.1) yielding the desired product (155 mg, 0.555 mmol) as a colorless solid in 31 %.

Chemical formula: $C_{13}H_{18}BNO_5$

Molecular weight: 279.10 g/mol

^{1}H-NMR (500 MHz, CD_2Cl_2, 298 K), δ [ppm]

7.78 - 7.74 (m, 2 H), 7.68 - 7.66 (d, *J* = 1.9 Hz, 1 H), 3.91 (s, 3 H), 1.35 (s, 12 H).

^{13}C-NMR (126 MHz, CD_2Cl_2, 298 K), δ [ppm]

164.5, 150.9, 137.5, 137.0, 114.8, 104.9, 84.1, 56.0, 24.6.

MS (EI, 70 eV), *m/z* (%)

279.3 (24) $[M]^{\bullet+}$; calculated: 279.13 Da.

Compound **92a** (PK-132, PK-133)

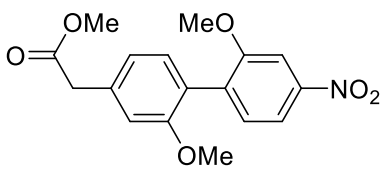

91 (1.602 g, 5.739 mmol, 1.000 eq.), **89** (1.873 g, 6.118 mmol, 1.066 eq.) and K_2CO_3 (4.997 g, 36.15 mmol, 6.230 eq.) were placed in a *Schlenk* flask and it was evacuated and flooded with argon

three times. The compounds were then suspended in dry THF (50 mL) and the mixture was purged with argon for 30 min. After adding $PdCl_2(PPh_3)_2$ (201 mg, 0.287 mmol, 0.0499 eq.), the mixture was heated to 70 °C for five days. After cooling to room temperature, the solvent was removed under reduced pressure, the residue was suspended in DCM and aq. HCl (2M) and the phases were separated. The aqueous phase was extracted five times with DCM, the combined organic layers were washed with brine and dried over magnesium sulfate. After removal of the solvent under reduced pressure, the residue was purified *via* column chromatography (SiO_2, DCM, R_f = 0.5) yielding the desired product as a yellow solid (1.441 g, 4.173 mmol) in 73 %.

Chemical formula: $C_{17}H_{17}NO_6$

Molecular weight: 331.32 g/mol

^{1}H-NMR (500 MHz, CD_2Cl_2, 298 K), δ [ppm]

7.89 - 7.86 (dd, *J* = 8.3 Hz, *J* = 2.2 Hz, 1 H), 7.79 (d, *J* = 2.2 Hz, 1 H), 7.32 - 7.29 (d, *J* = 8.2 Hz, 1 H), 7.13 - 7.10 (dd, *J* = 8.2 Hz, *J* = 0.6 Hz, 1 H), 6.93 - 6.89 (m, 2 H), 3.84 (s, 3 H), 3.82 (s, 3 H), 3.56 (s, 3 H), 3.41 (s, 2 H).

^{13}C-NMR (126 MHz, CD_2Cl_2, 298 K), δ [ppm]

171.8, 160.0, 157.6, 148.8, 137.0, 134.7, 132.4, 131.5, 129.6, 116.4, 116.1, 113.0, 106.0, 56.3, 55.7, 52.1, 39.2.

MS (EI, 70 eV), *m/z* (%)

331.1 (100) $[M]^{\bullet+}$, 299.1 (26) $[M\text{-}CH_3OH]^+$, 284.1 (10) $[M\text{-}CH_3OH\text{-}CH_3]^+$, 272.1 (12) $[M\text{-}CO_2CH_3]^+$, 240.1 (13) $[M\text{-}CO_2CH_3\text{-}CH_3OH]^+$, 210.1 (13) $[M\text{-}CO_2CH_3\text{-}2\ CH_3O]^+$; calculated: 331.11 Da.

Compound **93a** (PK-134)

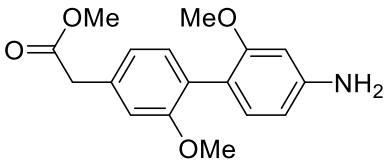

This synthesis applies a procedure published by He et al.[133]

92a (272 mg, 0.819 mmol, 1.00 eq.) and anhydrous tin(II) chloride (611 mg, 3.22 mmol, 3.93 eq.) were suspended in ethanol (15 mL) and the resulting suspension was heated to 90 °C overnight. After cooling to room temperature, the solvent was removed under reduced pressure, the residue was suspended in DCM and aq. NaOH (10 %) and the phases were separated. The aqueous phase was extracted four times with DCM, the combined organic layers were washed with brine and dried over magnesium sulfate. Removing the solvent under reduced pressure yielded the desired product (191 mg, 0.632 mmol) in 77 % as a colorless solid without further purification.

Chemical formula: $C_{17}H_{19}NO_4$

Molecular weight: 301.34 g/mol

^{1}H-NMR (500 MHz, CD_2Cl_2, 298 K), δ [ppm]

7.08 - 7.06 (d, J = 8.4 Hz, 1 H), 6.87 - 6.82 (m, 3 H), 6.32 - 6.27 (m, 2 H), 3.82 (s, 3 H), 3.65 (s, 3 H), 3.57 (s, 3 H), 3.43 (s, 2 H).

^{13}C-NMR (126 MHz, CD_2Cl_2, 298 K), δ [ppm]

172.4, 159.0, 157.9, 148.2, 135.3, 132.5, 132.1, 132.1, 119.6, 115.9, 112.6, 107.1, 98.3, 55.6, 55.4, 52.0, 39.3.

Compound **94a** (PK-136)

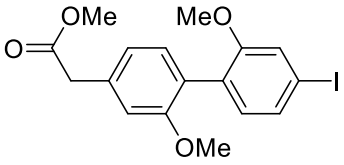

This synthesis applies a procedure published by He et al.[133]

93a (1.707 g, 5.663 mmol, 1.000 eq.) and *p*-TsOH·H_2O (3.022 g, 15.89 mmol, 2.805 eq.) were suspended in acetonitrile (50 mL). A solution of sodium nitrite (802 mg, 11.6 mmol, 2.05 eq.) in water (7 mL) was slowly added dropwise constantly keeping the temperature below 4 °C. After stirring for 10 min, an aq. solution of potassium iodide (2.803 g, 16.88 mmol, 2.981 eq.) was added dropwise keeping the temperature below 3 °C. The mixture was stirred overnight and was allowed to warm to room temperature. The reaction was terminated through the addition of aq. $NaHSO_3$ (40 %), the phases were separated, and the organic solvent was removed under reduced pressure. The residue was diluted with DCM and the phases were separated. The aqueous phase was extracted four times with DCM, the combined organic layers were washed with brine and dried over magnesium sulfate. After removal of the solvent under reduced pressure, the residue was purified *via* column chromatography (SiO_2, DCM, R_f = 0.6) yielding the desired product as a colorless solid (1.876 g, 4.551 mmol) in 80 %.

Chemical formula: $C_{17}H_{17}IO_4$

Molecular weight: 412.22 g/mol

^{1}H-NMR (500 MHz, CD_2Cl_2, 298 K), δ [ppm]

7.36 - 7.33 (dt, J = 7.8 Hz, J = 1.8 Hz, 1 H), 7.26 (d, J = 1.5 Hz, 1 H), 7.08 - 7.06 (d, J = 8.3 Hz, 1 H), 6.89 - 6.83 (m, 3 H), 3.82 (s, 3 H), 3.69 (s, 3 H), 3.56 (s, 2 H), 3.40 (s, 3 H).

^{13}C-NMR (126 MHz, CD_2Cl_2, 298 K), δ [ppm]

172.1, 159.5, 157.6, 135.0, 134.8, 133.5, 133.4, 131.6, 130.1, 120.4, 116.1, 112.8, 93.5, 56.0, 55.7, 52.0, 39.2.

MS (EI, 70 eV), *m/z* (%)

412.3 (100) $[M]^{\bullet+}$, 254.3 (6) $[M\text{-}I\text{-}OCH_3]^+$, 226.3 (30) $[M\text{-}I\text{-}CO_2Me]^+$, 211.3 (36) $[M\text{-}CO_2Me\text{-}I\text{-}Me]^+$; calculated: 412.02 Da.

Compound **92b** (PK-132V7)

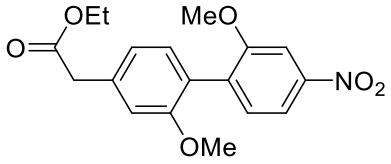

91 (502 mg, 1.80 mmol, 1.00 eq.), **89** (661 mg, 2.16 mmol, 1.20 eq.), PPh_3 (53.7 mg, 0.205 mmol, 0.114 eq.) and K_2CO_3 (1.502 g, 10.87 mmol, 6.048 eq.) were placed in a *Schlenk* flask and it was evacuated and flooded with argon three times. The compounds were then suspended in a mixture of toluene (16 mL) and ethanol (8 mL) and purged with argon for 30 min. After adding $PdCl_2(PPh_3)_2$ (60.0 mg, 85.5 μmol, 0.0478 eq.) the mixture was heated to 80 °C for two days. After cooling to room temperature, the solvent was removed under reduced pressure, the residue was suspended in DCM and aq. HCl (2M) and the phases were separated. The aqueous phase was extracted three times with DCM, the combined organic layers were washed with brine and dried over magnesium sulfate. After removal of the solvent under reduced pressure, the residue was purified *via* column chromatography (SiO_2, DCM, R_f = 0.5) yielding the desired product as a yellow solid (334 mg, 0.968 mmol) in 54 %.

Chemical formula: $C_{18}H_{19}NO_6$

Molecular weight: 345.35 g/mol

^{1}H-NMR (500 MHz, CD_2Cl_2, 298 K), δ [ppm]

7.89 - 7.86 (dd, *J* = 8.3 Hz, *J* = 2.2 Hz, 1 H), 7.79 (d, *J* = 2.2 Hz, 1 H), 7.32 - 7.30 (d, *J* = 8.2 Hz, 1 H), 7.13 - 7.09 (dd, *J* = 8.2 Hz, *J* = 0.6 Hz, 1 H), 6.93 - 6.88 (m, 2 H), 4.03 - 3.97 (q, *J* = 7.2 Hz, 2 H), 3.85 (s, 3 H), 3.83 (s, 3 H), 3.39 (s, 2 H), 1.17 - 1.12 (t, *J* = 7.1 Hz, 3 H).

^{13}C-NMR (126 MHz, CD_2Cl_2, 298 K), δ [ppm]

171.0, 159.6, 157.2, 148.4, 136.6, 134.5, 132.1, 131.0, 129.2, 115.9, 115.6, 112.5, 105.6, 60.7, 55.9, 55.3, 39.0, 13.9.

MS (EI, 70 eV), *m/z* (%)

345.1 (100) $[M]^{\bullet+}$, 299.1 (26) $[M\text{-}C_2H_5OH]^+$, 284.1 (10) $[M\text{-}C_2H_5OH\text{-}CH_3]^+$, 272.1 (12) $[M\text{-}CO_2C_2H_5]^+$, 240.1 (13) $[M\text{-}CO_2C_2H_5\text{-}CH_3OH]^+$, 210.1 (13) $[M\text{-}CO_2C_2H_5\text{-}2\ CH_3O]^+$; calculated: 345.12 Da.

Compound **93b** (PK-142)

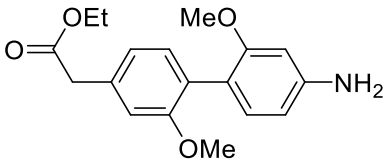

This synthesis applies a procedure published by He et al.[133]

92b (334 mg, 0.968 mmol, 1.00 eq.) and anhydrous tin(II) chloride (776 mg, 4.09 mmol, 4.23 eq.) were suspended in ethanol (15 mL) and the resulting suspension was heated to 90 °C overnight. After cooling to room temperature, the solvent was removed under reduced pressure, the residue was suspended in DCM and aq. NaOH (10 %) and the phases were separated. The aqueous phase was extracted four times with DCM, the combined organic layers were washed with brine and dried over magnesium sulfate. Removing the solvent under reduced pressure yielded the desired product as a pale-yellow solid (326 mg). Due to impurities in the NMR spectra, it was not possible to give a reliable yield. The synthesis was continued with the crude product.

Chemical formula: $C_{18}H_{21}NO_4$

Molecular weight: 315.37 g/mol

MS (ESI+), *m/z* (%)

338.1 (100) $[M+Na]^+$; calculated: 315.2 Da.

Compound **94b** (PK-143)

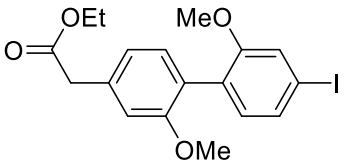

This synthesis applies a procedure published by He et al.[133]

The crude product of **93b** (326 mg) and *p*-TsOH·H_2O (490 mg, 2.57 mmol) were suspended in acetonitrile (20 mL). A solution of sodium nitrite (305 mg, 4.42 mmol) in water (5 mL) was added dropwise constantly keeping the temperature below 3 °C. After stirring for 10 min, an aq. solution of potassium iodide (985 mg, 5.93 mmol) was also slowly added dropwise keeping the temperature below 3 °C. The mixture was stirred overnight and was allowed to warm to room temperature. The reaction was terminated through the addition of aq. $NaHSO_3$ (40 %), the phases were separated, and the organic solvent was removed under reduced pressure. The residue was diluted with DCM and the phases were separated. The aqueous phase was extracted four times with DCM, the combined organic layers were washed with brine and dried over magnesium sulfate. After removal of the solvent under reduced pressure, the residue was purified *via* column chromatography (SiO_2, DCM, R_f = 0.6) yielding the desired product as a pale-yellow solid (192 mg, 0.141 mmol) in 46 % over two steps.

Chemical formula: $C_{18}H_{19}IO_4$

Molecular weight: 426.25 g/mol

^{1}H-NMR (500 MHz, CD_2Cl_2, 298 K), δ [ppm]

7.37 - 7.33 (dd, *J* = 7.9 Hz, *J* = 1.6 Hz, 1 H), 7.26 (d, *J* = 1.6 Hz, 1 H), 7.09 - 7.05 (dd, *J* = 8.3 Hz, *J* = 0.6 Hz, 1 H), 6.89 - 6.83 (m, 3 H), 4.05 - 3.97 (q, *J* = 7.1 Hz, 2 H), 3.83 (s, 3 H), 3.70 (s, 3 H), 3.39 (s, 2 H), 1.19 - 1.14 (t, *J* = 7.1 Hz, 3 H).

^{13}C-NMR (126 MHz, CD_2Cl_2, 298 K), δ [ppm]

171.3, 159.1, 157.2, 134.6, 133.1, 131.2, 130.2, 129.7, 129.3, 120.0, 115.7, 112.4, 93.1, 60.6, 55.6, 55.2, 39.0, 14.0.

MS (EI, 70 eV), *m/z* (%)

426.1 (39) $[M]^{\bullet+}$, 380.0 (7) $[M\text{-}C_2H_6O]^+$, 300.1 (6) $[M\text{-}I\text{+}H]^+$, 211.1 (19) $[M\text{-}I\text{-}CO_2Et\text{-}CH_3]^+$, 194.1 (43) $[M\text{-}I\text{-}CO_2Et\text{-}CH_4O]^+$; calculated: 426.0 Da.

Compound **95** (PK-137, PK-144)

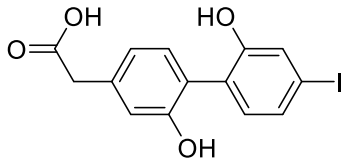

This synthesis applies a procedure published by He et al.[133]

94a (142 mg, 0.343 mmol, 1.00 eq.) was dissolved in dry DCM (15 mL) and the solution was purged with argon for 20 min. Afterwards, it was cooled to -78 °C and a solution of BBr_3 (1.40 mL, 1.40 mmol, 4.08 eq., 1M in DCM) was added dropwise. The mixture was stirred for 20 min and allowed to warm up to room temperature overnight. After dilution with water, the phases were separated and the aqueous phase was extracted five times with DCM. The organic layers were combined and the solvent was removed under reduced pressure yielding the desired product as a colorless solid (111 mg, 0.301 mmol) in 88 % without any further purification.

Chemical formula: $C_{14}H_{11}IO_4$

Molecular weight: 370.14 g/mol

^{1}H-NMR (500 MHz, CD_2Cl_2, 298 K), δ [ppm]

7.68 - 7.64 (m, 2 H), 7.52 - 7.49 (d, *J* = 8.4 Hz, 1 H), 7.32 - 7.29 (d, *J* = 8.1 Hz, 1 H), 6.98 - 6.95 (dd, *J* = 8.5 Hz, *J* = 2.6 Hz, 1 H), 6.88 - 6.86 (d, *J* = 2.6 Hz, 1 H), 3.66 - 3.48 (m, 2 H).

^{13}C-NMR (126 MHz, CD_2Cl_2, 298 K), δ [ppm]

168.5, 157.5, 150.0, 135.1, 133.1, 131.5, 130.4, 129.8, 127.4, 116.3, 115.5, 92.8, 40.4.

MS (EI, 70 eV), *m/z* (%)

370.1 (100) $[M]^{\bullet+}$; calculated: 370.0 Da.

Compound **96a**/**96b** (PK-138, PK-144)

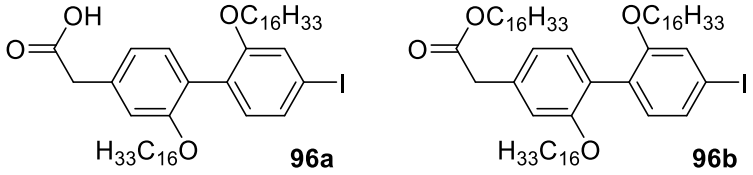

This synthesis applies a procedure published by He et al.[133]

95 (101 mg, 0.263 mmol, 1.00 eq.), K_2CO_3 (202 mg, 1.46 mmol, 5.55 eq.), substoichiometric amounts of potassium iodide and 1-bromohexadecane (0.4 mL, 1.3 mmol, 5.0 eq.) were suspended in acetone (20 mL) and the mixture was heated to 60 °C for 20 h. After cooling to room temperature, the solvent was removed under reduced pressure, the residue was diluted with DCM and aq. HCl (2M) and the phases were separated. The aqueous phase was extracted with DCM four times, the combined organic layers were washed with brine and dried over magnesium sulfate. After removal of the solvent under reduced pressure, the crude product was purified *via* column chromatography (SiO_2, Cy:DCM 1:1) yielding **96a** (16.3 mg, 19.6 μmol, R_f = 0.5) in 8 % and **96b** (77.9 mg, 74.7 μmol, R_f = 0.7) in 28 % both as colorless resins.

96a

Chemical formula: $C_{46}H_{75}IO_4$

Molecular weight: 819.01 g/mol

^{1}H-NMR (500 MHz, CD_2Cl_2, 298 K), δ [ppm]

7.33 - 7.30 (dd, *J* = 7.9 Hz, *J* = 1.6 Hz, 1 H), 7.26 (d, *J* = 1.6 Hz, 1 H), 7.06 - 7.03 (d, *J* = 8.3 Hz, 1 H), 6.86 - 6.81 (m, 3 H), 4.00 - 3.95 (t, *J* = 6.6 Hz, 2 H), 3.90 - 3.84 (t, *J* = 6.6 Hz, 2 H), 3.53 (s, 2 H), 1.27 (bs, 56 H), 0.90 - 0.86 (t, *J* = 7.1 Hz, 6 H).

^{13}C-NMR (126 MHz, CD_2Cl_2, 298 K), δ [ppm]

171.4, 158.6, 156.8, 134.5, 133.2, 131.2, 130.2, 129.8, 129.5, 121.3, 115.9, 112.7, 92.9, 68.7, 68.0, 39.2, 31.9, 29.7, 29.6, 29.5, 29.5, 29.4, 29.4, 29.3, 29.2, 28.9, 26.1, 25.8, 22.7, 13.9.

MS (MALDI-TOF pos, DCTB), *m*/*z* (%)

819.1 (100) $[M]^{\bullet+}$; calculated: 818.5 Da.

96b

Chemical formula: $C_{62}H_{107}IO_4$

Molecular weight: 1043.44 g/mol

^{1}H-NMR (500 MHz, CD_2Cl_2, 298 K), δ [ppm]

7.32 - 7.29 (dd, *J* = 7.9 Hz, *J* = 1.6 Hz, 1 H), 7.25 (d, *J* = 1.6 Hz, 1 H), 7.05 - 7.03 (d, *J* = 8.3 Hz, 1 H), 6.86 - 6.80 (m, 3 H), 4.00 - 3.95 (t, *J* = 6.6 Hz, 2 H), 3.93 - 3.84 (m, 4 H), 3.53 (s, 2 H), 1.27 (bs, 84 H), 0.91 - 0.86 (t, *J* = 7.1 Hz, 9 H).

^{13}C-NMR (126 MHz, CD_2Cl_2, 298 K), δ [ppm]

171.4, 158.6, 156.8, 134.5, 133.2, 131.2, 130.2, 129.8, 129.5, 121.3, 115.9, 112.7, 92.9, 68.7, 68.0, 60.5, 39.2, 31.9, 29.7, 29.6, 29.5, 29.5, 29.4, 29.4, 29.3, 29.2, 28.9, 26.1, 25.8, 22.7, 13.9.

MS (MALDI-TOF pos, DCTB), *m/z* (%)

1042.7 (100) $[M]^{\bullet+}$; calculated: 1042.7 Da.

Compound **97** (PK-140)

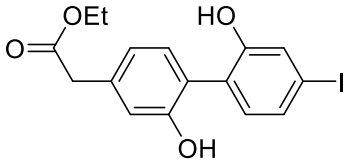

95 (270 mg, 0.730 mmol, 1.00 eq.) was suspended in ethanol (50 mL), five droplets of sulfuric acid were added and the mixture was heated to 90 °C overnight. After cooling to room temperature, the suspension was diluted with water and ethanol was removed under reduced pressure. The residue was diluted with DCM and aq. HCl (1M) and the phases were separated. The aqueous phase was extracted three times with DCM, the combined organic layers were washed with brine, dried over magnesium sulfate and dried over magnesium sulfate. After removal of the solvent, the product was received as a colorless solid (248 mg, 0.623 mmol) in 85 % without further purification.

Chemical formula: $C_{16}H_{15}IO_4$

Molecular weight: 398.20 g/mol

^{1}H-NMR (500 MHz, CD_2Cl_2, 298 K), δ [ppm]

7.34 (d, *J* = 1.8 Hz, 1 H), 7.30 - 7.27 (dd, *J* = 8.0 Hz, *J* = 1.8 Hz, 1 H), 7.09 - 7.07 (d, *J* = 8.7 Hz, 1 H), 6.79 - 6.76 (m, 3 H), 5.82 (s, 1 H), 5.62 (s, 1 H), 4.09 - 4.04 (q, *J* = 7.1 Hz, 2 H), 3.51 - 3.40 (m, 2 H), 1.20 - 1.17 (t, *J* = 7.1 Hz, 3 H).

^{13}C-NMR (126 MHz, CD_2Cl_2, 298 K), δ [ppm]

172.8, 156.2, 154.4, 135.1, 132.3, 132.1, 129.5, 127.8, 126.8, 125.2, 117.6, 115.1, 93.3, 61.5, 38.8, 13.8.

MS (EI, 70 eV), *m/z* (%)

398.0 (62) $[M]^{\bullet+}$, 352.0 (100) $[M\text{-}OEt]^+$, 197.1 (51) $[M\text{-}CO_2Et\text{-}I+H]^+$; calculated: 398.0 Da.

Compound **98** (PK-141)

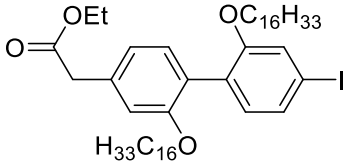

This synthesis applies a procedure published by Zhuang et al.[134]

97 (1.522 g, 3.823 mmol, 1.000 eq.), K_2CO_3 (2.112 g, 15.28 mmol, 3.998 eq.), substoichiometric amounts of potassium iodide and 18-crown-6 (0.498 g, 1.88 mmol, 0.493 eq.) were placed in a *Schlenk* flask and the flask was evacuated and purged with argon in three cycles. 1-Bromohexadecane (5.0 mL, 16 mmol, 4.3 eq.) and dry acetone (50 mL) were added and the mixture was stirred at 60 °C for 5 d. After cooling to room temperature, the solvent was removed under reduced pressure, the residue was suspended in DCM and aq. HCl (2M) and the phases were separated. The aqueous phase was extracted three times with DCM, the combined organic layers were washed with brine and dried over magnesium sulfate. After removal of the solvent under reduced pressure, the residue was purified *via* column chromatography (SiO_2, Cy:DCM, R_f = 0.36) yielding the desired product as a colorless solid (1.476 g, 1.742 mmol) in 46 %.

Chemical formula: $C_{48}H_{79}IO_4$

Molecular weight: 847.06 g/mol

^{1}H-NMR (500 MHz, CD_2Cl_2, 298 K), δ [ppm]

7.33 - 7.29 (dd, *J* = 7.9 Hz, *J* = 1.6 Hz, 1 H), 7.25 (d, *J* = 1.6 Hz, 1 H), 7.06 - 7.02 (d, *J* = 8.3 Hz, 1 H), 6.86 - 6.80 (m, 3 H), 4.01 - 3.93 (m, 4 H), 3.91 - 3.83 (m, 2 H), 3.41 (s, 2 H), 1.27 (bs, 56 H), 0.91 - 0.85 (t, *J* = 7.1 Hz, 9 H).

^{13}C-NMR (126 MHz, CD_2Cl_2, 298 K), δ [ppm]

171.8, 159.0, 157.2, 134.9, 133.6, 131.6, 130.6, 130.2, 129.9, 121.7, 116.3, 113.1, 93.3, 69.2, 68.4, 60.9, 39.6, 32.4, 30.1, 30.1, 30.1, 30.1, 30.1, 30.1, 30.0, 30.0, 30.0, 29.9, 29.8, 29.8, 29.6, 29.3, 26.5, 26.2, 23.1, 14.3, 14.3.

MS (MALDI-TOF pos, DCTB), *m*/*z* (%)

846.5 (100) $[M]^{\bullet+}$; calculated: 846.5 Da.

Compound **99** (PK-147)

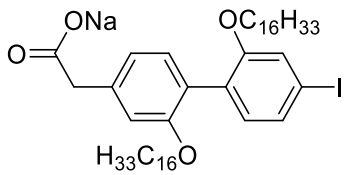

In a round-bottom flask, *tert*-butanol (50 mL) was molten at 40 °C. **96a** (1.388 g, 1.694 mmol, 1.000 eq.) and sodium *tert*-butoxide (0.162 g, 1.69 mmol, 0.996 eq.) were added and the mixture was

stirred for 2.5 h at 40 °C. The solvent was removed under reduced pressure yielding the product as a pale-yellow resin in quantitative yield.

Chemical formula: $C_{46}H_{74}INaO_4$

Molecular weight: 840.99 g/mol

Due to the similarity of **96a** *and* **99***, no spectra were recorded.*

Compound **100** (PK-148)

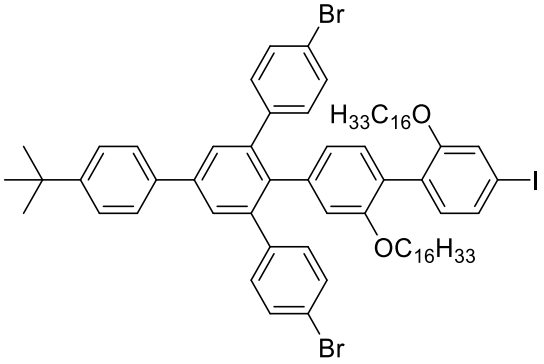

This synthesis applies a procedure published by Idelson et al.[96]

99 (500 mg, 0.595 mmol, 1.00 eq.) and **14**[105] (380 mg, 0.624 mmol, 1.05 eq.) were placed in a round bottom flask. Benzoic anhydride (1.40 g, 6.20 mmol, 10.4 eq.) was added and the mixture was heated to 150 °C for 4 h. Sublimed benzoic anhydride was molten by external heating every 15 minutes so that it drops back down into the suspension. The mixture was allowed to cool to room temperature. The crude product was purified *via* column chromatography (SiO_2, Cy:DCM 10:1, R_f = 0.5) yielding the desired product as a yellow resin (227 mg, 0.177 mmol) in 30 %.

Chemical formula: $C_{72}H_{95}Br_2IO_2$

Molecular weight: 1279.26 g/mol

^{1}H-NMR (500 MHz, CD_2Cl_2, 298 K), δ [ppm]

7.62 - 7.58 (d, *J* = 8.5 Hz, 2 H), 7.51 (s, 2 H), 7.50 - 7.47 (d, *J* = 8.5 Hz, 2 H), 7.27 - 7.23 (d, *J* = 8.5 Hz, 4 H), 7.15 - 7.12 (d, *J* = 8.6 Hz, 1 H), 6.91 - 6.83 (m, 6 H), 6.73 - 6.69 (dd, *J* = 8.7 Hz, *J* = 2.7 Hz, 1 H), 6.45 (d, *J* = 2.7 Hz, 1 H), 6.25 - 6.22 (d, *J* = 8.0 Hz, 1 H), 3.62 - 3.57 (t, *J* = 6.6 Hz, 2 H), 3.50 - 3.46 (t, *J* = 6.6 Hz, 2 H), 1.36 (s, 9 H), 1.27 (bs, 56 H), 0.90 - 0.86 (t, *J* = 6.9 Hz, 6 H).

^{13}C-NMR (126 MHz, CD_2Cl_2, 298 K), δ [ppm]

158.0, 157.2, 151.4, 141.6, 141.2, 140.6, 138.5, 137.3, 136.9, 133.4, 133.1, 131.6, 131.0, 129.6, 128.8, 128.8, 128.7, 126.9, 126.3, 120.9, 120.7, 118.8, 114.8, 92.1, 68.6, 68.2, 34.9, 32.4, 31.5, 30.1, 30.1, 30.1, 29.8, 29.4, 29.2, 27.3, 26.4, 26.3, 23.1, 14.3.

MS (MALDI-TOF pos, DCTB), *m/z* (%)

1387.4 (100) $[M+Ag]^+$, 1278.5 (21) $[M]^{\bullet+}$; calculated: 1278.5 Da.

Compound **101** (PK-146)

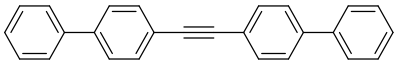

This synthesis applies a procedure published by Eichler et al.[135]

4-Iodobiphenyl (552 mg, 1.97 mmol, 2.08 eq.), bis(tributylstannyl)acetylene (0.50 mL, 0.94 mmol, 1.00 eq.) and PPh_3 (48 mg, 180 μmol, 0.19 eq.) were suspended in toluene (15 mL) and the mixture was purged with argon for 30 min. After adding $PdCl_2(PPh_3)_2$ (70 mg, 0.10 mmol, 0.105 eq.) the mixture was heated to 50 °C for 3 d. The solvent was removed under reduced pressure, the residue was diluted with DCM and aq. HCl (2M) and the phases were separated. The aqueous phase was extracted four times with DCM, the phases were separated and the combined organic phase was washed with brine and dried over magnesium sulfate. After removal of the solvent under reduced pressure, the residue was purified *via* column chromatography (SiO_2:K_2CO_3 9:1,[136] Cy:DCM 3:1, R_f = 0.55) yielding the desired product as an orange solid (110 mg, 0.333 mmol) in 35 %.

Chemical formula: $C_{26}H_{18}$

Molecular weight: 330.43 g/mol

^{1}H-NMR (500 MHz, CD_2Cl_2, 298 K), δ [ppm]

7.66 - 7.62 (m, 12 H), 7.50 - 7.40 (m, 4 H), 7.41 - 7.34 (m, 2 H).

^{13}C-NMR (126 MHz, CD_2Cl_2, 298 K), δ [ppm]

141.4, 140.7, 132.4, 129.3, 128.1, 127.5, 127.4, 122.6, 90.3.

MS (EI, 70 eV), *m/z* (%)

330.1 (100) $[M]^{\bullet+}$; calculated: 330.14 Da.

Compound **102** (PK-149)

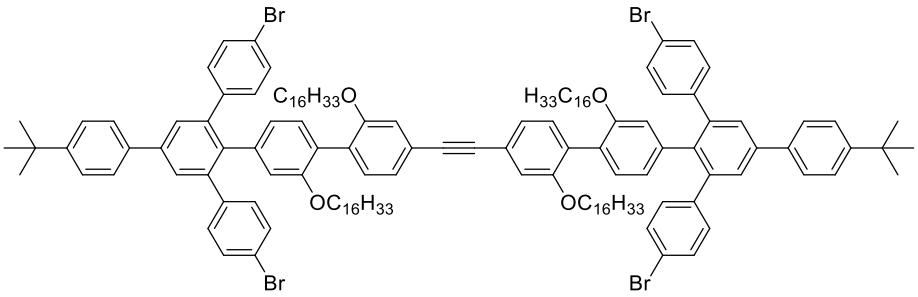

This synthesis applies a procedure published by Eichler et al.[135]

Inside a glove box, bis(tributylstannyl)acetylene (74.2 mg, 0.123 mmol, 1.00 eq.) and **100** (330 mg, 0.258 mmol, 2.01 eq.) were placed in a flamed *Schlenk* tube, toluene (4.5 mL) and $Pd(PPh_3)_4$ (16.9 mg, 14.6 μmol, 0.119 eq.) were added and the tube was sealed. The sealed tube was heated at 50 °C for 5 d. After removal of the solvent, the residue was purified *via* column chromatography (SiO_2:K_2CO_3 9:1, Cy:DCM 10:1, R_f = 0.7).[136] The collected crude product was further purified *via* recGPC (THF, unstabilized) yielding the desired product as a yellow resin (224 mg, 96.3 μmol) in 78 %.

Chemical formula: $C_{146}H_{190}Br_4O_4$

Molecular weight: 2328.74 g/mol

^{1}H-NMR (700 MHz, CD_2Cl_2, 298 K), δ [ppm]

7.61 - 7.59 (d, *J* = 8.2 Hz, 4 H), 7.52 (d, *J* = 8.2 Hz, 4 H), 7.49 - 7.47 (d, *J* = 8.5 Hz, 4 H), 7.28 - 7.25 (d, *J* = 8.2 Hz, 8 H), 7.21 - 7.18 (d, *J* = 8.6 Hz, 2 H), 6.89 - 6.86 (d, *J* = 8.1 Hz, 8 H), 6.76 (d, *J* = 1.6 Hz, 2 H), 6.74 - 6.70 (m, 4 H), 6.53 - 6.51 (d, *J* = 7.8 Hz, 2 H), 6.47 (d, *J* = 2.8 Hz, 2 H), 3.63 - 3.60 (t, *J* = 6.7 Hz, 4 H), 3.56 - 3.53 (t, *J* = 6.8 Hz, 4 H), 1.60 - 1.55 (p, *J* = 6.8 Hz, 4 H), 1.50 - 1.46 (p, *J* = 6.9 Hz, 4 H), 1.35 (s, 18 H), 1.27 (bs, 104 H), 0.90 - 0.87 (m, 12 H).

^{13}C-NMR (178 MHz, CD_2Cl_2, 298 K), δ [ppm]

157.5, 156.0, 150.9, 141.2, 140.8, 140.1, 138.2, 137.0, 136.7, 133.2, 131.3, 130.6, 129.6, 129.2, 128.2, 126.5, 125.8, 125.4, 122.5, 122.0, 120.5, 118.3, 114.3, 113.8, 89.3, 68.2, 67.5, 34.5, 31.9, 31.1, 29.7, 29.7, 29.7, 29.7, 29.7, 29.6, 29.6, 29.6, 29.4, 29.4, 29.4, 29.3, 29.0, 28.9, 26.0, 22.7, 13.9, 13.9.

MS (MALDI-TOF pos, DCTB), *m*/*z* (%)

2436.0 (100) $[M+Ag]^+$, 2328.1 (24) $[M+H]^+$; calculated: 2327.1 Da.

Compound **103** (PK-150)

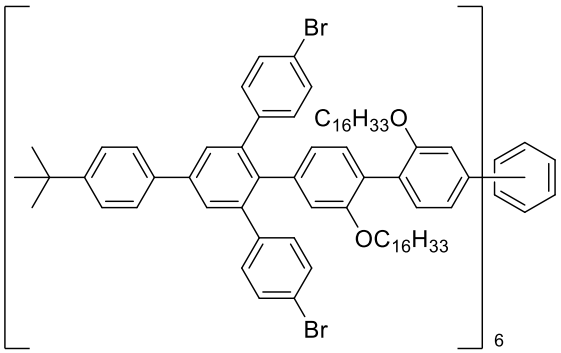

This synthesis applies a procedure published by Idelson et al.[96]

102 (118 mg, 50.7 μmol, 1.00 eq.) was dissolved in toluene (18 mL) and the solution was purged with argon for 40 min. In a sealable glass vessel, $Co_2(CO)_8$ (7.3 mg, 21 μmol, 0.42 eq.) was dissolved in toluene (0.5 mL) inside a glove box. The catalyst solution was transferred into the reaction solution with a syringe and the resulting mixture was heated to 135 °C for 5 d. The progress of reaction was controlled every 24 h *via* analytical GPC and more catalyst was added on the second (6.3 mg, 18 μmol, 0.36 eq.), third (6.7 mg, 20 μmol, 0.39 eq.) and fourth (6.6 mg, 19 μmol, 0.38 eq.) day of reaction. The mixture was allowed to cool to room temperature and the solvent was removed under reduced pressure. The crude product was purified by filtration through a plug of silica gel (DCM) and subsequent recGPC (THF, unstabilized) to give the desired product as a yellow resin (5.7 mg, 2.4 μmol) in 5 % yield.

Chemical formula: $C_{438}H_{570}Br_{12}O_{12}$

Molecular weight: 6986.21 g/mol

No NMR spectra could be recorded under various conditions.

MS (MALDI-TOF pos, DCTB), *m/z* (%)

7093.4 (100) $[M+Ag]^+$, 6985.4 (29) $[M]^{\bullet+}$; calculated: 6981.4 Da.

Compound **MSW-H** (PK-158)

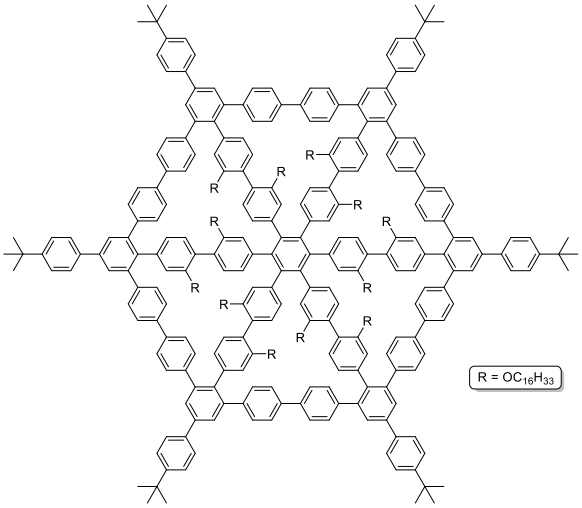

This synthesis applies a procedure published by Idelson et al.[96]

Inside a glove box, **103** (9.5 mg, 0.71 μmol, 1.0 eq), $Ni(COD)_2$ (9.8 mg, 36 μmol, 50 eq.) and 2,2´-bipyridine (10.5 mg, 67.2 μmol, 94.3 eq.) were placed inside a microwave tube. Under the exclusion of light, the tube was filled with a solvent mixture consisting of THF (8 mL) and COD (0.25 mL), immediately sealed and heated in a microwave reactor (12 min, 300 W, 120 °C). The solvent was removed under reduced pressure and after pre-purification *via* column chromatography (SiO_2, DCM), the crude product was isolated *via* recGPC (THF, unstabilized) as a yellow resin (6.6 mg, 0.53 μmol) in 75 % yield.

Chemical formula: $C_{438}H_{570}O_{12}$

Molecular weight: 6027.37 g/mol

^{13}C-NMR (178 MHz, CD_2Cl_2, 298 K), δ [ppm]

161.1, 159.2, 153.9, 142.5, 142.1, 139.9, 138.2, 136.3, 132.7, 132.3, 131.0, 128.9, 128.6, 128.5, 127.1, 126.5, 126.3, 121.8, 115.8, 106.1, 101.1, 70.5, 68.6, 32.4, 31.6, 30.4, 30.3, 30.1, 30.1, 30.1, 30.1, 30.0, 30.0, 29.8, 29.8, 26.5, 23.1, 14.3.

MS (MALDI-TOF pos, DCTB), *m/z* (%)

6136.3 (100) $[M+Ag]^+$; calculated: 6027.4 Da.

It was not possible to record any reliable ^{1}H-NMR spectra.

Compound **105** (PK-151)

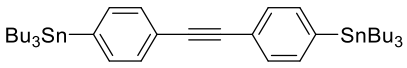

This synthesis applies a procedure published by Nechaev et al.[138]

1,2-Bis(4-bromophenyl)ethyne (500 mg, 1.49 mmol, 1.00 eq.) and PCy_3 (24.4 mg, 87.0 μmol, 0.0584 eq.) were suspended in hexabutyldistannane (2.00 mL, 3.96 mmol, 2.66 eq.) and the mixture was purged with argon for 30 min. Afterwards, $Pd(OAc)_2$ (10.3 mg, 4.59 μmol, 0.0308 eq.) was added and the suspension was heated to 110 °C for 21 h. After cooling to room temperature, the crude product was purified *via* column chromatography (SiO_2, Cy, R_f = 0.7) yielding the desired product as a colorless oil (489 mg, 0.647 mmol) in 43 %.

Chemical formula: $C_{38}H_{62}Sn_2$

Molecular weight: 756.33 g/mol

^{1}H-NMR (500 MHz, CD_2Cl_2, 298 K), δ [ppm]

7.49 - 7.44 (m, 8 H), 1.60 - 1.52 (m, 12 H), 1.38 - 1.30 (m, 12 H), 1.11 - 1.06 (m, 12 H), 0.91 - 0.87 (t, J = 7.3 Hz, 18 H).

^{13}C-NMR (126 MHz, CD_2Cl_2, 298 K), δ [ppm]

143.9, 136.9*, 130.9*, 123.0, 90.0, 29.5, 27.8*, 13.8*, 10.0* (signals with satellites = *).

^{119}Sn (186.4 MHz, CD_2Cl_2, 298 K), δ [ppm]

-39.8.

MS (MALDI-TOF pos, DCTB), *m*/*z* (%)

699.2 (100) $[M\text{-}C_4H_9]^+$; calculated: 756.3 Da.

Compound **106** (PK-160)

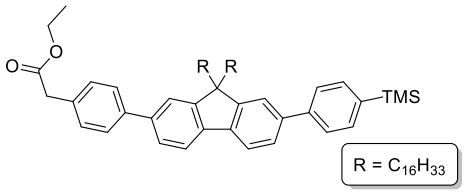

32 (1.202 g, 1.331 mmol, 1.000 eq.), 4-(trimethylsilyl)phenyl boronic acid (343 mg, 1.77 mmol, 1.33 eq.), K_2CO_3 (704 mg, 5.09 mmol, 3.83 eq.) and PPh_3 (50.4 mg, 0.192 mmol, 0.144 eq.) were suspended in toluene (12 mL) and ethanol (6 mL) and the mixture was purged with argon for 30 min. Afterwards, $PdCl_2(PPh_3)_2$ (49.9 mg, 0.071 mmol, 0.053 eq.) was added and the mixture was heated to 90 °C overnight. After checking the reaction progress, more $PdCl_2(PPh_3)_2$ (49.8 mg, 0.071 mmol, 0.053 eq.) was added and the mixture was heated for another 2 d at 90 °C. After cooling to room temperature, the solvent was removed under reduced pressure and the residue was suspended in DCM and aq. HCl (1M). The phases were separated and the aqueous layer was extracted three times with DCM. The combined organic phases were washed with brine, dried over magnesium sulfate and

the solvent was removed under reduced pressure. After purification *via* column chromatography (SiO_2, DCM:Cy 3:1, R_f = 0.2), the product was received as a colorless oil (484 mg, 0.523 mmol) in 39 % yield.

Chemical formula: $C_{64}H_{96}O_2Si$

Molecular weight: 925.56 g/mol

^{1}H-NMR (500 MHz, CD_2Cl_2, 298 K), δ [ppm]

7.81 - 7.71 (m, 2 H), 7.69 - 7.62 (m, 6 H), 7.62 - 7.57 (m, 3 H), 7.40 - 7.36 (dd, *J* = 8.4 Hz, *J* = 3.1 Hz, 2 H), 7.35 - 7.30 (m, 1 H), 4.19 - 4.13 (q, *J* = 7.1 Hz, 2 H), 3.67 (s, 2 H), 1.24 (bs, 60 H), 1.17 - 1.13 (m, 3 H), 0.90 - 0.85 (t, *J* = 7.1 Hz, 6 H), 0.32 (s*, 9 H).

^{13}C-NMR (126 MHz, CD_2Cl_2, 298 K), δ [ppm]

171.3, 151.7, 141.8, 140.3, 140.1, 140.1, 139.9, 139.6, 139.5, 139.1, 133.8, 133.4, 129.7, 127.1, 126.3, 125.9, 125.8, 121.6, 121.5, 119.9, 60.8, 55.3, 40.8, 31.9, 29.9, 29.6, 29.6, 29.6, 29.6, 29.5, 29.5, 29.5, 29.3, 29.2, 26.9, 23.8, 23.8, 22.6, 14.0, 13.8, -1.5.

MS (MALDI-TOF pos, DCTB), *m/z* (%)

924.720 (100) $[M]^{\bullet+}$; calculated: 924.72 Da.

*Signals marked with * feature satellites from couplings with isotopes of low abundance.*

Compound **107** (PK-161)

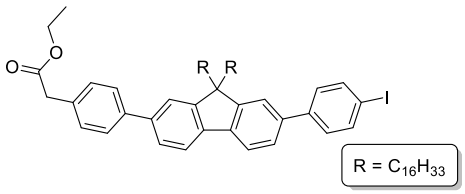

This synthesis applies a procedure published by Idelson et al.[96]

106 (473 mg, 0.511 mmol, 1.00 eq.) was dissolved in DCM (20 mL) and the mixture was purged with argon for 30 min. After adding iodine monochloride (0.51 mL, 0.51 mmol, 1.0 eq., 1M in DCM) the mixture was stirred overnight at room temperature under the exclusion of light. The reaction was terminated through the addition of aq. $NaHSO_3$ (40 %) until the organic phase became colorless and the phases were separated. The aqueous phase was extracted three times with DCM, the combined organic phases were washed with brine and dried over magnesium sulfate. After removal of the solvent, the crude product was purified *via* column chromatography (SiO_2, DCM:Cy, R_f = 0.64) yielding the desired product as a pale-yellow oil (498 mg, 0.508 mmol) in 99 %.

Chemical formula: $C_{61}H_{87}IO_2$

Molecular weight: 979.27 g/mol

^{1}H-NMR (500 MHz, CD_2Cl_2, 298 K), δ [ppm]

7.82 - 7.71 (m, 4 H), 7.69 - 7.63 (d, *J* = 8.2 Hz, 2 H), 7.63 - 7.56 (m, 4 H), 7.46 - 7.43 (d, *J* = 8.5 Hz, 2 H), 7.40 - 7.35 (dd, *J* = 8.5 Hz, *J* = 2.8 Hz, 2 H), 4.19 - 4.13 (q, *J* = 7.1 Hz, 2 H), 3.67 (s, 2 H), 1.24 (bs, 60 H), 1.17 - 1.13 (m, 3 H), 0.90 - 0.85 (t, *J* = 7.1 Hz, 6 H).

^{13}C-NMR (126 MHz, CD_2Cl_2, 298 K), δ [ppm]

171.8, 152.4, 152.3, 141.6, 141.0, 140.7, 140.4, 140.3, 139.2, 138.3, 133.9, 130.2, 129.4, 127.6, 126.3, 126.2, 122.0, 121.7, 120.5, 120.5, 93.0, 61.3, 55.8, 41.3, 32.4, 30.4, 30.1, 30.1, 30.1, 30.1, 30.0, 30.0, 30.0, 29.8, 29.7, 27.4, 24.3, 23.1, 14.5, 14.3.

MS (MALDI-TOF pos, DCTB), *m*/*z* (%)

978.6 (100) $[M]^{\bullet+}$, 852.7 (7) $[M\text{-}I]^{+}$; calculated: 978.6 Da.

Compound **108** (PK-162)

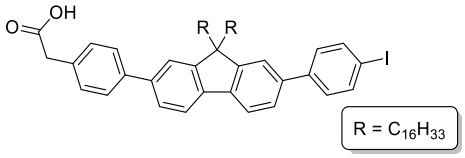

107 (486 mg, 0.496 mmol, 1.00 eq.) was dissolved in a mixture of THF (15 mL) and water (3 mL). After adding $LiOH{\cdot}H_2O$ (399 mg, 9.50 mmol, 19.2 eq.), the mixture was heated to 60 °C for 19 hours. After removal of the solvent, the residue was suspended in DCM and aq. HCl (1M). After separating, the aqueous layer was extracted three times with DCM. The combined organic phases were washed with brine, dried over magnesium sulfate and the solvent was removed under reduced pressure. The crude product was purified *via* column chromatography (SiO_2, DCM, R_f = 0.1), receiving the product as an orange oil (467 mg, 0.490 mmol) in 99 % yield.

Chemical formula: $C_{59}H_{83}IO_2$

Molecular weight: 951.22 g/mol

^{1}H-NMR (500 MHz, CD_2Cl_2, 298 K), δ [ppm]

7.82 - 7.78 (m, 3 H), 7.68 - 7.64 (d, *J* = 8.2 Hz, 2 H), 7.62 - 7.59 (dd, *J* = 6.0 Hz, *J* = 1.5 Hz, 2 H), 7.58 - 7.56 (dd, *J* = 6.0 Hz, *J* = 1.5 Hz, 2 H), 7.46 - 7.43 (d, *J* = 8.4 Hz, 2 H), 7.41 - 7.38 (d, *J* = 8.2 Hz, 2 H), 7.38 - 7.31 (m, 1 H), 3.73 (s, 2 H), 1.25 (bs, 60 H), 0.89 - 0.86 (t, *J* = 7.1 Hz, 6 H).

^{13}C-NMR (126 MHz, CD_2Cl_2, 298 K), δ [ppm]

171.3, 151.9, 151.7, 141.1, 140.5, 140.2, 139.9, 139.8, 138.7, 137.8, 133.4, 129.7, 129.7, 128.9, 127.1, 125.8, 125.7, 121.5, 121.2, 120.0, 92.5, 60.8, 55.3, 40.2, 31.9, 29.9, 29.6, 29.6, 29.6, 29.5, 29.5, 29.5, 29.3, 29.2, 29.1, 26.9, 23.8, 22.6, 13.8.

MS (MALDI-TOF pos, DCTB), *m*/*z* (%)

950.6 (100) $[M]^{\bullet+}$; calculated: 950.5 Da.

Compound **109** (PK-163)

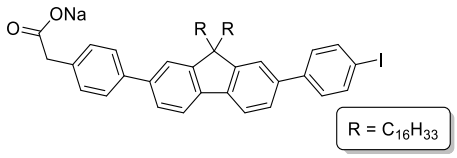

In a round-bottom flask *tert*-butanol (30 mL) was molten at 40 °C. **108** (458 mg, 0.479 mmol, 1.00 eq.) and sodium *tert*-butoxide (46.1 mg, 0.480 mmol, 1.00 eq.) were added and the mixture was stirred for three hours at 40 °C. The solvent was removed under reduced pressure yielding the product as a pale-orange resin in quantitative yield.

Chemical formula: $C_{59}H_{82}IO_2Na$

Molecular weight: 973.20 g/mol

Due to the similarity of **108** *and* **109***, no spectra were recorded.*

Compound **110** (PK-164)

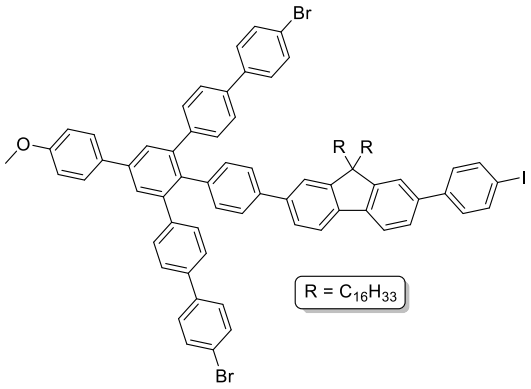

This synthesis applies a procedure published by Idelson et al.[96]

109 (443 mg, 0.455 mmol, 1.00 eq.), **65** (360 mg, 0.489 mmol, 1.07 eq.) and benzoic anhydride (1.21 g, 4.54 mmol, 9.98 eq.) were mixed and heated to 150 °C for 5 h. Sublimed benzoic anhydride was molten back into the flask by external heating with a heat gun every 15 minutes. The mixture was allowed to cool to room temperature. The crude product was purified *via* column chromatography (SiO_2, Cy:DCM 5:1, R_f = 0.2) yielding the product as an orange resin (145 mg, 95.0 μmol) in 21 %.

Chemical formula: $C_{94}H_{105}Br_2IO$

Molecular weight: 1537.59 g/mol

^{1}H-NMR (500 MHz, CD_2Cl_2, 298 K), δ [ppm]

7.81 - 7.78 (d, *J* = 8.5 Hz, 2 H), 7.77 - 7.73 (m, 2 H), 7.72 - 7.69 (m, 4 H), 7.56 - 7.52 (m, 8 H), 7.49 - 7.45 (dd, *J* = 8.6 Hz, *J* = 2.0 Hz, 8 H), 7.44 - 7.41 (m, 4 H), 7.32 - 7.30 (d, *J* = 8.5 Hz, 4 H), 7.10 - 7.07 (d, *J* = 8.2 Hz, 2 H), 7.04 - 7.02 (d, *J* = 8.8 Hz, 2 H), 3.87 (s, 3 H), 1.25 (bs, 60 H), 0.89 - 0.86 (t, *J* = 7.0 Hz, 6 H).

^{13}C-NMR (126 MHz, CD_2Cl_2, 298 K), δ [ppm]

160.1, 152.3, 152.2, 142.5, 142.1, 141.6, 141.0, 140.4, 140.3, 139.9, 139.9, 139.4, 139.2, 138.9, 138.3, 138.2, 137.5, 133.1, 132.7, 132.3, 131.3, 131.0, 129.4, 128.9, 128.6, 128.5, 126.5, 126.3, 126.2, 123.4, 121.8, 121.7, 121.5, 120.5, 120.4, 114.8, 93.0, 55.8, 40.7, 32.4, 30.1, 30.1, 30.1, 30.1, 30.1, 30.1, 30.0, 30.0, 29.8, 29.6, 27.4, 24.3, 23.1, 14.3.

MS (MALDI-TOF pos, DCTB), *m*/*z* (%)

1536.6 (100) $[M]^{\bullet+}$; calculated: 1536.6 Da.

Compound **111** (PK-166)

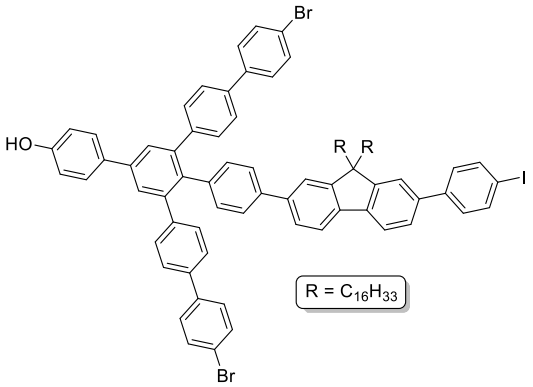

This synthesis applies a procedure published by Idelson et al.[96]

110 (145 mg, 0.0945 mmol, 1.00 eq.) was placed in a *Schlenk* flask and it was evacuated and purged with argon in three cycles. Dry DCM (15 mL) was added, the solution was cooled to -78 °C and a solution of BBr_3 (0.50 mL, 0.50 mmol, 5.29 eq., 1M in DCM) was added dropwise. The mixture was stirred overnight and thereby allowed to warm to room temperature. Afterwards, the reaction was quenched through addition of water, aq. HCl (1M) was added, the phases were separated, and the aqueous phase was extracted three times with DCM. The combined organic layers were washed with brine, dried over magnesium sulfate and the solvent was removed under reduced pressure. The crude product was purified *via* column chromatography (SiO_2, DCM, R_f = 0.65) yielding the product as a colorless resin (116 mg, 0.076 mmol) in 80 %.

Chemical formula: $C_{93}H_{103}Br_2IO$

Molecular weight: 1523.56 g/mol

^{1}H-NMR (500 MHz, CD_2Cl_2, 298 K), δ [ppm]

7.81 - 7.78 (d, *J* = 8.4 Hz, 2 H), 7.77 - 7.74 (d, *J* = 8.6 Hz, 1 H), 7.73 - 7.71 (d, *J* = 7.9 Hz, 1 H), 7.70 (s, 2 H), 7.66 - 7.63 (d, *J* = 8.7 Hz, *J* = 8.5 Hz, 2 H), 7.57 - 7.51 (m, 8 H), 7.48 - 7.45 (d, *J* = 8.8 Hz, 8 H), 7.45 - 7.42 (dd, *J* = 8.5 Hz, *J* = 4.5 Hz, 4 H), 7.32 - 7.29 (d, *J* = 8.5 Hz, 4 H), 7.10 - 7.07 (d, *J* = 8.4 Hz, 2 H), 6.97 - 6.95 (d, *J* = 8.7 Hz, 2 H), 1.24 (bs, 60 H), 0.89 - 0.85 (t, *J* = 6.8 Hz, 6 H).

^{13}C-NMR (126 MHz, CD_2Cl_2, 298 K), δ [ppm]

155.7, 151.8, 151.7, 142.0, 141.6, 141.1, 140.5, 139.9, 139.8, 139.4, 138.9, 138.7, 138.4, 137.8, 137.7, 137.0, 132.8, 132.2, 131.8, 130.5, 128.9, 128.4, 128.3, 128.0, 126.1, 125.9, 125.7, 122.9, 122.4, 121.4, 121.2, 121.0, 120.0, 120.0, 115.7, 92.5, 55.3, 40.2, 31.9, 29.9, 29.7, 29.6, 29.6, 29.6, 29.6, 29.5, 29.5, 29.3, 29.1, 23.8, 22.6, 13.8.

MS (MALDI-TOF pos, DCTB), *m/z* (%)

1523.5 (100) $[M]^{\bullet+}$; calculated: 1523.5 Da.

Compound **112** (PK-167)

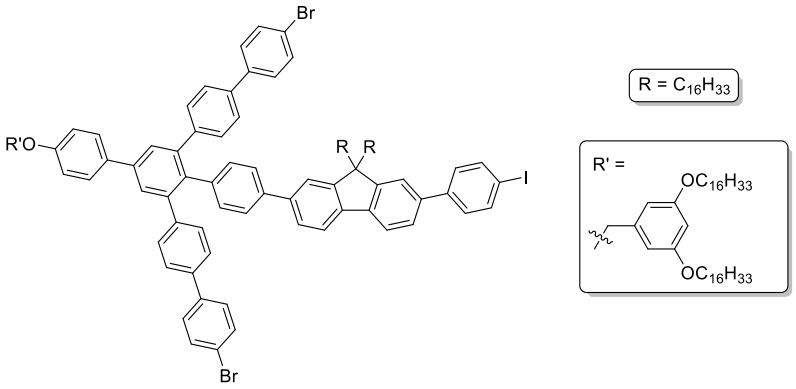

This synthesis applies a procedure published by Idelson et al.[96]

111 (116 mg, 76 μmol, 1.00 eq.), **68b** (56 mg, 92 μmol, 1.2 eq.) and Cs_2CO_3 (108 mg, 92.4 μmol, 4.37 eq.) were suspended in acetone (20 mL) and water (5 mL) and the mixture was heated for 48 h at 80 °C. After cooling to room temperature, the solvent was removed under reduced pressure and the residue was suspended in DCM and aq. HCl (1M). The phases were separated and the aqueous layer was extracted three times with DCM. The combined organic layers were washed with brine, dried over magnesium sulfate and the solvent was removed under reduced pressure. After purification *via* column chromatography (SiO_2, Cy:DCM 1:1, R_f = 0.76) the product was received as a yellow oil (103 mg, 48.9 μmol) with impurities of **68b** alongside recovered substrate (55 mg, 36 μmol, 48 %).

Chemical formula: $C_{132}H_{173}Br_2IO_3$

Molecular weight: 2094.55 g/mol

^{1}H-NMR (500 MHz, CD_2Cl_2, 298 K), δ [ppm]

7.81 - 7.79 (d, *J* = 8.4 Hz, 1 H), 7.77 - 7.74 (dd, *J* = 7.7 Hz, *J* = 0.8 Hz, 1 H), 7.73 - 7.71 (d, *J* = 7.9 Hz, 1 H), 7.71 (s, 2 H), 7.70 - 7.68 (d, *J* = 9.0 Hz, 2 H), 7.56 - 7.52 (d, *J* = 8.7 Hz, 8 H), 7.49 - 7.46 (dd, *J* = 8.6 Hz, *J* = 2.8 Hz, 8 H), 7.44 - 7.41 (m, 3 H), 7.32 - 7.30 (d, *J* = 8.5 Hz, 4 H), 7.10 - 7.07 (dd, *J* = 8.6 Hz, *J* = 2.8 Hz, 3 H), 6.58 (d, *J* = 2.2 Hz, 2 H), 6.51 (d, *J* = 2.3 Hz, 2 H), 6.41 - 6.39 (m, 2 H), 5.06 (s, 2 H), 3.97 - 3.92 (m, 4 H), 1.79 - 1.73 (m, 8 H), 1.28 (bs, 108 H), 0.90 - 0.85 (m, 12 H).

^{13}C-NMR (126 MHz, CD_2Cl_2, 298 K), δ [ppm]

160.6, 160.5, 158.7, 151.8, 142.0, 141.6, 140.5, 139.8, 139.5, 139.2, 137.8, 137.7, 137.0, 132.9, 132.2, 131.8, 130.5, 128.9, 128.4, 128.1, 126.7, 126.0, 125.8, 125.7, 121.3, 120.0, 115.3, 106.8, 105.6, 101.2, 100.6, 70.0, 68.2, 55.3, 31.9, 29.9, 29.6, 29.6, 29.6, 29.5, 29.4, 29.3, 29.3, 29.2, 26.9, 26.0, 26.0, 23.8, 22.6, 13.8.

MS (MALDI-TOF pos, DCTB), *m*/*z* (%)

2202.0 (100) $[M+Ag]^+$, 2094.1 (28) $[M]^{\bullet+}$; calculated: 2095.1 Da.

Compound **113** (PK-153)

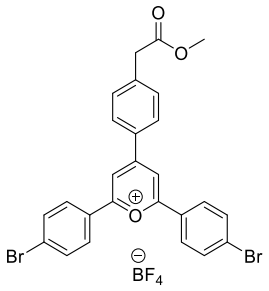

This synthesis applies a procedure published by Kotra et al.[104]

Methyl 2-(4-formylphenyl)acetate (1.502 g, 7.547 mmol, 1.000 eq.) and 4-bromoacetophenone (2.299 g, 15.31 mmol, 2.028 eq.) were placed in a *Schlenk* flask and it was evacuated and flooded with argon in three cycles. DCE (2 mL) was added and the mixture was purged with argon for 20 min. Boron trifluoride diethyl etherate (8.0 mL, 63 mmol, 8.4 eq.) was added and the suspension was heated to 80 °C for 4 h. After cooling to room temperature, the residue was precipitated from diethyl ether. The precipitate was filtered off, dissolved in acetone and precipitated once more. The received solid was dried overnight under vacuum yielding the product as a yellow solid (1.609 g, 1.752 mmol) in 23 %.

Chemical formula: $C_{26}H_{19}BBr_2F_4O_3$

Molecular weight: 626.05 g/mol

^{1}H-NMR (500 MHz, CD_2Cl_2, 298 K), δ [ppm]

9.18 (s, 2 H), 8.59 - 8.55 (d, *J* = 8.5 Hz, 2 H), 8.52 - 8.48 (d, *J* = 8.8 Hz, 4 H), 8.04 - 8.00 (d, *J* = 8.8 Hz, 4 H), 7.71 - 7.68 (d, *J* = 8.5 Hz, 2 H), 3.95 (s, 2 H), 3.67 (s, 3 H).

^{13}C-NMR (126 MHz, CD_2Cl_2, 298 K), δ [ppm]

171.4, 169.6, 165.3, 143.3, 133.4, 132.3, 131.6, 131.4, 131.0, 130.7, 130.0, 128.8, 115.8, 52.5, 31.2.

MS (ESI+), *m*/*z* (%)

538.968 (100) $[M-BF_4]^+$; calculated: 626.0 Da.

114 (PK-154)

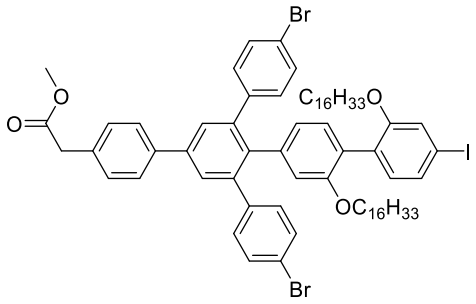

This synthesis applies a procedure published by Idelson et al.[96]

99 (499 mg, 0.594 mmol, 1.00 eq.) and **113** (381 mg, 0.624 mmol, 1.05 eq.) were placed in a round bottom flask. Benzoic anhydride (1.40 g, 6.20 mmol, 10.5 eq.) was added and the mixture was heated to 150 °C for 4 h. Sublimed benzoic anhydride was molten by external heating every 15 minutes so that it drops back down into the suspension. The mixture was allowed to cool to room temperature. The crude product was purified *via* column chromatography (SiO_2, Cy:DCM 1:1, R_f = 0.6) yielding the desired product as an orange oil (220 mg, 0.170 mmol) in 29 %.

Chemical formula: $C_{71}H_{91}Br_2IO_4$

Molecular weight: 1295.22 g/mol

^{1}H-NMR (400 MHz, CD_2Cl_2, 298 K), δ [ppm]

7.64 - 7.61 (d, *J* = 8.3 Hz, 2 H), 7.51 (s, 2 H), 7.38 - 7.35 (d, *J* = 8.3 Hz, 2 H), 7.28 - 7.23 (d, *J* = 8.5 Hz, 4 H), 7.15 - 7.12 (d, *J* = 8.6 Hz, 1 H), 6.92 - 6.89 (m, 2 H), 6.88 - 6.83 (m, 4 H), 6.73 - 6.69 (dd, *J* = 8.6 Hz, *J* = 2.7 Hz, 1 H), 6.45 (d, *J* = 2.7 Hz, 1 H), 6.26 - 6.23 (d, *J* = 8.0 Hz, 1 H), 3.69 (s, 3 H), 3.68 (s, 2 H), 3.62 - 3.58 (t, *J* = 6.6 Hz, 2 H), 3.50 - 3.46 (t, *J* = 6.6 Hz, 2 H), 1.27 (bs, 56 H), 0.90 - 0.86 (t, *J* = 6.7 Hz, 6 H).

Due to impurities, it was not possible to reliably assign the signals recorded in the ^{13}C-NMR spectrum.

MS (MALDI-TOF pos, DCTB), *m*/*z* (%)

1295.2 (100) $[M+H]^+$; calculated: 1294.4 Da.

115 (PK-156)

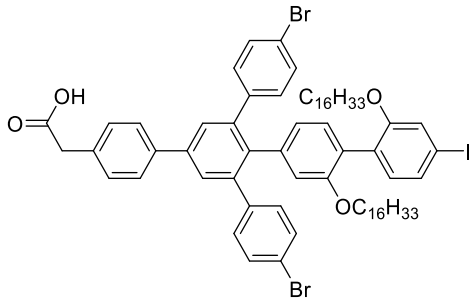

114 (220 mg, 0.170 mmol, 1.00 eq.) was dissolved in a mixture of THF (15 mL) and water (3 mL). After adding $LiOH \cdot H_2O$ (136 mg, 3.24 mmol, 19.0 eq.), the mixture was heated to 60 °C for 19 hours. The reaction mixture was diluted with DCM and neutralized using aq. HCl (2M). After phase separation, the aqueous layer was extracted three times using DCM. The combined organic phases were washed once with brine, dried over magnesium sulfate and the solvent was removed under reduced pressure. The crude product was purified *via* column chromatography (SiO_2, DCM:EA 1:1), receiving the product as a yellow oil (95.7 mg, 74.7 μmol) in 44 % yield.

Chemical formula: $C_{70}H_{89}Br_2IO_4$

Molecular weight: 1281.19 g/mol

^{1}H-NMR (500 MHz, CD_2Cl_2, 298 K), δ [ppm]

7.65 - 7.63 (d, J = 8.3 Hz, 2 H), 7.52 (s, 2 H), 7.39 - 7.37 (d, J = 8.2 Hz, 2 H), 7.27 - 7.24 (d, J = 8.5 Hz, 4 H), 7.15 - 7.13 (d, J = 8.6 Hz, 1 H), 6.91 - 6.87 (m, 2 H), 6.86 - 6.83 (d, J = 7.9 Hz, 4 H), 6.73 - 6.70 (dd, J = 8.6 Hz, J = 2.7 Hz, 1 H), 6.45 (d, J = 2.7 Hz, 1 H), 6.26 - 6.23 (d, J = 8.0 Hz, 1 H), 3.72 (s, 2 H), 3.62 - 3.58 (t, J = 6.6 Hz, 2 H), 3.50 - 3.46 (t, J = 6.8 Hz, 2 H), 1.27 (bs, 56 H), 0.90 - 0.87 (t, J = 6.8 Hz, 6 H).

^{13}C-NMR (126 MHz, CD_2Cl_2, 298 K), δ [ppm]

175.8, 157.5, 156.7, 141.2, 140.6, 139.8, 138.9, 137.9, 136.9, 133.1, 133.0, 132.6, 131.2, 130.6, 129.9, 129.1, 128.3, 127.0, 120.5, 118.3, 91.7, 68.1, 67.7, 31.9, 29.7, 29.6, 29.6, 29.6, 29.6, 29.3, 29.3, 29.1, 28.9, 28.8, 25.9, 25.9, 22.7, 13.8.

MS (MALDI-TOF pos, DCTB), m/z (%)

1280.4 (100) $[M]^{\bullet+}$; calculated: 1280.4 Da.

10 Appendix

10.1 List of Schemes, Figures and Tables

10.1.1 Schemes

10.1.2 Figures

10.1.3 Tables

10.2 Abbreviations

°C	degree *Celsius* (unit of temperature)
15-C-5	15-crown-5 (reagent)
18-C-6	18-crown-6 (reagent)
Å	*Ångström* (1 Å equals 10^{-10} meters)
a.u.	atomic unit
abs.	absolute
Ac	acyl (functional group)
Ac_2O	acetic anhydride
AcOH	acetic acid
APCI	atmospheric pressure chemical ionization (mass spectrometry)
aq.	aqueous
BHT	dibutylhydroxytoluene
BINOL	1,1’-bi-2-naphthol (ligand)
bipy	2,2´-bipyridine
BISBI	bis(diphenylphosphinomethyl)-1,1'-biphenyl (ligand)
Boc	*tert*-Butyloxycarbonyl (protecting group)
Bpin	4,4,5,5-Tetramethyl-1,3,2-dioxaborolan-2-yl (functional group)
bs	broad singlet (NMR)
Bu	butyl (functional group)
Bz	benzoyl (functional group)
c	concentration
CD	cyclodextrine
COD	cylcoocta-1,5-diene
comp.	compare
conc.	concentrated
CPD*i*PS	(3-Cyanopropyl)diisopropylsilyl (protecting group)
CPDMS	(3-Cyanopropyl)dimethylsilyl (protecting group)
Cy	cyclohexane
d	day(s)
d	diameter
d	distance
d	dublet (NMR)
Da	*Dalton* (unified atomic mass unit)
dba	dibenzylideneacetone

DCE	1,2-dichloroethane
DCM	dichloromethane
DCTB	*trans*-2-[3-(4-*tert*-Butylphenyl)-2-methyl-2-propenylidene]malononitrile (matrix)
DCvC	dynamic covalent chemistry
DFT	density-functional theory
DIOP	2,3-*O*-isopropylidene-2,3-dihydroxy-1,4-bis(diphenylphosphino)butane (ligand)
DMF	*N*,*N*-dimethylformamide
DMSO	dimethyl sulfoxide
EA	ethyl acetate
EI	electron ionization (mass spectrometry)
eq.	equivalents
ESI	electron spray ionization (mass spectrometry)
Et	ethyl (functional group)
et al.	*et alii*, (*latin*: and others)
eV	electron volt
EWG	electron-withdrawing group
Fmoc	fluorenylmethyloxycarbonyl (protecting group)
g	gram
GPC	gel permeation chromatography
h	hour(s)
bhess	biased Hessian approach
HOPG	highly oriented pyrolytic graphite
Hz	Hertz (unit of coupling constants)
I	inductive (electronic effect)
*i*Pr	isopropyl (functional group)
J	coupling constant (NMR)
K	Kelvin (unit of temperature)
log	logarithmic
M	mesomertic (electronic effect)
m	*meta*
m	meter
M	molar (mol/L)
M	molecule (mass spectrometry signal)
m	multiplet (NMR)
m/*z*	mass to charge-ratio in *Dalton* (mass spectrometry)

MALDI	matrix-assisted laser desorption ionization
MCW	Molecular cobweb
MD	molecular dynamics (type of quantum chemical calculations)
Me	methyl
MeOH	methanol (CH_3OH)
mg	milligram
MHz	megahertz
min	minute(s)
mL	milliliter
mmol	millimol
MS	mass spectrometry
MSW	molecular spoked wheel
mw	microwave
nm	nanometer
NMR	nuclear magnetic resonance
norm.	normalized
o	*ortho*
OA	octylic acid
OLED	organic light-emitting diodes
p	*para*
p	perimeter
p	quintet (NMR)
PCy_3	tricyclohexylphosphine (ligand)
PG	protection group
Ph	phenyl (functional group)
PhH	benzene (solvent)
PhMe	toluene (solvent)
PHO	1-phenyloctane
PPh_3	triphenylphosphine (ligand)
ppm	parts per million
QPhos	pentaphenyl(di-*tert*-butylphosphino)ferrocene (ligand)
QPP	quinoxalinophenanthrophenazine
quant	quantitative
R	residue
rac	racemate

recGPC	recycling gel permeation chromatography
R_f	retention factor
rt	room temperature
s	singlet (NMR)
s	second(s)
SAM	self-assembled monolayers
S_EAr	Electrophilic Aromatic Substitution (reaction)
SPM	shape-persistent macrocycle
STM	scanning tunneling microscopy
t	triplet (NMR)
TBAF	tetra-*n*-butylammonium fluoride
*t*Bu	*tert*-butyl (functional group)
TCB	1,2,4-trichlorobenzene
TFP	tri(2-furyl)phosphine (ligand)
THF	tetrahydrofuran
THP	tetrahydropyran
T*i*PS	triisopropylsilyl (protecting group)
TLC	thin layer chromatography
TMS	trimethylsilyl (protecting group)
TOF	time of flight (MALDI spectrometry)
TsOH	toluenesulfonic acid
UV	ultraviolet (electromagnetic radiation)
UV/Vis	ultraviolet and visible electromagnetic radiation
V	Volt
VE	valence electrons
Vis	visible (wavelength region of light)
vs	versus (*latin*: against, towards)
W	Watt
XPhos	dicyclohexyl[2',4',6'-tris(propan-2-yl)[1,1'-biphenyl]-2-yl]phosphane (ligand)
δ	chemical shift in ppm
λ	wavelength

10.3 Literature

[1] in *The IUPAC Compendium of Chemical Terminology* (Editor V. Gold), International Union of Pure and Applied Chemistry (IUPAC), Research Triangle Park, NC. **2019**.

[2] A. W. Hull, *Phys. Rev.* **1917**, *10*, 661–696.

[3] A. Hirsch, *Nat. Mater* **2010**, *9*, 868–871.

[4] M. Jawaid, M. S. Salit, O. Y. Alothman, *Green Biocomposites*, Springer International Publishing, Cham, **2017**.

[5] M. A. Shampo, R. A. Kyle, D. P. Steensma, *Mayo Clin. Proc.* **2010**, *85*, e58.

[6] Donald R. Askeland, Pradeep P. Fulay, *The Science & Engineering of Materials,* 5. Aufl., Van Nostrand Reinhold Company, New York, **2005**.

[7] S. Mukherjee, *Applied Mineralogy*. Applications in Industry and Environment, Springer Netherlands, Dordrecht, **2011**.

[8] Conférence Générale des Poids et Mesures, 'Quatrième Conférence Générale des Poids et Mesures', https://www.bipm.org/documents/20126/17314988/CGPM4.pdf/c0169d86-7b95-b5a0-6460-87a120e8ce94#page=89, accessed: 21.05.2024.

[9] Lamborghini Automobili, 'Sesto Elemento', https://www.lamborghini.com/de-en/geschichte/sesto-elemento, accessed: 21.05.2024.

[10] K. Tamao, K. Sumitani, M. Kumada, *J. Am. Chem. Soc.* **1972**, *94*, 4374–4376.

[11] E. Negishi, T. Takahashi, S. Baba, D. E. van Horn, N. Okukado, *J. Am. Chem. Soc.* **1987**, *109*, 2393–2401.

[12] O. Diels, K. Alder, *Justus Liebigs Ann. Chem.* **1928**, *460*, 98–122.

[13] Nobel Media AB, 'The Nobel Prize in Chemistry 1950 - Press Release', https://www.nobelprize.org/prizes/chemistry/1950/summary/.

[14] B. L. Oliveira, Z. Guo, G. J. L. Bernardes, *Chem. Soc. Rev.* **2017**, *46*, 4895–4950.

[15] R. Brückner, *Reaktionsmechanismen*. Organische Reaktionen, Stereochemie, moderne Synthesemethoden, 2. Aufl., Spektrum, Akad. Verl., Heidelberg, Berlin, **2003**.

[16] S. Danishefsky, T. Kitahara, *J. Am. Chem. Soc.* **1974**, *96*, 7807–7808.

[17] R. B. Woodward, T. J. Katz, *Tetrahedron* **1959**, *5*, 70–89.

[18] a) C. Friedel, J.-M. Crafts, *Compt. Rend.* **1877**, 1392–1395; b) C. Friedel, J.-M. Crafts, *Compt. Rend.* **1877**, 1450–1454.

[19] S. Hauptmann, *Organische Chemie,* 3. Aufl., Dt. Verl. für Grundstoffindustrie; Wiley-VCH, Leipzig, Weinheim, **1991**.

[20] S. K. Weber, F. Galbrecht, U. Scherf, *Org. Lett.* **2006**, *8*, 4039–4041.

[21] A. Loibl, W. Oschmann, M. Vogler, E. A. Pidko, M. Weber, J. Wiecko, C. Müller, *Dalton Trans.* **2018**, *47*, 9355–9366.

[22] J. Kay, *Krebs' citric acid cycle*, Biochemical Society symposia, London, **1987**.

[23] J. J. Li, *Contemporary Drug Synthesis,* 1. Aufl., John Wiley & Sons Incorporated, Hoboken, **2004**.

[24] F. Ullmann, J. Bielecki, *Ber. Dtsch. Chem. Ges.* **1901**, *34*, 2174–2185.

[25] J. K. Stille, *Angew. Chem. Int. Ed.* **1986**, *25*, 508–524.

[26] K. Sonogashira, *J. Organomet. Chem.* **2002**, *653*, 46–49.

[27] N. Miyaura, K. Yamada, A. Suzuki, *Tetrahedron Lett.* **1979**, *20*, 3437–3440.

[28] Y. Hatanaka, T. Hiyama, *J. Org. Chem.* **1988**, *53*, 918–920.

[29] J. F. Hartwig, *Organotransition metal chemistry*, University Science Books, Sausalito, Calif, **2010**.

[30] C. A. Tolman, *J. Am. Chem. Soc.* **1970**, *92*, 2956–2965.

[31] L. Kürti, B. Czakó, *Strategic applications of named reactions in organic synthesis*. Background and detailed mechanisms ; 250 named reactions, Elsevier Acad. Press, Amsterdam, Heidelberg, **2009**.

[32] A. L. Casado, P. Espinet, *Organometallics* **1998**, *17*, 954–959.

[33] C. Amatore, G. Le Duc, A. Jutand, *Chem. Eur. J.* **2013**, *19*, 10082–10093.

[34] M. N. Hopkinson, C. Richter, M. Schedler, F. Glorius, *Nature* **2014**, *510*, 485–496.

[35] M. Gomberg, W. E. Bachmann, *J. Am. Chem. Soc.* **1924**, *46*, 2339–2343.

[36] P. Hahn, T. Bruggmann, *Lexikon Lebensmittelrecht,* 2. Aufl., Behr's Verlag, Hamburg, **1998**.

[37] L. Xiao, X. Ai, Y. Cao, H. Yang, *Electrochim. Acta* **2004**, *49*, 4189–4196.

[38] M. P. Johansson, J. Olsen, *J. Chem. Theory Comput.* **2008**, *4*, 1460–1471.

[39] B. Testa in *New Comprehensive Biochemistry*, Elsevier. **1982**, 18.

[40] L. Pu, *Chem. Rev.* **1998**, *98*, 2405–2494.

[41] M.-N. Birkholz, Z. Freixa, P. W. N. M. van Leeuwen, *Chem. Soc. Rev.* **2009**, *38*, 1099–1118.

[42] P. C. Kamer, P. W. van Leeuwen, J. N. Reek, *Acc. Chem. Res.* **2001**, *34*, 895–904.

[43] R. Pschorr, *Ber. Dtsch. Chem. Ges.* **1896**, *29*, 496–501.

[44] S. A. Chandler, P. Hanson, A. B. Taylor, P. H. Walton, A. W. Timms, *J. Chem. Soc.* **2001**, 214-228.

[45] K. Laali, M. Shokouhimehr, *Curr. Org. Synth.* **2009**, *6*, 193–202.

[46] F. G. Bordwell, *Acc. Chem. Res.* **1988**, *21*, 456–463.

[47] K. V. Ponmuthu, D. Kumaraguru, J. B. Arockiam, S. Velu, M. Sepperumal, S. Ayyanar, *Res. Chem. Intermed.* **2016**, *42*, 8345–8358.

[48] L. A. Carpino, *Acc. Chem. Res.* **1987**, *20*, 401–407.

[49] B. Liu, W.-L. Yu, Y.-H. Lai, W. Huang, *Chem. Mater.* **2001**, *13*, 1984–1991.

[50] D. Burns, J. Iball, *Nature* **1954**, *173*, 635.

[51] M.-J. Park, J.-H. Lee, D.-H. Hwang, *Curr. Appl. Phys.* **2006**, *6*, 752–755.

[52] B. Liu, W.-L. Yu, Y.-H. Lai, W. Huang, *Macromolecules* **2002**, *35*, 4975–4982.

[53] M. Leclerc, *J. Polym. Sci., Part A: Polym. Chem.* **2001**, *39*, 2867–2873.

[54] D.-H. Hwang, S.-K. Kim, M.-J. Park, J.-H. Lee, B.-W. Koo, B.-W. Kang, S.-H. Kim, T. Zyung, *Chem. Mater.* **2004**.

[55] Y. Xin, G.-A. Wen, W.-J. Zeng, L. Zhao, X.-R. Zhu, Q.-L. Fan, J.-C. Feng, L.-H. Wang, Wei, B. Peng, Y. Cao, W. Wei, *Macromolecules* **2005**, *38*, 6755–6758.

[56] Y. Han, Z. Fei, M. Sun, Z. Bo, W.-Z. Liang, *Macromol. Rapid Commun.* **2007**, *28*, 1017–1023.

[57] a) Y. Zou, T. Ye, D. Ma, J. Qin, C. Yang, *J. Mater. Chem.* **2012**, *22*, 23485; b) X. Yin, J. Miao, Y. Xiang, H. Wu, Y. Cao, C. Yang, *Macromol. Rapid Commun.* **2015**, *36*, 1658–1663.

[58] A. K. Yudin, *Chem. Sci.* **2015**, *6*, 30–49.

[59] G. Crini, *Chem. Rev.* **2014**, *114*, 10940–10975.

[60] G. Crini, S. Fourmentin, É. Fenyvesi, G. Torri, M. Fourmentin, N. Morin-Crini, *Environ. Chem. Lett.* **2018**, *16*, 1361–1375.

[61] H.-S. Byun, N. Zhong, R. Bittman, *Org. Synth.* **2000**, *77*, 220.

[62] A. Motoyama, A. Suzuki, O. Shirota, R. Namba, *J. Pharm. Biomed. Anal.* **2002**, *28*, 97–106.

[63] T. Wimmer in *Ullmann's Encyclopedia of Industrial Chemistry*, Wiley-VCH Verlag GmbH & Co. KGaA, Weinheim, Germany. **2000**.

[64] C. J. Pedersen, *J. Am. Chem. Soc.* **1967**, *89*, 7017–7036.

[65] G. W. Gokel, J. F. Stoddart, *Crown Ethers and Cryptands*, The Royal Society of Chemistry, **1991**.

[66] F. L. Cook, C. W. Bowers, C. L. Liotta, *J. Org. Chem.* **1974**, *39*, 3416–3418.

[67] D. A. Wynn, M. M. Roth, B. D. Pollard, *Talanta* **1984**, *31*, 1036–1040.

[68] J. W. Steed, J. L. Atwood, *Supramolecular Chemistry*, Wiley, Chichester, **2009**.

[69] C. Yoo, H. M. Dodge, A. J. M. Miller, *Chem. Commun.* **2019**, *55*, 5047–5059.

[70] R. Alberto, K. Ortner, N. Wheatley, R. Schibli, A. P. Schubiger, *J. Am. Chem. Soc.* **2001**, *123*, 3135–3136.

[71] The Nobel Prize Foundation, 'MLA style: The Nobel Prize in Chemistry 1987', https://www.nobelprize.org/prizes/chemistry/1987/summary/.

[72] S. Höger, *J. Polym. Sci., Part A: Polym. Chem.* **1999**, *37*, 2685–2698.

[73] M. D. S. Healy, A. J. Rest in *Advances in Inorganic Chemistry and Radiochemistry*, Elsevier. **1978**, 1–40.

[74] W. Zhang, J. S. Moore, *Angew. Chem. Int. Ed.* **2006**, *45*, 4416–4439.

[75] D. Zhao, J. S. Moore, *J. Org. Chem.* **2002**, *67*, 3548–3554.

[76] H. A. Staab, K. Neunhoeffer, *Synthesis* **1974**, *1974*, 424.

[77] S. Höger, V. Enkelmann, *Angew. Chem. Int. Ed.* **1996**, *34*, 2713–2716.

[78] J. S. Moore, J. Zhang, *Angew. Chem. Int. Ed.* **1992**, *31*, 922–924.

[79] J. Zhang, J. S. Moore, Z. Xu, R. A. Aguirre, *J. Am. Chem. Soc.* **1992**, *114*, 2273–2274.

[80] S. Höger, A.-D. Meckenstock, H. Pellen, *J. Org. Chem.* **1997**, *62*, 4556–4557.

[81] J. C. Moore, J. G. Hendrickson, *J. Polym. Sci., Part A: Polym. Chem.* **1965**, *8*, 233–241.

[82] P. K. Hansma, J. Tersoff, *J. Appl. Phys.* **1987**, *61*, R1-R24.

[83] G. Binnig, H. Rohrer, C. Gerber, E. Weibel, *Phys. Rev. Lett.* **1982**, *49*, 57–61.

[84] Nobel Media AB, 'The Nobel Prize in Physics 1986 - Press Release', https://www.nobelprize.org/nobel_prizes/physics/laureates/1986/press.html.

[85] M. Schmid, 'The Scanning Tunneling Microscope', http://www.iap.tuwien.ac.at/www/surface/stm_gallery/stm_schematic#copyright_notice.

[86] S.-S. Jester, A. Idelson, D. Schmitz, F. Eberhagen, S. Höger, *Langmuir : the ACS journal of surfaces and colloids* **2011**, *27*, 8205–8215.

[87] Y. Kuk, P. J. Silverman, *Rev. Sci. Instrum.* **1989**, *60*, 165–180.

[88] T. J. Keller, C. Sterzenbach, J. Bahr, T. L. Schneiders, M. Bursch, J. Kohn, T. Eder, J. M. Lupton, S. Grimme, S. Höger, S.-S. Jester, *Chem. Sci.* **2021**, *12*, 9352–9358.

[89] S.-S. Jester, E. Sigmund, S. Höger, *J. Am. Chem. Soc.* **2011**, *133*, 11062–11065.

[90] A. Ziegler, W. Mamdouh, an ver Heyen, M. Surin, H. Uji-i, M. M. S. Abdel-Mottaleb, F. C. de Schryver, S. de Feyter, R. Lazzaroni, S. Höger, *Chem. Mater.* **2005**, *17*, 5670–5683.

[91] D. Mössinger, J. Hornung, S. Lei, S. de Feyter, S. Höger, *Angew. Chem. Int. Ed.* **2007**, *46*, 6802–6806.

[92] D. Mössinger, *Dissertation*, University of Bonn, **2009**.

[93] a) V. Aggarwal, *Dissertation*, University of Bonn, **2012**; b) J. Burdyńska, Y. Li, A. V. Aggarwal, S. Höger, S. S. Sheiko, K. Matyjaszewski, *J. Am. Chem. Soc.* **2014**, *136*, 12762–12770.

[94] R. May, S.-S. Jester, S. Höger, *J. Am. Chem. Soc.* **2014**, *136*, 16732–16735.

[95] R. May, *Dissertation*, University of Bonn, **2014**.

[96] A. Idelson, C. Sterzenbach, S.-S. Jester, C. Tschierske, U. Baumeister, S. Höger, *J. Am. Chem. Soc.* **2017**, *139*, 4429–4434.

[97] P. Krämer, J. Kohn, D. A. Hofmeister, M. Kersten, C. Sterzenbach, A. Gres, A. Hansen, S.-S. Jester, S. Grimme, S. Höger, *Angew. Chem. Int. Ed.* **2024**, e202411092.

[98] W. G. L. Aalbersberg, A. J. Barkovich, R. L. Funk, R. L. Hillard, K. P. C. Vollhardt, *J. Am. Chem. Soc.* **1975**, *97*, 5600–5602.

[99] T. Yamamoto, S. Wakabayashi, K. Osakada, *J. Organomet. Chem.* **1992**, *428*, 223–237.

[100] T. Zimmermann, G. W. Fischer, *J. Prakt. Chem.* **1987**, *329*, 975–984.

[101] G. N. Dorofeenko, L. B. Olekhnovich, *Chem. Heterocycl. Compd.* **1972**, *8*, 800–802.

[102] A. T. Balaban, W. Schroth, G. Fischer in *Advances in Heterocyclic Chemistry*, Elsevier. **1969**, 241–326.

[103] Y. Li, H. Wang, X. Li, *Chem. Sci.* **2020**, *11*, 12249–12268.

[104] A. M. Bello, L. P. Kotra, *Tetrahedron Lett.* **2003**, *44*, 9271–9274.

[105] M. Kersten, *Dissertation*, University of Bonn, **2021**.

[106] L. zur Horst, *Dissertation*, University of Bonn, **2023**.

[107] V. Percec, M. Peterca, Y. Tsuda, B. M. Rosen, S. Uchida, M. R. Imam, G. Ungar, P. A. Heiney, *Chem. Eur. J.* **2009**, *15*, 8994–9004.

[108] C. Sterzenbach, *Dissertation*, University of Bonn, **2019**.

[109] T. Schneiders, *Bachelor Thesis*, University of Bonn, **2017**.

[110] J.-M. Lehn, *Supramolecular Chemistry*, VCH, Weinheim, New York, **1995**.

[111] J. B. Wittenberg, L. Isaacs in *Supramolecular Chemistry* (Editors P. A. Gale, J. W. Steed), Wiley. **2012**.

[112] R. P. Matthews, T. Welton, P. A. Hunt, *Phys. Chem. Chem. Phys.* **2014**, *16*, 3238–3253.

[113] B. Kohl, M. V. Bohnwagner, F. Rominger, H. Wadepohl, A. Dreuw, M. Mastalerz, *Chem. Eur. J.* **2016**, *22*, 646–655.

[114] B. Kohl, K. Baumgärtner, F. Rominger, M. Mastalerz, *Eur. J. Org. Chem.* **2019**, *2019*, 4891–4896.

[115] A. Idelson, *Dissertation*, University of Bonn, **2015**.

[116] S. Becker, *Dissertation*, University of Bonn, **2018**.

[117] M. Takase, A. Nakajima, T. Takeuchi, *Tetrahedron Lett.* **2005**, *46*, 1739–1742.

[118] A. Klapars, S. L. Buchwald, *J. Am. Chem. Soc.* **2002**, *124*, 14844–14845.

[119] P. Krämer, *Master Thesis*, University of Bonn, **2020**.

[120] Z.-T. He, J. F. Hartwig, *Nat. Commun.* **2019**, *10*, 4083.

[121] K. Kamtekar, A. Steudel, M. Humphries, US2015274890 (A1), **3/31/2015**.

[122] T. Hama, S. Ge, J. F. Hartwig, *J. Org. Chem* **2013**, *78*, 8250–8266.

[123] S. Rickert, *Dissertation*, University of Bonn, **2024**.

[124] G. G. Abashev, K. Y. Lebedev, I. V. Osorgina, E. V. Shklyaeva, *Russ. J. Org. Chem.* **2006**, *42*, 1873–1876.

[125] R. Grisorio, G. Allegretta, P. Mastrorilli, G. P. Suranna, *Macromolecules* **2011**, *44*, 7977–7986.

[126] A. Gres, *Bachelor Thesis*, University of Bonn, **2022**.

[127] P. K. Mandali, D. K. Chand, *Catal. Commun.* **2014**, *47*, 40–44.

[128] X. Lei, A. Jalla, M. Abou Shama, J. Stafford, B. Cao, *Synthesis* **2015**, *47*, 2578–2585.

[129] S. E. Yoon, S. J. Shin, S. Y. Lee, G. G. Jeon, H. Kang, H. Seo, J. Zheng, J. H. Kim, *ACS Appl. Polym. Mater.* **2020**, *2*, 2729–2735.

[130] M. Mamone, T. Bura, S. Brassard, E. Soligo, K. He, Y. Li, M. Leclerc, *Mater. Chem. Front.* **2020**, *4*, 2040–2046.

[131] S. S. Kim, S. Sar, P. Tamrakar, *Bull. Korean Chem. Soc.* **2002**, *23*, 937–938.

[132] L. Mayer, R. Kohlbecher, T. J. J. Müller, *Chem. Eur. J.* **2020**, *26*, 15130–15134.

[133] C. He, P. Liu, P. J. McMullan, A. C. Griffin, *Phys. Status Solidi* **2005**, *242*, 576–584.

[134] J. Zhuang, H. Seçinti, B. Zhao, S. Thayumanavan, *Angew. Chem., Int. Ed.* **2018**, *130*, 7229–7233.

[135] A. E. Brown, B. E. Eichler, *Tetrahedron Lett.* **2011**, *52*, 1960–1963.

[136] D. C. Harrowven, D. P. Curran, S. L. Kostiuk, I. L. Wallis-Guy, S. Whiting, K. J. Stenning, B. Tang, E. Packard, L. Nanson, *Chem. Commun.* **2010**, *46*, 6335–6337.

[137] T. Furuya, A. E. Strom, T. Ritter, *J. Am. Chem. Soc.* **2009**, *131*, 1662–1663.

[138] P. S. Gribanov, Y. D. Golenko, M. A. Topchiy, L. I. Minaeva, A. F. Asachenko, M. S. Nechaev, *Eur. J. Org. Chem.* **2018**, *2018*, 120–125.

[139] N. G. Andersen, B. A. Keay, *Chem. Rev.* **2001**, *101*, 997–1030.

[140] G. Ohlendorf, C. W. Mahler, S.-S. Jester, G. Schnakenburg, S. Grimme, S. Höger, *Angew. Chem. Int. Ed.* **2013**, *52*, 12086–12090.

[141] A. Roth, *unpublished results*, University of Bonn, **2024**.

[142] S. Schimmelpfennig, *unpublished results*, University of Bonn, **2024**.

[143] S. Höger, K. Bonrad, *J. Org. Chem.* **2000**, *65*, 2243–2245.

[144] M. D. Hanwell, D. E. Curtis, D. C. Lonie, T. Vandermeersch, E. Zurek, G. R. Hutchison, *J. Cheminform.* **2012**, *4*, 17.

[145] C. Bannwarth, S. Ehlert, S. Grimme, *J. Chem. Theory. Comput.* **2019**, *15*, 1652–1671.

[146] Grimme Lab, 'Semiempirical Extended Tight-Binding Program Package xtb', https://github.com/grimme-lab/xtb, accessed: 2024.

[147] W. Humphrey, A. Dalke, K. Schulten, *J. Mol. Graph.* **1996**, *14*, 33-8, 27-8.

[148] S. Spicher, S. Grimme, *Angew. Chem., Int. Ed.* **2020**, *132*, 15795–15803.

[149] S. Ehlert, M. Stahn, S. Spicher, S. Grimme, *J. Chem. Theory. Comput.* **2021**, *17*, 4250–4261.

[150] S. Grimme, A. Hansen, S. Ehlert, J.-M. Mewes, *J. Chem. Phys.* **2021**, *154*, 64103.

[151] A. Klamt, *WIREs Comput. Mol. Sci.* **2011**, *1*, 699–709.

[152] F. Furche, R. Ahlrichs, C. Hättig, W. Klopper, M. Sierka, F. Weigend, *WIREs Comput. Mol. Sci.* **2014**, *4*, 91–100.

[153] B. Peters, A. Heyden, A. T. Bell, A. Chakraborty, *J. Chem. Phys.* **2004**, *120*, 7877–7886.

[154] F. Neese, *Software update: The ORCA program system—Version 5.0,* **2022**.

[155] a) A. Klamt, *J. Phys. Chem.* **1995**, *99*, 2224–2235; b) J. G. Brandenburg, C. Bannwarth, A. Hansen, S. Grimme, *J. Chem. Phys.* **2018**, *148*, 64104.

[156] M. Müller, A. Hansen, S. Grimme, *J. Chem. Phys.* **2023**, *158*, 14103.

[157] D. Göbel, P. Rusch, D. Duvinage, N. C. Bigall, B. J. Nachtsheim, *Chem. Commun.* **2020**, *56*, 15430–15433.

[158] R. Grisorio, C. Piliego, P. Cosma, P. Fini, P. Mastrorilli, G. Gigli, G. P. Suranna, C. F. Nobile, *Tetrahedron* **2008**, *64*, 8738–8745.

10.4 Spectra

10.4.1 NMR spectra

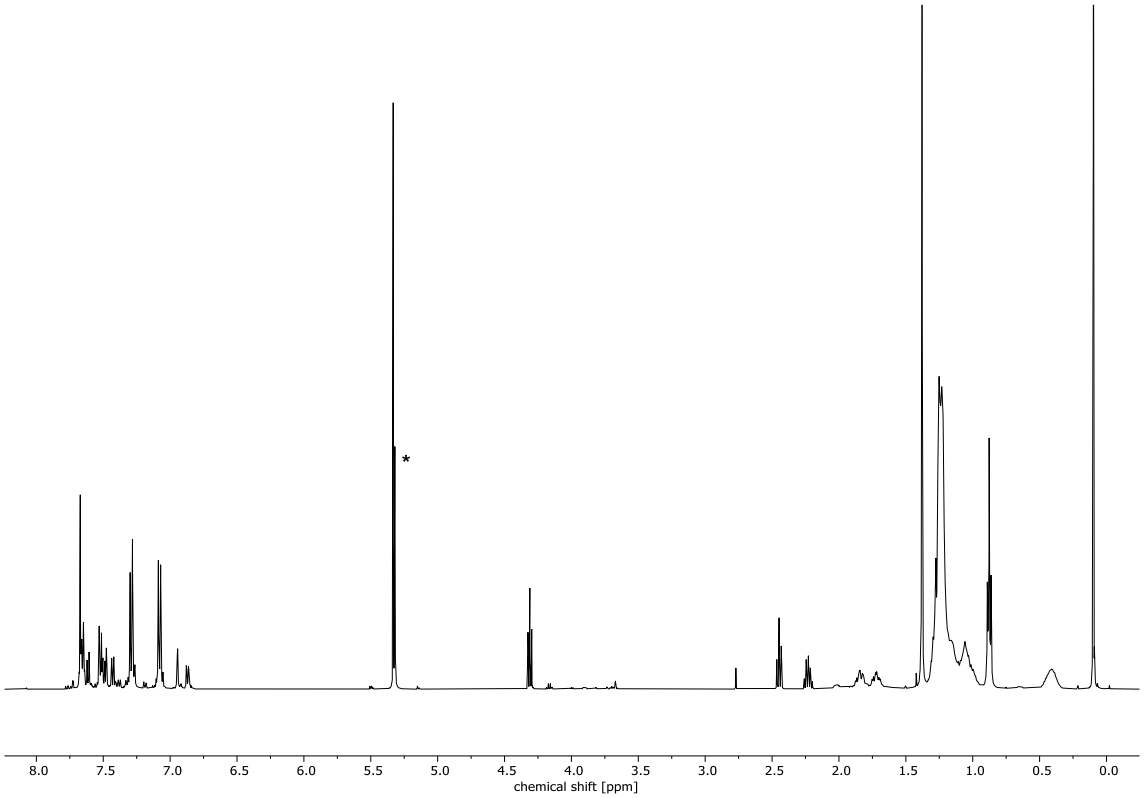

Figure 87: ^{1}H-NMR spectrum of **17a** (500 MHz, CD_2Cl_2, 298 K), solvent marked with *.

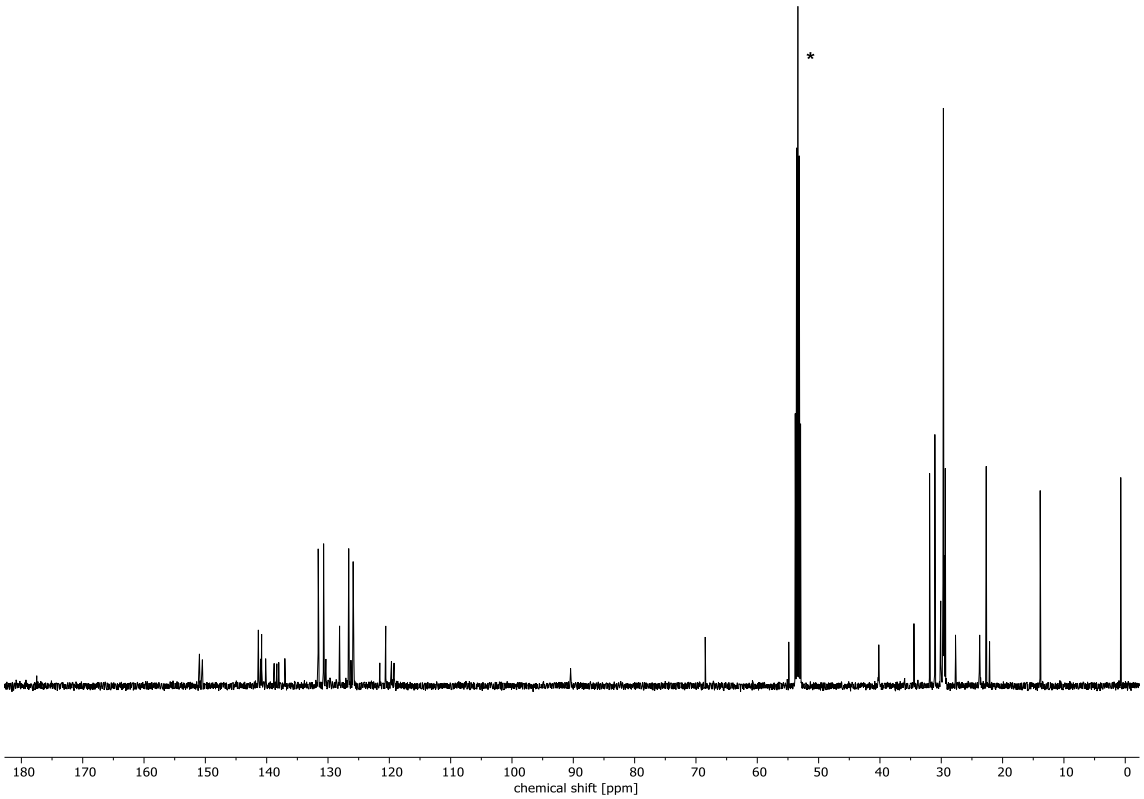

Figure 88: ^{13}C-NMR spectrum of **17a** (126 MHz, CD_2Cl_2, 298 K), solvent marked with *.

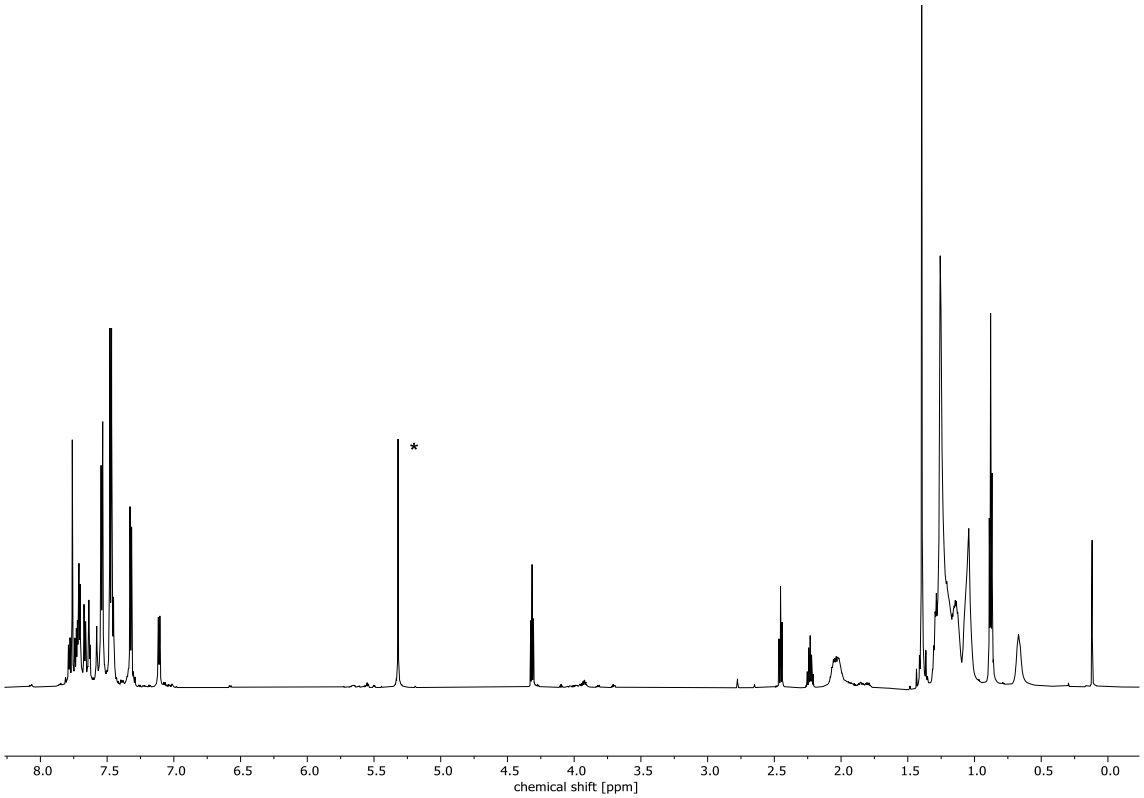

Figure 89: ^{1}H-NMR spectrum of **39** (700 MHz, CD_2Cl_2, 298 K), solvent marked with *.

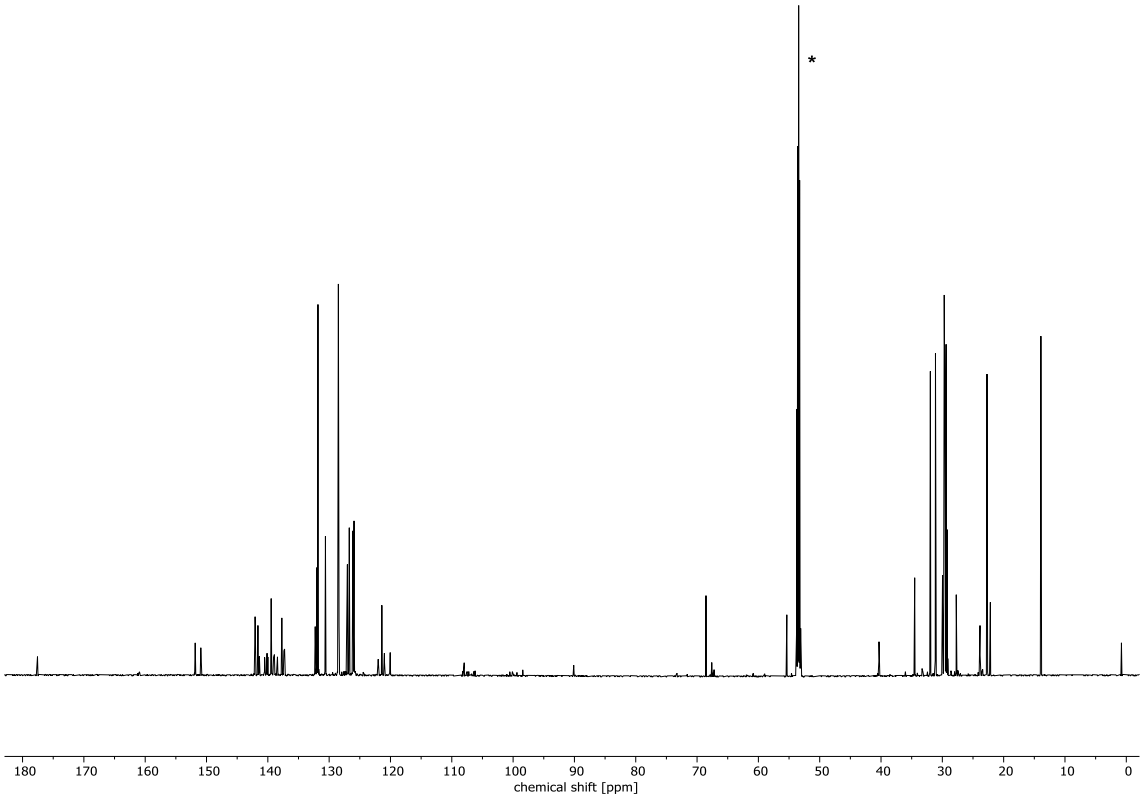

Figure 90: ^{13}C-NMR spectrum of **39** (176 MHz, CD_2Cl_2, 298 K), solvent marked with *.

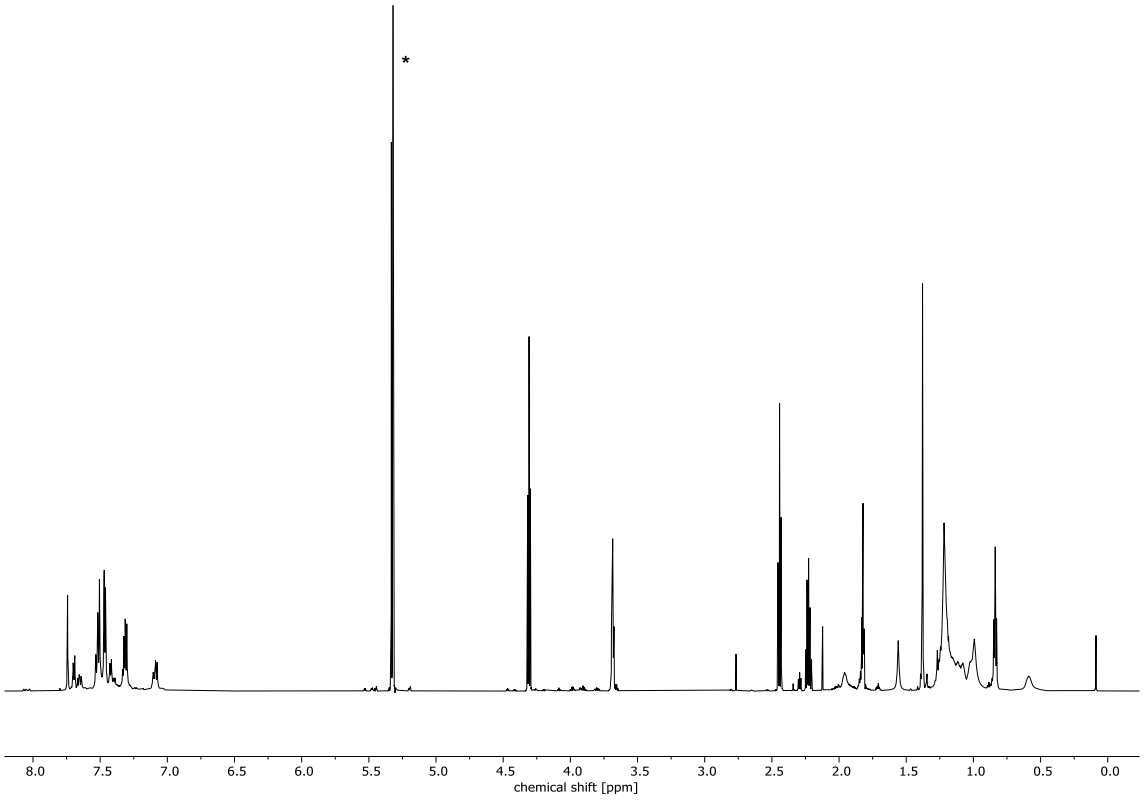

Figure 91: ^{1}H-NMR spectrum of **40** (700 MHz, CD_2Cl_2, 298 K), solvent marked with *.

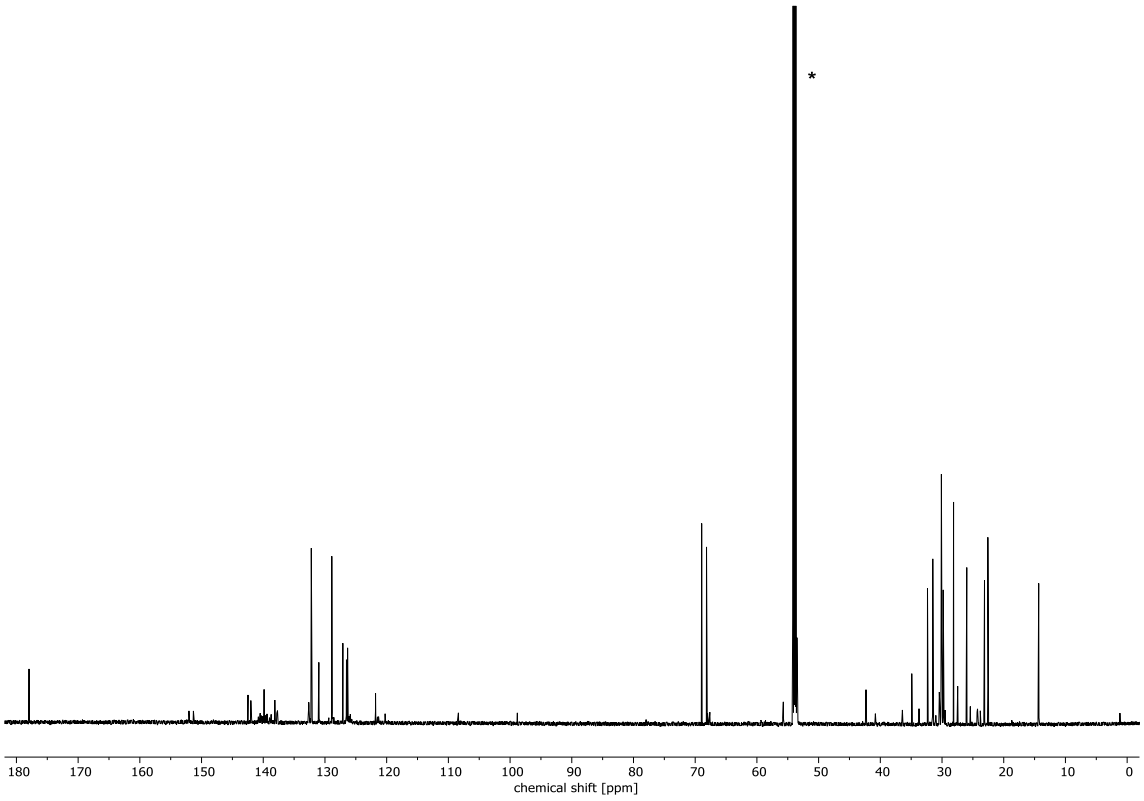

Figure 92: ^{13}C-NMR spectrum of **40** (176 MHz, CD_2Cl_2, 298 K), solvent marked with *.

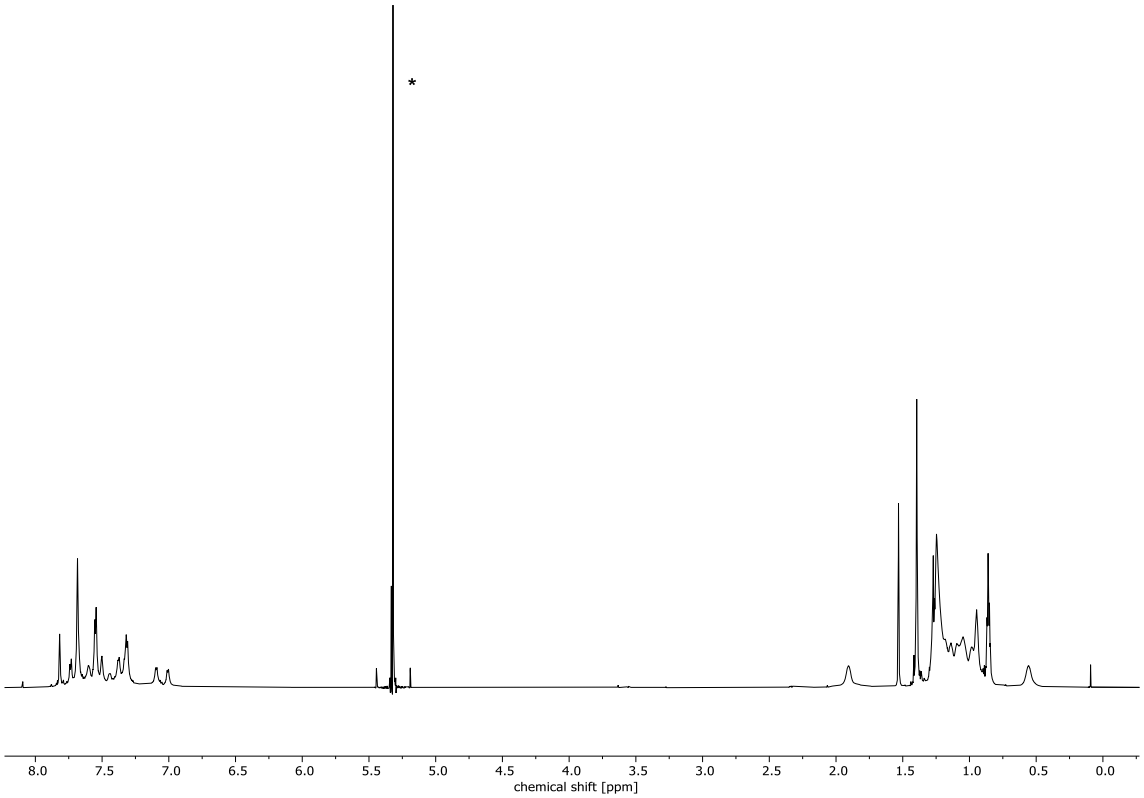

Figure 93: ^{1}H-NMR spectrum of **MSW-C** (700 MHz, CD_2Cl_2, 298 K), solvent marked with *.

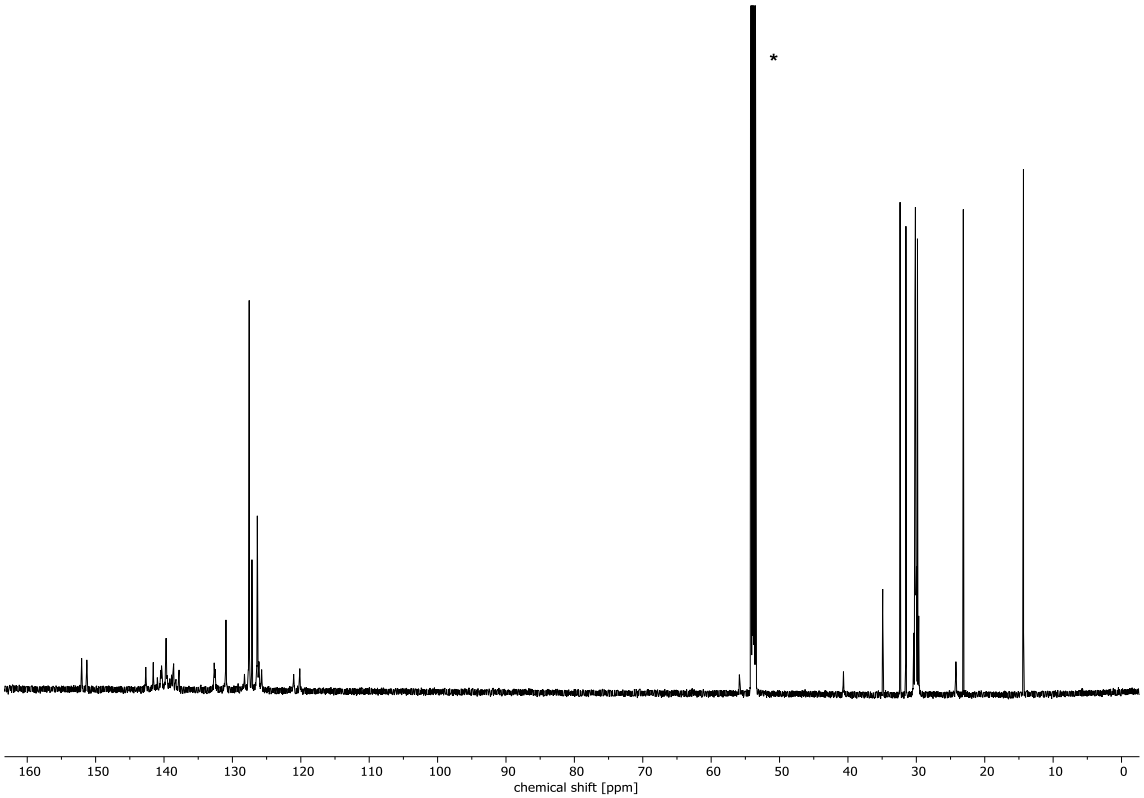

Figure 94: ^{13}C-NMR spectrum of **MSW-C** (176 MHz, CD_2Cl_2, 298 K), solvent marked with *.

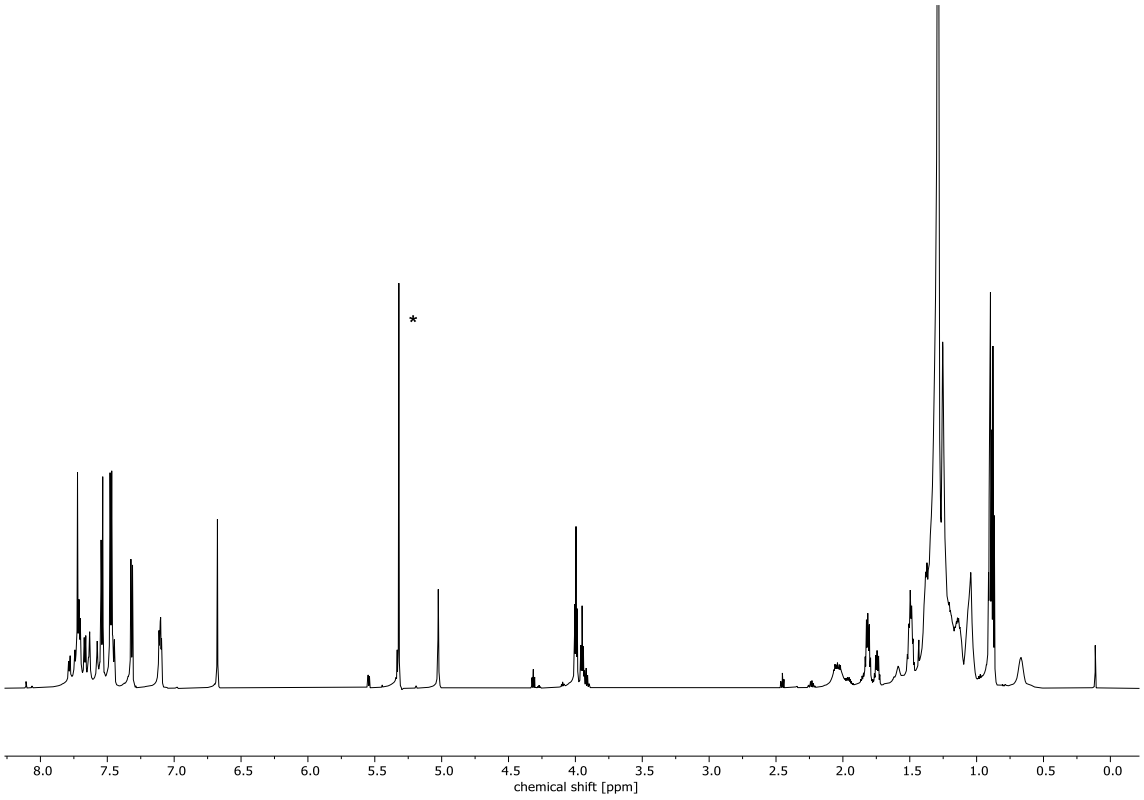

Figure 95: ^{1}H-NMR spectrum of **70a** (500 MHz, CD_2Cl_2, 298 K), solvent marked with *.

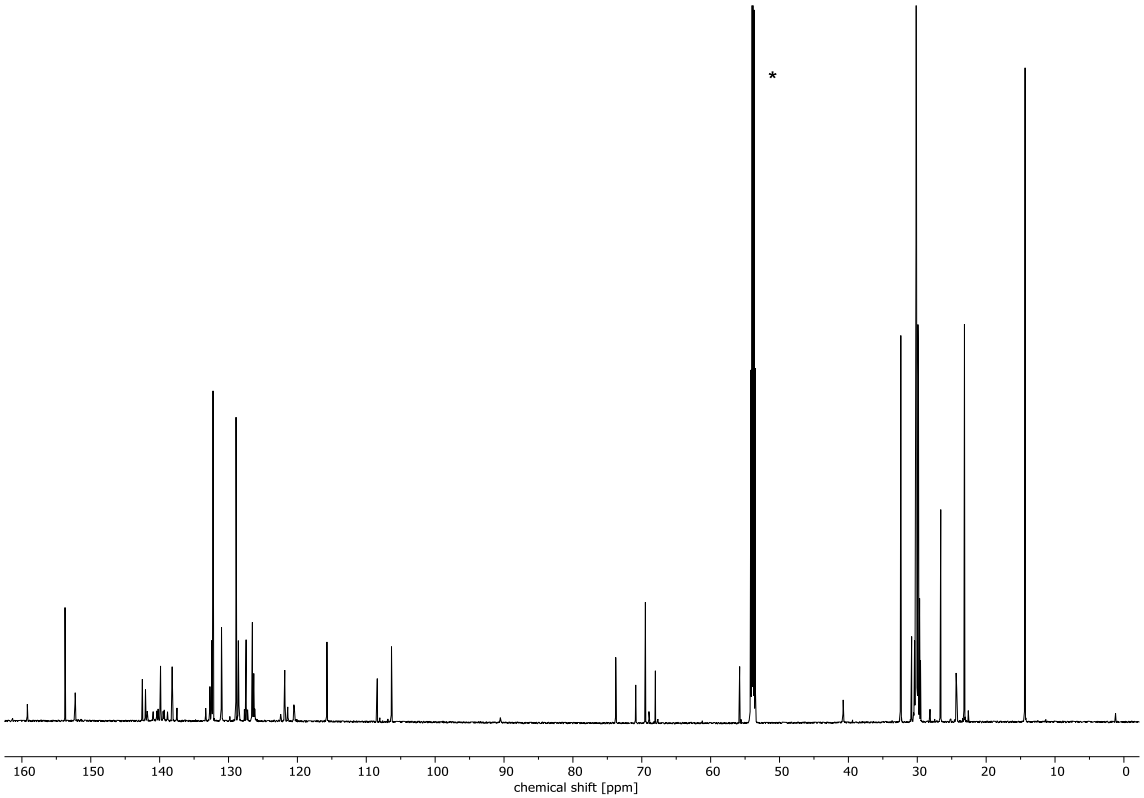

Figure 96: ^{13}C-NMR spectrum of **70a** (126 MHz, CD_2Cl_2, 298 K), solvent marked with *.

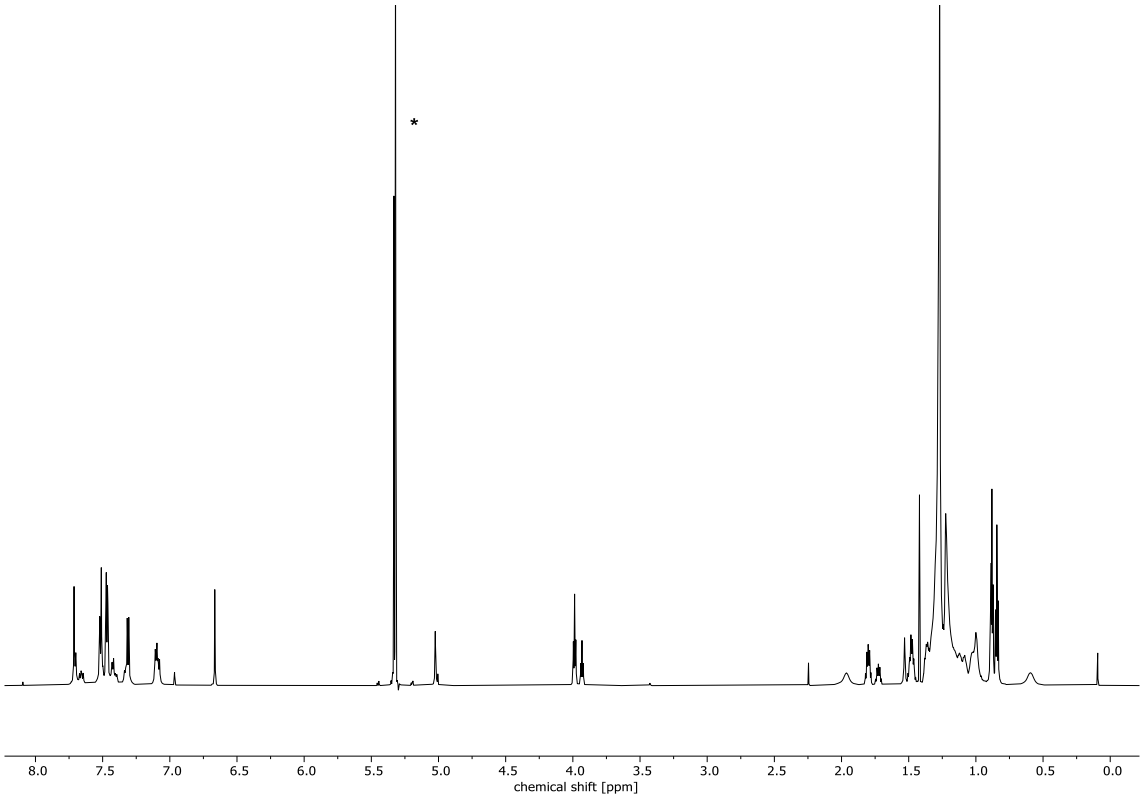

Figure 97: ^{1}H-NMR spectrum of **71a** (700 MHz, CD_2Cl_2, 298 K), solvent marked with *.

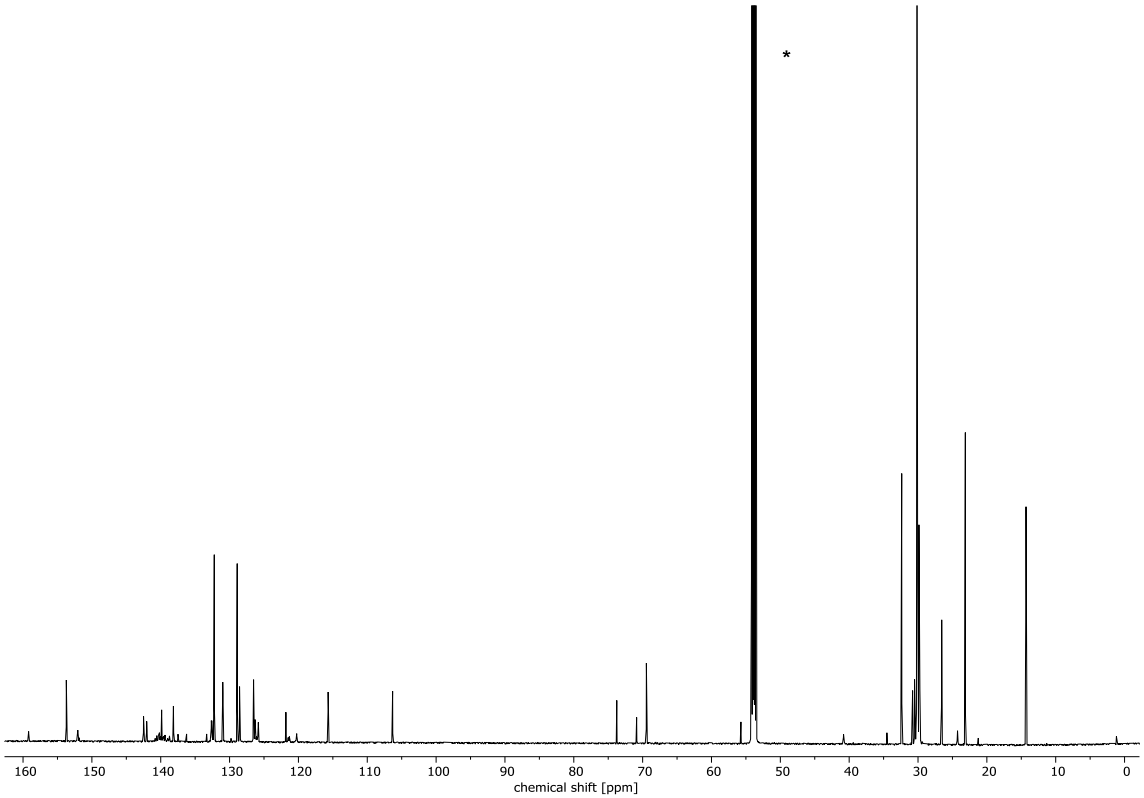

Figure 98: ^{13}C-NMR spectrum of **71a** (176 MHz, CD_2Cl_2, 298 K), solvent marked with *.

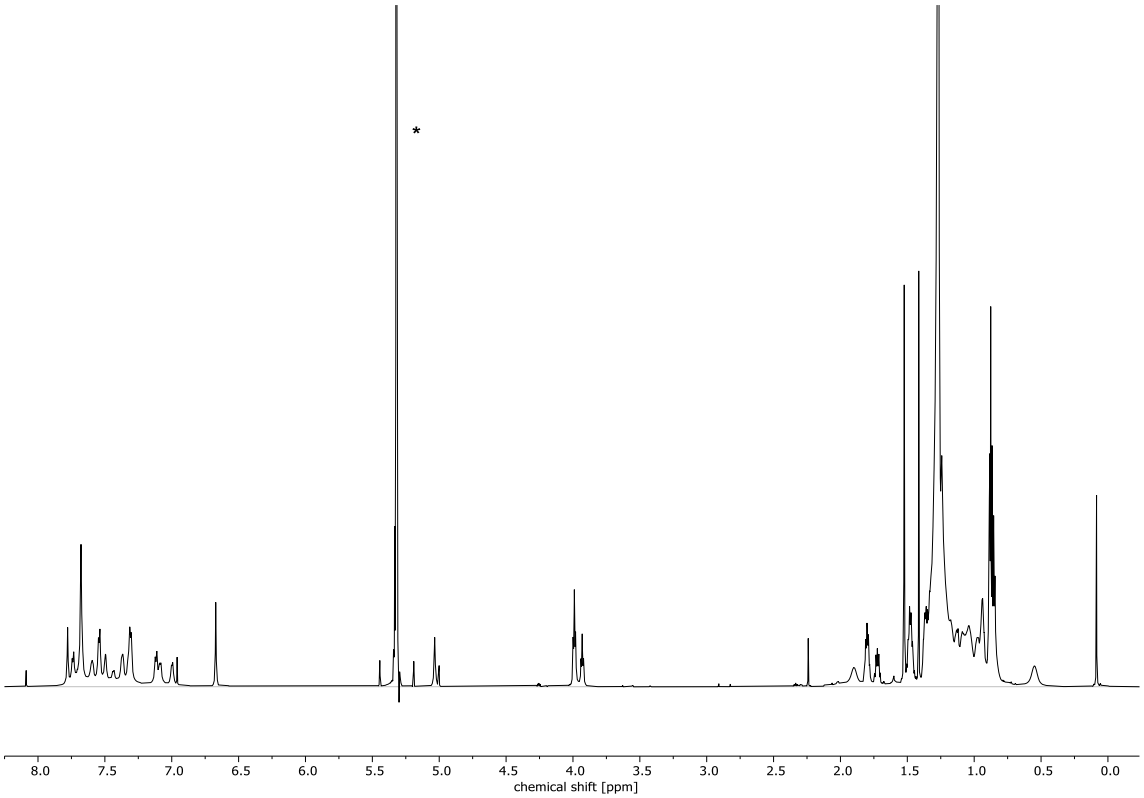

Figure 99: ^{1}H-NMR spectrum of **MSW-Fa** (700 MHz, CD_2Cl_2, 298 K), solvent marked with *.

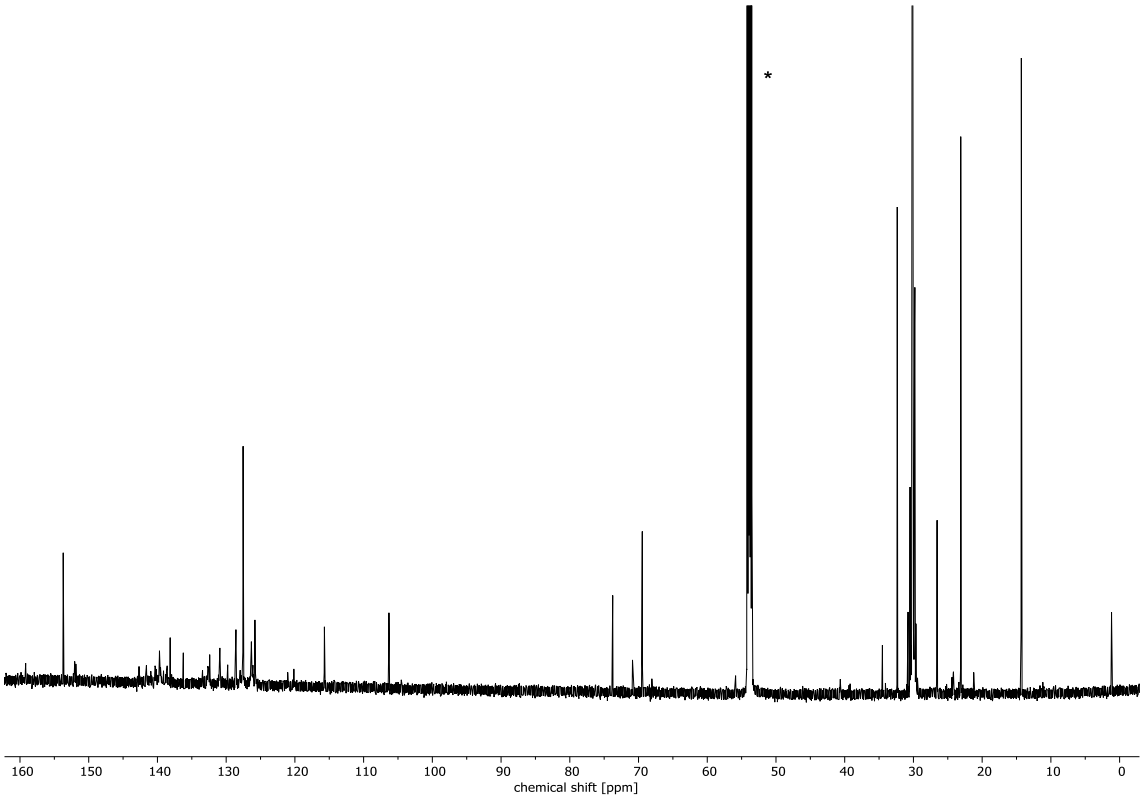

Figure 100: ^{13}C-NMR spectrum of **MSW-Fa** (176 MHz, CD_2Cl_2, 298 K), solvent marked with *.

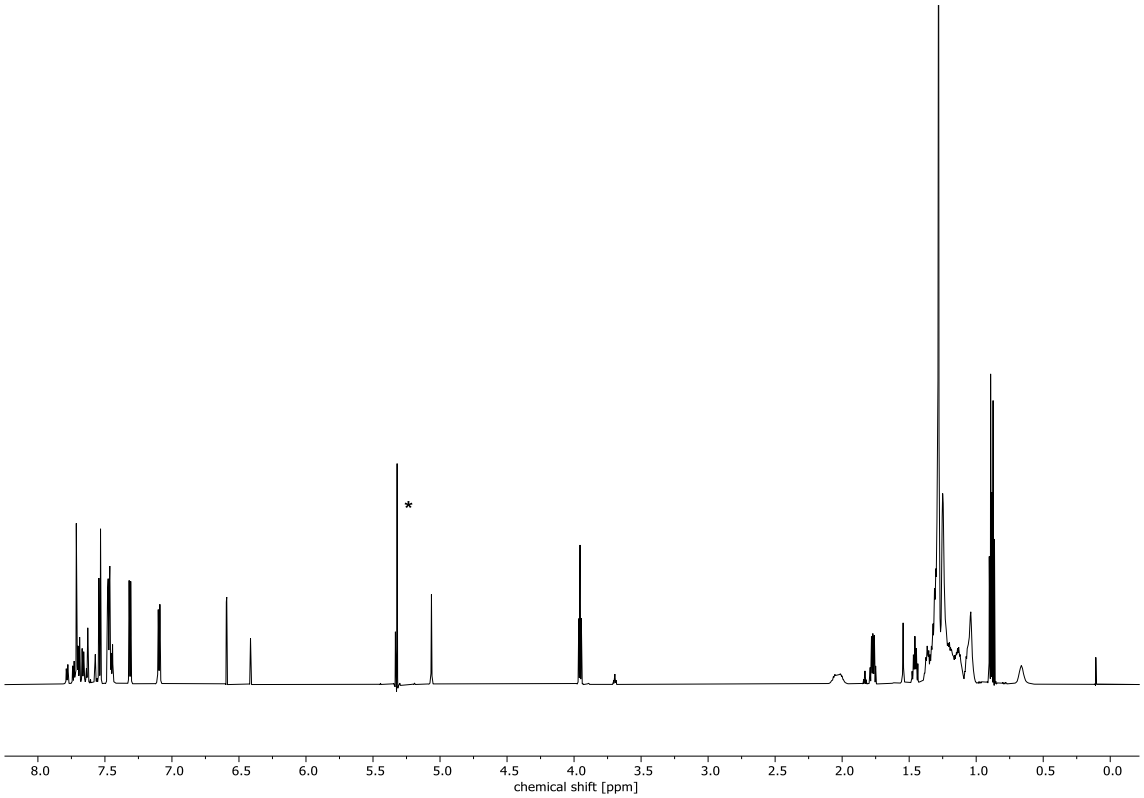

Figure 101: ^{1}H-NMR spectrum of **70b** (700 MHz, CD_2Cl_2, 298 K), solvent marked with *.

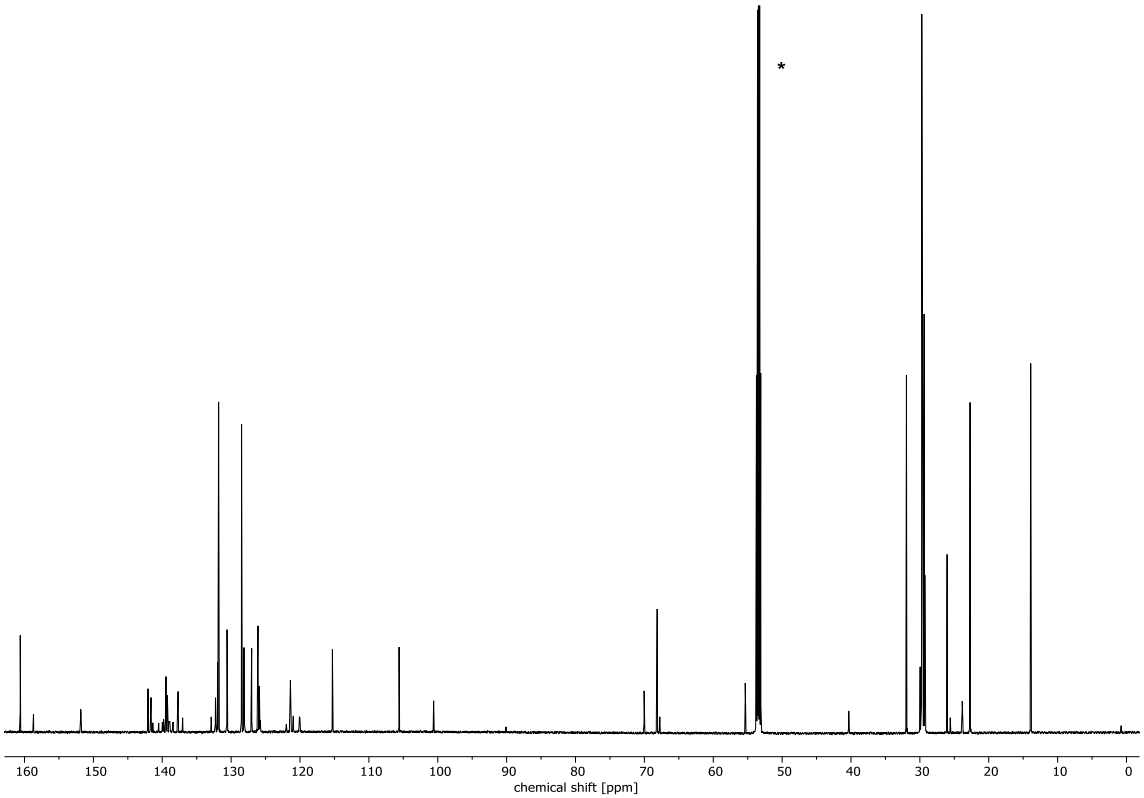

Figure 102: ^{13}C-NMR spectrum of **70b** (176 MHz, CD_2Cl_2, 298 K), solvent marked with *.

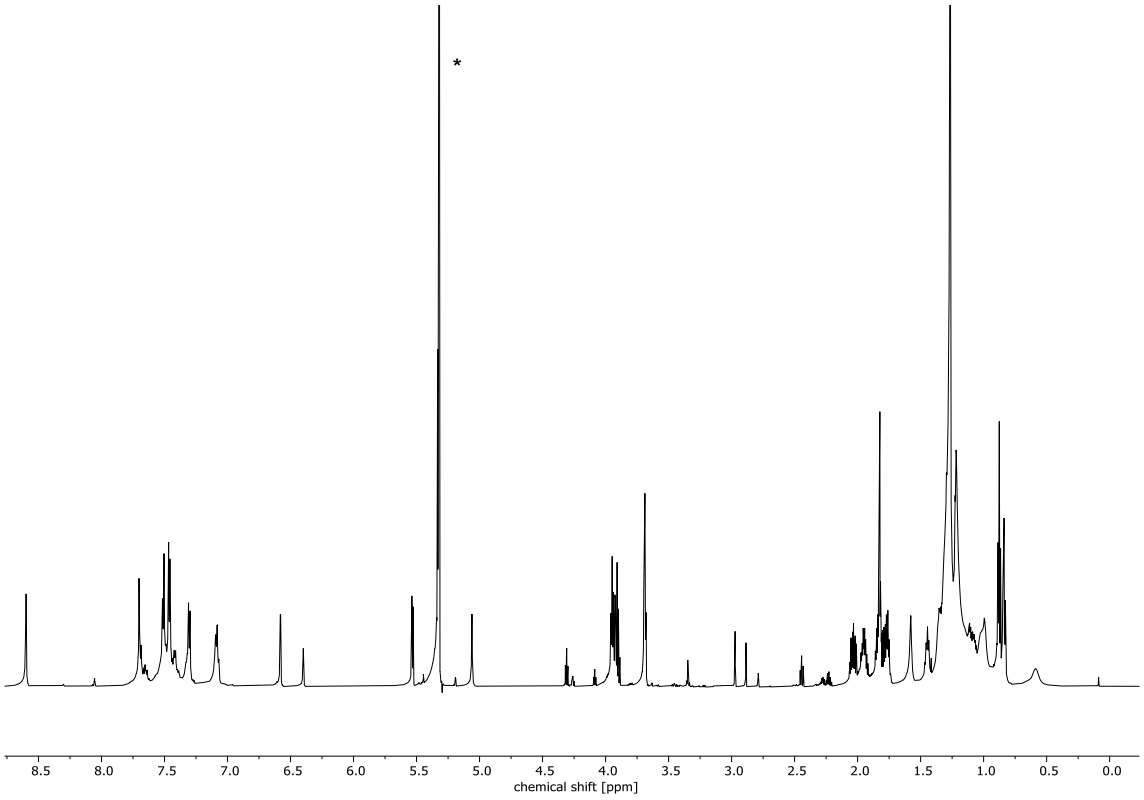

Figure 103: ^{1}H-NMR spectrum of **71b** (700 MHz, CD_2Cl_2, 298 K), solvent marked with *.

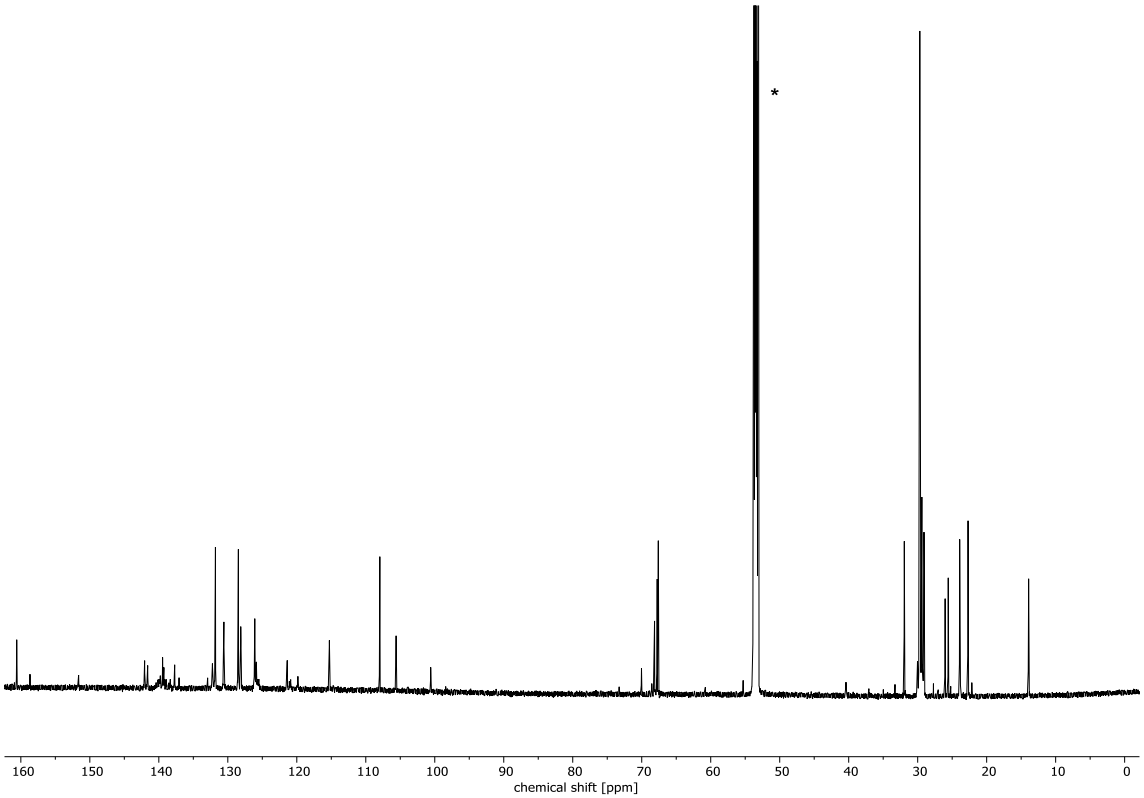

Figure 104: ^{13}C-NMR spectrum of **71b** (176 MHz, CD_2Cl_2, 298 K), solvent marked with *.

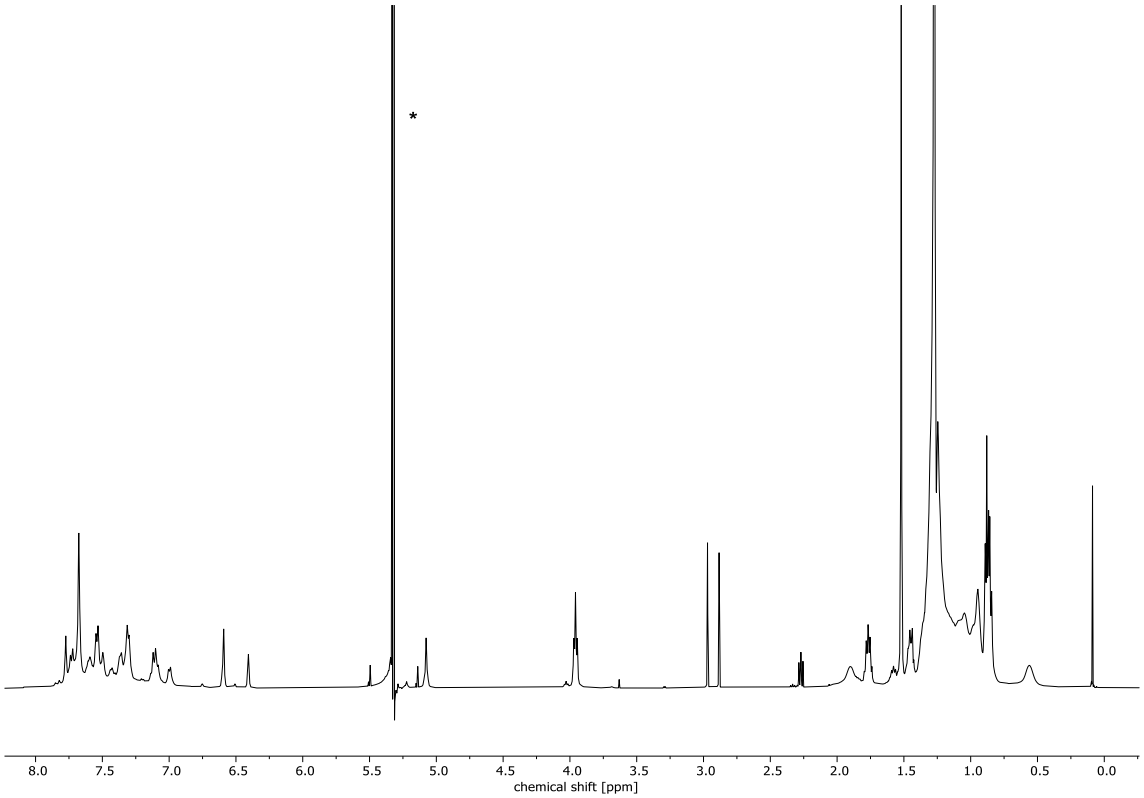

Figure 105: ^{1}H-NMR spectrum of **MSW-Fb** (700 MHz, CD_2Cl_2, 298 K), solvent marked with *.

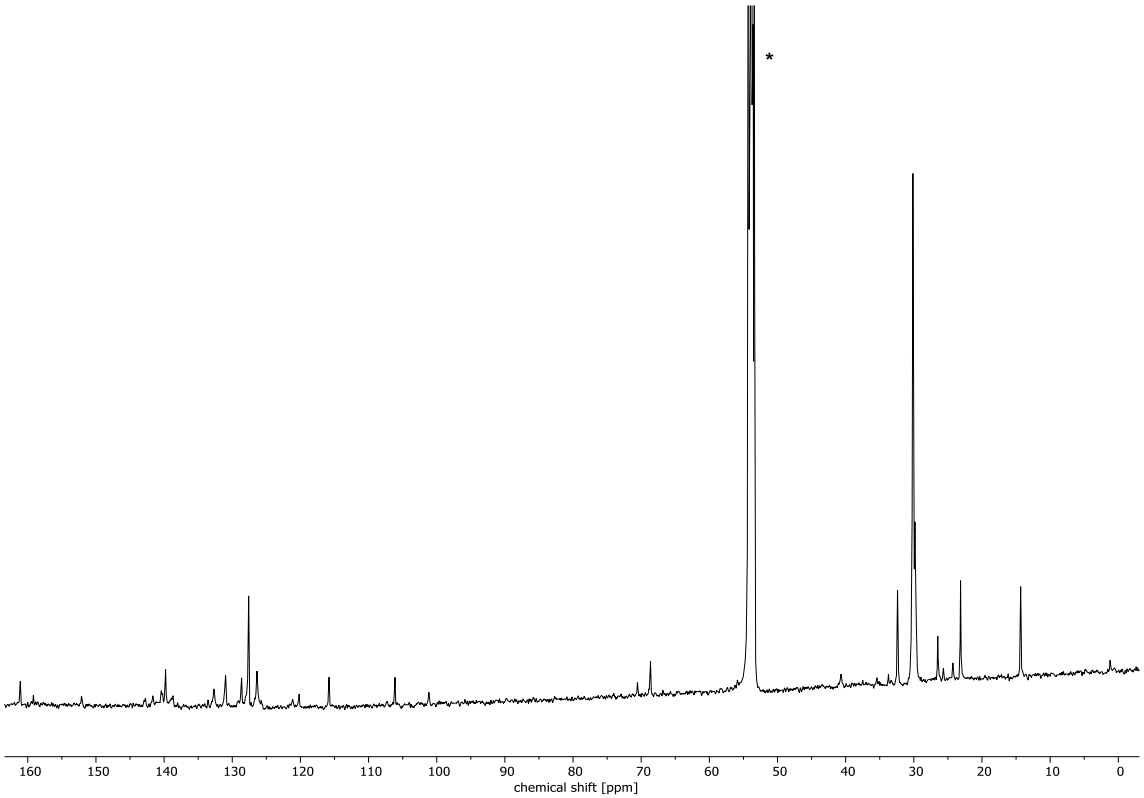

Figure 106: ^{13}C-NMR spectrum of **MSW-Fb** (176 MHz, CD_2Cl_2, 298 K), solvent marked with *.

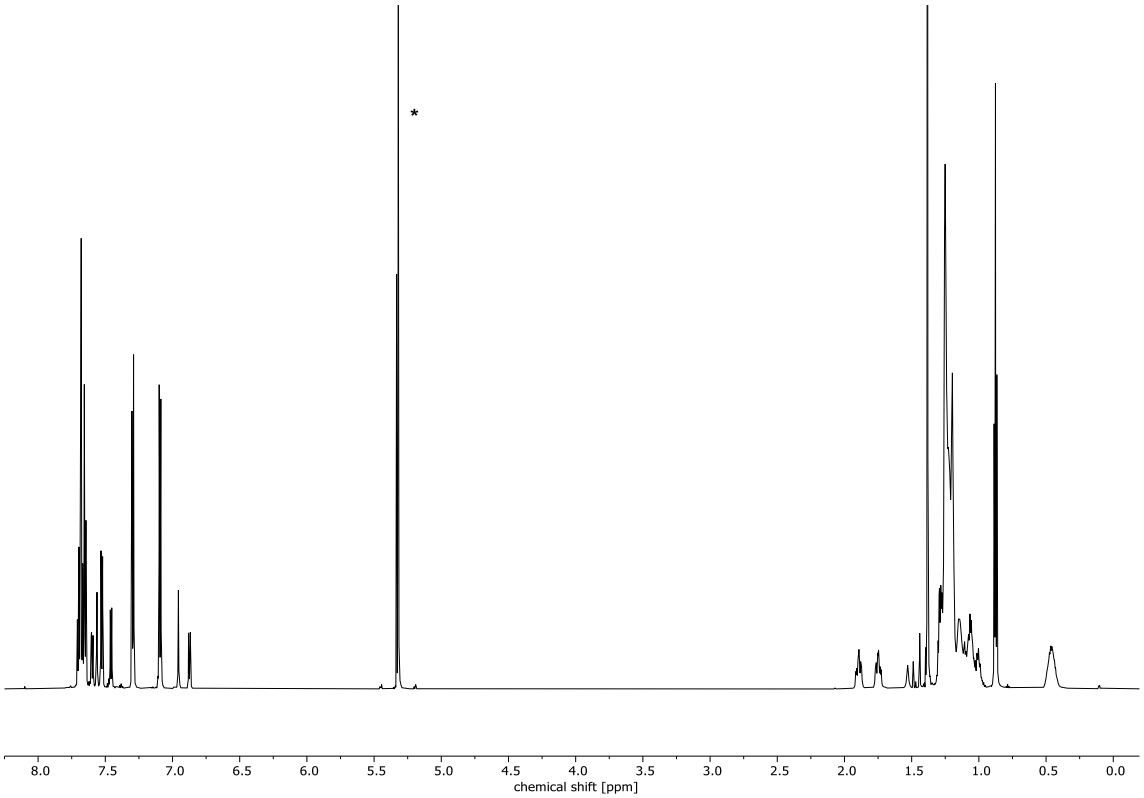

Figure 107: ^{1}H-NMR spectrum of **73** (700 MHz, CD_2Cl_2, 298 K), solvent marked with *.

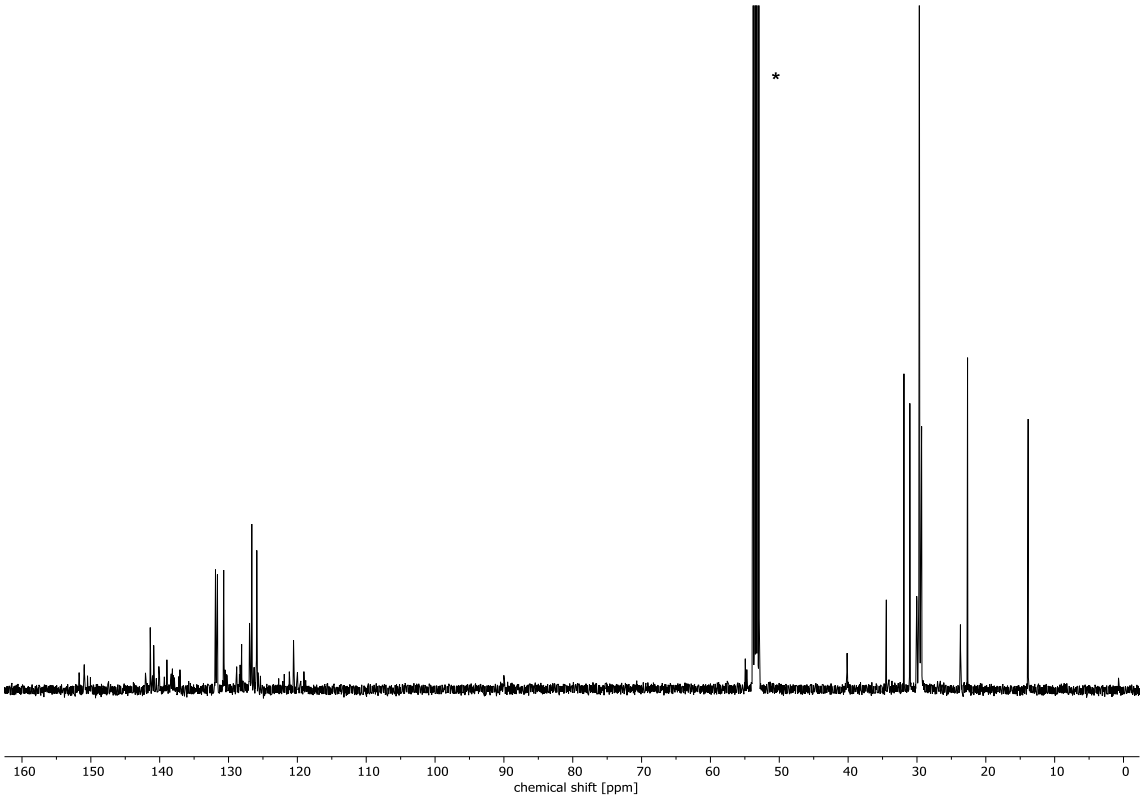

Figure 108: ^{13}C-NMR spectrum of **73** (176 MHz, CD_2Cl_2, 298 K), solvent marked with *.

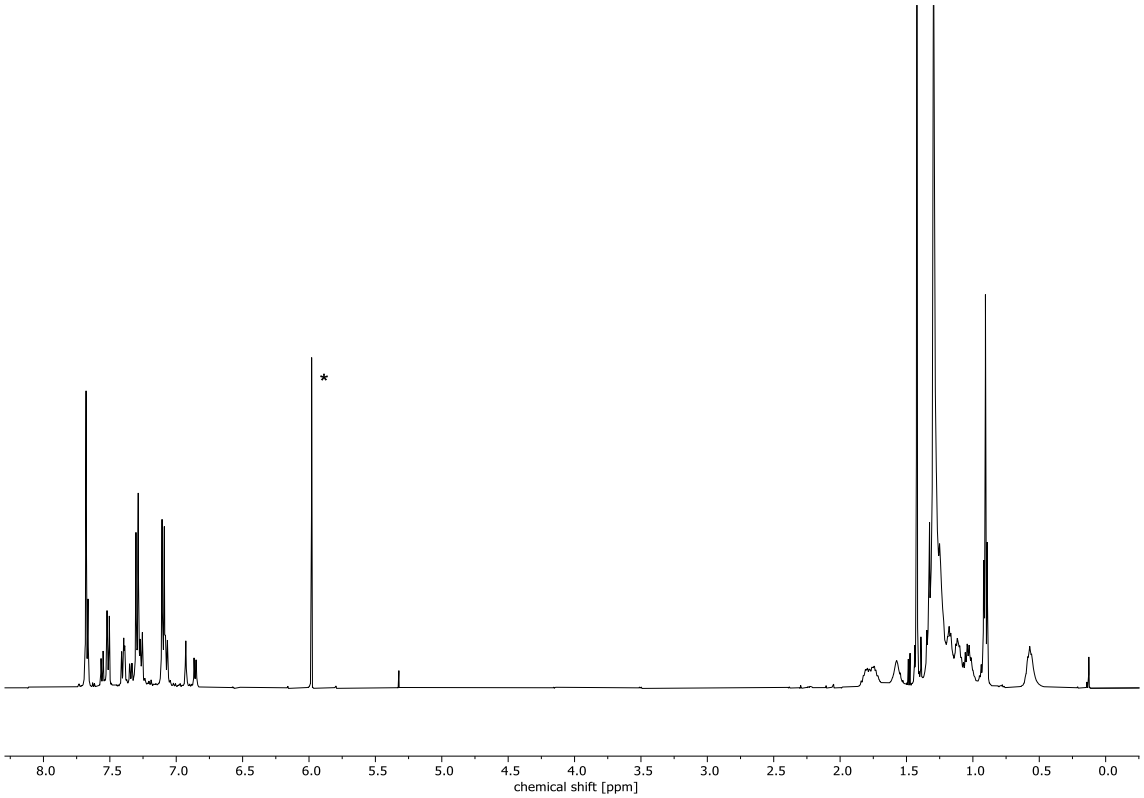

Figure 109: ^{1}H-NMR spectrum of **74** (700 MHz, $C_2D_2Cl_4$, 373 K), solvent marked with *.

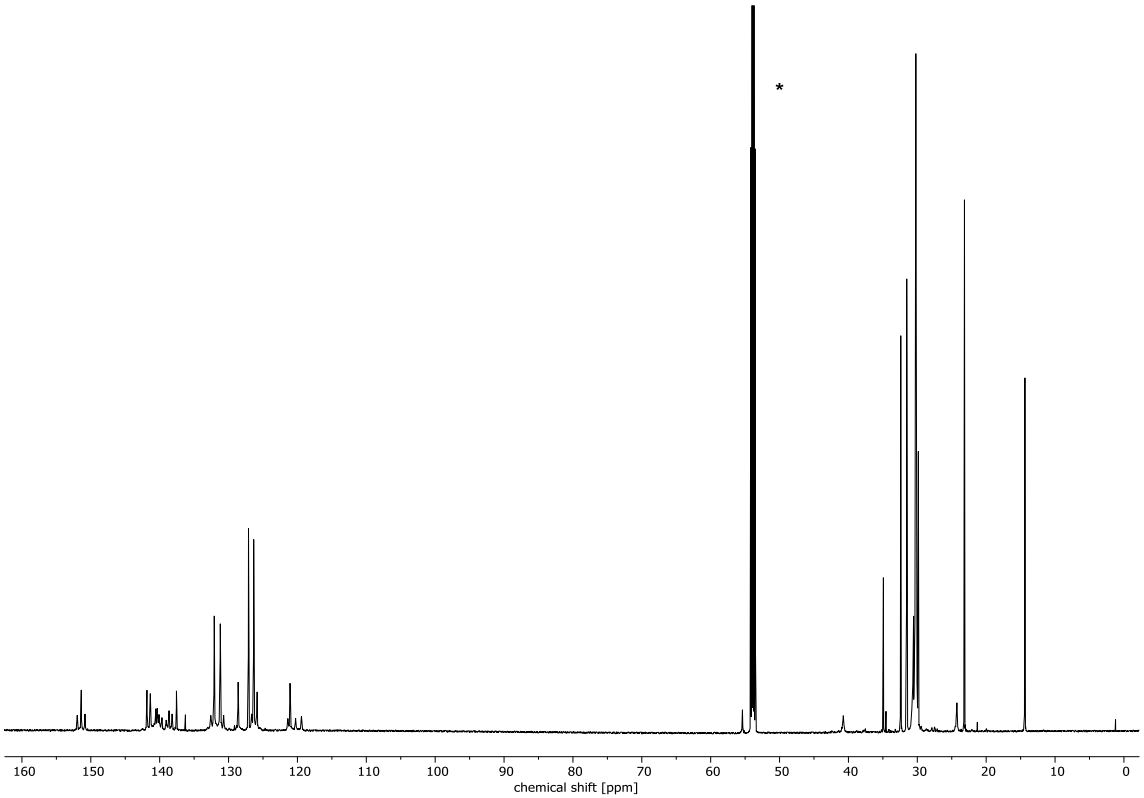

Figure 110: ^{13}C-NMR spectrum of **74** (176 MHz, CD_2Cl_2, 298 K), solvent marked with *.

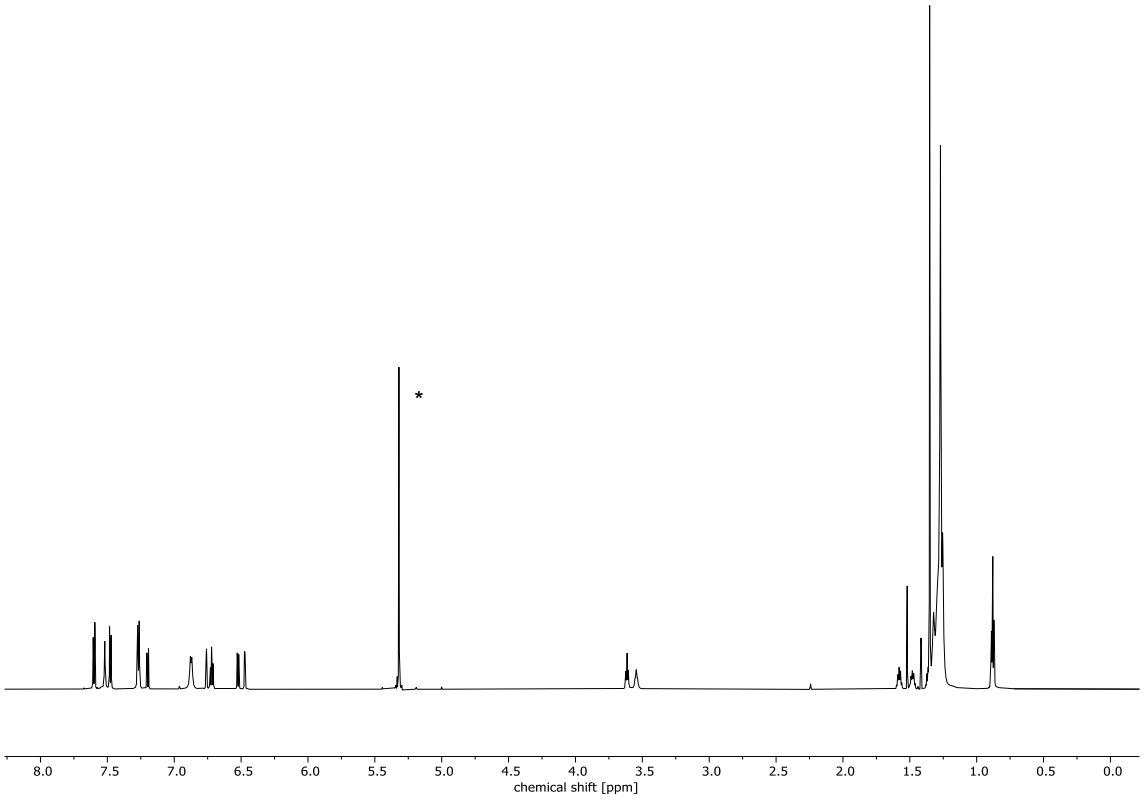

Figure 111: ^{1}H-NMR spectrum of **102** (700 MHz, CD_2Cl_2, 298 K), solvent marked with *.

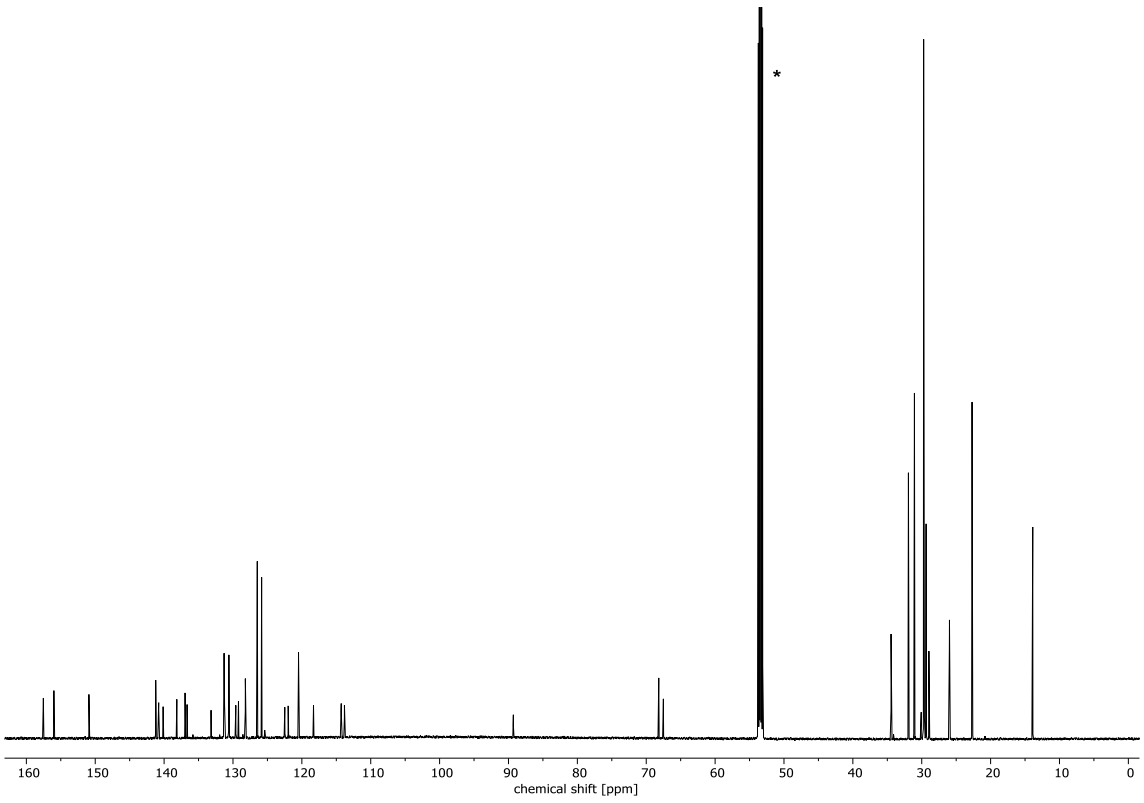

Figure 112: ^{13}C-NMR spectrum of **102** (176 MHz, CD_2Cl_2, 298 K), solvent marked with *.

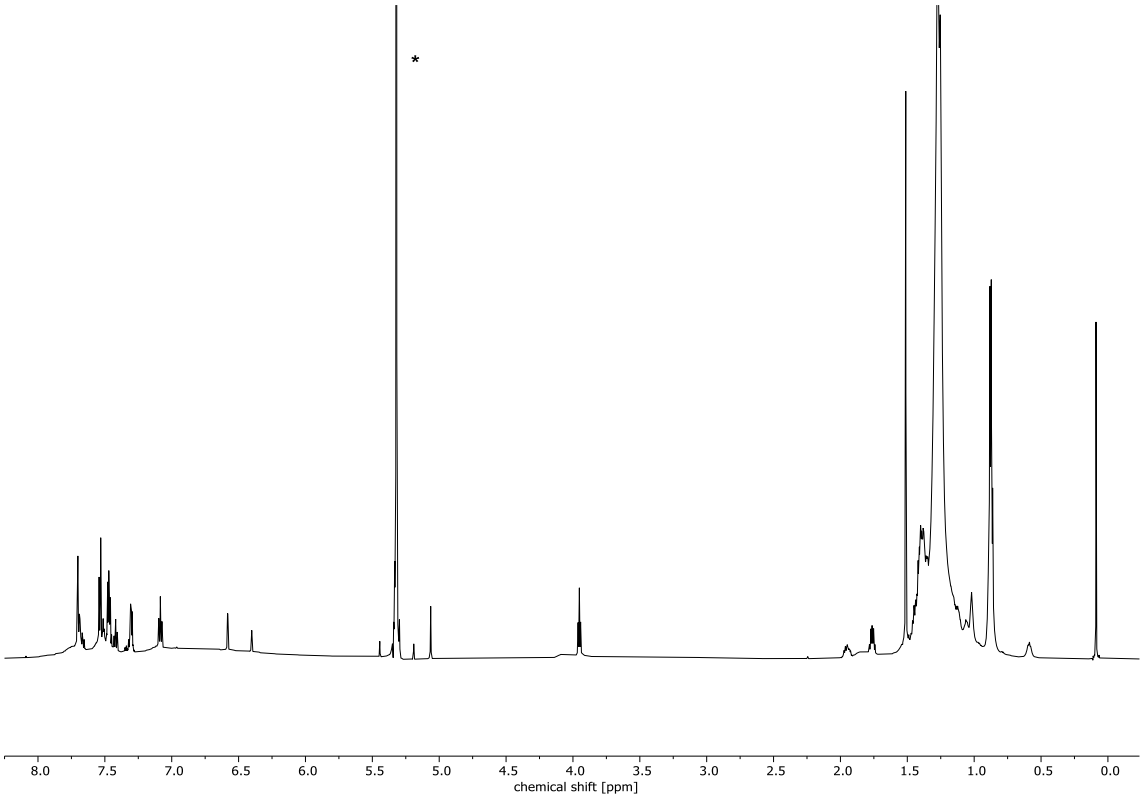

Figure 113: ^{1}H-NMR spectrum of **MSW-H** (700 MHz, CD_2Cl_2, 298 K), solvent marked with *.

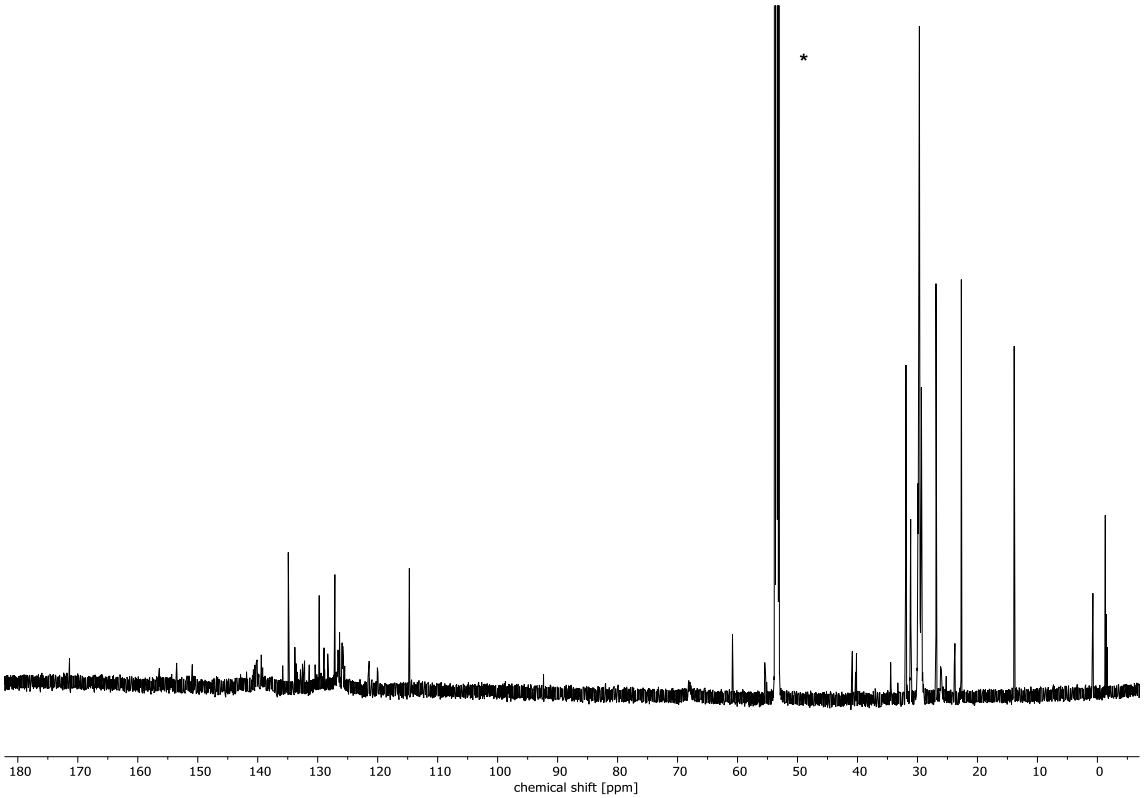

Figure 114: ^{13}C-NMR spectrum of **MSW-H** (176 MHz, CD_2Cl_2, 298 K), solvent marked with *.

10.4.2 Mass spectra

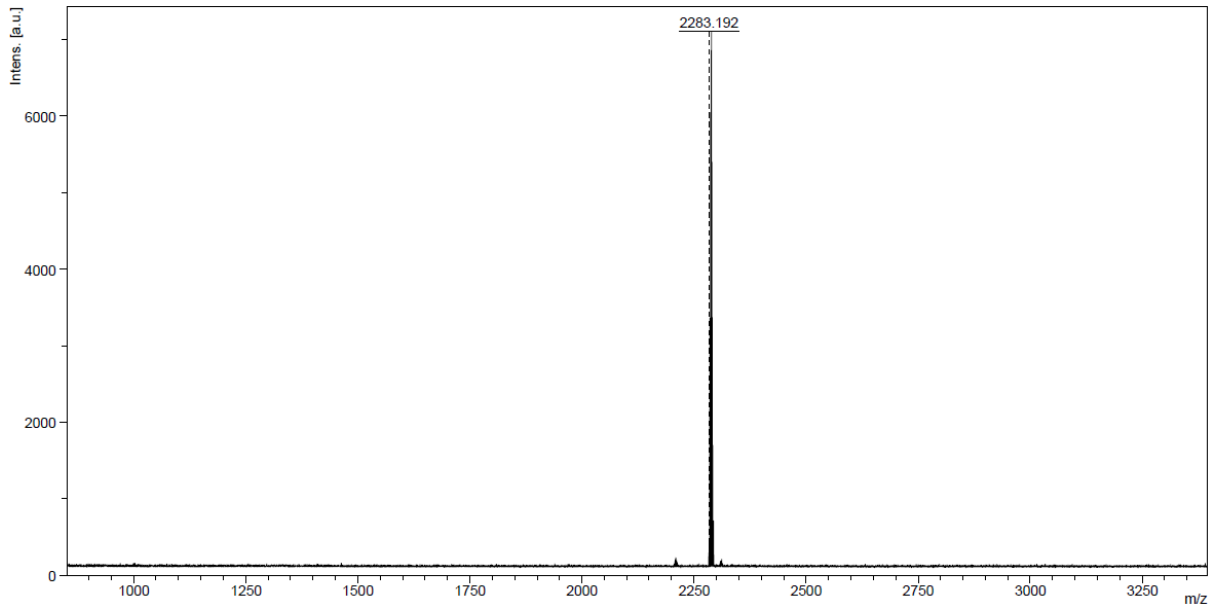

Figure 115: MALDI-TOF mass spectrum of **17a** (matrix: DCTB).

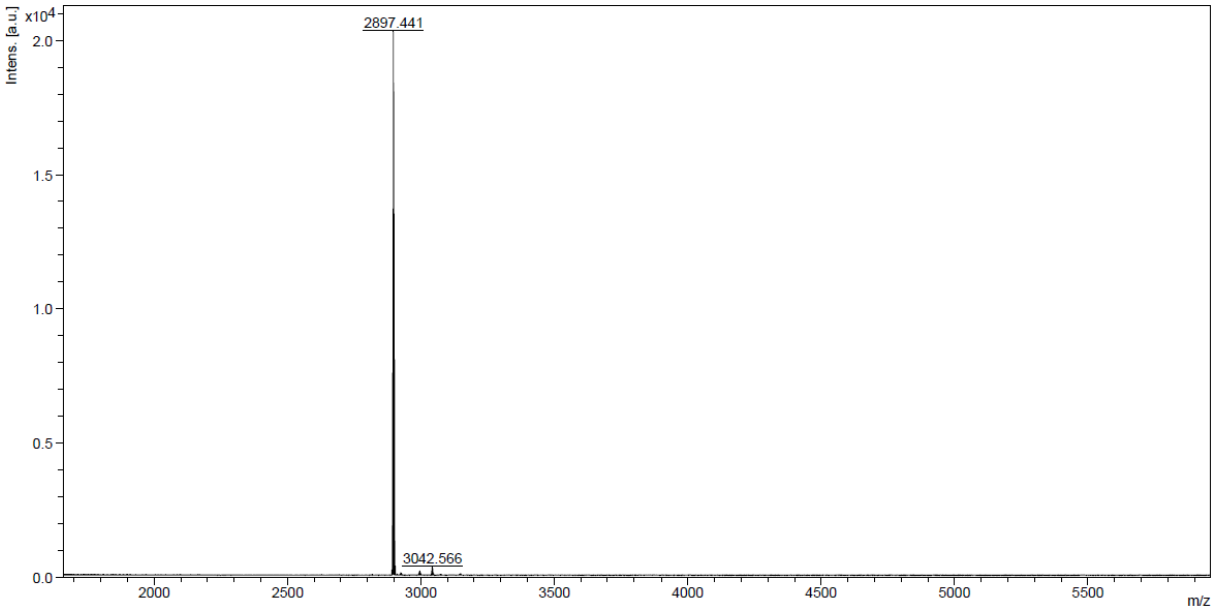

Figure 116: MALDI-TOF mass spectrum of **39** (matrix: DCTB).

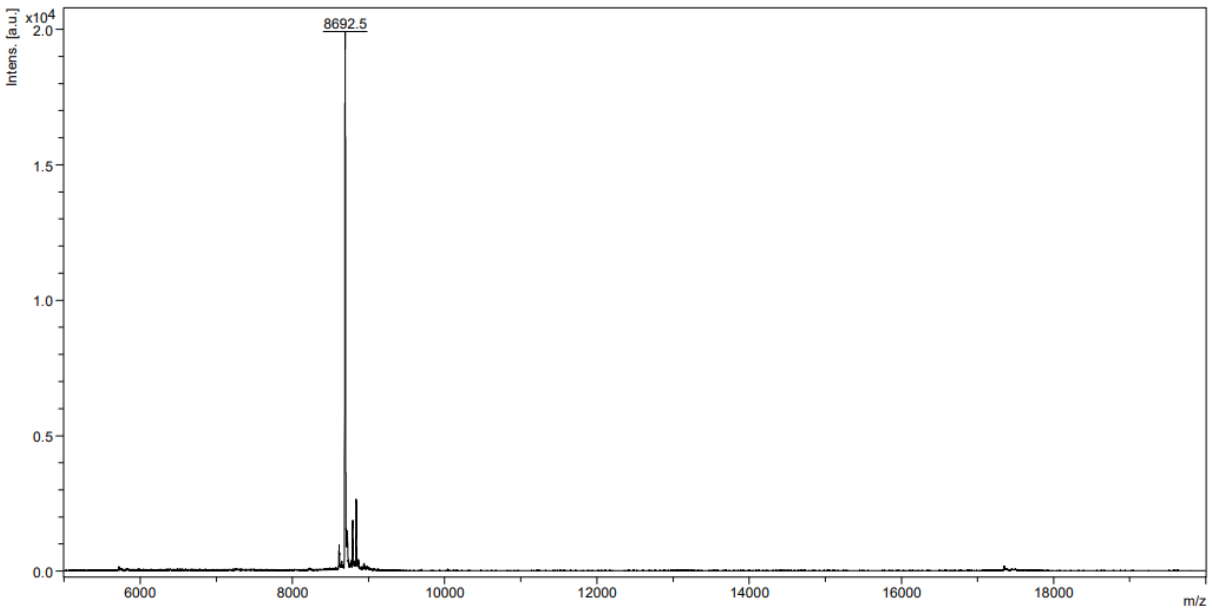

Figure 117: MALDI-TOF mass spectrum of **40** (matrix: DCTB).

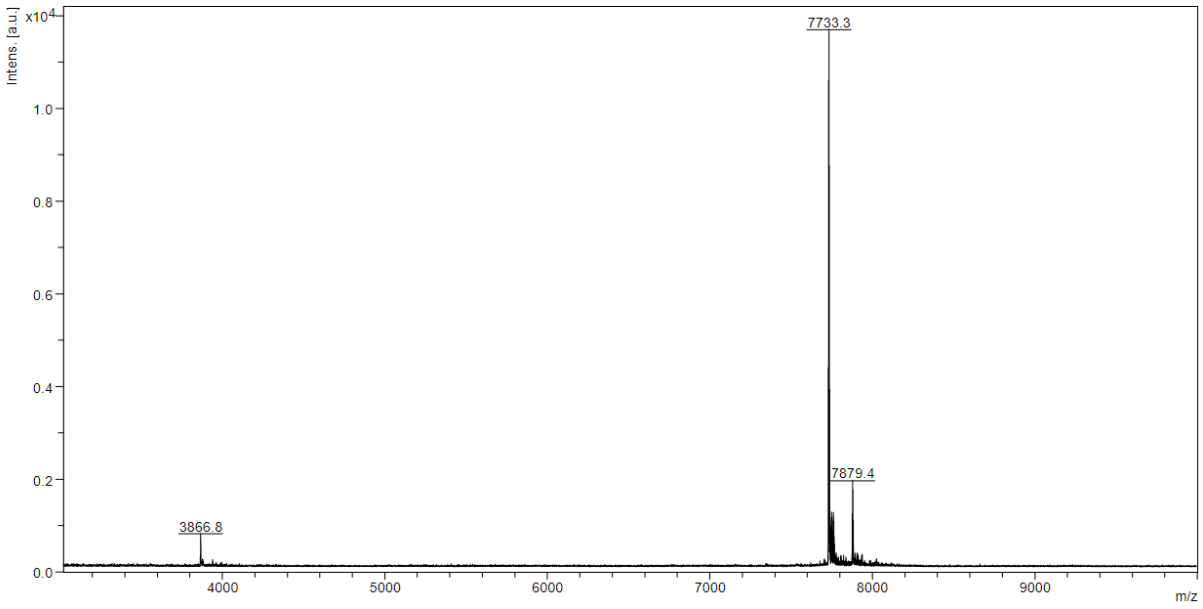

Figure 118: MALDI-TOF mass spectrum of **MSW-C** (matrix: DCTB).

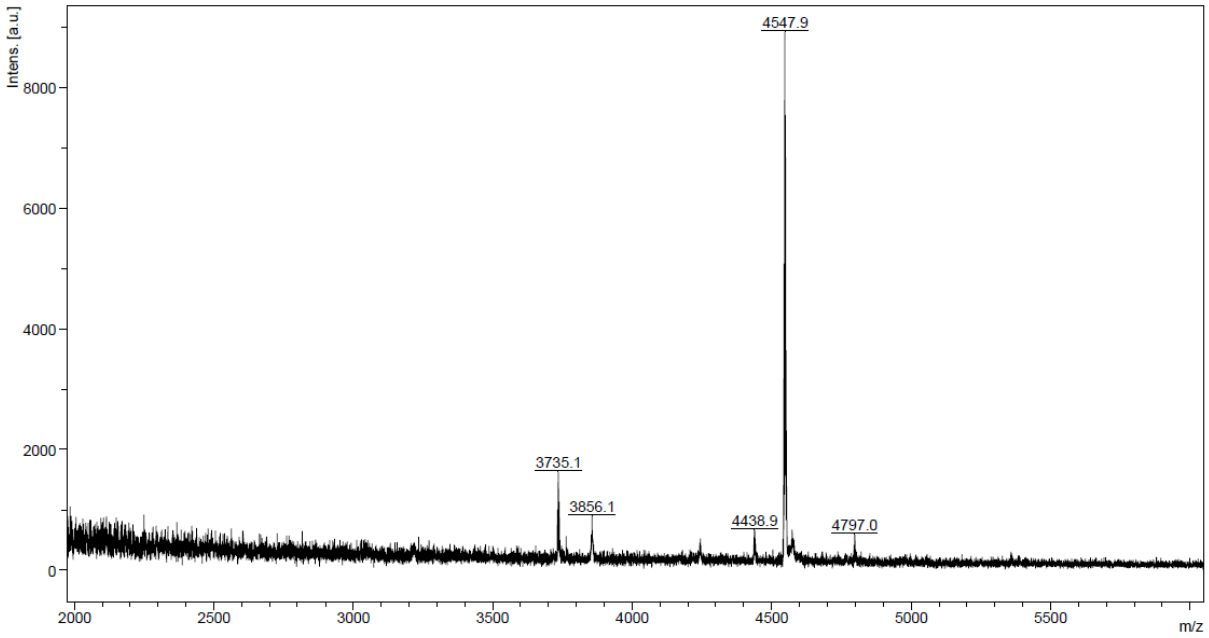

Figure 119: MALDI-TOF mass spectrum of **70a** (matrix: DCTB).

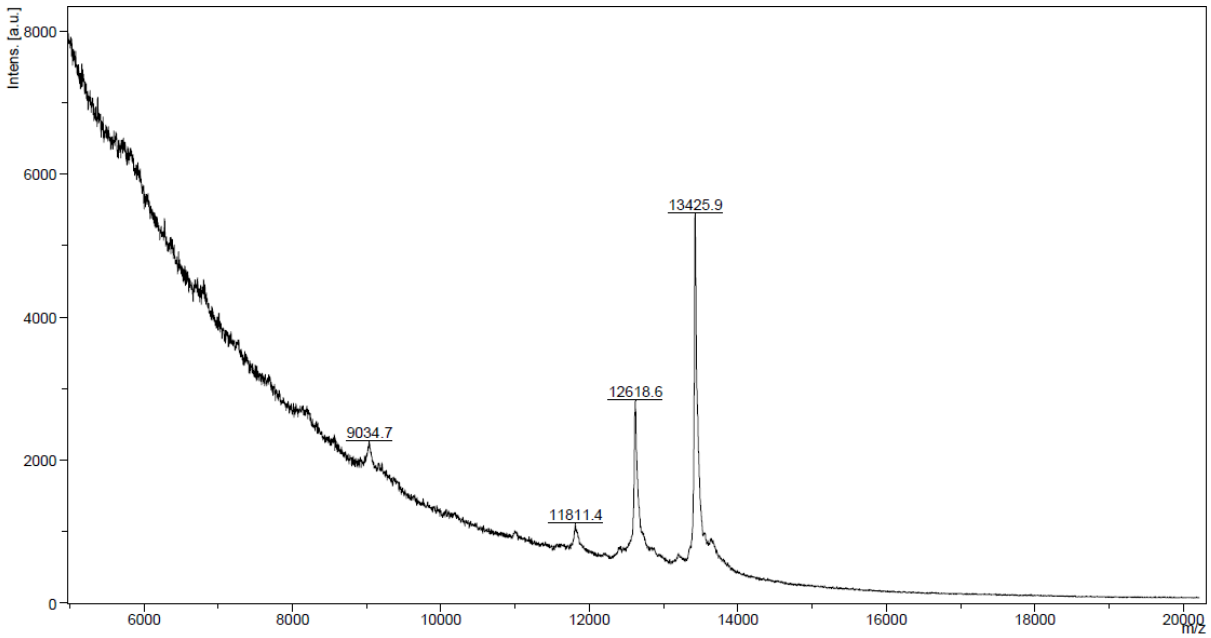

Figure 120: MALDI-TOF mass spectrum of **71a** (matrix: DCTB; added Ag^+-salts).

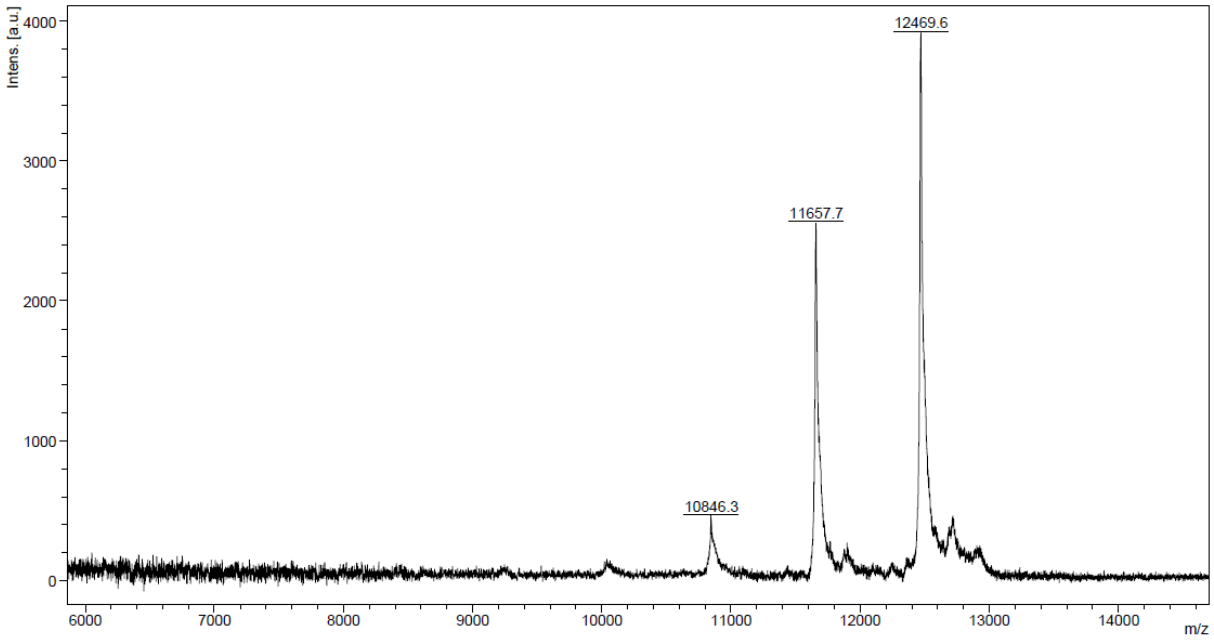

Figure 121: MALDI-TOF mass spectrum of **MSW-Fa** (matrix: DCTB; added Ag^+-salts).

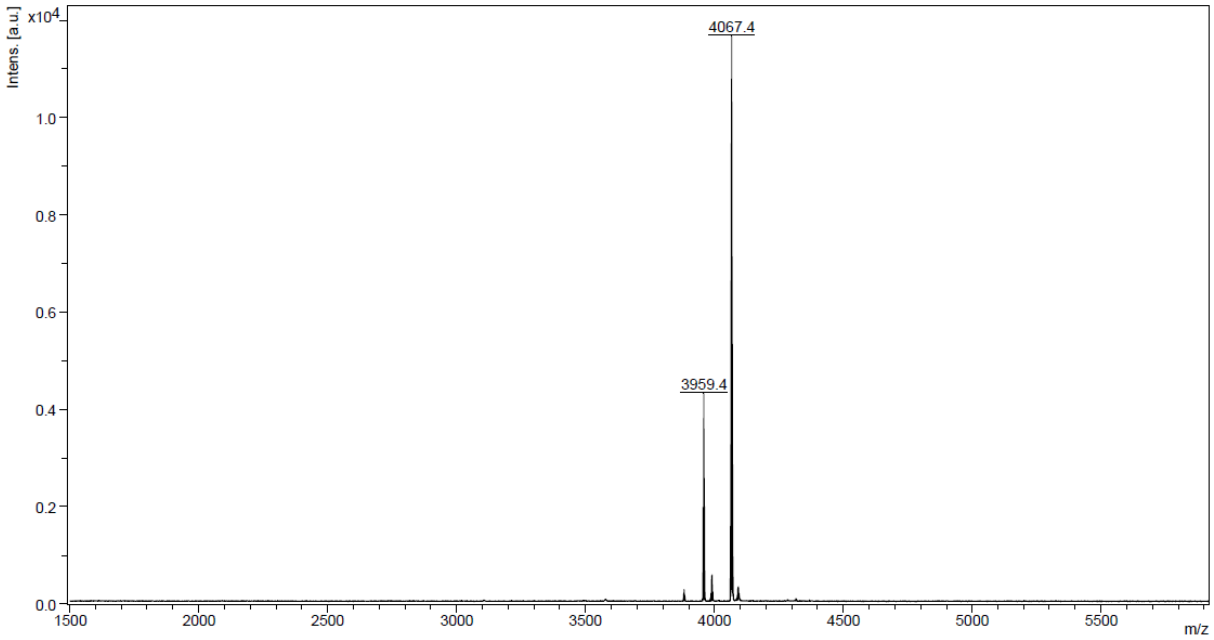

Figure 122: MALDI-TOF mass spectrum of **70b** (matrix: DCTB; added Ag^+-salts).

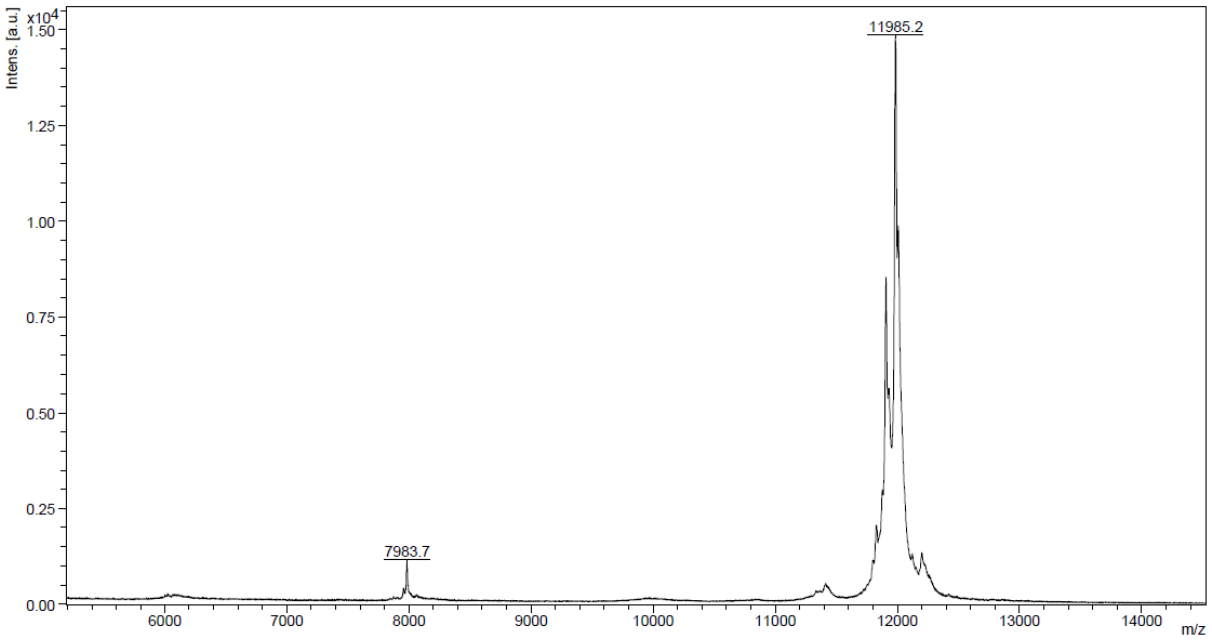

Figure 123: MALDI-TOF mass spectrum of **71b** (matrix: DCTB; added Ag^+-salts).

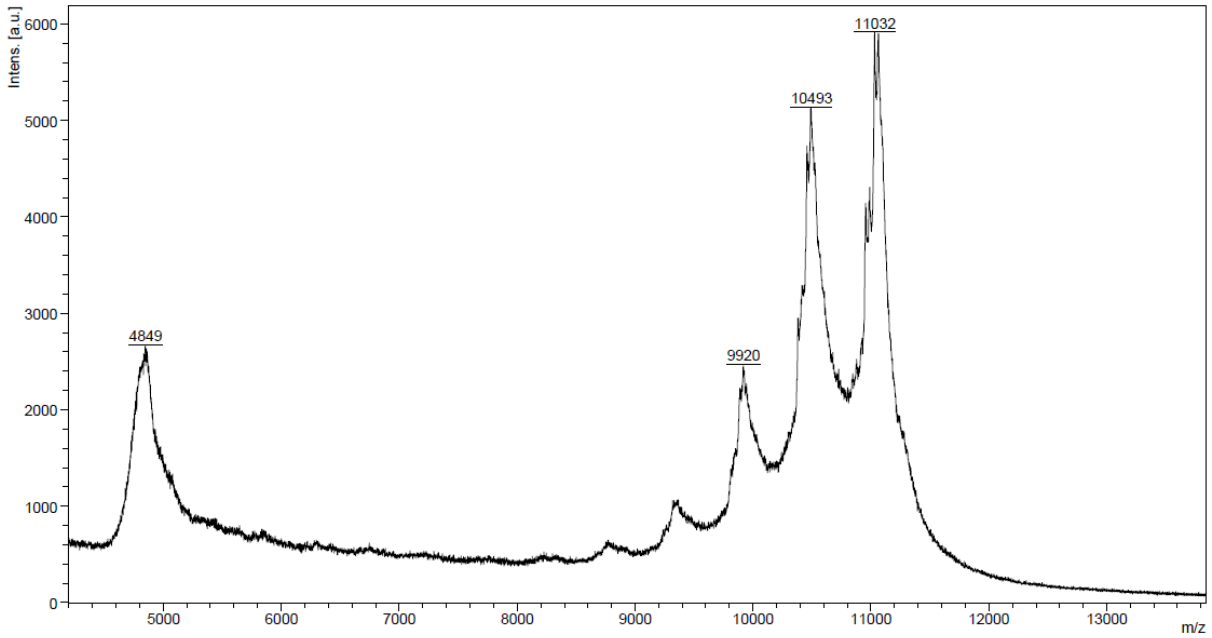

Figure 124: MALDI-TOF mass spectrum of **MSW-Fb** (matrix: DCTB; added Ag^+-salts).

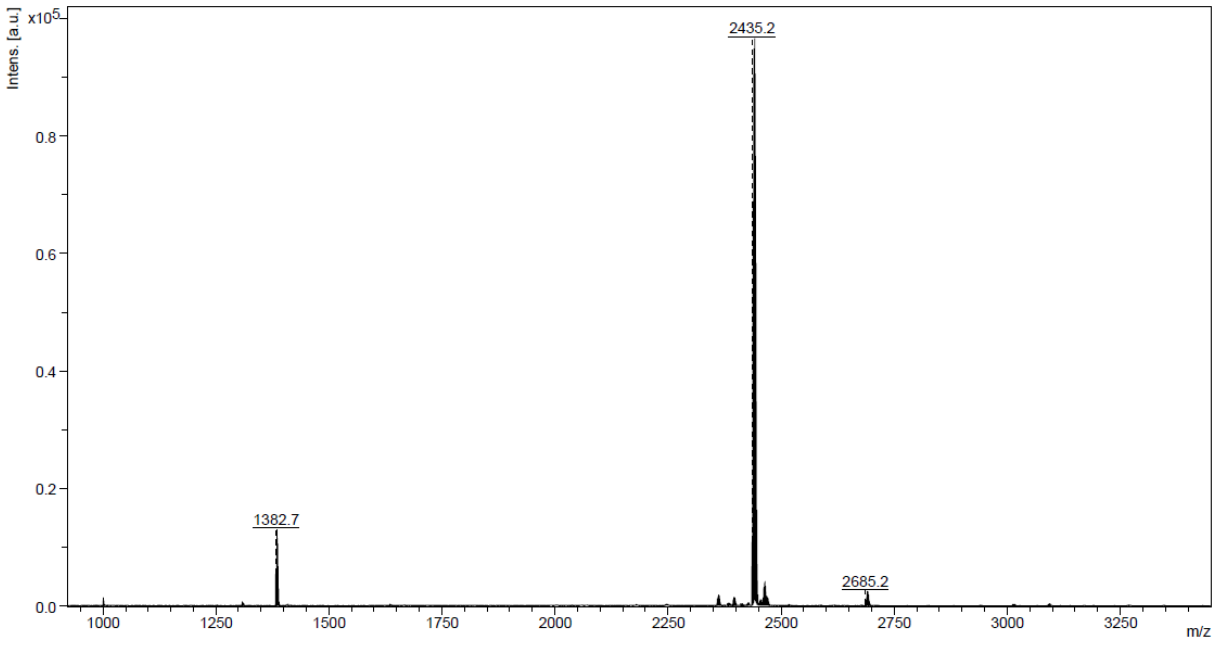

Figure 125: MALDI-TOF mass spectrum of **73** (matrix: DCTB).

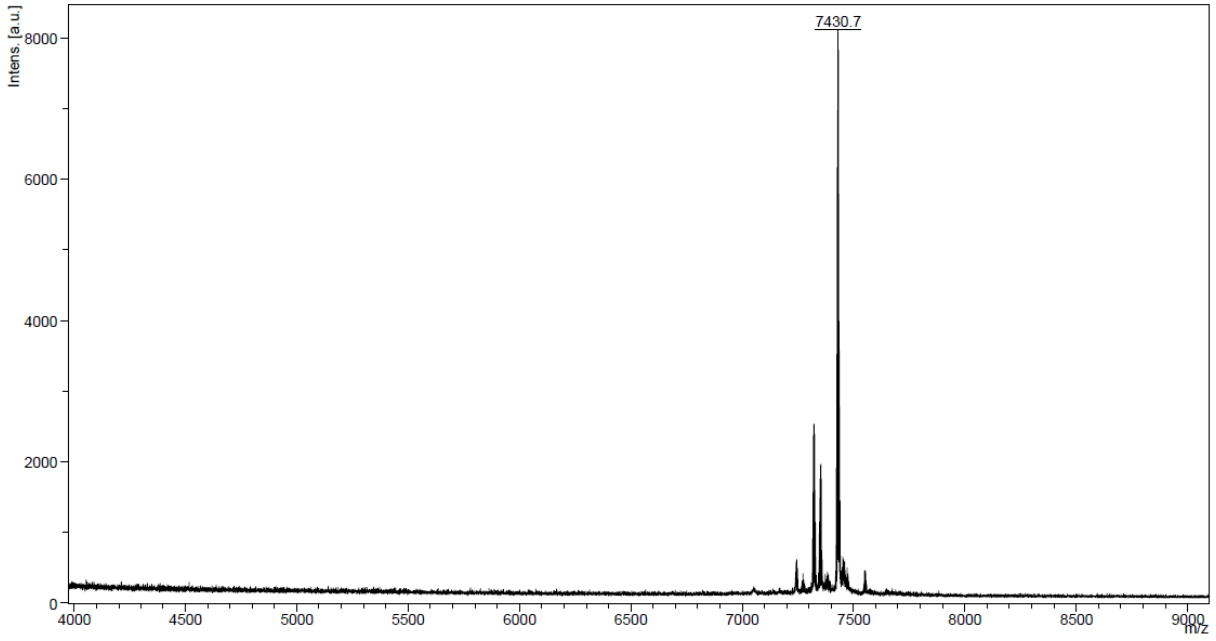

Figure 126: MALDI-TOF mass spectrum of **74** (matrix: DCTB; added Ag^+-salts).

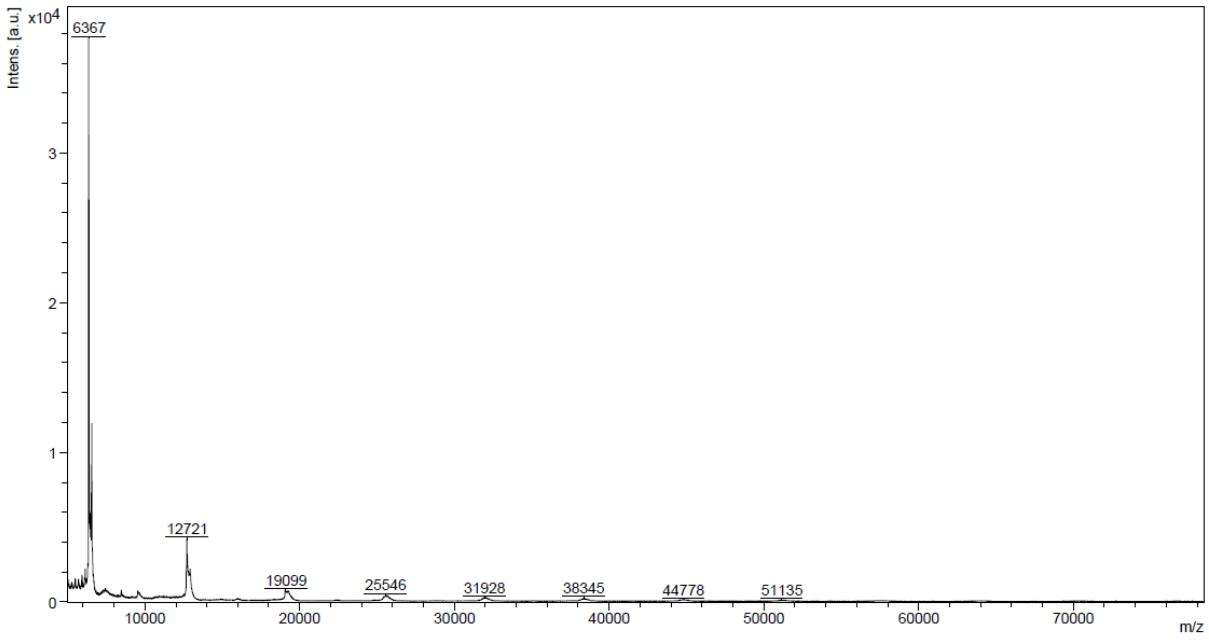

Figure 127: MALDI-TOF mass spectrum of the crude cyclization product of **74** (matrix: DCTB; added Ag^+-salts).

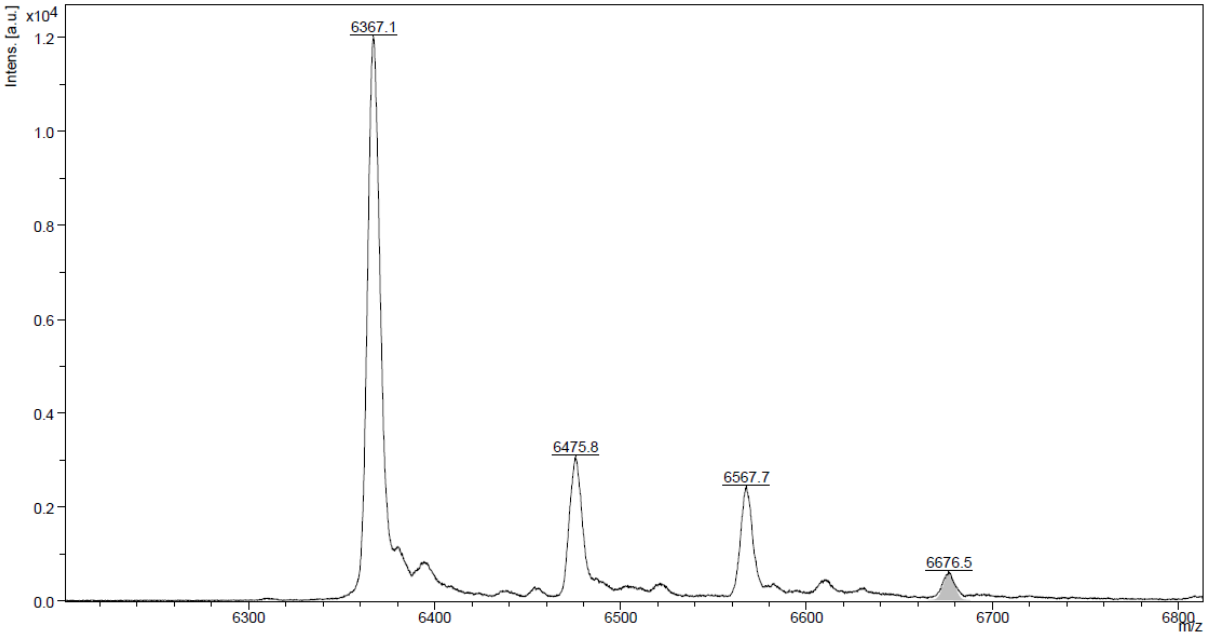

Figure 128: MALDI-TOF mass spectrum of **75** (matrix: DCTB; added Ag^+-salts).

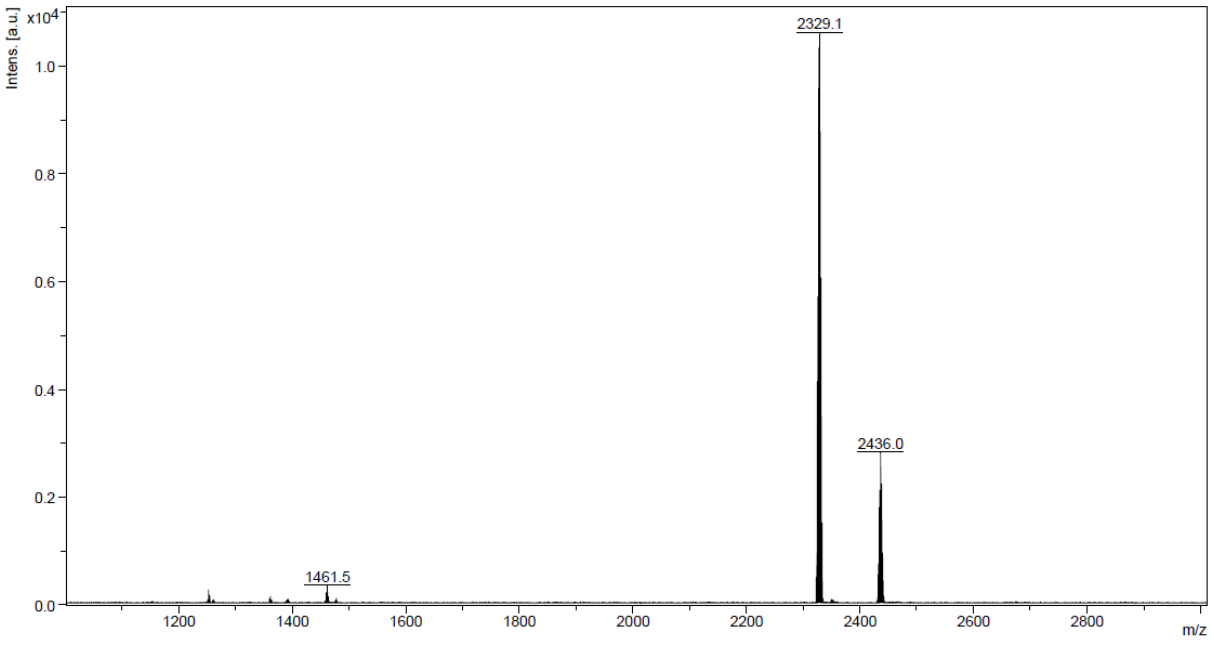

Figure 129: MALDI-TOF mass spectrum of **102** (matrix: DCTB; added Ag^+-salts).

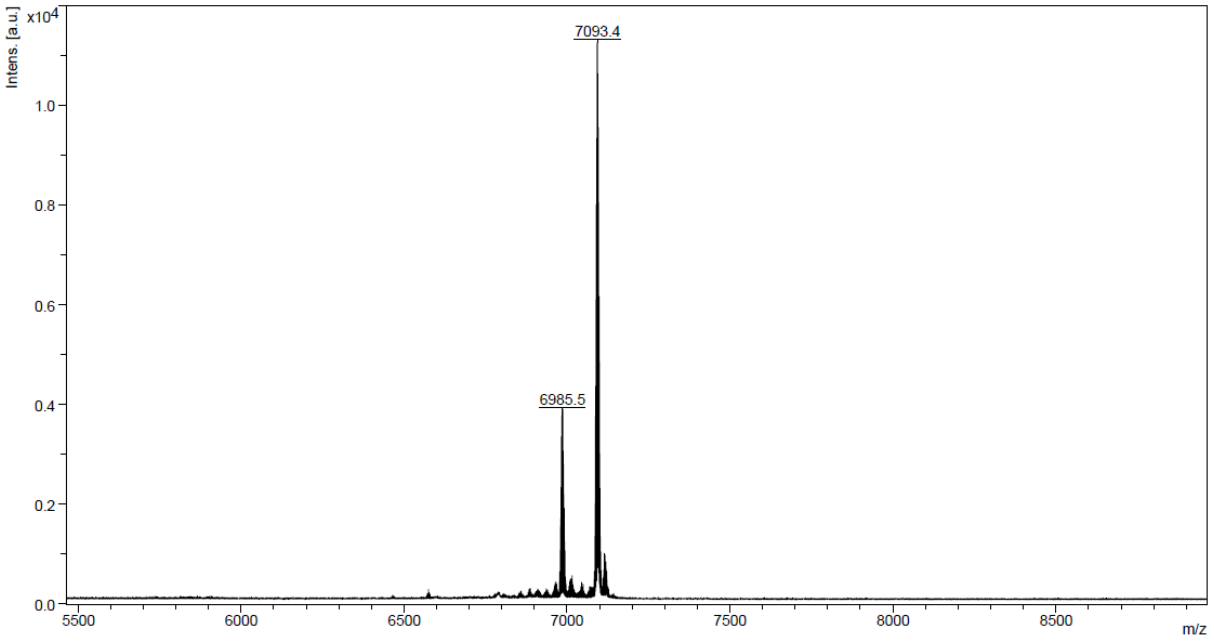

Figure 130: MALDI-TOF mass spectrum of **103** (matrix: DCTB; added Ag^+-salts).

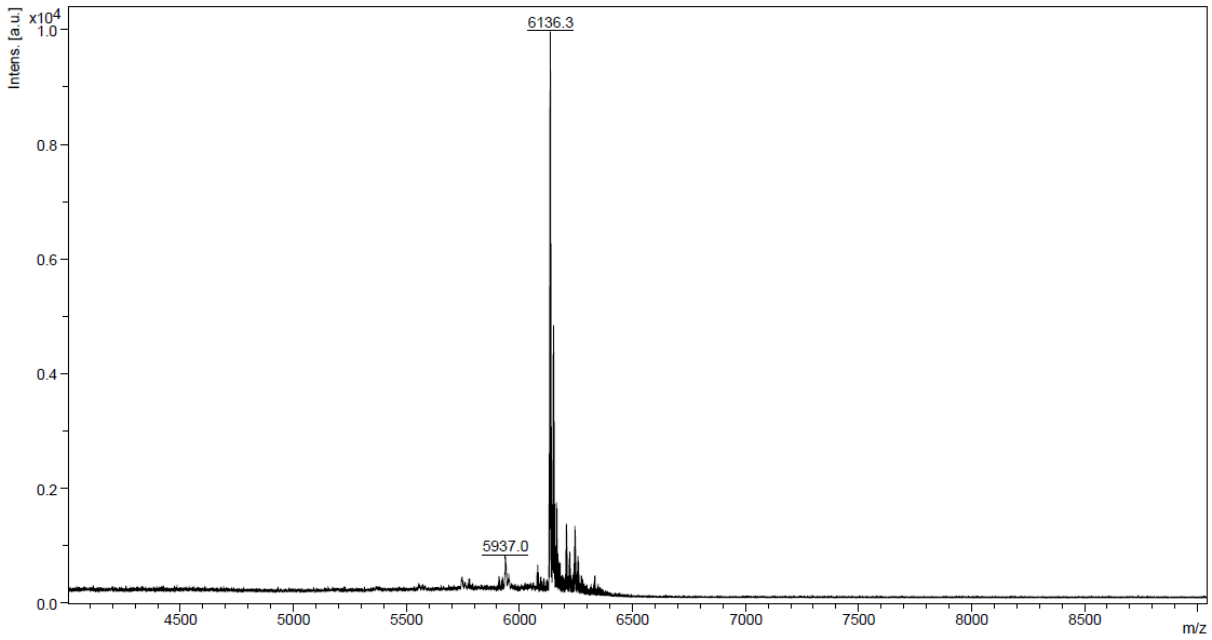

Figure 131: MALDI-TOF mass spectrum of **MSW-H** (matrix: DCTB; added Ag^+-salts).